EPA-650/2-75-009

JANUARY 1975 Environmental Protection Technology Series

FABRIC FILTER CLEANING STUDIES

Office of Research and Development
U.S. Environmental Protection Agency
Washington, DC 20460

RESEARCH REPORTING SERIES

Research reports of the Office of Research and Development, U. S. Environmental Protection Agency, have been grouped into series. These broad categories were established to facilitate further development and application of environmental technology. Elimination of traditional grouping was consciously planned to foster technology transfer and maximum interface in related fields. These series are:

1. ENVIRONMENTAL HEALTH EFFECTS RESEARCH
2. ENVIRONMENTAL PROTECTION TECHNOLOGY
3. ECOLOGICAL RESEARCH
4. ENVIRONMENTAL MONITORING
5. SOCIOECONOMIC ENVIRONMENTAL STUDIES
6. SCIENTIFIC AND TECHNICAL ASSESSMENT REPORTS
9. MISCELLANEOUS

This report has been assigned to the ENVIRONMENTAL PROTECTION TECHNOLOGY series. This series describes research performed to develop and demonstrate instrumentation, equipment and methodology to repair or prevent environmental degradation from point and non-point sources of pollution. This work provides the new or improved technology required for the control and treatment of pollution sources to meet environmental quality standards.

EPA-650/2-75-009

FABRIC FILTER CLEANING STUDIES

by

Richard Dennis and John Wilder

GCA Technology Division
Burlington Road
Bedford, Massachusetts 01730

Contract No. 68-02-0268
ROAP No. 21ADJ-049
Program Element No. 1AB012

EPA Project Officer: Dale L. Harmon

Control Systems Laboratory
National Environmental Research Center
Research Triangle Park, North Carolina 27711

Prepared for

OFFICE OF RESEARCH AND DEVELOPMENT
U.S. ENVIRONMENTAL PROTECTION AGENCY
WASHINGTON, D.C. 20460

January 1975

EPA REVIEW NOTICE

This report has been reviewed by the National Environmental Research Center - Research Triangle Park, Office of Research and Development, EPA, and approved for publication. Approval does not signify that the contents necessarily reflect the views and policies of the Environmental Protection Agency, nor does mention of trade names or commercial products constitute endorsement or recommendation for use.

This document is available to the public for sale through the National Technical Information Service, Springfield, Virginia 22161.

CONTENTS

		Page
List of Figures		xiii
List of Tables		xxi
Nomenclature		xxiv
Conversion Factors for British and Metric Units		xxvii
Section	Title	
I	INTRODUCTION	1
	ROLE AND CAPABILITIES OF FABRIC FILTER SYSTEM	1
	PROBLEMS IN AEROSOL FILTRATION	1
	PROBLEMS IN FABRIC FILTER CLEANING	2
	PROGRAM OBJECTIVES	3
	SELECTION AND SEQUENCE OF STUDY OF FABRIC CLEANING METHODS	4
	SUMMARIZED CONCLUSIONS AND RECOMMENDATIONS	6
	Conclusions	6
	Recommendations	8
	REFERENCES	9
II	MECHANICAL SHAKING STUDY	11
	OBJECTIVES AND APPROACH	11
	BACKGROUND AND THEORY	13
	Adhesion and Removal Mechanisms Including Acceleration	14
	Bag Motion Theory	21
	Basic Concepts	21
	Waves and Wave Velocity	24
	Tension Changes	25
	Damping and Reflection	28

CONTENTS (Continued)

Section	Title	Page
	Bag Acceleration	29
	Shaking Energy and Power	30
	Bag Life	32
	Collection Efficiency	32
	APPARATUS, TECHNIQUES AND MATERIALS	36
	Shaker Apparatus	36
	Test Fabrics	41
	Bag Properties and Measurement Techniques	41
	Lineal Density	45
	Bag Weight and Bag Tension	45
	Bag Modulus	46
	Shaking Energy and Power	49
	Motion of the Shaking Bag	50
	Test Dusts	50
	Dust Measurements	53
	Aerosol Concentration and Particle Size	53
	Dust Filtering Rate	60
	Dust Removal	60
	Residual Dust	60
	Pressure, Air Flow and Air Properties Measurements	62
	RESULTS	63
	Cleaning Forces and Bag Motion	63

CONTENTS (Continued)

Section	Title	Page
	Bag Tension versus Shaking Frequency	63
	Bag Acceleration	69
	Bag Power Consumption	80
	Dust Removal	86
	Dust Removal versus Number of Shakes	89
	Dust Removal versus Shaking Frequency	92
	Dust Removal versus Shaking Amplitude	94
	Dust Removal versus Acceleration	100
	Dust Removal versus Initial Bag Tension	107
	Dust Removal versus Cloth Loading	107
	Dust Removal versus Fabric Type	113
	Dust Removal versus Dust Type	115
	Summary of Dust Removal Studies	119
	Collection Efficiency and Emission	121
	General Observations	122
	Effluent Concentration versus Filtration Time	124
	Effluent Concentration versus Shaking Amplitude	131
	Effluent Concentration versus Shaker Frequency	131
	Effluent Concentration versus Bag Life and Bag Stretch	134
	Efficient Concentration versus Fabric Type	137

CONTENTS (Continued)

Section	Title	Page
	Efficient Concentration versus Dust Type	138
	Discussion of Particle Emission Studies	144
	Filter Resistance	146
	Linearity of Resistance-Time Curves	149
	Specific Resistance Coefficient, K	149
	Effective Residual Resistance	154
	Discussion of Operating Parameters for Various Filter Systems	157
	Bag Life	158
	CONCLUSIONS TO MECHANICAL SHAKING STUDY	167
	General Conclusions	167
	Particulate Emissions	168
	Dust Removal by Mechanical Shaking	171
	Filter Resistance and Power Requirements	172
	REFERENCES	173
III	PULSE CLEANING STUDIES	175
	OBJECTIVES AND APPROACH	175
	BACKGROUND	176
	Applications and Advantages	176
	Problem Areas	177
	Collector Performance	178
	Resistance and Particle Removal	178
	Factors Involved in Dust Removal	181

CONTENTS (Continued)

Section	Title	Page
	Adhesion	181
	Dislodgement	181
	Reverse Air Transport	182
	APPARATUS, MATERIALS AND TECHNIQUES	182
	Filter Assembly	183
	Pulse Jet Cleaning Equipment	185
	Test Fabrics	188
	Bag Properties and Measurement Techniques	190
	Bag Motion	191
	Accelerometer	191
	Strain Gage	191
	High Speed Photography	192
	Test Dusts	192
	Dust Measurements	192
	Pressure and Flow Measurements	194
	RESULTS	196
	Particulate Emission Characteristics	196
	Compressed Air Pressure	197
	Cleaning Frequency (Operating Cycle)	204
	Cleaning Pulse Duration	210
	Felt Type	210
	Dust Type	213
	Filtration Parameters	215

CONTENTS (Continued)

Section	Title	Page
	Design Modifications	218
	Particle Size and Concentration Changes During Filtration Cycle	224
	Residual Filter Resistance	233
	Concentration Profiles, Dust Emissions	236
	Operating Filter Resistance	237
	Compressed Air Pressure	242
	Pulse Interval	242
	Pulse Duration	245
	Felt Type	245
	Dust Type	245
	Filtration Parameters	248
	Design Modifications	250
	Control of Operating Resistance	252
	Residual Resistance	253
	Transition Pressure	268
	Operating Resistance	269
	Factors in the Selection of Optimum Operating Conditions	270
	CONCLUSIONS TO PULSE JET CLEANING STUDIES	272
	General Conclusions	272
	Particulate Emissions	273
	Dust Removal and Filter Resistance	275
	System Design and Operating Factors	276

CONTENTS (Continued)

Section	Title	Page
	REFERENCES	278
IV	REVERSE FLOW STUDIES	281
	OBJECTIVES AND APPROACHES	281
	BACKGROUND	282
	Postulated Cleaning Actions	282
	Basic Design Concepts	284
	APPARATUS, MATERIALS AND TECHNIQUES	285
	Modified Mechanical Shaking System	285
	Modified Pulse Jet System	288
	Test Fabrics	289
	Measurements and Instrumentation	289
	Test Dusts	290
	RESULTS	290
	Low Pressure, Reverse Flow with Mechanical Shaking	290
	Low Pressure, Reverse Flow With Pulse Jet Equipment	295
	Slow Inflation Rate, Reverse Flow Only	296
	Pressure Rise Rate, Reverse Flow Only	299
	Frequency of Cleaning, Reverse Flow Only	302
	Reverse Flow Duration - Reverse Flow Only	304
	Reverse Flow With Reverse Pulse Cleaning	307
	CONCLUSIONS TO REVERSE FLOW CLEANING STUDIES	310
	General Conclusions	311

CONTENTS (Continued)

Section	Title	Page
	Augmentation of Mechanical Shaking by Reverse Flow	312
	Felt Bags Cleaned by Reverse Flow	313
	REFERENCES	314
V	CONCLUSIONS AND RECOMMENDATIONS	315
	CONCLUSIONS	316
	Limits of Data Application	316
	Outlet Versus Inlet Concentrations	316
	Fractional Particle Size Efficiencies	317
	Filter Effluent Concentrations	317
	Filter Cleaning Action	318
	Energy Requirements and System Capabilities	319
	RECOMMENDATIONS	319
	Equipment Application and Operating Parameters for Mechanically Shaken Filters	319
	Equipment Applications and Operating Parameters for Pulse Jet Filter Systems	320
	Research and Instrumentation Needs	321
Appendix		
A	AUTOMATIC FLOW CONTROL SYSTEM	325
B	FORCE AND VELOCITY MEASURING INSTRUMENTATION	331
	FORCE AND PRESSURE MEASUREMENTS	331
	VELOCITY MEASUREMENT	338
C	PHOTOELECTRIC DETECTION OF SHAKEN BAG MOTION	339

CONTENTS (Continued)

Appendix	Title	Page
D	THEORETICAL AVERAGE WAVE VELOCITY	341
E	BAG STRETCH AND TENSION DURING SHAKING	345
F	DAMPING AND AVERAGE BAG AMPLITUDE THEORY	349
G	ENVELOPE PHOTOGRAPHS OF BAG MOTION	351
H	DATA SHEETS FOR MECHANICAL SHAKING STUDIES	359
	DYNAMIC SHAKING TESTS	359
	Dust Removal Tests	360
	Effluent Size Properties	367
I	THEORY FOR LATERAL FORCES IN SHAKING	373
J	SYSTEM PRESSURE DIFFERENTIAL VERSUS SINGLE ELEMENT PRESSURE DIFFERENTIAL	379
	CONCLUSIONS	385
	Mathematical Model of a Five-Compartment Baghouse	386
	Results	387
K	DUST TRANSPORT DURING PULSE CLEANING	389
L	FABRIC ACCELERATION IN PULSE CLEANING	397
	MECHANICAL PROPERTIES OF THE BAG	398
	Dynamics of Bag Motion	400
	Estimating Fabric Deceleration	401
	STIFF, LIGHT FABRICS	401
	Flexible, Heavy Fabrics	402
	Moderately Stiff, Moderately Heavy Fabrics	403
	Velocity of Removed Agglomerates	404

CONTENTS (Continued)

Appendix	Title	Page
M	SUPPLEMENTARY DATA ON PRECISION OF MEASUREMENT TECHNIQUES	407
	ANDERSEN "OUTSTACK" IMPACTOR	407

LIST OF FIGURES

No.	Title	Page
1	Potential Dust Fabric Stresses Developed During Shake Cleaning	15
2a	Concepts of Cleaning Via Acceleration (a) High Adhesive/Cohesion Ratio	16
2b	Concepts of Cleaning Via Acceleration (b) Low Adhesive/Cohesion Ratio	16
3	Internally Illuminated 10-Foot by 6-Inch Diameter Cotton Bag, After Cleaning (Photo Approximately 4 Feet From Lower End)	20
4	Appearance of Shaking Sateen Weave Cotton Bag 10-Feet Long by 6-Inch Diameter (4 cps, 2-Inch Amplitude, 7.4 Pound Shaking Tension)	23
5	Variation of Bag Tension With Position of Shaker Arm	26
6	Schematic Frawing, Bag Mounting and Shaking Assembly	39
7	Mountings Used to Support Bottom of Shaken Bags	40
8	Bag Dimensions and Loop Design	44
9	Tensile Properties for a 10-Foot by 6-Inch Sateen Bag	48
10	Inlet Fly Ash Size Distributions by Andersen Cascade Impactor	56
11	Shaking Tension as a Function of Frequency for Cotton Sateen Bag	65
12	Predicted Versus Observed Resonant Frequencies	66
13	Maximum and Minimum Envelope Curves and Average Shaking Tension for Cotton Sateen Bag	67
14	Bag Displacement Versus Driven Frequency and Indicated Dynamic Tension	71
15	Effect of Shaker Amplitude on Shaking Tension	75
16	Effect of Fabric Type on Shaking Tension With 10 Ft. x 6 In. Bags (1 In. Shaking Amplitude)	76

LIST OF FIGURES (Continued)

No.	Title	Page
17	Effect of Length/Diameter Ration on Shaking Tension	77
18	Effect of Initial Tensioning on Shaking Tension With Unnapped, 10 Ft. x 6 In. Cotton Sateen Bags	78
19	Comparison of Average Bag Amplitudes as Calculated by Equation (2.8) or Equations (2.17) and (2.18)	81
20	Measured Power Inputs to Shaker Motor	82
21	Power Consumption, Phase Angle and Frequency Relationships for a 10 Ft. x 6 In. Cotton Sateen Bag (1 In. Amplitude)	84
22	Force and Velocity Versus Shaking Frequency and Period	85
23	Percent Fly Ash Removal Versus Number of Shakes and Shaking Frequency at 1-Inch Amplitude	91
24	Effect of Shaking Frequency on Filter Capacity for 1-Inch Shaking Amplitude	93
25	Effect of Resonance on Dust Removal	95
26	Effect of Number of Shakes, 8 cps, and Shaking Amplitude on Dust Removal From 10 Ft. by 6 In. Cotton Bags	97
27	Effect of Shaking Amplitude and Shaking Frequency, 350 Shakes, on Dust Removal From 10 Ft. by 6 In. Unnapped Cotton Bags	98
28	Effect of Shaking Frequency and Shaking Amplitude, 350 Shakes, on Dust Removal From 10 Ft. by 6 In. Cotton Bags	99
29	Dust Removal Versus Bag Acceleration for Cotton Bags, 350 Shakes	103
30	Dust Removal Versus Bag Acceleration for Cotton Bags, 40 Shakes	104
31	Filter Capacity Versus Average Bag Acceleration for Sateen Weave Cotton Bags	106

LIST OF FIGURES (Continued)

No.	Title	Page
32	Cloth Loading and Filter Drag Characteristics for Typical Shaking Regimes - Composite Curve	108
33	Dust Removal Versus Cloth Loading for Fixed Shaking Regime	109
34	Residual Fabric Loading Versus Average Bag Acceleration	111
35	Residual Fabric Loading Versus Total Number of Shakes at Three Acceleration Levels for Unnapped Sateen Weave Cotton	112
36	Residual Fabric Loadings for Various Fabrics With Fly Ash Aerosol (8 cps, 1 In. Amplitude Shaking)	114
37	Residual Fabric Loadings for Various Fabrics With Talc Aerosol (8 cps, 1-In. Amplitude Shaking)	116
38	Fabric Loading Versus Filter Drag for Woven Cotton and Dacron Bags With a Talc Aerosol (360 Shakes at 8 cps and 1-In. Amplitude)	117
39	Calculated Effluent Concentration Versus Time for Fly Ash and Ambient Dust Based on B&L Measurements	125
40	Calculated Effluent Number Concentration Versus Time and Particle Diameter for Fly Ash Filtration With Sateen Weave Cotton	129
41	Changes in Effluent Size Properties With Filtering Time for New ($< 10^4$ Shakes) and Old (2×10^7 Shakes) Bags (Sizing by Optical, B&L, Counter)	130
42	Calculated Concentration Versus Shaker Amplitude at Constant Shaking Frequency	132
43	Calculated Effluent Concentration Versus Shaking Frequency at Constant Amplitude	133
44	Inlet Concentration Versus Percent Weight Penetration, Ambient Temperature	136
45	Comparative Effluent Concentrations for Fly Ash With Different Fabrics	140

LIST OF FIGURES (Continued)

No.	Title	Page
46	Total Dust Emitted Per Filter Cycle Versus Fabric Type and Residual Dust Holding	141
47	Comparative Effluent Concentrations for Talc and Fly Ash With Cotton and Dacron Fabrics	143
48	Resistance Changes During Fly Ash Filtration (see Table 15)	150
49	Effect of Insufficient (Non-Equilibrium) Shaking on "K", Filter Drag and Fabric Loading With Fly Ash at 3.5 grains/ft.^{3} and 3 ft./min. Filter Velocity 10 Ft. x 6 In. Cotton Sateen Bag	153
50	Residual Filter Resistance and Residual Fabric Loading (Figure 34) Versus Bag Acceleration for Fly Ash/Sateen Weave Cotton System	155
51	Bag Elongation Versus Total Number of Shakes for Used and Clean, 10 Ft. x 6 In. Sateen Weave Cotton Bags	161
52	Bag Elongation Versus Total Number of Shakes for Various Used 10 Ft. x 6 In. Fabric Bags	164
53	Schematic of Pulse Jet Cleaning Assembly	184
54	Standard Pulse Delivery System	186
55	Average Outlet Concentrations for Fly Ash Versus Reservoir Pressure With Direct and Damped Pulses; (a) All Variables Averaged Except Pressure and Pulse Type; (b) Variations in Velocity, Loading and Pulse Type Shown Individually	198
56	Effect of Direct and Delayed Pulses on Bag Differential Pressure for Valve Open Time of 0.15 Second	200
57	Effect of Reservoir Pressure and Pulse Damping on Effluent Concentration for Fly Ash Filtration With Dacron Felt (Note: Inlet Mass Concentration Converted to Equivalent Number Concentration and Scaled by 10^{-4} for Comparison)	201
58	Effect of Frequency of Cleaning on Average Outlet Concentrations for Fly Ash Filtration With Dacron Felt	205

LIST OF FIGURES (Continued)

No.	Title	Page
59	Effect of Frequency of Cleaning on Average Outlet Concentrations for Fly Ash Filtration With Dacron Felt	207
60	Effect of Pulse Duration and Pulse Interval on Effluent Concentration for Fly Ash Filtration With Dacron Felt, Direct Pulse (Note: Inlet Mass Concentration Converted to Equivalent Number Concentration and Scaled by 10^{-4} for Comparison)	208
61	Effect of Pulse Duration and Pulse Interval on Effluent Concentration for Fly Ash Filtration With Dacron Felt, Damped Pulse (Note: Inlet Mass Concentration Converted to Equivalent Number Concentration and Scaled by 10^{-4} for Comparison)	209
62	Comparative Performance Between Wool and Dacron Felts With Fly Ash Filtration	211
63	Effect of Felt Type on Fly Ash Particulate Emissions	212
64	Comparative Filtration Characteristics for Talc and Fly Ash With Dacron Felt	214
65	Particle Concentration Versus Time for Selected Sizes	226
66	Particle Concentration Versus Time for Selected Sizes	227
67	Particle Concentration Versus Time for Selected Sizes	228
68	Particle Concentration Versus Time for Selected Sizes	229
69	Particle Concentration Versus Time for Selected Sizes	230
70	Particle Concentration Versus Time for Selected Sizes	231
71	Relationship Between Residual Dust Deposit and Residual Filter Resistance	234
72	Average Outlet Concentration Versus Average Filter Resistance (Reservoir Pressure 40 to 100 psig, Pulse Interval 1 min., and Pulse Duration 0.06 to 0.15 sec.	235
73	Dust Concentration Profile on Exit Side of Bag, Bottom to Top	238

LIST OF FIGURES (Continued)

No.	Title	Page
74	Resistance Characteristics for Fly Ash and Dacron Felt, Inlet Conc. 12 grains/ft.^{3}, Filtration Velocity 8.5 ft./min.	240
75	Resistance Characteristics for Talc and Dacron Felt, Inlet Conc. 1.53 grains/ft.^{3}, Filtration Velocity 8.5 fpm	241
76	Average Filter Resistance Versus Reservoir Pressure, Direct and Damped Pulses, for Fly Ash Filtration With Dacron Felt	243
77	Effect of Pulse Interval on Average Filter Resistance for 70 psig Pulses	244
78	Comparative Resistance Properties of Wool and Dacron With Fly Ash Filtration	247
79	Relationship Between Rate of Pressure Rise and Residual Filtration Resistance at 8.5 ft./min. Filtration Velocity	256
80	Residual Filter Resistance Versus (a) Pressure Rise Rate and (b) Reservoir Pressure (see Figures 76 and 79, Respectively)	258
81	Postulated Removal Mechanism for Reverse Air Drag Through a Loaded Felt	263
82	Schematic of Mechanical shaking System as Modified for Reverse Flow Cleaning	286
83	Schematic View, Pulse Jet Assembly With Low Pressure Reverse Air and High Pressure Nozzle Removed	287
84	Resistance Characteristics for Fly Ash/Unnapped Cotton Filtration With Mechanical Shaking and/or Reverse Flow	293
85	Resistance Characteristics for Fly Ash/Dacron (Plain Weave) Filtration With Mechanical Shaking and/or Reverse Flow	294
86	Controlled Variations in Rate of Differential Pressure Change Across Felt Bags (See Table 31)	300

LIST OF FIGURES (Continued)

No.	Title	Page
87	Air Volume Ejected Per Pulse With Commercial 1/4-in. Nozzle and Solenoid Valve Assembly	303
88	Characteristic Pressure/Time Traces for Variations in Reverse Pulse Duration (see Table 33)	306
89	Differential Pressures Across Dacron Felt Bag for Indicated Cleaning Conditions	309
A-1	Automatic Flow Control System	327
B-1	Load Cell Mounting for Shaken Bags, Model 1	332
B-2	Revised Design for Load Cell Mounting for Shaken Bags	333
B-3	Load Cell Mounting for Weighing the Pulsed Bag Assembly	335
B-4	Circuit Diagram, Signal Output From Load Cell	336
C-1	Description of Bag Motion by Interception of Light Beam	340
G-1	Position of Photographs Relative to Resonant Frequencies	351
G-2	Bag Displacement Versus Shaking Frequency	352
H-1	Sample Data Sheet for Dust Removal Tests	363
H-2	Typical Effluent Concentrations Versus Particle Size Category and Filtration Time	368
J-1	Operating Variables in a Multicompartment Baghouse	380
K-1	Transport Effects on Particle Disposition; s: Small Particles, M: Medium Particles, l: Large Particles	390
K-2	Particle (or Agglomerate) Sizes Which are Supported by Upward Air Flow	394
L-1	Static Displacement of Fabric Surface at Constant Differential Pressure, Used Bags	399
M-1	Comparative Mass Loading Measurements With All-Glass Filters and Andersen Impactor (Foundry Dust, MMD = ~1 μm)	408

LIST OF TABLES

No.	Title	Page
1	Shaker Motion and Bag Suspension Used in Commercial Equipment	37
2	Properties of Woven Fabrics Selected (Manufacturers' Data)	42
3	Properties of Bags Tested in Mechanical Shaking Systems	43
4	Summary of Test Dust Size Properties	51
5	Comparative Aerosol Concentrations as Determined by Various Instrumental Methods	61
6	Envelopes of Motion for a Sateen Weave Cotton Bag	72
7	Calculated and Measured Average Bag Amplitudes	74
8	Sample Test Data Tabulation	90
9	Experimental Shaking Conditions	100
10	Dust Removal Versus Average Bag Amplitude Measured and Calculated Test Parameters	102
11	Filtration Characteristics of Various Dust/Fabric Combinations	118
12	Collection Efficiency and Effluent Concentrations for Various Cleaning Regimes	135
13	Effluent Concentrations Versus Averaging Period (Fly Ash; Unnapped Cotton Sateen Bags, 10 IN. X 6 FT.)	137
14	Fly Ash Emission Parameters for Different 10 FT. X 6 IN. Fabric Bags	139
15	Talc and Silica Emissions From New ($< 10^4$ Shakes) Cotton and Dacron Bags	142
16	Fly Ash Filtration Characteristics for New ($< 10^4$ Shakes) and Well-Used (2×10^7 Shakes) Bags	151

LIST OF TABLES (Continued)

No.	Title	Page
17	Effect of Extended Shaking on Tensile Properties of Clean and Dust Laden Cotton Bags, Fly Ash Aerosol	160
18	Tensile Measurements on New and Used Fabric Strips With Instron Tester	166
19	Properties of Test Felts	189
20	Outlet Concentration and Fraction Penetration for Various Reservoir Pressures and Direct and Damped Pulses	203
21	Talc and Fly Ash Filtration With Dacron Felt at 8.5 ft./min.	216
22	Effect of Variations in Filtration Velocity and Inlet Loading on Fly Ash Emissions With Dacron Felt	217
23	Summary of Test Parameters for Fly Ash and Talc Filtration With Dacron and Wool Felts	219
24	Effect of Pulse Duration on Average Filter Resistance for Various Dusts and Fabrics	246
25	Effect of Inlet Concentration and Filtration Velocity on Average Filter Resistance for Fly Ash and Dacron	249
26	Fly Ash Effluents From Pulsed Dacron Bags as a Function of Pulse Form	251
27	Typical Descriptors of Pulsed Bag Motion (Dacron Felt)	259
28	Parameters for Use in Equation (3.2)	260
29	Fly Ash Filtration With Mechanical Shaking and/or Low Pressure Reverse Flow Cleaning	292
30	Dust Removal Versus Reverse Flow Velocity, Volume, Pressure and Duration	297
31	Effect of Varying Rate of Pressure Change on Filter Resistance and Effluent Concentration.	301

LIST OF TABLES (Continued)

No.	Title	Page
32	Effect of Cleaning Frequency on Filter Resistance and Effluent Concentration With Reverse Flow Cleaning	304
33	Effect of Low Pressure PUlse Duration on Filter Resistance and Effluent Concentration	305
34	Effect of Pulse Jet and/or Reverse Flow Cleaning on Filter Resistance and Effluent Concentrations With a Fly Ash/Dacron Felt System	308
H-1	Summary Listing of Data Sheets for Tension/Shaking Frequency Studies	361
H-2	Summary Listing of Data Sheets for Typical Filtration and Mechanical Shaking Tests	364
H-3	Summary Listing of Data Sheets for Effluent Size and Concentration Properties for Various Dusts and Fabrics	370
I-1	Comparison of Measured and Predicted Lateral Forces	377
M-1	Weight Losses for Loaded Lubricated, Petri Dish Impactor Stages After Repeated Weightings	409

NOMENCLATURE

A	Shaker arm amplitude
C_i	Inlet concentration
D_f	Characteristic collector diameter
E'	Instantaneous energy in travelling wave per unit length
E_{cyc}	Energy per shaking cycle
F	Lateral force normal to shaker arm
F_{max}	Maximum lateral force
G	Flexibility modulus
K	Specific resistance coefficient
L	Length (bag)
M	Elastic (tensile) modulus of bag
M''	Shear modulus
N	Number of individual shakes or particles
P_c	Compressed air manifold pressure
$\overline{P}$	Average steady state power consumption
R_A	Shaker arm radius
S_e	Effective (initial) filter drag
S_t	Terminal filter drag
T	Tension
T_A	Initial midpoint bag tension (static) at maximum amplitude
T_d	Dynamic tension produced by shaking
T_i	Initial tension (static) at top of bag
$T_{i,m}$	Initial average midpoint tension (static)
T_m	Midpoint bag tension (dynamic)
T_p	Pulse duration
T_V	Initial midpoint tension, (static) shaker arm vertical
V	Velocity
$\overline{V}$	Average velocity
V_a	Lateral velocity of shaker arm
V_{amax}	Maximum lateral velocity of shaker arm
V_o	Initial particle ejection velocity
V_R	Average air velocity at resumption of air flow
V_T	Particle terminal velocity

NOMENCLATURE (continued)

W	Filter bag weight
W_R	Residual fabric dust holding, weight/unit area
W_T	Terminal fabric dust holding, weight/unit area
Y	Bag amplitude
$\overline{Y}$	Average bag amplitude
a	Acceleration
a_m	Maximum acceleration
c_i	Inlet concentration
cps	Cycles/second
d	Diameter or bag separation distance
e	2.71828....
f	Frequency
f_c	Pulse frequency or cleaning frequency
f_N	Resonant frequency
g	Acceleration in gravity field (32.2 ft./sec.^{2}) or gram
gr	Grain
h	Filter pressure drop or fabric thickness
h_r	Residual filter pressure drop (effective)
H_t	Terminal filter pressure drop
n	Exponent
t	Time
x	Distance (along bag)
α	Attenuation parameter (wave energy), dimensionless
β	Exponential damping rate, length^{-1}
Δp	Pressure lose, any filter bed
ΔT_E	One-half tension excursion at resonance
ΔY_E	Difference in bag amplitude for resonant and nonresonant states
ζ	Dust transport effectiveness parameter
θ	Phase angle relating force and velocity at shaker arm
λ	Wave length
$\overline{\lambda}$	Average wave length

NOMENCLATURE (continued)

μ	Viscosity
μm	Micrometer
π	3.14159....
ρ	Bag and/or dust mass per unit length
σ_g	Geometric standard deviation
τ	Relaxation time or period
ϕ	Function symbol

CONVERSION FACTORS FOR BRITISH AND METRIC UNITS

To convert from	To	Multiply by	To	Multiply by
^{o}F	^{o}C	$\frac{5}{9}$ (^{o}F-32)	———	———
ft.	meters	0.305	centimeters	30.5
$ft.^2$	$meters^2$	0.0929	$centimeters^2$	929.0
$ft.^3$	$meters^3$	0.0283	$centimeters^3$	28,300.0
ft./min. (fpm)	centimeters/sec.	0.508	meters/sec.	5.08×10^{-3}
$ft.^3$/min.	$centimeters^3$/sec.	471.9	$meters^3$/hr.	1.70
in.	centimeters	2.54	meters	2.54×10^{-2}
$in.^2$	$centimeters^2$	6.45	$meters^2$	6.45×10^{-4}
oz.	grams	28.34	grains	438.0
$oz./yd.^2$	$grams/meter^2$	33.89	$grams/centimeter^2$	3.39×10^{-3}
grains	grams	0.0647	———	———
$grains/ft.^2$	$grams/meter^2$	0.698	———	———
$grains/ft.^3$	$grams/meter^3$	2.288	———	———
lb. force	dynes	4.44×10^5	Newtons	0.44
lb. mass	kilograms	0.454	grams	454.0
$lb./ft.^2$	$grams/centimeter^2$	0.488	$grams/meter^2$	4880.0
in. H_2O/ft./min.	cm. H_2O/cm/sec.	5.00	$Newtons/meter^2$/cm/sec.	490.0

CHAPTER I

INTRODUCTION

ROLE AND CAPABILITIES OF FABRIC FILTER SYSTEM

Fabric filtration provides a highly effective means of dust control provided that the filter medium can be cleaned periodically at reasonable cost without impairing collection efficiency or disturbing the system gas flow. Although some electrostatic precipitators and wet scrubbers also provide high efficiency collection, ~ 99 to 99.9 percent in some applications, the greater collection capabilities of a fabric filter system should be sought for very hazardous materials such as asbestos, beryllium and plutonium. On the basis of equivalent inlet concentrations, for example, weight collection efficiencies for fabric filters range from 99.9 to 99.999+ percent and the effluent dust concentrations are about 10 to 1000 times lower than those attainable with wet scrubbing or electrostatic precipitation.[1] In terms of dollar investment, fabric filter systems represent some 25 percent of the commercial market and an estimated 10^5 fabric filter units are treating about 7.5×10^8 $ft.^3/min.$ of industrial effluents.[1]

PROBLEMS IN AEROSOL FILTRATION

Two specific problem areas have prevented more extensive usage of fabric filter systems. The first relates strictly to the working environment where high temperatures and/or corrosive materials lead to rapid degradation or at least abbreviated service lives for the filter media. Additionally, the inability to maintain highly humid gas streams at

temperatures safely above the dewpoint can also prevent effective application of fabric filters. The second problem area is that associated directly or indirectly with the fabric cleaning process, the principal reason for conducting the research described in this report.

PROBLEMS IN FABRIC FILTER CLEANING

Specific problem areas related to fabric cleaning, which must be carried out on an intermittent or continuous basis to provide uninterrupted, high efficiency gas filtration, are summarized below:

- Failure to remove sufficient dust in cleaning to maintain acceptable filter resistance.
- Fabric damage and frequent replacement due to excess or poorly distributed cleaning energy.
- Excessive cleaning energy requirement due to inefficient conversion of energy into mechanical stresses at the dust-fabric interface.
- Excessive time required for cleaning, requiring long filter compartment down-times and extra system capacity.
- Improper selection of cleaning method for a given application and improper selection of fabric for that cleaning method.
- Improper matching of dust and/or fabric properties and cleaning method.

Benefits to be derived from improved cleaning should: (1) make filtration technology feasible for new field applications; (2) reduce the chance of filter tearing or perforation with the ensuing release of particulate; and, (3) provide for significant reductions in emissions by avoiding over-cleaning in some applications.

Good fabric cleaning, with specific reference to the actual cleaning process used, may be judged by the following yardsticks:

- No significant reduction in collection efficiency immediately following and during cleaning of filter elements.
- Minimal average resistance to air flow over an extended operating period.
- Minimal time required for cleaning.
- Minimal reduction of fabric service life due in any way to cleaning including application of cleaning energy, mechanical wear of fabric during cleaning, or changes in the abrasive or plugging properties of dust due to cleaning.
- Minimal cleaning energy requirement.

Ideally, the costs to meet the above criteria in conjunction with all other costs related to the owning and operating of the filter system should be at a minimum for treating the prescribed volume of gas at the prescribed efficiency level.

The additional recovery of particulate accomplished by improved cleaning for many existing installations is estimated to be of the order of 0.1 percent of the amount presently under control (or collected). Unless the dust has a high intrinsic value, there might be little economic advantage to the added recovery and probably some cost disadvantage for increased handling or waste disposal. On the other hand, since most fabric filters operate in the 99 to 99.9 percent efficiency range, very significant reductions may be seen in terms of the discharge rate of particulates to the atmosphere, ~ 5 to 10 times, depending upon the specific installation.

PROGRAM OBJECTIVES

The objectives of the research program presented in this report were to:

- Determine how the effectiveness and utilization of fabric filter systems can be increased through a better understanding and application of filter cleaning methods.

- Design and construct a laboratory pilot plant testing facility and appropriate instrumental techniques that provide maximum flexibility for the investigation of existing and experimental fabric filtration and cleaning systems.

- Investigate currently used or proposed cleaning methods to identify and define the basic mechanisms responsible for dust removal.

- Suggest design and operating parameters for maximum utilization of existing cleaning methods and any new or improved techniques that might arise from this study.

SELECTION AND SEQUENCE OF STUDY OF FABRIC CLEANING METHODS

A very brief discussion of the principal methods of filter cleaning and the rationale for the selection and sequence of study of the fabric cleaning methods investigated in this program are presented in the following text. More detailed background data, including appropriate background and reference material, are provided in the individual chapters of this report.

The major program effort was directed to a study of mechanical shaking methods used with woven fabrics and reverse pulse-jet systems used with felted fabrics. It was estimated that some 35 and 22 percent, respectively, of existing filtration equipment are cleaned by the above methods.[1] Time restrictions dictated that a lesser effort be directed to low pressure, reverse-flow cleaning approaches which, taken as a broad class, are used in about 25 percent of existing filter systems.[1]

Although high pressure, pulse-jet systems appear to be increasingly popular filter cleaning methods, field surveys have indicated that mechanically shaken systems, because of their basic design simplicity, will continue to control a large fraction of the particulate emission potential for some time in the future. More important, properly selected woven fabrics in conjunction with mechanical shaking can provide much

greater particle retention than pulse-jet cleaned, felted media in most applications.

Pulse-jet systems, on the other hand, afford significant advantages in reduced space occupancy because of their high air-to-cloth ratios and a high degree of stability in exhaust ventilation rates which is essential for good source control of dust generating processes. In contrast to woven fabric filtration systems with mechanical shaking, pulse-jet systems have also been reported as better adapted for the filtration of very high dust loadings.

Despite the fact that filtration technology and its related fabric cleaning methods have been used for a long time, the design criteria for many systems depend mainly upon prior field experience and empirical projections of very limited laboratory data. Although the qualitative aspects of filter performance derive readily from theory and the cleaning action of various filter surface restoration methods can be explained satisfactorily on a qualitative basis, the existing literature provides very few quantitative guidelines to aid in the choice, method of application, and the evaluation of filter cleaning methods.

In that the overall effectiveness of any fabric filter system hinges upon the operator's ability to clean the media on some periodic basis so that resistance levels are moderate, the system gas flow relatively constant, and the particulate removal consistent either with process needs or emission control regulations, it was believed that a detailed investigation of fabric filter cleaning methods would represent a significant contribution to the state-of-the-art.

The results of the studies on mechanical shaking, high pressure pulse-jet cleaning and low pressure reverse-flow cleaning are described in the order named along with a detailed outlining of specific conclusions and recommendations in Chapters II, III, and IV, respectively. As pointed out previously the above cleaning techniques have been estimated to

represent about 82 percent of the market. Reverse jet (traveling blow ring) designs, units cleaned by high frequency mechanical (or sonically produced) vibrations and miscellaneous combinations of all cleaning methods typify the remaining collector designs in current usage. Time priorities did not allow for investigations of all possible cleaning systems.

Several new instrumental methods were developed exclusively for these studies that permitted measurements heretofore impossible either in the the laboratory or in the field. Unfortunately, most devices were restricted to laboratory use (or would at least be restricted to single bag collectors) because of the need to integrate sensor and filter system components. Details on the fabrication and the operation of special instrumentation are provided in the appendices. The development of theoretically and/or empirically derived relationships for describing overall collector function; i.e., bag motion, dust dislodgment forces and other aspects of particle and fabric kinetics are also presented in the appendices to amplify their treatment in the main text.

SUMMARIZED CONCLUSIONS AND RECOMMENDATIONS

Detailed conclusions appear in Chapters II, III and IV and slightly abbreviated versions of the conclusions and recommendations evolving from this study have been consolidated in Chapter V. Because of their large number and diversity, only a brief summation of the principal conclusions and recommendations is given here.

Conclusions

- Unless indicated to the contrary, the operating and performance parameters cited for the specific dust/fabric combinations investigated in this program cannot be applied safely to other dust/fabric systems without supporting data.

- Fabric filter performance is best judged by the concentration and size properties of the particulate

effluent. There are no simple relationships for predicting the above properties on the basis of the concentration and size distribution of the inlet dust and the clean fabric properties.

- Particle size distributions for filter effluents may more often be controlled by the agglomerating and dust release characteristics of the filter fabric (and method of cleaning) than by the inlet dust properties.

- Residual and average fabric resistance, dust holding capacity and dust retention characteristics can be predicted for specified dust/fabric combinations and specific cleaning systems.

- Filter effluent concentrations from mechanically shaken filters are, on the average, some 10 to 100 times lower than those for high pressure, pulse-jet systems.

- Dust removal by mechanical shaking results mainly from the acceleration/deceleration action of the bag produced by the shaker arm. Actual dust separation takes place when tensile forces exceed the adhesive and cohesive forces binding the dust to the fabric.

- Shaking frequency, shaking amplitude and duration of the shaking interval define the performance of mechanically-shaken, woven fabrics.

- Dust removal by high pressure pulse-jet action also results from the acceleration/deceleration action imparted to the fabric and the interaction of tensile and adhesive/cohesive forces.

- The waveform, the rate of differential pressure change across the fabric (a function of reservoir pressure, jet location and the opening time for solenoid values), and the average differential pressure over the duration of the pulse determine the performance of felted media cleaned by high pressure pulse-jet action.

- Aerodynamic forces per se play a very minor role in dust removal both in high pressure, pulse-jet systems where reverse cloth velocities seldom exceed 2 ft./sec. and in low pressure, reverse air cleaning where reverse velocities are seldom much greater than filtration velocities. In most instances, bag collapse and/or flexure caused by flow reversal are the major dust dislodging forces.

Recommendations

- Fabric filter systems cleaned by mechanical shaking should be used whenever highly toxic or harmful particulates are encountered. Insofar as possible, a woven fabric such as sateen weave cotton or its synthetic or mineral equivalent in terms of filtration properties should be selected.

- Woven fabric filters should always be maintained at sufficient tension to guarantee transmission of shaking energy over the complete length of the bag.

- No attempt should be made to use the shaking parameters suggested by laboratory studies in the field until the structural integrity of the bag enclosure and supporting members are determined.

- The use of felted fabrics cleaned by high pressure, pulse-jet air is recommended when the advantages of reduced space requirements, minimal air flow variations at critical exhaust points, and adaptability to high inlet dust loadings are important. The above features must be weighted, however, against higher outlet loadings and higher power needs.

- Net power requirements for pulse-jet systems may be lower at reduced compressed air pressure; e.g., 40 versus 100 psig despite greater fabric resistance while significant reductions ($\sim$ 5 times) are attainable in effluent concentrations.

- Regardless of reservoir pressure levels, a pulse-jet unit must employ fast acting valves to produce rapid changes in system pressure levels $>$ 1,500 in. water/sec.

- It is recommended that pilot plant and field engineering measurements be performed to determine the appropriate "K" values for dust/fabric combinations encountered in industrial practice.

- Fundamental studies should be performed to determine which particle and fiber (fabric) parameters, taken singly or in combination, are most important in determining characteristic "K" and residual resistance values for a specified dust/fabric combination in conjunction with a specified fabric cleaning technique.

- Carefully controlled laboratory pilot studies should be performed to define accurately the role of filtration velocity, dust loading, method of jet pulse admission, and bag dimensions (particularly length) with pulse-jet systems.

- Rigorous tests should be performed, initially on a bench scale and later on a pilot scale, to determine how the following factors control or may be utilized to improve the filterability of various dusts: electrostatic charge, its presence or absence on particles and/or fibers; particle size distribution with shape factor constant; humidity control; particle size versus fabric pore size; surface deposition versus interstitial deposition; and the use of conditioning methods such as induced agglomeration.

REFERENCES

1. Billings, C. E. and J. E. Wilder. Handbook of Fabric Filter Technology. GCA Corporation, Bedford, Massachusetts, Contract No. CPA-22-69-38, Available From National Technical Information Service, U.S. Department of Commerce, Springfield, Virginia 22151, Document No. PB 200-648. December 1970.

CHAPTER II

MECHANICAL SHAKING STUDY

OBJECTIVES AND APPROACH

Although shaking has been used for many years to remove accumulated dust from fabric filters, no quantitative analyses of the physical mechanisms controlling the cleaning process were published until about 1962. At that time, Walsh and Spaite[1] reported a series of experiments that related bag cleaning to the peak acceleration of the shaken end of the bag. Their tests showed distinct, nonlinear relationships between peak acceleration and the dust removed by shaking and the resultant pressure drop across the fabric. No data were presented on collection efficiencies, changes in fabric properties and expected bag service lives, nor was the acceleration of the shaker arm related to the motion of other parts of the bag. The optimization of the performance of a filter system, however, may be presumed to require a beforehand knowledge of all these factors.

In the present study attention was directed first to extending the relationship between shaker arm motion and cleaning and resistance characteristics to the overall motion of fabric bags. Secondly, the effects of shaking on dust collection efficiency, bag service life and the power needed to provide effective cleaning were investigated. This was accomplished by first identifying a mechanism whereby bag acceleration might reasonably promote dust removal, followed by a detailed study of the motion of clean bags. The latter step was necessary to avoid the complication of variable bag and system properties arising from

progressive loss of dust. The same motion mechanics were then applied to dust-laden bags with respect to the resulting dust removal and pressure differentials. Other tests were also conducted to determine collection efficiency and shaker power consumption as described in the following sections.

In order to represent accurately the force and motion patterns of typical shaken filter bags, apparatus was designed and constructed that would simulate typical fabric filter equipment.* The apparatus utilized cylindrical filter bags suspended from a horizontally-aligned rocker shaft. For convenience in manipulation of instrumentation external to the bags, the filter was operated on a positive pressure basis (fan upstream).

The ranges and magnitudes of the operating variables were selected so that test results might be applied to field filtration systems with minimal extrapolation. Tests were performed on a variety of woven fabric bags, each of which depicted a commonly used size or fabric type. A prime objective of this study was to investigate the underlying physical processes that contribute to either good or poor field performance in existing fabric filter systems. Although areas for improvement attainable by redesign or operational changes in existing systems were not overlooked, most tests were aimed at the need to define first the cleaning processes now in common usage before initiating any development work on new or novel designs.

*The apparatus and various instruments and techniques for measuring bag tension, bag displacement, dust concentration, and other variables, which were developed during the program are described under APPARATUS, TECHNIQUES AND MATERIALS, pages 36 to 63, and in more detail in Appendices A, B and C.

BACKGROUND AND THEORY

The qualitative aspects of dust removal by mechanical shaking are fairly well recognized. The harmonic motion that is imparted to the dust-laden bag accelerates and decelerates the fabric-dust system producing tensile and shearing forces at dust-particle and dust-fabric interfaces. When these forces exceed local cohesive and adhesive forces, the dust is dislodged. The magnitude of the latter forces depends upon several factors; e.g., physical properties of the dust and/or fabric system, gas velocity, dust aging and compaction, and temperature and humidity of the gas.

The first constructive analyses of mechanical shaking processes were reported by Walsh and Spaite in 1962.[1] The tests performed on a single bag system established practical limits for the number of shakes needed to remove fly ash from sateen weave cotton fabrics. Measurements made at various shaking frequencies, amplitudes and shaking times also indicated that dust removal could be related to the peak acceleration of the shaken end of the bag. No data were reported on collection efficiency, projected bag service life, and the kinetics of the bag motion. Thus, the above findings, although providing useful guidelines for the present study, did not furnish the necessary data inputs to establish optimum shaking conditions.

Aside from the work of Walsh and Spaite[1] little additional understanding of mechanical shaking processes has been achieved up to the present time. Investigations have been made, however, on adhesive phenomena, collection efficiency, fabric design factors, and various other filter operating characteristics that contribute to an understanding of cleaning by mechanical shaking. This work is summarized in the following sections.

Adhesion and Removal Mechanisms Including Acceleration

All fabric shaking involves some combination of:

- Stress in a direction normal to the dust-fabric interface (tension).
- Stress directed parallel to the interface (shear).
- Stresses developed during warping, bending or flexing of the fabric surfaces.

These stress conditions are illustrated in Figure 1. In addition to shaking per se, there are two other general methods of cleaning, the first relying on air pressure or viscous drag to remove dust and the second relying on direct physical contact as with vibration, manual rapping or sonic and shock cleaning. In the later instances, contact stresses such as those produced by mechanical shaking appear responsible for cleaning. While Figure 1 depicts the types of stresses encountered in all cleaning systems, the intensity and/or repetition factors may differ between those of simple mechanical shaking and the other cleaning techniques.

According to theory, adhesive or cohesive bonds will fail whenever or wherever the local stresses exceed the bonding strength. Examination of the stress models illustrated in Figure 1 shows that of the four, only the first, (a), involves stresses directed away from the fabric. Thus, although the other three mechanisms may loosen the deposited dust and prepare it for separation, only when the tensile force produced by acceleration directly opposes the adhesive and/or cohesive forces will there be a true separation of the dust from the fabric.

Without a high-speed microscopic study of the dust separation process (something beyond the scope of the present study) there is no way to describe precisely the dust removal mechanisms. Two conceptual models of separation by acceleration are indicated in Figures 2a and 2b. Bond

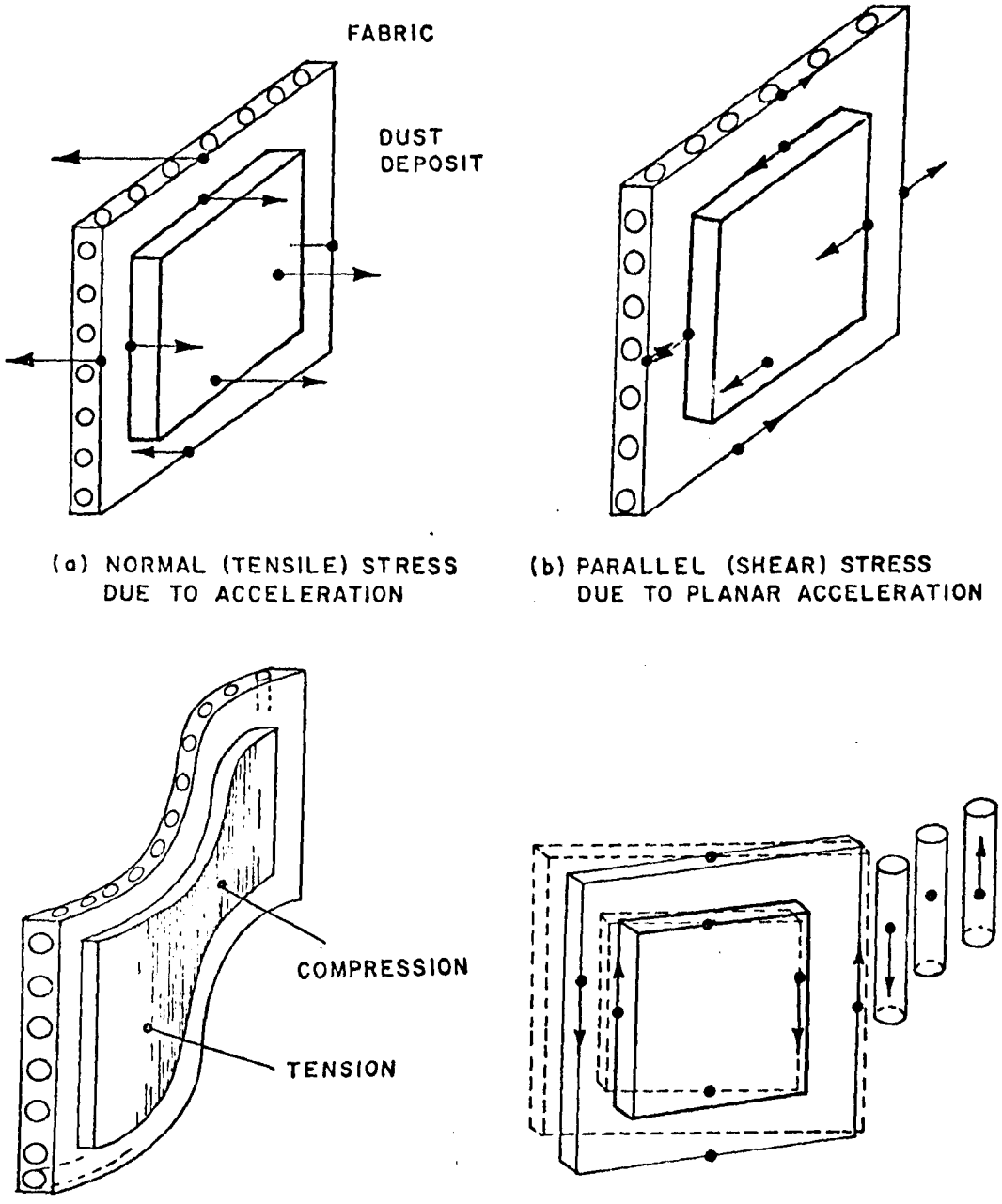

(a) NORMAL (TENSILE) STRESS DUE TO ACCELERATION

(b) PARALLEL (SHEAR) STRESS DUE TO PLANAR ACCELERATION

(c) STRESSES DUE TO FABRIC FLEXING

(d) STRESS DUE TO PLANAR YAW, OR YARN TO YARN SHEAR

Figure 1. Potential dust fabric stresses developed during shake cleaning

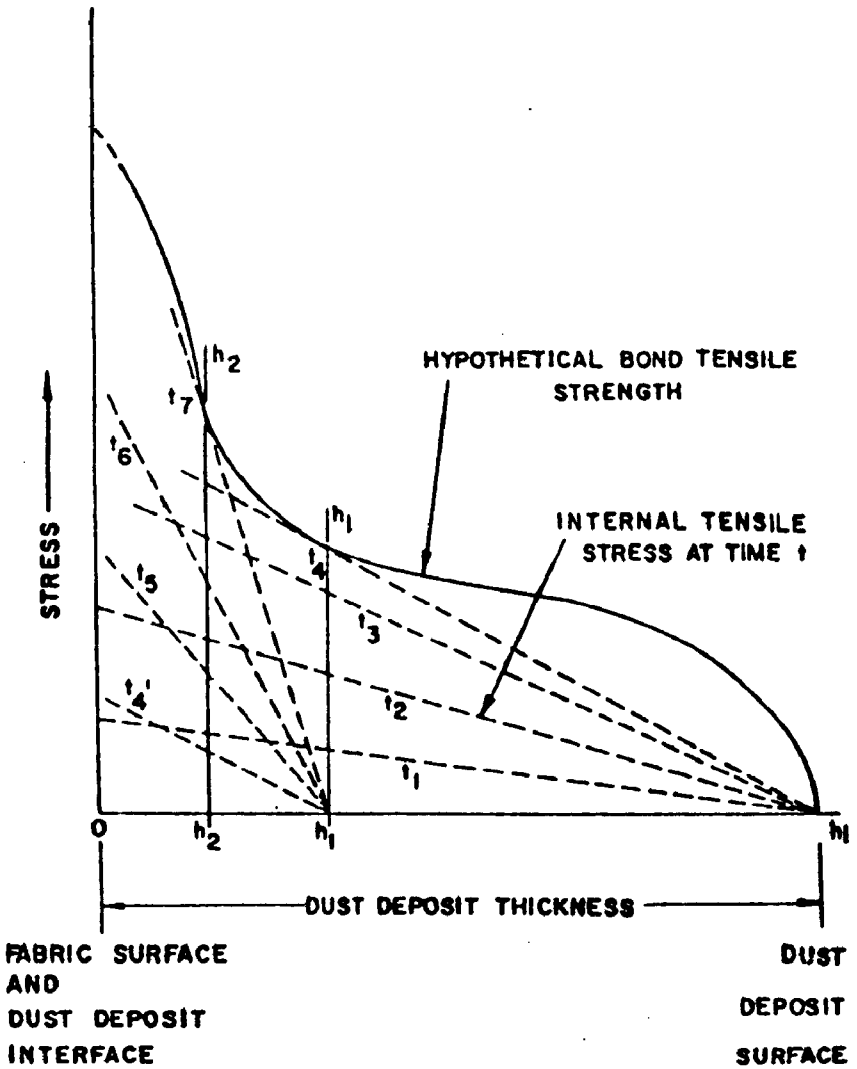

Figure 2a. Concepts of cleaning via acceleration (a) High adhesive/cohesive ratio

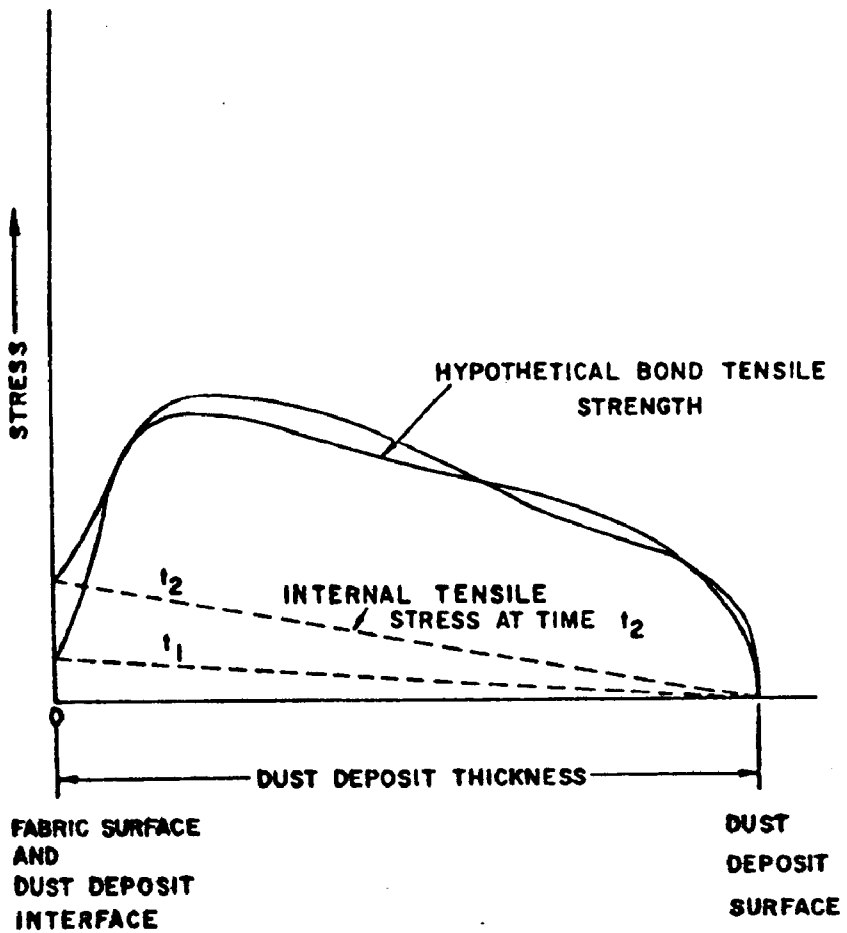

Figure 2b. Concepts of cleaning via acceleration (b) Low adhesive/cohesive ratio

strengths are characterized hypothetically by the solid curves. In the first case, the adhesion of the dust to the fabric surface is higher than the cohesive strength within the dust deposit.

As one moves from the interface to the surface of the deposit, the cohesive strength is assumed to diminish because the aerodynamic stresses tending to compact the deposit also diminish. In order for separation to occur, it is necessary that the tensile stress caused by acceleration must equal or exceed the bond strength at some specified depth in the deposit. When this occurs a flake or layer of dust is removed down to that depth. Beginning at time zero, successive instantaneous tensile stresses are represented by the dotted lines in Figure 2a. As acceleration begins, the tensile stresses rise from a zero value at the surface of the deposit to a value at a given depth in the deposit that is proportional to the mass per unit area above that depth. At successive times during each cycle, t_1, t_2, t_3, ... the acceleration of the fabric rises until at time t_4 the tensile stress finally equals the tensile strength at depth (h_1). At this time, a dust layer of depth (h_1-h_1) is detached, leaving the remainder of the deposit unchanged. Immediately the tensile stress at the new surface drops to zero and the stresses within the remaining cake become proportional to the remaining mass (line t_4'). If the fabric acceleration continues to increase, another layer of thickness (h_1-h_2) will dislodge at time t_7. Whatever depth remains at the end of the shaking period becomes the new residual deposit along with the dust within the fabric structure.

After many consecutive cleanings, the residual dust deposit is composed of those particles most difficult to remove. Thus, this material may adhere more strongly than any fresh surface deposits. This is the reason for showing relatively strong residual bonds in Figure 2a. Although the bonding strength decreases as particle diameter decreases, the particle mass (and hence the tensile stresses produced by acceleration) decrease at an even more rapid rate. As the finer particles are more difficult to dislodge than the larger ones, they probably

tend to concentrate in the residual deposit. Their small size would tend to increase the flow resistance of the filter or even blind it in extreme cases. Filter system operators often report a gradual increase of filter operating pressure over a period of several hours or days operation with a specified cleaning cycle. They also report that temporarily increasing the cleaning intensity usually lowers the pressure drop within a short period such that the regular cleaning cycle can be resumed. It is postulated that this increase is due to a well-bonded layer of selectively retained fine particles. It appears that the residual layer can be reduced by periodically resorting to a more intense cleaning cycle.

In contrast to the strong interfacial adhesive forces shown in Figure 2a, the opposite situation is described in Figure 2b. In the latter case, it is suggested that the cohesive, particle-to-particle bonding exceeds the adhesive forces at the particle-fabric interface. The dust detaches from the fabric more cleanly, leaving a negligible residual deposit. Lower separation forces are required and larger dust agglomerates are removed. Smooth-fibered, shallow-surface fabrics such as glass and certain synthetics, if suitably woven, are believed to perform in the above manner. The results of the present study have shown a much lower residual dust weight on Dacron than on cotton fabrics, probably because of the mechanism postulated in Figure 2b. Heavily napped fabrics, felts, or fabrics with deeply woven surfaces may be expected to accumulate substantial deposits of dust beneath the surface. The dust may be physically interlocked with the fibers and consequently adhere strongly irrespective of particle size. The overall effect should be similar to that indicated in Figure 2a. The size and range of pore sizes probably account for the differences in behavior between deeply woven and smooth shallow fabric surfaces.

The factors that determine cohesion and adhesion have been shown in studies of interfacial phenomena to include the molecular characteristics of the materials as well as the properties of adsorbed or

absorbed surface films. In practice, the surfaces of most materials are contaminated by gas molecules, liquids, or solid particles. For example, Durham and Harrington[2] found a small effect of humidity on the effective residual pressure differential of a filter that might be explained by a change in the surface characteristics of either the fiber or the dust particles. Other possible factors are the porosity of the deposit, its degree of compaction, and electrostatic effects.

In those cases where high surface adhesion predominates, the depth to which dust is removed may depend upon local variations in any one of the several factors that appear to determine removal depth. Insufficient tensile stress to produce removal in one cleaning cycle will result in a heavier than usual deposit at that location after the next filtration cycle. The added dust mass will tend to increase tensile stress, thus increasing the probability of removal at that location in subsequent cleaning. It appears probable, therefore, that in successive cleaning cycles, the removal of dust at a given location on the filter bag may vary over a considerable range from one cycle to another. If so, one would predict a non-uniform deposit over the filter surface at any given time. Just such a spotty effect was observed in this study when a light bulb was placed inside a filter bag and the light transmission viewed in a darkened room, as shown in Figure 3. Some areas of the fabric expected to have little normal acceleration, however, were also well cleaned, particularly the pleats around the top of the bag. The latter removal probably was due to Type c and Type d stresses as shown in Figure 1. All the stresses in Figure 1 contribute something to loosening the dust, even though acceleration predominates.

Walsh and Spaite[1] in their studies of shaker arm acceleration found that about 1 g (32.2 ft./sec.^{2}) was required to cause discernible dust removal and 2 g's was sufficient to attain significant cleaning. In view of the fact that the dust is deposited in a gravitational field of 1 g, it is understandable that accelerations should exceed 1 g to

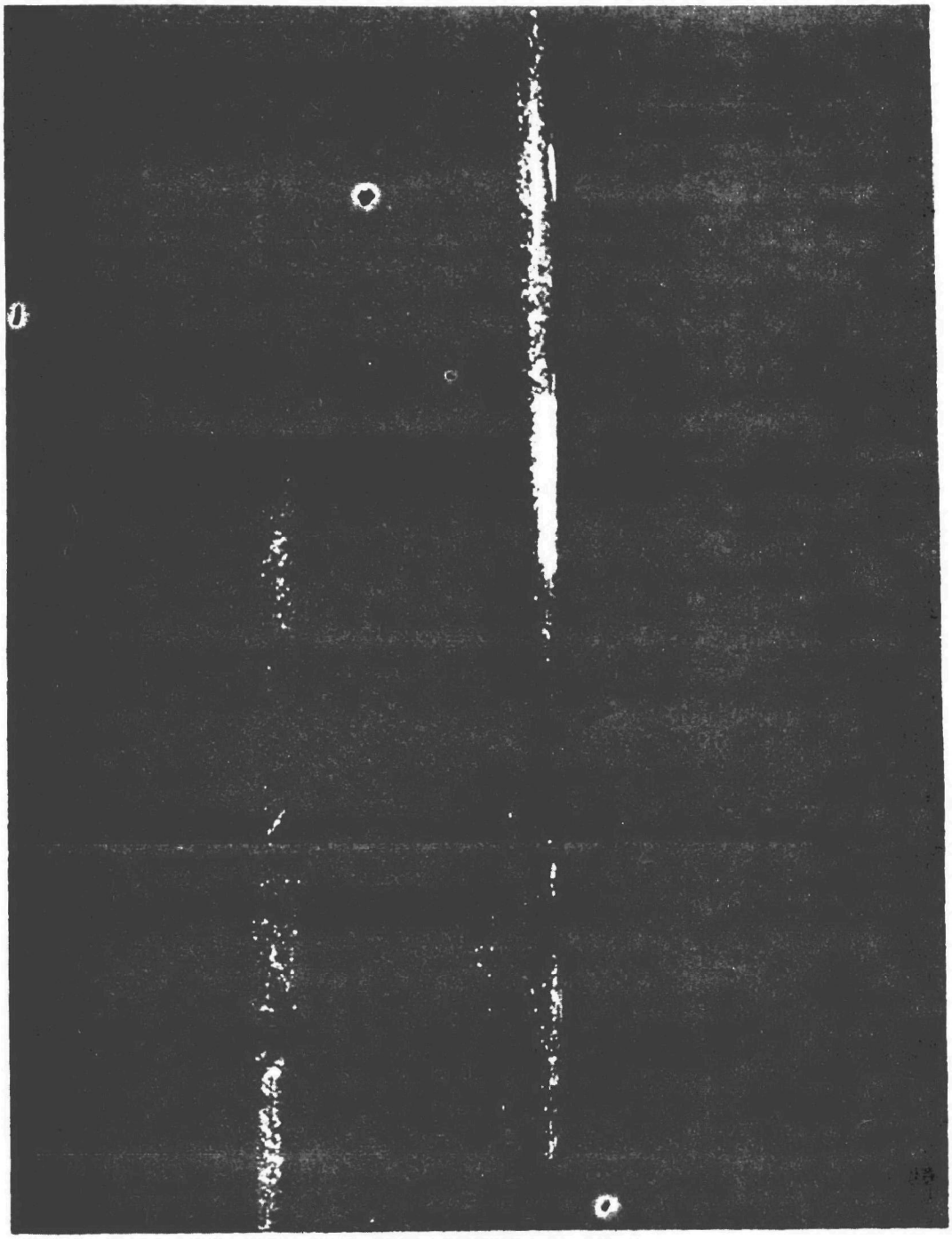

Figure 3. Internally illuminated 10-foot by 6-inch diameter cotton bag, after cleaning (photo approximately 4 feet from lower end). Shake direction is normal to the page.

remove dust deposits. Walsh and Spaite found that accelerations below 1 g lowered the residual drag, probably because the dust deposit was made more permeable by fabric and dust flexing.

In this program, the residual fly ash dust deposits on cotton fabrics were typically 300 grains/ft.^{2} following an extended shaking with a 10 g maximum acceleration. Based upon bag kinetics and observed dust removal, average adhesive forces of the order of 200 dynes/cm.^{2} were estimated. No directly comparable data could be found in the literature. However, Zimon[3] has reported effective adhesive strengths of the order of 100 to 300 dynes/cm.^{2} for layers of various particle materials (under 50 microns diameter) bonded to various substrate materials. Thus, the postulated mechanism of dust removal by acceleration appears acceptable as far as the magnitude of separation forces are concerned.

Bag Motion Theory

In the preceding section, fabric acceleration was established as one important factor in dust removal by mechanical shaking. Although Walsh and Spaite[1] found a correlation between the acceleration of the shaker arm, per se, and dust removal, their studies did not indicate the actual acceleration undergone by the fabric. A theory has been developed in this study, based on classical mechanics and laboratory measurements, that provides reasonable definition of fabric motion. Although this theory is actually a result of the study, it is summarized here to establish a framework for the experimental results reported later.

Basic Concepts - Periodic lateral motion applied to one end of a flexible tubular body (or filter bag) produces lateral waves that travel downward along the bag with a characteristic translational velocity. Wave amplitude is progressively diminished, depending upon the system damping properties. At the bottom of the bag, which is

rigidly fastened, there may be further attenuation of the wave while the unattenuated portions of the incident waves are reflected and experience further damping as they travel back up the bag. The reflected wave adds to the oncoming downward wave, producing a standing wave marked by a characteristic nodal pattern along the bag. At the antinodes, the bag undergoes a large, sometimes violent lateral oscillation. At the nodal positions, the bag undergoes a slight oscillation, in contrast to remaining stationary as it should for the "ideal vibrating string."* Figure 4a shows the instantaneous sinusoidal shape of the shaken bag. Figure 4b, a time exposure, indicates the maximum lateral displacements of the same bag while generating a standing wave pattern. Although standing waves are present at all shaking frequencies, the loop pattern is clearly defined only at certain resonant frequencies when the reflected wave has sufficient strength to return for constructive combination with its successor wave. The constructive combination of return and successor waves at resonant frequencies depends on the phase relationship as determined by bag length and wave velocity. At other frequencies, destructive interference of these waves diminishes the standing wave.

Because the bag assumes a sinusoidal form while it is shaking, it must be stretched by an amount necessary to produce the curvature. The added stretching causes more tension in the bag, depending upon its elastic modulus. This added tension, in conjunction with whatever tension the bag displayed while stationary, may exceed by several times that produced by its weight alone. Despite this tension increase and the variations in stiffness and damping properties, the shaken bag behaves much like the classical ideal string. The main effect of dust

---

*Ideal String: Uniform mass and tension at all points and all times; zero stiffness; zero damping.[4]

(a)

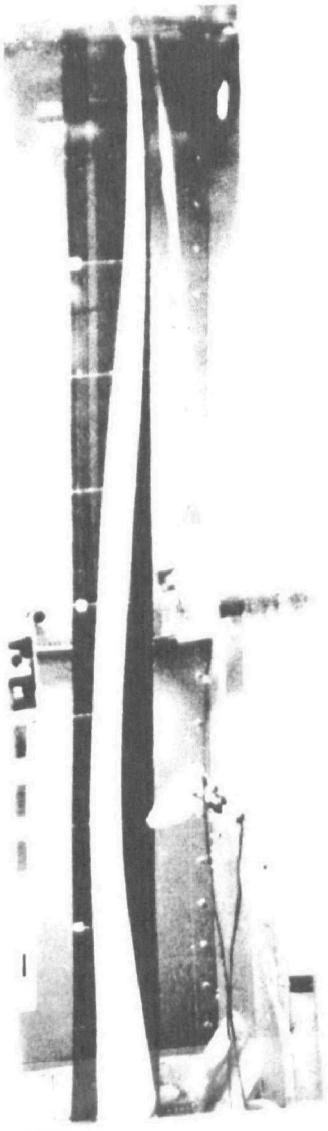

(b)

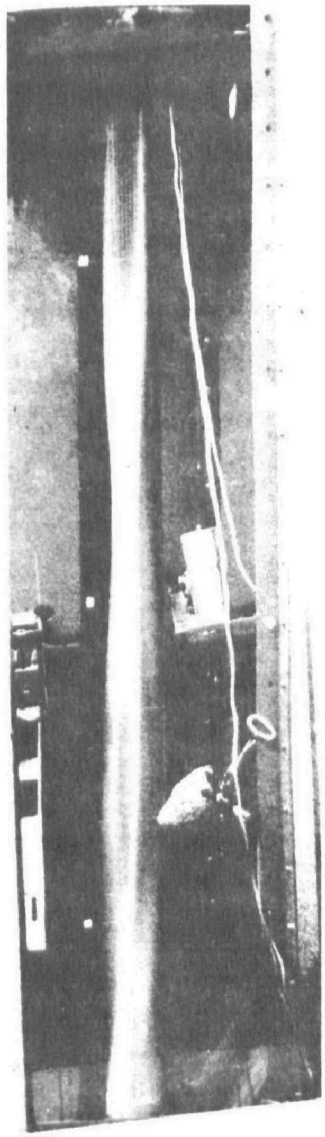

(a) Exposure time 1/120 sec.

(b) Exposure time 2 sec.

Figure 4. Appearance of shaking sateen weave cotton bag 10-feet long by 6-inch diameter (4 cps, 2-inch amplitude, 7.4 pound shaking tension)

accumulation on the bag is to increase its weight per unit length, a term used in the classical wave equations. The dust appears to exert only minor effects on the other bag properties such as stretching, damping and stiffness.

When a stationary bag is first shaken, energy is required to initiate the shaking action. Once the motion is established, a fraction of the energy is retained in the bag as kinetic and/or potential. All bags undergo some degree of damping, however, thus requiring a continual input of shaking energy to maintain a steady motion. The mechanical power required to maintain steady shaking is typically a few watts. The damping loss is mainly due to air drag and to friction between fiber, yarn, and dust particles. If the dust projected from the bag during shaking has appreciable kinetic energy, further make-up energy is required.

Waves and Wave Velocity - In an ideal string (a uniform density cylindrical structure with its length much larger than its diameter) lateral waves travel axially along the string with a velocity given by

$$V = \sqrt{\frac{T}{\rho}} \qquad (2.1)$$

where T is the tension and ρ is the mass per unit length.[4] To a first approximation, waves traveling in a shaking bag behave the same way, allowing for the qualification set forth in Appendix D. If the wave travels down the string or bag of length L and returns to its origin while the shaker arm has made exactly N cycles, the returning wave will coincide (and reinforce) the input wave to produce a resonant state. In this case, the resonant frequency is represented approximately as

$$f_N = \frac{N}{2L} \cdot \sqrt{\frac{T}{\rho}} \qquad (2.2)$$

A correction factor amounting to about plus 10 percent is developed in Appendix D to correct empirically for a stiffness factor not encountered with the ideal string. Additionally, the weight of the bag produces a variation in tension from top to bottom that is ignored with the ideal string. It is shown later that if the average tension half way down the bag is used in Equation (2.2) the calculated frequency usually compares well with the observed resonant frequency.

Tension Changes - The total tension in a shaking bag is the sum of the initial static tension in the bag prior to shaking, T_i, and an additional amount caused by the shaking called the dynamic tension, T_d. The initial tension, T_i, is the sum of the weights of bag and dust, the clamping tension (if any) applied statically to the bottom of the bag, plus any stretching due to deflection of the shaker arm. At a given point along the length of the bag, the gross weight of material below that point must be supported; thus T_i has its maximum value at the top of the bag. For most purposes, the average initial tension along the bag at its midpoint $T_{i,m}$, may be used.

Bag tension also varies with the position of the shaker arm Figure 5. The midpoint tension, T_V, increases from the vertical position of the shaker arm to a value T_A when the arm is swung outward a distance A from the vertical (or zero amplitude) position. At static conditions or very slow shaking frequencies, the tension difference is given by

$$T_A - T_V = \frac{MA^2}{2}\left(\frac{1}{R_A} + \frac{1}{L}\right) \qquad (2.3)$$

where R_A is the radius of the shaker arm, L is the bag length and M is the elastic modulus of the bag (see Bag Modulus, pages 46 to 49). Consequently, the time averaged initial tension is

$$T_{i,m} = \frac{T_V + T_A}{2} = T_V + \frac{MA^2}{2}\left(\frac{1}{2R_A} + \frac{1}{2L}\right) \cong T_V + \frac{MA^2}{4R_A} \qquad (2.4)$$

when the bag is much longer than the shaker arm.

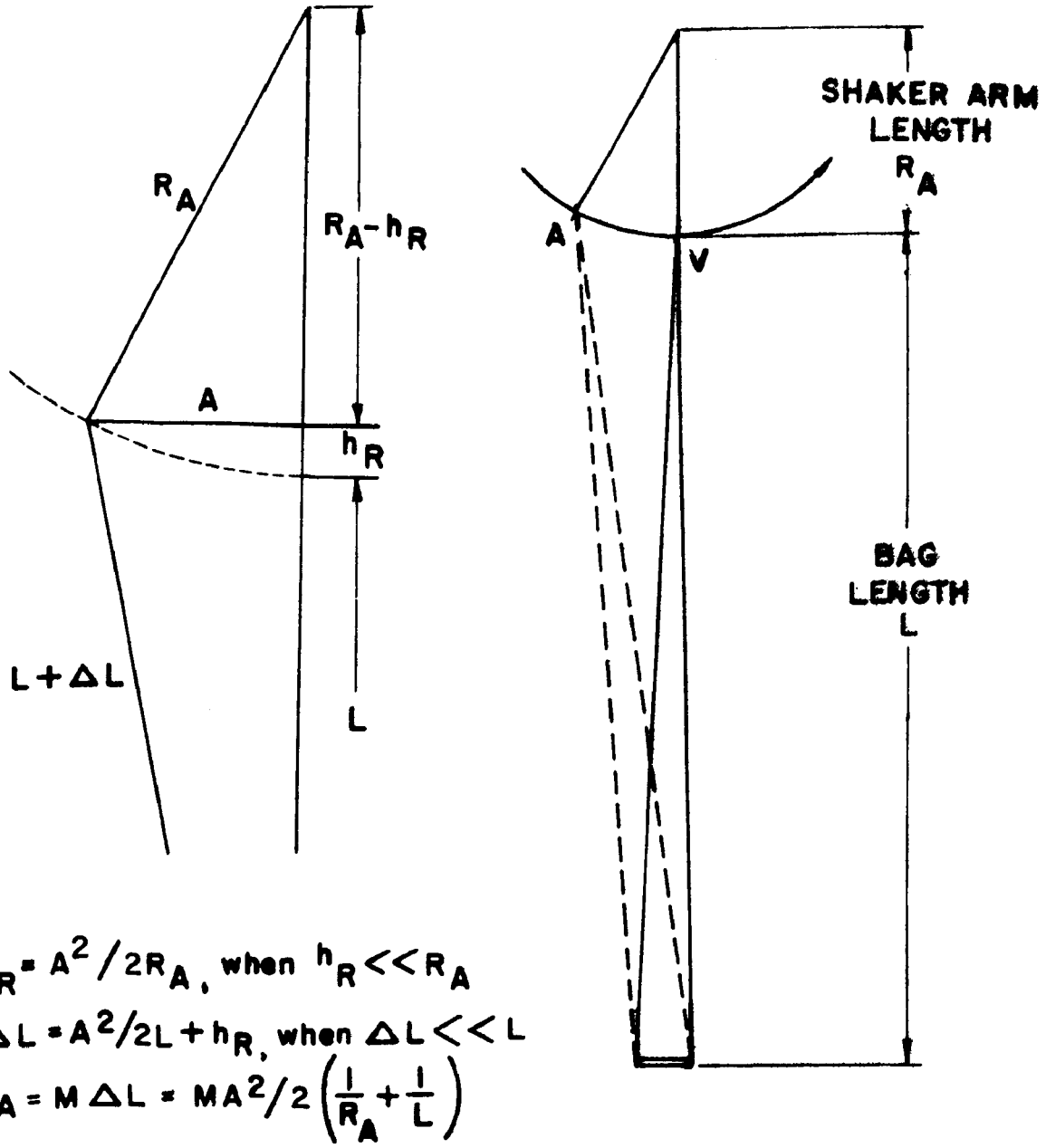

$$h_R = A^2/2R_A, \text{ when } h_R << R_A$$

$$\Delta L = A^2/2L + h_R, \text{ when } \Delta L << L$$

$$T_A = M\Delta L = MA^2/2\left(\frac{1}{R_A} + \frac{1}{L}\right)$$

Figure 5. Variation of bag tension with position of shaker arm

Normal shaking takes place at 5 to 10 cycles per second, a speed at which the wave shape of the bag requires that it be stretched more than at very low shaking frequencies. This elongation produces an additional tension, T_d, that depends upon both the amplitude and the length of the waves produced in the bag. In Appendix E, the formula for estimating T_d is developed

$$T_d = ML\left(\frac{\pi Y}{\lambda}\right)^2 \tag{2.5}$$

where λ is the wavelength and Y is wave amplitude. Equation (2.5) indicates that for a fixed bag amplitude, Y, the dynamic tension varies inversely with the wavelength (and directly with shaking frequency). The proper tension value to use in Equation (2.2) is the one that reflects the combined effects of bag weight, applied tension, shaker arm position, and wave shape; i.e.,

$$T_m = T_{i,m} + T_d \tag{2.6}$$

where the right hand terms are defined as in Equations (2.4) and (2.5) respectively.

The average wavelength of the shaking bag can be estimated from Equation (2.1) as

$$\bar{\lambda} = \frac{V}{f} = \frac{1}{f}\sqrt{\frac{T_m}{\rho}} \tag{2.7}$$

By combining Equations (2.5), (2.6), and (2.7), the following expression can be derived for calculating average bag amplitude, $\bar{Y}$.

$$\bar{Y} = \frac{1}{f}\sqrt{\frac{1}{ML\rho}}\sqrt{T_m\left(T_m - T_{i,m}\right)} \tag{2.8}$$

In Equation (2.8), bag motion is related to three basic bag properties (tensile modulus, length and mass per unit length) and to three parameters depicting the shaking conditions (shaking frequency, initial tension at the bag midpoint, and average shaking tension at the midpoint).

All variables cited in Equation (2.8) are readily determined without special measuring techniques except for shaking tension. During the experimental phase of this study, however, methods for calculating shaking tension in terms of readily measured system variables were developed. Therefore, Equation (2.8) can be used to predict bag shaking amplitude so that dust removal and related filter performance criteria can be estimated.

Damping and Reflection - According to general theories of undamped oscillations, bag amplitude at resonant frequencies should become extremely large in comparison to the driving motion.[5] Since the actual oscillations in the shaking bag seldom exceed the shaker arm amplitude, there must be considerable damping. In fact, the appearance of the wave when the shaker is suddenly stopped indicates that the wave is only slightly reflected from the lower cuff fastening. This must be due either to heavy damping of the downward wave, or to energy absorption in the reflection process, or both. When a rather slack bag is shaken the waves tend to disappear before reaching the bottom of the bag, particularly at the higher frequencies and lower amplitudes. It is assumed, therefore, that the degree of damping and reflection in a shaken bag can be responsible for the extremes of no motion at all in parts of the fabric to violent motion in other cases. Thus, it appears that next to shaker amplitude, damping and reflection are the most important considerations in determining bag amplitude.

Closely associated with damping is bag stiffness that tends to increase the bag's wave velocity above that of an ideal string. Damping, reflection, and stiffness factors are very complex because they depend on the cross-sectional contour of the bag. As the bag shakes, its cross section changes from circular to elliptical, the amount of flattening depending on tension and other factors. The flatter the cross section, the less the stiffness and probably the lower the damping rate.

In theory, one might develop a mathematical or computer model of a shaking bag that would predict damping, reflection, and stiffness. This model would have to include not only the wave mechanics cited above, but also the flexural and shear stiffnesses of the fabric-dust combination. The model would consist of a thin shell cylinder, with significant adjustments to describe the pleated top and shape changes found with shaken bags. Because of the lack of accuracy in defining major variables and the expected complexity of mathematical treatment, such a sophisticated approach was not considered worthwhile.

Instead, useful results were obtained by an alternative empirical approach in which minor correction factors were added to the mechanics outlined previously, Equations (2.1) through (2.8). Despite the acknowledged simplicity of these relationships, they appear to provide a strong predictive capability.

Bag Acceleration - Based upon measurements performed during this study the oscillation of a shaking bag was determined to be essentially a simple harmonic motion. In such motion, a given point on the bag attains a maximum acceleration given by

$$a_m = 4\pi^2 f^2 Y \qquad (2.9)$$

where f is the frequency of oscillation and Y is the local amplitude. Amplitude is defined herein as one-half the peak-to-peak displacement.

By stroboscopic viewing, it was determined that all points on the bag move with essentially the same frequency as that of the shaker arm driving the bag. As a wave of amplitude Y moves along the bag, successive points on the bag undergo a maximum acceleration given approximately by the above formula. Consequently, the problem of determining the local bag acceleration is reduced to one of determining the amplitude of motion along the bag. In order to determine the

average acceleration, which is presumed to control average dust removal, it is only necessary to establish the average bag amplitude. One can neglect, therefore, the variation in amplitude along the bag due to damping, changes in tension, and variations in dust deposit weight. In a later section, results will be presented that show that averaged bag acceleration, as computed from tension data, can be correlated with dust removal.

Shaking Energy and Power

Based upon many commercial shaking systems, it appears that a one horsepower motor can shake simultaneously about 200 filter bags. Thus, the power required for a single bag should be of the order of three to five watts. The chief consideration with respect to the power requirement is not its cost, but the effect the dissipated energy may have on the service life of the bag and on the removal of dust. Damping in the bag is associated with dissipation of mechanical energy through friction, air current generation, and extraneous random motion.

To maintain steady shaking, there must be constant and sufficient energy replenishment at the driven end of the bag to transmit the motion to the bottom of the bag without excessive damping. The instantaneous energy in a lateral wave traveling in a flexible string is defined by classical wave mechanics as

$$E' = 2\pi^2 f^2 Y^2 \rho \qquad (2.10)$$

per unit length of string.[6] The motion in a shaking bag, however, is complicated by both damping and a reflection factor, such that it is difficult to establish from a theoretical standpoint the precise energy density at any point along the bag. Nevertheless, Equation (2.10) is useful for estimating the energy flow into the bag under the tacit assumption that most of the motion near the top of the bag is due to

the downward wave. The above approach predicts a bag power consumption that is directly proportional to the squares of bag amplitude and shaking frequency and to the weight of the bag. Experimental results presented later in this report appear to substantiate the above relationships.

Power consumption can be measured at the top of the bag where the instantaneous energy flow through the linkage point is determined by the vector product of force and velocity. In the present case, the energy transmission rate is the product of the lateral velocity, V_a, of the suspension point of the bag and the lateral force, F, at this point taken at right angles to the shaker arm. The instantaneous product of arm lateral force and arm velocity, averaged over a full cycle, represents the energy input per cycle, from which steady state power consumption can be computed:

$$\bar{P} = (E_{cyc})\ (f) = \frac{1}{t} \int F\ V_a\ dt \qquad (2.11)$$

Alternatively, since both lateral force and velocity are periodic and have the same frequency, their maxima can be used:

$$\bar{P} = (F_{max}\ V_{amax})\ \frac{\cos\ \theta}{2} \qquad (2.12)$$

where cos θ expresses the phase relationship and is analogous to a power factor in electric power transmission termission terminology.[7]

The lateral forces discussed later in this report can be measured directly or, alternatively, they can be estimated from shaking tension data as given by the theory developed in Appendix I. By using the latter formulas in conjunction with Equation (2.12) for computing power input to the shaking bag, it is shown in a subsequent section of this report, pages 80 to 86, that power consumption can be predicted with fair reliability.

Bag Life

Limited field data indicate that filter bags may last from a few weeks or less to 13 years or longer, with one survey showing an average life of about 1 year.[8] Bag failure may result from abrasion, excessive temperature or burning particles, fiber degradation from acid or chemical attack, mechanical problems such as seam failures or tears, and blinding or plugging. Quantitation of the above failure conditions is very poor. It is sometimes claimed that grit, having penetrated a fabric, can abrade fibers during mechanical shaking to the point that the yarns are severed. No good quantitative data are available, however, to evaluate this effect. Glass fabrics are known to be seriously damaged by mechanical shaking. It appears that nicks or scratches produced by abrasion increase fiber breakage during flexure.[9,10] The breakdown of glass fiber fabrics is a special case, however, not typical of filter fabrics in general. In the present study, fabric life was measured by the number of individual shakes given the bags during the testing period, up to 2×10^7.

At the outset of the study there was no background evidence or theory that related the concurrent mechanical effects of tension, flexure, shear, and dust to fabric deterioration in filter systems cleaned by mechanical shaking. For this reason, a portion of this study was devoted to the assessment of this problem.

Collection Efficiency

An information survey has shown that the relationship between mechanical shaking and collection efficiency has not been examined in any great detail.[8] Although numerous investigations have shown a perceptible correlation between efficiency and pressure differential across the fabric, (and weight of dust deposited on the fabric) these investigations generally embraced a narrow experimental range. The results have not been summarized in such a way that they can be applied to

other situations.[8] As noted above, the relationship between mechanical shaking and pressure differential has only been partially studied, chiefly by Walsh and Spaite.[1]

The fractional particle size efficiencies of various filter systems are even less clearly defined. In 1961, Whitby and Lundgren[11] studied the relationship between cleaning intensity and efficiency of particle collection for diameters between 0.06 and 3 micrometers. They loaded a fabric filter with three standard test dusts, cleaned the fabric with a varying number of shakes, and then measured the effectiveness of the partially cleaned filter in collecting uranine dye particles of known diameter. Their measurements showed, first, that collection efficiency was reduced by additional cleaning but at a decreasing rate and, second, that collection efficiency was practically constant for particles less than 0.3 micrometers, and increased steadily for all larger sizes. Collection efficiencies from about 70 to 99.9 percent were reported.

A substantial amount of data relating efficiency to various fabrics, humidities, dust types, inlet concentrations and system capacity has been reported.[8,12] Draemel recently described an investigation of several fabric design parameters and related collection efficiencies, including analyses of filter pore geometry.[13] While all these investigations suggest that pore dimensions play an important role in determining collection efficiency, the effects of cleaning methods on efficiency are not described by these investigations. Therefore it appeared at the outset of the present study that a considerable effort would be necessary to relate, for example, the shaker arm motion, through several cause and effect steps, to particle collection.

Applied filtration technology is based upon two distinct particulate collector designs. The first involves the use of woven fabrics with relatively flat, shallow surfaces upon which a closely compacted or sealing layer of dust accumulates. Subsequent filtration is primarily

a sieving process that is usually very efficient as the aerosolized and filter bed particles are the same size. On the other hand, napped fabrics and felted materials present deep, open surfaces that may not become completely sealed. The widely spaced fibers present a statistical barrier to airborne particle penetration, thus gradually reducing particle concentration as the bed depth increases. This deep-bed or mat filtration concept may involve any of the classical collection mechanisms - impaction, interception, or diffusion as well as sieving in locations where the bed has become heavily loaded. Since few commercial filter systems operate completely either as sieves or deep-bed filters several collecting mechanisms must be considered in explaining or predicting their performance.

Efficiency depends on several factors as shown in the following tabulation.[8]

- Dust Properties

  Size - particles between 0.1 and 1.0 micrometers diameter may be more difficult to capture;

  Seepage characteristics - small, spherical solid particles tend to escape;

  Inlet dust concentration - the deposit is likely to seal over sooner at high concentrations.

- Fabric Properties

  Surface depth - shallow surfaces form a sealant dust cake sooner than napped surfaces;

  Weave tightness - fabrics with high permeabilities, when clean, show lower efficiencies. Also monofilament yarns, without fibrils protruding into the yarn interstices, show lower efficiencies than more "fuzzy" staple yarns having similar interstitial spacing;

  Electrostatics - known to affect efficiency.

- Dust Cake Properties

  Residual weight - the heavier the residual loading the sooner the filter is apt to seal over.

  Residual particle size - the smaller the base particles, the smaller (and fewer) the particles likely to escape.

- Air Properties

  Humidity - with some dusts and fabrics, 60 percent RH is much more effective than 20 percent RH.

- Operational Variables

  Velocity - increased velocity usually gives lower efficiency, but this can be reversed depending on the collection mechanisms.

  Pressure - probably not a factor except that increase of pressure after part of the dust cake has formed can fracture it and greatly reduce efficiency until the cake reseals.

  Cleaning - relatively unstudied (see following discussion).

A stabilized residual deposit often has the appearance of close-packed tufts or aggregates. Between these aggregates lie pores or slits leading to much more permeable regions of the fabric beneath the residual layer. As filtration begins, some particles escape through the pores while others attach to and enlarge the aggregated structures (and reduce the pore dimensions). As the pores become blocked, further passage of air and particles through these regions is greatly reduced because of the considerable loss of pressure. The flow resistance of the filter continues to increase due to dust deposition on the surface of the filter.

The usual process of cleaning consists of removing most of the fresh (external) relatively loose deposit. The older, relatively firmly bonded (internal) residual deposit often remains. Some areas of the

fabric are cleaned more thoroughly than others and the degree of cleaning in any one location may vary from one operational cycle to another.

Most efficiency data reported in the literature are based on lengthy sampling periods (hours to days) and conventional gravimetric methods. Although these measurements provide a practical estimate of the average emission rate (weight basis) they do not indicate the variations in effluent concentration that usually take place over individual filtering cycles. The deviations from average efficiency are highly significant with respect to understanding the mechanics of the fabric cleaning and filtration processes.

APPARATUS, TECHNIQUES AND MATERIALS

The requirement to test on a realistic dimensional scale led to the design and construction of an experimental fabric filter system accomodating bags 10 feet long by 6 inches diameter. This filtration equipment and the testing facilities are described in Appendices A and B. The lower end of each bag was clamped to a thimble through which dusty air entered the bag during the filtration cycle. The upper end of each bag was fastened to an oscillating shaker arm that imparted a vigorous shaking motion to the bag during the cleaning interval. The motion of the bag and the forces in the bag during filtration and cleaning were determined as well as the dust concentrations entering and leaving the system. Several types of fabrics and dusts were tested.

Shaker Apparatus

Prior to designing bag shaking apparatus, a survey was made of the different methods of shaking used in commercial equipment, the results of which are summarized in Table 1. The travel of a bag(s) suspension point may follow nearly horizontal or vertical paths as well as several intermediate combinations with amplitudes up to 2.5 inches. The motion

Table 1. SHAKER MOTION AND BAG SUSPENSION USED IN COMMERCIAL EQUIPMENT

Manufacturer	Number of collectors[a]	Shaker motion[b]			Bag suspension			
		Radius (inches)	Estimated amplitude (inches)	Sketch	Cap	Grommet	Buckle	Other
American Air Filter	33	3	1 V				X	
Buffalo Forge	12	3	1.5 V				X	
Cox	5	1	0.4 H		X			
Fuller Dracco	60	12	-- H		X			
Fuller Dracco	60	3	1.5 V				c	c
Dusty Dustless	5	7	0.75 H			X		
Johnson March	1	6	0.5 H			X		
Pangborn	90	4	2.5		X			
Rees	5	4	0.75 V				d	d
Research Cottrell	60	7	1.3 H				X	
Ruemelin	3	10	2 H				X	
Seversky	1	7	--			X		
Tailor	1		-- H		X			
Wheelabrator	40	7	2.5				d	d

[a] Based on 1969 sales data and type of shaking motion specified.

[b] Based upon manufacturers data; V = nominally vertical motion; H = nominally horizontal motion.

[c] Clip used with buckle and strap.

is usually produced by a pivoting radial arm, up to 12 inches long, that describes a progressively flatter arc as the arm length increases and the amplitude decreases.

The 6-inch radius arm selected for the present study afforded a nearly horizontal motion with but a slight upward displacement at the points of maximum amplitude. The shaker arm was attached to a horizontal shaft, Figure 6, that was given a rapid alternating rotation by an eccentric drive. By varying the speed of a 1 hp dc motor, shaking frequencies from 0 to 20 cps were readily attainable. Careful balancing permited operation up to 80 cps. The amplitude of the harmonic motion at the top of the bag was easily controlled by varying the arm length. The top of each bag was tented and sewn into a loop, the latter connected to a light but rigid wire loop attached to the end of the shaker arm. The shaking motion reached full speed in 0.2 second or less and the stop action was made very abrupt by the addition of a resistance in series with the motor armature.

The top of the shaken bag was fixed in position by the location of the thimble at the lower end of the bag. The shaft, however, was designed to be moved to two other positions on a 6-inch arc, leaving the suspension loop in the same rest location. The net result was that a vertical or a 45° motion was obtainable as an alternative to a horizontal motion. Additionally, the uniform hole spacing in the structural frame of the baghouse allowed the entire shaker mechanism to be lowered in 6-inch increments to accomodate bags shorter than 10 feet.

Because the top of the bag was fixed in location, tension was usually adjusted from the bottom of the bag by one of the various mechanisms indicated in Figure 7. The simplest but least effective adjustment method, "a", required trial and error shifting of the bag cuff until the desired tension level was attained. In an improved design, "b", the thimble was floated on a long radius arm that was locked in place during filtration and shaking. When released, however, the weight of

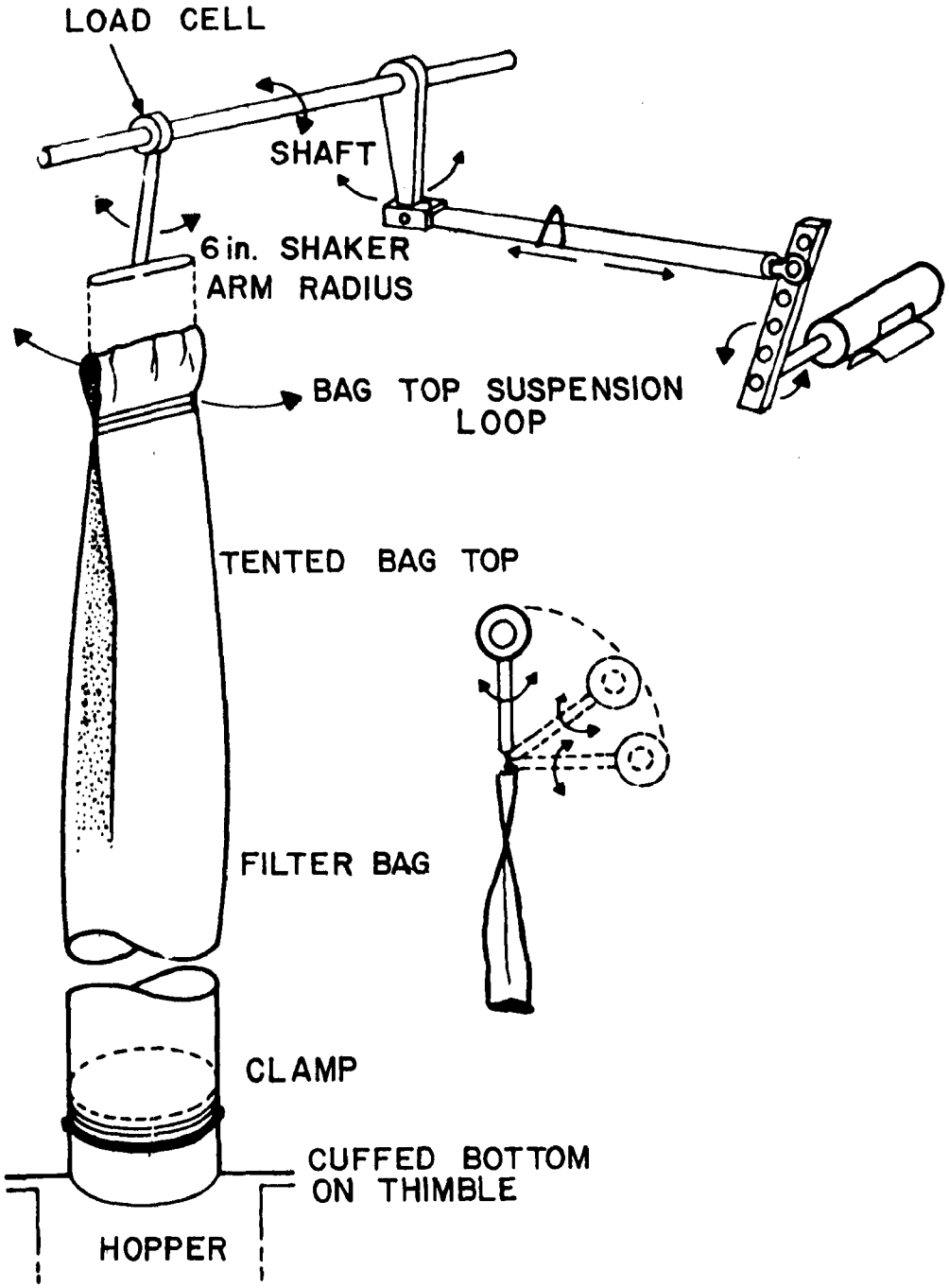

Figure 6. Schematic drawing, bag mounting and shaking assembly

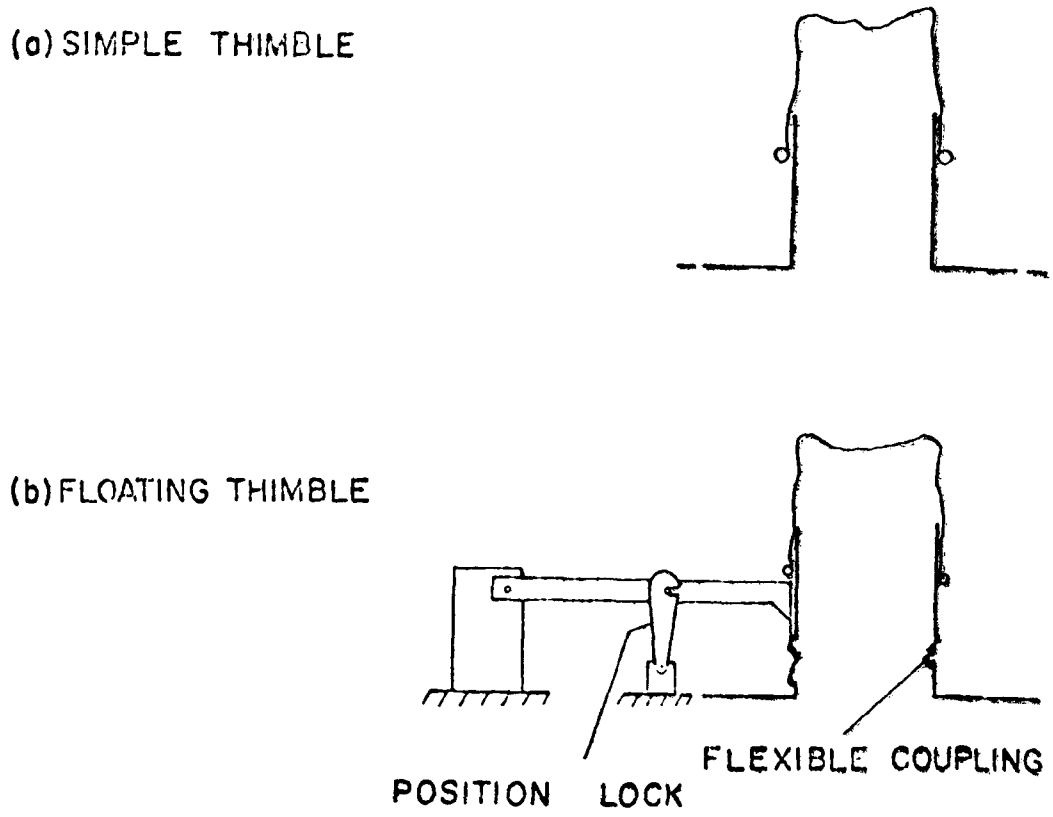

Figure 7. Mountings used to support bottom of shaken bags

the thimble was counterbalanced by a supporting spring so that the bag (and dust) weight could be determined in situ. In the final design, "c", the thimble was permitted to float horizontally. The thimble was readily positioned by a hand screw for adjustment of tension and it could be completely detached from the bag so that very accurate weighings could be made. These successive mountings evolved as the nonlinear and time dependent properties of the bags became more evident. Simultaneously, modifications were also made in the load cell mounting at the top of the bag.

Test Fabrics

While many commercial or specially woven filter fabrics might have been selected in this program, practical considerations dictated that testing be restricted to the most commonly used fabric media. Cotton sateen is used for a wide variety of dusts at low to moderate temperatures because of its relatively low cost and high efficiency. Since it is obtainable from several manufacturers, it appeared to be a good choice as the primary test fabric. To extend the study, the same cotton fabric in napped form and several types of Dacron® fabrics were also utilized as shown in Table 2. Although the above fabrics were not necessarily designed for exclusive use in shaking filter equipment, they did represent a broad range of mechanical properties that might be encountered in shaking systems, as well as typical variations in permeability and surface properties.

Bag Properties and Measurement Techniques

The selected fabrics were sewn into the specified bag configurations shown in Table 3, by the firm supplying the fabric. The design of the cuffs and seams for the bags, Figure 8, was left entirely to the sewing

---

® DuPont Trademark

Table 2. PROPERTIES OF WOVEN FABRICS SELECTED (MANUFACTURERS' DATA)

Fabric	Weight	Weave	Yarn count	Permeability	Mfgr. no.	Mfgr.'s comment
1) Cotton	10	Sateen	95x58	13	960	For shaking
2) Cotton (Napped)	10	Sateen	95x58	13	960C	
3) Dacron®	5	3/1 Twill	66x56 (Filament)	12	C892B	For reverse flow
4) Dacron®	10	Plain	30x28 (Staple)	55	862B	For shaking
5) Dacron®	10	1/3 Crowfoot	71x51 (Filament)	33	865B	For both shaking and reverse flow

Definitions

Weight: ounces per square yard

Yarn count: yarns per inch, warp x fill

Permeability: $ft.^3/min.$ of air passing through 1 $ft.^2$ of clean, new fabric at 1/2 inch H_2O pressure drop

Manufacturer: Albany International Corporation, Industrial Fabrics Division

® DuPont Trademark

Table 3. PROPERTIES OF BAGS TESTED IN MECHANICAL SHAKING SYSTEMS

Bag size and state	Weight[a] (lbs.)	Lineal density[b] (slugs/ft. x 10^3)	Modulus[c] (lbs./in.)	Effective filter area ($ft.^2$)
Unnapped cotton, 10 ft. x 6 in. clean	1.11	3.58	16.5	14.60
Unnapped cotton, 10 ft. x 6 in. used, $< 10^4$ shakes	1.33	4.22	16.5	14.60
Unnapped cotton, 10 ft. x 6 in. used, 2×10^7 shakes	1.78	5.70	31 - 45 tension dependent	14.60
Unnapped cotton, 10 ft. x 4 in. clean	0.77	2.45	9.66	9.63
Unnapped cotton, 10 ft. x 4 in. used, $< 10^4$ shakes	1.26	4.06	9.66	9.63
Unnapped cotton, 5 ft. x 6 in. clean	0.60	3.58	33.0	6.92
Plainweave Dacron, 10 ft. x 6 in. clean	1.11	3.58	13.9	14.60
Multifilament Dacron, 10 ft. x 6 in. clean	0.56	1.80	73.0	14.60

[a] Total weight of bag including cuffs and seams.
[b] Mass per unit length of the uniform portion of the bag; i.e., excluding cuffs but including the lengthwise seam, $lb.\text{-}sec.^2/ft.^2$.
[c] The elastic stretch modulus for the overall bag, including the normal stretch characteristics of the cuff, lbs./inch of stretch.

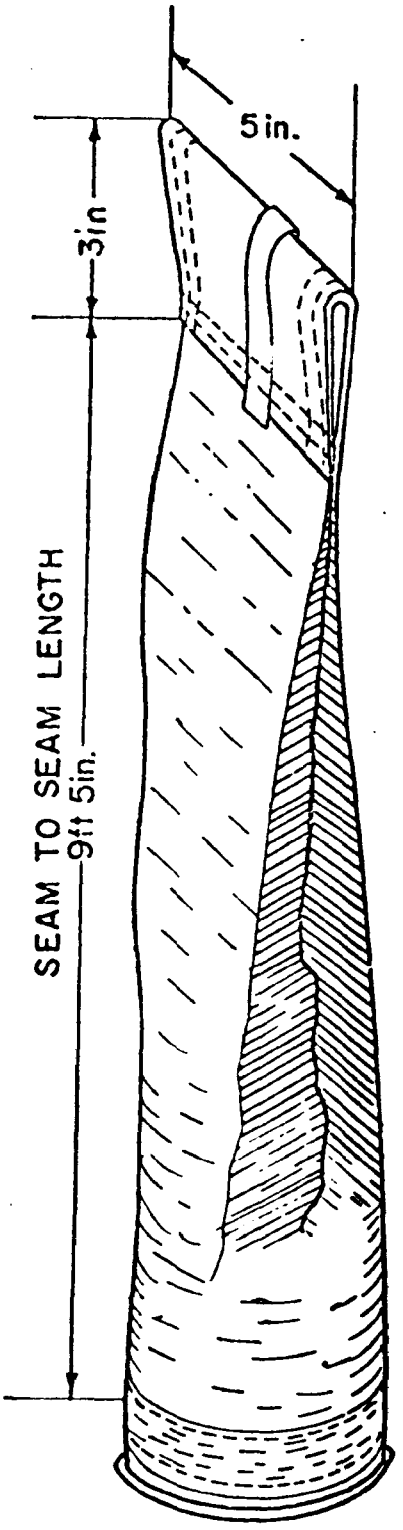

Figure 8. Bag dimensions and loop design

shop's normal procedures except for specifications as to the style of cuff; e.g., "sewn loop at top" or "slip fit at bottom." The selected bag dimensions included two diameters, 6 inches and 4 inches, and two bag lengths, 5 feet and 10 feet, providing length/diameter ratios of 10, 20 and 30. The mechanical characteristics of these bags were representative of standard commercial bags.

Lineal Density - The weight of fabric filter media, often expressed as ounces per square yard, Table 3, provides a rough index of anticipated collection efficiency, bag life, and possibly pressure drop. Sewing a fabric of a given weight into a cylinder with a fixed amount of folding in the seam (see Figure 8) results in a bag having a fixed mass per unit length or lineal density, ρ, defined by the unit slugs/ft. The above factor has a direct bearing on wave velocity and also influences initial bag tension, damping properties and power consumption.

In normal filtering operations, the weight of dust on and in the fabric may increase the lineal density of new, clean, fabric by a factor of 2 or more. Since the dust is usually not distributed uniformly along the bag, both before and after cleaning, the lineal density varies along the bag. Thus, it is probably best to consider the average value over the entire bag. As dust is shaken from the bag, lineal density decreases with time thus changing the bag's tension, its resonant frequencies, and probably its damping properties. Analysts may take these variations into account in a step-by-step analysis of the cleaning process, or they may opt to use a time-averaged value of lineal density in computation processes.

Bag Weight and Bag Tension - A load cell was incorporated in the shaker arm, Figure 6, to provide an indication of the tension at the top of the bag. The original load cell assembly used for determination of static or dynamic (shaking) tension is shown in Figure B-1, Appendix B. Compression of the load cell attached to the movable slide rod frame against the metal block clamped to the oscillating shaft, provided a

direct measure of axial tension. Because of sliding friction between the lubricated rods and the shaft block, however, the response to higher shaking frequencies was attenuated to an unknown degree. An improved design again utilizing load cell compression to define axial tension, is shown in Figure B-2, Appendix B. By providing a pivoting action between the shaker arm frame and the oscillating shaft, a relatively frictionless (and fast response) linkage was achieved. Connecting the load cell to a pivoting member resulted in a varying mechanical advantage across the top of the bag, such that tension on one side of the bag contributed more to the voltage signal than tension on the other side. The fact that the load cell seldom compressed more than 0.001 inch under the maximum safe load of 25 lb. minimized the above problem. The instrument provided a stable and linear response (Appendix B) with fairly reliable time-averaged and instantaneous tension data for static and shaking conditions.

During one series of tests, tension had to be maintained at a constant level in a three bag system. Rather than design and fabricate additional load cells, a simple tension measuring device was fashioned from a U-shaped loop of copper tubing. When slipped over a slack bag, the loop was supported at an angle determined by the bag tension. An adjustable side arm with a bubble gauge allowed for calibration against any preset tension, see Appendix B. By installing turnbuckles in bag shaker arms, any desired tension level could be attained.

Bag Modulus - The tension required to produce a unit change in bag length, defined as the elastic modulus in this study, was shown to be an important bag property. The elastic modulus of the fabric was not included in any materials specifications furnished by bag suppliers. It was measured on fabric samples in our laboratory by applying a known tension to a strip, (about 4 inches wide and 18 inches long) and measuring the resulting change in length. The above approach gave only an approximation of the elastic modulus of an actual filter bag

($\sim \pm$ 30 percent) because the overall bag modulus depended not only on the basic fabric properties but also on the style or tightness of the seam, the method of cuff stitching, and the folds in the upper (tented) end of the bag. It was preferred, therefore, to measure the modulus of the bag directly by suspending a known weight from the bottom of the bag and measuring the resulting bag elongation. Alternatively, the modulus was measured in situ by lowering the clamped lower end of the bag a known distance, and measuring the resulting tension increase with a load cell. Typical results are shown in Figure 9. Bag modulus values did not vary linearly with increasing tension, due mainly to the uncrimping of yarns prior to the normal stretching of individual fibers. Because of this nonlinearity, the reciprocal slope of the line (or elastic modulus) was arbitrarily taken as the average value over the range of typical shaking tensions.

Many composite materials show nonlinear rheology due to friction between their separate elements. Such a material usually displays a tension hysteresis as it is cycled repetitively through a fixed linear displacement. Since the degree of hysteresis may depend on the rate of cycling, there was reason to suspect that the bag modulus might depend on the shaker frequency. A limited attempt to measure this property was made with a 10-ft. x 6-in. cotton bag by allowing the lower bag cuff mounting to move up and down at variable frequency, through a stroke of approximately 0.1 inch, while the top of the bag remained rigidly fastened to the load cell. The average bag tension that resulted was essentially independent of frequencies up to about 20 cps. The range of instantaneous tension values approximately doubled, however, as frequency increased indicating some degree of bag hysteresis. These results suggested that bag modulus values would display similar variations. The hysteris factor was also demonstrated when the tension-elongation measurements were made over extended time periods. With respect to the calculations performed in this study, average tension and average modulus values were used to estimate bag displacements, energy requirements and dust removal.

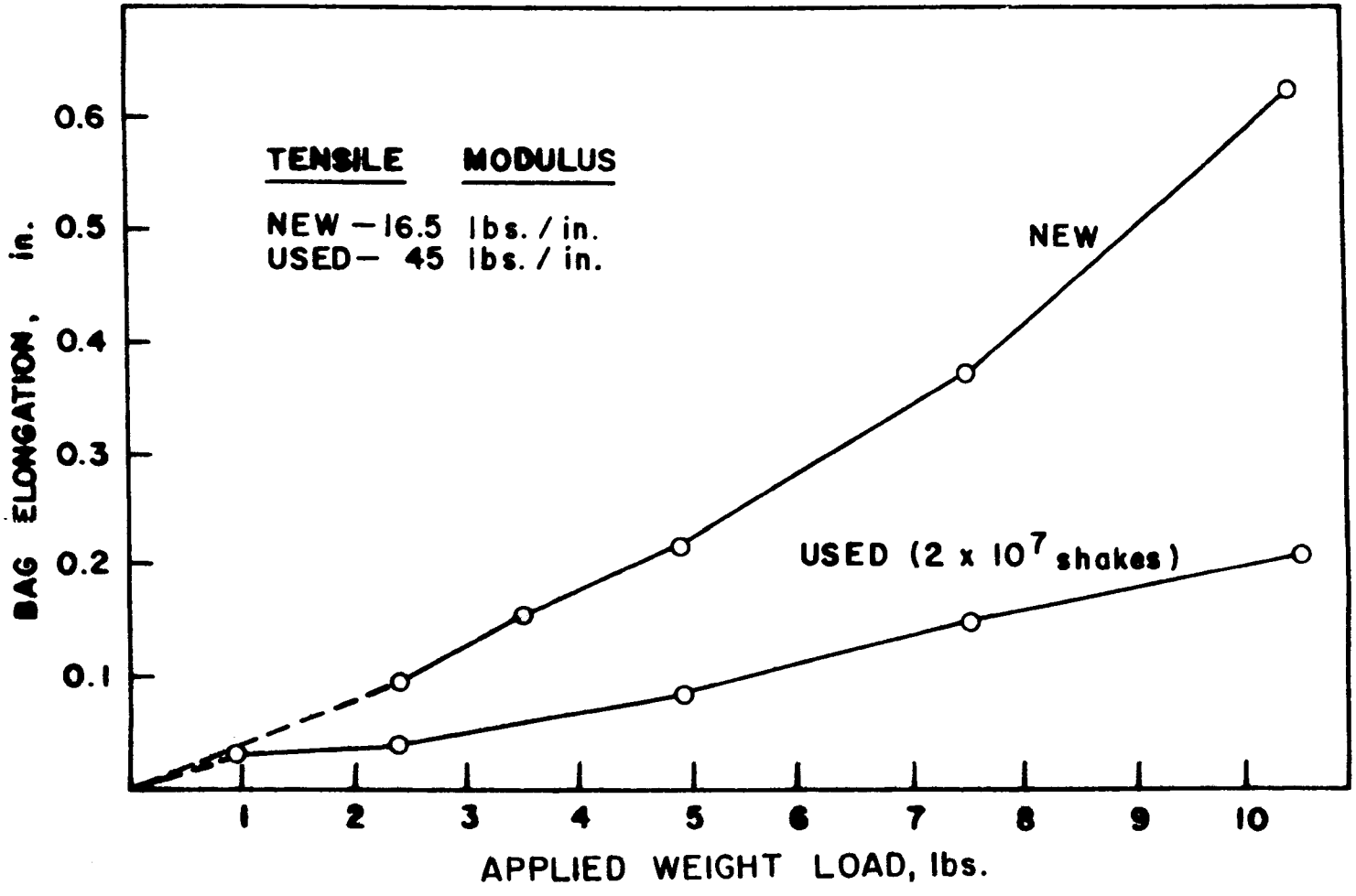

Figure 9. Tensile properties for a 10-foot by 6-inch sateen bag

The elastic properties of a bag may be expected to vary not only in the short term (frequency dependence) but also in the long run as many materials are made less elastic or "work hardened" by repeated stretching or flexure. To determine the durability of cotton filter bags, they were shaken about 20×10^6 times which is equivalent to several (3 to 5) years of normal bag use. The net effect on modulus was to increase it by a factor of 2 or more. One can infer that the static modulus of a new filter bag might be controlled by preconditioning, a process that would reduce its "break in" time when put into service.

During shaking, flexure of the sides of the bag parallel to the direction of motion probably causes some shearing action. Therefore, the bag's resistance to shear, or its shear modulus, may influence its motion. Although any detailed analysis of such motion was beyond the scope of this study, shear modulus was examined superficially for possible future reference. A swatch of cotton filter fabric was mounted between parallel jaws, one of which was free to move in a direction parallel to itself. The force-displacement relationship as the jaw was moved indicated an approximate modulus $M'' h = 1.5$ lb./in. where M'' is the customary shear modulus (lb./in.^{2}) and h the fabric thickness.

Shaking Energy and Power - The power needed to operate a shaking bag filter system depends on the velocity of the top of the bag and the force at the top of the bag tangent to the arc of motion (or roughly normal to the bag axis). The velocity of the top of the bag, equal to that of the end of the shaker arm, was readily computed since the motion was essentially a simple harmonic type. The tangential or "side" force was measured by strain gauges mounted on the shaker arm as shown in Appendix B. In addition, a magnet-and-coil device mounted on the shaker shaft indicated the phase relation between velocity and side force. The latter device was also useful in studying the timing of the bag tension excursions with respect to the position of the shaker arm. Bag power consumption was also approximated by ammeter and voltmeter measurements on the field and armature

circuits of the shaker motor. A significant part of the energy transmitted to the bag at the shaker arm juncture was lost because of damping processes. The rate of energy loss along the bag depends on the characteristic damping properties of the fabric and also its particular geometry. In this study, damping was inferred by observations of tension changes and motion during shaking, there being no simple way to measure it directly. The results are discussed in a later section of this report.

Motion of the Shaking Bag - Bag motion was measured by photographic, stroboscopic and photometric methods. The most common approach involved time exposure photographs of the shaking bag that showed the maximum excursions of the fabric. Stroboscope observations were made of the bounding wave patterns and local fabric motions. Still (short exposure) photographs of instantaneous fabric positions enabled quantitative analyses of the wave patterns. A light beam and photocell technique, described in Appendix C, was also used to monitor the maximum excursions of single points along the bag. The measurement techniques and results are discussed further under RESULTS pages 63, to 167.

Test Dusts

Coal fly ash was selected as a primary test dust for several reasons. With respect to density and size properties (see Table 4) it is representative of many industrial dusts that are collected by fabric filtration. It can be successfully redispersed by high pressure, $\geq$ 90 psig, compressed air ejectors to produce a particulate suspension with size characteristics approximating those of the parent material. Since most fly ash particles from pulverized coal combustion are spheroids (cenospheres), the analysis of aerodynamic behavior is simplified. On the other hand, the sphericity leads to increased particle penetration, relative to that for irregularly shaped particles having the same settling velocity.

Table 4. SUMMARY OF TEST DUST SIZE PROPERTIES

	MMD μm	σ_g
Coal Fly Ash		
Source: Hopper of electrostatic precipitator, cyclone boiler. Sold by concrete block manufacturer ($0.025/lb. in 50-lb. bags in 5-ton lots).		
Size properties:		
Light field microscopy		
As received bulk dust	5.0	2.13
Dust shaken from bags	2.4	1.77
Andersen cascade impactor[a]		
Aerosolized dust	8.0	2.0
Coulter count		
Aqueous dispersion	14.2	2.4
Sieve analysis	27.0	3.7
Talc		
Source: Sierra Talc and Clay Co., So. Pasadena, California. "EMTAL 599" ($0.0844/lb. in 50-lb. bags).		
Size properties:		
Andersen cascade impactor[a]		
Aerosolized dust	3.2	2.9
Light field microscopy		
As received bulk dust	3.6	2.0
Silica		
Source: Cabot Corp., Boston, Mass. "M-5 Cab-O-Sil" ($2.00/lb. in 10-lb. bags).		
Size properties:		
Andersen cascade impactor[a]	-	-
Manufacturer	0.012	-

[a]Andersen impactor data used as particle size standard for upstream samples.

Another reason for selecting fly ash was that it has been used by several investigators in related studies.[1,13] As far as can be determined, the aerosols used in past and present studies were sufficiently similar to allow comparisons of experimental results. Additionally, fly ash is available in large quantities at little expense (50-lb bags at $1.25) in contrast with some specially prepared powders for microscale testing costing as much as $25.00 per gram. The nature of the production process for fly ash is such that there should be minimal variation from bag to bag or from ton to ton. The present fly ash was collected by electrostatic precipitator from a cyclone fired boiler. Thus, its size was somewhat smaller than the ash from a conventional pulverized coal fired system.

Dusts from other industrial processes, if available in large quantities, may prove to be useful test aerosols. There are apt to be problems, however, such as very broad size ranges from aggregate drying kilns, hygroscopic properties with some calcined materials, and redispersability with metal fumes. Although dust recovered by fabric filter systems appears desirable from the size point of view, the presence of short fibers shed by the filter may lead to atypical collection properties.

To extend the range of aerosols studied, two other materials, talc and silica were selected to depict other size and shape properties encountered in the field (see Table 4). Both dusts are commercially available in bag quantities at reasonable prices.

Fly ash and talc dusts were sized initially by conventional microscopy wherein small amounts of the bulk dust were dispersed in an immersion oil. The above approach provides only a rough estimate of size since one can never be certain whether the final state of dispersion is representative of the aerosol phase. The same dispersibility problem also applied to screen analyses and Coulter counter measurements. Generally the cascade impactor measurements were considered to provide

better estimates of aerodynamic size although it was necessary here to assume an average particle density. Because agglomerates were known to be present in the aerosol, the assumption of a particle specific gravity of 2.0 is at best an approximation.

It was observed that the aerosolized state of the talc dust based upon Andersen impactor measurements suggested a finer suspension than the fly ash. Higher resistance characteristics noted for the talc were consistent with its smaller particle size. In that the talc and fly ash aerosols did not differ radically in size, it was expected that any apparent difference in filtration characteristics might be attributable to particle shape factor (and packing density).

Re-precipitated silica is composed mainly of highly agglomerated submicron particles. Its pneumatic redispersion was expected to produce a cloud composed of agglomerates of the order of 1-micron diameter, corresponding to an aged fume. The high resistance observed during its filtration suggested that the aerosolized material was considerably smaller than 1 micron. Extremely high efficiencies were obtained when filtering silica particles, possibly due to electrostatic properties of the particles being very different from fly ash and talc. No satisfactory size measurements were obtained on the inlet aerosols with the cascade impactor.

Dust Measurements

Aerosol Concentration and Particle Size - Inlet dust concentrations for the various fabric filter systems investigated during this study were determined directly by gravimetric methods. The following approaches were used:

- Material balance by dust feed rate - The dust delivery rate for the Acrison Dust Feeder* was shown to be controllable to within ± 1 percent for feed rates in the range of 0.032 lb./min. (14.4 grams/min.) and averaging periods of 1 minute or greater. In conjunction with the recorded system airflow rate, the dust concentration entering the hopper section was readily measured. The actual dust concentration arriving at the fabric surface was found to be about 30 percent lower than the gross inlet loading because of settlement in the hopper section.

- Filters, all-glass or membrane types - Readily weighable quantities of dust (~ 0.5 gram) were collected on high efficiency filter media at typical inlet concentrations, ~ 1 to 10 grains/ft.^{3}, to the fabric filter testing assembly. Sampling was performed isokinetically at 7 to 15 liters/min. for 10 minute periods. Since replication in filter circle weights was of the general order of ± 0.2 mg. for 100 mg. filters, filter weight gains could be determined easily within ± 1 percent. Ordinarily, no change in inlet concentration occurred during any one testing sequence.

- Cascade impactor measurements - A standard Andersen impactor (6 stage, 1 ft.^{3}/min., outstack design) was used whenever practicable to determine the mass concentrations and size distributions of upstream and downstream aerosols. Duct dimensions were too small in the test system to permit use of the newer instack models. In the case of highly efficient filter systems, it was not possible to collect weighable amounts of dust from the effluent air streams within reasonable sampling periods, ~ 2 hours. Usually, outlet concentration levels > 0.001 grain/ft.^{3} could be determined by the Andersen impactor.

Comparison between parallel filter and Andersen impactor measurements indicated that the Andersen values could be considered accurate to within ± 10 percent at the 95 percent confidence level, Appendix M. It is assumed here that because of far greater ease in sample handling,

*Acrison Model 120 Volumetric Feeder, Acrison, Inc., Carlstadt, New Jersey, 07072.

the filter values are usually correct. Since the individual impactor stages could be weighed to within ± 0.3 mg., Appendix M, no appreciable errors were introduced with the collection of 10 mg. or larger amounts of dust on each stage.

Repetitive determinations of the size distribution of the fly ash aerosol showed fairly good agreement, Figure 10. Size distributions Nos. 1 and 2 show mass median diameters, MMD, of 8.7 and 7.2 μm, respectively, and similar geometric standard deviations. Why Distribution 3 should indicate a slightly higher MMD, 9 μm, is not clear although the difference might be attributed to the lower concentration level or to variations in humidity. Generally, it is expected that the reproducibility in MMD values should parallel that observed for total mass concentrations determined by Andersen impactor.

Characterizing stage diameters for the Andersen device were based upon the manufacturer's specifications for spherical particles of specific gravity 2.0 at a 1 $ft.^3$/min. flow rate:

Stage	Particle diameter, μm
Filter	0.36
6	0.7
5	1.4
4	2.3
3	3.9
2	6.5
1	> 6.5

In view of variations in physical and chemical composition, shape factor, and degree of agglomeration, the assumption of a density of 2.0 grams/cc for fly ash appeared acceptable.

Figure 10 also shows the size parameters for the fly ash aerosol as determined by the light field microscope sizing of an oil dispersion of the dust. Frequently, this approach produces a better redispersion

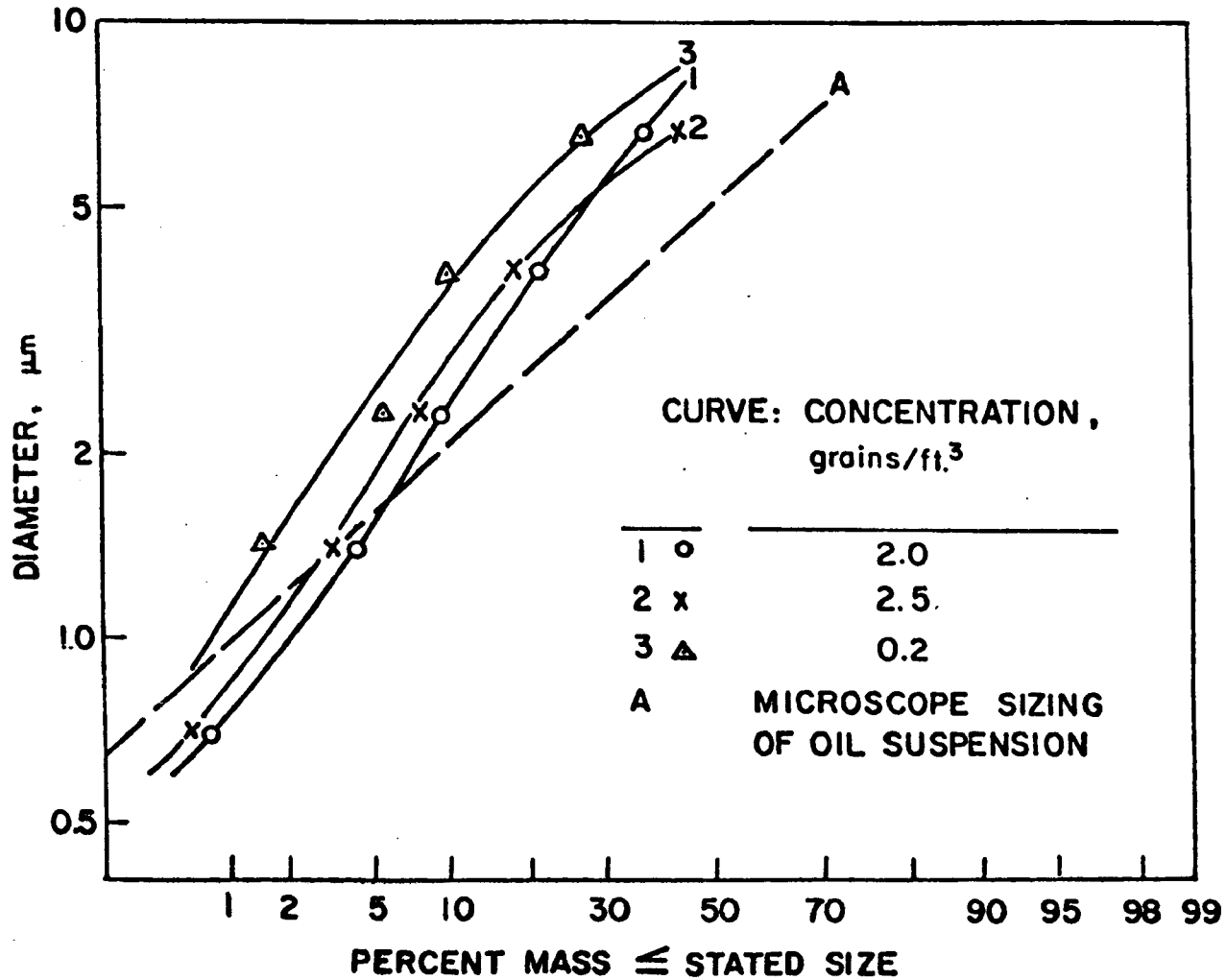

Figure 10. Inlet fly ash size distributions by Andersen cascade impactor

of a dry powder than that obtainable by air ejector systems. For the purposes of the present study, it was assumed that the Andersen impactor measurements indicated the effective size of the aerosol.

Outlet dust concentrations for the various investigations conducted during the program were measured by the following methods:

- RDM, respirable dust monitor - Mass concentration measurements in the range of 0.001 to 0.01 grains/ft.^{3} were made with an RDM* sampler. This device operates on the principle of collecting a short term, ~ 1 min., dust sample on a single impactor stage and determining the mass of the dust spot by its beta attenuation characteristics. The measurement accuracy for this instrument ranges from about ± 25 percent at the low end to about ± 6 percent at midscale. The principal use for this device was with fairly permeable woven fabrics cleaned by mechanical shaking and felt bags cleaned by reverse air pulse. Except for B&L measurements to be discussed later, this instrument provided the only way to estimate low mass concentrations within a 1 min. sampling period.

- Single particle light scattering counter - The size properties of the inlet dust loadings could be established for periods as brief as a few minutes by cascade impactor sampling. Such measurements, however, were not ordinarily needed in this study because the inlet aerosol was maintained at a nearly constant concentration level. On the other hand, the outlet dust concentrations from the various filter systems studied changed constantly over each filtration cycle. The fact that the outlet concentrations often ranged from 10^3 to 10^8 times lower than the inlet levels precluded the use of impactors except for the long term measurements cited previously. Although it might have been possible to collect very brief samples, ~ 10 to 30 sec., on special membrane filter assemblies, the time needed for visual assessment of sufficient samples to portray accurately changes in both size and concentration properties was prohibitive.

*RDM-101 Respirable Dust Monitor, GCA/Technology Division, Bedford, Mass. 01730.

Therefore, the use of a fast response device, designed for the detection and measurement of low particle concentrations was indicated. A Bausch and Lomb* (B&L) counter was found in many ways to be singularly effective for the needs of this study. Even when used with a single channel dial or digital display, changes in the concentration of specified size ranges could be established in 0.1 minute and within 0.5 minute five size ranges could be scanned. It was possible, therefore, to follow sequentially the changes in concentration for a broad range of particle diameters as the filter process continued. As expected, particle emissions were greatest when filtration was resumed with a "just cleaned" filter. However, use of the B&L instrument provided unusual insights into the effects of type of fabric (and dust), and the method and intensity of cleaning.

It was recognized at the outset of the study that size measurements by different systems could present correlation problems. Light scattering equipment is highly sensitive to particle shape, surface smoothness, and to refractive index. Furthermore, the working particle concentration range for these units is generally near ambient dust levels. Thus, unless special air dilution apparatus is used, electronic "choking" or no display conditions may occur in the lower size channels at concentrations levels in excess of 10^6 particles/ft.^{3}. Because the gating with the B&L device is designed to show the number of particles greater than the indicated size, choking in the lowest channel; e.g., > 0.3 μm does not completely invalidate measurements for the higher channels, 0.5, 1.0, 2.0, 5.0 and 10 μm. Some error is expected, however, possibly in the factor of two range, when one computes mass concentrations from the indicated number concentrations.

The B&L measurements provide a data output from which one can calculate immediately a size distribution (with respect to particles > 0.3 μm)

*Bausch & Lomb Dust Counter 40-1, Bausch & Lomb Inc., Rochester, New York 14602.

and the total number of concentration. If the distribution can be described by some convenient mathematical function; e.g., logarithmic normal distribution, and a constant density assumed over the size range, the dust distribution with respect to mass, volume, or surface area can also be readily calculated. In the absence of a rigorous mathematical relationship, a conventional incremental method is employed in which particles are grouped within size ranges characterized by some mean diameter. This approach was used in the present study with the B&L size groupings described as shown below:

Size range, μm	Average diameter,* $\bar{d}$
0.3 - 0.5	0.424
0.5 - 1.0	0.826
1.0 - 2.0	1.65
2.0 - 3.0	2.60
3.0 - 5.0	4.24
5.0 - 10.0	8.26

The accuracy of the conversion from number to mass concentration depends upon the initial particle concentration and the validity of assumptions relative to density of either discrete particles or agglomerates, optical properties, possible particle losses in sampling lines and the stability of the aerosol concentration over the 0.5 to 0.75 minute period required to scan all size channels.

It was not intended that the B&L measurements be used for direct comparisons with other sampling methods; i.e., cascade impactor, filter or RDM unit. Its primary function was to determine the relative changes in aerosol properties taking place over the filtration cycle. Calibration procedures were carried out, however, in the form of parallel

---

*$\bar{d}^3 = (d_1^3 + d_2^3)/2$

sampling of the same aerosol streams with the B&L instrument and other devices. The results of some of these tests, summarized in Table 5, show the general order of the agreement between the B&L instrument and the RDM unit. Although our reaction to differences of up to a factor of 5 may appear to be rather casual it should be kept in mind that effluent concentration levels over a nominal filtration cycle with sateen weave cotton bags sometimes varied by 4 to 5 orders of magnitude.

Dust Filtering Rate - Dust filtering rate was determined either by an overall system material balance, or by weighing the filter bag before and after dust loading. In the balance method, the dust from the screw feeder was collected in a weighing pan for various time intervals and the hopper fallout was collected and weighed after a fixed filtering time at a constant air flow. The differencing of these two quantities represented the amount of dust actually reaching the fabric. In the weighing method, the bag was freed at the bottom whereupon the load cell used in tension measurements was used as a conventional weighing device. Readings before and after filtering indicated the weight of dust deposit. For greater precision, however, the filter bag was carefully removed and weighed on standard laboratory scales.

Dust Removal - Various techniques were used to determine the dust removed during a single cleaning process. When cleaning by mechanical shaking, the hopper was immediately opened following filtration and as the bag was shaken, the falling dust was caught in a pan inserted under the bag. Weighing the dislodged dust permitted precise determination of the rate of removal after successive shaking intervals of varying duration.

Residual Dust - The residual dust holding of a bag following cleaning bore no relationship to the amount of dust deposited during the filtration cycle. Although the residual accumulation was related

Table 5. COMPARATIVE AEROSOL CONCENTRATIONS AS DETERMINED BY VARIOUS INSTRUMENTAL METHODS[a]

Test dust	Concentration - grains/ft.^{3} x 10^3		Concentration ratio
	B&L[b]	RDM[c]	RDM/B&L
Fly ash	8.2	11.8	1.44
	10.4	7.0	0.67
	0.048	0.13	2.71
	0.083	0.34	4.1
	0.11	0.23	2.1
	0.92	2.0	2.17
Talc	0.14	0.23	1.64
	0.027	0.10	3.70
	0.071	0.23	3.25
	0.076	0.23	3.03
	0.11	0.25	2.27

[a]Based upon outlet concentrations from wool and Dacron felt bags cleaned by pulse jet air.

[b]Bausch and Lomb Dust Counter, 40-1.

[c]RDM-101, Respirable Dust Monitor.

approximately to the energy input of the cleaning cycle, the electrical charge, relative humidity and the age and prior service of the bag also had some effect on residual dust holding.

A beta radiation instrument was constructed according to a procedure devised by Stephan, et al[14] to measure the dust distribution on small (~ 1 in.^{2}) areas of the fabric. Some measurements of dust distribution along the shaken bags with this instrument showed changes in cloth loading after successive short periods of shaking. Variations in dust loading during the actual shaking could not be measured, however, because the instrument was sensitive to the position of the fabric. The instrument was found to be about three times as sensitive to dust on one side of the bag cylinder as the other side, due to lack of radiation collimation in this type of instrument. The above problem, coupled with the sensitivity of positioning, limited the usefulness of the instrument in most tests.

A simple and very qualitative technique for observing the residual dust deposit density in shaken bags was to run a light bulb up and down inside the filter bag. As little as 40 grains/ft.^{2} of additional deposit was sufficient to completely block the transmission of a 50 watt light when observed in a darkened room. Thus, small variations in residual dust were clearly seen as variations in the bag brightness.

Pressure, Air Flow and Air Properties Measurements

The system for regulating airflow to the filter bag is described in Appendix A. The pressure differential across a Stairmand disc, normally about 1 inch water, was automatically monitored by a pneumatic indicating, controlling, and recording system (Appendix A).

A Stairmand disc is a circular plate, symmetrically located within a round duct, that diverts the gas flow through the outer annular region.

When the disc area is one half of the duct cross section, its resistance properties are nearly the same as that of an orifice of similar size. In addition to acting as a flowmeter, this device promotes good mixing of suspended particulates so that centerline sampling alone is sufficient at downstream locations, ~ 4 to 5 pipe diameters. Accuracy and precision of the flows indicated by this system are estimated to be within about 5 percent.

The pressure differential across the filter bag was monitored by a pneumatic indicator similar to that used in the flow control system and also by a sensitive Bourdon-type Magnehelic gauge and a liquid manometer. The Magnehelic device with its fast response and high precision (better than 1 percent), was used when moderate accuracy was acceptable (within 5 percent). The manometer was used as a standard and for highly accurate measurements.

The air used for filtration was drawn from the room in which the filter system was located, such that considerable recirculation was involved. Nominal room conditions of about $70^{\circ} \pm 3^{\circ}F$ and 50 percent $\pm$ 4 percent RH were maintained during most of the tests. Based on measurements reported by Durham and Harrington,[2] the variations in relative humidity during present testing were not expected to have any significant effect on cotton fabric tests. Dacron multifilament weaves might have shown some changes in both collection efficiency and specific resistance coefficient due to the $\pm$ 4 percent RH range.

RESULTS

Cleaning Forces and Bag Motion

Bag Tension versus Shaking Frequency - Theoretical relationships, summarized in a previous section, indicate that shaking tension should increase with shaking frequency and show characteristic maximum values at resonant frequencies. Confirming experiments, summarized in

Figure 11, with a typical filter bag indicate distinct resonant frequencies of about 2, 4.5 and 7.5 cps. The dynamic shaking tension, T_d, increases more or less steadily with increasing frequency, except for the periodic resonant states noted above.

A comparison of predicted versus observed resonant frequency values for the fundamental frequency and the first few harmonics is shown in Figure 12. The predicted values, computed by formulas developed in Appendix D, confirmed the fact that observed tension maxima were associated with resonance points. The rather narrow scatter of data points around the regression line suggested that the relationships developed in this study to describe bag motion were fundamentally sound.

The shaking tension at a specified frequency was not constant as implied by Figure 11, because the display dial shows only the average or integrated reading. It was actually the time average of a rapidly varying force that was measured by a fast response load cell mounted at the upper end of the bag in conjunction with an oscilloscope display. A typical force envelope is shown in Figure 13. In each excursion of the shaker arm from the vertical, the tension passed through a maximum and a minimum (i.e., two maxima per shaking cycle). The average width of the envelope appeared to be similar in magnitude to the variation in static tension as the arm was fully displaced from the vertical, Equation (2.3). On the other hand, the range in envelope width depended upon proximity to the resonant state. The position of the arm at the instant of maximum tension was found to vary from full displacement at zero frequency to the vertical position at very high frequencies (or at resonance conditions at moderate frequencies). Although the instantaneous forces at the top of the bag were probably related to small permutations in the bag's standing wave pattern, the analysis of this relationship in greater detail did not prove fruitful.

According to classical mechanics, the amplitude at which a body resonates is highly dependent on the degree of damping in the system. A

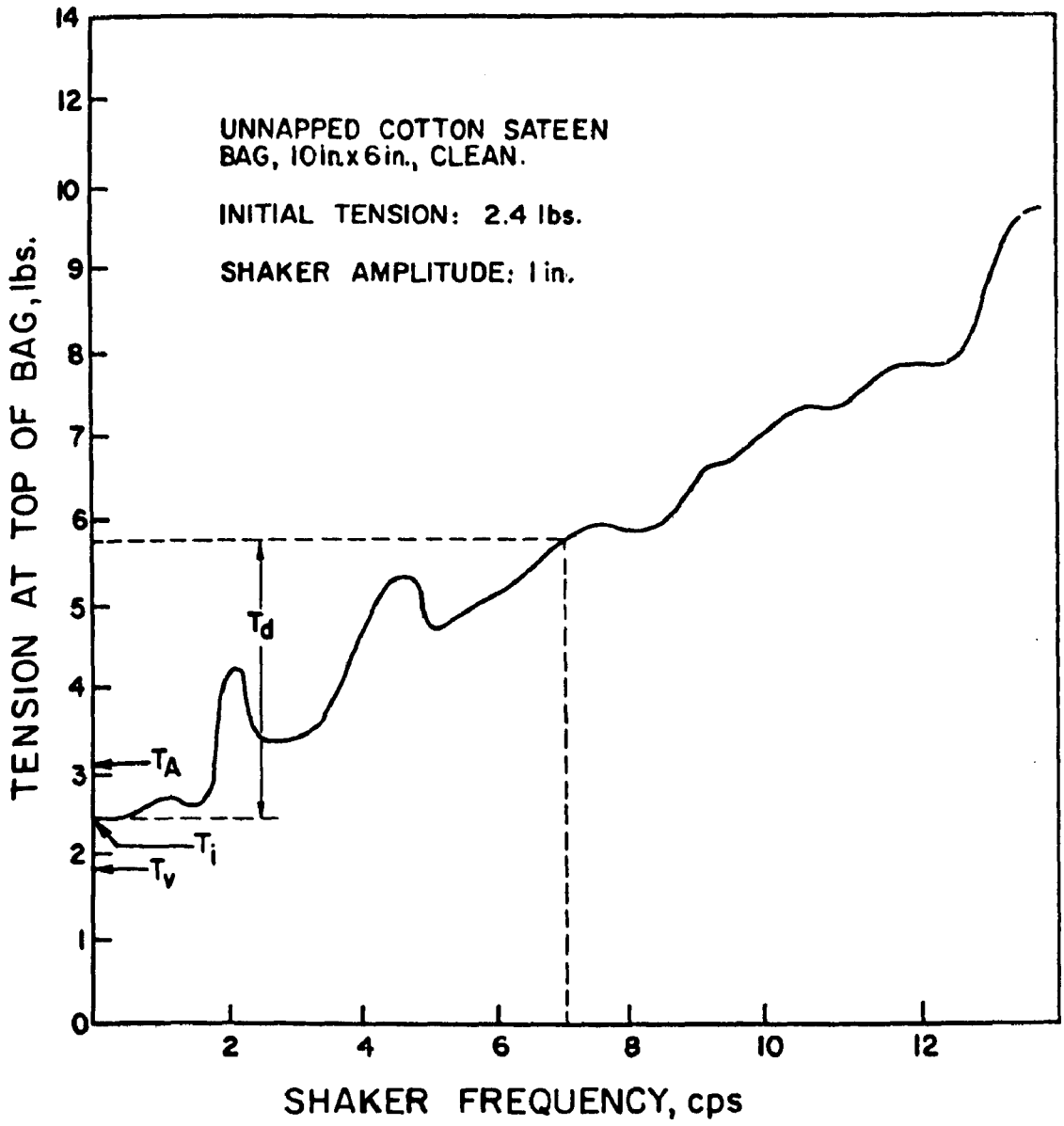

Figure 11. Shaking tension as a function of frequency for cotton sateen bag

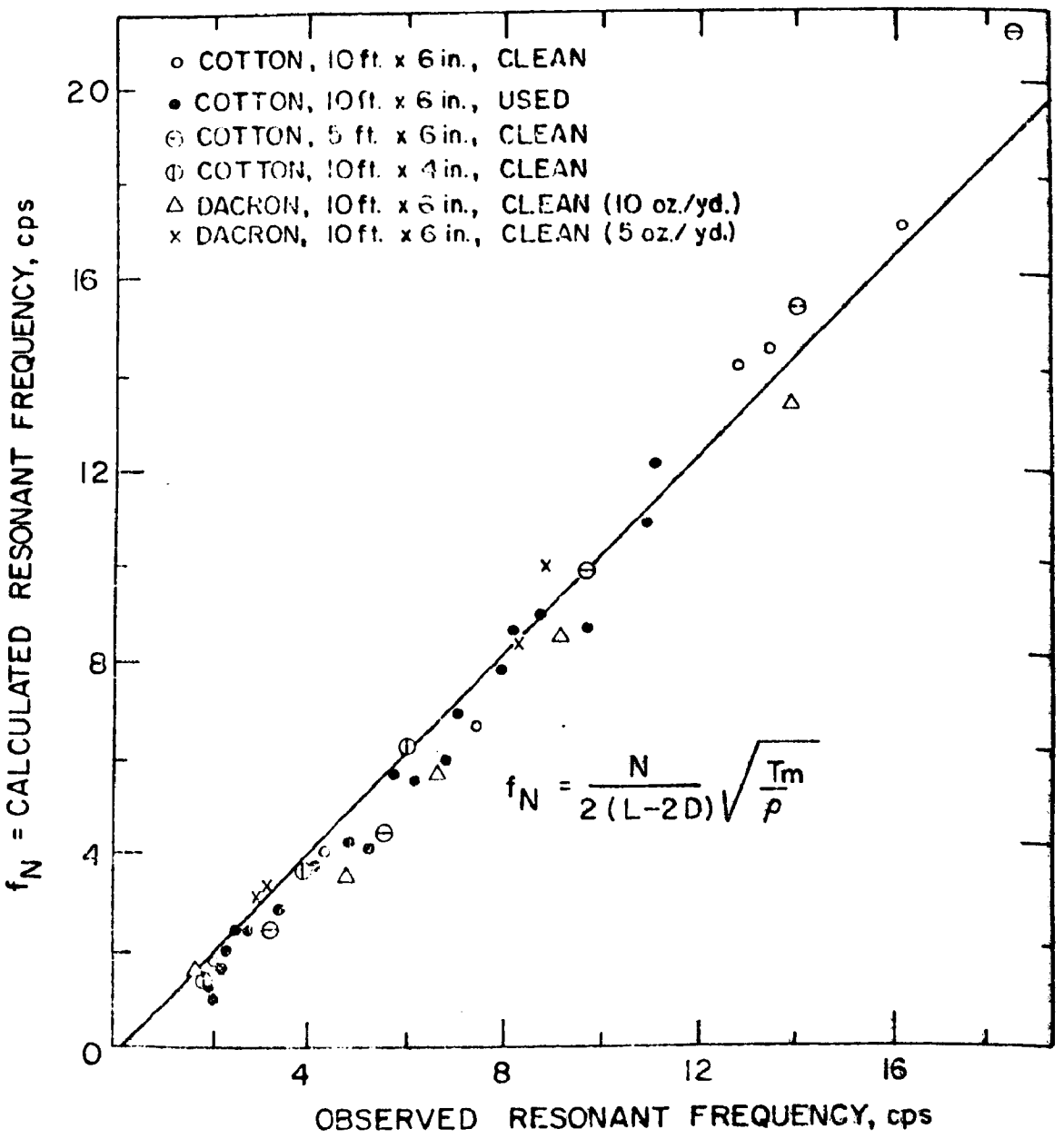

Figure 12. Predicted versus observed resonant frequencies

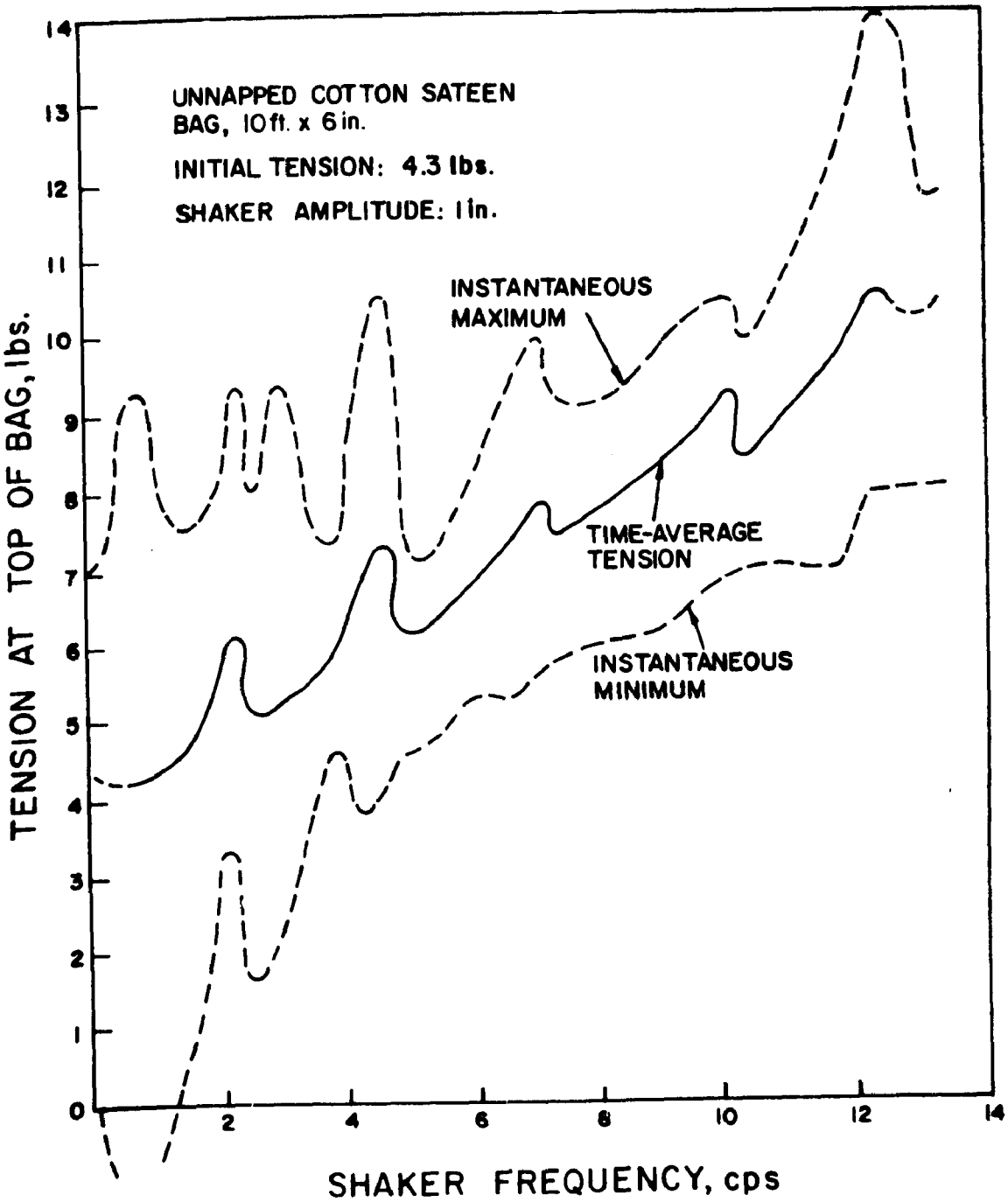

Figure 13. Maximum and minimum envelope curves and average shaking tension for cotton sateen bag

high damping rate will greatly attenuate system amplitudes, while a low damping rate may produce amplitudes large enough to destroy the vibrating member. In the case of an oscillating filter bag, observations indicated that damping and reflection were partially dependent on bag tension, bag weight, and shaker frequency and amplitude. The main causes of the energy dissipation, or damping process, were considered to be friction between fibers, yarns, and dust particles, as well as flexural heating within the fibers and air resistance to the moving bag. Dust separated from the surface of the bag with appreciable velocity also represents a significant kinetic energy loss.

Although a rigid quantitative theory of damping might be developed for shaken bags, it appeared that too many parameters would be required to yield practical damping coefficients. As an alternative, the classical damped wave equation shown below

$$Y = A\, e^{-\beta x} \sin (2\pi\, x/\lambda) \qquad (2.13)$$

was applied to a single shaken bag (Appendix F). It was shown that the average bag amplitude, Y, could be related to the amplitude of the driven end, A, by an attenuation parameter, α, for specific shaking conditions; i.e.,

$$\alpha \equiv \frac{Y}{A} \approx (2\beta L)^{-\frac{1}{2}} \qquad (2.14)$$

The ratio Y/A was usually less than one except near resonant frequencies in low-damped bags where it sometimes exceeded unity. If the classical exponential damping rate, β, can be defined, the attenuation coefficient for Equation (2.10) needed to obtain average bag amplitude can be easily computed. At this time, shaking tension data for various bags and shaking regimes have been analyzed to obtain empirical values of α. On this basis, α can be estimated roughly in accordance with procedures described later in this section.

The wave damping properties of the bag presumably bear some relation to those of the fabric. An approximate measure of damping tendency was made by stretching a strip of cotton filter fabric between fixed supports and tapping the center of the strip to initiate oscillation. The ensuing oscillation and its decay were observed on an oscilloscope by magnetically sensing a tiny bit of steel cemented to the fabric strip. Each successive amplitude displacement was about 0.91 times its predecessor, indicating a 20 percent energy loss per cycle. To obtain meaningful data, damping in a fabric sample should be studied at tensions, frequencies, and angles of flexure similar to those seen in a real filter bag. Generally, it is preferred to make measurements on a full scale bag under normal conditions of use as discussed earlier under APPARATUS, TECHNIQUES, AND MATERIALS (pages 36 to 61).

Bag Acceleration - As pointed out under BACKGROUND AND THEORY (pages 13 to 36) the maximum acceleration seen by a point on the filter bag can be approximated by Equation (2.9). The specific acceleration assumed to relate quantitatively to dust removal is the average value of the maxima seen by all the points on the filter bag. The time-wise phasing of these maxima from point to point is expected to exert second order effects only on dust removal. Since all parts of the bag were observed to shake at essentially the same frequency the determination of average bag acceleration requires only a measure of average bag amplitude.

Bag frequency - In almost every case, all points on a bag moved with the same frequency as that of the shaker arm according to stroboscopic measurements and a light beam interception method (see Appendix C). Consequently, it was concluded that the average bag frequency needed to compute average bag acceleration was simply the shaker arm frequency. The light-beam interception technique also revealed that the motion was essentially simple harmonic (i.e., not appreciably saw-toothed or skewed). Limited measurements by the above method suggested that at shaking frequencies greater than nine cps, the bag motion indicated the

possible presence of beat frequencies (higher harmonics). Their intensities, however, relative to the driving frequency of the shaker arm, were sufficiently low to justify neglecting them.

Envelopes of motion - As a means of estimating the average bag amplitude needed to compute average bag acceleration, time exposure photographs were made over ten or more bag oscillations. A series of photographs of a 10 foot by 6 inch used cotton bag with a residual dust holding of about 1.2 pounds were made at selected frequencies to depict resonant, antiresonant and immediate frequencies. Typical tracings, Figure 14, show the largest lateral excursions made by the opposite edges of the bag. Reference to the rest position of the bag, which is normally a tented Vee, yields the approximate amplitude of bag motion at any axial location. Action photographs of different bags at a variety of tensions and frequencies were used to obtain an average bag amplitude for comparison with dynamic tension data.

The motion envelopes deriving from the above photographs (Figure 14) depict clearly the resonant and anti-resonant states. The latter state, which occurs at a frequency slightly above a resonant level, is characterized by minimum tension and amplitude values. Additional envelope photographs are discussed in Appendix G.

Typical motion envelope measurements are summarized in Table 6. Over the range of frequencies investigated, 0 to 11.4 cps, the maximum lateral displacement at the nodal points was 1.69 inches from the rest position at a shaking frequency of 3.95 cps. Midway between the nodes, the fabric only moved about 0.74 inches from the rest position, indicating about 44 percent as much acceleration in that region. These data demonstrated that the bag amplitude became more uniform as frequency was increased and that the average amplitude of the bag diminished as the frequency increased.

PHOTO	TENSION, lbs.	FREQUENCY, cps
2	3.01	2.0
3	2.20	2.60
4	2.93	3.70
5	3.66	4.4
6	3.18	4.75
7	3.94	6.15
8	4.56	8.0

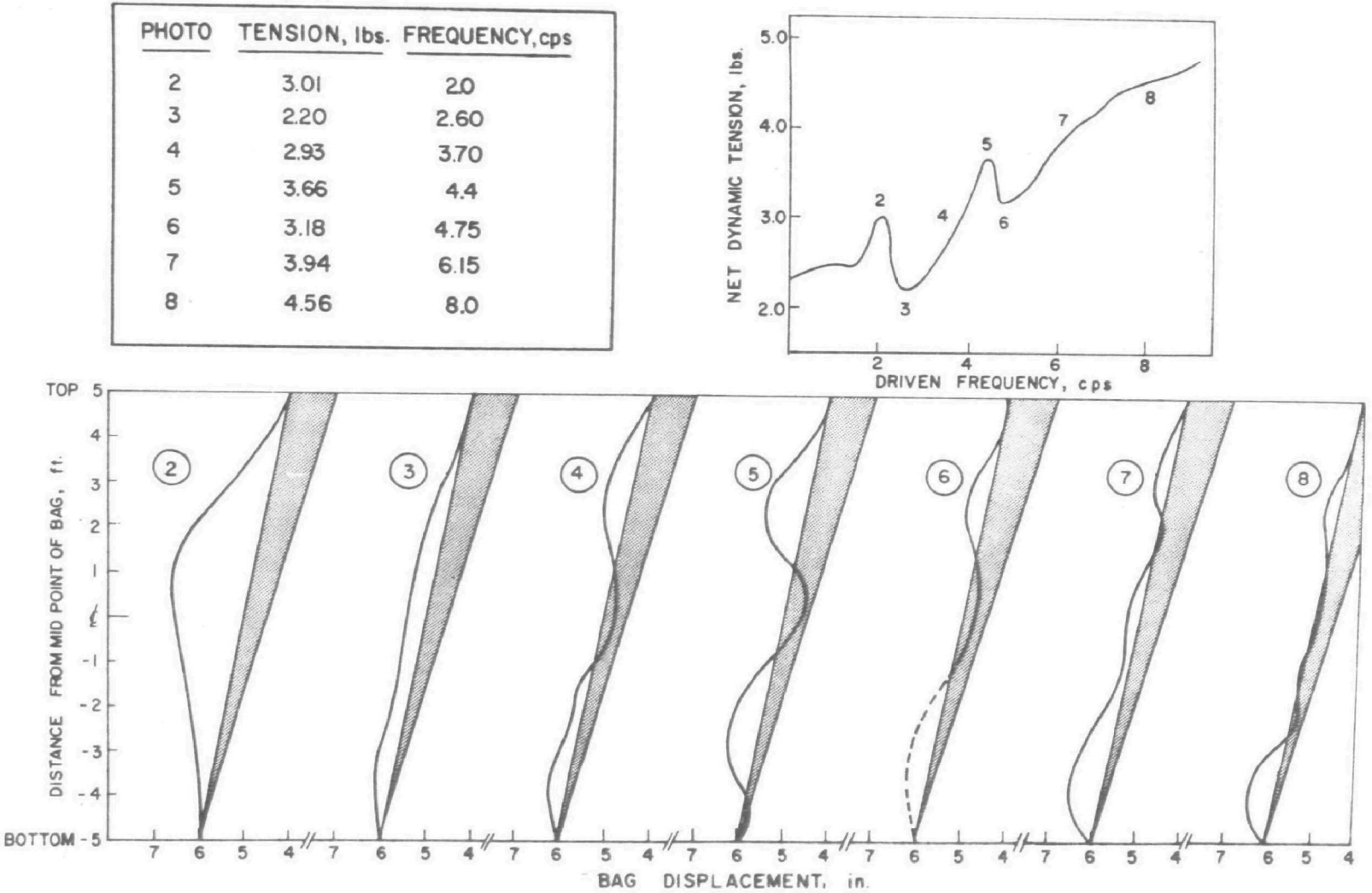

Figure 14. Bag displacement versus driven frequency and indicated dynamic tension

Table 6. ENVELOPES OF MOTION FOR A SATEEN WEAVE COTTON BAG[a]

Photo number	Frequency (cps)	Resonance state	Average shaking[b] tension-T_m (lbs.)	Bag amplitude[c] -Y (in.)		
				max.	min.	avg.
1	1.8	1st Res.	3.23	1.62	-	(1.81)
2	2.2	Anti Res.	2.19	1.35	1.06	1.21
3	3.3	Midpoint	3.38	1.40	0.90	1.15
4	3.95	2nd Res.	4.27	1.69	0.74	1.22
5	4.1	Anti Res.	3.46	1.60	0.72	1.16
6	5.4	Midpoint	4.18	1.22	0.88	1.05
7	5.95	3rd Res.	4.75	1.30	0.84	1.07
8	6.4	Anti Res.	4.59	1.10	0.70	0.91
9	8.6	4th Res.	6.03	1.20	0.88	1.04
10	8.9	Anti Res.	5.39	1.14	0.90	1.02
11	11.0	5th Res.	7.13	1.20	0.94	1.07
12	11.4	Anti Res.	6.19	1.16	0.93	1.05

[a]10 in. x 6 ft. bag with light residual dust holding, gross lineal weight = 0.135 lbs./ft. Initial tension ($T_{i,m}$) = 1.55 lb., shaker amplitude = 1 in.

[b]Total time-averaged tension at bag midpoint.

[c]Maximum at node points, minimum at anti-node points.

Our major difficulty in interpreting these data is that the rest position of the fabric probably changed during shaking partly due to flexure along the bag. This flexure in conjunction with the increased tension tended to straighten bags that were initially tented unevenly or were creased from storage. Downward traveling waves produced a detectable downward air draft outside the bag that also contributed to the flattening process. Thus, the maximum displacements seen in envelope photographs represent only approximately the true amplitude at a given point along the bag.

The tension data in Table 6 provide a means to compute the average bag amplitude using Equations (2.5) through (2.7). The results are compared in Table 7 with the apparent average bag amplitude estimated from the envelope photographs. The same trends are seen with increasing frequency and/or resonance. However, the computed tension-based amplitude is about 30 percent lower probably because the photograph displays only the maximum displacement, while the calculated tension depicts an average around the bag. The lower amplitude values are more in keeping with the visual observation that bag amplitudes are usually less than the shaker amplitude, especially in situations involving heavy damping. We believe that the tension approach yields a more accurate average bag amplitude with respect to correlations with dust removal.

Amplitude from basic bag properties - Before undertaking dust removal studies, three types of fabrics and three length to diameter ratios were tested at different installed tensions, shaking frequencies, and shaking amplitudes (see Table 3). The purpose of the tests was to enlarge upon and validate the general concepts developed in the previous section. Appendix H provides detailed summaries of all tension versus frequency measurements. Typical results for various experimental conditions are provided in Figures 15, 16, 17, and 18.

Table 7. CALCULATED AND MEASURED AVERAGE BAG AMPLITUDES[a]

Photo no.	Average dynamic tension T_d (lbs.)	Bag wavelength (ft.)	Average bag amplitude - $\bar{Y}$ (in.)	
			Calculated[b]	Photograph
1	1.68	15.4	1.68	(1.81)
2	0.64	10.4	0.70	1.21
3	1.85	8.6	0.98	1.15
4	2.74	8.1	1.13	1.22
5	1.98	7.0	0.83	1.16
6	2.70	5.9	0.81	1.05
7	4.32	5.6	0.98	1.07
8	3.16	5.2	0.78	0.91
9	4.60	4.4	0.79	1.04
10	3.96	4.0	0.67	1.02
11	5.70	3.8	0.76	1.06
12	4.76	3.4	0.62	1.05

[a]See Table 6 for operating data.

[b]Based upon tension data, shaking parameters and bag properties:

$$\bar{Y} = \frac{1}{\pi f} \sqrt{\frac{1}{ML\rho}} \cdot \sqrt{T_m \cdot T_D} \qquad \text{Equation (2.15)}$$

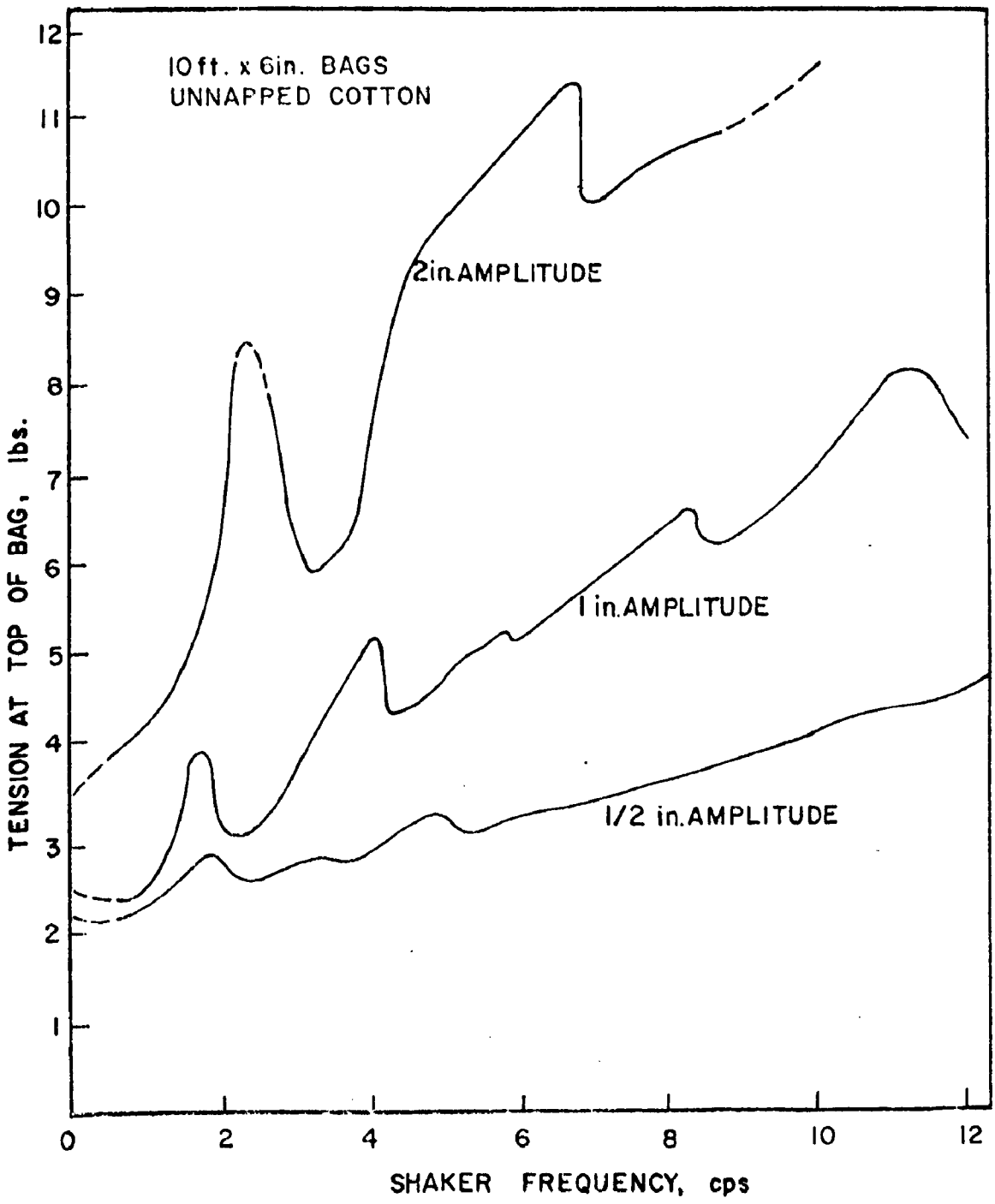

Figure 15. Effect of shaker amplitude on shaking tension

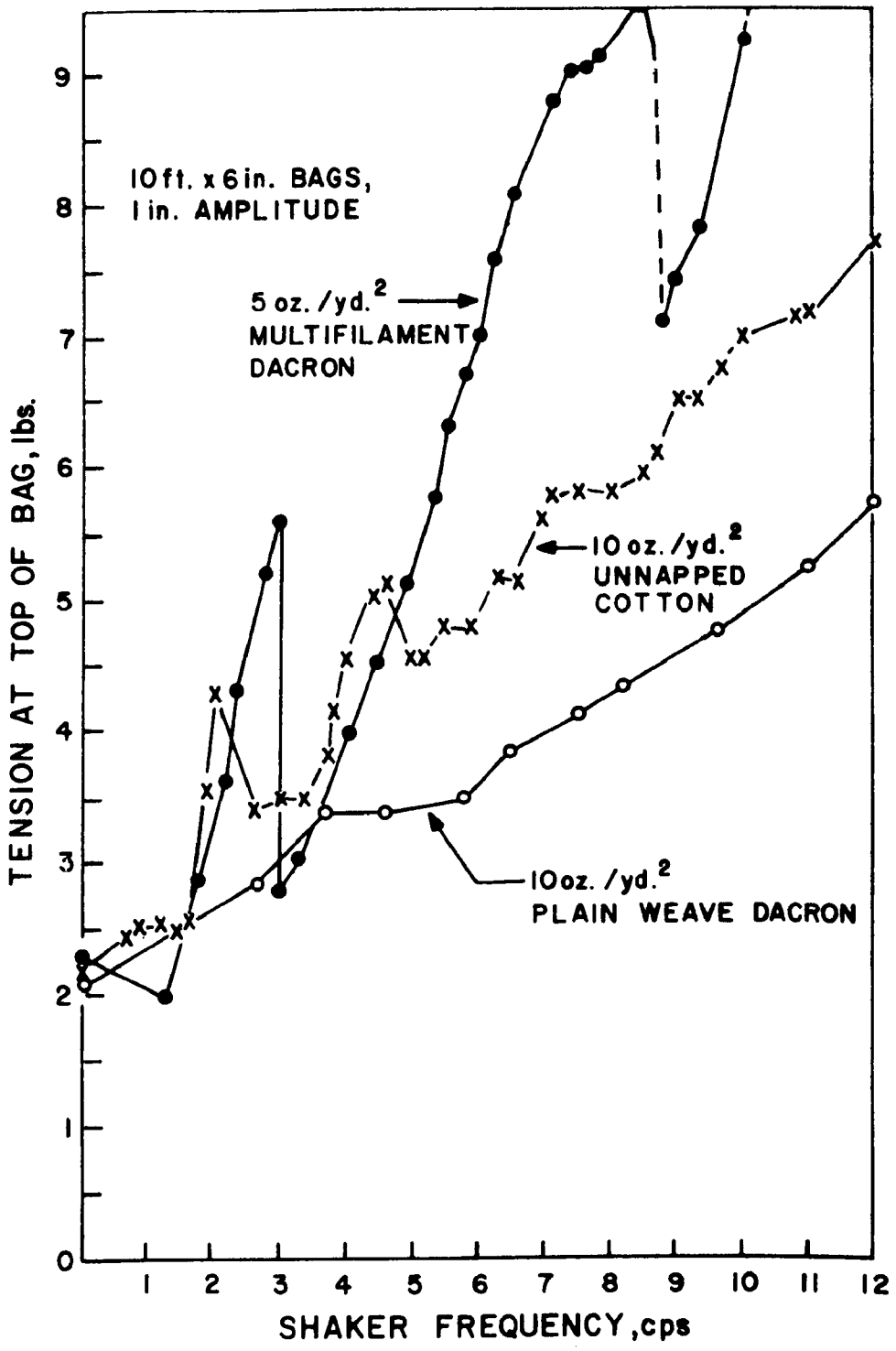

Figure 16. Effect of fabric type on shaking tension with 10 ft. x 6 in. bags (1 in. shaking amplitude)

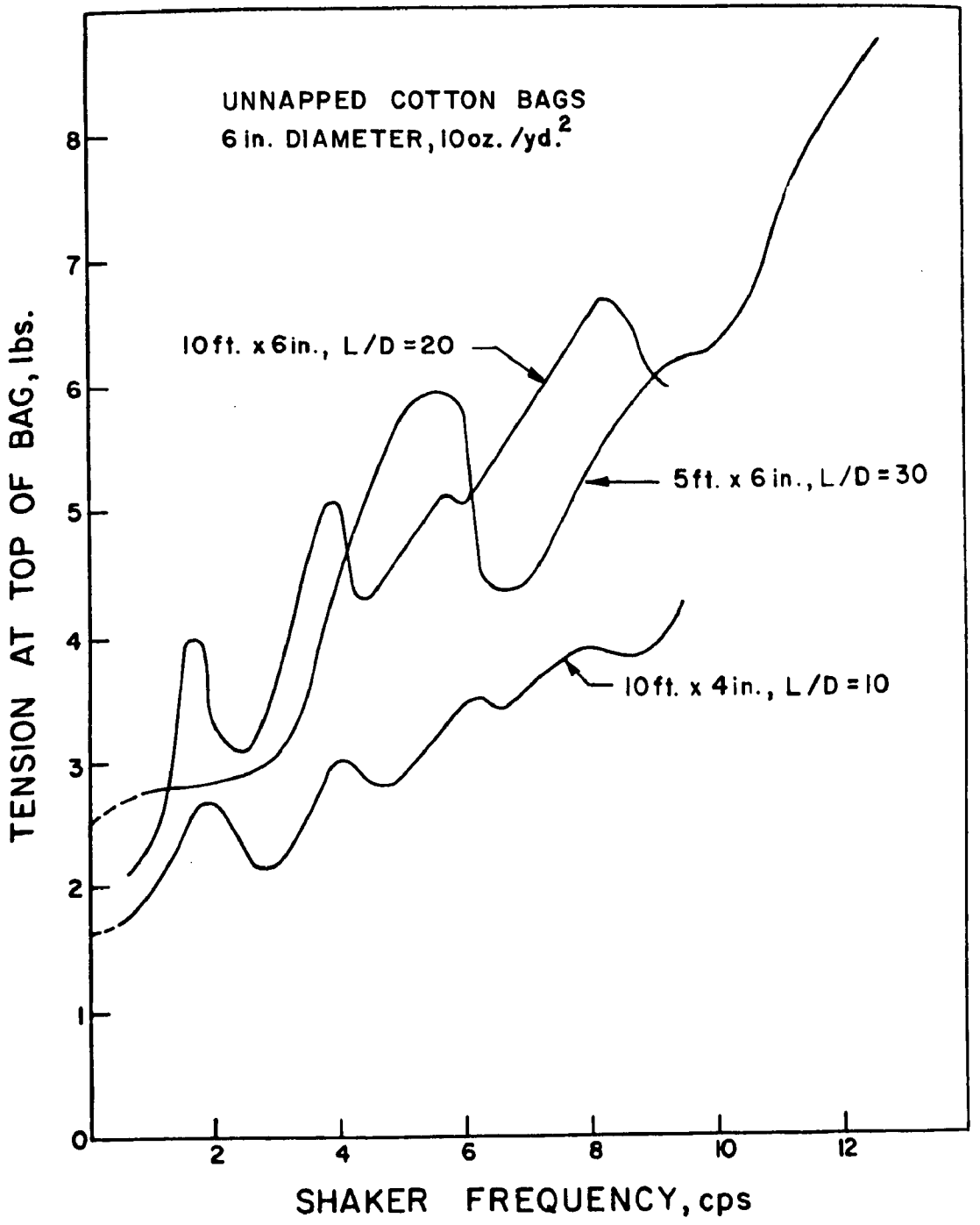

Figure 17. Effect of length/diameter ratio on shaking tension

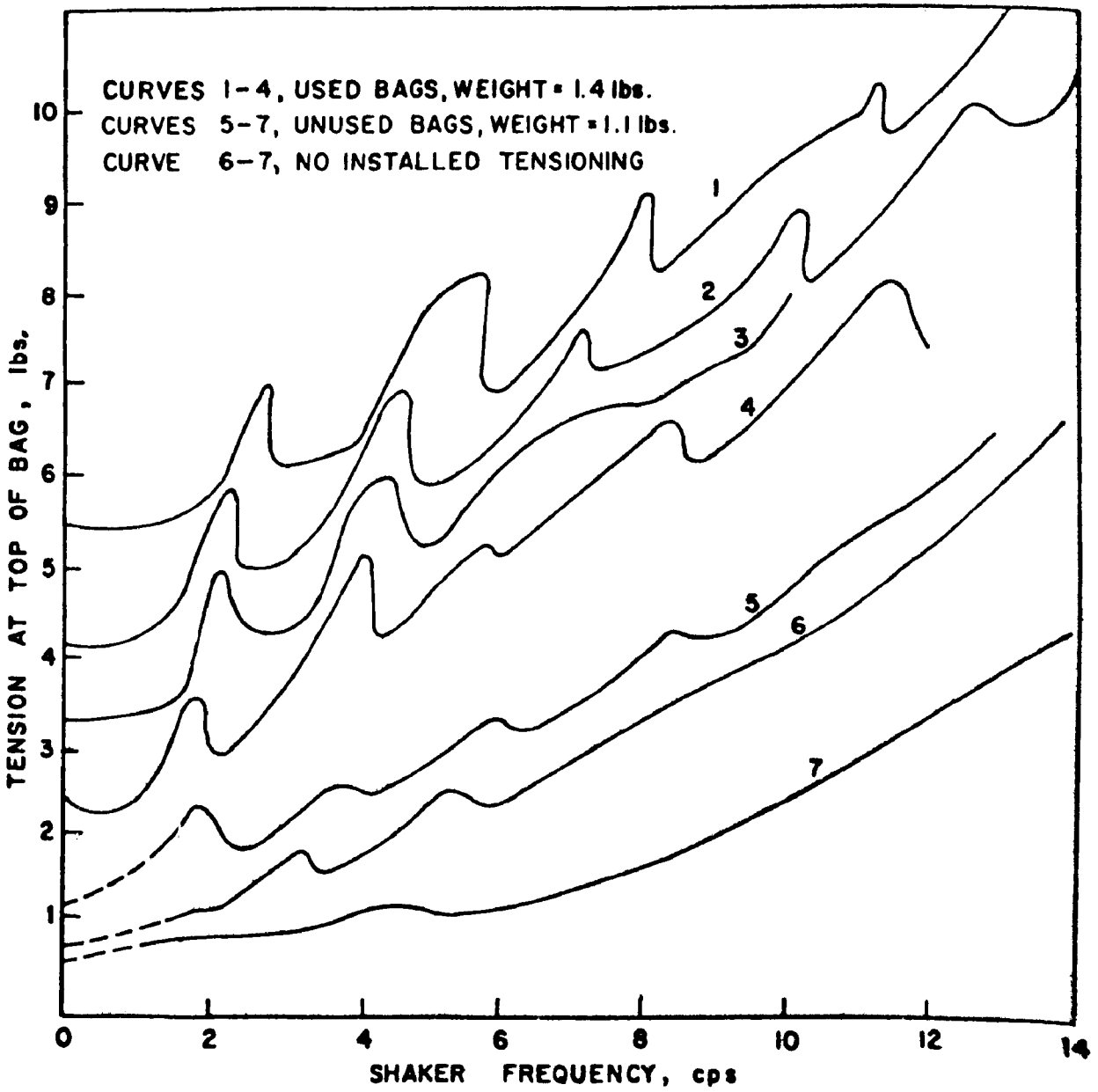

Figure 18. Effect of initial tensioning on shaking tension with unnapped, 10 ft. x 6 in. cotton sateen bags

Regardless of the fabric configuration or shaking conditions, all tension-frequency curves exhibited several common features. Starting from specified T_i values that depended only upon initial tensioning and bag weight, all curves described upwards paths with periodic excursions or oscillations from the mean associated with resonance phenomena.

The mean curves of Figure 18 (excluding oscillations) can be described approximately by a combination of Equations (2.16) and (2.17).

$$(T_m - T_i, m) = \frac{ML\rho}{T_m} (\pi A f \alpha)^2 \qquad (2.16)$$

The term α given in Equation (2.16) can be estimated readily from the tension-frequency data given in Appendix H and the following empirical relationship:

$$\alpha = \left[1 - 7.1 \left(\frac{A}{L/D}\right)\left(\frac{W}{T_i}\right)^{\frac{1}{2}}\right] \left[\frac{f - 2.65 + \left(\frac{T_i}{W} - 0.75\right)^{\frac{1}{4}}}{f - 2}\right] \qquad (2.17)$$

In Equation (2.17), the term T_i refers to the initial average tension at the top rather than at the middle of the bag and W is the total bag weight.

The predicted average bag amplitude can be adjusted to take into account the tension variations cited above by the following empirical equation

$$\Delta T_E \approx 0.35 \left(\frac{MA^2}{2R_A}\right) \qquad (2.18)$$

where ΔT_E is one-half the peak-to-peak tension excursion that occurs near each resonant frequency.* The magnitude of this tension excursion is about one-third of the tension difference noted when a bag is stretched from its vertical position (T_V) to maximum displacement (T_A), Equation (2.15).

Equation (2.17), in conjunction with Equation (2.18), provide a second means to estimate average bag amplitude without the need to perform actual shaking tests as required by Equation (2.16). All terms in Equation (2.17) can be evaluated prior to performing any shaking measurements. A comparison of average bag amplitudes as calculated by both approaches, Figure 19, indicates fair agreement.

The corresponding deviation in average bag amplitude, ΔY_E, at the resonance and nonresonance points may be approximated from the following expression

$$\Delta Y_E = \Delta T_E \frac{\bar{Y}}{T_m} \qquad (2.19)$$

noting that the coefficient in Equation (2.18) decreases with increasing frequency. The primary value of Equation (2.19) is that a better estimate of bag amplitude can be made for the resonant state.

Bag Power Consumption - The most direct way to estimate bag power consumption is to measure the electrical power needed to operate the shaker with and without the bag. Figure 20 indicates that typical bag power consumption, which is roughly a few watts, increases with frequency.

*The coefficient 0.35 is an average that appears to depend on which harmonic is excited. Review of data gives the following average coefficients for the 1st through 5th harmonic as 0.43, 0.39, 0.31, 0.26, and 0.21 respectively.

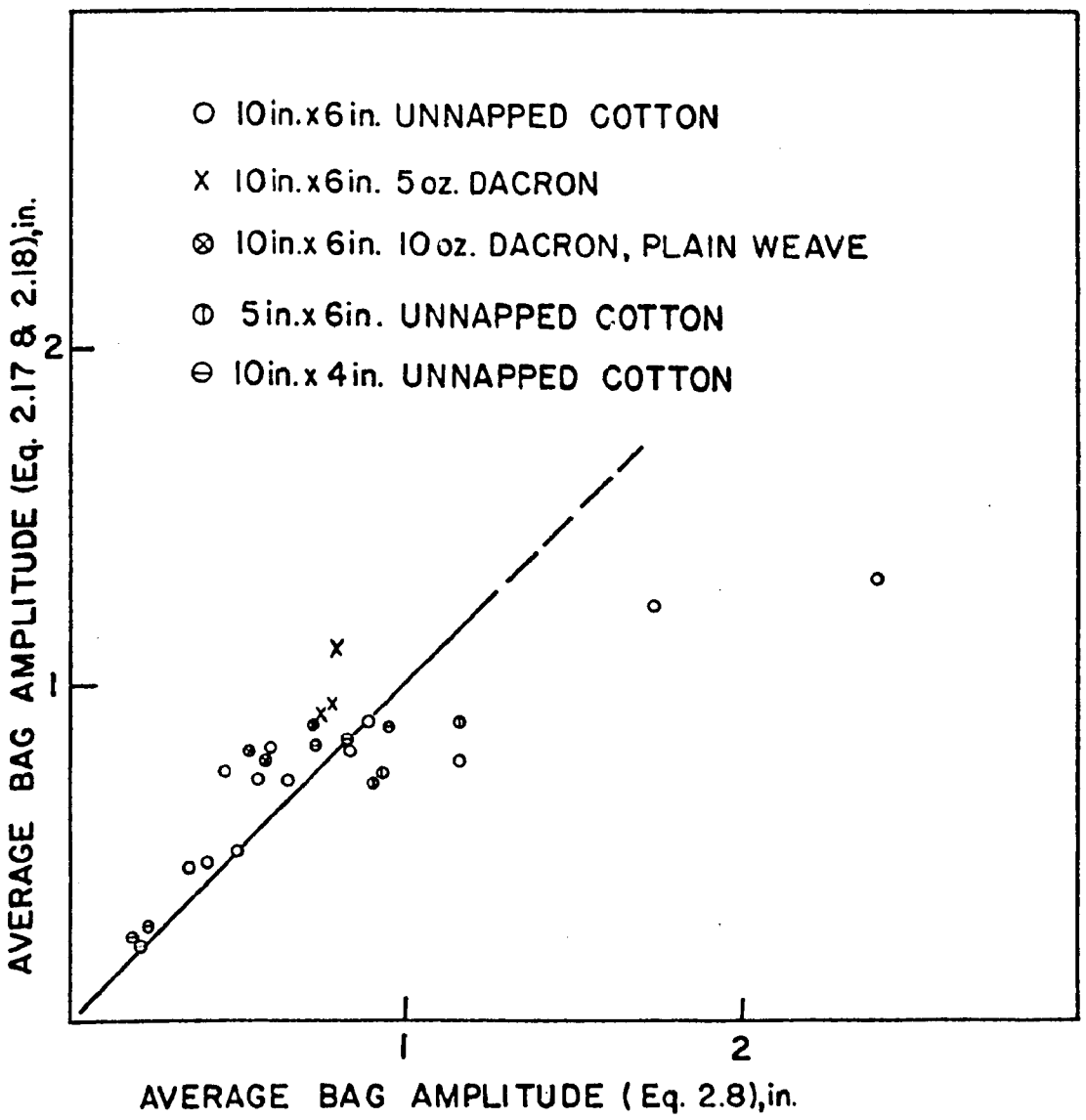

Figure 19. Comparison of average bag amplitudes as calculated by Equation (2.8) or Equations (2.17) and (2.18)

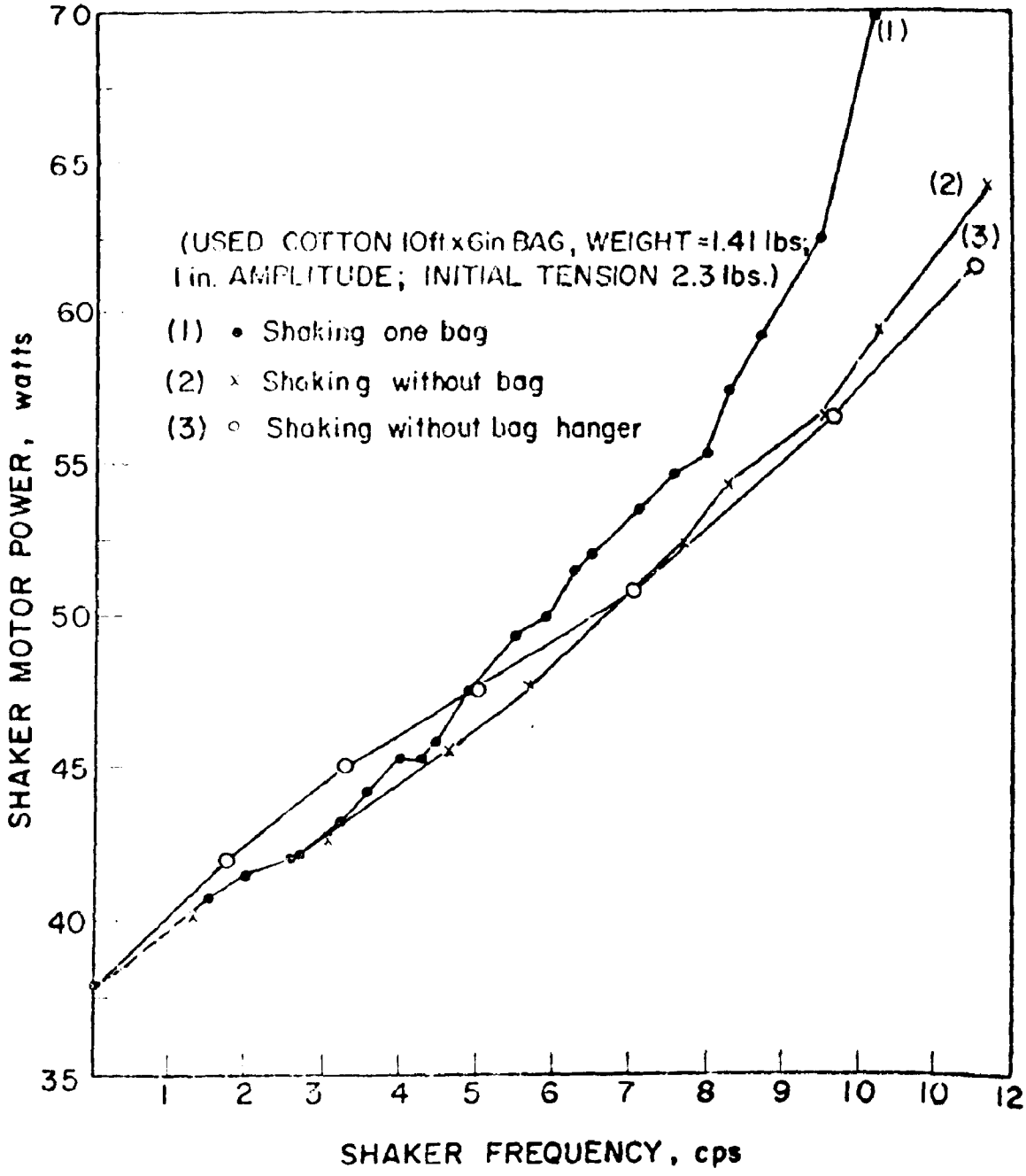

Figure 20. Measured power inputs to shaker motor

During laboratory tests, the power requirements were so low that accurate current/voltage measurements were difficult, particularly so because of the special, solid-state switching circuit required to vary shaking frequency. It was decided, therefore, that a better indication of bag power consumption would be the measurement of the force/velocity relationship at the juncture of the bag and the shaker arm. A concurrent oscilloscope display of the signal tracings denoting lateral force and the position of the shaker arm, respectively, enabled determination of the phase angle between the lateral (horizontal) force and the horizontal component of the arm velocity. The latter quantity was determined readily by the classical wave equations and the shaking amplitude and frequency.

Figure 21 summarizes typical results for tension, lateral force and computed power levels based on tests with a 10 ft. x 6 in. cotton sateen bag. Both tensile and lateral forces are seen to increase with shaking frequency and to show peak values at resonance points. The phase angle between the lateral force and the horizontal component of the shaker arm velocity decreases from 90° at very low, < 1 cps, frequencies to approximately 0° at 8 cps or greater. Shaker power consumption for a single bag increases approximately as the 1.5 power of the shaking frequency because of the decreasing phase angle. Although calculated power consumption is slightly higher at the lower frequencies, the differences are not significant at those frequency levels where the bag cleaning appears the most effective.

Since all shaken bags ordinarily assume the same phase relationship between the instantaneous lateral force and the suspension point velocity, the key variable to define is the lateral force. Figure 22 and Appendix I show that the instantaneous maximum lateral force is roughly proportional to the average tension when plotted against frequency. In Appendix I, the ratio of maximum lateral force to average tension was postulated to be as follows:

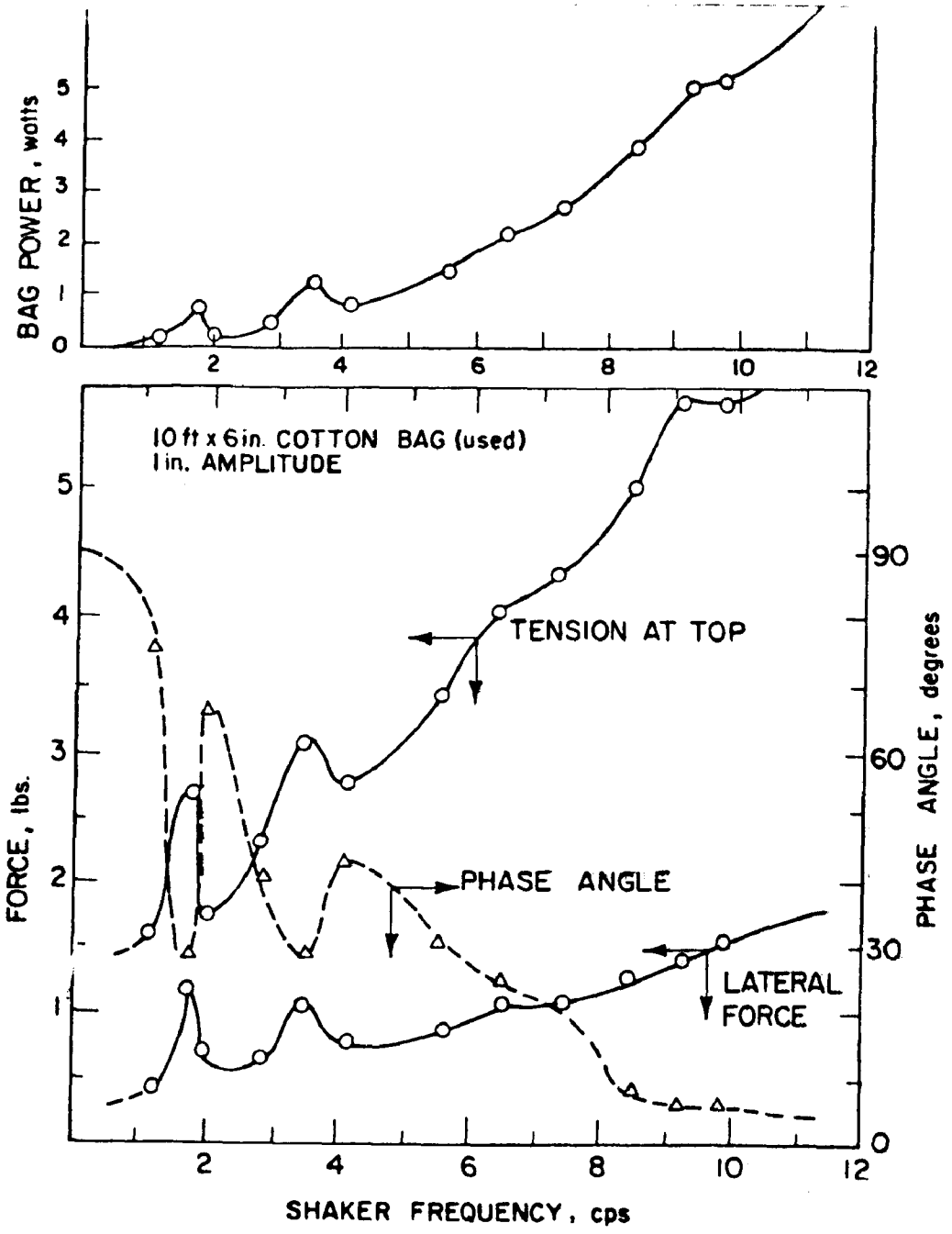

Figure 21. Power consumption, phase angle and frequency relationships for a 10 ft. x 6 in. cotton sateen bag (1 in. amplitude)

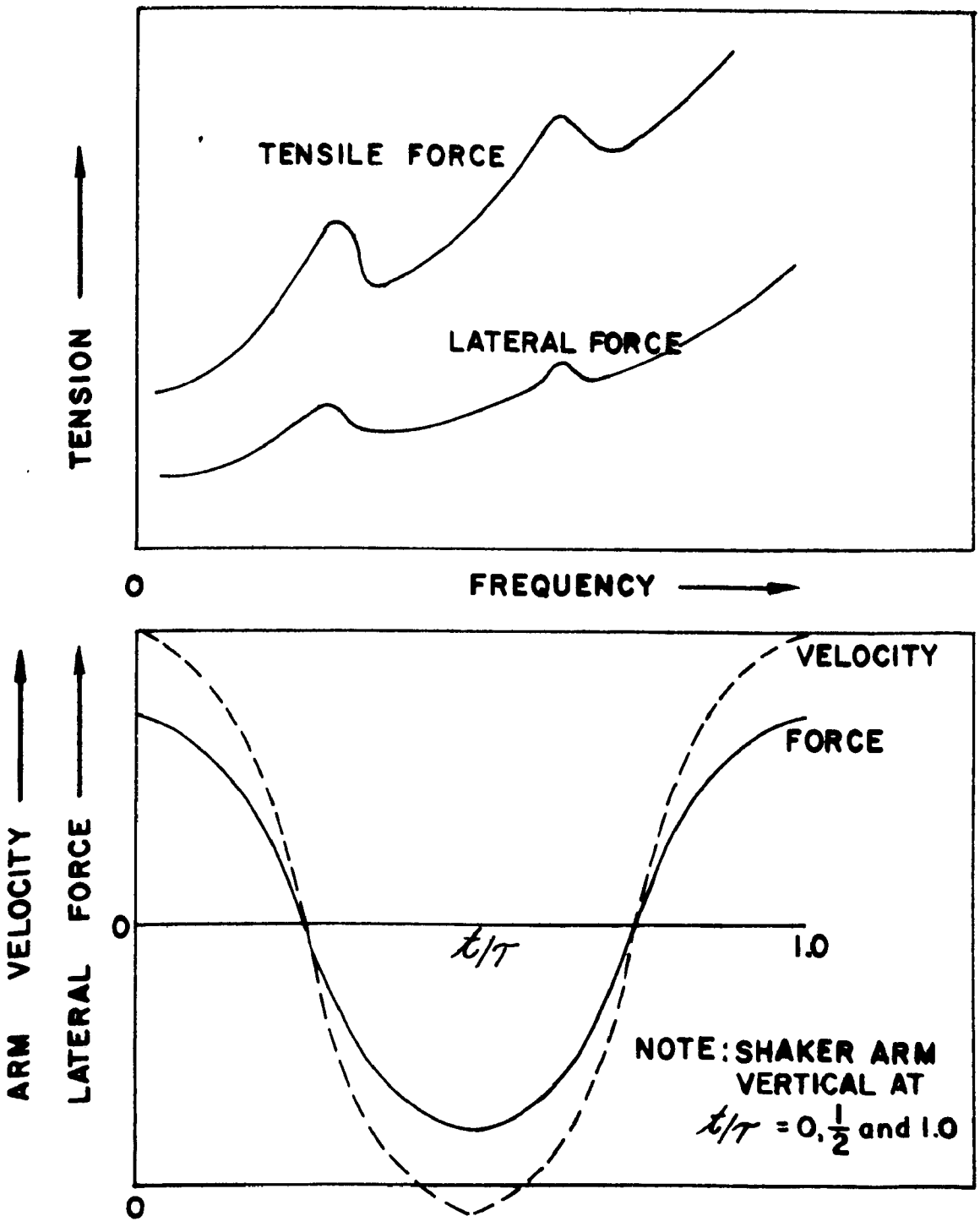

Figure 22. Force and velocity versus shaking frequency and period

$$\frac{F_{max}}{T_{avg}} = \frac{A}{R_A}\left(1 + \frac{MA^2}{4R_A T_m}\right) \approx \frac{A}{R_A} \qquad (2.20)$$

The actual ratios determined for a variety of bags, Appendix I, were about 1.5 times greater than the theoretical ratio, Equation (2.20). Noting that T_{avg} in Equation (2.20) refers to the shaking tension at the midpoint of the bag, T_m, Equation (2.12) may be revised to read

$$\overline{P} \approx \left(1.5\,\frac{A\,T_m}{R_A}\right)(2\pi fA)\left(\frac{\cos\,\theta}{2}\right) \qquad (2.21)$$

The second right hand term in Equation (2.21) expresses maximum arm velocity as a function of the shaking conditions. As indicated previously, T_m can be estimated from the known physical properties of a bag and the operating parameters for the shaking system.

Dust Removal

Dust removal was investigated over a broad range of fabric loadings and cleaning methods by several controlled experiments. Generally, the range of cleaning parameters studied was much broader than that expected in most field applications. To facilitate comparisons, inlet dust concentrations and fabric dust holdings were held as near constant as possible at typical field levels. Except for limited tests at a cloth velocity of 6 ft./min., most filtration was performed at 3 ft./min. and inlet concentrations were 5 grains/ft.^{3}. As the result of elutriation losses in the dust hopper, dust concentrations arriving at the fabric surfaces were reduced by 30 percent. At the same time the mass median diameter (MMD) and the geometric standard deviation (σ_g) for the inlet fly ash particles were reduced from 5.0 μm to 2.4 μm and 2.4 to 1.8, respectively.

Prior to starting a filtration cycle, the static tension (no shaking, no airflow) as measured at the top of the bag was adjusted to some

preselected level. During the succeeding filtering intervals, the tension values at the same location and the pressure differential across the bag were monitored periodically. Dynamic tension levels, which always exceeded the initial static values, increased with dust accumulation.

Stopping the airflow at the end of the filtration cycle dislodged but a small amount of dust, < 60 grains, as the result of bag deflation. The gradual flexure induced in the fabric may have promoted some surface loosening that enhanced dust release during subsequent shaking. About one minute after cessation of air flow, the shaking operation was initiated.

The procedure used to establish the relationship between dust removal and the number of shakes (the product of frequency and shaking time) was to shake the loaded filter intermittently for several brief shaking periods. The amount of dust dislodged and collected in a special tray inserted beneath the bag was measured after each shaking interval. Since the dust release rate decayed roughly exponentially, the length of successive cleaning intervals was increased such that about 20 seconds of continuous shaking were used for the final shake period. The same time increments were used for those tests designed to establish the relative cleaning effectiveness of different cleaning regimes. Although variations in shaking time increments affected intermediate dust releases, the total amount of dust removed by either continuous or interrupted shaking, was essentially constant, depending mainly on the total number of shakes and the specific shaking conditions. The total number of shakes was normally about 360, with some deliberate variation.

The dust release per increment of shaking was also determined by independent weighings of the bag before and after shaking by using the tension measuring load cell as a simple weighing scale. As a supplementary measurement, the total amount of dust collected in the

hopper (fallout plus bag shakedown) was compared to that delivered by the dust generating system. The latter technique was applicable only for long term, steady state operations.

The dynamic tension (top of bag) was recorded during each successive step of the incremental shaking process. During certain special tests, the lateral forces exerted at the top of the bag were also measured.

Filter bags used for the evaluation of selected cleaning regimes were alternately loaded and cleaned on a cyclical basis until no discernible changes could be detected in the pressure loss (or drag) versus time or cloth loading relationship. During the course of these measurements, no significant behavior differences were observed for bags operated anywhere between 2 and 24 hours. Therefore, a reasonably constant base line was established for comparing various shaking systems. It is emphasized, however, that under long term service conditions, a gradual increase in residual drag often takes place at a rate determined by the combined properties of the specific dust/fabric system and the working environment.

Since the amount of dust removed was variable from test to test, the residual drag and residual cloth holdings also differed from test to test. Therefore, in order to establish a standard rating technique, all filters were given an extra cleaning (called supercleaning in this study) to reduce all fabric residual loading and drag values to the same starting level. The special shaking regime for the supercleaning process consisted of a continuous 20 second shaking period at about 11 cps and a 1-inch shaker arm amplitude. This resulted in a residual holding of approximately 0.9 lb./bag (430 grains/ft.^{2}) at the start of the experimental filtration cycles. The weight gain per 30 minute filtration cycle (0.7 lb. or 300 grains/ft.^{2}) represented the difference between the dust entering the baghouse hopper and that settling immediately to the dust bin. The total dust accumulation on each bag at the end of the loading cycle was approximately 1.6 pounds.

A typical experimental data sheet is shown in Table 8. Detailed information for all measurements in this series and related technical nomenclature is presented in Appendix H. The terms "taut" and "loose" refer respectively to the top tension in pounds when the bag is attached for filtration, and to the total bag weight when suspended free for determination of dust loading. Most tests were conducted with the bag tension adjusted to a near "slack" condition; i.e., with the top tension ranging from about the weight of the free hanging bag to 1.0 pound in excess. These tension levels conform to those cited for related experiments performed by EPA personnel in past studies.[1]

Dust Removal versus Number of Shakes - The dust removal curves of Figure 23 indicate that the dust is dislodged in decreasingly smaller increments as the shaking process continues. The unloading process can be approximated by an exponential decay. All curves indicate that a practical upper limit in dust removal is approached, regardless of shaking frequency, after 200 to 250 individual shakes. The leveling off point is reached with fewer shakes at the higher shaking frequencies. It appears that extending the shaking beyond 200 to 250 shakes represents a needless power expenditure, a reduction in gas handling capacity, and in the long term a possible reduction in service life due to extra shaking motion.

It was noted that the rate of dust removal during the first phase of the shaking operation was significantly less for the lower shaking frequencies. This suggested that with less applied shaking energy, the initial flexing motion served mainly to diminish the bonding forces prior to the actual dust dislodgement by subsequent shaking. Generally, the form of the removal curves at low frequencies indicates that more shaking is needed to reach a limiting level of dust removal. From a practical viewpoint, increased frequency and/or amplitude appear to provide the better approach to cleaning.

Table 8. SAMPLE TEST DATA TABULATION

DUST REMOVAL TEST

Date: 4 May 71

Test No. 4

LOADING DATA:	Bag No. 4	Bag type: 10'x6" cotton, Well Used	
Inlet conc.: 5 gr/ft^3	CFM: 43.8	% RH	
Initial tension (lbs.) Taut: 2.54	Loose: 2.03	Re-taut: ____	

Time(min)	Δp(in)	Filtering Tension (lbs.)
0	1.40	8.12
1	1.58	8.12
10	2.28	8.12
21	3.08	9.33
30	3.65	9.50

Notes:

CLEANING DATA: Amplitude: ± 1 inches Frequency: 10 cps

Cum. seconds shaken	cps (increm't ave.)	Cum. No. shakes	Shake tension range	Dust off (grams)	Cum. dust off	Cum. % dust off	Result Δp (in.)	Resulting tension				Total dust grams
								taut	loose	net	retaut	
0		0		0	0	0	3.65	3.05	2.73	.32		732
5	10.	50	7.98	233	233	31.8		2.50	2.19	.31		
10	10.	100	8.12	107	340	46.5		2.62	2.14	.48		
15	11.5	150	8.30	30	370	50.5		2.56	2.06	.50		
25	10.0	250	8.5-8.6	16	386	52.7		2.35	2.03	.32		
45	10.1	452	8.6-8.8	11	397	54.3		2.30	1.98	.32		755
SUPERCLEANING:												
20	11.5	2.30	9.1-9.3				1.20	2.22	1.90	.32		

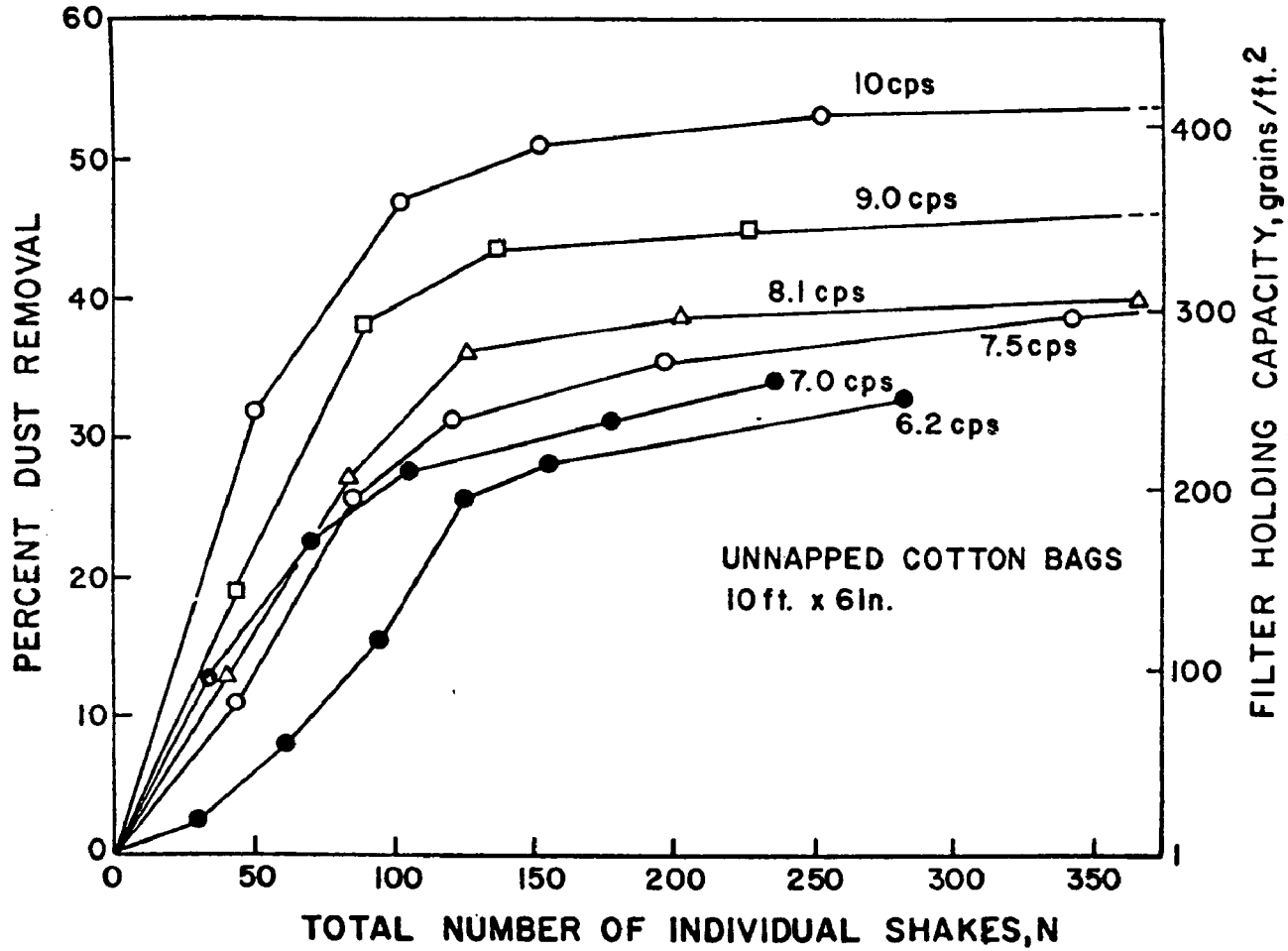

Figure 23. Percent fly ash removal versus number of shakes and shaking frequency at 1-inch amplitude

Since the total cloth loading for the tests described in Figure 23 was essentially constant at 740 grains/ft.^{2}, the actual weight of dust removed is directly proportional to the cumulative percent removed. This weight is a measure of the fabric filtration or dust capacity per filtration cycle. This parameter shows how much dust can be collected with a specified filtration and cleaning system. If the maximum cloth loading is held constant, any cleaning process that reduces the residual dust holding such as increased frequency, shaking amplitude and, up to a point, the number of shakes will also increase the filtration capacity.

Experimental data shown in Figure 23 are in qualitative agreement with earlier tests reported by Walsh and Spaite,[1] Figure 24. Although fewer shakes were required to achieve optimum cleaning, 60 to 80 versus 100 to 200 in the present tests, filtration capacity and shaking frequency followed the expected relationships. The higher capacities indicated in Figure 24 are attributed to somewhat coarser fly ash size properties that provide a more permeable dust deposit and to a slightly different shaking motion. Because certain key measurement defining static and dynamic tension conditions were not made, no further attempt is made here to compare the data of Figures 23 and 24.

Dust Removal versus Shaking Frequency - Examination of Figure 23 shows that for a fixed number of shakes at a constant driving amplitude, the amount of dust removed is an increasing function of frequency. This result, which confirms earlier tests,[1] is consistent with the basic theory relating the dust removal forces to the fabric's acceleration.

During successive shaking intervals, it was observed that the bag amplitude and axial tension increased after partial dust removal had taken place. This behavior is explained by the bag motion studies described earlier in the BACKGROUND AND THEORY section (pages 13 to 36). According to theory, near-resonant frequencies can exist only over limited ranges of dust holding. As the bag becomes lighter, it can pass into a resonant state causing the amplitude of motion and shaking

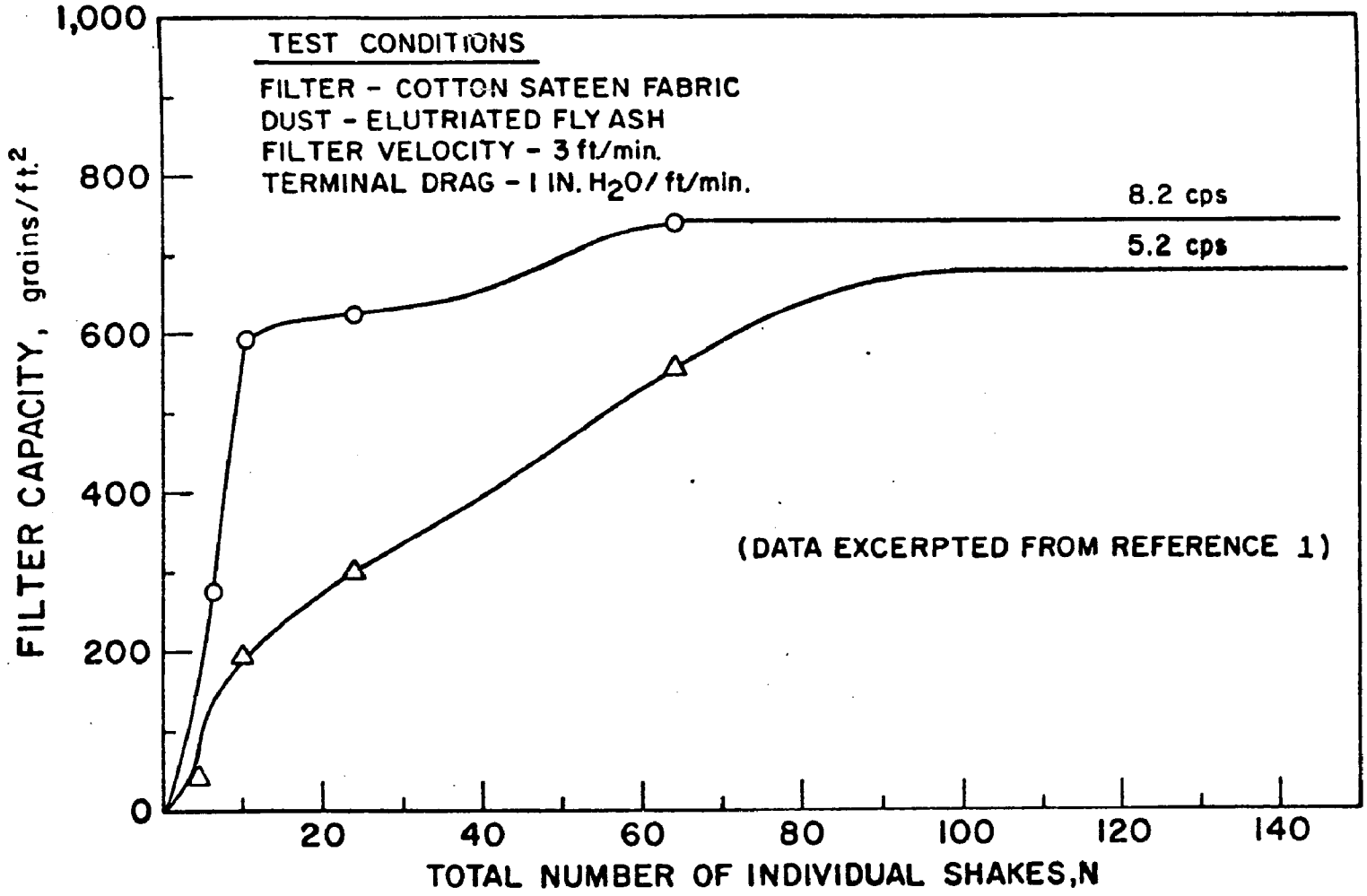

Figure 24. Effect of shaking frequency on filter capacity for 1-inch shaking amplitude

tension to increase. In addition, removal of dust probably diminishes the damping characteristics of the bag, thus promoting greater amplitudes of motion. A point-by-point computation of the varying resonant frequencies during dust removal indicated that during a typical cleaning cycle, a bag is likely to achieve a resonant state for at least one frequency.

One might infer that more vigorous cleaning might be accomplished by continually adjusting or "tuning" the applied frequency to compensate for dust loss. Results of such an attempt are shown in Figure 25 where in the upper curve frequencies were varied to produce a maximum tension. In a separate test, the frequency was shifted to minimize the tension as shown in the lower curve. Since several different maxima and minima might have been selected over the complete range of shaking frequencies, maximum and minimum tension values were sought which were as close as possible to 9 cps. The results suggest that 10 percent greater dust removal might be obtainable by holding to a resonant condition.

During prior motion studies on clean bags, the bag amplitude, when computed over a range of frequencies, was found to increase only 10 percent or so above the average level at resonant frequencies. Thus it is concluded that while resonance does enhance dust removal, the improvement is a very modest one. In view of the postulated complexity of the instruments and controls necessary to maintain resonance, the "tuning" approach does not appear justified at this time. On the other hand, it does appear advisable to estimate and operate at the resonant frequency of the combined bag and dust weight during the latter part of its cleaning cycle.

Dust Removal versus Shaking Amplitude - In a separate series of experiments, the shaker arm amplitude was varied from 0.5 to 1.5 inches during sequential tests, while keeping the shaking frequency constant at 8 cps. Complete loading and cleaning cycles were carried out at

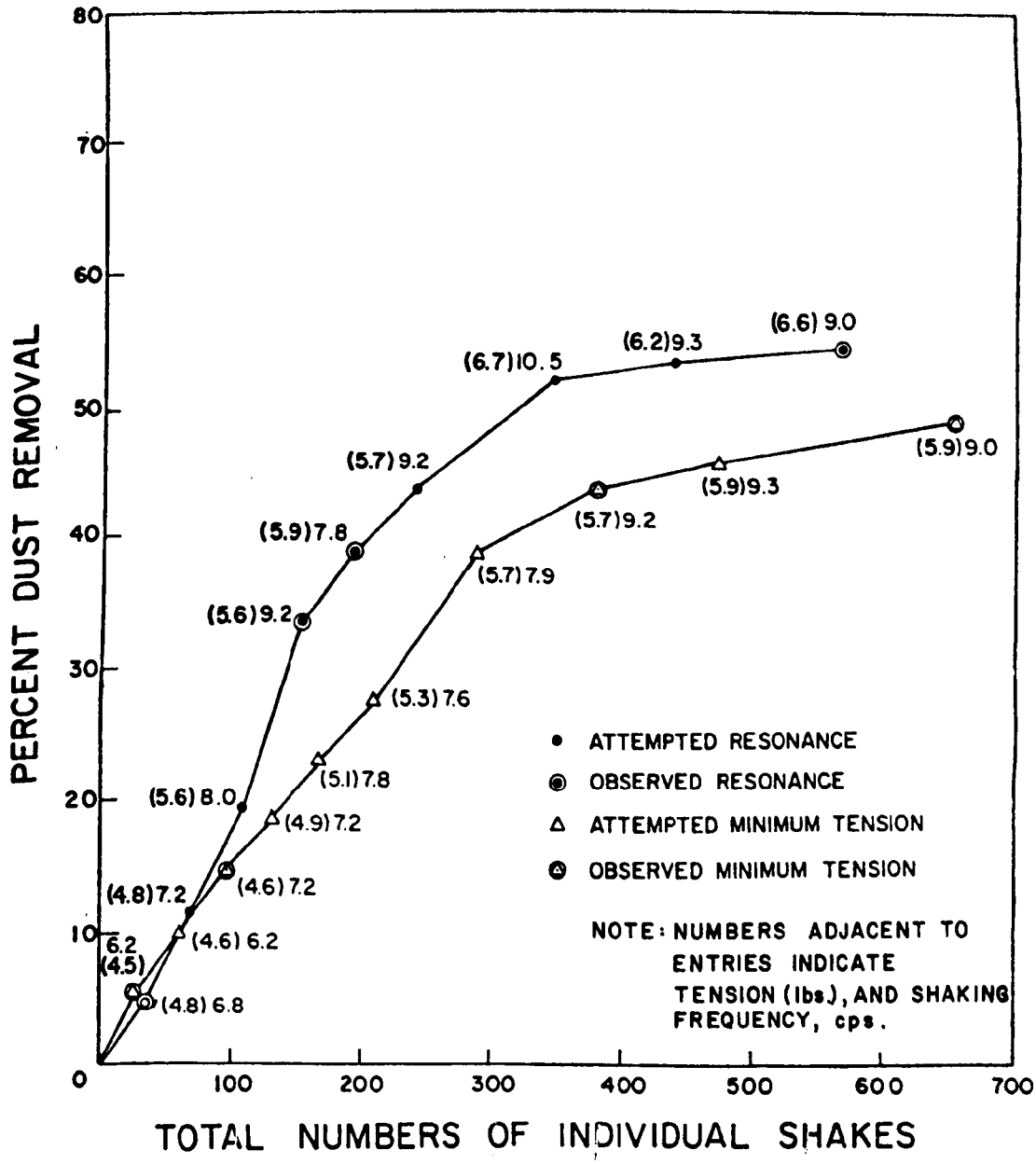

Figure 25. Effect of resonance on dust removal

selected amplitudes as shown in Figure 26. It appears that amplitudes less than 0.75 to 0.50-inch were ineffective, at least over the first few hundred shakes. This is because the wave motion is rapidly damped at small amplitudes such that a large part of the bag sees no motion at all. From 0.50 to 1-inch, amplitude increases were very effective in promoting dust removal. The waves reached the bottom of the bag and underwent reflection so that generally uniform bag motion was obtained.

Although further removal was attained at higher shaking amplitudes, the actual increases were relatively small in comparison to the total amount of dust removal.

The relationship between dust removal and shaker amplitude is indicated in Figure 27 by several constant frequency curves. The measurements suggest that below certain threshold amplitudes, ~ 0.5 inches, poor dust removal is attained regardless of shaking frequency. Over a limited range of amplitude increase, the dust removal is also increased significantly with the greatest improvement shown at the higher shaking frequencies.

Although shaking amplitudes greater than 2 inches were not studied, the shapes of the curves of Figure 27, indicate that there are practical upper limits beyond which further dust removal is small.

A related graphing of dust removal characteristics is given in Figure 28 for shaking frequency variations at several amplitudes. Again similar trends are suggested; i.e., at very low frequency energy transmission throughout the entire bag is ineffective leading to poor dust removal.

There is no apparent limit to the improvement over the frequency range tested, although above 50 percent removal, proportionately less dust is removed. Frequency is, of course, limited in practice by other considerations such as bag tension and equipment vibration.

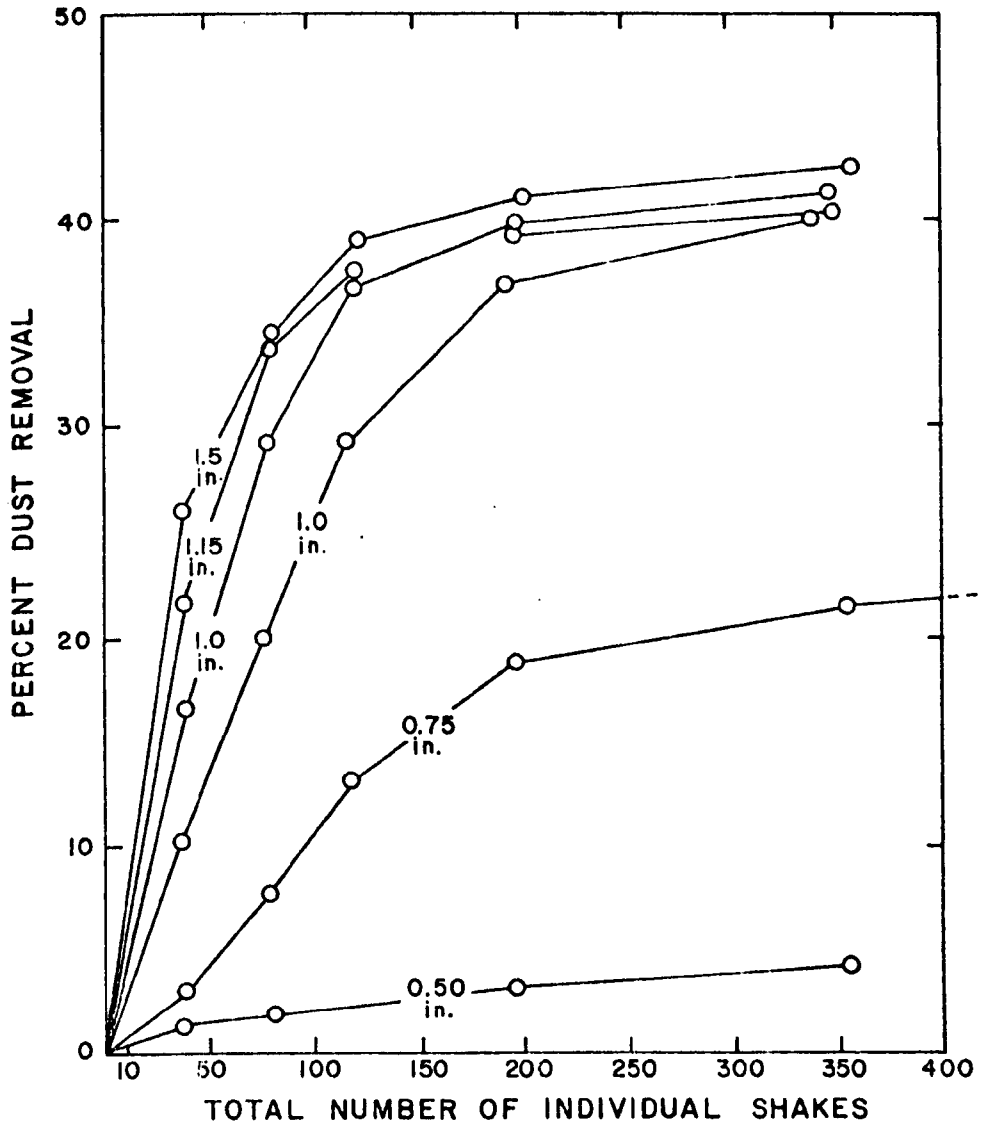

Figure 26. Effect of number of shakes, 8 cps, and shaking amplitude on dust removal from 10 ft. by 6 in. cotton bags

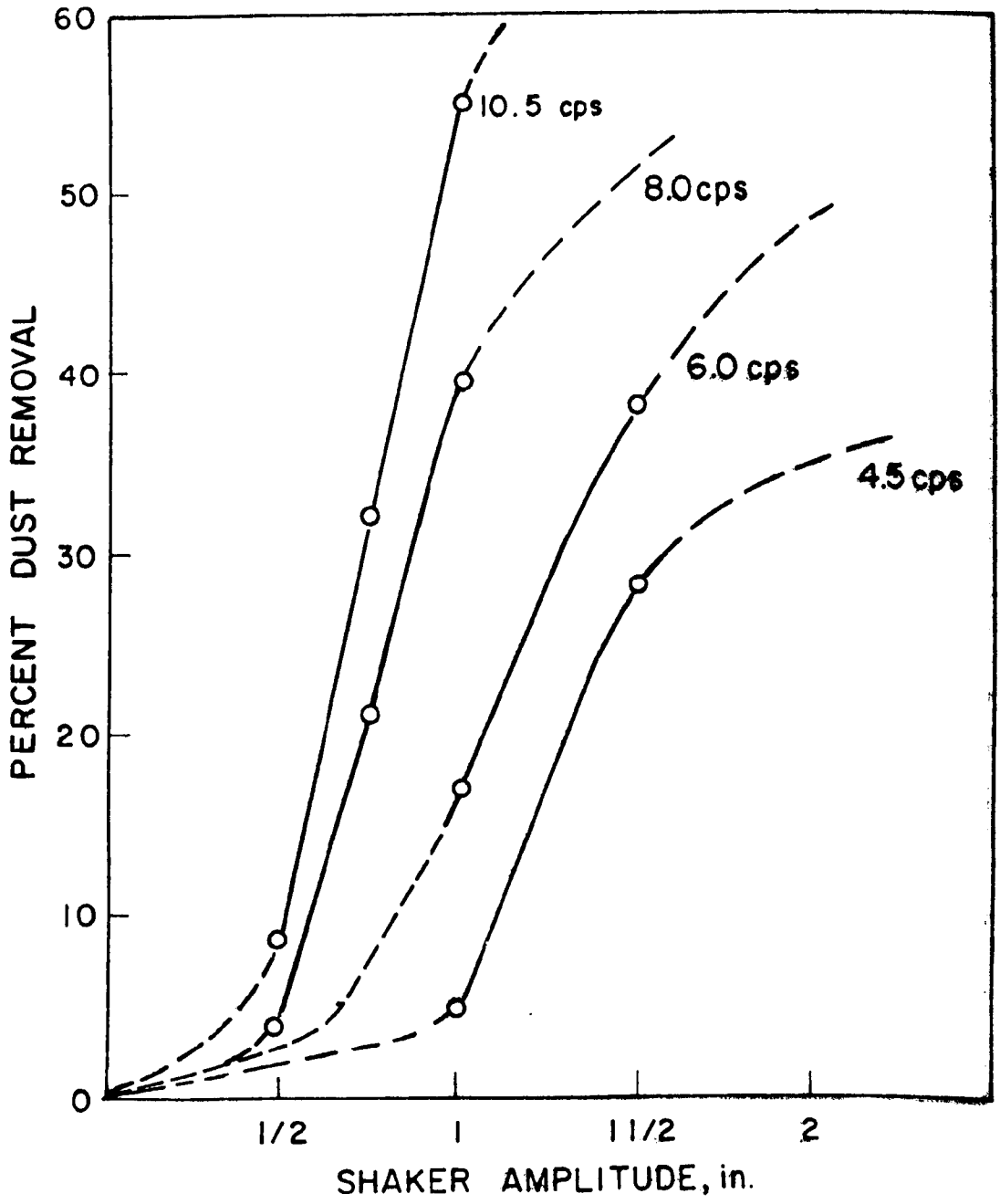

Figure 27. Effect of shaking amplitude and shaking frequency, 350 shakes, on dust removal from 10 ft. by 6 in. unnapped cotton bags

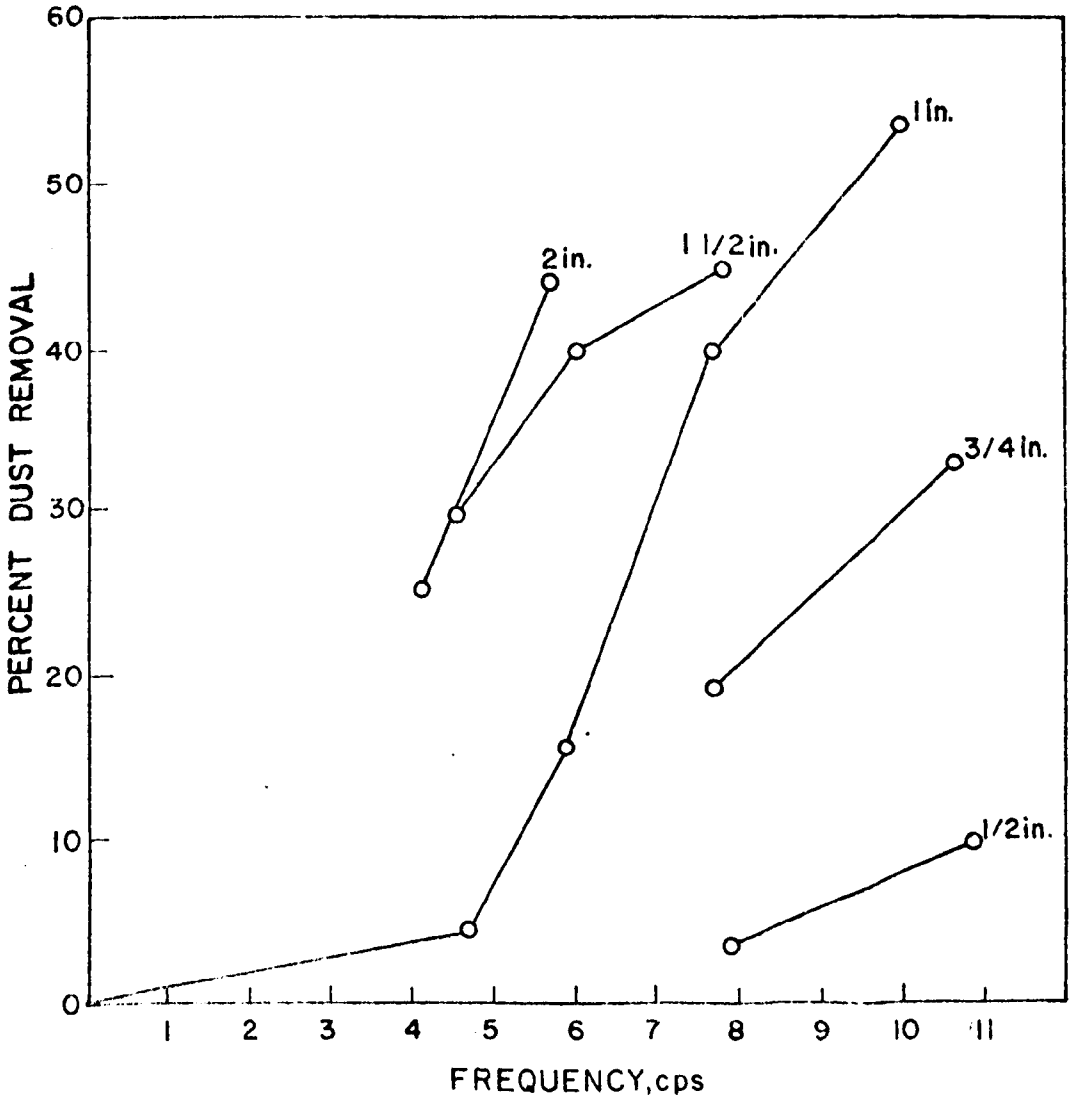

Figure 28. Effect of shaking frequency and shaking amplitude, 350 shakes, on dust removal from 10 ft. by 6 in. unnapped cotton bags

The effects of amplitude and frequency are combined in the concept of fabric acceleration in the following section.

Dust Removal versus Acceleration - Previous EPA investigators[1] have indicated that the dust holding capacity of fabric filters could be related to the maximum acceleration, a_m, of the shaker arm:

$$a_m = 4\pi^2 f^2 A \qquad (2.22)$$

In Equation (2.22), f is the shaking frequency and A the shaking amplitude. According to the EPA tests performed with sateen weave cotton bags and a fly ash aerosol, there existed a strong correlation between filtration capacity and acceleration for accelerations less than 46.2 ft./sec.^{2} (1.44 g's). Above this critical acceleration level, no significant improvements in filtration capacity were obtained. As defined in the present discussions, filtration capacity describes the quantity of dust that can be placed upon a filter during its normal filtration cycle (grains/ft.^{2} or grams/m^2). Under steady state operations, it must also depict the quantity of dust removed by the specific cleaning method. In conjunction with the reported drag values (effective and terminal) the filtration capacity enables one to determine the collector size and power requirements for a given dust/fabric system.

Table 9. EXPERIMENTAL SHAKING CONDITIONS

Shaker arm frequency (cps)	Shaker arm amplitude (maximum) (in.)
4.7	1.0, 1.5, 2.0
6.0	1.C, 1.5, 2.0
8.0	0.5, 0.75, 1.0, 1.15, 1.5
11.0	0.5, 0.75

Note: Inlet dust concentration, 3.5 grains/ft.^{3}
Filtration velocity, 3 ft./min.
Filtering interval, 30 min.
Number of shakes, 350.

Several experiments were performed during the present study to provide a broader range of amplitude-frequency combinations with which to test the dust removal-acceleration relationship. Table 9 indicates the various shaking systems investigated.

The results of dust removal tests under the shaking conditions described in Table 10 are presented graphically in Figure 29. Here the ordinate refers to the average bag amplitude and the abscissa depicts the bag shaking frequency which is the same as the driving frequency. The parallel broken lines, which represent lines of constant input acceleration (1, 3, and 10 g's), are drawn with a slope of -2 on the log-log plots.

The bag amplitude-frequency coordinate for each cleaning condition cited in Table 10 has been identified by a number showing the related percent dust removal. Dashed lines representing approximately lines of constant dust removal appear to have a slope of -2. The encircled number flagging each dashed line is the best estimate of dust removal efficiency along that line. Despite the broad point scatter, the experimental data suggest that the amount of dust removed is a function of the product $(\bar{Y}f^2)$ and hence the average bag acceleration, as shown in the following Equation:

$$R = \Phi\ (\bar{a}) = \Phi\ (4\pi^2 f^2 \bar{Y}) \qquad (2.23)$$

Figure 30 shows the results of similar measurements except that the shaking action was restricted to 40 shakes. Although the dust removal followed the same pattern shown in Figure 29, the absolute quantities removed were considerably lower in accordance with the reduced number of shakes.

The point scatter exhibited in Figures 29 and 30 was attributed to several effects; the neglect of individual differences in bag tensioning with respect to resonant frequencies, statistical variations due to

Table 10. DUST REMOVAL VERSUS AVERAGE BAG AMPLITUDE, MEASURED AND CALCULATED TEST PARAMETERS

Test number	Shaker amplitude (in.)	Shaker frequency (cps)	Bag[a] amplitude average (in.)	Bag[a] acceleration average (g's)	Tension		Dust removal (%)	Filter[c] capacity (gr./ft.^{2})	Residual[c] fabric loading (gr./ft.^{2})
					Shaking (lb.)	Static[b] (lb.)			
S1	1	9.0	0.72	5.96	7.9	3.1	44	326	373
S2	1	7.0	0.75	3.75	7.1	2.9	33	246	494
S3	1	10.0	0.73	7.45	8.3	2.5	54	414	324
S4	1	6.2	0.85	3.34	6.8	2.2	36	264	476
S5	1	8.1	0.77	5.16	7.4	2.7	42	312	428
S6	1	7.2	0.77	4.08	6.8	2.2	39	289	440
S7	1	7.8	0.73	4.55	7.1	1.9	42	314	426
S8	1	7.5	0.83	4.75	9.5	6.1	39	289	451
S9	1	7.7	0.69	4.18	7.5		41	304	436
S10	0.75	7.7	0.46	2.79	6.0	2.9	27	202	538
S11	1.15	8.0	0.76	4.97	8.1	2.5	47	350	390
S12	0.5	7.9	0.23	1.47	4.5		4.2	31	709
S13	1	7.5	0.75	4.31	7.2	2	40	296	445
S14	1.5	7.8	1.4	8.70	11.9	2.6	45	336	404
S15	1	5.9	0.74	2.63	6.4	2.5	24	179	561
S16	1.5	6.0	1.1	4.05	8.4	2.0	40	300	440
S17	2	5.7	2.2	7.30	14.3	1.9	47	348	392
S18	1	4.7	0.58	1.31	5.1	2.0	8.2	61	679
S19	1.5	4.5	1.8	3.72	10.4	2.0	31	233	507
S20	2	4.1	1.6	2.75	9.4	1.6	27	197	543
S21	0.5	10.9	0.18	2.18	3.9	1.6	11	83	657
S22	0.75	10.7	0.37	4.33	5.4	1.6	34	255	485

[a] Calculated values.

[b] At 0 cps, shaker arm vertical.

[c] After 350 shakes.

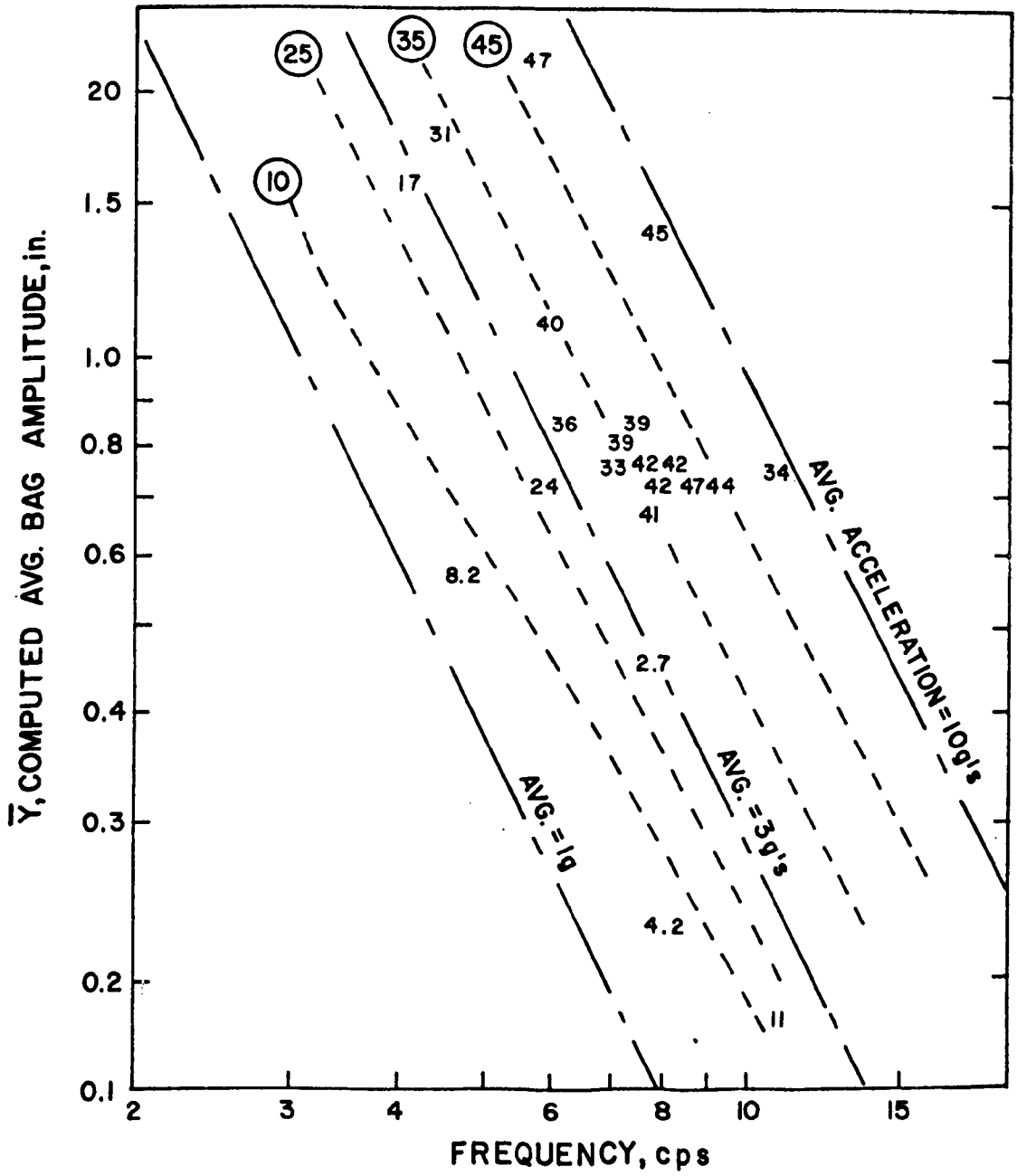

Figure 29. Dust removal versus bag acceleration for cotton bags, 350 shakes. Broken line indicates constant acceleration contours. Dashed line and circled number shows constant dust removal contour. Uncircled numbers show actual dust removal at Y-cps coordinates.

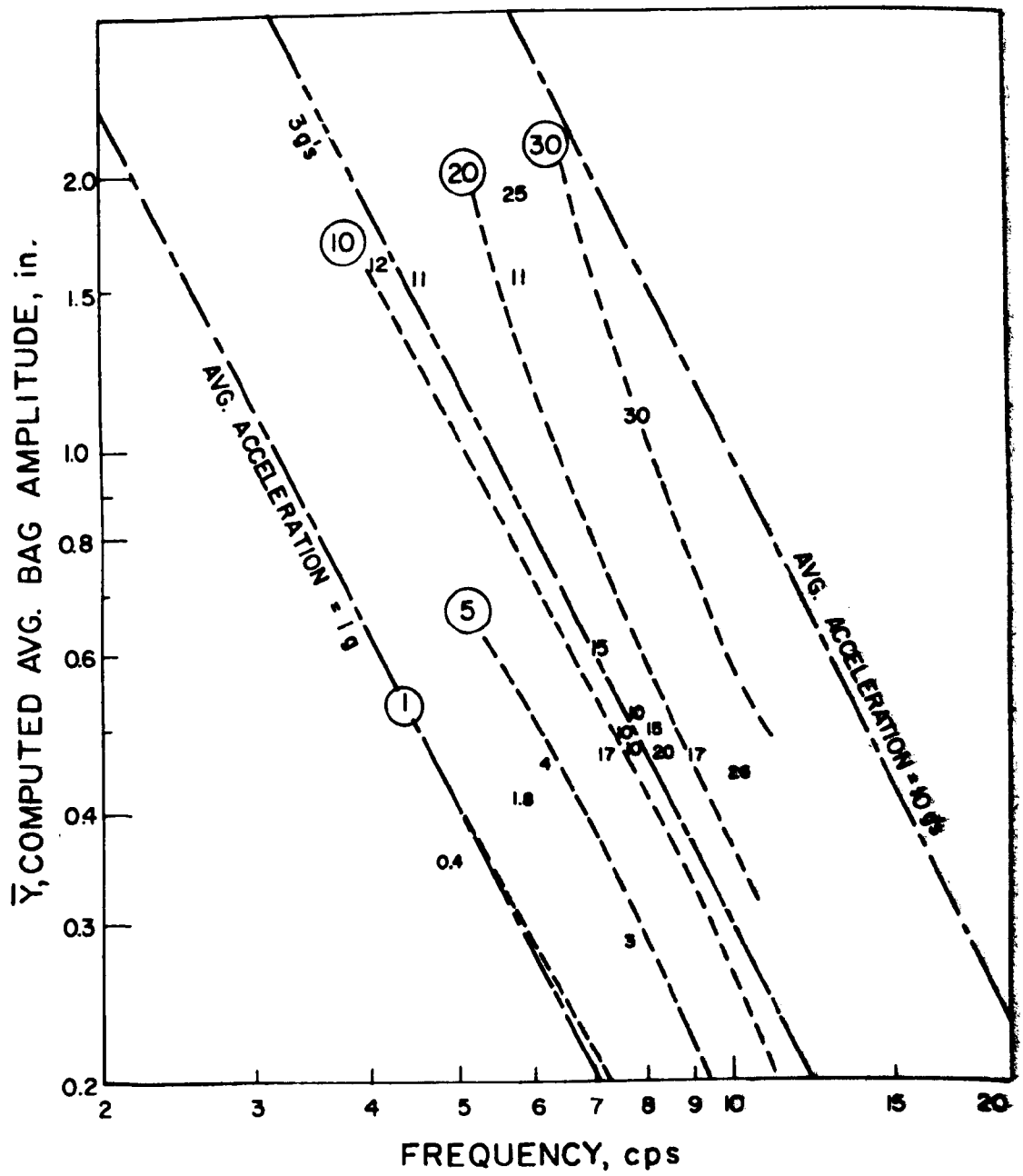

Figure 30. Dust removal versus bag acceleration for cotton bags, 40 shakes. Broken line indicates constant acceleration contour. Dashed line and circled numbers show constant dust removal contour. Uncircled numbers show actual dust removal at Ȳ-cps coordinates.

accuracy limitations in instrumental methods or control of operating parameters, and the basic assumption that the acceleration force, acting normally to the bag surface, was the predominant dust removal factor. It was also noted that the dust removal rate did not always follow an exponential decay pattern when the total number of shakes was small (< 75). This is shown by the inflection points on some of the curves of Figure 23 at the lower shaking frequencies. It was concluded that the initial shaking, particularly at the lower frequencies, was effective in loosening, but not necessarily dislodging, the dust deposit until at some critical threshold the bonding forces were exceeded. Practically speaking, the above variations are relatively unimportant since the net dust removal after 200 shakes undergoes little change. In addition, the lower frequencies at which the abnormal unloading effects were noted, would not ordinarily be selected for optimum cleaning. Although it has not been possible to distinguish between loosening and separation forces in the cleaning process, it is postulated that increased fabric stretching with increased shaker amplitude might enhance the interfacial shear between the fabric structure and the dust deposit.

Above certain critical acceleration levels, the present measurements and those of earlier investigators suggest that dust removal (and filtration capacity) increases only slightly. Therefore, the postulated linear relation between dust removal and acceleration should be expected to hold only over a limited range, roughly 3 to 10 g's.

In Figure 31, the relationship between average bag acceleration and filter capacity is given for all data shown in Table 10. These measurements indicate that the filter capacity for low acceleration systems varies (on an empirical basis) with the square of the average bag acceleration. Beyond the 4 g level, however, subsequent filtration capacities are much less dependent on acceleration, varying approximately as the square root of g. Over the central range of 2.5 to 6 g's the hypothesized direct relationship between filter capacity and

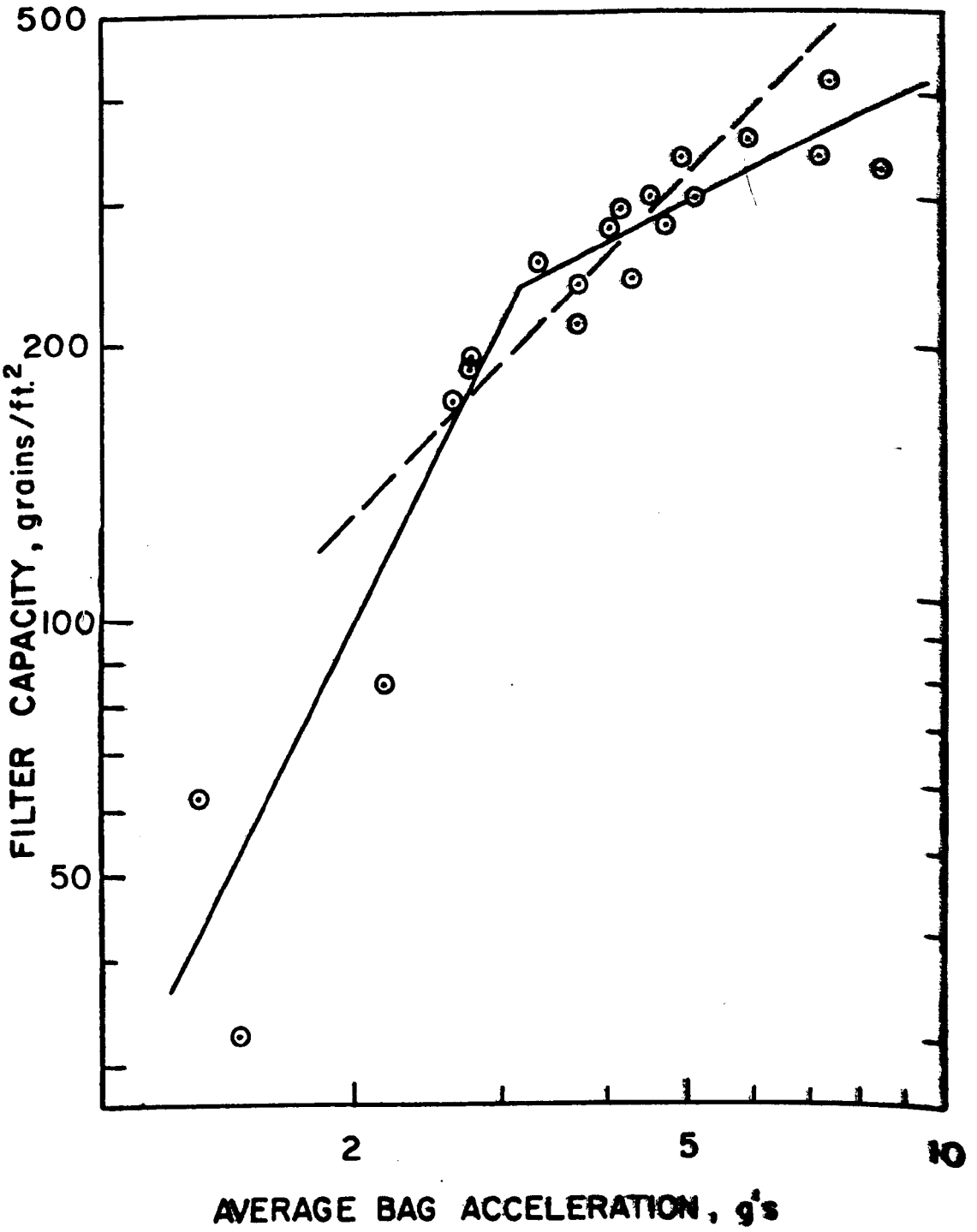

Figure 31. Filter capacity versus average bag acceleration for sateen weave cotton bags

acceleration appears to prevail as indicated by the dashed 45° line. The relationships suggested above are intended as rough approximations only of a process too complex for rigorous description at this time.

Dust Removal versus Initial Bag Tension - It was shown earlier that after the complete bag is set in motion, good cleaning will result provided that the proper combination of acceleration and number of shakes is used. It has also been shown that a minimum initial tension is necessary to establish good bag motion. Although the effects of bag tension on dust removal were not investigated separately, it appeared that a minimum initial bag tension was required to obtain good cleaning. This threshold level was considered to be equal to the combined tension at the shaker arm produced by the free hanging, dust-laden bag plus an added tensioning of 25 percent of the loaded bag weight. Further tensioning might hasten the development of bag motion as the shaking begins, but unless it were important to minimize the shaking period, the added tension would afford no advantages. In fact, fabric wear as well as dust penetration properties might be increased.

Dust Removal versus Cloth Loading - The effects of given cleaning systems (frequency, amplitude, and duration) on dust removal, described in the preceding sections, were determined with a constant terminal cloth loading, W_T, on the fabric, approximately 760 grains/ft.^{2}. Under these circumstances, the residual cloth holding, W_R, decreases and the holding capacity, $W_T - W_R$, increases as the energy applied during the cleaning cycle is increased. This is illustrated by the composite curve in Figure 32 that shows the differences in W_R values for selected cleaning regimes as well as the corresponding filter drag and resistance characteristics.

The data presented in Figure 33 show that the residual dust loading for any specified cleaning system is independent of the cloth loading on

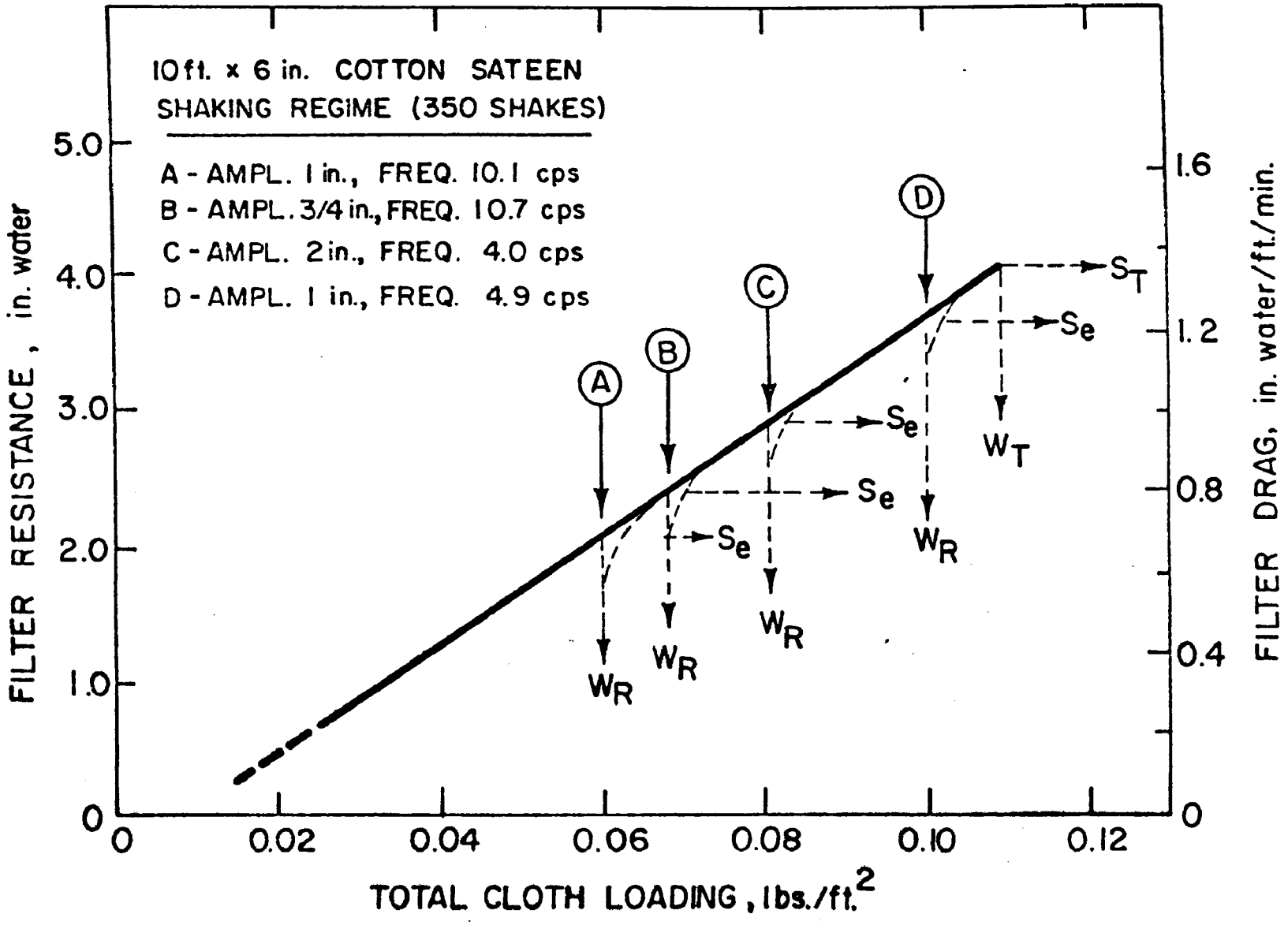

Figure 32. Cloth loading and filter drag characteristics for typical shaking regimes - composite curve

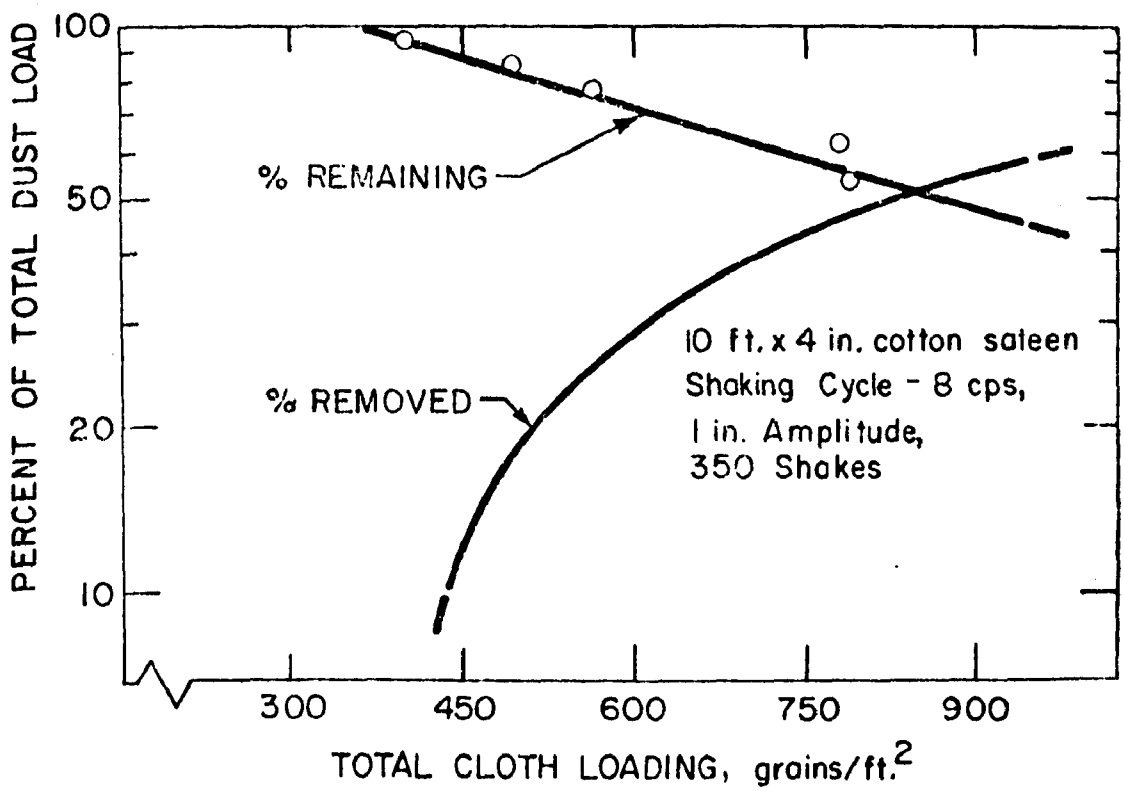

Figure 33. Dust removal versus cloth loading for fixed shaking regime

the filter at the start of cleaning. Both the fraction and absolute quantity of dust removed, however, increase with cloth loading, the latter the result of increased inlet dust concentration, filtration velocity, or filtration interval.

With respect to measurements on a 10 ft. by 4 in. cotton sateen bag (using an 8 cps, 1-inch amplitude, 350 shake cleaning system) no dust removal was observed for initial cloth loadings less than 330 grains/ft.^{2}. When cloth loading was allowed to increase to 800 grains/ft.^{2}, the same cleaning system caused approximately 60 percent (470 grains/ft.^{2}) of the total cloth holding to be dislodged. For all final cloth loadings, however, represented in Figure 33, the residual cloth loading was the same. On a fractional basis, the quantity of dust removed for a specified dust-fabric cleaning method is expressed by the ratio $(W_T - W_R)/W_R$.

The data provided in Figure 33 and in earlier figures, in which the percent of dust removed was used as an experimental performance parameter, is meaningful when a specific fabric has the same terminal dust loading. For field applications of laboratory findings, however, the effect of the mechanical shaking operation is best described by the relationship between residual fabric dust holding and the average acceleration imparted to the bag as shown in Figure 34. According to the data presented in this figure the residual dust loading, W_R, varies inversely with the square root of the average bag acceleration over the range 1.5 to 7.5 g's. These tests were based upon 360 individual shakes per bag. Examination of the effect of varying the number of shakes at different acceleration levels, Figure 35, indicates again that there is little to be gained by too extensive a shaking period. Beyond 100 shakes, the dependency between residual cloth holding, W_R, and number of shakes, N, is relatively weak; i.e., $W_R = \phi\ (N)^{-0.09}$. Although the linear curve fits do not apply for shaking levels less than 100, the practical consideration is that the dust removal is generally inadequate and unpredictable for N values less than 100.

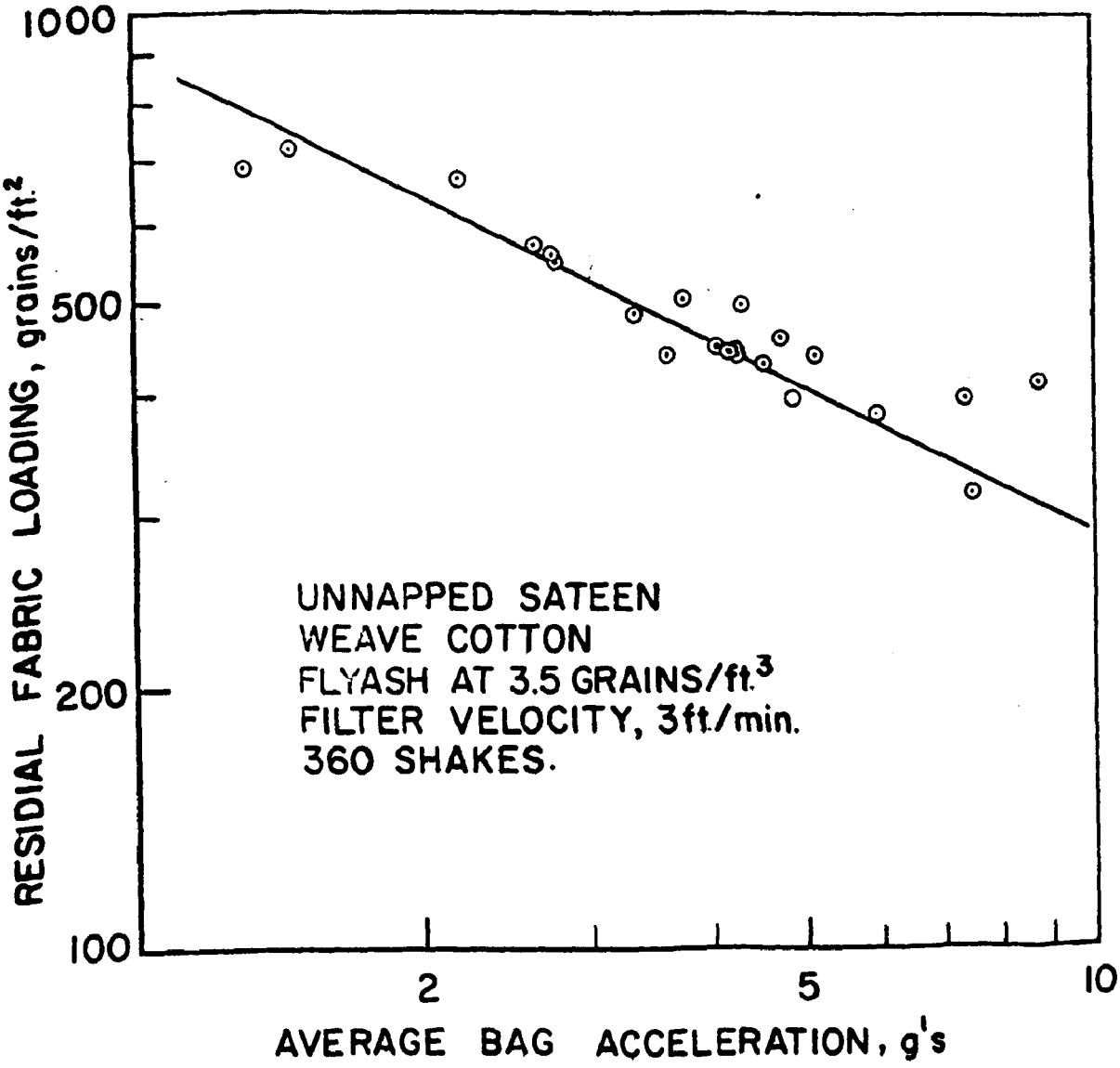

Figure 34. Residual fabric loading versus average bag acceleration

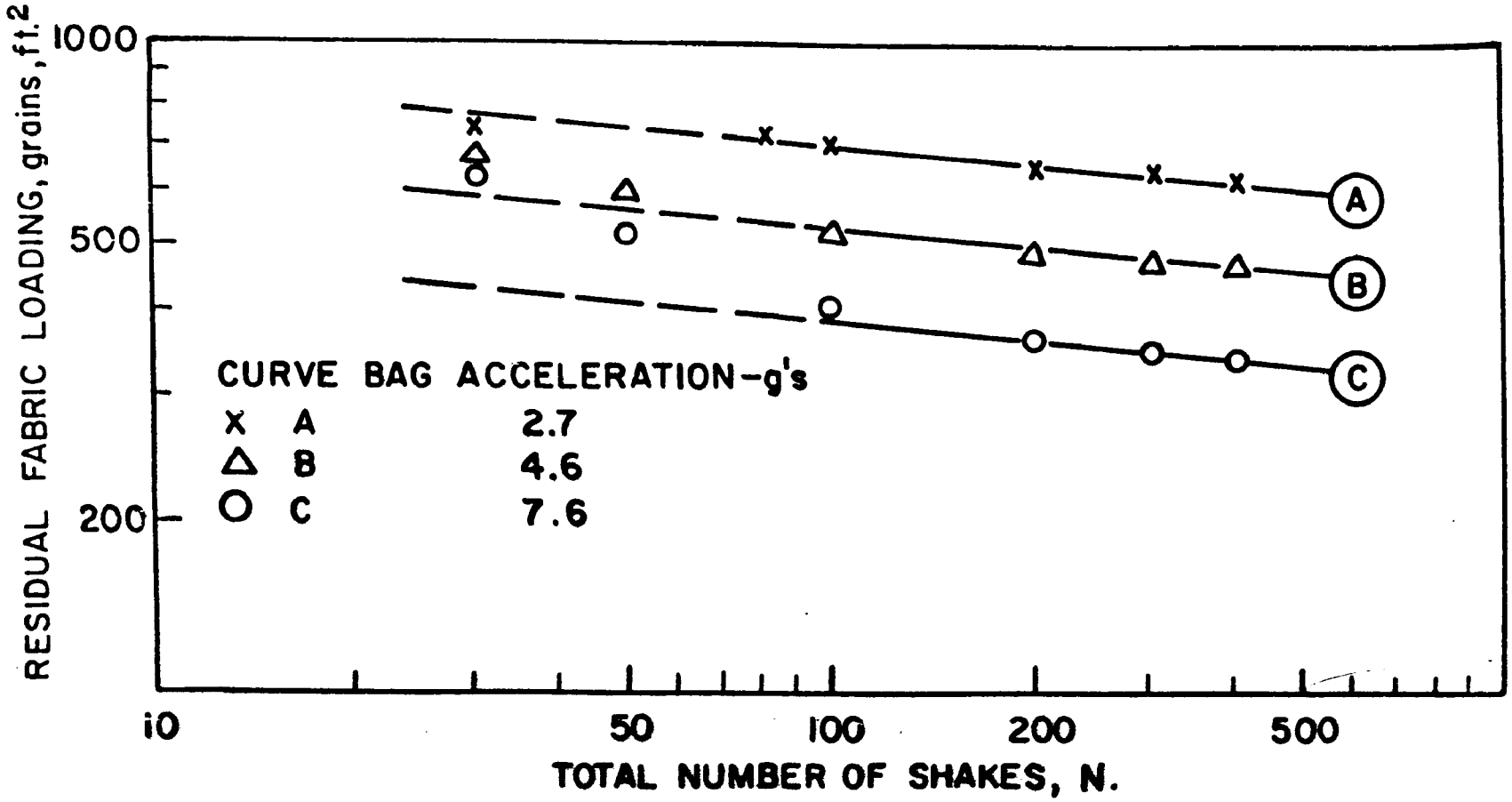

Figure 35. Residual fabric loading versus total number of shakes at three acceleration levels for unnapped sateen weave cotton

By combining the empirical relationships shown in Figures 34 and 35, the residual fabric loading can be expressed in the following manner as a function of both average bag acceleration, $\bar{a}$, and total number of shakes, N,

$$W_R = 1433\ (a)^{-0.5}\ (N)^{-0.09} \qquad (2.24)$$

Equation 2.24 applies specifically to the fly ash aerosol and the sateen weave cotton bags used in this study. The amount of dust that can be accommodated by the fabric; i.e. its filter capacity, is the difference between the selected terminal and residual fabric loadings. For a given cleaning system, the filter capacity is usually limited by the maximum allowable resistance across the fabric or the available fan capacity. As discussed previously, knowledge of the K value for the specific dust-fabric combination, in conjunction with the residual cloth loading and related resistance, permit ready estimation of either the terminal filter drag and the terminal fabric holding, Figure 32.

Dust Removal versus Fabric Type - Further tests were performed with the previously described fly ash aerosol to permit comparison of filtration behavior of different fabrics. Again, inlet loadings were approximately 3.5 grains/ft.^{3} and the filtration velocity 3 ft./min. The bag dimensions were also the same, 10 feet long by 6 inches diameter, as well as the mechanical shaking system, 8 cps at 1-in. amplitude for 360 individual shakes. Test results are shown in Figure 36 for two Dacron weaves, plain and crowfoot, and a napped sateen weave cotton.

The curve shapes follow closely those for the unnapped cottons shown in Figure 35. In fact, there does not appear to be any significant difference between the two cotton fabrics based upon the limited experimental data. After extended use as simulated by the accelerated life testing procedures, the residual dust holding capacity of all bags decreased after 2×10^7 shakes. The observation that outlet dust concentrations were generally higher after 2×10^7 shakes suggested that irreversible stretching in the media had enlarged the pores.

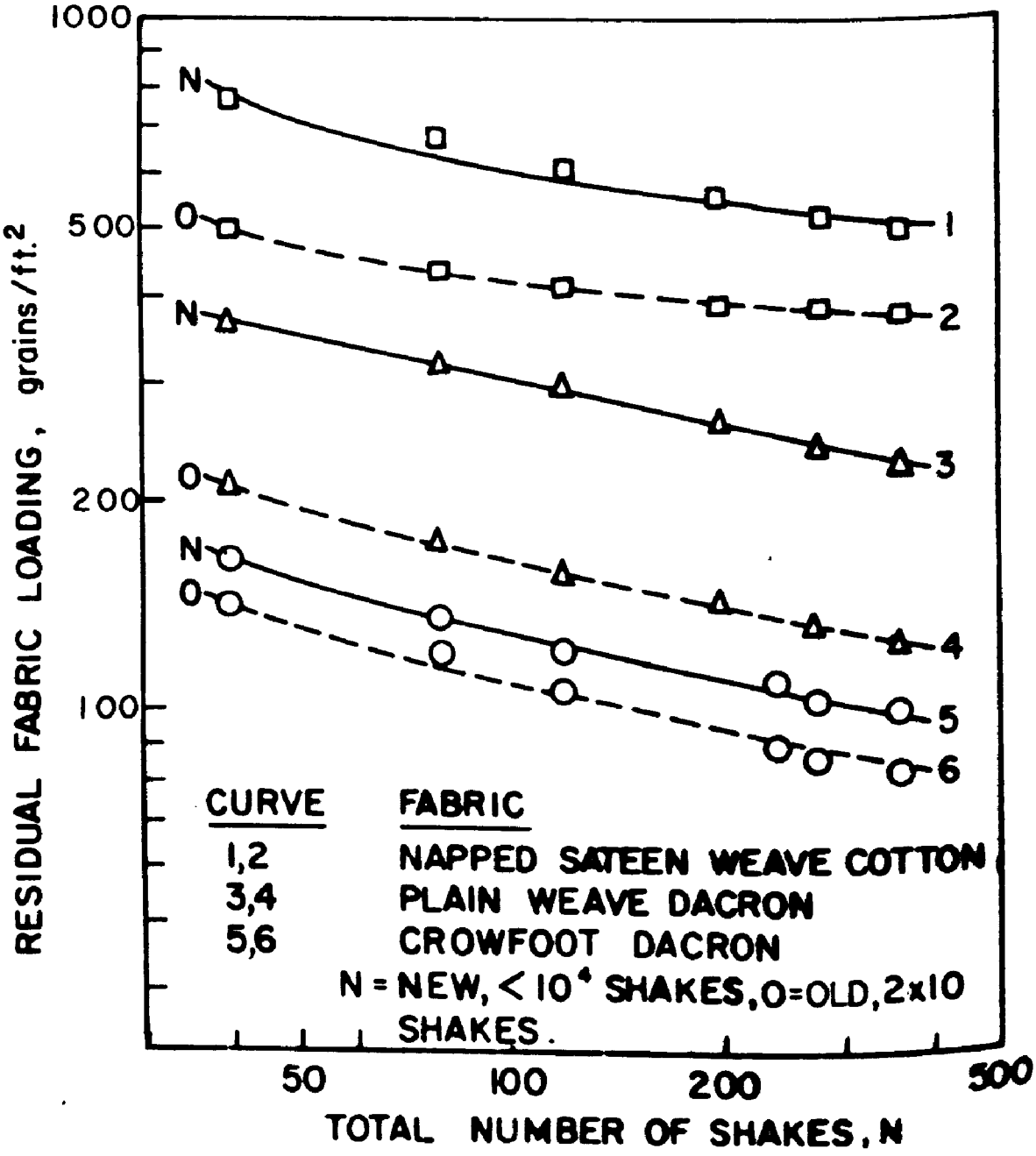

Figure 36. Residual fabric loadings for various fabrics with fly ash aerosol (8 cps, 1 in. amplitude shaking)

In contrast to the cotton fabrics, the steeper slopes of the curves for Dacron media, Figure 36, indicate that the dust release process is more gradual. Approximately 20 percent of the total dislodged dust was removed between the 100th and 360th shake of the Dacron bags in contrast to only 10 percent for the cotton fabrics over the same shaking interval.

Dust Removal versus Dust Type - Limited tests were performed to investigate the filtration characteristics of other dusts with the previously described cotton and Dacron fabrics. Measurements with a resuspended talc dust having approximately the same size parameters determined for the aerosolized fly ash (see Table 4) are shown in Figure 37. The residual fabric loadings varied approximately as the -0.2 power of the number of shakes. The approach to equilibrium cleaning for both cotton and Dacron media appeared to follow the same pattern in contrast to the distinctly different slopes shown in Figure 36 for fly ash filtration.

The difference in release characteristics for fly ash and talc may be associated with the relative strengths of adhesive and cohesive bonds. One possible explanation is that a higher adhesive force between dust and fibers may lead to a gradual spalling-off of dust rather than a scaling-off at the dust/fabric interface.

The relationship between filter drag and fabric loading given in Figure 38 shows that residual fabric loadings and residual (effective) drags were lower for talc dust than for fly ash. This comparison is also indicated in Table 11 along with the filter capacities for both talc and fly ash with cotton and Dacron fabrics. Filter capacities were based upon a filtration velocity of 3 ft./min. a 360 shake cleaning cycle at 8 cps and 1-in. amplitude, and a terminal drag, S_t, of 1-in. water/ft./min.

According to Figure 38, the K values for talc are generally in the range of 2.5 to 3 times greater than those for fly ash. The fact

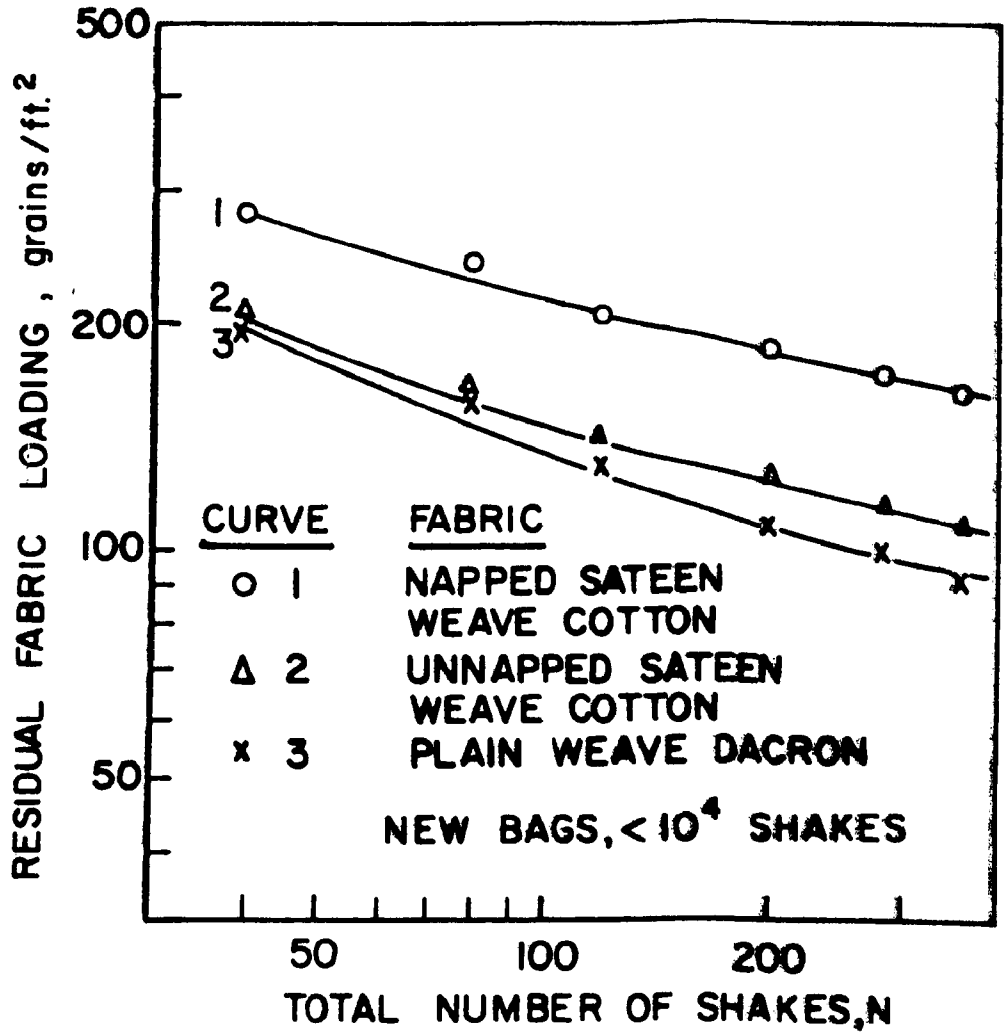

Figure 37. Residual fabric loadings for various fabrics with talc aerosol (8 cps, 1-in. amplitude shaking)

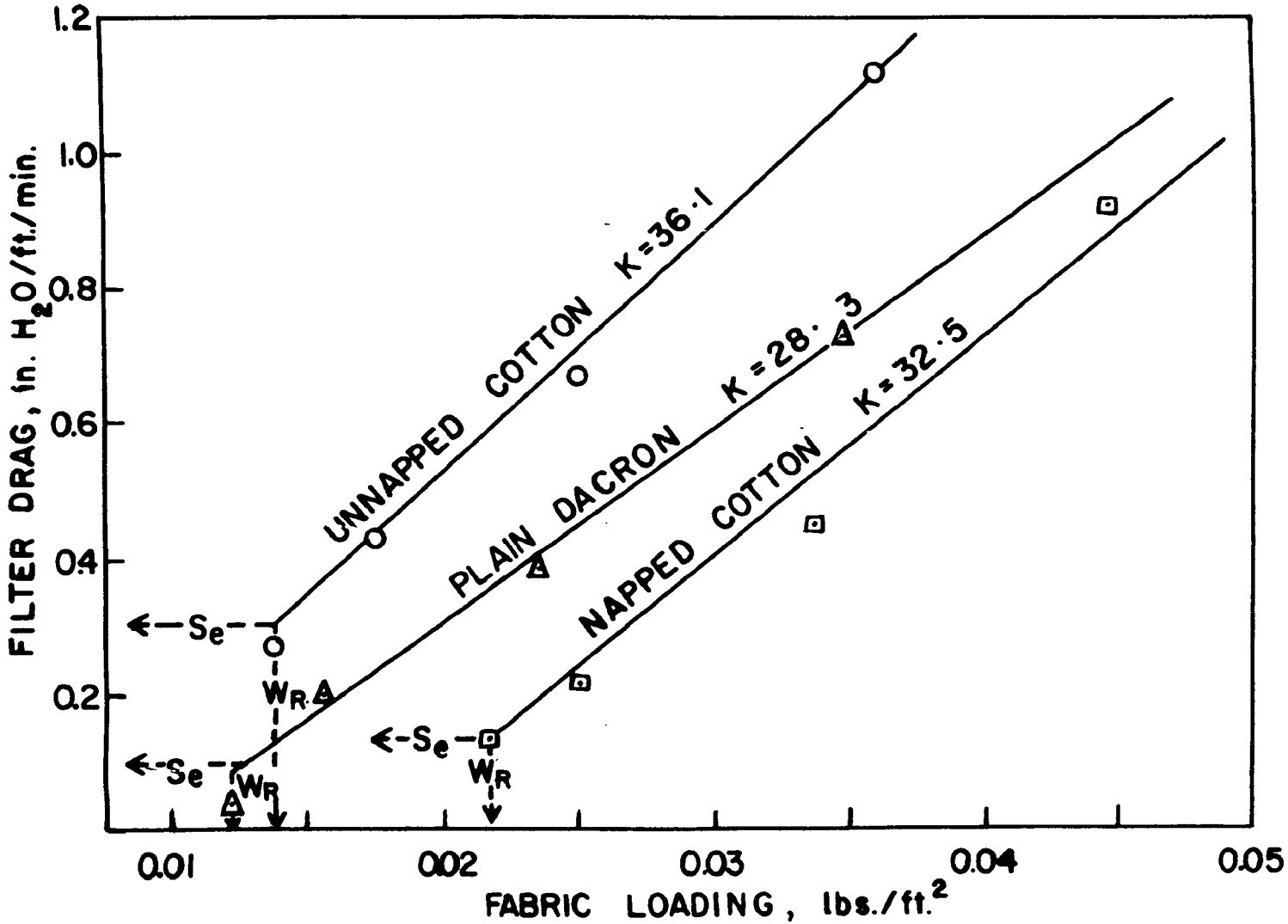

Figure 38. Fabric loading versus filter drag for woven cotton and Dacron bags with a talc aerosol (360 shakes at 8 cps and 1-in. amplitude)

Table 11. FILTRATION CHARACTERISTICS OF VARIOUS DUST/FABRIC COMBINATIONS[a]

Fabric	Effective drag (in. H_2O/ft./min.)		Filter capacity[c] $W_T - W_R$ (lbs./ft.^{2})	
	Fly ash[b]	Talc[b]	Fly ash	Talc
Unnapped cotton	0.67	0.3	0.024	0.019
Napped cotton	0.23	0.13	0.058	0.027
Plain Dacron	0.35	0.08	0.059	0.032
Crowfoot Dacron	0.43	-	0.035	-

[a]Mechanical shaking, 360 shakes at 8 cps and 1-inch amplitude.
[b]See Table 4 for aerosol size properties.
[c]Filter capacity, $W_T - W_R$, at a terminal drag of 1 inch H_2O/ft./min.

that the filter capacities appear in the ratio of 1.7:1 is attributed to the greater ease with which the talc is dislodged from the fabric. As a result, filtration is begun at a lower resistance or drag. One explanation for the lower residual fabric loadings may be that a larger fraction of the talc reaching the filter face remains as a superficial deposit. If, in fact, the estimated pore deposits for talc are composed of loosely agglomerated particles as suggested previously, it follows logically that the superficial layer may predominate.

The limited data obtained for talc and fly ash filtration point out significant differences in dust behavior despite similar size properties. Although the differences can be partially attributed to shape factor, electrical and hygroscopic properties, and surface smoothness, a more important consideration is whether certain of the basic relationships postulated for fly ash; i.e., residual fabric loading versus average bag acceleration and the number of shakes needed to approach a practical limit in cleaning capability can be applied directly to other dust. It has been shown, for example, in Figures 35, 36, and 37

that the dust unload properties versus number of shakes does follow different patterns for talc and fly ash. Generally, the results indicate that more studies are required to pinpoint critical relationships where dust/fabric interactions are involved as shown by differences in K values.

Attempts were made to establish filtration parameters for a resuspended amorphous silica with sateen weave cotton fabrics. Generally, no approach to steady-state filtration could be reached until inlet concentrations were reduced to 0.075 grains/ft.^{3} (versus 3.5 grains/ft.^{3} for talc and fly ash tests) and filter velocities to 1.5 ft./min. Finally, at 11.6 cps shaking frequency and 1-in. amplitude, 360 shakes appeared sufficient to stabilize the filtration process. It was noted that the dust shaken from the bags was composed of chip-like agglomerates such as those often found when filtering zinc oxide fumes. Examination of the bag suggested that some areas were poorly cleaned, leading to an appreciable dust layer that displayed surface cracks when the bag was flexed. The results of the silica tests are too limited to warrant any but the obvious conclusions that certain fine particles are very difficult to filter and that existing shake cleaning methods require considerable improvement.

Summary of Dust Removal Studies - Test results given in this section have indicated the following relationships and/or interactions among dust removal characteristics, dust type, fabric type and the intensity and duration of mechanical cleaning:

- After 200 shakes, practically all of the dust removable by a specified combination of shaker frequency and amplitude was dislodged. Tests indicated, however, that the fraction of dust removed at 200 shakes ranged from 80 to 95 percent of the dust dislodgable by extending the cleaning period to 360 shakes (~ 1 min. at 6 cps). The variations cited above depended upon the single or combined effects of dust and fabric properties.

- Although dust removal was shown to increase with an increase in either shaker amplitude or frequency, the most useful parameter describing dust removal was the average bag acceleration. The above term is readily defined in terms of the average bag amplitude, $\overline{Y}$, and the shaking frequency, f.
- The residual fabric loading for a specified dust/fabric combination correlated well with the reciprocal of the square root of the average bag acceleration (expressed in g's) over the test range of 1.5 to 7 g's.
- The residual fabric loading and residual filter drag also appeared as unique functions of the dust/fabric combination under study and the specified cleaning approach. Regardless of the initial fabric loading, application of the same mechanical shaking routine (frequency, amplitude, and total number of shakes) led to the same residual cloth holding.
- Filter capacity, defined as the amount of dust that can be collected upon the fabric surface during each successive filtration cycle, is a parameter that depends upon the acceptable terminal filter drag, available fan capacity, and the ability of the fabric to withstand and operate effectively at a specified pressure drop across the media.
- Because of the limited tests performed with dusts other than fly ash, it has not been clearly determined whether the shaking relationships and the effect of bag acceleration on dust removal can be treated independently, irrespective of dust and/or fabric types.
- The measurements presented in this and earlier sections enable one to estimate average resistance characteristics (power costs) and fabric area (collector size) for dust and fabrics very similar to those used in the experimental program.

In the following section, important performance parameters relating to the filter effluent properties are presented.

Collection Efficiency and Emissions

The following filtration and cleaning experiments were designed to determine effluent dust concentrations and particle size properties under the same test conditions described previously for inlet dust loadings, bag types, fabric loadings and methods of cleaning.

One test procedure involved the measurement of particulate emissions immediately upon resumption of filtration following the use of the superclean cycle described previously. In a second testing procedure, particulate properties were determined after steady state filtration conditions had been established for the selected cleaning conditions. No supercleaning was employed in the latter case.

To permit maximum accessibility for instrument placement, mechanical shaking systems were operated under positive pressure, (inside to outside) filtration. Thus, it was necessary to surround the lower 8 ft. of a 10-ft. bag by a grounded metal enclosure with a small exit port for venting a representative fraction of the effluent aerosol. Failure to use this design would have resulted in dilution of the bag effluent with the ambient air prior to sampling. In those cases where the particulate concentrations were very low, 10^{-8} to 10^{-3} grains/ft.^{3}, the B&L sampler was the only effective measuring instrument. On some occasions, the RDM sampler provided an index of mass concentrations when exit concentrations were in the 10^{-3} to 10^{-2} grains/ft.^{3} range or larger.

The use of these instruments and the quality of the resulting data have been discussed under Aerosol Concentration and Particle Size, pages 53 to 60. Again, because of the rapid response and high sensitivity of the B&L unit, it was possible to categorize the effluent aerosol in five size fractions within a 0.5 min. sampling interval. By repeating this process as long as necessary throughout the filtration cycle, the initial and subsequent particle concentrations could be

measured until they decreased to levels below the detection limit, $\sim 10^{-8}$ grains/ft.^{3}. This lower limit of detectability was usually reached after 4 to 5 min. of filtration.

As described previously, it was possible to estimate roughly the total mass concentrations at various times during the filtration cycle by summing up the computed masses within each size fraction. On a relative basis, the changes in number concentration and size distribution were probably in agreement within at least a factor of two. Comparisons of B&L and RDM measurements on an absolute basis indicated that the ratio of mass concentrations, RDM/B&L, ranged from 2 to 5 on the average. With respect to this study, where concentration changes of five orders of magnitude were not uncommon, the discrepancies between B&L and standard measuring devices, such as the RDM, were considered unimportant.

General Observations - The experimental results described in this section suggest that the particulate emissions from a filter can be attributed to some combination of the following sources:

1. Inlet dust that because of its small size passes directly through the filter, usually in progressively smaller amounts as the filter pore structure becomes plugged.
2. Dust that migrates through the filter by successive deposition and re-entrainment under the combined effects of aerodynamic and mechanical (vibrational) forces. Such dust penetration is often referred to as "seepage" in commercial parlance. It may be more pronounced in the case of multifilament yarns, spherical or smooth surfaced regular particles, and in the absence of electrostatic or other forces enhancing adhesion or cohesion.
3. Dust dislodged from the shaken fabric during cleaning that has penetrated to the clean air region. Resumption of air flow flushes out the clean air side of the system, often producing a visible puff of dust.

4. Dust loosened during the cleaning process whose bonding to the fibers or interstitial dust structure is not sufficiently strong to resist the combined dislodging forces (aerodynamic and mechanical flexure) when system air flow is resumed.

Although it appears difficult to weigh the relative importance of the above sources, it is suspected that items (3) and (4) may account for a large fraction of the total mass emission, probably in the form of a few large particles, whereas items (1) and (2) are responsible for the discharge of most of the submicrometer material.

One can infer from the above that effluent concentrations based upon long-term measurements represent the combined, unresolvable effects of these four emission sources. On the other hand, short-period measurements, of the order of seconds to minutes, provide an opportunity to identify the dust source and to assign reasonable values to particle sizes and number concentrations.

The four suggested sources of dust emission contribute in some degree to the total emission from all types of fabric filters. The predominant source with respect to particle number is probably emission during filtration. According to theory,[8] this emission should relate inversely to the pressure drop across the filter, since both are dependent on the degree to which the pores in the fabric and dust deposit have become filled and sealed. In other words, the total emission of dust per unit area of filter over a given period of operation should relate to the weight of dust on the filter.

Based upon the relationship between adhesive and/or cohesive forces and particle size, it appears that particles collected singly on the filter surfaces will most likely be dislodged in the form of agglomerates. One could conceive of the extreme case where a freshly

generated fume composed of particles less than 0.5 μm could very readily produce a filter effluent composed of much coarser particles despite a high overall mass collection efficiency.

Effluent Concentration versus Filtration Time - Comparison of the concentration properties of filter effluents when the inlet aerosols consisted of ambient dust at $< 10^{-4}$ grains/ft.^{3} and fly ash at 3.5 grains/ft.^{3}, respectively, is given in Figure 39. The time scale in Figure 39 and many similar figures has been terminated at 5 min. because subsequent emissions over the remainder of the 30 min. filtration cycle used in most tests were below the limit of detection, $\sim 10^{-8}$ grains/ft.^{3}. In both cases, steady state conditions had been established for fly ash filtration in conjunction with a 360 shake cleaning cycle at 7.2 cps and 1-in. amplitude. The results indicated that effluent concentrations at the resumption of filtration were roughly equivalent to the prevailing atmosphere levels, regardless of the inlet aerosol. Furthermore, both effluents decayed by more than three orders of magnitude within 5 minutes time and both decay curves suggested that the total mass emissions over the filter cycle were similar and hence practically independent of the inlet concentration to the filter.

Since very little dust accumulation was expected during atmospheric dust filtration, the initial concentration level and the subsequent decrease in effluent concentration were attributed to two factors. The first was the dislodgement of interstitial and surface deposits loosened by prior shaking, and the second was the transient inlet loading produced at the resumption of air flow by material dislodged from the inlet duct system.

The fact that resumption of full dust load, Curve B, Figure 39, led to emission levels of the same order as the "clean air" tests points out that effluent concentrations are not related in any simple fashion to inlet loadings as one finds with many centrifugal collectors.

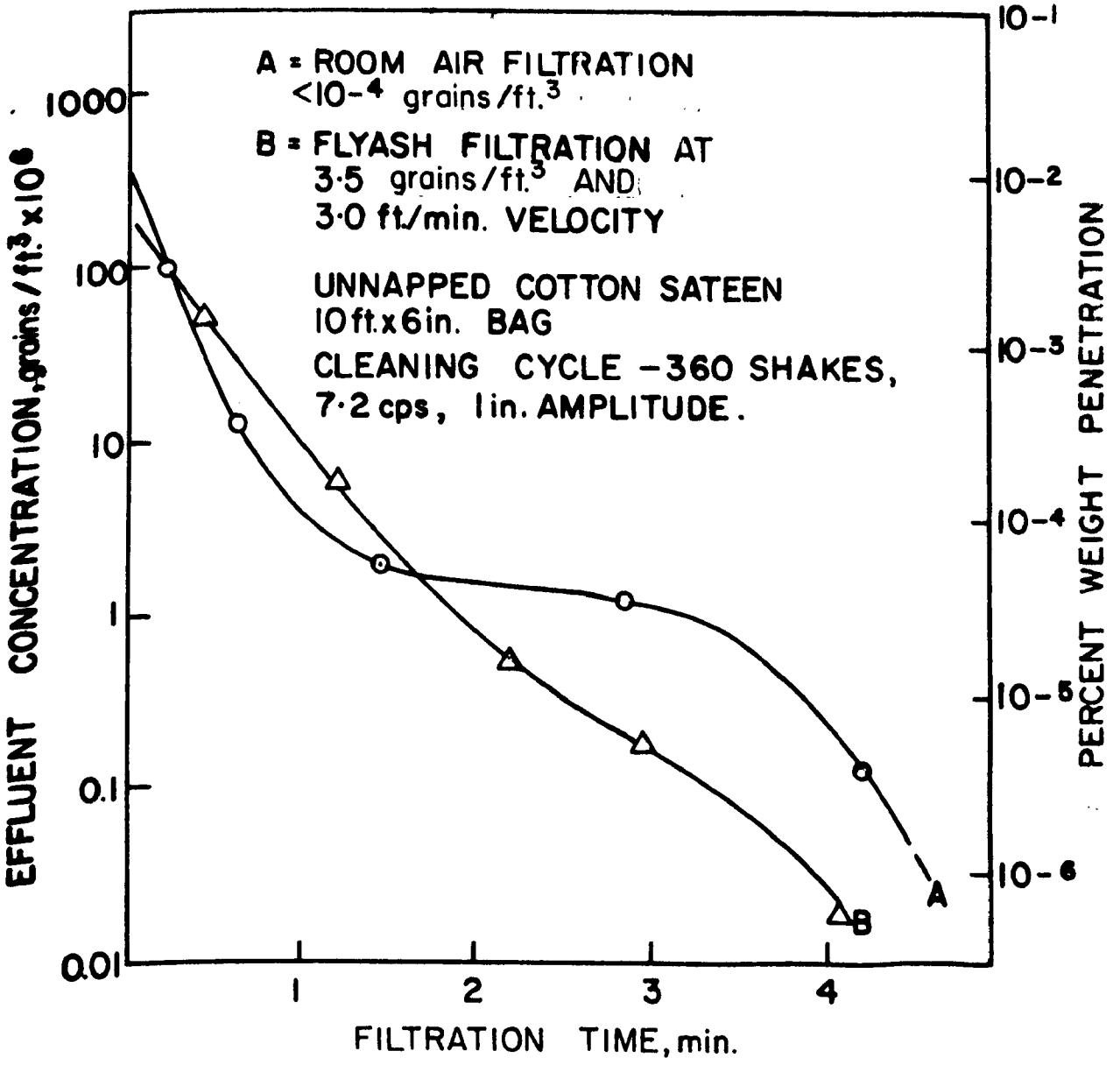

Figure 39. Calculated effluent concentration versus time for fly ash and ambient dust based on B&L measurements

Actually, the effluent concentration appears to be almost independent of inlet dust loading. In addition, the dust that penetrates the filter probably represents a composite of inlet particles that pass unchanged through the filter plus particle agglomerates and perhaps discrete particles that are swept from their former deposition sites by the entraining air stream.

It is also important to note that approximately 90 percent of the total quantity of dust emitted during the complete 30 min. filtration cycle was released during the first minute of filtration. During this period the filtration surface underwent partial restoration. Similar results were shown by Durham and Harrington[2] at 50 and 60 percent relative humidities.

The dust penetration characteristics shown in Figure 39 typify nearly all tests with fly ash and cotton sateen fabrics in which the effluent concentrations fell to levels below the limit of detection by the B&L instrument in about 5 minutes. On the other hand, similar tests with Dacron fabrics showed a continuing emission throughout the entire filtration period.

Figure 39 shows an initial fly ash weight penetration of about 0.006 percent, which means that initially only one out of every 33,000 entering particles passed through the filter. The above statement is based upon the simplifying assumption that the aerosol is monodisperse. The emission then decreased about one order of magnitude for every 6 grains/ft.^{2} deposited. If distributed evenly among the number of yarn interstices (about 5500 pores/in.^{2}) in this cotton fabric, a deposit of about 30,000 average-sized particles per interstitial pore would result. Thus, it appears that the probability of a single particle passing through a pore is reduced one order of magnitude following each successive filtration interval of about 0.55 minutes. This assumes that all filtration and emission occurs at the inter-yarn pores, which may not necessarily be true in all cases.

It was estimated that a fabric dust holding of 6 grains/ft.^{2} on a per-pore basis would occupy a volume characterized by an 85 μm cube. In comparison, the inter-yarn pores of the fabric with their residual loading were estimated to be of the order of 75 μm diameter, based on the residual drag.

Despite the broad assumptions made in the above analysis, it is easy to visualize why the dust depositing within the first few minutes of filtration is so effective in reducing particulate emission levels, Figure 40.

Effluent Concentration versus Particle Size - Upon restoration of the filter surface, the larger particles are the first to be effectively retained as shown in Figure 40. Because of difficulties in performing these measurements, the data points may appear quite scattered as shown in Appendix H. The larger particles, > 2 μm, are emitted for such brief periods as to make accurate measurement difficult. Whether they come from the surface of the fabric as seepage dust or are actually penetrating particles is difficult to ascertain. Based upon the ambient dust filtration results described in Figure 39, it is believed that dislodgement of particles loosened by prior shaking may constitute a significant fraction of the early, < 1 minute, emissions. Discharge of the large particles is usually diminished at a greater rate than for the small particles and with cotton sateen filtration not even the smallest particles (> 0.3 μm class) could be found after 3 to 5 minutes.*

Other fabrics, mainly Dacron weaves, apparently sealed incompletely such that particles greater than 0.3 μm continued to penetrate throughout the 30 minute filter cycle, following a moderately rapid initial

---

*The lowest equivalent mass concentration detectable by the B&L device was estimated to be 10^{-9} grains/ft.^{3}, roughly 10^3 times lower than typical clean air concentrations of approximately 10^{-5} grains/ft.^{3} or 20 μg/m^3.

decrease in penetration. The larger particles, 0.5 to 1.0 μm, however, usually ceased to be emitted after a few minutes. Therefore, the poorer the filtration, the greater the divergency of the particle size curves in Figure 40.

A review of a number of tests with cotton fabrics (Appendix H) showed that the size distributions of the emitted dust were fairly similar in all cases. The size distributions were truncated at the high ends by some limiting characteristics of the filter in its just-cleaned state, probably the size of the largest pore in the media. Smaller particles appeared to be emitted in concentrations controlled by the parent aerosol size distribution. This applied not only immediately after cleaning, but throughout the filtration process, with the concentrations of all but the extreme particle sizes diminishing at about the same rate. As time progressed, first the largest size and then the next smaller passed below the detectable range (150 particles/ft.^{3}). The rate of decrease of individual particle sizes was about the same as that for the total mass emission; i.e., roughly one order of magnitude for each additional deposit of 6 grains/ft.^{2}.

The decrease in effluent size properties with filtration time is indicated in Figure 41 for times ranging from 0.7 to 2.8 minutes. After 2.8 minutes, the indicated size distribution parameters for the effluent, CMD = 0.75 μm, σg = 2.1, appear to be approaching those for the typical room air, CMD = 0.5, σg = 1.5, as determined by membrane filter sampling and oil immersion, light field microscopy.

Based upon an average efficiency in the range of 99.9999 percent for a typical 30-minute filtration period (Curve B, Figure 39) the following rough estimates of fractional size efficiencies can be made:

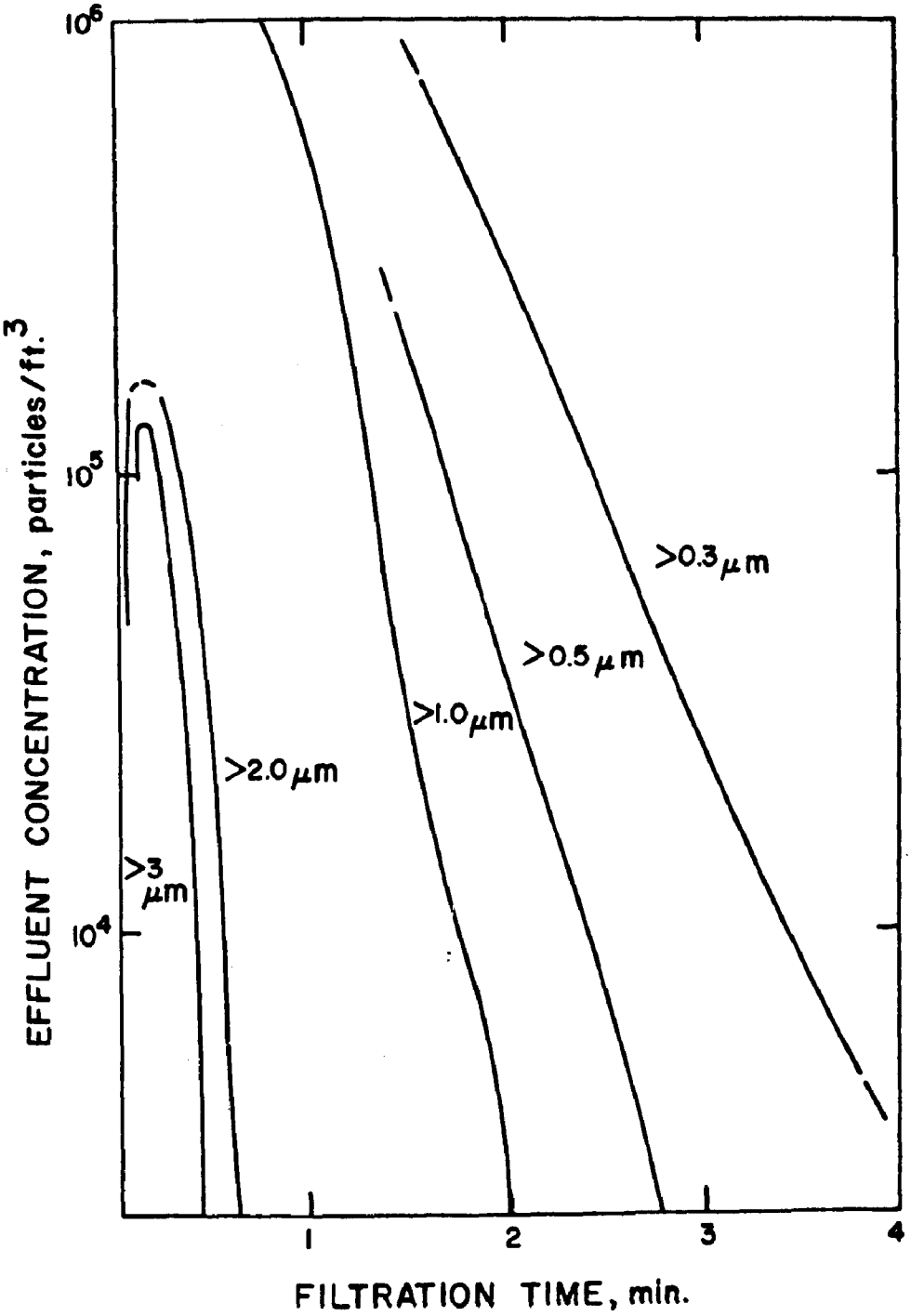

Figure 40. Calculated effluent number concentration versus time and particle diameter for fly ash filtration with sateen weave cotton. Filtering and cleaning conditions of Figure 39.

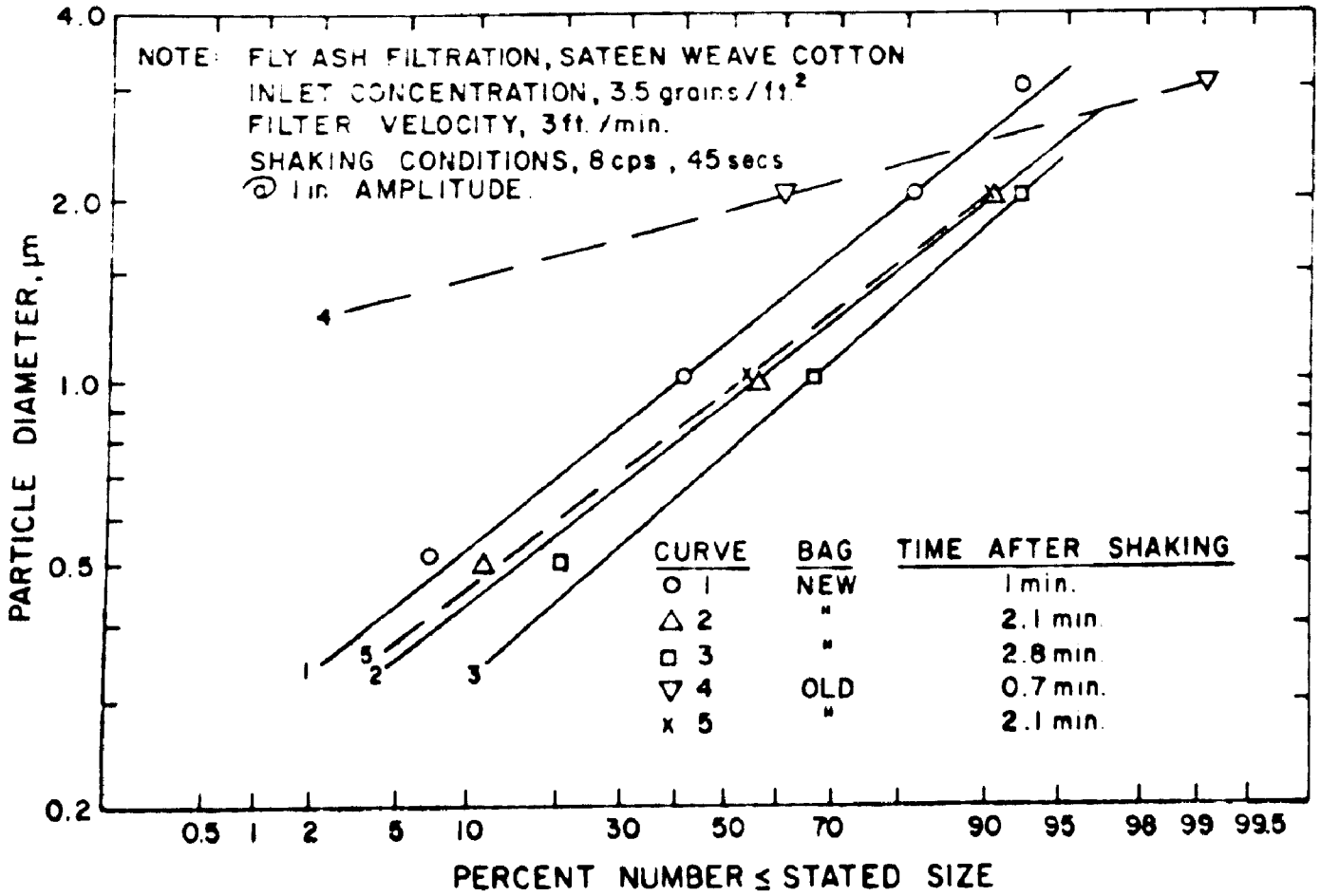

Figure 41. Changes in effluent size properties with filtering time for new (<10^4 shakes) and old (2 x 10^7 shakes) bags. Sizing by optical, B&L, counter

Size range, μm	Efficiency, percent
0.3 - 0.5	99.9970
0.5 - 1.0	99.9965
1.0 - 2.0	99.9992
2.0 - 5.0	99.9999+

The above calculations derive from cascade impactor measurements of mass distribution for the inlet aerosol and effluent size properties estimated to be similar to atmospheric dust, MMD = 1 μm, σg = 1.5. Although the larger sizes were collected at the higher efficiencies as theory would predict, highly efficient collection was also observed for particles as small as 0.3 μm.

Effluent Concentration versus Shaking Amplitude - Effluent concentrations were found to be strongly dependent on shaking amplitude based on a series of tests with 10 ft. by 6 in. unnapped cotton sateen bags. This is most evident in Figure 42a which shows differences in effluent concentration when filtering room air after shaking the bags at amplitudes of 1/2, 1 and 2 inches. A similar but less pronounced trend was indicated when filtration was resumed with fly ash at inlet loadings of 3.5 grains/ft.^{3}, Figure 42b. The best explanation seems to be that the residual dust cake experiences more breakup with greater stretching of the fabric, thus creating larger gaps between the residual deposits and prolonging the sealing process. It was noted that a factor of two increase in amplitude caused a factor of ten increase in average effluent concentration. This difference could be of considerable importance in marginal applications.

Effluent Concentration versus Shaker Frequency - In a series of related tests, shaker frequency was found to have little effect on effluent concentration. Results of tests at three different frequencies and a constant of 1-inch amplitude are shown in Figure 43. The higher shaking tensions and greater rates of fabric deformation associated with higher

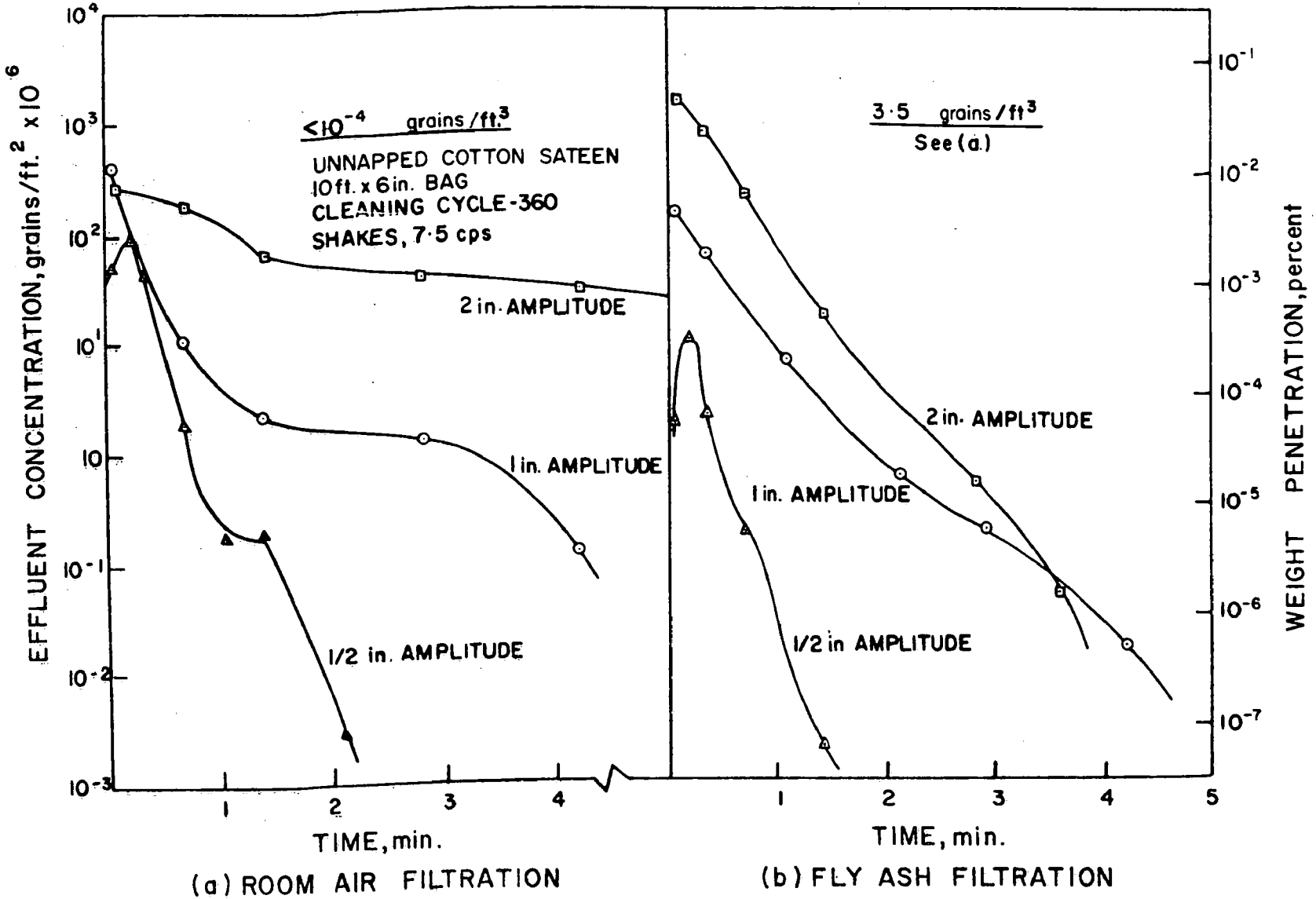

Figure 42. Calculated effluent concentration versus shaker amplitude at constant shaking frequency

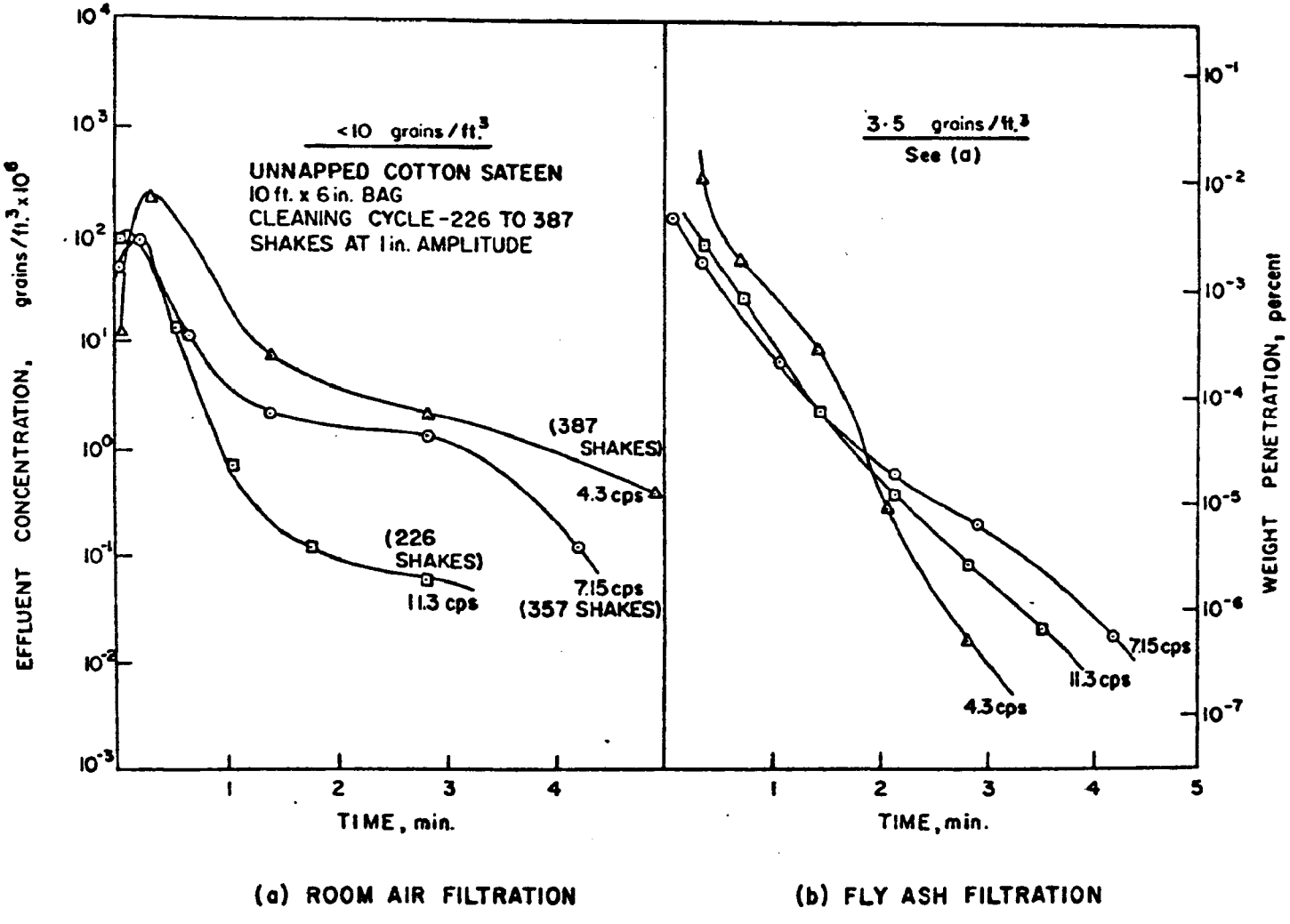

Figure 43. Calculated effluent concentration versus shaking frequency at constant amplitude

shaking frequencies did not appear to influence dust penetration even though more dust was removed from the fabric at the higher frequencies. The finding that the degree of stretching and not the rate of fabric flexure determined filter emission levels was consistent with the view that the effective pore dimensions after cleaning were controlled by the cracks in the dust cake.

A summary of test measurements showing the effects of amplitude and frequency variations in given in Table 12. On the average, effluent concentrations during the first minute of filtration were 30 times greater than those for the complete 30-minute filtering cycle, irrespective of the inlet concentration. The highest tension level was associated with the largest shaking amplitude and also the largest effluent concentration.

The average emissions for the fly ash/sateen weave cotton system were at first suspected of being too low, possibly because of the limitations of the B&L instruments. This impression was based partly on several tests reported by Draemel[13] in which outlet concentrations for several fly ash/Dacron systems were found to be in the 10^{-3} grains/ft.^{3} range. Examination of measurements on several different sateen weave cotton, industrial filter systems, Figure 44, showed that GCA fly ash data were in excellent agreement with the field data.[15] Since the size properties of the foundry dust, Figure 44, were similar to those for the GCA fly ash, it appeared that the mass concentration data developed from B&L number count measurements were well within an order of magnitude of the true values.

Effluent Concentration versus Bag Life and Bag Stretch - As part of the accelerated life testing procedure for cotton sateen filter bags, particulate measurements were made periodically in an attempt to detect potential signs of bag failure. After 2×10^7 shaking cycles, equivalent to 3 to 5 years of normal bag usage, no physical damage could be discerned visually. Effluent concentrations for fly ash

Table 12. COLLECTION EFFICIENCY AND EFFLUENT CONCENTRATIONS FOR VARIOUS CLEANING REGIMES[a]

Shaking system		Average effluent concentration - grains/ft.^{3}				Shaking tension (lbs.)	Fabric[d] dust holding grains/ft.^{2}
		Fly ash filtration[b]		Ambient air filtration[c]			
cps	Ampl. (in.)	First minute	30 minutes	First minute	30 minutes		
7.5	2	3×10^{-4}	1×10^{-4}	2×10^{-4}	2×10^{-5}	10.7	200
7.5	1	3×10^{-5}	1×10^{-6}	2×10^{-5}	1×10^{-6}		300
7.5	1/2	1×10^{-6}	3×10^{-7}	1×10^{-5}	3×10^{-7}	3.5	410
4.3	1	1×10^{-4}	3×10^{-6}	2×10^{-4}	1×10^{-6}	4.8	420
7.15	1	5×10^{-5}	2×10^{-6}	2×10^{-5}	1×10^{-6}		290
11.3	1	5×10^{-5}	2×10^{-6}	2×10^{-5}	1×10^{-6}	7.5	200

[a] 360 shakes per cleaning cycle.

[b] Fly ash, 5 grains/ft.^{3}, CMD = 2.4 μm, σg = 1.77.

[c] Ambient air, $< 10^{-4}$ grains/ft.^{3} CMD ~ 1 μm, σg ~ 1.5

[d] At resumption of filtration.

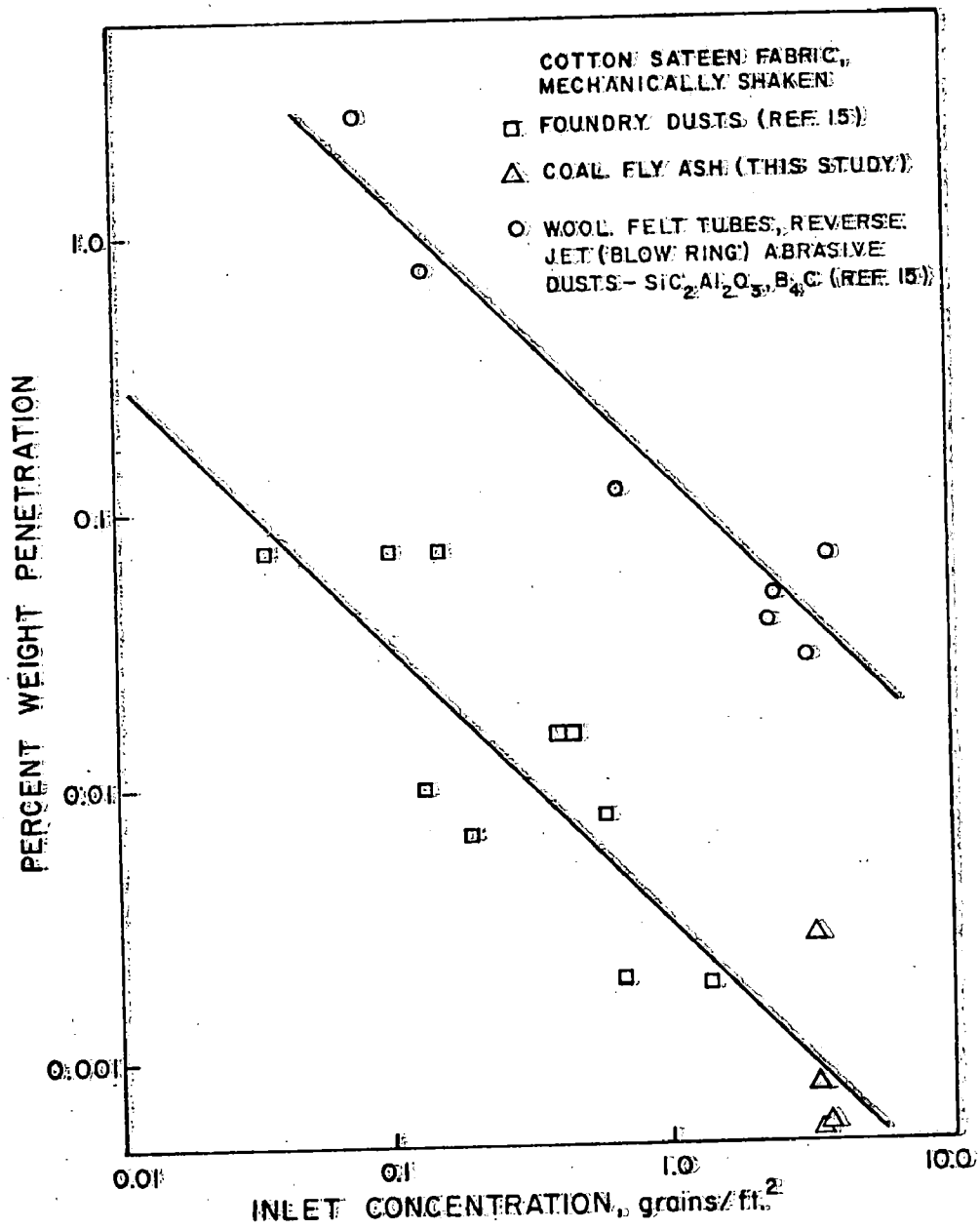

Figure 44. Inlet concentration versus percent weight penetration, ambient temperatures.

increased gradually throughout the shaking process, however, as indicated in Table 13. The factor of two or three increase is almost negligible when compared with some of the other changes encountered in this study.

During the extended shaking process, the bags underwent progressive stretching. This must have opened the inter-yarn pores in the longitudinal direction, possibly accounting for the modest concentration increase. Tests with the more highly tensioned bag indicated slightly higher outlet concentrations.

Table 13. EFFLUENT CONCENTRATIONS VERSUS AVERAGING PERIOD (FLY ASH; UNNAPPED COTTON SATEEN BAGS, 10 IN. X 6 FT.)

Number of shaking cycles[b]	Average effluent concentration - grains/ft.^{3} x 10^6 [a]			
	Taut bag[c]		Loose bag[d]	
	First minute	30 minutes	First minute	30 minutes
6 x 10^6	750	25	250	8.7
10 x 10^6	750	25		8.3
15 x 10^6	500	17	350	12
20 x 10^6	900	30	450	15

[a]Measurements made after loading filter to ~ 700 grains/ft.^{2}, and then cleaning.

[b]Shaking cycle 8 cps, 1-inch ampl. 360 shakes.

[c]Static tension = 3.1 lbs., shaking tension 6.5 lbs.

[d]Static tension = 1.3 lbs., shaking tension 4.5 lbs.

Efficient Concentration versus Fabric Type - In conjunction with life tests on four types of fabrics, comparative emission measurements were made on equilibrated nearly new bags (< 10^4 shakes) and on equilibrated bags shaken 2 x 10^7 times. Generally, the two cotton fabrics had very high efficiencies compared with the Dacron media. All four fabrics, however, showed efficiencies in excess of 99 percent, and the Dacron fabric performance would be completely acceptable in many applications

despite the higher effluent concentrations. Test conditions and results are summarized in Table 14 and Figure 45.

The napping of the cotton sateen fabric appeared to improve its performance. The net emission was slightly lower, although it took slightly longer for the napped surface to seal. The effect of the napped surface was almost insignificant when compared with the emission differences noted for the Dacron fabrics. Although there is no reason why the weight of the dust on a fabric should uniquely determine the penetrating properties of a dust, the general correlation shown in Figure 46 was expected. Deviations from the mean curves are readily explained by differences in deposit density, fabric weave, pore structure and other physical factors.

Efficient Concentration versus Dust Type - Summary measurements in Table 13 indicate that the effect of extended cleaning, up to 2×10^7 shakes, on various fabrics was to increase emission levels by a factor of 2 to 4 over the outlet concentrations for new filter media. In some cases, the greater penetration may have resulted from lower residual deposits. Additionally, the stretching of all fabrics over the life testing period undoubtedly produced a more open pore structure that contributed to increased dust emissions.

Limited tests were performed with talc and silica to study the effect of particle properties on dust penetration. Test results shown in Table 15 and Figure 47 indicate that higher efficiencies were obtained with talc than for fly ash. The greatest improvement was noted for the plain weave Dacron bags although the talc/unnapped cotton emissions were also slightly less than those for the fly ash/unnapped cotton combination tested previously. On the other hand, a slightly higher talc emission was noted with a napped cotton bag than that determined for fly ash. Estimated residual drag values for talc and fly ash tests, 0.27 and 0.13 in./ft./min., respectively, appear consistent with the higher emission level for fly ash although the difference may not

Table 14. FLY ASH EMISSION PARAMETERS FOR DIFFERENT 10 FT. X 6 IN. FABRIC BAGS[a]

	Unnapped cotton	Napped cotton	Plain-weave Dacron	Crowfoot Dacron	
Nearly new fabrics < 10^4 shakes					
Residual drag	0.47	(0.20)[b]	(0.17)	(0.37)	in./ft./min.
Residual dust	437	475	219	97	gr./ft.^{2}
Peak exit concentration	136	26	3,600	10,400	gr./ft.^{3} x 10^6
Avg. exit concentration for 1st min.	50	20	1,900	(6,000)	gr./ft.^{3} x 10^6
Avg. exit concentration for 30 min.	1.9	1.2	1,635	(2,330)	gr./ft.^{3} x 10^6
Total emission per 30 min. cycle	180	110	147,000	(210,000)	gr./ft.^{2} x 10^6
Avg. efficiency, 30 min.	99.99994	99.99997	99.95	99.93	percent
Well used fabrics 2 x 10^7 shakes					
Residual drag	(0.60)	(0.53)	(0.00)	(0.02)	in./ft./min.
Residual dust	397	355	120	77	gr./ft.^{2}
Stretch, 20 x 10^6 period	1.40[c]	1.20	0.79	0.69	inches
Peak exit concentration	710	80	17,000	20,000	gr./ft.^{3} x 10^6
Avg. exit concentration for 1st min.	170	(60)	(12,000)	(15,000)	gr./ft.^{3} x 10^6
Avg. exit concentration for 30 min.	5.7	2.5	8,200	10,400	gr./ft.^{3} x 10^6
Total emission per 30 min. cycle	510	222	738,000	939,000	gr./ft.^{2} x 10^6
Avg. efficiency, 30 min.	99.9998	99.99993	99.77	99.71	percent

[a]Measurements made after equilibration at 3 ft./min. velocity and 3.5 gr./ft.^{3} inlet loading. Cleaning cycle of 360 shakes of 1-inch amplitude at 8 cps.

[b]Parenthesis indicates questionable data.

[c]Bag tension adjusted periodically to 3 lbs.

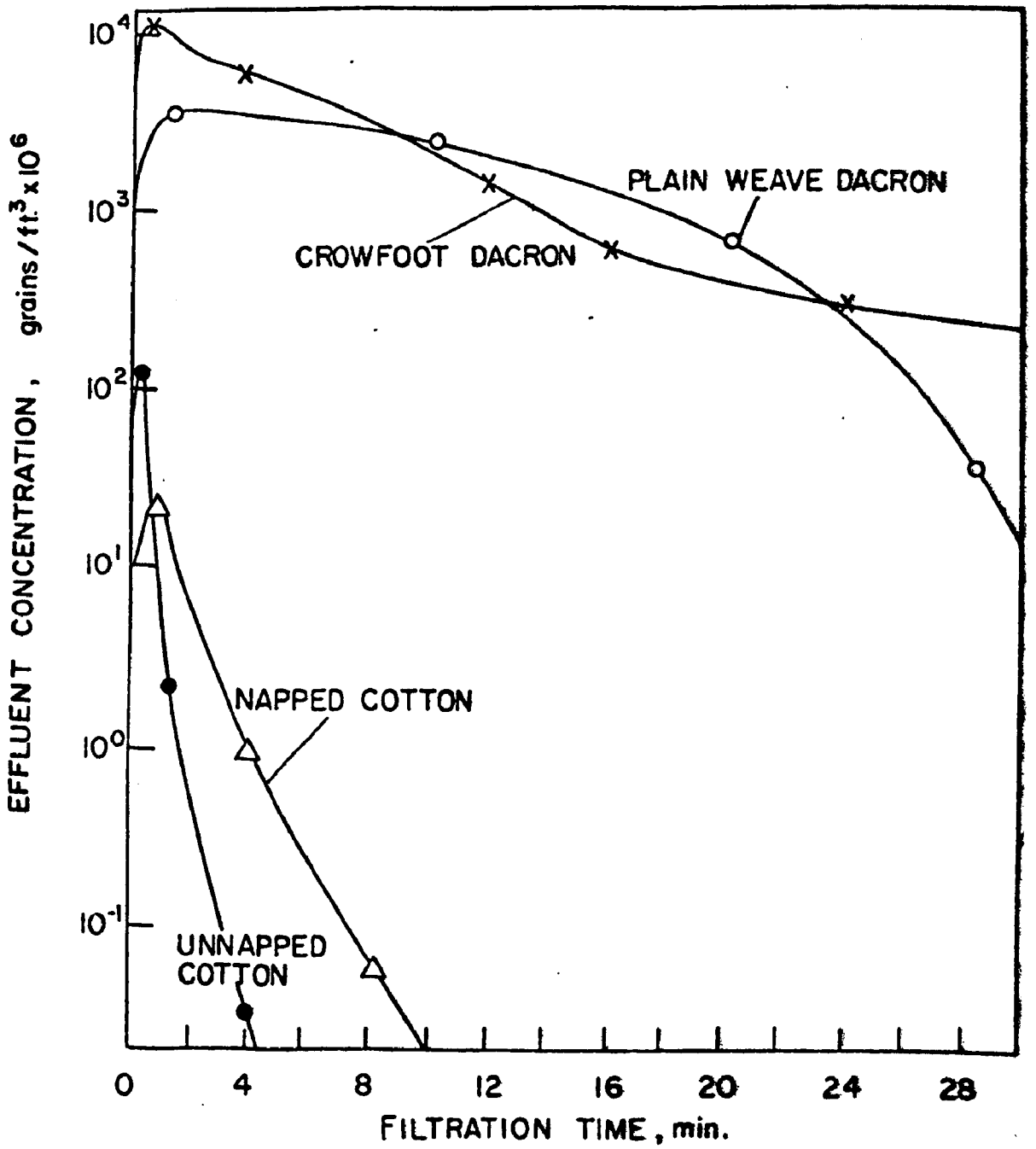

Figure 45. Comparative effluent concentrations for fly ash with different fabrics

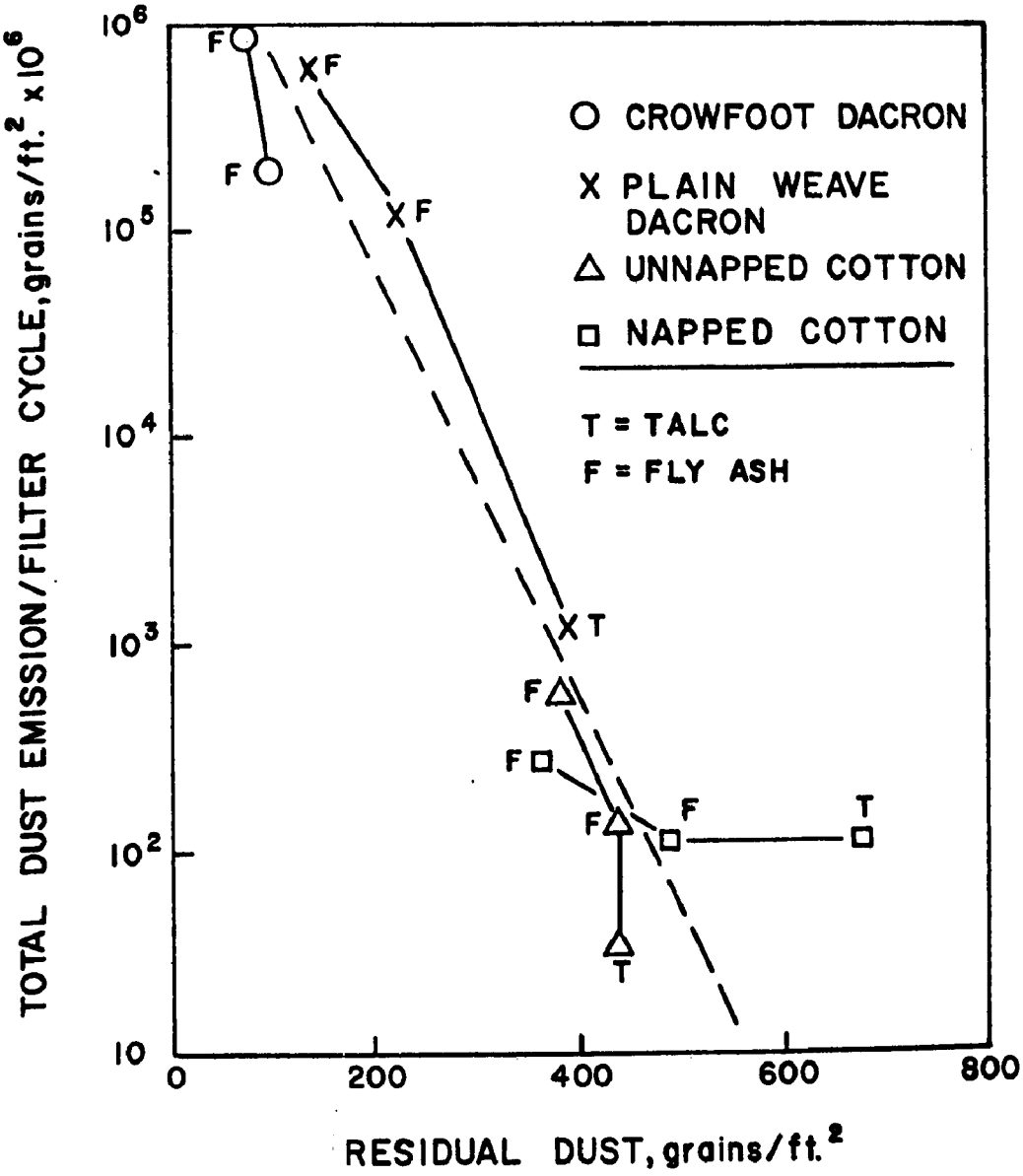

Figure 46. Total dust emitted per filter cycle versus fabric type and residual dust holding

Table 15. TALC AND SILICA EMISSIONS FROM NEW ($< 10^4$ SHAKES) COTTON AND DACRON BAGS

	Talc[a]			Silica[b] unnapped cotton	
	Unnapped cotton	Napped cotton	Plain-weave Dacron		
Residual drag	0.27	0.13	0.047	1.3	in./ft./min.
Residual dust	97	152	86	--[b]	gr./ft.^{2}
Peak exit concentration	32	92	713	0.012	gr./ft.^{3} x 10^6
Avg. exit concentration for 1st min.	12	40	358	~0.001	gr./ft.^{3} x 10^6
Avg. exit concentration for 30 min.	0.38	1.6	14	~0.0001	gr./ft.^{3} x 10^6
Total emission per 30 min. cycle	34	140	1,300	~0.01	gr./ft.^{2} x 10^6
Avg. efficiency, 30 min.	99.99999	99.99996	99.99996	> 99.99999[c]	percent

[a]Inlet loading ~ 3.5 grains/ft.^{3}, filter velocity 3 ft./min., 20 min. filter cycle. Cleaning 8 cps, 1-in. amplitude and 360 shakes.

[b]Equilibrium not attained.

[c]Based on reduced inlet loading of 0.1 grain/ft.^{3}.

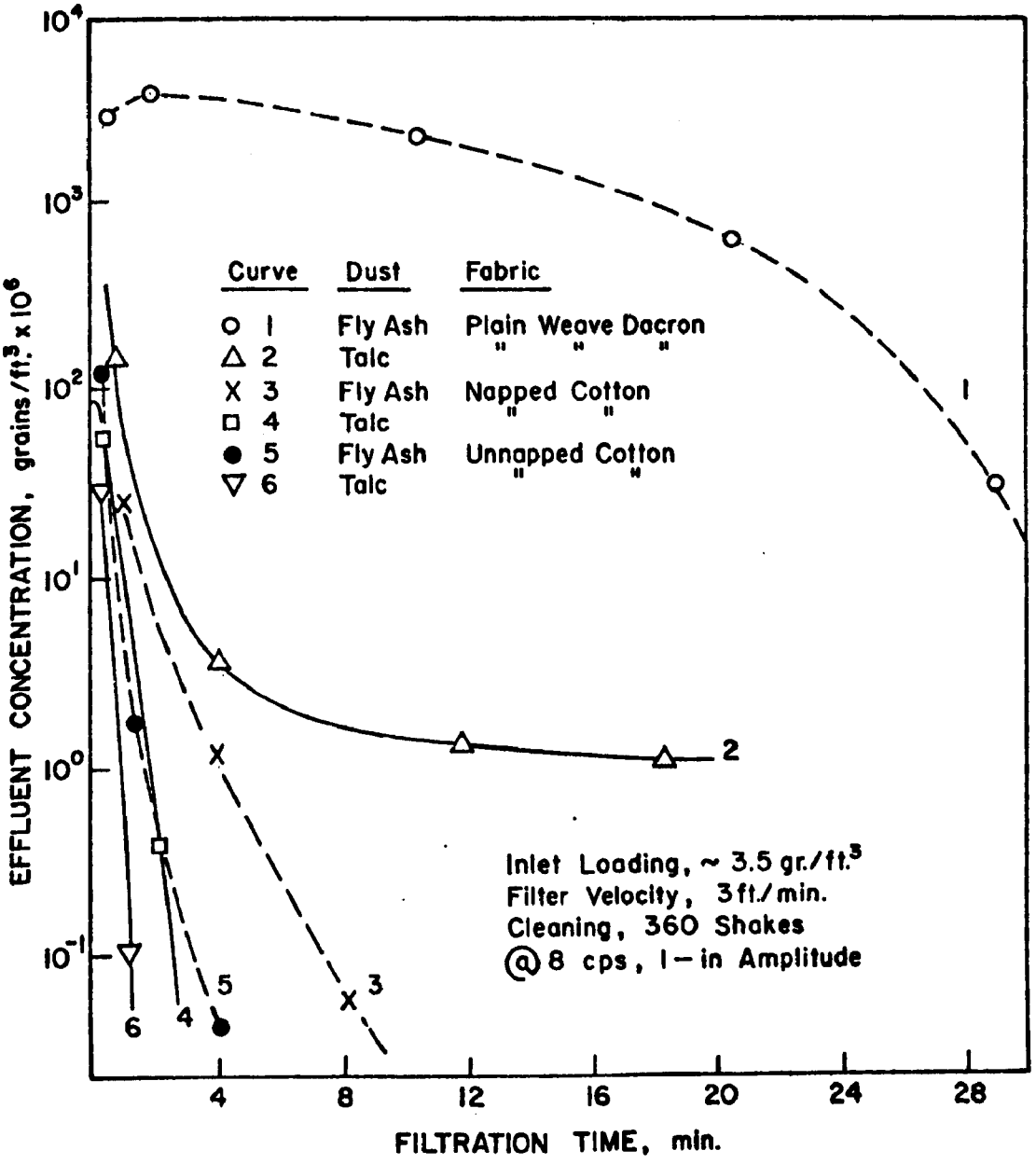

Figure 47. Comparative effluent concentrations for talc and fly ash with cotton and Dacron fabrics

be significant. The same situation seems to apply to the talc emissions for napped and unnapped cotton, Table 15. Again, the outlet concentrations and total emissions varied inversely with the residual drag levels as expected.

As indicated previously, it has been postulated that the characteristically fluffier deposit formed by the talc (roughly one quarter the bulk density of fly ash) probably leads to less interstitial and greater superficial deposition. Therefore, a larger fraction of the dust is released during cleaning. Because of its irregular form, however, there is assumed to be less talc migration or "seepage" during the actual filtration cycle.

Exceptionally high efficiencies were noted during the silica/unnapped cotton tests although the minimal holding capacity, high resistance, and cleaning difficulties did not make the system attractive from the power cost or capacity perspectives. Actual outlet concentrations were estimated to be several orders of magnitude lower than those determined for the other test dusts. One can infer that the high resistance and low dust holding capacity demonstrated by the silica/unnapped cotton system is related largely to the extremely low bulk density of the silica pigment, $\sim$ 0.04 g/cc.

Based upon the limited tests performed with talc and silica and the numerous measurements made with fly ash, it appears that filter resistance and holding capacity is more closely related to the volume than to the mass of dust residing on the filter surface.

Discussion of Particle Emission Studies - Dust collection for the highly efficient filter bags tested in this study can best be viewed in terms of the particles penetrating the bag as a function of time during the filtration cycle. The particulate emission may be related to the following factors:

- Weight and/or volume of dust residing on filter - The quantity of dust discharging to the atmosphere over any time interval depends upon the degree of fill of the interstitial or pore volume of the fabric. Present tests suggest that deposition of sufficient dust to fill the estimated pore volume reduces particulate emissions by a factor of 10. The time to achieve this condition depends upon the inlet dust concentration, gas flow rate and, as noted in the previous section, the bulk density of the collected dust. The accumulation of successive increments of dust (equal to that of the initial deposit) leads to an exponential decay in outlet concentrations that may embrace several orders of magnitude during a single filtration cycle.

- Particle size - The larger particles are the first to be blocked from further penetration followed by progressively smaller particles as the filtration cycle progresses. The smallest size blocked appears to be inversely proportional to the mass or volume of dust deposited on the filter.

According to Draemel,[13] it appears that complete filling or bridging-over of the pore openings may be expected if the mass median diameter of the dust is greater than 0.1 the average pore diameter. This estimate must, of course, be tempered by the nominal packing density assumed by the dust as determined by particle shape and electrical charge properties and the uniformity of the pore structure. Failure to attain complete bridging was evidenced by pinhole leaks through which dust penetrated in the form of high velocity jets.[13] Such dust penetration was observed during this study with Dacron media when filtering fly ash.

- Shaking amplitude and rate of flexure - Increasing shaking amplitude from 1 to 2 inches led to a nearly tenfold increase in mass emission rates whereas variations in shaking frequency from about 4 to 12 cps had little impact on total dust discharge. This leads to the conclusion that it is the stretching or enlarging of the pore openings rather than the rate of flexure that causes increased particle emissions.

- Bag life - After an extended shaking period, equivalent to 3 to 5 years of service, the average fly ash emission rates for cotton fabrics increased by 2 to 3 times. Because of the very low effluent concentrations determined for fly ash, Table 14, this increase was not considered important.

After a similar shaking period, a 4- to 5-fold increase in fly ash emissions was observed for the Dacron fabrics. In the latter case, the fact that the absolute quantities of dust released to the atmosphere were 1000 to 2000 times greater may be very important with toxic materials. Irreversible stretching and related pore enlargement were assumed to be responsible for the increased emissions.

- Dust type - Aside from differences in size, shape, charge or hygroscopic properties, the single factor that appears to influence most the resistance and dust holding capacity of a specified dust/fabric combination is the bulk density of the dust as it actually deposits on and within the filter structure. Therefore, in searching for characterizing parameters with which to predict filter performance one might use bulk density as one means of defining the interaction of several independent variables.

Filter Resistance

On the resumption of filtration, the pressure differential across the filter bag was recorded as a function of time. Due to the initial rapid rate of pressure increase during the brief period of accelerating flow, it was difficult to determine accurately the true residual pressure differential. However, since pressure data were reasonably accurate after about 10 seconds of filtration, it was possible to determine the effective residual pressure differential in most cases by extrapolation of the nominally linear portion of the resistance-time curve.

A single filter element (or compartment) may be operated in two ways. First, it can be loaded with dust until a predetermined terminal resistance is reached at which point the flow is stopped and the filter cleaned. Alternatively, it can be cleaned at predetermined time intervals. In the first instance, the average operating pressure loss across the element, $\bar{h}$, is given by

$$\bar{h} = (h_r + h_t)/2 \qquad (2.25)$$

where h_r is the effective residual resistance immediately after cleaning and h_t the terminal resistance. The term "effective residual resistance" refers to the time zero intercept value of the linear extrapolation of the resistance-time curve that appears as a nearly reproducible quantity during repetitive filtration and cleaning cycles. In contrast, the instantaneous values of resistance when filtration is resumed, and those during the first few minutes of filtration, are difficult to measure and may vary from cycle to cycle because of rapidly changing cake structure. In practice, use of the more readily determined "effective residual resistance", results in a slightly conservative (higher) estimate of average operating pressure from Equation (2.25). Thus, the cost of fan power, a major consideration in filtration, is dependent on cleaning only insofar as the effective residual pressure resistance is determined by the specific method of cleaning.

It should also be recognized that the use of Equation (2.25) to estimate the average filter resistance over a filter cycle applies only to the time interval over which filter resistance increases from its h_r to h_t levels. If only a negligible change (decrease) in air flow rate takes place over the filter cycle, the average resistance, $\bar{h}$, calculated by Equation (2.25) provides a good estimate of power requirements for the specified filtration cycle. Variability in inlet concentration will require a time weighting of calculated power levels for successive averaging periods.

When a filter system is operated on a time cycle, the resistance increases for successive filtration cycles will vary directly with changes in inlet concentration. In principle, Equation (2.25) again will indicate the average pressure loss with respect to defining power requirements except that the terminal resistance, h_t, may vary with time and the other terms cited below.

$$\bar{h} = (h_r + KV^2C_it)/2 \qquad (2.26)$$

if the filtration velocity, V, the inlet concentration, C_i, and presumably the specific resistance coefficient, K, for the specified dust/fabric combination remain invariant over the period of filtration, the estimation of $\bar{h}$ depends only upon the filtering interval, t. Variation in the other parameters merely requires that Equation (2.26) be modified to show their time dependencies.

It is not readily apparent that when several filter bags or compartments are cleaned sequentially, the overall average system resistance may be expressed in terms of the same variables describing a single element or chamber. Because the mathematical procedures necessary to illustrate the above approach are cumbersome although actually quite simple, the details have been relegated to Appendix J. It is shown that if a linear relationship exists between resistance increase and time, and the specific resistance coefficient is independent of the method of shaking, the average system resistance can be calculated on the basis of single bag (or compartment) parameters.

As shown in Appendix J, the average system (multi-compartment) filter drag may be expressed in the alternate forms given by Equations (2.27) and (2.28).

$$\frac{\bar{h}}{\bar{V}} = \frac{S_t + S_e}{2} \tag{2.27}$$

$$\frac{\bar{h}}{\bar{V}} = \frac{Se + KV\, C_i t}{2} \tag{2.28}$$

If it is assumed that the average air flow (and filtration velocity) does not change significantly with time, Equations (2.27) and (2.28) reduce to the same form and involve the same parameters appearing in Equations (2.25) and (2.26).

Linearity of Resistance-Time Curves - Resistance versus time curves based upon constant filtration velocity and constant inlet concentration are shown in Figure 48 for various fabrics and a fly ash aerosol. Despite the variations between the intercepts for the actual and effective residual resistance values, a good approximation to linearity was usually achieved within 5 minutes. Generally, these findings are substantiated by performance data for woven fabrics appearing in the literature.[8] In the case of heavily napped media or the typical felts discussed in Chapter III, non-linear resistance versus time curves are often encountered. As pointed out in the literature, high seepage rates or cake compression may also lead to non-linearity. Inspection of Figure 48 indicates clearly that the use of Equations (2.25) through (2.28) to estimate average resistance and power requirements will provide slightly conservative results seldom more than 5 percent higher than the true values.

Specific Resistance Coefficient, K - While comparing the results of fly ash filtration with four different fabrics, K values* were determined for relatively new and well-used fabrics shaken $\sim 2.0 \times 10^7$ times, Table 16. In each instance, the bag was repetitively loaded and cleaned many times to equilibrate it before making measurements. Althouth the residual dust holdings of all fabrics were substantially reduced, ~ 25 percent, by the extended shaking, no consistent nor large changes were noted for K values. Considerably more variation was found among different fabrics, suggesting that the surface structure of a fabric affects the average pressure drop during filtration more than differences in cleaning method. For example, Figure 32 indicates that K values were substantially unaltered despite a broad range in shaking frequencies and shaking amplitudes.

---

*K = Specific Resistance Coefficient = $\frac{\text{Resistance Change}}{\text{Filter Velocity} \cdot \text{Cloth Loading}}$

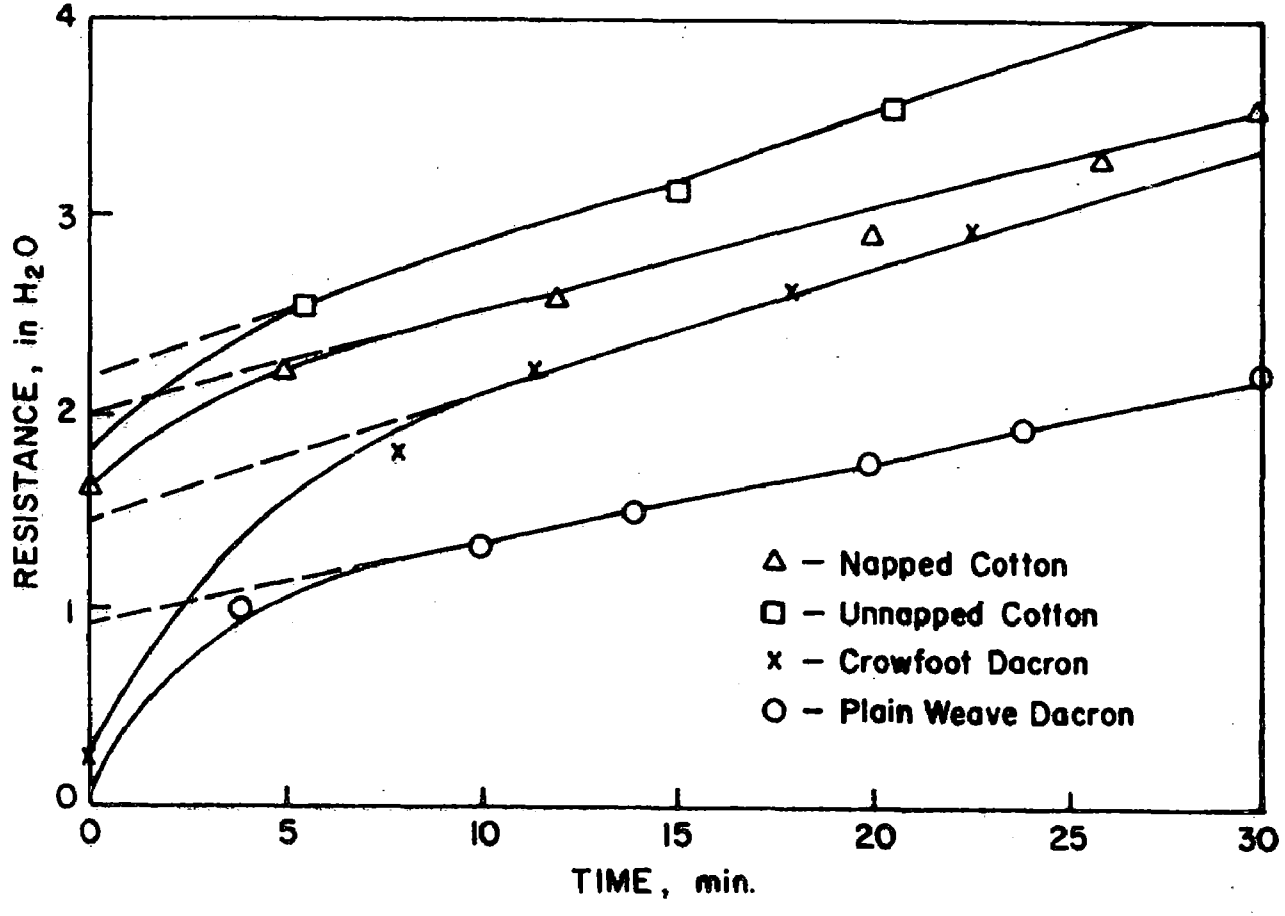

Figure 48. Resistance changes during fly ash filtration for well used fabrics (see Table 16)

Table 16. FLY ASH FILTRATION CHARACTERISTICS FOR NEW (< 10^4 SHAKES) AND WELL-USED (2 X 10^7 SHAKES) BAGS

	Fabric type[a]							
	Plain weave Dacron		Crowfoot Dacron		Napped		Unnapped	
					Cotton	Sateen	Cotton	Sateen
	N	U	N	U	N	U	N	U
Residual drag in H_2O/ft./min.	0.17	-	(0.37)	(0.02)	(0.20)	(0.53)	0.47	(0.60)
Effective residual drag in H_2O/ft./min.	(0.35)	0.30	0.43	0.47	0.23	0.67	0.67	(0.73)
Terminal drag in H_2O/ft./min.	(0.81)	0.73	1.12	1.11	0.82	1.17	1.24	1.41
Dust collected[b] per cycle grains/ft.^{2}	278	255	288	275	295	312	284	290
"K" value in H_2O ft./min./ lbs./ft.^{2}	11.6	11.0	16.8	16.3	14.0	11.2	14.1	16.4
Residual dust grains/ft.^{2}	207	113	92	73	449	336	413	375
% dust removed[c] by shaking	57	69	76	79	48	48	41	41

[a] 10 ft. long x 6 in. diam. bags, N = New, U = Well used.

[b] Inlet loading ~ 3.5 grains/ft.^{3}, Filter velocity - 3 ft./min., 30 min. filter cycle.

[c] Cleaning cycle - 360 shakes, 1 in. amplitude, 8 cps.

In another series of tests, the fabric was deliberately undercleaned with respect to the number of shakes to determine the impact upon K. Figure 49 shows the relationship between filter drag and total fabric dust holding for four successive filtration and cleaning cycles. Tests were initiated with a bag that had been shaken at 11 cps for 10 minutes. In real practice, no such cleaning cycle would be used because of loss of service (filtration) time and fabric overstressing. The first cleaning, however, provided a base line with which to compare the effect of shaking duration on performance parameters for a fixed shaking technique (1 in. amplitude and 6.8 cps).

During the first filtration cycle the average value for K was 12.4 as the fabric dust holding rose to 450 grains/ft.^{2}. Use of the standard cleaning regime, ~ 360 shakes, reduced residual filter drag to roughly the starting level although the residual dust holding was considerably greater, ~ 210 grains/ft.^{2}. A slight increase in "K" was observed for the second filtration cycle. Of more significance, however, was the fact that use of only 86 shakes led to a still higher residual drag and a nearly doubled residual fabric loading, roughly 400 grains/ft.^{2}. A third filtration interval indicated that "K" values were continuing to increase, 14.3 to 16.5, as the number of shakes were reduced. A minimal shaking process, 30 shakes, led to a large decrease in filter drag but was quite ineffective in removing dust. Along with a large residual dust holding of 620 grains/ft.^{2}, the K value was almost doubled during the last filtration cycle.

These tests, which confirm the earlier measurements of Walsh and Spaite,[1] indicate that the number of shakes required to maximize filtration capacity exceeds those needed to reach a minimum drag value. According to data presented earlier, Figure 32, the K value for a fixed dust/fabric system undergoes little change provided that the number of shakes is in excess of 200. It is postulated that with less shaking, the dust residing upon the filter undergoes compaction and thereby

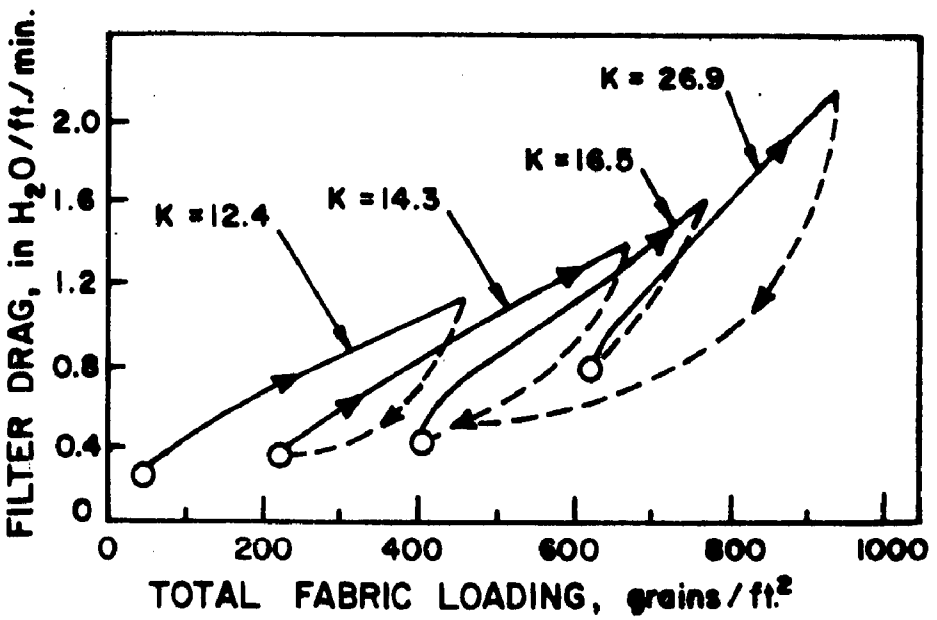

Initial Fabric State	Subsequent "K" Value*
Extended (Excess) Cleaning	12.4
356 Chakes, in ampl., 6.8 cps	14.3
83 shakes, in ampl., 6.8 cps	16.5
30 shakes, in ampl., 6.8 cps	26.9

*in H_2O/ft./min. x lb/ft.^{2}

Figure 49. Effect of insufficient (non-equilibrium) shaking on "K", filter drag and fabric loading with fly ash at 3.5 grains/ft.^{3} and 3 ft./min. filter velocity 10 ft. x 6 in. cotton sateen bag

presents a more resistant path for air flow. As indicated previously, K values depend not only upon dust properties but also upon the surface properties of the filter media as shown in Table 16.

Effective Residual Resistance - The filter resistance immediately following cleaning was examined with respect to the energy imparted to the shaken bag at various acceleration levels. According to Figure 50, an inverse relationship is suggested despite the scatter of points. Exclusion of the flagged point, however, indicates a progressive reduction in residual resistance as the shaking intensity (acceleration) is increased. The solid line, Curve C, depicts the normalized linear regression line having a correlation coefficient, r = -0.83, and a slope of -0.26. The dashed line, Curve A, represents an empirical fit to a slope of -0.5 to simplify rough calculations. Curve A′, which shows the approximate relationship between residual fabric loading and bag acceleration, also appears in Figure 34.

In that the actual slope of this curve, -0.39, as shown by the linear regression line Curve B (r = -0.93) was roughly -0.5, the force fit curve with a slope of -0.5 was presented in Figure 34 for calculation purposes when estimated bag accelerations are in the 3 to 6 g range.

It was not unexpected that a broad spread of data points would obtain for the residual resistance measurements because fabric flexure upon resumption of air flow, and re-entrainment and re-deposition of system dust deposits upon the filter surface could well cause wide variations in the character of the residual dust/fabric structure.

From a practical viewpoint, the actual magnitude of the resistance changes do not appear to be very large relative to the range of accelerations over which most fabric filters would be expected to operate. In the limiting case depicted by extended shaking periods, the resultant dust holdings and resistance, respectively, would ultimately be expected to converge, regardless of the intensity of shaking.

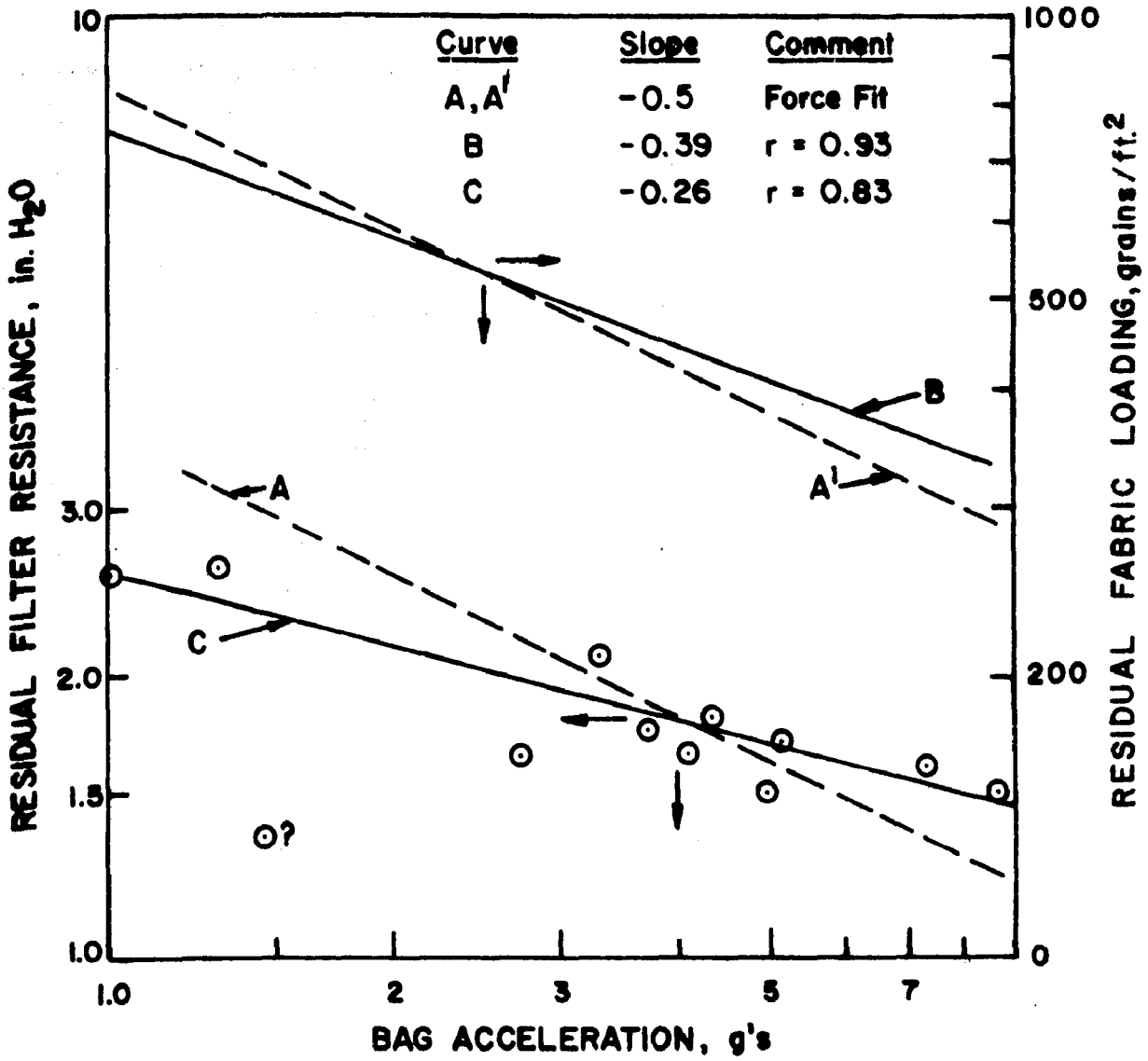

Figure 50. Residual filter resistance and residual fabric loading (Figure 34) versus bag acceleration for fly ash/sateen weave cotton system

Past studies by Walsh and Spaite[1] appear to confirm the latter observation.

As a matter of interest, the relationship between fabric dust holding and residual resistance may be inferred by comparing the curves of Figure 50. First, in the strictly hypothetical case where dust removal is assumed to result from the spallation of an essentially superficial dust layer, a linear relationship should prevail between resistance and the amount of dust remaining on the filter. In the above situation, it is assumed that no significant change in pore structure takes place and that a decrease in dust holding is reflected by a proportionate decrease in dust layer thickness. Were this concept valid, the slopes of Curves B and C would be identical. The fact that they differ, however, is understandable if one assumes that in addition to increased acceleration removing more dust, the increased intensity of shaking also compacts and thereby decreases the porosity of the interstitial dust deposits. In accordance with a simplified expression of the factors determining resistance to air flow in filter beds,

$$\Delta p = \phi\left(\frac{\mu V \beta^{n} L}{D_f^{2}}\right) \qquad (2.29)$$

gas velocity, (V), gas viscosity (μ) and characteristic collector diameter (D_f) are assumed to be constants. Despite the fact that the dislodgement of dust will lead to a decrease in effective bed depth (L), the compaction process will increase the overall packing density (β) of the residual dust/fabric structure. Since the exponent for n is about 1.5, the residual filter resistance should be proportional to the residual fabric holding raised to the same power, $n < 1.0$.

Insofar as fly ash was concerned, the range of effective residual resistances was small, approximately 1.5 to 2.4 in. water and equivalent to residual drag levels of 0.5 to 0.8 in. water/ft./min. During the early use period for the bags, up to 10^4 shakes, a gradual increase in residual resistance was noted, roughly 25 to 35 percent, indicating a plugging of fabric interstices.

After extended usage as simulated by accelerated shaking (up to 2×10^7 shakes), cotton fabrics appeared to develop slightly higher residual and terminal drag levels. Thus, power requirements for treating equivalent gas volumes would increase in roughly the same proportion. According to tests with the Dacron fabrics, Table 16, extensive shaking did not appear to change significantly the resistance characteristics nor the dust holding capacity. It should be noted, however, that the Dacron media were also less efficient than either the napped or unnapped cotton bags.

Discussion of Operating Parameters for Various Filter Systems - Tests results summarized in Tables 11 and 16 and Figure 36 provide basic operating parameters that enable estimation of power requirements, cloth area for arbitrary limits set for terminal drag, and frequency of cleaning. It was pointed out previously that the holding capacity of a given fabric for certain dusts appeared to be a combined function of both dust and fabric properties. Thus, K values for fly ash ranged from 11.0 to 16.8 depending upon whether plain weave Dacron or Crowfoot Dacron were the filter media, with cotton fabric generally lying in the 11.2 to 14 range. On the other hand, talc filtration with various fabrics, Figure 38, showed much smaller variations for K.

As far as fly ash was concerned, extended shaking did not appear to have any significant bearing on K values, regardless of the fabric used. Therefore, power requirements would increase in direct proportion to the average filter resistance over the cleaning cycle,

Equation (2.25), provided that a rise in terminal drag were permissible. If a definite upper limit were set for terminal drag, it would be necessary to either increase the cloth area or increase the cleaning frequency to handle the inlet dust loading.

Napping of cotton sateen appeared to reduce resistance characteristics appreciably for relatively new media but the advantage diminished after an extended shaking period. Nevertheless, according to Table 16, the dust holding capacity for the napped cotton appears to be about twice that for the unnapped material when a constraint of 1 in. water/ft./min. is set for terminal drag.

In that residual resistance (and drag) values were consistently lower for talc, irrespective of filter media, the average resistance and power level would also be consistently lower with a 1 in. H_2O/ft./min. set for the terminal drag. On the other hand, the dust handling capacity for equivalent filter cycles would be about half as much for talc as shown in Table 11 and implied by the higher K values for talc, Figure 38.

Bag Life

It is reasonable to assume that bag motion will always contribute to fabric deterioration whether by fatigue or embrittlement, by abrasion between dust and/or fibers or by some heretofor unidentified mechanisms. Degradation due specifically to fabric motion is difficult to isolate in commercial practice because heat, abrasion and corrosive atmospheres may also augment the damage done by flexure alone.

Because the cost of filter media represents a significant fraction of overall system operating costs, a portion of this study was devoted to determining the effect of lengthy mechanical flexure on filter performance. As described previously, life tests, based upon a conventional shaking procedure, exposed various full-size filter bags to

some 2 x 10^7 individual shakes, representing a nominal 3 to 5 year's continuous field service. Periodic loading of the filters with fly ash to their normal dust holding capacities permitted the investigation of the combined effects of mechanical flexure and abrasion on filter performance.

A summary of test parameters and the observed changes in bag length and tensile modulus after 2 x 10^7 shakes is given in Table 17 for parallel accelerated life tests on three unnapped, cotton bags. Turnbuckles were installed in the bag suspending arms as a means of adjusting the tension to the initial values as stretching progressed. After the first few days, during which time frequent tension adjustments were necessary, tension was adjusted once per day over the remainder of the test period.

In Figure 51, the elongation properties for the test media described in Table 17 are shown as a function of the cumulative number of shakes. As a rough estimate, the total stretch varied as the 1/4 power of the cumulative number of shakes given the bag.

Over the test period of about 4 weeks, the unnapped cotton bags stretched approximately 1-in. while the elastic moduli of the bags more than doubled. In these tests, the new bags stretched about 1/8 of an inch in the first 2 minutes of shaking, the rate of stretching decreasing significantly thereafter. Note that this amount of stretching without re-tensioning would produce a tension decrease of 2 to 4 pounds, depending on the individual bag modulus. These tests clearly show the need for frequent adjustment of tension, particularly during the early life of a bag, if excessive slack conditions are to be avoided. They also suggest that bags should also be well-broken in, prestretched or decrimped before installation, to minimize early maintenance problems.

Following the above tests, these bags were hung in storage (top support only) for about 2 months. At that time, the modulus of bag

Table 17. EFFECT OF EXTENDED SHAKING ON TENSILE PROPERTIES OF CLEAN AND DUST LADEN COTTON BAGS, FLY ASH AEROSOL

Bag number[a]	Initial tension (lbs.)	Shaking[b] tension (top) (lbs.)	Maximum[c] dust loading (grains/ft.^{2})	Cumulative stretch (in.)	Elastic[d] modulus (lbs./in.)	
Unnapped cotton						
Reference[e]	-	-	-	0	16.5	
8	Top 3.1 Avg. 2.2	6.5	420	1.4	44.5	
9	Top 0.9 Avg. 0.4	3.0	None (clean)	0.81	31.4	
10	Top 1.3 Avg. 0.4	4.5	420	1.03	39.6	
					Initial[f]	Final
Napped cotton						
11	Bottom 0.5	-	420	1.2	26.5	37.2
Plain-weave Dacron						
12	Bottom 0.5	-	420	0.79	10.1	10.1
Crowfoot Dacron						
13	Bottom 0.5	-	420	0.69	33.0	39.1

[a] 10 ft. x 6 in. bags.

[b] Shaking system, 8 cps, 1 in. amplitude, 2 x 10^7 shakes.

[c] One 30 minute filtration cycle per day.

[d] Special modulus applying only to a 10 ft. x 6 in. bag of specified fabric.

[e] Clean, unused bag, no prior shaking.

[f] Measured after 30 minutes continuous shaking.

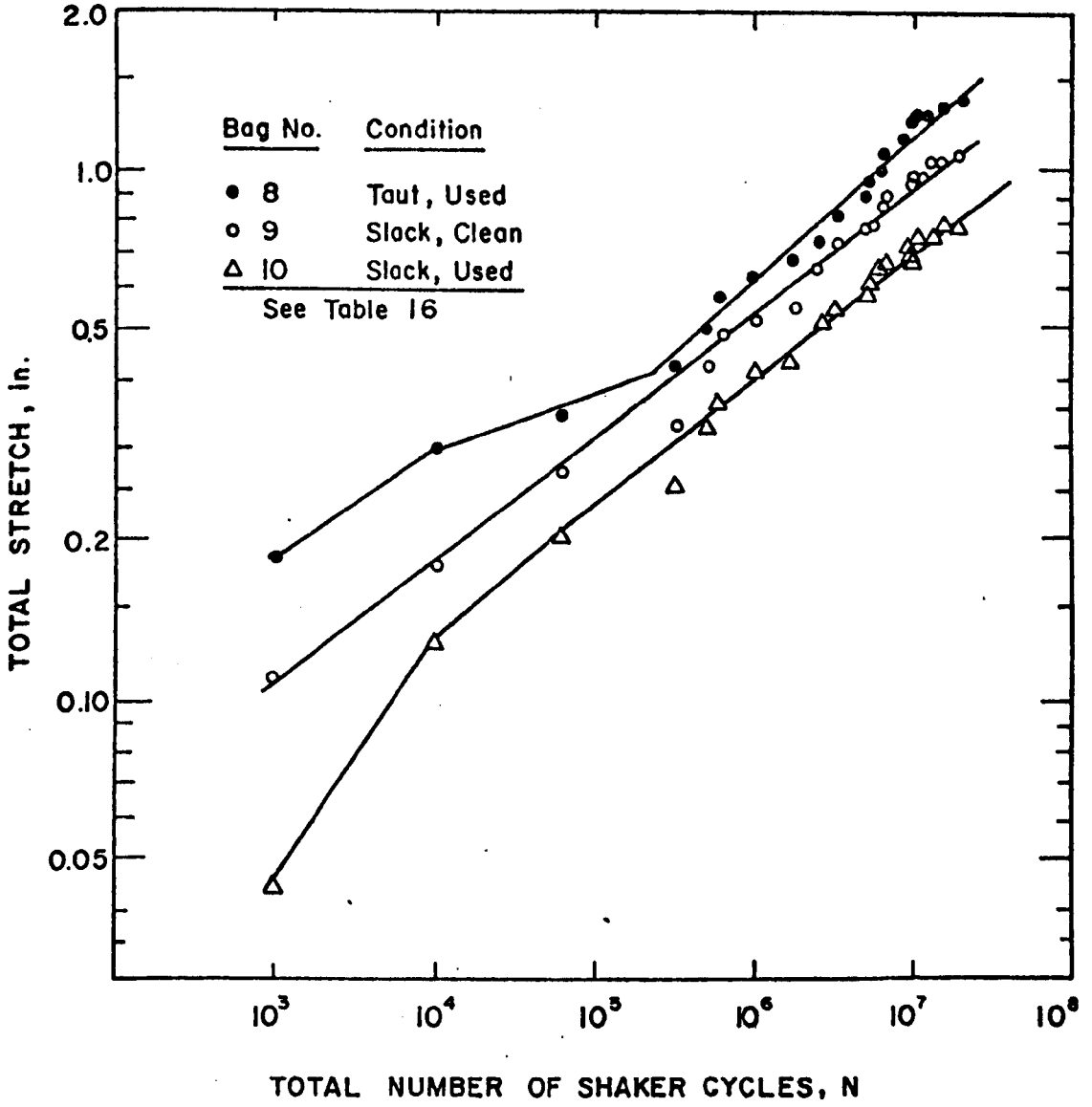

Figure 51. Bag elongation versus total number of shakes for used and clean, 10 ft. x 6 in. sateen weave cotton bags

No. 10 was found to have recovered to approximately 20 lbs./in. Since the moduli values in Table 17 were measured a few hours following the end of the extended shaking period, the bags may have already undergone partial recovery. Because of this hysteresis factor, it is possible that the bag moduli were actually higher during the shaking period.

Practically no sign of bag wear was observed. Dust collection efficiency tests conducted once per week during the life testing process indicated a gradual increase of dust penetration to about 10 times the initial level, Table 13. Despite the tenfold increase in effluent concentration, the cotton fabric efficiencies for fly ash were so high that outlet concentrations were still about 10^3 times lower than normal atmospheric levels.

There was absolutely nothing that could be termed a bag failure with respect to filtration capability. The outer surfaces of the bags showed no fabric deterioration except for some raising of a light nap on the lower portions of all three bags. The outer (clean) surfaces of the loaded bags were stained by low level seepage of dust through the fabric, particularly in the lower portions of the bags near the nodal areas and in folds of the bags near the tented tops (probably the areas of greatest flexure). The clean filter bag being shaken adjacent to the two loaded bags also acquired a staining in the vicinity of the nodes due to external contamination. However, no changes in the mechanical properties nor the filtration capabilities of the bags were observed that could be attributed to the fly ash particles beyond the effect of deposit weight on shaking tensions. Since a large fraction of the fly ash particles is spherical (cenospheres), it is expected that they would cause less damage than hard, jagged particles.

Frictional wear of the bag suspending loops was observed at their contact points between the loop and the supporting 1/8th-inch steel

rods. At some points the loops were perforated by either a rod end or by rough spots on the rod surface. Presumably, the same type of inconsequential wear occurs in field installations (assuming that the above damage is external to the enclosed filtering volume).

The degradation of glass filter fabrics due to shaking has been extensively studied by several laboratories.[17] This deterioration is of a unique type, however, in which abrasive scratching or corrosive pitting of the surface of individual glass fibers produces stress points that lead to complete fracture under subsequent flexure. Because most filtration fibers are not as brittle as glass, their service lives are usually much longer.[8] Most fibers and fibrous materials are tested for their chemical, thermal, and mechanical resistance properties by the manufacturers. Unfortunately, manufacturers are often not cognizant of the ultimate use of their materials in filter bags nor to the types of stresses and abuse encountered in the field. As a result, the effects of filter cleaning, including mechanical shaking, on filter life are generally poorly defined.

Life tests were also performed on three other bag types; napped cotton, plain-weave Dacron, and crowfoot Dacron, Table 17. The total elongation features for these bags, Figure 52, were approximately the same as those of the unnapped, Figure 51. Napping of the cotton bag apparently raised its initial modulus relative to that of the unnapped media, perhaps because the bag was mechanically stretched in the process of napping. Note that even the crowfoot Dacron with multifilament yarns was stretched moderately by the extended shaking. It is not clear why the plain-weave fabric had the same modulus after shaking in contrast to the other fabrics tested. Again, the three fabrics continued to filter effectively after lengthy shaking and no mechanical wear of the fabric surfaces was visible.

The results of special tensile tests performed by an independent laboratory with an Instron Tester on several 16 in. x 2 in. wide samples

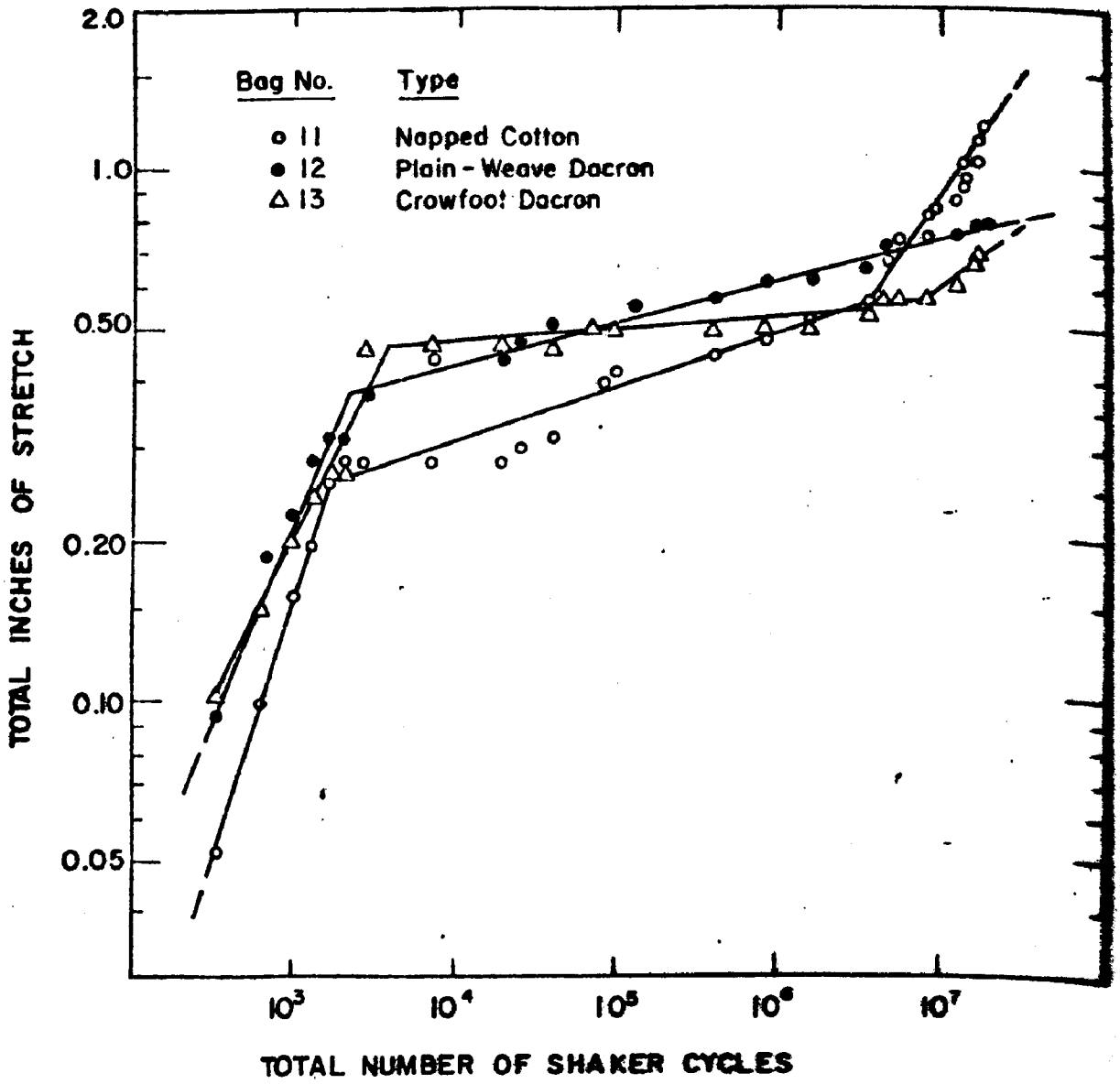

Figure 52. Bag elongation versus total number of shakes for various used 10 ft. x 6 in. fabric bags

of new (unshaken) and used (2 x 10^7 shakes) fabrics are summarized in Table 18. The purpose of these measurements was to determine by conventional textile rating apparatus whether any important changes in fabric mechanical properties had resulted from extensive shaking.

Fabric specimens were clamped between jaws 6 in. apart and stretched at a rate of 2 in./sec.

As far as the unnapped cotton bags are concerned, it can be seen that there are no significant differences between descriptive parameters for new and well-used bags. Furthermore, no specific locations on the surface of a bag appeared to show signs of excess stress and/or strain. The ultimate load (failure) levels for cotton were approximately 200 times greater than the dynamic tensions seen by the bags during shaking. Generally, the negligible impact upon filter performance both efficiency- and resistance-wise and the lack of visual signs of damage or changes is supported by the tests described in Table 18.

Initial "ultimate loads" for both Dacron fabrics were considerably higher than those determined for cotton bags. Extended shaking, however, appeared to have a weakening effect on the Dacron bags, although not at a level to suggest any impairment of filter function.

The results of the test series indicated that mechanical shaking, per se, of woven cotton and nonmineral synthetic fabrics does not damage the media over relatively long simulated working periods, 3 to 5 years. Additionally, nonabrading type dusts having smooth surfaces do not appear to detract from effective field service over the previously stated time period. With respect to the media described in Table 18, it is suggested that thermal effects and chemical corrosion singly or in combination with mechanical flexure are major causes for bag failure. One might also include such factors as installation at excessive tension

Table 18. TENSILE MEASUREMENTS ON NEW AND USED FABRIC STRIPS WITH INSTRON TESTER

Bag number	Ultimate[a] load (lbs./in.)	Standard[b] deviation (lbs./in.)	Ultimate[c] strain	Break point[d] modulus (lbs./in.)
Unnapped cotton				
Reference bag[e]	100	7.7	0.24	416
8U[f]	106	6.7	0.24	441
9U	103	5.0	0.25	413
10U	103	8.7	0.24	430
Napped cotton				
Reference bag	107	7.2	0.24	446
11U	112	6.0	0.22	508
Plain-weave Dacron				
Reference bag	173	18.9	0.43	402
12U	152	4.0	0.40	380
Crowfoot Dacron				
Reference bag	421	5.5	0.40	1060
13U	366	19.5	0.29	1260
Unnapped cotton - bag 88[g]				
Top, left	101	8.5	0.26	–
Top, rear	107	4.1	0.24	–
Center, front	106	7.6	0.24	–
Bottom, rear	107	5.8	0.25	–
Bottom, right	104	7.4	0.26	–

[a]Maximum stress per inch of strip width at break point.

[b]Standard deviation of break point stress.

[c]Strain immediately before breaking, clamps set at 6 in.

[d]Point function only.

[e]Reference bag, no prior shaking.

[f]U indicates 2×10^7 shakes, see Table 17.

[g]Five strips from various sections of single bag.

or slackness and the failure to prevent the formation of cementlike deposits by hydration reactions.

CONCLUSIONS TO MECHANICAL SHAKING STUDY

In the following section we summarize the major conclusions that can be drawn from the mechanical shaking studies discussed in Chapter II. With respect to the order in which these conclusions are presented, two key factors have been considered. First, one of the most pressing concerns is the effectiveness of various particulate control systems in the removal of fine particles, ≤ 1 μm. Our current efforts are now directed not only to overall mass collection efficiencies but also to the actual concentration and size composition of collector effluents. Second, given the specification that particulate emissions from a given source must not exceed certain boundaries, the use of mechanical shaking has been examined with respect to optimizing methods to achieve these criteria while minimizing those factors contributing to capital and operating costs.

General Conclusions

To avoid misinterpretation and misapplication of the results of this study we present the following general conclusions.

1. Limits of data application - Unless it is clearly indicated that a conclusion may be given broad interpretation, the reader should assume that descriptive and operating parameters cited for a specific dust and fabric combination may apply only to that specified dust/fabric combination.

   Measurements reported in this study and also in the literature indicate that test results for a single dust or fabric are not sufficient to permit a generalized extrapolation to other dusts or fabrics. This problem results from the large number of independent variables needed to describe completely a dust and/or fabric and their respective interactions.

2. Need for further research - A major conclusion based upon the previous paragraph is that much more research on a

bench and pilot scale is required if one is to be able to predict the field performance characteristics of a fabric filter system without preliminary trials with the dust/fabric system involved.

3. Outlet versus inlet concentrations - It is strongly emphasized that no simple relationship exists between typical outlet and inlet concentrations for most fabric filters. More often, for a specified dust/fabric combination and a fixed operating mode for the collector, the average mass emission and its related size properties may be nearly independent of the concentration and size of the inlet dust. Furthermore, the fact that the dust penetrating a filter consists partly of agglomerates (which are formed within the filter from single particles but detached as clusters) prevents any accurate analysis of collector fractional particle size efficiencies.

It is also emphasized that the particle concentrations departing the fabric filter may vary by several orders of magnitude over a complete filter cycle. Thus, for all practical purposes, the only useful size parameters that can be generated for field application are those describing average performance over a complete and representative filter cycle.

Particulate Emissions

Those conclusions relating to specific tests on various dust/fabric combinations are presented first with respect to the impact of the mechanical shaking process upon particulate effluent characteristics. Whenever possible, an attempt has been made to indicate the limit to which test results may be extrapolated to other dusts and fabrics.

1. Fly ash and talc aerosols or other particulates having similar size properties can be filtered at very high efficiencies with sateen weave cotton bags, ~99.9999 percent for inlet concentrations of 3.5 grains/ft.^{3}. Filtration efficiencies for Dacron media are high, 99.7 to 99.9+ range, but based upon an inlet concentration of 3.5 grains/ft.^{3}, outlet concentrations are much greater as pointed out below.

2. Average outlet concentrations for the cotton fabrics range from 10^{-7} to 10^{-4} grains/ft.^{3} depending upon the number of shaking cycles, the degree of tension in the bag, the precise mode of shaking, and the residual dust holding. Average outlet concentrations for the Dacron media with fly ash and talc aerosols are about 10^{-3} to 10^{-2} grains/ft.^{3}, about 1000 times greater than those for the cotton fabrics. One concludes that where dust toxicity is important the fabric performance should always be examined on the basis of the outlet concentrations and not efficiency alone.

3. For a specified set of operating conditions, the magnitude of the average outlet concentration is nearly independent of the inlet dust concentration. Thus, an order of magnitude increase in the inlet loading may result in a corresponding rise in collection efficiency but a negligible change in the mass and size distribution of the discharged particulates.

4. Effluent particle size distributions for fly ash and talc aerosols, as measured by instruments having 0.3 μm as the smallest resolvable size, were about the same as for atmospheric dust, CMD = 0.5 μm, σg = 1.5.

5. Instantaneous values for outlet concentrations measured from the beginning to the end of a normal filtration cycle may decrease by less than one to several orders of magnitude. The greatest changes take place with the fabrics having the highest efficiencies.

6. The fact that as much as 90 percent of the total dust emission from a filter may take place during the first minute of use following cleaning suggests strongly that a recycle of the early effluent would greatly improve the system performance.

7. The key factor determining how rapidly the restoration of an efficient filtering layer is accomplished is the rate at which the inlet dust can completely fill the pores within the fabric weave.

8. The filling or bridging-over of the fabric pore structure appears to depend upon the characteristic specific volume of the dust within the filter interstices as well as the pore diameter, and the ratio of particle to pore diameter.

9. The slightly lower outlet concentrations observed for talc (relative to fly ash) result from a low bulk density that facilitates closure of the pore deposits and the irregularity in shape that retards seepage or slippage such as found for spherical particles; e.g., fly ash cenospheres.

10. Variations in mechanical shaking parameters have the following impact upon fabric filter effluent concentrations.

- An increase in shaking frequency from 4 to 11 cps does not produce significant increases in effluent concentrations. Thus, the rate of fabric flexure is not considered an important factor in determining particulate emissions.
- An approximate 10 times increase in outlet concentration occurs when shaking amplitude is increased from 1 to 2 inches. It is concluded that it is not the amplitude per se but the tension increase on the filter bags and the resultant increase in pore dimension that leads to greater emissions.
- Particulate emissions relate inversely to the number of shakes given a filter up to about 200 shakes. Beyond this point, further dust removal is negligible and filter emissions are essentially constant.

11. Accelerated life testing of cotton and Dacron bags by shaking each approximately 2 by 10^7 times (equivalent to about 3 to 5 years' field service) leads to inconsequential increases in the outlet particle concentrations, 2.5 times for the napped and unnapped cotton and 4.3 times for the Dacron media. It is concluded that increased dust penetration results from the slightly lower residual dust holdings observed for both media after extended shaking.

12. Average particle outlet concentrations (or the amount of dust leaving the filter over a representative filter cycle) can be related approximately to the residual or terminal fabric loadings (corrected to equivalent volume) by a simple exponential decay; e.g., a one order of magnitude decrease in the mass release for the addition of 90 grains of fly ash per square foot of fabric.

13. If the average outlet concentrations prove excessive for certain dusts, wherein there is little latitude in the choice of fabric media, the intensity of the cleaning action may be reduced at the expense of a higher residual resistance but a corresponding increase in collection efficiency. The above approach entails either added cost for increased fabric area or increased power costs because of higher resistance levels.

Dust Removal by Mechanical Shaking

The following conclusions are concerned with the relationships between the mechanical shaking process and the system performance parameters exclusive of particle effluent description.

1. Dust removal by mechanical shaking is best defined by relating the energy supplied by the shaking process to the adhesive and/or cohesive forces binding the dust to the fabric.
2. An increase in shaking frequency and/or shaking amplitude has a direct effect on shaking power and dust removal.
3. For a specified dust/fabric combination there is a characteristic residual dust loading (grains/ft.^{3}) and an effective residual resistance for each specific mode of shaking that are nearly independent of the fabric loading at the end of a filtration cycle.
4. The total number of shakes at a specified shaking frequency and amplitude should not be carried much beyond 200 to 300 since further dust removal and reduction of filter resistance is negligible. Continued shaking will only decrease the effective filter on-line time, increase the probability of shortened service life by unnecessary stress and abrasion damage to the fabric, and as stated previously increase the effluent concentration levels.
5. With respect to a given dust/fabric combination, the residual dust holding is best related to the average acceleration imparted to the bags during the shaking process. Based upon readily measurable (or predictable) physical properties of the fabric bags; the assigned shaking parameters (frequency, amplitude and duration); and the installed and dynamic tension, average bag accelerations are readily computed.
6. Residual fabric dust loadings correlate well with average bag accelerations for fly ash/sateen weave cotton systems. Over the acceleration range, 1.5 to 10 g's, residual dust holding varies approximately with the inverse square root of average bag acceleration.
7. Increase of accelerations beyond 6 to 8 g's does not lead to any significant decrease in residual dust holding.
8. For all practical purposes, there are upper limits to both the intensity and duration of the shaking process. Given sufficient shaking under strictly experimental

conditions, the residual dust holdings of many filters cleaned at different acceleration levels would ultimately converge. Thus, a mathematical description of the fabric cleaning process is necessarily constrained to operate within pre-set limits.

9. Installed bag tensioning does not appear to exert any significant effect upon the average bag acceleration provided that the initial values are in the 0.5 to 5 lb. range. It is the difference between shaking tension and averaged installed tension that determines average bag shaking amplitude and acceleration.

10. Installed bag tension levels should be as close as possible to a true slack condition where the top tension is that of the bag weight alone. If too slack, however; i.e., no actual stretching of the bag occurs even when the shaker arm sees its maximum displacement from center, transmission of shaking energy over the entire bag length is incomplete and cleaning is poor and nonuniform. Over-tensioning of the fabric bags affords no advantages with respect to dust removal but will expand the pore structure (greater dust penetration) and possibly shorten fabric life through excessive stretching.

11. Although slightly greater dust removal, ~ 10 percent, was obtained by adjusting shaking frequencies to resonance levels, it was concluded that the cost and complexity of constant "tuning" to compensate for dust loss was not justified.

Filter Resistance and Power Requirements

1. The actual energy expenditure for mechanical shaking is very small, approximately a few watts per bag, such that the cleaning power requirement is negligible compared to that needed to overcome the resistance to air flow through the filter media.

2. The residual (effective) filter resistance (and/or filter drag) can be related to the residual dust holding on a weight or volume basis for a specified dust/fabric system. Additionally, the residual resistance for different dusts may be related approximately on the basis of the volume of dust residing on the filter after cleaning.

3. Dusts with low bulk densities such as talc are collected more as superficial rather than as interstitial deposits. Therefore, dust is dislodged

more readily such that lower residual resistance levels obtain.

4. Specific resistance coefficients appear to be a combined function of both dust and fabric properties. In the absence of field data it is risky to attempt to predict "K" values without some trial data.

5. Undercleaning of a filter; i.e., less than the recommended 200 shakes, has an adverse effect on its K values, leading to decreased system filtration capacity for a specified working resistance range.

6. Filtration capacity, per se, is an indeterminate quantity unless one defines the upper allowable working resistance for the filter.

7. Average filter resistance with respect to estimating fan power requirements is the arithmetic average of the residual (effective) and terminal resistance values. This will apply for single bags or sequentially cleaned multicompartment units just so long as the system gas flow is reasonably constant.

REFERENCES

1. Walsh, G. W. and P. W. Spaite. An Analysis of Mechanical Shaking in Air Filtration. J. Air Poll. Control Assoc., 12:57, 1962.

2. Durham, J. R. and R. E. Harrington. Influence of Relative Humidity on Filtration Resistance and Efficiency. NAPCA, PHS, U.S. DHEW, AICHE 63rd Annual Meeting paper, Chicago, Ill., November 1970.

3. Zimon, A. D. Adhesion of Dust and Powder. Plenum Press, New York, 1969.

4. Lindsay, R. B. Mechanical Radiation. McGraw-Hill, New York (1960).

5. Shortley, G. and D. Williams. Elements of Physics. Vol. II, 4th Ed. Prentice-Hall, Inc., Englewood Cliffs, New Jersey (1965).

6. Sears, F. W. and M. W. Zemansky. University Physics. 3rd Ed., Part 1. Addison-Wesley Publishing Company, Inc., Reading, Massachusetts (1963).

7. Fink, D. and J. Carroll. Standard Handbook for Electrical Engineers. 10th Edition. McGraw-Hill, New York (1968).

8. Billings, C. E. and J. E. Wilder. Handbook of Fabric Filter Technology. GCA Corporation, Bedford, Massachusetts, Contract No. CPA-22-69-38, Prepared for National Technical Information Service, U.S. Department of Commerce, Springfield, Virginia 22151, Document No. PB 200-648, December 1970.

9. Spaite, P. W., J. E. Hagan and W. F. Todd. A Protective Finish for Glass-Fiber Fabrics. Chem. Engg. Prog., 59:54, April 1963.

10. Hicks, R. E. and W. G. B. Mandershoot. Flexing Fatigue of Glass-Fiber Filter Cloth. Textile Res. J., 942, September 1968.

11. Whitby, K. T. and D. A. Lundgren. Fractional Efficiency Characteristics of a Torit Type Cloth Collector. Torit Manufacturing Company, St. Paul, Minnesota, August 1961.

12. Spaite, P. W. and G. W. Walsh. Effect of Fabric Structure on Filter Performance. Am. Ind. Hyg. Assoc. J., 24:357, 1963.

13. Draemel, D. C. Relationship Between Fabric Structure and Filtration Performance in Dust Filtration. Control Systems Laboratory, U.S. Environmental Protection Agency, Research Triangle Park, Report No. EPA-R2-73-288, July 1973.

14. Stephan, D. G. et al. A New Technique for Fabric Filter Evaluation. AIHA J., 28:276, 1958.

15. Dennis, R., G. A. Johnson, M. W. First, and L. Silverman. How Dust Collectors Perform. Chem. Eng., 59:196, 1952.

16. Robinson, J. W., R. E. Harrington and P. W. Spaite. A New Method of Analysis for Multicompartmented Fabric Filtration. Atmos. Envir., 1:495, 1967.

17. Spaite, P. W. and R. E. Harrington. Endurance of Fiberglas Filter Fabrics. JAPCA, 17:310, 1967.

CHAPTER III

PULSE CLEANING STUDIES

OBJECTIVES AND APPROACH

Within the last 15 years, reverse pulse cleaning has seen increased use for many types of dust and fume control. Nearly every large manufacturer of fabric filter equipment offers at least one model cleaned by this method.[1] Because of the growing utilization of filter systems cleaned by high pressure reverse air pulses, it is important that the mechanics of this cleaning process be fully understood. Accordingly, a study of reverse pulse cleaning, as reported in this chapter, was instituted to achieve the following objectives:

- To determine the effect of design and operating parameters on the performance of pulse-cleaned equipment with special emphasis on the particle size and concentration of the effluent dust.
- To determine the power requirements for various operating modes.
- To establish an improved base for future studies, field testing, design modifications, and preparation of operating guidelines.

In order to represent commercial equipment as it operates in the field, a full-scale, pulse-cleaned fabric filter system was constructed. Considerable flexibility was incorporated in the design to permit simulation of several common configurations and operating conditions. Instrumentation was provided for measuring bag motion, bag weight, and the

instantaneous pressure differential across the bag. These variables, which are seldom monitored in the field, were considered fundamental to describing the pulse cleaning process.

Two types of filter bags (Dacron and wool felt) and two test dusts (fly ash and talc) were used in the test program. The various cleaning cycles and filtration conditions evaluated in the study encompassed those conditions commonly encountered in industry. Operating pressure differentials, cleaning power requirements, and dust concentrations emitted by the filter were measured for all test runs, since these factors represent the main criteria for assessing cost and performance. Additional details concerning the equipment and test procedures used are discussed under APPARATUS, MATERIALS AND TECHNIQUES.

The approach taken in the study was to determine first the variations in operating pressure differential and outlet dust concentration with selected operating and design parameters. These variations were then examined in terms of more fundamental parameters such as bag motion and particle adhesion versus removal mechanisms, in an attempt to explain the observed results.

BACKGROUND

Applications and Advantages

Pulse cleaning is accomplished by admitting a short-duration pulse of reverse flow, high pressure air to the clean air side of the filter bag. This method of cleaning was introduced in the mid-fifties by Pulverizing Machinery Co.[2] It has proven to be a utilitarian means of filter bag cleaning that is now offered by all large manufacturers of bag filter equipment. While there are no published statistics to indicate the proportion of the market represented by pulse-cleaning equipment, it is estimated that about one-third of current sales or about 3,000 installations per year are of the pulse-cleaned type. This equipment is employed

for many dust control applications as well as for chemical process operations.[1] Its application has been less common in areas where the gas temperatures are high, the dust loadings low (infrequent cleaning) or the dust especially fine (freshly generated fume).

Several characteristics of reverse pulse cleaning make this system very attractive for a large number of applications. Because the pulse of high pressure air is brief, typically 0.1 second in duration, the primary air flow does not have to be shut off during the cleaning. Instead, the pulse temporarily reverses the flow through the fabric due to the transient reversal of pressure gradient. The particle agglomerates dislodged by the pulse and reversed flow are sufficiently large so that much of the dust can settle to the hopper during the brief interruption of filtration. Thus, the equipment operates essentially on a continuous basis and with almost no moving parts except for solenoid valve elements. The fabric receives little mechanical wear when properly installed and thus has a long service life, unless damaged by some other environmental factor. Felts rather than woven fabrics are generally used in this equipment, because woven fabrics tend to be over-cleaned by pulsing, resulting in excessive leakage following cleaning. In addition, the frequent fabric cleaning rate permits filtering velocities typically three to four times greater than those used in shaken or reverse flow equipment without an accompanying pressure increase. Because the bags move less during cleaning, they may be packed together more closely. Additionally, little or no extra capacity need be installed to replace the filter surface temporarily removed from service during cleaning. The latter factor is especially advantageous with high dust loadings. In combination, the above features contribute to a reduced space (and volume) requirement for cleaning a specified gas volume.

Problem Areas

Despite the attractive features of the pulse jet system, there are still insufficient data to properly assess its cost and performance in many

field applications. Because of the need to use compressed air, it is recognized that the power costs associated with cleaning may often be higher than those for mechanically shaken systems of equivalent capacity. At the same time, however, the increased air-to-cloth ratios may provide compensating cost advantages with respect to reduced collector size and space occupancy requirements. If no alternate method is available to perform the required filtration process, however, any added cost must be accepted as a prerequisite to meeting the control needs.

An important disadvantage in certain cases is the generally lower efficiency provided by a pulse-jet system. For example, typical effluent concentrations from pulse-cleaned filters are about 100 times greater than those attainable with mechanically shaken fabrics. Additionally, because the energy of the high pressure air-pulse tends to dissipate rapidly as it travels down a bag, the length of pulse-cleaned bags is limited to 10 feet or less in most models.[1] If the felt does plug, it is usually the result of interstitial rather than surface deposition. This may require the removal and external cleaning of the bags (an expensive procedure) or a media replacement, both of which add to operating cost.

Collector Performance

Resistance and Particle Removal - The filter operating pressure differential and its relation to the cleaning regime has been studied by Dennis, et al.[3] Based upon tests with fly ash on one of the first types of reverse pulse equipment, the authors found the average operating pressure differential to be defined approximately by the following relation:

$$P\ (\text{in. } H_2O) = 1.1 + \frac{3.8\ (c_i)^{0.25}}{\left(\frac{P_c}{100}\right)^2 (f_c)^{0.5}} \qquad (3.1)$$

where dust loading (c_i) varied from 1 to 14 grains/ft.^{3}, the manifold compressed air pressure (P_c) varied from 60 to 120 psig, and the cleaning frequency (f_c) varied from 1 to 6 pulses per min. per bag.

Equation (3.1) applies to a nine-bag, single compartment, sequentially pulsed system using wool felt (6 ft. x 4.5 in.) bags at a filtering velocity of 8 ft./min. Pulse duration, nominally about 0.16 seconds, had no apparent effect on resistance or efficiency, at least with a nine-bag unit.

The same quantitative relationship was shown for a fine silica dust except that the resistance was considerably higher. Freshly generated iron oxide could not be filtered successfully with the fabrics available at the time of the earlier studies. Transient pressure levels were also estimated within filter bags during the pulse interval, but only during nonflow conditions.[3] Therefore, although these tests indicated the general wave form and magnitude of pressure pulses, they did not reflect true operating conditions.[3]

Although considerable laboratory and field data have been reported with respect to operating pressures,[3,4,5] data on collection efficiency and effluent dust properties for pulse cleaned filters are very sparse. Dennis, et al.[3] reported weight penetrations ranging from 0.1 to 0.01 percent for wool felt bags with fly ash and vaporized silica, respectively. No apparent correlation of the efficiency with any of the operating variables was noted. Berg[5] reported 0.1 percent particle penetration for Nomex felt in asphalt-concrete plant operations at gas temperatures of 400°F and inlet dust loadings (sand and limestone) of about 25 grains/ft.^{3}. There are several reasons for the scarcity of information in the above areas:

- In a very practical sense, the lack of any visible emissions coupled with the accepted generalization that all fabric filters operate at the 99 percent efficiency level or greater is often the basis for selection and favorable acceptance of fabric filter systems. Many users of filter equipment are disinterested in any details of particulate emissions so long as no complaints arise and no product loss is involved.

- Collection efficiency may be so high, or possibly so difficult to measure because of accessibility problems, that the sampling process is undesirably long.

- Because efficiency depends upon several factors; e.g., particle size, humidity, charge characteristics, state of fabric surface (just cleaned to fully loaded), all of which may vary considerably at a given plant site, one cannot rely on a few measurements to give an accurate portrayal of collector performance. Since a lengthy sampling period may not be acceptable, often for economic reasons, the net result is that few, if any, efficiency measurements are performed.

There are reasons to suspect that many factors affect cleaning effectiveness and dust collection efficiency, including dust particle size and physical properties; air temperature, velocity, and humidity; individual fiber properties; fabric weave, surface depth, porosity, and mechanical characteristics; the dimensions and physical properties of the filter bags; the arrangement of bags in the dust collector; the cleaning pulse - its intensity, duration, and frequency, and the accompanying reverse flow of air through the filter.

The experiments performed during this study were designed to accomplish the following objectives:

- Show the relative importance of several of the design and operating parameters cited above.

- Determine how these parameters can be controlled to attain optimum collector performance for specified dust removal criteria.

Factors Involved in Dust Removal

During one complete filtration cycle for a single bag at equilibrium conditions, fresh dust is deposited upon and within the fabric structure while an equal amount of dust consisting partly of the newly arrived material and partly of previously deposited dust is dislodged by the cleaning action. Of the total amount of dust dislodged by the pulse, a large fraction immediately redeposits when normal air flow is resumed. Some particles may remain within the fabric structure indefinitely, becoming part of a residual deposit such as described under Shake Cleaning.

Adhesion - The residual and fresh dust is seldom deposited as a uniform layer as postulated for smooth-surfaced fabrics. The dust is usually concentrated in the form of tufts because the medium is thicker, much more open, and the pore structure more irregular. Thus, although the deposited dust may have an average internal strength profile analogous to that discussed under a postulated spallation theory for shake cleaning, the average profile concept may be misleading in the case of felted media. Individual fiber-to-particle and particle-to-particle bonds should be similar regardless of cleaning method. However, because the deposit on a felt is formed and dislodged at frequent intervals with pulse cleaned systems, the adhesive strengths and also the cleaning stresses can vary considerably from location to location.

Dislodgement - To the extent that the fabric moves or is deformed during pulse cleaning, the same four dust removal mechanisms apply as discussed in Chapter II for shaking cleaning; i.e., acceleration, sheer, flexure-stretch, and warping. However, the motion of a pulsed bag is less complex than that of a shaken bag, since it consists mostly of radial displacements. Therefore, acceleration and one-dimensional flexure appear to be the most probable mechanical removal mechanisms. In addition, a substantial reverse flow of air occurs during the pulse cleaning interval. This contributes additional removal stresses as

well as transporting the dislodged dust from the fabric interstices. One major goal of the pulse cleaning experiments was to determine the relative importance of the four mechanisms contributing to cleaning; i.e., acceleration and flexure coupled with reverse drag and re-entrainment.

Reverse Air Transport - The reverse flow of air through the fabric during the pulse interval flushes loosened particles from the fabric pores. Although not considered a primary dislodgement mechanism, the effect of the reverse flow on system operation may be considerable. After the bag is pulsed, there is little time before the flow recovers and filtering is resumed. During this interval, the particles must either fall into the hopper or else be re-deposited on the fabric. Only the largest agglomerates may have sufficient weight to continue falling after normal filtration flow has been resumed. Many agglomerates, however, will be drawn toward the fabric as they descend and be re-deposited at some lower station. The major transport processes associated with pulse cleaning are discussed in detail in Appendix L. It is shown on theoretical grounds that the main effect of extending the pulse duration is to provide added time for the agglomerates to fall. The benefit gained depends on the fall velocity of the agglomerates and hence their size and density. Thus one suggestion is that the performance of a filter might be improved by controlling the properties of the agglomerates removed in pulse cleaning.

APPARATUS, MATERIALS AND TECHNIQUES

A description of the apparatus, materials, and experimental techniques used in the pulse cleaning study is presented in this section. When appropriate, reference is made to Chapter II for previously detailed descriptions of test procedures, apparatus and test aerosols.

Filter Assembly

The basic filter assembly used in the pulse cleaning study is shown in Figure 53, which indicates schematically the major operating and design features. Dusty gas enters the hopper section at the base of the bag enclosure losing some of its particulate loading by gravity and inertial separation to the collection drum attached to the hopper. Filtration of the gas then follows via outside to inside flow through the felt bag, the latter supported by a wire cage to prevent its collapse. Cleaned gas departs through the upper exit plenum from which reverse pulse air is ejected into the bag exit in accordance with the programmed cleaning schedule.

The equipment was designed with sufficient flexibility to represent in principle, if not exactly in dimensional scaling, the more common types of commercial equipment. The 4-1/2 inch diameter bags were enclosed in an 8-inch by 8-inch chamber to provide the normal upward dust transport velocities found in the field. Bags of any length up to 8 feet could be accommodated in the housing by adding extension sections.

The volume of the housing surrounding the filter bag, including the dust collection drum indicated in Figure 53 was about 7 cu. ft. To facilitate observation of the bag during filtration and cleaning, a 3/8 inch thick Plexiglas window was installed in one wall of the housing. The other three walls of the housing were fabricated as a single movable section to allow rapid access to the filter bag and the instruments attached to it. It was constructed from a sheet of 10 gauge steel bent into channel shape and suspended on rollers to form a sliding enclosure. This enclosure was held in place by quick disconnect clamps and 1/8 to 1/4 inch neoprene sponge gasketing was used to prevent gas leakage.

The supporting wire cage for the filter consisted of 10, 1/8 inch steel rods spaced at equal intervals around the circumference of the bag, and

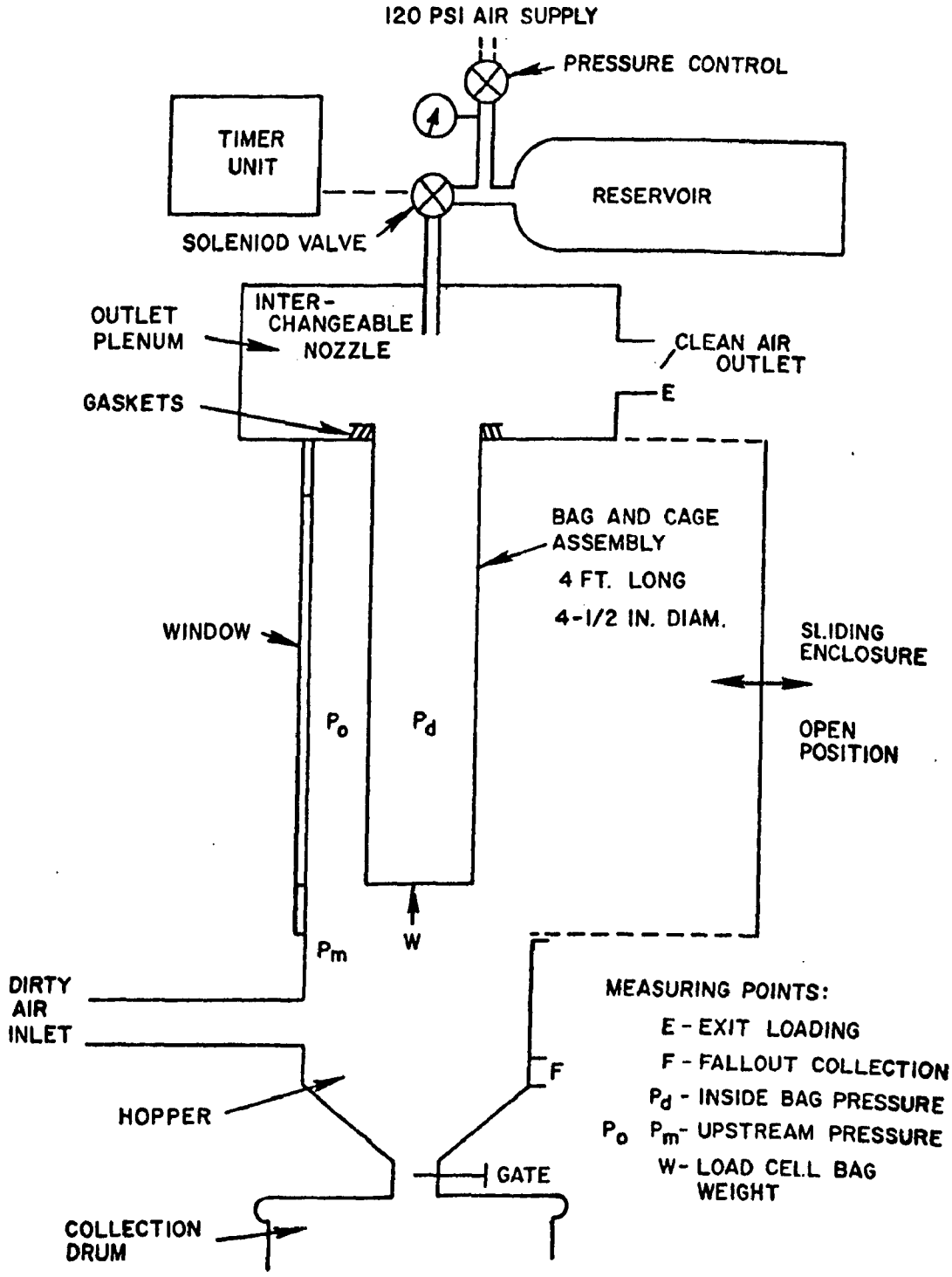

Figure 53. Schematic of pulse jet cleaning assembly

five stiffening rings spaced at equal intervals along the length of the bag. The cage was fastened to a steel thimble by a 4-1/2 inch diameter steel strap clamp that also served to prevent any by-pass leakage. A Venturi nozzle was attached to the steel thimble usually in the configuration shown in Figure 54. The Venturi section, wire cage, compressed air valves and also the pulse control apparatus discussed below were assembled from commercially available components.

Pulse Jet Cleaning Equipment

The system used to deliver compressed air to the bag, which was designed to adapt to a number of pulse cleaning configurations, is shown in Figure 54. All components were standard shelf items, black iron pipe, hose, and sheet metal, with the exception of the diaphragm and solenoid valve system, which was a commercial system purchased from a major manufacturer of pulse cleaning equipment. The damping tank and valve shown in Figure 54 were introduced in some tests to determine how the form of the pressure wave affected dust removal and dust penetration properties. The nozzle was a 1/4 inch diameter section of black iron pipe, adjustable in the vertical direction with respect to the location of the Venturi nozzle. The jet of compressed air through the Venturi induced a secondary clean air flow from the top plenum in addition to the primary jet air.

In operation, the compressed air reservoir was maintained at the desired cleaning pressure via the regulator valve. Release of the electrically controlled solenoid valve tripped the diaphragm valve, dumping air from the reservoir through the nozzle for as long as the valve remained open, usually about 0.1 second. During this time, the reservoir pressure usually decreased to about two-thirds of its initial level. This pressure difference, in conjunction with any necessary temperature adjustment, a reservoir volume of 0-1/2 ft.^{3}, and an assumed adiabatic expansion provided one means of estimating the compressed air requirement.

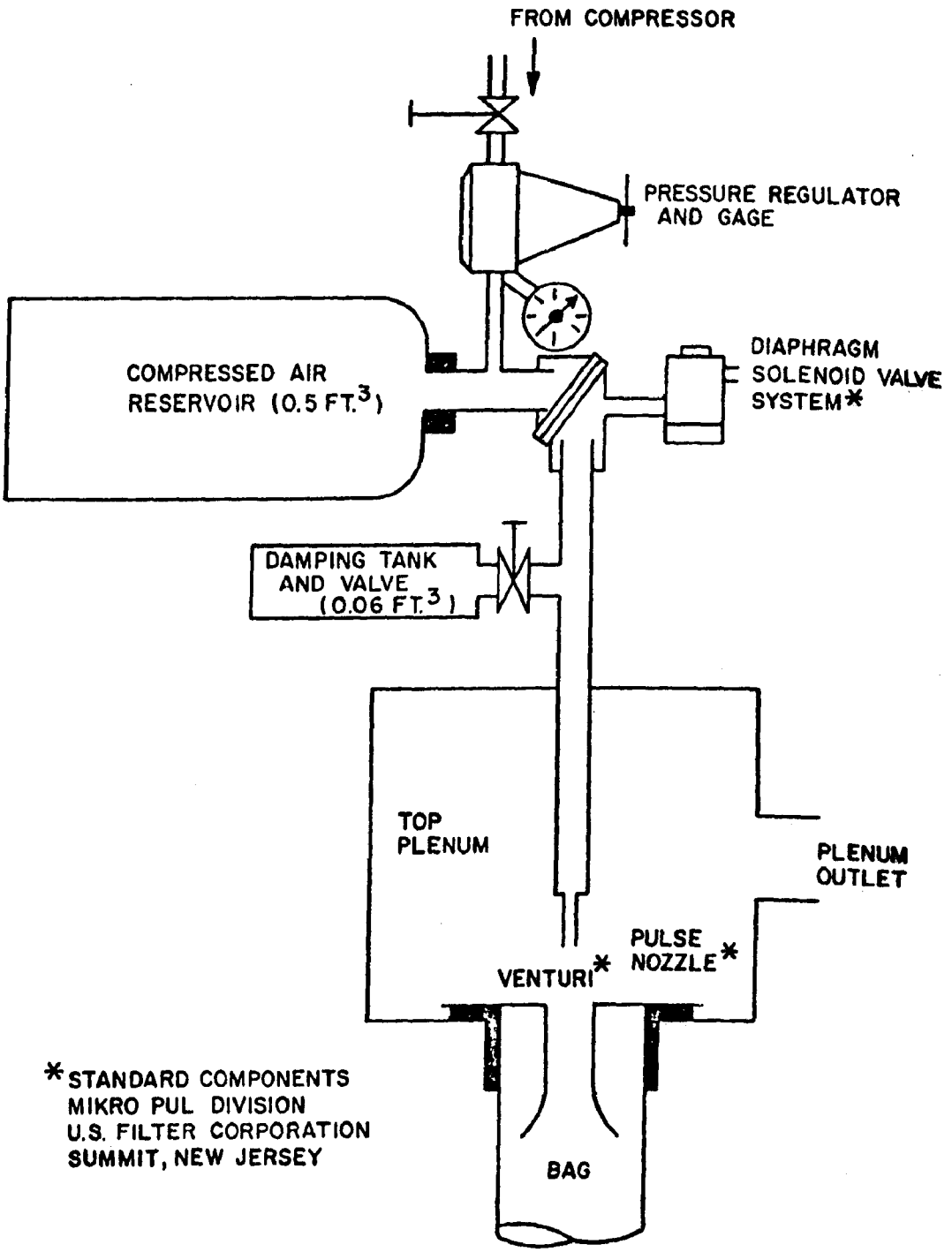

Figure 54. Standard pulse delivery system

For repetitive operation of the pulse system, two solid-state timers were used, one controlling the interval between pulses; i.e., the length of the operating cycle, and the other controlling the length of time the solenoid valve was open. These timers had capabilities of 0.01 to 99.99 min., and 0.01 and 99.99 sec., respectively, with precisions of about 0.008 sec. according to the manufacturer.

The source of compressed air was a compressor operating at 120 psig that delivered air at room temperature and essentially free of water droplets. The pulse properties as delivered to the bag depend on the pressure-flow characteristics of the compressed air supply, and the nozzle shape and location relative to the bag inlet. The effective pulse volume depends on the induction action of the Venturi, if a Venturi is used. The total air volume entering the bag is controlled by the nozzle induction capacity that depends, in turn, upon plenum dimensions and the absolute pressure within the plenum. The reverse pressure differential across the bag caused by the pulse depends strongly on the pressure that rapidly builds up on the dirty side of the bag. This build-up depends not only on the volume of reverse flow air, but also on the pressure-flow characteristics of the main fan when it is momentarily blocked. Additionally, the pressure build-up also depends on the volume of the housing surrounding the bag including the hopper volume and perhaps on the length/width (aspect) ratio of the housing. Thus, in practice, the presence of other filter bags in the same housing may affect the cleaning whether they are cleaned simultaneously or not.

It should be noted that the pressures measured inside the filter bag during the pulse interval were of the order of 1.0 psig or less above atmospheric, much lower than that of the reservoir pressures. This follows from the fact that the air pressure beyond the nozzle discharge depends only upon the reservoir venting rate, the external pressure, and the external system pressure release capability. For the purposes of analyzing dust penetration, dust removal, and operating pressure drop, one should consider the pressure within the bag and not that of

the compressed air reservoir. However, tank pressure, which is much more easily measured, is commonly used as a descriptor for the cleaning process. For this reason, compressed air pressure will be reported in this study as an operating parameter, while bag differential pressure will be used to explain filter performance.

The apparatus shown in Figure 54 provided most of the pulse control capability needed in the study. For other special tests, the gate valve above the collection drum was sometimes closed, a pressure release valve was installed in the inlet duct ahead of the hopper, and a supplementary fan system was used to inject cleaning air into the top plenum outlet. This secondary system included a damper, blower, and timers, as described in Chapter IV of this report.

Test Fabrics

Felted fabrics are commonly used in filtration equipment cleaned by high pressure reverse pulsing. The Dacron felt used in the majority of tests discussed in this section was representative of fabric media used in commercial practice. However, an abbreviated series of comparative tests were also run with a woolen felt that also sees frequent commercial application. Wool felts were used for many years in equipment cleaned by other than pulsing methods, notably by the traveling blow ring method.[1] They are still being used to some extent in various kinds of equipment including the pulse type. Table 19 provides a description of the properties of the two fabrics used in the tests. The similarity of the two fabric structures is further reflected in their essentially similar filtration performance as shown later in this Chapter.

The Dacron and wool felts supplied by the manufacturers were very similar in fiber diameter, fabric thickness and density. The felt density or volume fraction of fiber was computed from the felt weight and thickness using discrete fiber densities of 1.40 and 1.30 gram/cc for the

Table 19. PROPERTIES OF TEST FELTS

Property	Dacron	Wool
Type	felted, needled	felted, without scrim, HCE silicone treatment
Style	A136B[a]	M1778[b]
Weight (oz./yd.^{2})	18	16
Permeability (air flow, ft./min. 1/2 in. pressure drop)	35	30 to 40
Fiber diameter (micrometer), D_f	20	20
Felt thickness (cm)	0.17	0.20
Fiber volume fraction, α	0.26	0.21
Pore size (micrometer), D_p[c]	34	39

[a] Albany International Corp., Globe Albany Division, North Monmouth, Maine.

[b] Menardi and Co., Augusta, Georgia.

[c] $D_p = D_f \left(\frac{1 - \alpha}{\alpha} \right)^2$.

Dacron and wool, respectively. Calculated pore sizes and air flow permeabilities were also very similar.

Felt structures differ from woven fabrics in many important respects. They are depth type media and generally contain many more pores and a larger free area than woven filter fabrics. The performance of felted media has been the subject of numerous investigations.[6,7,8] Although the performance of clean (previously unused) media can be adequately predicted by classical filtration theory, the behavior of media containing substantial amounts of residual dust cannot be quantitatively depicted because of the complexity of the geometrical array of fibers

and collected dust. There is great need for a systematic study of the effect of dust size/pore size on felted fabric performance similar to that conducted by Draemel[9] on a multiplicity of woven fabric structures using dust loadings representative of those encountered industrially.

The average pore size can be expected to play an important role in the penetration of test dusts. An extensive investigation of pore size/dust size correlations with filter efficiency has been conducted by Draemel[9] for several woven fabrics. Extensive penetration was noted when the average pore size was more than 10 times the mass median particle diameter. Earlier workers have also noted the same relationship between woven fabric structures and filter performance.[10,11]

Bag Properties and Measurement Techniques

Bag weights before and after cleaning were measured to determine the gross bag weight and/or the amount of dust collected upon the filter. The mounting plate was clamped against the bottom of the top plenum using a neoprene sponge seal to facilitate easy removal. Because this method was time consuming, a much quicker but less accurate method was devised to weigh the bag in place. The mounting plate was unclamped, and a piezoelectric load cell located beneath the bottom of the bag cage was elevated until it came in contact with the bag. Pressing the load cell against the bag produced a signal proportional to the weight of the bag, cage, Venturi, and mounting plate. The method selected depended upon the accuracy requirement.

The elastic modulus of the bag was determined by inflating a bladder inserted inside the bag and noting the differential changes in circumference and length with increasing pressure. The static position of the bag as it draped around the supporting cage was measured by calipers. Small increases of pressure inside the bag reduced the dimpling and ultimately caused it to balloon out into a smooth surfaced cylinder. The relationship between displacement and pressure, which afforded a

measure of the bag's flexibility, was used in computing the motion of the fabric during a pulse.

Bag Motion

Motion of the bag during pulses was also measured in three different ways.

Accelerometer* - A piezoelectric accelerometer weighing only 0.15 grams was attached to the bag and the output signal displayed on an oscilloscope screen during the bag pulse. Some electronic diffulties were encountered; i.e., any motion of the two wires carrying the extremely small signal apparently produced electromagnetic noise even when the wires and accelerometer were shielded. Additionally, high-frequency vibrations, apparently present either in the pulsed air or in the bag cage, sometimes overwhelmed the desired lower-frequency signal. Sufficient information was obtained, however, to confirm other instrumental measurements despite the limitations of this technique.

Strain Gage+ - A special strain gauge sensor, similar in principle to a phonograph pick-up cartridge, was designed for measuring small fabric displacements (up to 1/2 inch). The device consisted of a lightweight finger in light but positive contact with the bag and with the strain gauges bonded to opposite sides. Bag motion flexed the finger causing imbalance in a resistance bridge. Photographs of the resulting signals displayed as distance/time coordinates on an oscilloscope screen permitted estimation of fabric velocity and acceleration as well as physical displacement of the bag during pulsing.

---

*Accelerometer: Model 91 piezoelectric accelerometer from Wilcoxon Research, P.O. Box 5798, 9 Ericsson Road, Bethesda, Md. 20014.

+Pressure transducer: Model PT-H2 Pitran Pressure Transistor, nominal linear pressure range, 015 psid; from Stow Lab., Inc., Kane Industrial Drive, Hudson, Mass. 01749.

High Speed Photography - Cinematography at approximately 3500 frames per second produced a viewing time magnification of about 220X. The movies were also used to make estimates of the displacement, velocity, and acceleration of the fabric and also to depict the dust cloud leaving the fabric.

By and large, pressure differential measurements provided the best indication of bag motion, using mechanical properties of the bags and computing the motion. The above techniques were used during the study to verify the computational approach.

Test Dusts

The fly ash and talc dusts described earlier in Chapter II of this report were also used in pulse cleaning tests. They were reaerosolized in the same way; i.e., using an aspirator with a jet of 90 psig compressed air.

Dust Measurements

Generally, the same procedures were used in the pulse jet studies as were used in the Mechanical Shaking Studies. Dust was metered and monitored in the same ways. A portion of the dust introduced to the system was lost to the hopper as fallout without reaching the filter bag. For fly ash, this was of the order of 50 percent, depending on air flow rate, whereas practically all the talc reached the bag. The most accurate method of determining rate of dust filtering was by bag weighing techniques described above. Weighing techniques were accurate to within about 8 grams, or 2 percent.

Dust removed by mechanical shaking, Chapter II, could be determined readily by weighing the dust shaken into a special container placed in the dust hopper. Because there was no air flow during and for 1 minute after shaking, it was estimated that the dust reaching the hopper

represented most, ~ 99 percent, of the dust dislodged by shaking. Once steady state conditions were established, the dust removed by a specific mode of shaking also depicted the filtration or holding capacity of the fabric for the indicated increase in resistance to airflow. In cleaning by pulsing, however, a large portion of the dislodged dust deposits on the walls of the enclosure around the bag, where it mixes with dust previously deposited during the filtering state. Furthermore, there was no direct method of measuring the amount of dust dislodged from the bag that would not interfere either with the inlet flow or the flow reversal during the pulse interval. More important, the amount of dust falling to the hopper per pulse does not depict the actual quantity of dust removed by the pulse, but only that fraction of the dislodged material that reaches the hopper. The remaining dust mixes with the oncoming air stream and then redeposits, usually at some lower position along the filter tube. From a practical standpoint, however, the true filtration capacity of each bag at steady state is the quantity of dust conveyed to the filtration surface between pulse cleaning intervals. In turn, this quantity represents the difference between the amount of dust dislodged by each pulse and the amount of dust that redeposits on the filtering surface before reaching the hopper.

Emission of dust from the filter bag was determined by the B&L counter and the RDM monitor described in Chapter II. The B&L instrument indicated particle size and concentration based upon light scattering phenomena, while the RDM instrument provided mass concentration only. The B&L instrument was used principally to observe variations in outlet concentration with time over the operating cycle with a time resolution of about 0.1 minute.

Mass concentration and particle count measurements were determined for the effluent air stream at the exit from the clean air plenum (see Figure 54). The size of the device required that an 18-in. tygon sampling tube (dwell time, 4 sec.) be used between the plenum outlet and the instrument. For measurements along the length of the bag a

longer Tygon tube was inserted via the plenum into the bag to the desired sampling height. While some particle diffusional losses were unavoidable, the B and L test results are comparable on a relative basis and also show moderately good agreement with concurrent RDM measurements.

Pressure and Flow Measurements

The instrument systems for measuring operating pressure differential across the filter bag and controlling the system air flow to the bag were described earlier in Chapter II and are described in detail in Appendix A. These devices, which relied on pneumatic sensing of pressures at various points in the system, provided accuracies and precisions of the order of 5 percent.

Operating pressure differentials were also monitored using manometers as reference standards and Bourdon-type dial indicators* for fast response direct readout. Neither instrument, however, was suited for measuring the rapid pressure changes during pulse intervals. For the latter application, two good quality diaphragm-type pressure transducers+ were used, one inside the bag and the other outside and with one side of each transducer sealed. Each was calibrated to have identical linear responses and zero points so that when their separate signals were subtracted on an oscilloscope, the pressure differential trace was displayed. Alternatively, the individual pressure signals also could be viewed. Although response times of the transducers and circuits were excellent, there was a problem of a drifting zero point that occasionally allowed one transducer or the other to shift into a

*Magnehelic gauges, 0 to 10-inch water range.

+Pitran silicon transistor, 10 microsecond rise time, 2 microinch diaphragm displacement, 1/3 gram weight, 14-inch water nominal linear range. Model PT-H2, Stow Laboratories, Inc., Kane Industrial Drive, Hudson, Mass.

region of nonlinear response. Infrequently, dust caked over the diaphragm of the dirty-side transducer, causing an erratic response and making it difficult to calibrate until cleaned. Photographs of the pulse differentials recorded on the oscilloscope are included with the data in Appendix M.* These two pressure transducers were mounted on opposite sides of the fabric, at a point about half way down the bag. Compared to the typical pulse duration of about 0.1 sec., air shock fronts traversed the 4-ft. bag in about 0.004 sec. Thus, the pressures measured by the transducers were very nearly equal to the time averaged pressures throughout the entire bag.

The regulating circuits for the establishment of pulse intervals and pulse durations were standard commercial hardware items. It should be noted, however, that the dial settings of 0.01 and 0.1 second for controlling valve open times actually produced 0.06 and 0.15 second pulses, respectively. The above values were derived by examination of oscilloscope traces depicting the transient pressure changes within the filter bags as discussed later in this Chapter.

The volume of air delivered during a single pulse was determined by attaching a 2 ft. diameter meteorological balloon to the nozzle and by accumulating sufficient volume, ~ 2 ft.^{3}, by sequential pulsing so that the balloon contents could be determined with a laboratory spirometer. The primary air volume per pulse was also calculated on the basis of critical flow through the 1/4 in. nozzle and the absolute pressure and temperature of the reservoir air.

---

*In retrospect, a single transducer element across the bag to provide a direct differential signal would probably have been a better approach. It was rejected in this program because of the anticipated difficulties of grommeting a pneumatic tube through the bag without picking up mechanical vibrations to which these transducers were sensitive; the possibility of dust plugging the pneumatic tube, and the inability to view separately the inside and outside pressures.

Although the automatic flow control and recording system was adequate for normal flow regulation, it could not respond to sudden surges in flow. Therefore, the reduced resistance of the "just-cleaned" filter bag caused a flow increase which took the flow control system about 10 seconds to return to the preset level. The residual filter pressure drops reported in the following chapters have been adjusted to reflect normal filtering velocities.

RESULTS

The results of extensive tests with a single bag, full-scale pulse jet system in which system performance was studied with wool and Dacron felt bags are presented next. Test aerosols, sampling equipment and the design and operating features of the filter system have been described previously in this chapter and/or in Chapter II.

Although the laboratory system was designed to simulate full scale industrial systems to enable maximum use of experimental data, it was heavily instrumented to provide information that could not be obtained practically under normal field conditions. The primary functions of the special measurement systems were to relate the particle collection and resistance characteristics to the key operating variables of the compressed air pulse jet system.

Particulate Emission Characteristics

Effluent dust concentrations from pulse cleaned bags are appreciably higher than those for the mechanically shaken bags described in Chapter II. Penetrations of the order of 0.01 percent, however, can be obtained with suitable choice of felt and operating conditions. As with shaken bags, filter emissions are highest immediately after cleaning. The effect of the cleaning cycle and other system operating and equipment design parameters on dust penetration are reviewed in the following paragraphs.

Compressed Air Pressure - The pulse of air used to clean the bag was released from a reservoir tank by a quick-acting solenoid valve. The air pressure within the reservoir, 30 to 100 psig, was found to be a major factor in controlling filter efficiency and fabric resistance. Because of the ease with which pressure adjustments could be made, reservoir pressure was treated as a primary variable in this study.

Figures 55a and b indicate particulate emissions measured by the RDM for a series of experimental runs in which fly ash was filtered with Dacron felt. The reservoir pressure was varied between 40 and 100 psig and the mode of introduction of the cleaning pulse to the bag was either direct or damped. Analyses of the data indicate that the emission increases with reservoir pressure (statistically significant at < 1 percent level of confidence). A pressure of 40 psig was determined to be the approximate minimum level necessary to obtain any appreciable cleaning of the bag. These results indicate that, at least with fly ash, one should be able to control collection efficiency by the proper choice of reservoir pressure.

The data points shown in Figure 55a represent the combined effects of variations in inlet concentration, filtration velocity, pulse interval and pulse duration for each reservoir pressure level. It was intended that the smoothing and averaging process would provide an improved picture of the emission/reservoir pressure relationship. The right hand graph, Figure 55b, shows a family of curves in which the operating parameters were separated for each curve. The latter data have been used to assess concentration and velocity effects in later discussions.

The difference between the effluent concentrations resulting from the application of the cleaning pulse to the bag by the direct and damped modes is significant at a < 1 percent level of confidence. The decrease in effluent concentration resulting from damped or delayed pulses is attributed to two factors. When the valve is opened to the damping tank shown

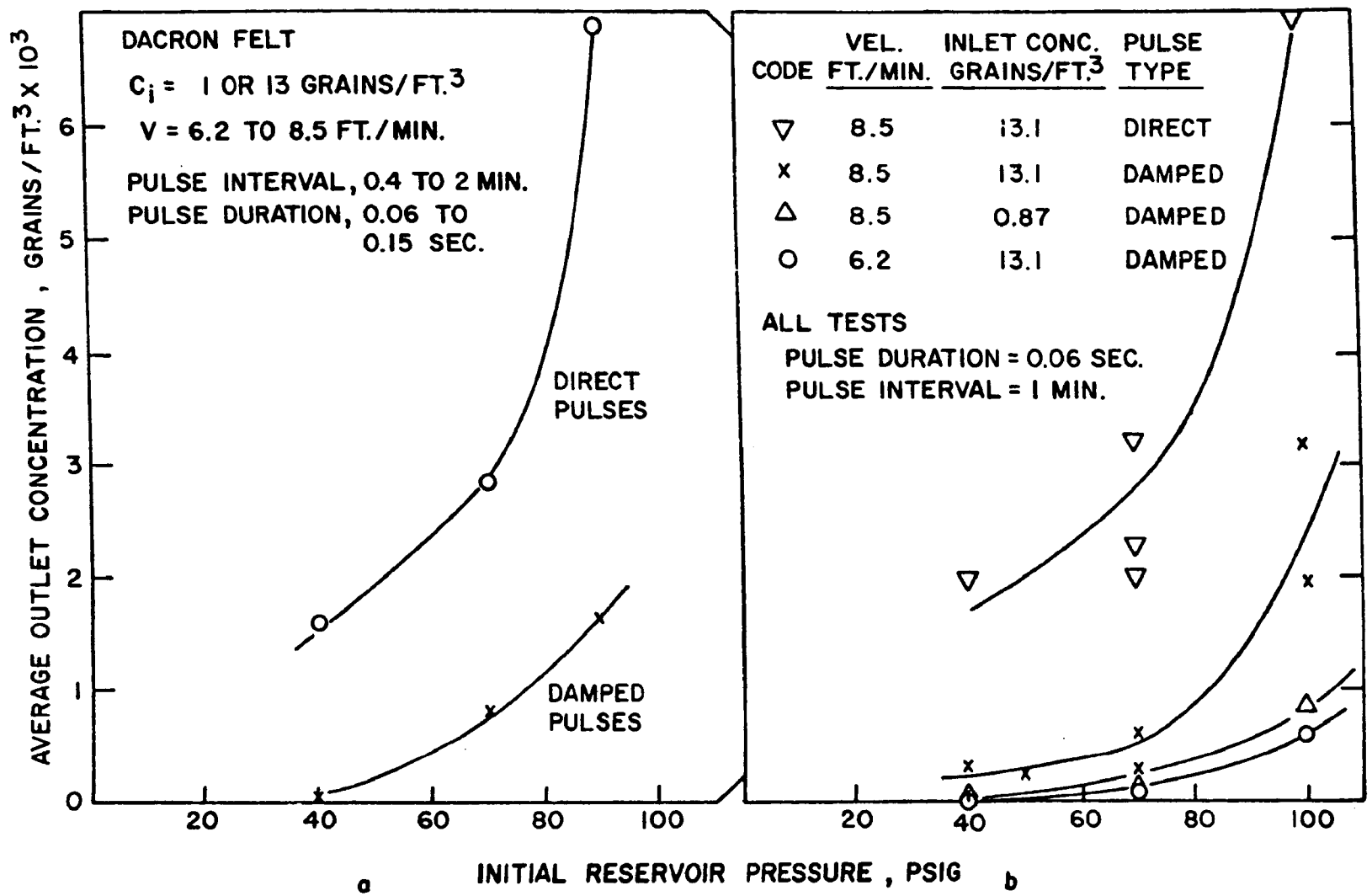

Figure 55. Average outlet concentrations for fly ash versus reservoir pressure with direct and damped pulses. (a) All variables averaged except pressure and pulse type; (b) variations in velocity, loading and pulse type shown individually.

in Figure 54, part of the compressed air vented from the main pressure reservoir (about 10 percent) is diverted to the damping tank. There it remains until closure of the solenoid valve in the vent line from the main pressure reservoir. Because part of the total air volume released from the main reservoir is temporarily stored in the damping tank, the transient reverse pressure gradient across the bag during the open time of the valve and the rate of pressure change in the system are slightly reduced. Both factors contribute to less effective cleaning such that the greater residual dust holding leads to improved particle collection.

Another distinguishing feature of the delayed pulse is that upon closure of the solenoid valve to the reservoir tank, the contents of the damping tank vent to the clean air side of the bag thus forestalling a too rapid resumption of filtration. In the case of the direct pulse, there is no back pressure to oppose the transient flow and pressure drop increases that often occur at the end of the pulse. The higher air flow coupled with a transient stretching of the felt augments the higher effluent concentration caused by the greater rate of pressure rise and larger reverse pressure gradient associated with the direct pulse. Figure 56 illustrates simplified tracings and actual photographs of typical pressure/time relationships shown by oscilloscope display of the differential pressures across direct and delayed pulse systems.

The interaction between reservoir pressure and the mode of presentation to the bag (i.e., direct or damped) was found to be significant (< 1 percent level of confidence) indicating that the cleaning effectiveness of a pulse delivered from a reservoir operating at a given pressure is also a function of the pulse form. Thus, the collection efficiency and the average pressure drop can be optimized within the system by properly selecting the reservoir pressure and the mode of admission to the bag.

Overall particulate emissions presented in Figure 55 have been resolved into specific size fractions in Figure 57 to show the separate effects of reservoir pressure and pulse damping on the effluent

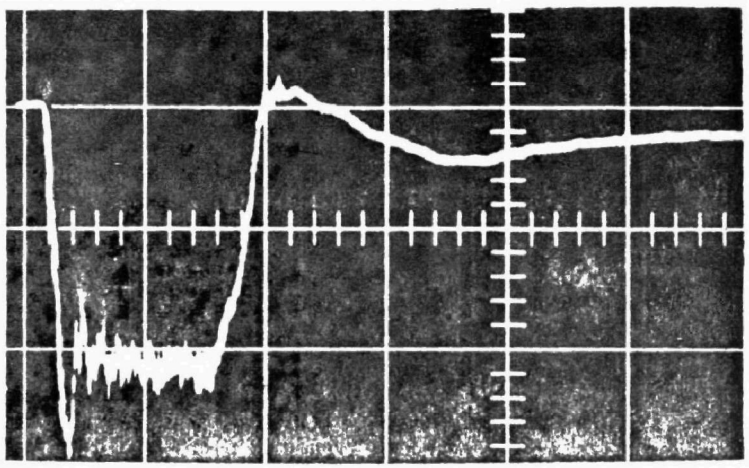

PHOTOGRAPH, DIRECT

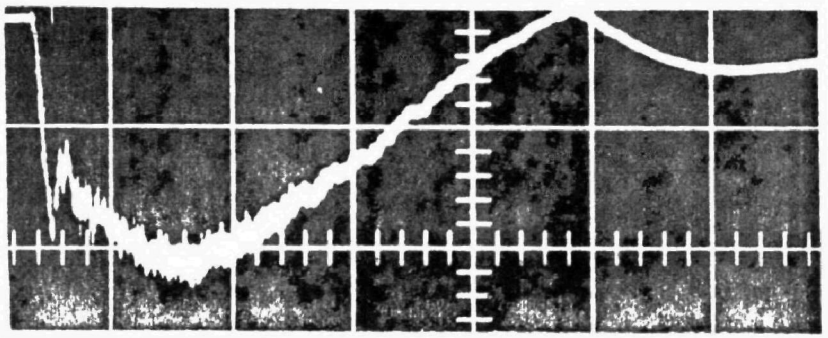

PHOTOGRAPH, DELAYED

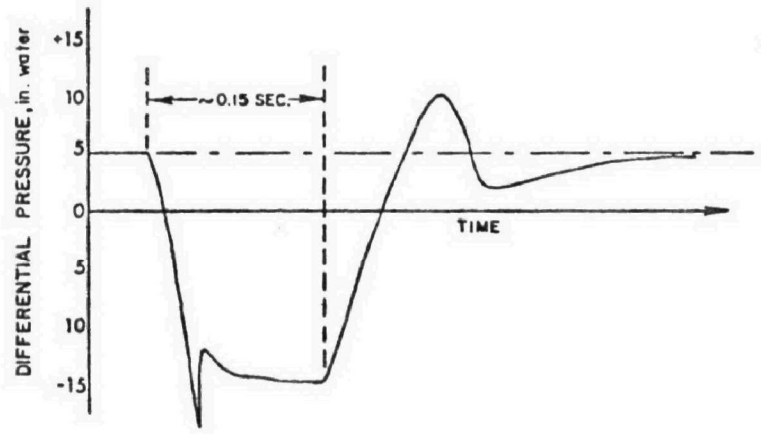

TRACE, DIRECT

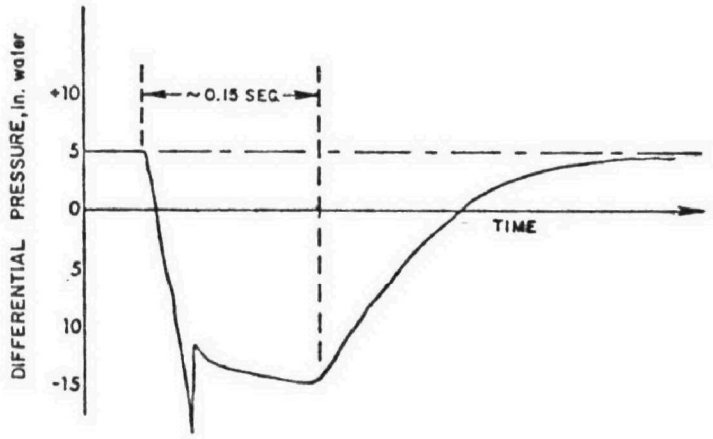

TRACE, DELAYED

Figure 56. Effect of direct and delayed pulses on bag differential pressure for valve open time of 0.15 sec.

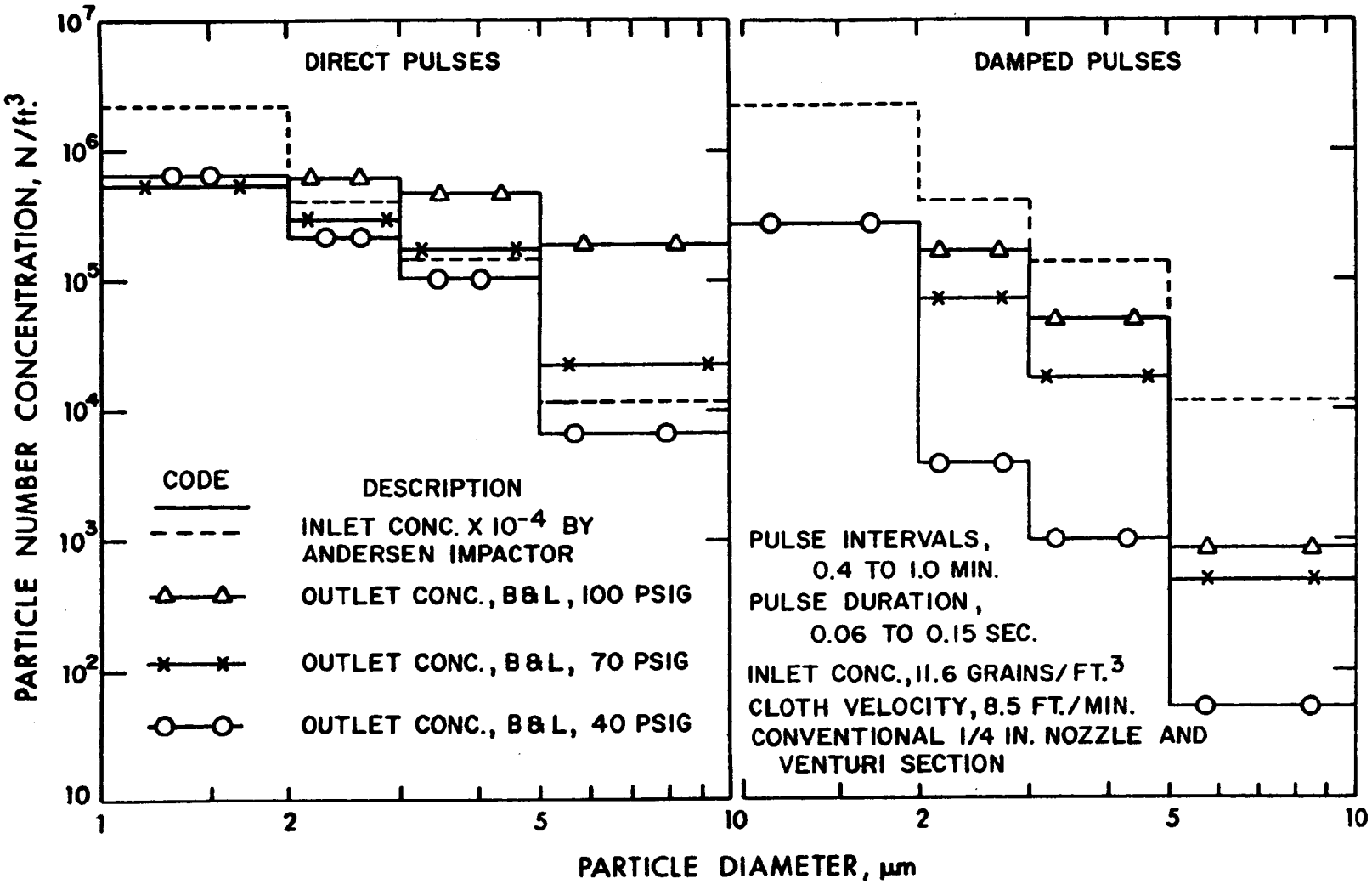

Figure 57. Effect of reservoir pressure and pulse damping on effluent concentration for fly ash filtration with Dacron felt (note: inlet mass concentration converted to equivalent number concentration and scaled by 10^{-4} for comparison)

characteristics. To allow comparisons between inlet and outlet concentrations with the fly ash/Dacron felt system, the inlet concentrations estimated by Andersen impactor have been converted to their equivalent number concentrations and classified according to the B&L size intervals. The inlet values appearing on the graph have also been reduced by four orders of magnitude to facilitate the comparison. When the dashed impactor lines and those depicting the effluent are exactly superimposed on Figure 57, the collection efficiency for the indicated size category is 99.99 percent (or the fractional pentration 1×10^{-4}).

Examination of the histogram bars of Figure 57, aside from a conforming qualitatively the results in Figure 55, shows that a higher proportion of coarse particles appear in the collector effluent during direct pulse cleaning. This effect, which is most pronounced at the higher pressure levels, is more clearly shown in Table 20. Inspection of the calculated fractional particle size penetration values indicates that the apparent collection efficiencies decrease with increasing particle diameter for direct pulse cleaning at 70 and 100 psig. What actually takes place is that previously deposited dust is loosened and flushed out in the form of agglomerates when the normal filter flow resumes. Therefore, the effluent particles usually represent two populations, those upstream particles that would ordinarily penetrate the felted media with its residual dust holding and the agglomerate fraction dislodged as a result of the cleaning process.

The damping procedure appears to reduce effluent concentrations significantly, particularly so at the lower reservoir pressures. The improved effluent conditions are attributed in large part to the less rapid change in bag pressure differential, Figure 56, when the main solenoid valve is closed. It appears that the "snap" of the bag when filtration is removed coupled with the higher transient filtration velocity are the principal causes of the higher average dust penetration. It should be noted that the experimental points in Figure 57 and Table 20 include variations in pulse duration and pulse frequency. Therefore,

Table 20. OUTLET CONCENTRATION AND FRACTION PENETRATION FOR VARIOUS RESERVOIR PRESSURES AND DIRECT AND DAMPED PULSES. FLY ASH FILTRATION WITH DACRON FELT (SEE FIGURE 57)

Size range (μm)	Dust concentration particles/ft.^{3}				Apparent fraction penetration		
	Inlet[a]	Outlet[b]			Outlet[c]		
		100	70	40	100	70	40
Direct pulse							
1- 2	2.2×10^{10}	--	5.7×10^{5}	6.3×10^{5}	--	2.6×10^{-5}	2.9×10^{-5}
2- 3	1.0×10^{10}	6.2×10^{5}	2.9×10^{5}	2.2×10^{5}	6.2×10^{-5}	2.9×10^{-5}	2.2×10^{-5}
3- 5	1.5×10^{9}	5.1×10^{5}	1.8×10^{5}	1.1×10^{5}	3.4×10^{-4}	1.2×10^{-4}	7.3×10^{-5}
5-10	1.2×10^{8}	2.2×10^{5}	2.3×10^{4}	7.0×10^{3}	1.8×10^{-3}	1.9×10^{-4}	5.8×10^{-5}
Damped pulse							
1- 2	2.2×10^{10}	--	--	2.7×10^{5}	--	--	--
2- 3	1.0×10^{10}	1.7×10^{5}	7.1×10^{4}	4.2×10^{3}	1.7×10^{-5}	7.1×10^{-6}	4.2×10^{-7}
3- 5	1.5×10^{9}	5.1×10^{4}	1.7×10^{4}	1.0×10^{3}	3.4×10^{-5}	1.1×10^{-5}	6.7×10^{-7}
5-10	1.2×10^{8}	9.0×10^{2}	5.0×10^{2}	5.0×10	7.5×10^{-6}	4.2×10^{-6}	4.2×10^{-7}

[a] Based on Andersen impactor data converted to equivalent number concentration.

[b] Based on B&L measurements. Outlet concentration levels partly attributable to agglomerates re-entrained immediately after pulsing.

[c] Many coarse particles dislodged from fabric as agglomerates. Not due to direct penetration.

although the data appear to align logically on a qualitative basis, they should be used only as guidelines until more precise measurements can be made.

Cleaning Frequency (Operating Cycle) - Several tests were performed to determine the effect of cleaning frequency on particulate effluent properties. If one assumes that two filtering operations are identical in every respect except for a difference in cleaning frequency it would appear that the more rapid pulsing process might cause increased dust emissions. This follows from the fact that the filter surface is presented more frequently in the "just cleaned" state in which greater particle penetration occurs. Increased emissions during the very early filtrations phase are attributed to two effects, first the expected increased penetration due to the more open filter structure and second the re-entrainment of particles (usually agglomerates) whose bonds have been weakened by the preceding cleaning process.

The above mechanisms may be counterbalanced by two additional effects. The amount of dust associated with the transient puff is probably directly associated with the prior dust holding of the filter. Thus a greater dust release should occur when the cleaning frequency is reduced; i.e., more dust on the filter. Figure 55b, for example, indicates that the filter effluent concentration is strongly dependent on filter loading for a fixed cleaning system. Although part of the total dust penetration is presumed to be due to a less complete sealing of the fabric surface, it is suspected that most of the effluent is associated with the initial puff. In turn, the "puff" concentration depends upon the transient concentration produced on the dirty air side of the filter immediately after pulsing. On the other hand, the filter with the greater dust loading should also show decreased penetration in accordance with all filtration logic. The net result of these opposing effects is that cleaning or pulse frequency may not exert a strong influence on effluent concentrations, as shown in Figure 58 with respect to cleaning frequencies greater than 0.4 minutes.

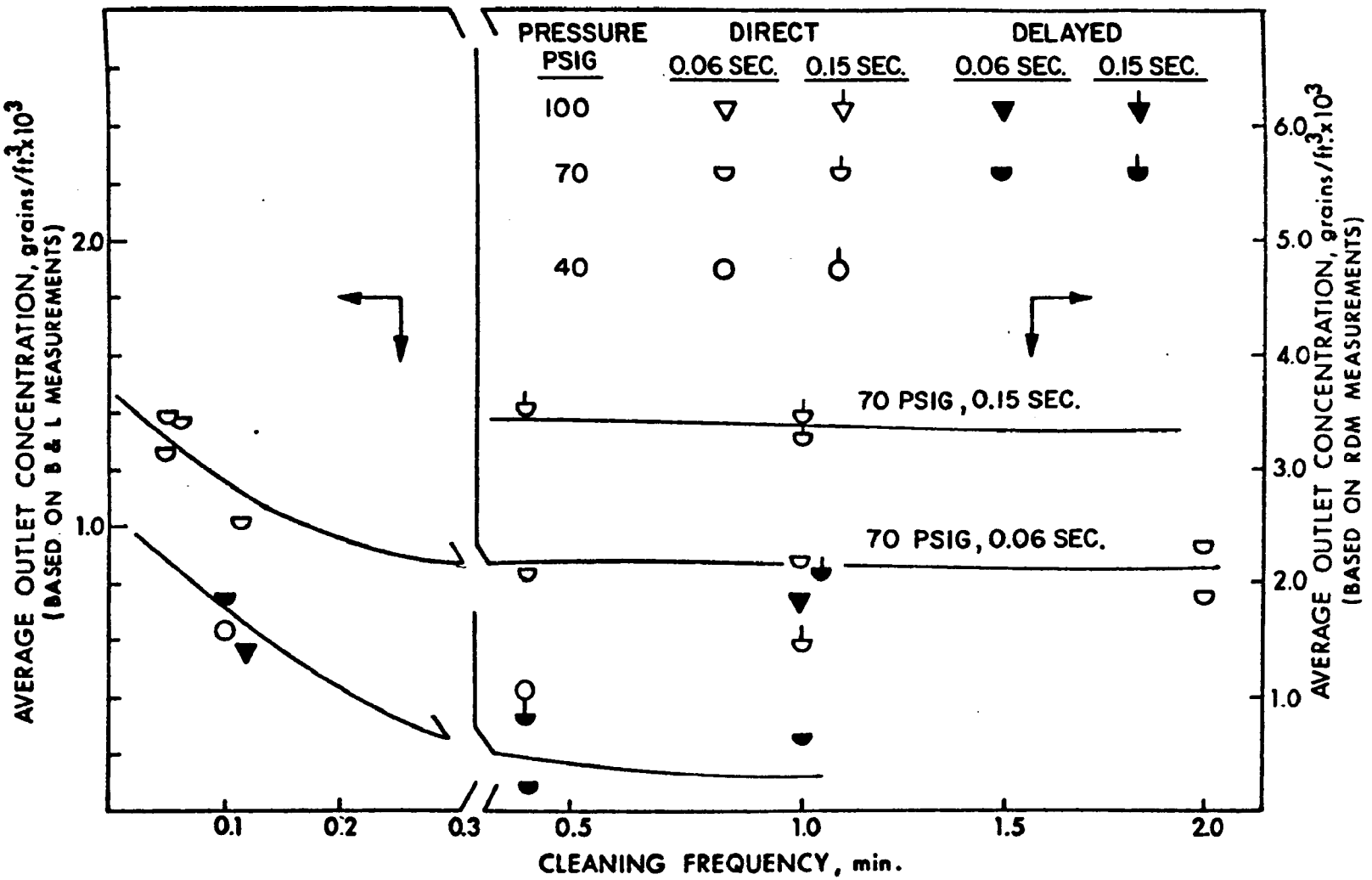

Figure 58. Effect of frequency of cleaning on average outlet concentrations for fly ash filtration with Dacron felt. Data reflect variations in reservoir pressure, pulse duration and pulse form for commercial 1/4 in. jet and Venturi system.

It should be noted, however, that very frequent pulses appear to increase significantly the effluent concentrations. Note that revised values for mass concentrations given by B&L samples should be at least as high as the values read from the right-hand ordinate. Actual calibrations under experimental conditions applying specifically to pulse jet tests suggest that the ratio of RDM to B&L concentrations is roughly 5.0.

Practically, the use of pulse intervals less than 0.5 minute would present severe compressed air requirements as well as increasing the particle emissions. The above high frequency measurements are confirmed by the plenum pulse tests shown in Figure 59. Here we see a very consistent structure to the concentration/pulse frequency relationship for time periods of up to 0.2 minute. The data align logically with respect to both reservoir pressure and pulse duration. Despite the fact that filter resistance levels were quite low, it is emphasized that the low pressure plenum pulses actually represented prohibitive compressed air demands (about six times greater than those for typical commercial 1/4-in. diameter jets). The main purpose of the plenum pulse tests was to permit a better understanding and definition of the pulse cleaning process.

Figures 60 and 61 examine the effects of cleaning frequency on the particle size distribution and number concentration of the filter effluent. The histograms also indicate the relative fractional concentrations of the inlet dust (fly ash). The term relative has been used because the actual number concentration levels have been reduced by 10^4 to permit rapid visual estimation of apparent efficiencies in the indicated size ranges. The effects of direct and damped pulses as well as pulse duration, 0.06 and 0.15 second, are also shown in Figures 60 and 61.

With respect to the size ranges resolvable by the particle measurement instruments (Andersen impactor and B&L counter) there appears to be

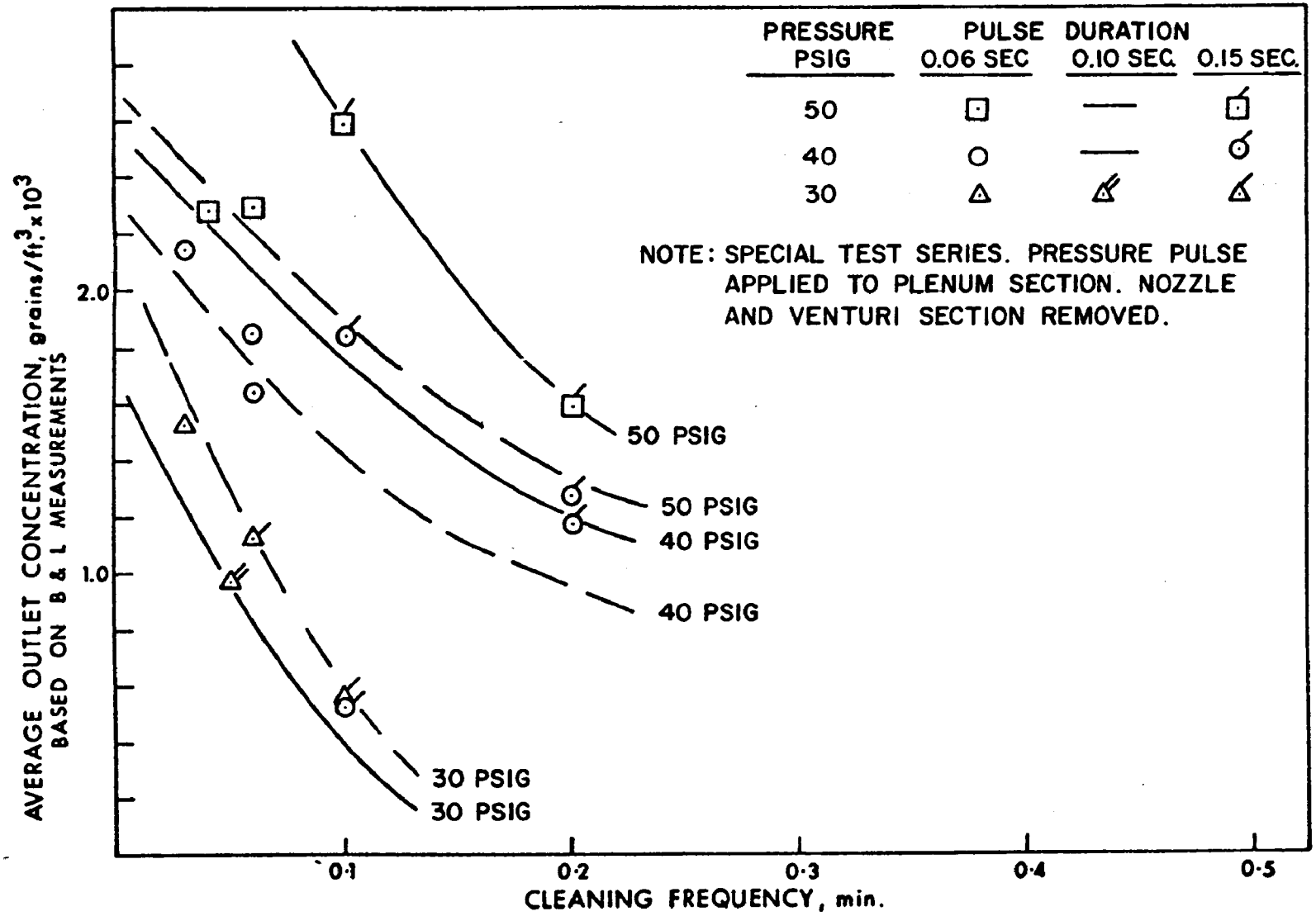

Figure 59. Effect of frequency of cleaning on average outlet concentrations for fly ash filtration with Dacron felt. Data reflect variations in reservoir pressure and pulse duration.

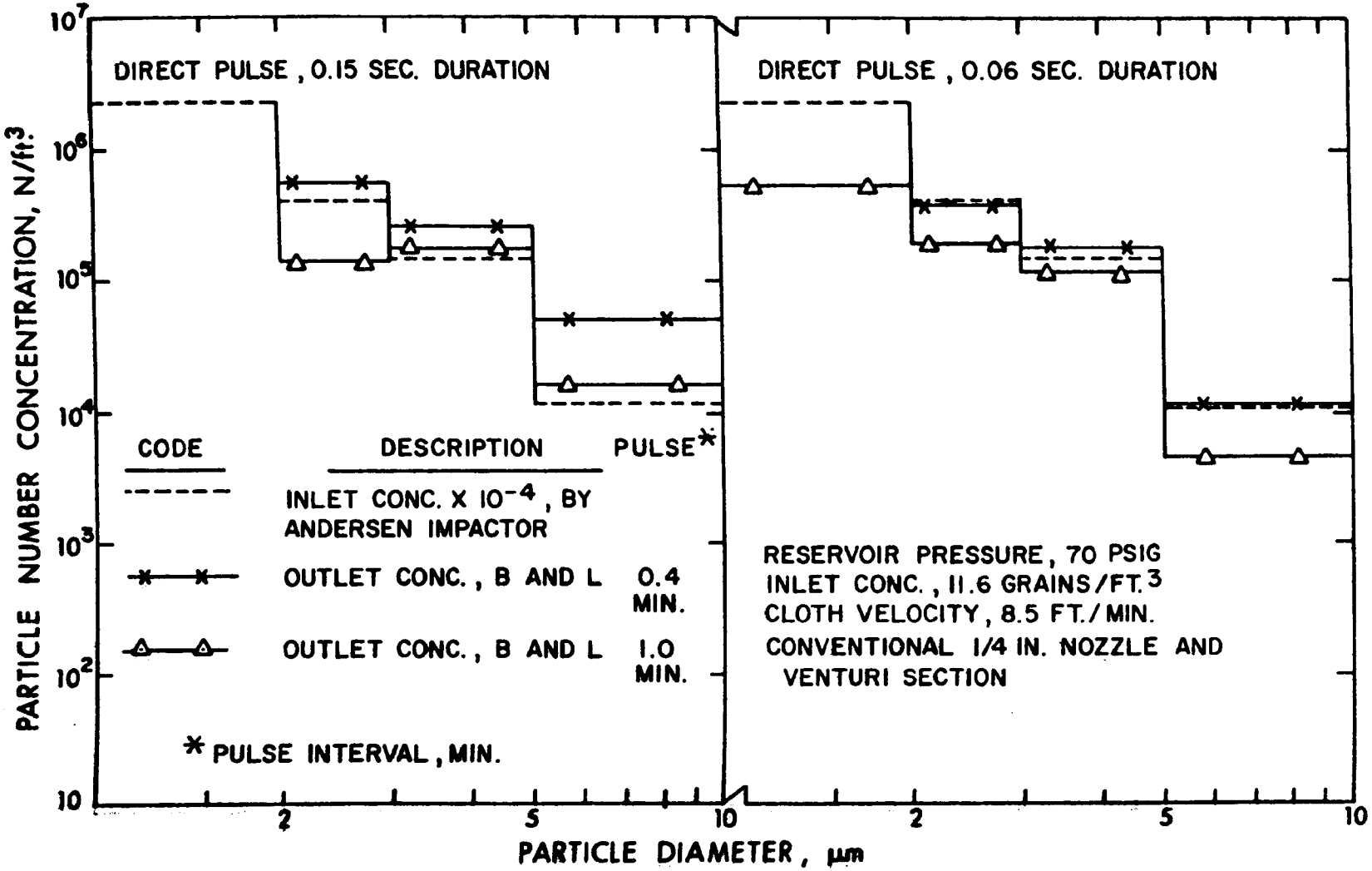

Figure 60. Effect of pulse duration and pulse interval on effluent concentration for fly ash filtration with Dacron felt, direct pulse (note: inlet mass concentration converted to equivalent number concentration and scaled by 10^{-4} for comparison)

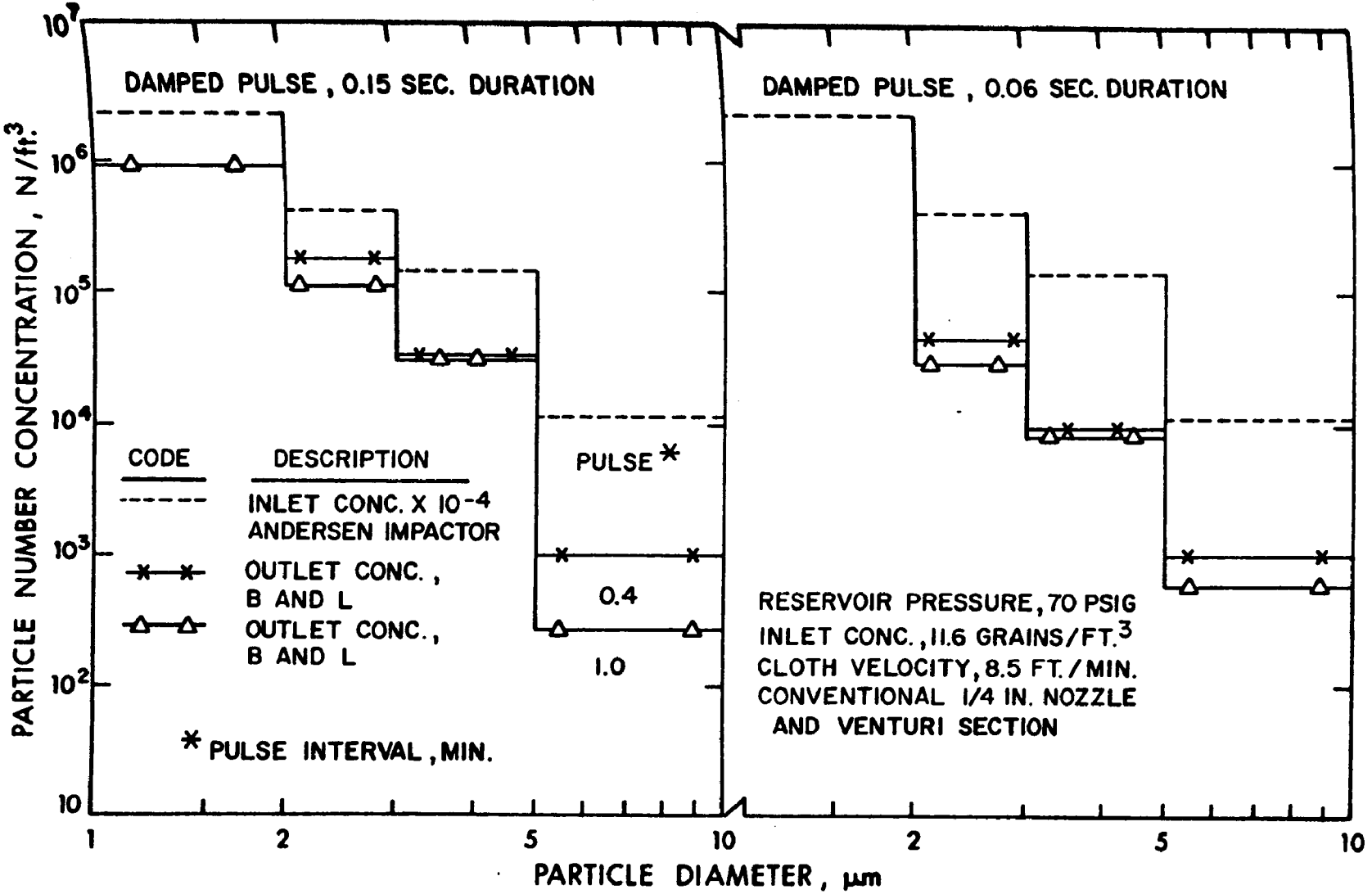

Figure 61. Effect of pulse duration and pulse interval on effluent concentration for fly ash filtration with Dacron felt, damped pulses (note: inlet mass concentration converted to equivalent number concentration and scaled by 10^{-4} for comparison)

no discernible evidence that the effluent particle size distribution is altered significantly with direct or damped pulses. Note that superposition of an effluent histogram bar with the corresponding dotted influent bar depicts a collection efficiency of 99.99 percent. As stated previously, the apparent "coarseness" of the effluent dust results from a large contribution from agglomerates released immediately after the pulse. Examination of particle size concentration versus filtration time curves given later in this section confirm this hypothesis. It should be noted that reservoir pressure variations depicted in Figure 57 exerted a significant effect on particle emission. At 100 psig, for example, the outlet aerosol was much coarser than the inlet aerosol despite the large, $> 10^3$ times, reduction in mass concentration.

Cleaning Pulse Duration - Preliminary tests during this study and earlier results reported by Dennis et al.[3] indicated that pulse duration had no significant effect on filter resistance. It is recognized that in comparing tests upon single bag and multi-bag collectors, any effects noted with a single bag may be obscured in the larger system. Figures 60 and 61 show that pulse duration does have a measurable effect upon effluent concentration. The most pronounced change, however, occurs with damped pulses where the effluent concentration appears to increase by about 3 times for the longer pulses in the 2 to 5 μm size range. The fact that there is less of a change for direct pulse systems is attributed to the fact that the initial emissions immediately following a pulse constitutes the major part of the total emission.

Felt Type - Comparative fly ash emissions for wool and Dacron felts are given in Figure 62 for direct and damped pulses over the reservoir pressure range 40 to 100 psig. Although wool felt emissions were slightly lower than those for felt, the differences in fabric density, permeability, residual dust holding and filtration resistance provide no clear cut explanation for the slightly improved performance. A second perspective on comparative performance is given in Figure 63

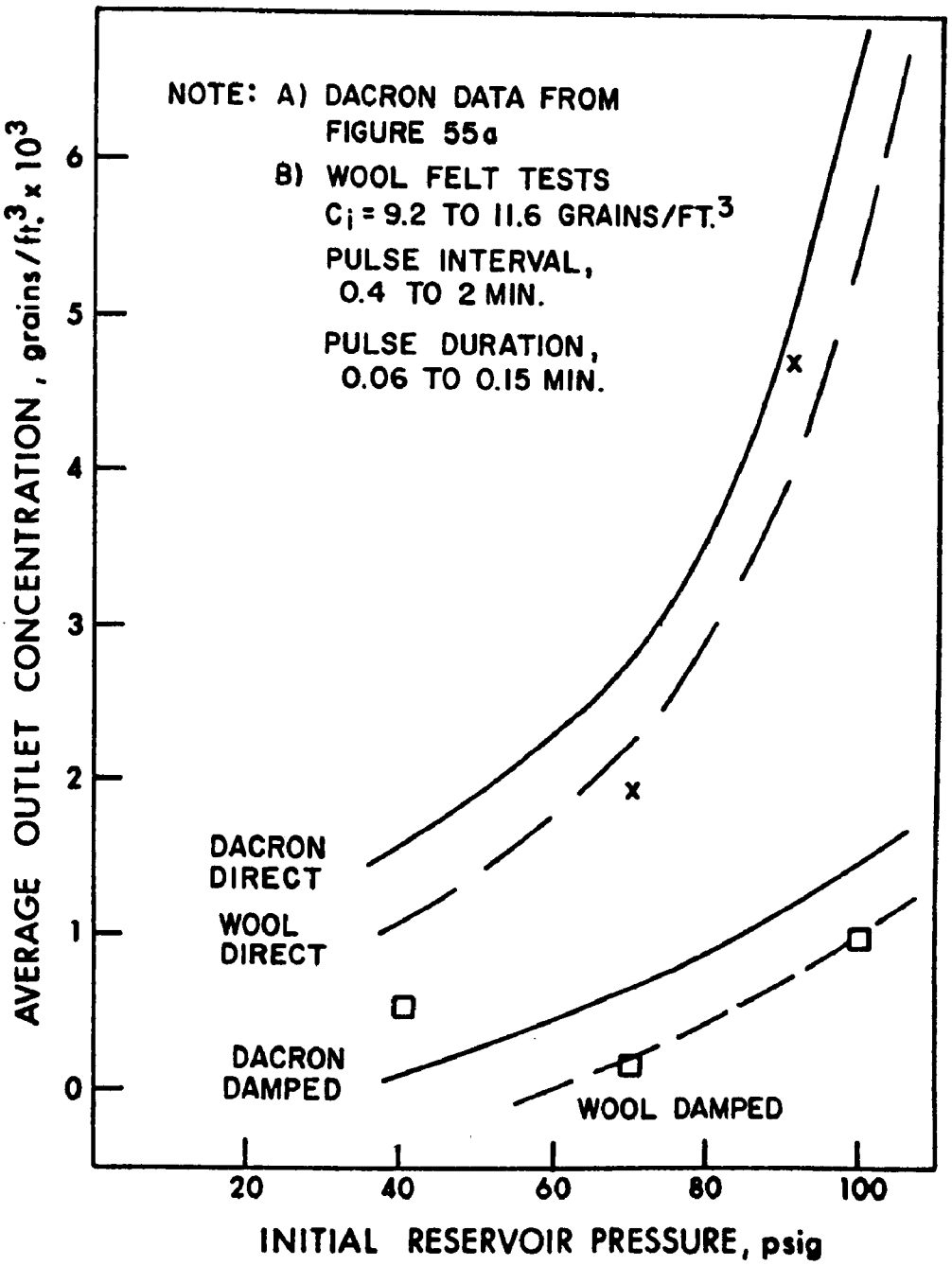

Figure 62. Comparative performance between wool and Dacron felts with fly ash filtration

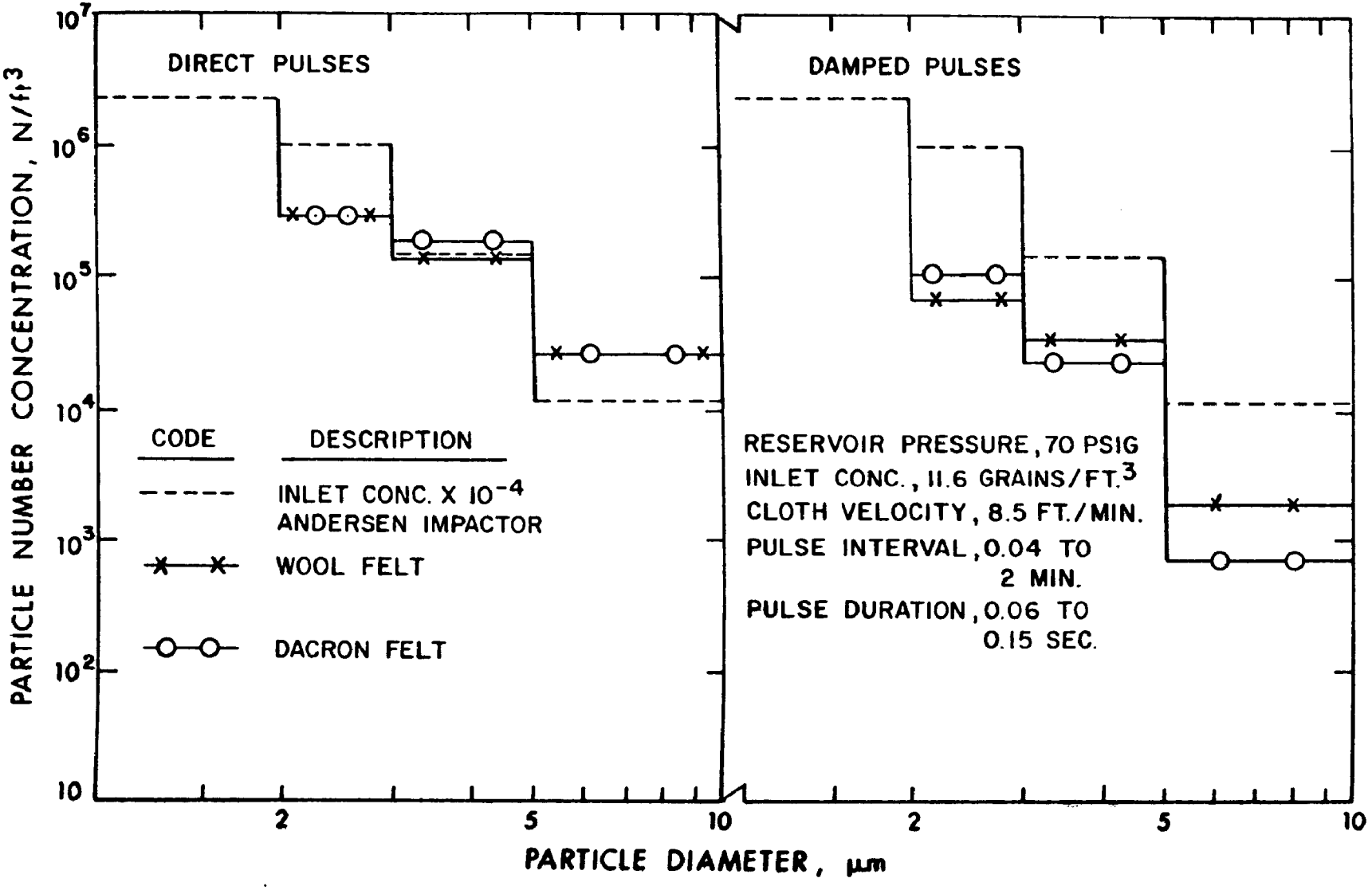

Figure 63. Effect of felt type on fly ash particulate emissions

in which the fractional emissions are shown for direct and damped pulse systems. According to the latter data, little distinction can be made between the Dacron and wool felts. It should be noted that wool emissions are also coarser for the direct pulse conditions.

Dust Type

Limited tests were performed with a resuspended talc dust which was slightly finer than the fly ash based upon cascade impactor measurements, Table 4. Microscope examination indicated that the particles were irregularly shaped with few spherical forms (cenospheres) as found in fly ash. Although the dispersed dust was finer than the fly ash, it appeared that it formed more loosely packed agglomerate structures according to filtration studies with mechanical shaking systems, Chapter II.

A comparison of filter effluent concentrations for talc and fly ash given in Figure 64 shows no extreme differences in performance. Generally, the apparent collection efficiencies for the indicated size ranges average close to 99.9 percent or greater for both talc and fly ash aerosols. The reason that talc concentrations were held at the 1.6 grains/ft.^{3} level was due to a handling problem with the dust feed system and not to limitations in pulse jet cleaning capacity. For example, the average filter resistance for the 40 and 70 psig talc tests shown in Figure 64 was 2.4 and 1.9 inch water, respectively, with the lower resistance associated with the higher pressure pulses as expected. On the other hand, it is also indicated that the pulse damping process exerted a greater effect on effluent concentration than does a lowering of pulse pressure from 70 to 40 psig.

The limited measurements performed with the talc/Dacron system showed that increased reservoir pressure and extended pulse duration led to increased particulate emissions, thus conforming to the pattern exhibited by the fly ash/Dacron tests.

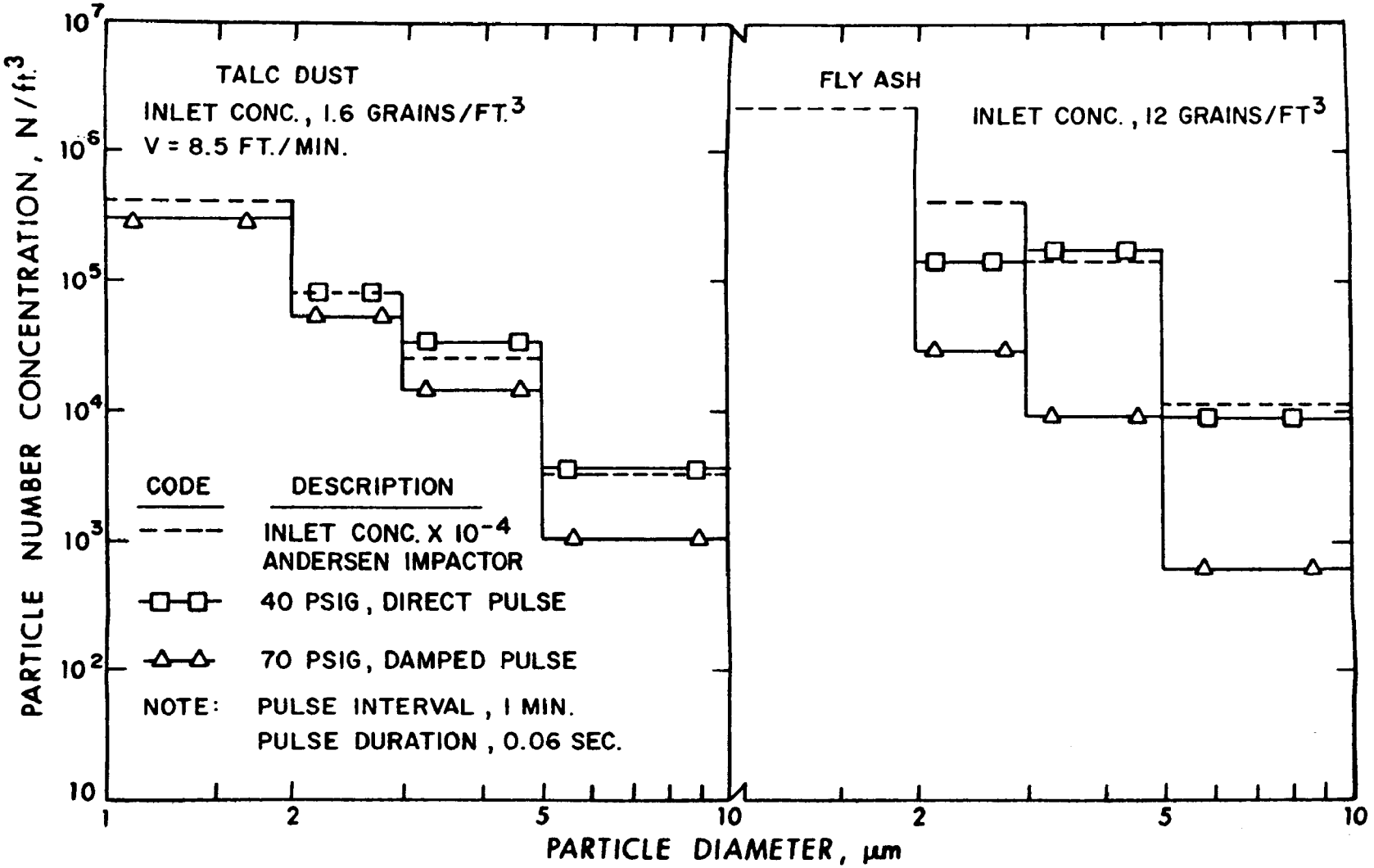

Figure 64. Comparative filtration characteristics for talc and fly ash with Dacron felt

A comparison of talc and fly ash filtration with Dacron felt tubes, Table 21 suggests that there are no dramatic differences between the capture characteristics of these two dusts. It should be noted, however, that the system capacity for talc is considerably lower than that for fly ash. For example, in tests to be discussed later, the effective K values for fly ash and talc, respectively, appear as 14.5 and 80 inch water/ft./min./lb./ft.^{2}. The fact that, on the average, the residual talc weight is 290 grains/ft.^{2} versus 583 grains/ft.^{2} for fly ash/Dacron tests and 492 grains/ft.^{2} for fly ash/wool tests indicates that proportionally more talc is retained on the basis of inlet loading (12 grains/ft.^{3} for fly ash and only 1.6 grains/ft.^{3} for talc).

Filtration Parameters - Limited tests were performed in which the inlet dust loadings were reduced by roughly 12 times. In contrast to prior shaken bag tests where outlet concentration correlated very weakly if at all with inlet loading, (Table 12) the pulse jet systems are seen to be highly responsive to loading changes. The outlet concentrations are 3 to 5 times greater at the higher load levels over the range of reservoir pressures studied. Based upon approximate measurements, the residual dust holdings immediately after cleaning are nearly the same for all operating conditions shown in the matrix of Table 22. After a 1-minute filtering interval, one should find that about 12 times as much dust has deposited under standard filtering conditions (11.6 grains/ft.^{3} and 8.5 ft./min. filtration velocity). It follows that dust penetrations should be appreciably lower if the majority of the dust particles escape the filter during the filtration period. The fact that the reverse is true can only be explained by assuming that most of the dust release takes place immediately upon cessation of pulsing. When normal air flow is resumed, the dust concentration on the dirty air side of the fabric momentarily exceeds the normal level due to enrichment by particles dislodged from the filter (but too small to have settled completely to the hopper). Several measurements by B&L counter presented later in this section suggest strongly that most of the dust escapes the bag during the early phase of filtration.

Table 21. TALC AND FLY ASH FILTRATION WITH DACRON FELT AT 8.5 ft./min.

Cleaning parameters	Talc emissions[a]		Fly ash emissions[b]	
	Concentration[c] grains/ft.^{3} x 10^6	Percent penetration	Concentration[c] grains/ft.^{3} x 10^6	Percent penetration
Direct pulse, 40 psig Pulse frequency, 1 min. Pulse duration, 0.06 sec.	251	0.016	1960	0.016
Damped pulse, 70 psig Pulse frequency, 1 min. Pulse duration, 0.06 sec.	218	0.014	613	0.051
Damped pulse, 40 psig Pulse frequency, 1 min. Pulse duration, 0.06 sec.			330	0.028
Pulse duration, 0.30 sec.	100	0.006		
Damped pulse, 70 psig Pulse frequency, 4 min. Pulse interval, 0.06 sec.	20	0.001		

[a] Inlet concentration = 1.6 grains/ft.^{3}.

[b] Inlet concentration = 12 grains/ft.^{3}.

[c] Concentration estimated gravimetrically by RDM mass monitor.

Table 22. EFFECT OF VARIATIONS IN FILTRATION VELOCITY AND INLET LOADING ON FLY ASH EMISSIONS WITH DACRON FELT

Outlet concentration grains/ft.^{3} x 10^6 [a]					
Reservoir pressure (psig)	Ci = 0.87 gr/ft.^{3} V = 8.5 ft./min. (low load)	Ci = 9.9 gr/ft.^{3} V = 6.2 ft./min. (low flow)	Ci = 11.6 gr/ft.^{3} V = 8.5 ft./min. (standard)	Ratio	
				Standard / Low load	Standard / Low flow
40	65 (177)[b]	44 (220)	250 (240)	3.8	5.7
70	102 (160)	98 (185)	500 (170)	4.9	5.1
100	852 (163)	607 (192)	2500 (167)	2.9	4.1

[a] Concentration measurements by RDM monitor

[b] Numbers in parenthesis are residual dust holdings in grams.

Note: Pulse interval, 1 min.; pulse duration 0.06 sec. Damped pulses.

A second sequence of tests in which the filtration velocity was reduced from 8.5 to 6.2 ft./min. (and the inlet concentration reduced slightly) also showed a significant; i.e., a 5-fold reduction in emissions. Part of the decrease in effluent concentration is charged to the fact that about 40 percent less dust is deposited on the filter over a 1-minute filtration cycle. It appears, however, that the magnitude of the filtration velocity may also be important during the first part of the filtering cycle. On the premise that the jet pulse loosens considerable dust without actually dislodging it, the lower (6.2 versus 8.5 ft./min.) filtration velocity should entrain fewer particles and therefore lead to lower effluent loadings.

Design Modifications - It has been pointed out previously that the experimental pulse jet system was constructed so that many operating and design features could be varied. During the present study, it was possible to examine in at least cursory fashion the following factors that were suspected to influence overall system performance:

- Pulse damping - Clean air side - In prior descriptions of the impact of reservoir pressure on particulate emissions, considerable data were presented showing the effect of pulse damping. Data reported in Figures 55 and 62 for fly ash and Dacron and wool felt bags indicated that use of the damped pulse technique resulted in about a 5-fold decrease in effluent concentrations. Although a secondary damping reservoir (Figure 54) was the means used to accomplish a more gradual return to the normal (filtration) pressure gradient, it appears that the same results could be attained more simply by changing the closing time of the solenoid valve.

- Pulse generation - Clean air side - In the normal arrangement for the jet pulse system, the nozzle tip is located about 2 inches above the inlet to the Venturi element attached to the exit end of the bag. The nozzle itself consists of a 2-inch length of 1/4-inch pipe with a true inside diameter of 0.364 inch. When the complete nozzle assembly is detached, however the air vents directly into the plenum through a 0.84 inch diameter opening located 12 inches above the bag exit. Limited measurements presented in Table 23, Tests 1 through 15 indicate that the

Table 23. SUMMARY OF TEST PARAMETERS FOR FLY ASH AND TALC FILTRATION WITH DACRON AND WOOL FELTS

Test number	Dust/[a] fabric	Air flow ($ft.^3/min$)	Inlet conc. $gr./ft.^3$	Outlet[b] conc. $gr./ft.^3 \times 10^3$	Filter resistance in. water		Reservoir pressure[c] (psig)	Pulse freq. $min.^{-1}$	Pulse duration (sec.)	Comment
					Average	Residual				
1	F/D	40	12.0	B 1.17	3.1	2.6	40	0.2	0.15	Plenum pulse, no
2	F/D	45	12.0	B 0.53	4.3	4.0	40	0.1	0.15	jet or Venturi;
3	F/D	40	12.0	B 0.97	4.5	4.4	30	0.05	0.10	Tests 1 through 14
4	F/D	40	12.0	B 1.13	5.0	4.8	30	0.06	0.13	
5	F/D	40	12.0	B 1.55	4.7	4.6	30	0.03	0.06	
6	F/D	40	12.0	B 0.56	5.1	5.0	30	0.1	0.15	
7	F/D	40	12.0	B 1.47	4.7	4.2	40	0.5	0.06	
8	F/D	40	12.0	B 2.12	2.1	2.0	40	0.03	0.06	
9	F/D	40	12.0	B 1.64	3.0	2.9	40	0.06	0.06	
10	F/D	40	12.0	B 2.60	2.3	1.7	50	0.1	0.15	
11	F/D	40	12.0	B 1.59	2.9	1.8	50	0.2	0.15	
12	F/D	40	12.0	B 2.30	1.5	1.3	50	0.06	0.06	
13	F/D	40	12.0	B 2.29	1.4	1.3	50	0.04	0.06	
14	F/D	40	12.0	B 1.66	3.0	2.7	40	0.1	0.15	
15	F/D	40	12.0	B 1.84	4.7	4.3	40	0.1	0.15	5/8-inch nozzle
16	F/D	40	12.0	B 1.27	5.3	4.8	40	0.2	0.15	and Venturi;
17	F/D	40	12.0	B 1.85	4.2	4.0	40	0.06	0.06	Tests 15 through 18.
18	F/D	40	12.0	B 1.62	5.6	5.4	40	0.06	0.06	No collection drum
19	F/D	40	12.0	B 1.31	4.6	4.2	60	0.1	0.06	Commercial con-
20	F/D	40	12.0	B 0.21	6.2	6.1	D 60	0.1	0.06	figuration, 1/4-
21	F/D	36	12.0	B 0.32	7.3	7.1	40	0.1	0.15	inch jet with
22	F/D	40	12.0	B 2.66	2.4	2.2	90	0.1	0.06	Venturi; Tests
23	F/D	40	12.0	B 0.57	4.6	4.2	D 90	0.1	0.06	19 through 33
24	F/D	40	12.0	B 1.00	6.2	5.9	40	0.1	0.15	

Table 23 (Continued). SUMMARY OF TEST PARAMETERS FOR FLY ASH AND TALC FILTRATION WITH DACRON AND WOOL FELTS

Test number	Dust/[a] fabric	Air flow ($ft.^3/min.$)	Inlet conc. $gr./ft.^3$	Outlet[b] conc. $gr./ft.^3 \times 10^3$	Filter resistance in. water		Reservoir pressure[c] (psig)	Pulse freq. $min.^{-1}$	Pulse duration (sec.)	Comment
					Average	Residual				
25	F/D	30	12.0	B 0.62	7.2	7.1	40	0.1	0.06	Commercial configuration, 1/4-inch jet with Venturi; Tests 19 through 33
26	F/D	40	12.0	B 1.08	5.3	4.9	70	0.1	0.06	
27	F/D	32	12.0	B 0.75	6.9	6.7	D 70	0.1	0.06	
28	F/D	40	12.0	B 0.59	6.0	5.7	D 100	0.1	0.06	
29	F/D	40	12.0	B 2.05	3.2	2.8	100	0.1	0.06	
30	F/D	40	12.0	B 1.05	4.6	4.3	90	0.1	0.06	
31	F/D	40	12.0	B 0.67	5.5	5.0	90	0.2	0.06	
32	F/D	40	12.0	B 0.95	5.5	5.0	90	0.2	0.10	
33	F/D	40	12.0	B 0.78	5.5	5.0	90	0.2	0.20	
35	F/D	40	11.6	R 1.46	4.4	3.4	D 70	1.0	0.15	
36	F/D	40	11.6	R 3.32	4.1	3.0	70	1.0	0.15	
37	F/D	40	11.6	R 0.80	3.5	2.9	D 70	0.4	0.15	
38	F/D	40	11.6	R 3.54	2.9	2.0	70	0.4	0.15	
39	F/D	40	11.6	R 2.07	3.7	2.8	70	0.4	0.06	
40	F/D	40	11.6	R 0.09	5.1	4.8	D 70	0.4	0.06	
41	F/D	40	11.6	R 1.09	5.6	5.3	40	0.4	0.06	
42	F/D	40	11.6	R 0.15	7.0	6.8	D 40	0.4	0.06	
43	F/D	40	11.6	R 2.06	5.5	4.8	D 70	1.0	0.15	
44	F/D	40	11.6	R 3.48	3.8	3.2	70	1.0	0.06	
45	F/D	40	11.6	R 2.24	5.5	4.4	70	1.0	0.06	
46	F/D	40	9.3	R 1.85	5.6	4.8	D 100	1.0	0.06	
47	F/D	40	0.87	R 0.85	3.7	3.3	D 100	1.0	0.06	Low loading tests, Tests 47 through 50
48	F/D	40	0.87	R 0.12	5.0	4.6	D 70	1.0	0.06	
49	F/D	40	0.87	R 0.07	6.5	6.0	D 40	1.0	0.06	
50	F/D	40	0.87	R 0.10	5.0	4.5	D 70	1.0	0.06	

Table 23 (Continued). SUMMARY OF TEST PARAMETERS FOR FLY ASH AND TALC FILTRATION WITH DACRON AND WOOL FELTS

Test number	Dust/[a] fabric	Air flow ($ft.^3/min.$)	Inlet conc. $gr./ft.^3$	Outlet[b] conc. $gr./ft.^3 \times 10^3$	Filter resistance in. water		Reservoir pressure[c] (psig)	Pulse freq. $min.^{-1}$	Pulse duration (sec.)	Comment
					Average	Residual				
51	F/D	29	9.9	R 0.10	4.4	4.0	D 70	1.0	0.06	Low flow tests;
52	F/D	29	9.9	R 0.61	3.8	3.5	D 100	1.0	0.06	Tests 51 through 53
53	F/D	29	9.9	R 0.04	4.7	4.4	D 40	1.0	0.06	
54	F/D	40	13.1	R 2.00	4.3	3.3	D 70	1.0	0.06	
55	F/D	40	13.1	R 0.26	5.0	3.8	D 50	1.0	0.06	
56	F/D	40	13.1	R 1.96	4.6	3.7	40	1.0	0.06	
57	F/D	40	13.1	R 0.33	6.4	5.5	D 40	1.0	0.06	
58	F/D	40	11.0	R 3.16	4.2	3.2	D 100	1.0	0.06	
59	F/D	40	11.6	R 6.87	3.3	2.4	100	1.0	0.06	
60	F/D	40	11.6	R 3.20	6.7	5.8	70	2.0	0.06	
61	F/D	40	11.6	R 1.88	7.4	6.5	70	2.0	0.06	
62	F/D	40	11.6	R 2.29	4.8	3.8	70	2.0	0.06	Nozzle raised
63	F/D	40	11.6	R 0.23	5.3	4.3	D 70	1.0	0.06	4 inches
64	F/D	40	11.6	R 0.61	5.2	4.2	D 70	1.0	0.06	
65	F/W	40	9.5	R 2.40	4.2	3.4	70	1.0	0.06	
66	F/W	40	9.2	B 0.58	3.4	2.5	100	1.0	0.06	
67	F/W	40	11.6	B 0.15	3.6	2.8	D 100	1.0	0.06	
68	F/W	40	11.6	R 1.00	4.0	3.1	D 90	1.0	0.06	
69	F/W	40	11.6	R 0.20	4.9	3.9	D 70	1.0	0.06	
70	F/W	40	11.6	R 0.66	7.2	6.7	D 40	1.0	0.06	
71	F/W	40	11.6	R 0.13	4.3	4.6	D 70	0.4	0.06	
72	F/W	40	11.6	R 1.96	6.4	3.4	D 70	2.0	0.06	
73	F/W	40	11.6	R 1.51	4.2	3.4	70	1.0	0.15	
74	F/W	40	11.6	B 0.38	4.2	3.9	70	1.0	0.06	

Table 23 (Continued). SUMMARY OF TEST PARAMETERS FOR FLY ASH AND TALC FILTRATION WITH DACRON AND WOOL FELTS

Test number	Dust/[a] fabric	Air flow ($ft.^3/min.$)	Inlet conc. $gr./ft.^3$	Outlet[b] conc. $gr./ft.^3 \times 10^3$	Filter resistance in. water		Reservoir pressure[c] (psig)	Pulse freq. $min.^{-1}$	Pulse duration (sec.)	Comment
					Average	Residual				
75	F/W	40	11.6	B 0.38	4.9	3.9	D 70	1.0	0.15	
76	F/W	40	11.6	R 1.33	5.3	--	70	1.0	0.06	
77	F/W	40	11.6	R 2.62	5.0	--	70	1.0	0.15	
78	F/W	40	11.6	R 4.85	4.1	--	70	1.0	0.10	Supplementary plenum pulse, 100 100 psig, 0.35 sec.
79	F/W	40	11.6	R 0.09	4.6	3.7	D 70	1.0	0.06	
80	F/W	40	11.6	R 0.29	4.7	3.6	D 70	1.0	0.06	Loose bag
81	F/W	40	11.6	R 0.30	5.2	4.3	D 70	1.0	0.06	Taut bag
82	T/D	40	1.53	R 0.22	1.9	1.4	D 70	1.0	0.06	
83	T/D	40	1.53	R 0.02	6.0	2.7	D 70	4.0	0.06	
84	T/D	40	1.53	R 0.05	4.7	2.4	D 70	4.0	0.30	
85	T/D	40	1.53	R 0.10	2.9	2.1	D 40	1.0	0.30	
86	T/D	40	1.53	R 0.22	2.4	1.4	40	1.0	0.30	
87	T/D	40	1.53	R 0.44	2.4	1.5	40	1.0	0.15	
88	T/D	40	1.53	R 0.25	2.5	1.7	40	1.0	0.06	
89	T/D	40	1.53	R 0.22	2.1	1.6	40	1.0	0.15	

[a] F/D = fly ash/Dacron; F/W = fly ash/wool; T/D = talc/Dacron

[b] B indicates B and L measurement; R indicates RDM measurement.

[c] D indicates damped pulse, otherwise direct.

pulse technique (no Venturi used) did not cause any significant difference in particle emissions relative to the conventional 1/4-inch nozzle system cited previously. The compressed air requirement is increased by about 10 percent, and the average filter resistance is somewhat lowered.

When a 0.622-inch nozzle was substituted for the 1/4-inch model, the outlet concentration was higher and, consistent with this higher emission, the average filter resistance was lower. Again the Venturi section was not used during the above tests.

- Nozzle location - Clean air side - Raising the 1/4-inch nozzle tip to a position 6 inches above the Venturi inlet rather than the noraml 4 inches, permitted improved bag cleaning during special tests in which the cleaning interval was extended to 2 minutes, Tests 62 and 63 in Table 23. It appeared that with an approximate doubling of the dust deposit upon the bag very poor dust removal was obtained over the upper 10 percent of the bag. Allowing the air jet to entrain more air from the plenum reduces the possibility of air entrainment from within the bag. The latter process can induce air from the dirty air side which reverses the flow direction sought during the cleaning interval.

- Baghouse volume - Dirty air side - During typical field operation, it is highly unlikely that more than 10 percent of the bags (or compartments) will be undergoing cleaning at the same time. Hence, during the transient cleaning period when a small fraction of the system gas handling capacity is lost, the remaining on-line components accommodate the diverted flow with but a small increase in chamber pressure.

  Unfortunately, in the single bag test unit, the pulse period interrupted all filtration flow. Therefore, the main fan continued to pump air into the dirty air side of the system up to its static pressure capacity. Because the chamber containing the bag was designed to provide gas approach velocities on the dirty air side typical of those found in large field assemblies, its volume was only about 3 ft.^{3} Therefore, even during brief, approximately 0.06 second pulses a transient back pressure increase of 5 inches of water might be expected. When the slide valve was open between the baghouse and the collection barrel beneath the hopper, an additional 4 ft.^{3} was added to the "dirty air" volume of the system. Thus, a 0.06 second pulse caused a smaller pressure increase, approximately

2-1/2 inch of water, on the dirty air side. The effect of varying the air volumes on the dirty air side of the system is shown by Tests 17 and 18, Table 23. Closing the slide damper led to a decreased pressure differential across the filter during the pulse interval. As a result, the cleaning was less effective, the effluent dust concentration slightly lower, and the operating resistance slightly higher. Although these data are far too limited to allow any firm conclusions, we do not believe that the volume factor introduced by the special test system had any serious effect on the simulation of field performance conditions.

- Bag tension - Dirty air side - The circumferential snugness of fit of the bag on its supporting cage was lessened by reducing the cage diameter by 3/8 inch. In a second test, a wedge was inserted between the bag and the frame to produce a tighter fit. The results of these variations are reflected by Tests 47 and 28 (Table 23) upon wool felt bags with fly ash. Surprisingly, the data showed negligible differences both for outlet concentration and average bag resistance. It had been expected that a slack bag might undergo a more vigorous motion (greater acceleration) and hence be cleaned more effectively.

Particle Size and Concentration Changes During Filtration Cycle

Data have been presented previously in this Chapter on those factors that exerted (or were expected to exert) measurable effects on particulate emissions from pulse cleaned fabric filters. We have shown that the reservoir pressure level, the pulse form as controlled by damping tank, the inlet loading level, the filtration velocity, and the duration of the compressed air pulse exert significant effects on effluent dust properties. On the other hand the behavior of Dacron and wool felts with respect to the collection of both fly ash and talc showed only minor differences. Likewise a reduction in the frequency of cleaning and minor permutations in nozzle dimensions and location did not produce any important changes in system performance, suggesting that other areas be examined for possible improvements in system operation.

In the following paragraphs, the observed changes in concentration for various particle diameters over the period of the filtration cycle are examined. Again, a single particle light scattering counter such as used for the mechanical shaking systems proved to be the only measurement technique capable of providing the desired time resolution.

It has been shown earlier in Figures 58 and 59 that when the fabric is cleaned very frequently (filtration interval < 0.2 minute) the emission increases with frequency, but with less frequent cleaning it is relatively independent of frequency. This suggests that emission is largely associated with the instant of cleaning and the transient period immediately thereafter. This hypothesis appears to be confirmed by Figures 65 through 70 which show particle concentrations by size and total mass concentration as estimated by light scattering measurements over typical operating cycles. In fact, after correcting for the delay in signal output (sampling time and particle counting time combined were approximately 0.1 minute) the emission peak appears to be almost coincident with the termination of the pulse.

Based upon the clean air volume (1.44 $ft.^3$) and the filtration flow (40 $ft.^3/min.$) any residual dust in suspension in the clean air side of the system would be rapidly flushed out. On a very conservative basis, a concentration reduction of at least 16 times at the end of 1 minute is predicted by an ideal logarithmic dilution process. This appears to be the apparent decay rate for the larger particle sizes during some tests although with high pressure pulses, large particles are found in the effluent over the complete filtration cycle. The data would tend to suggest, therefore, that the observed emissions can be only partially explained by a simple flushing out process. The remaining particles must represent a combination of those that penetrate continuously over the filtration cycle or those that are re-entrained from the filter over the same time period.

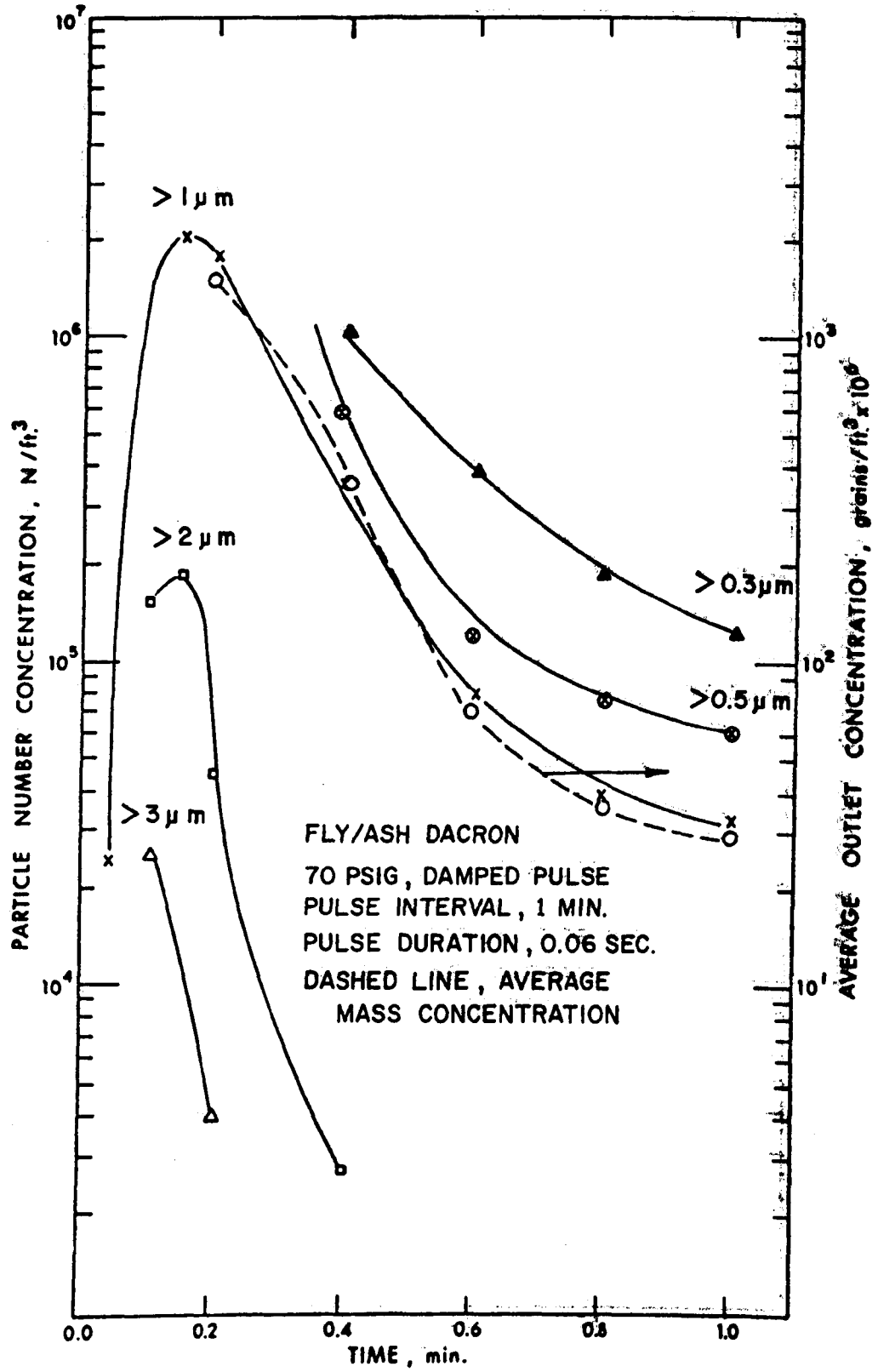

Figure 65. Particle concentration versus time for selected sizes

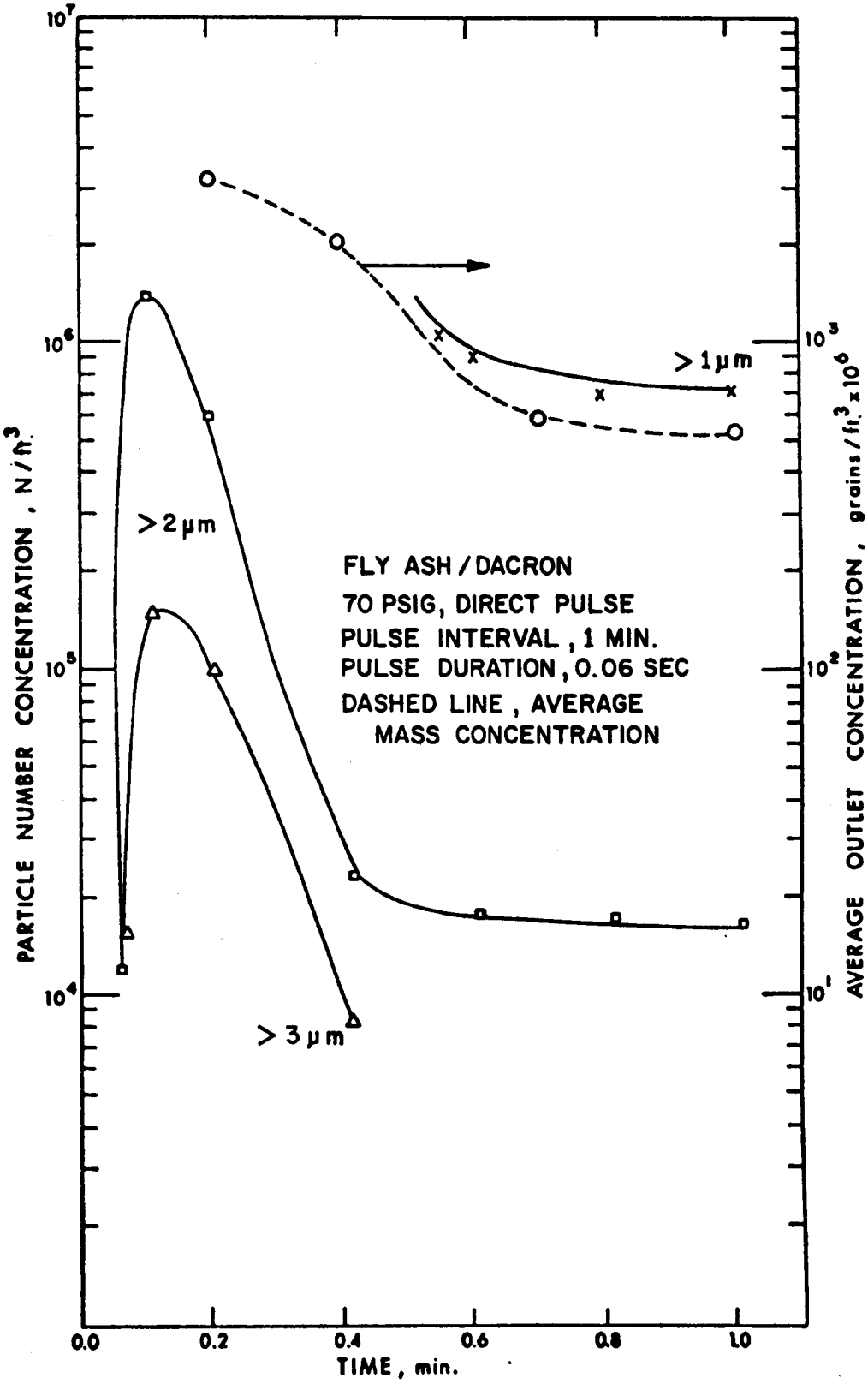

Figure 66. Particle concentration versus time for selected sizes

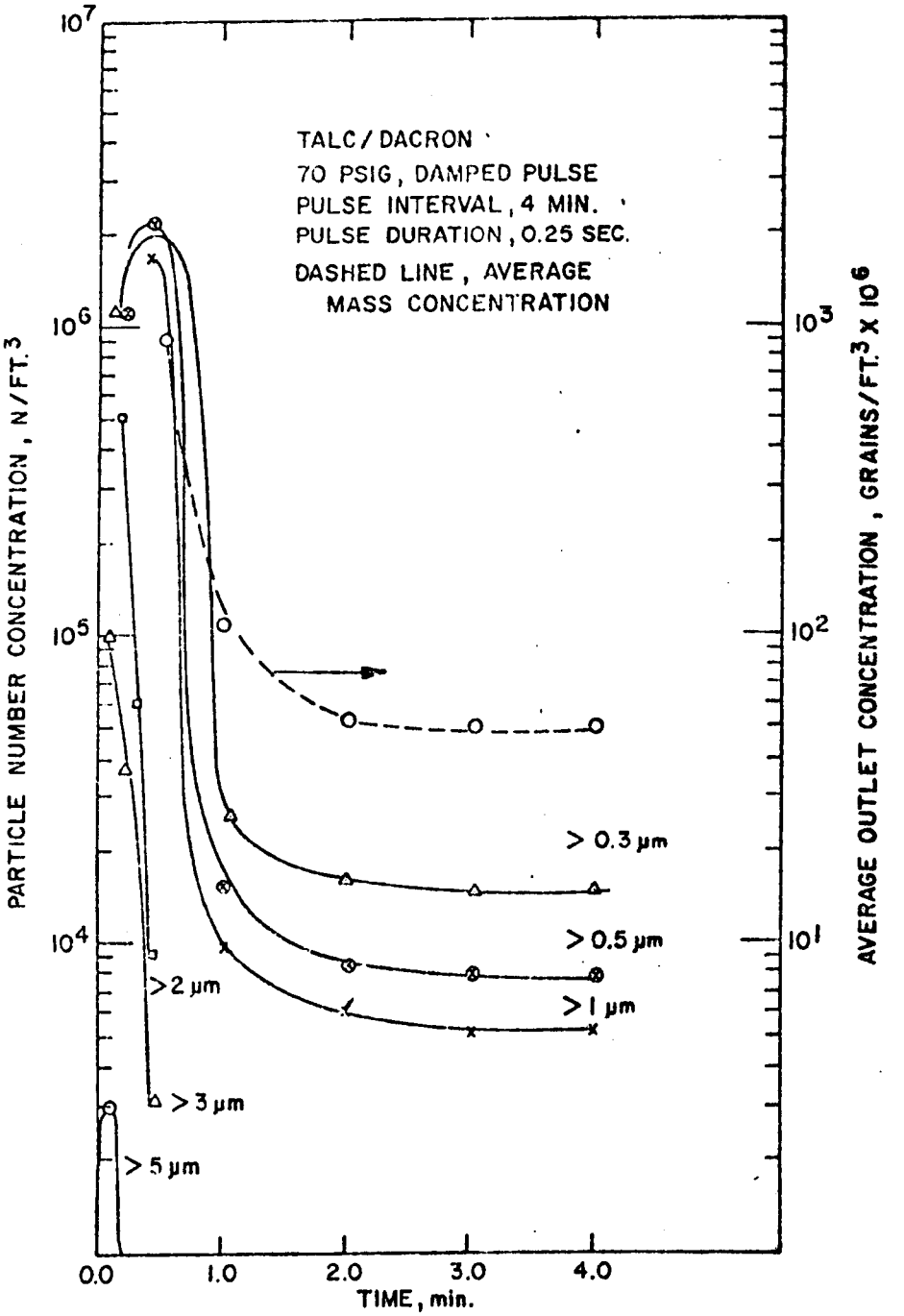

Figure 67. Particle concentration versus time for selected sizes

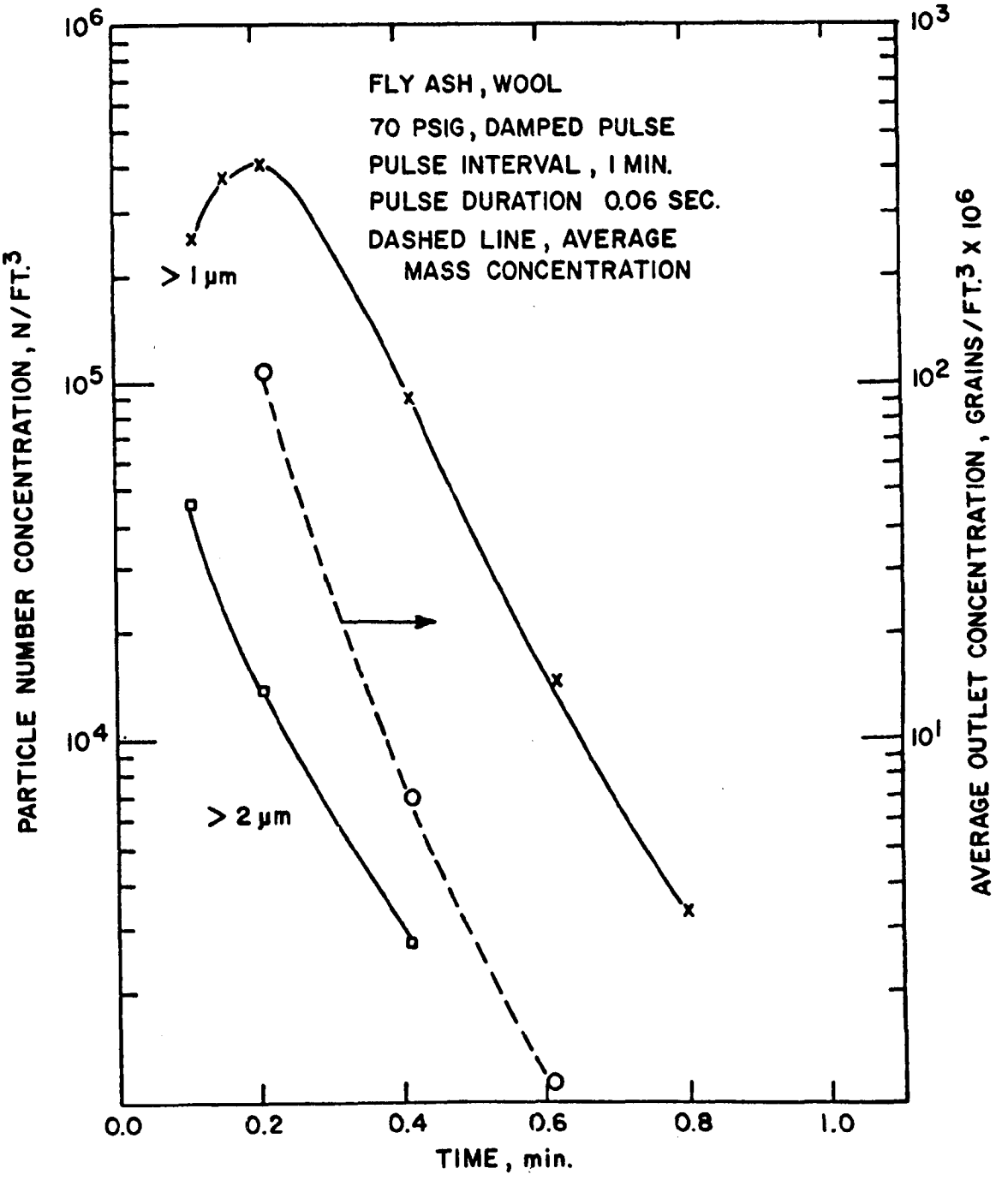

Figure 68. Particle concentration versus time for selected sizes

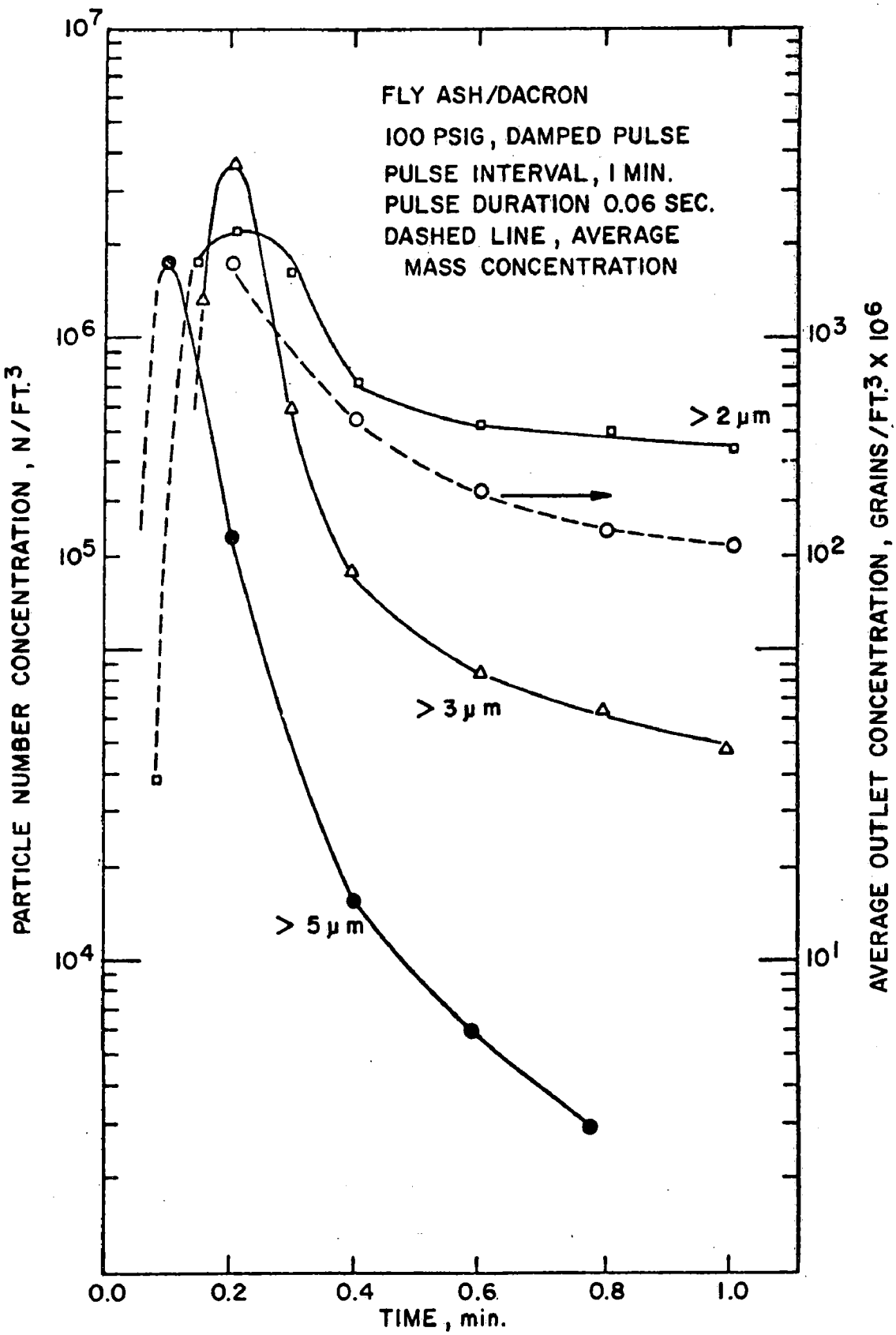

Figure 69. Particle concentration versus time for selected sizes

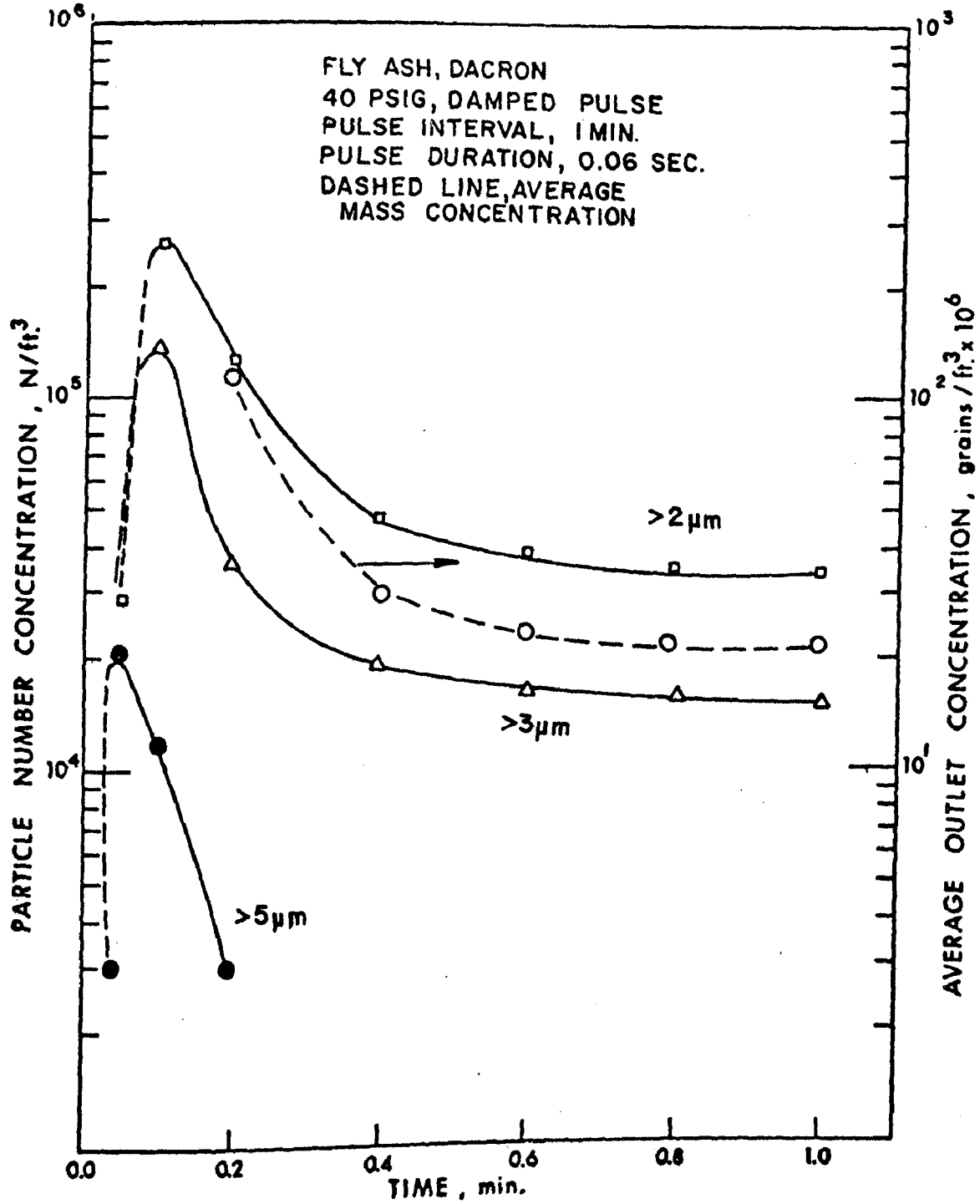

Figure 70. Particle concentration versus time for selected sizes

Generally speaking, dust penetration decreases progressively over the filtration cycle with the greatest changes observed for the larger particles. The estimated mass concentrations (calculated on the basis of the indicated number concentrations and an assumed particle specific gravity of 2.0) appear as the right hand ordinates of Figures 65 through 70. The decay paths for the overall mass concentrations, which are shown as dotted lines, tend to follow those of the predominant particle sizes. Prior filtration tests with mechanically shaken, cotton bags indicated that the overall weight collection efficiencies for fly ash decreased about one order of magnitude for each addition of 5 to 6 grains of dust per square foot of filter area. Based upon a cloth loading rate of approximately 100 grains/ft.^{2}/min. for pulse jet filtration, one might predict that efficiency would decrease one order of magnitude in 0.055 minute. The family of curves appearing in Figures 65 through 70, however, not only indicate much less rapid decay rates but even a tendency to level off in effluent concentrations after the first 1/2 minute of filtration.

It appears, therefore, that the filtration process is quite different for the felt media. Whereas experimental measurements and theoretical calculations indicated that the interstitial pore structure filled quite rapidly with mechanically shaken, woven fabrics, the predominant filtration process with pulse-cleaned felt media appears to be mainly a statistical or deep bed process in which particle and fiber size, fiber packing density, bed depth, filtration velocity and inlet concentrations may play very important roles.

Regardless of the mechanisms involved in the filtration process using damped pulses, the dust concentrations at the end of each 1 minute filter cycle ranged from 20 to 100 times less than that estimated after 0.1 minute of filtration for systems. High early emission rates are believed to be associated mainly with the pulse action upon already loosened particles and a transient dilation of the pore structure.

Residual Filter Resistance

The fact that about 95 percent of the operating pressure differential is due to imbedded dust rather than to the fiber matrix (clean media resistance at 8.5 ft./min. is 0.12-inch water) suggests that most of the particle collection is associated with the dust rather than with the fiber matrix. Unfortunately, the in-situ measuring technique used to estimate gravimetrically the residual or final filter dust holdings was insufficiently accurate to establish useful correlations between filter dust holding and average particulate emissions or residual resistance. It is believed, however, that the amount of dust initially present on the filter should relate closely to the average, initial, or final filter resistance for a fixed set of filtration and cleaning parameters. Figure 71 indicates a fairly high correlation ($\sim = 0.66$) between residual dust deposit and residual filtration resistance despite the fact that the data were collected under wide range of dust, fabric and pulsing conditions.

In Figure 72, the average filter emission (assumed to be proportional to the peak emission after cleaning) is plotted against the average filter resistance. A consistent relationship is indicated in which the outlet concentration decreases approximately an order of magnitude for each additional 2-1/2 inch water of pressure differential. The data points depicted on Figure 72 should be considered in three general categories. The first represents a sample population based upon fly ash/Dacron measurements in which the pulse interval was constant at 1 minute and the inlet dust concentration was 12 grains/ft.^{3}. Otherwise, reservoir pressures ranged from 40 to 100 psig, pulse durations were 0.06 and 0.15 second and the pulses were eigher direct or damped. Despite the indicated variations, the effluent concentration seems to depend mainly on the filter resistance as shown by the regression line labeled A. A second data set depicts a limited test sequence in which the inlet fly ash loading was reduced to 0.87 grains/ft.^{3}. Previous analyses of the measurements shown on Curve B (also shown in Figure 55), suggested that

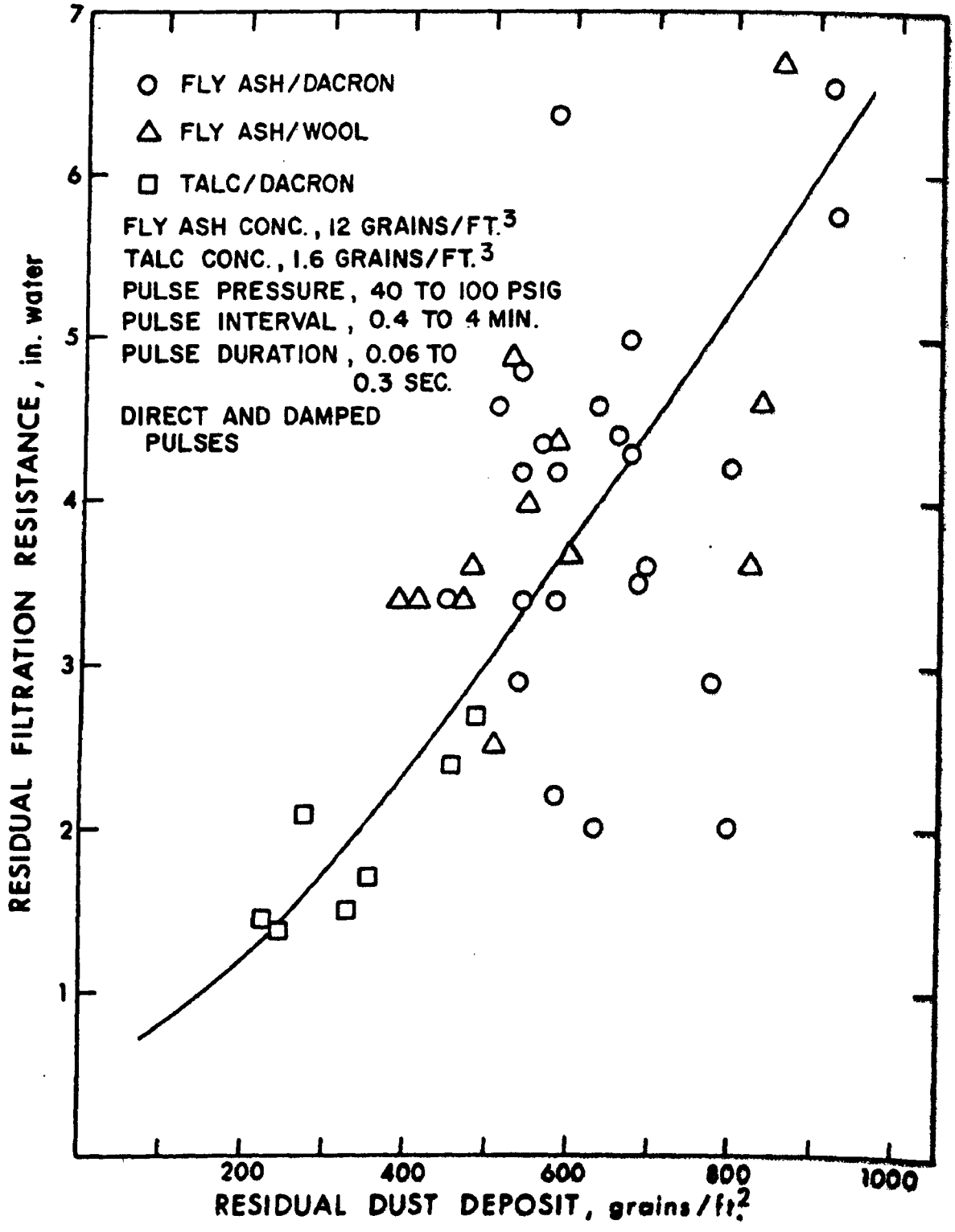

Figure 71. Relationship between residual dust deposit and residual filter resistance

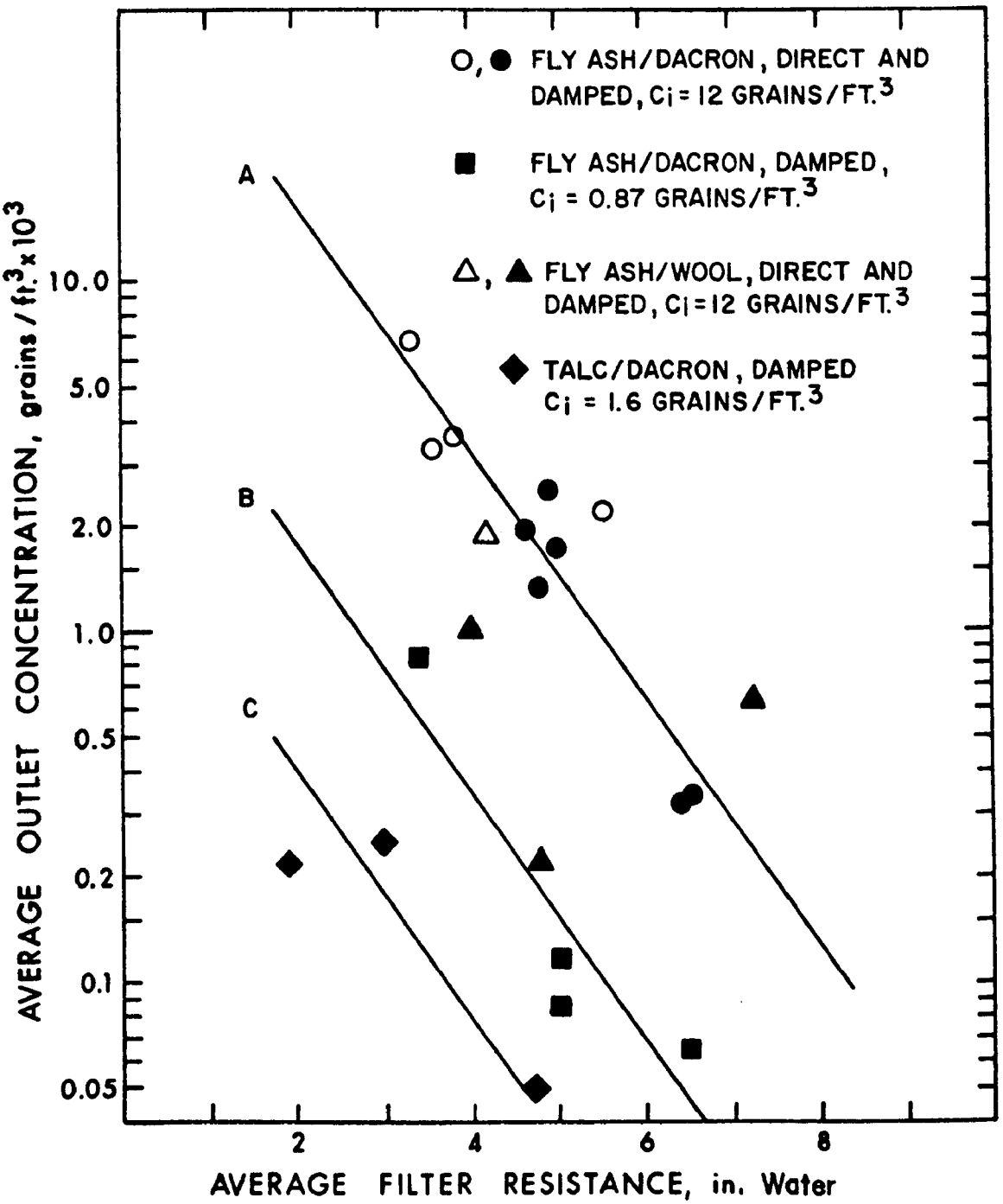

Figure 72. Average outlet concentration versus average filter resistance (reservoir pressure 40 to 100 psig, pulse interval 1 min., and pulse duration 0.06 to 0.15 sec.

the emission related not only to the filter average dust holding but also to the inlet concentration. In view of the limited information available, there appears to be no reason to assume a different slope for Curves A and B.

The third data set, Curve C, is based upon talc filtration with a Dacron felt. Except for the fact that the loading was 1.6 grains/ft.^{3}, the variables were the same as cited for Curves A and B. It was not expected that the talc data would fall on Curve A, because inlet loading had already been shown to have a significant effect on outlet loading. The fact that filter resistance is appreciably lower for talc filtration than for fly ash based upon equal outlet concentrations, is attributed to the lower bulk density of the talc as it deposits within the fiber matrix. It is assumed that the volume and not the mass of dust within the filter pores is the key factor in determining efficiency. This concept has been discussed earlier in Chapter II in which filter efficiency for shaken bags has been related to the volume of dust upon the filter.

Although the few data points based upon fly ash filtration with wool felt are scattered broadly, they appear to fall within the realm of the fly ash/Dacron results.

Concentration Profiles, Dust Emissions

In the preceding discussions, the reported emissions are those at the outlet of the top plenum which depict the weighted average concentrations over the entire filter bag. Based on the premise that emission is related to the degree of cleaning, one expects that effluent concentrations may vary along the filter bag. By lowering a flexible sampling line (attached to the inlet of the B&L counter) into a fourth long bag it was possible to extract samples at selected locations. A vertical (upward) traverse of the bag interior provided a series of data points, each describing the average concentration of particles in the effluent air up to the point of sampling. Some particle loss took place in the

sampling lines and the shock of the cleaning pulses probably caused intermittent sloughing off of particles from the walls of the sampling tube. Despite the above problems, the measurements were considered useful as an indication of concentration variations along the bag.

Figure 73 shows that the local dust concentration levels increase as one traverses from the bottom to the top of the bag. The greatest increases takes place from the mid position to the top end of the bag in which region the cleaning appears to be the most vigorous. Based upon inspection of the bag, the densest deposits appear to be at the bottom with a steady decrease noted up to approximately the end of the Venturi section (roughly 6-inches from the top of the bag). From the Venturi element upwards, the cleaning is poor according to the apparent thickness of the residual deposit after pulsing.

Since average filter emission correlates with average pressure differential (Figure 72), it is probable that the filter bag was poorly cleaned at the lower end and over-cleaned in the region just below the Venturi. Since a concentration gradient appears with a 4 foot bag it is proposed that the potential for non-uniform cleaning might be much greater for longer bags.

Operating Filter Resistance

One of the major costs in operating a gas cleaning system is that for moving the dusty gas through the collection device. In the case of filter systems, the resistance to gas flow through the fabric medium may represent a large part of the fan total static pressure requirement. Therefore, a full understanding as to how such filtration resistance may be minimized while meeting a specific effluent criterion, is very important. In the case of mechanically shaken bags, the resistance increased linearly with time (and cloth loading) over more than 80 percent of a 30 minute filtration cycle, (see Figure 45, Chapter II). Therefore, the average operating resistance was readily determined. On

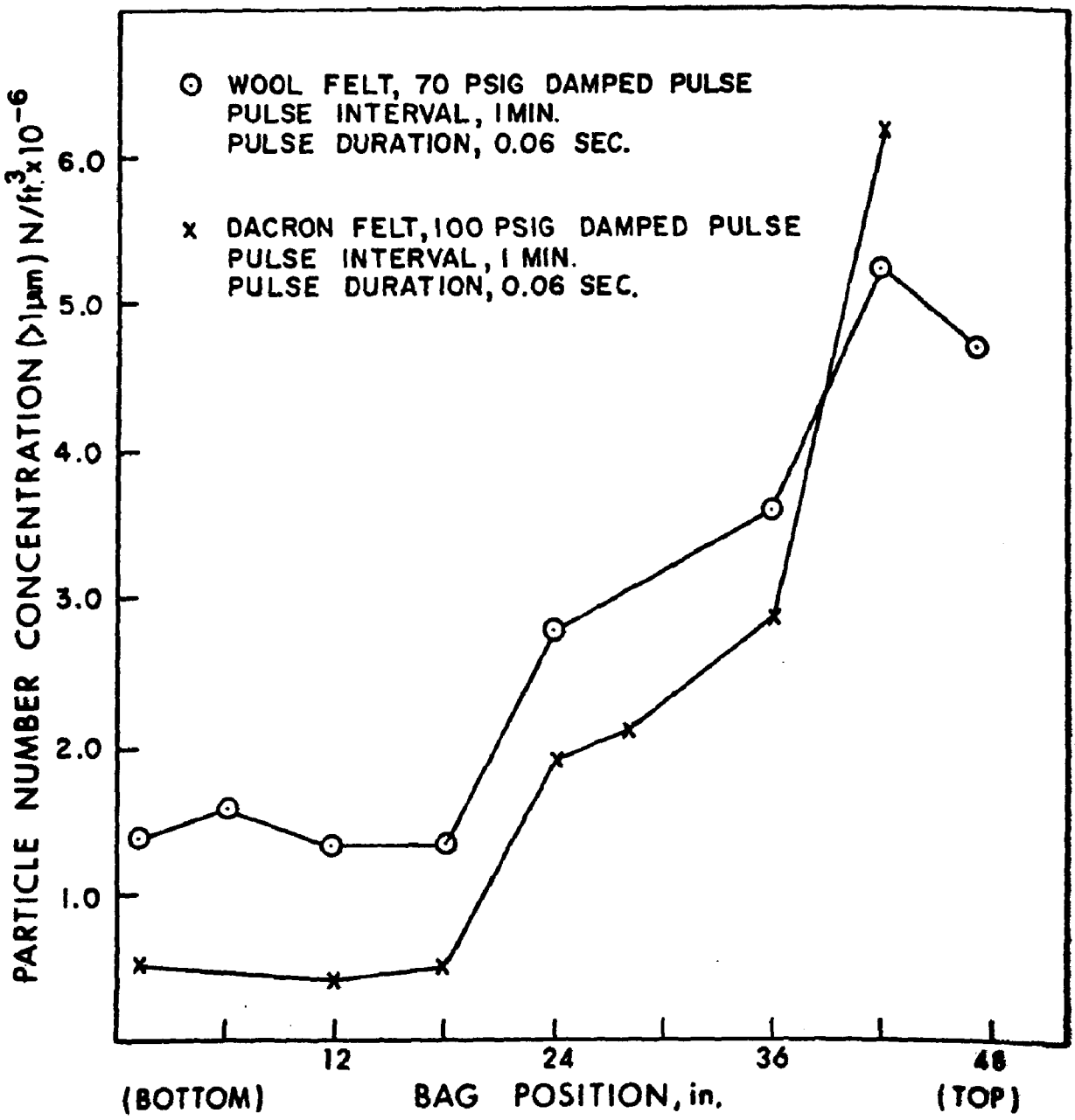

Figure 73. Dust concentration profile on exit side of bag, bottom to top. Fly ash filtration at 12 grains/ft.^{3} and 8.5 ft./min.

the other hand, it was noted that only during the last 60 percent of a normal, 1 minute filtering cycle was the resistance/time curve essentially linear for a pulse jet system, Figure 74. If the resistance curves are examined in terms of the quantity of dust deposited on the filter (expressed as grains/ft.^{2}) then 0.4 minute of pulse jet operation at 8.5 ft./min. and 12 grains/ft.^{3} should be equivalent to approximately 4 minutes of filtration with the mechanically shaken system described in Chapter II at 3 ft./min. and 3.5 grains/ft.^{3}. Therefore, it appears that the amount of fly ash required to seal over of the fabric surface is roughly the same for both the mechanically shaken cotton fabric and the pulse jet cleaned Dacron felt. If one compares the relative effluent concentrations for the mechanically shaken and the pulse jet systems, it is also seen that the greatest reduction in effluent concentration takes place during the initial 4 minute and 0.4 minute filtration periods, respectively.

Because of the rapid changes in the system when normal air flow resumes, it is impossible to define accurately the fabric resistance immediately after cleaning. It was found, however, that consistent relationships were obtained for all resistance values measured 0.1 minute after the resumption of filtration, Figure 74. Furthermore, when the average resistance of the filter for the complete (1 minute) filtration cycle was estimated by taking the actual curve path into account, it was found that it differed from the 0.5 minute value by no more than a few percent. Therefore, it was considered acceptable to use the resistance at the midpoint of the filtration cycle as the average value.

Filter resistance characteristics for talc dust and Dacron felt are given in Figure 75 for an inlet loading of 1.53 grains/ft.^{3} and a filtration velocity of 8.5 ft./min. The slopes of several curves were essentially constant irrespective of cleaning frequency, 1 to 4 minutes, and the apparent "K" value was 80 as compared to 14.5 for fly ash. In contrast to fly ash measurements, the linearity of the curves extends over a much broader range even though the surface dust loading is about

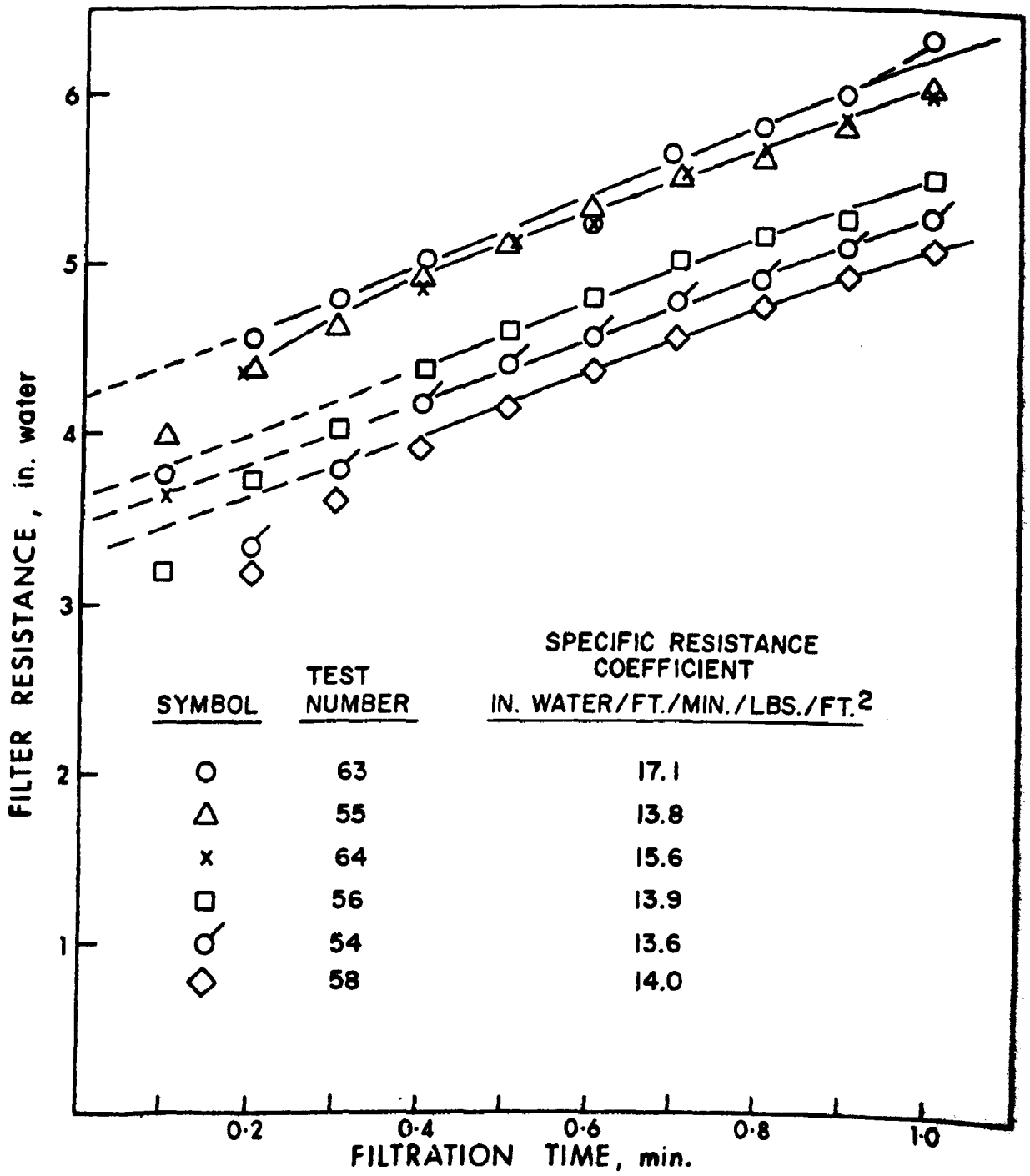

Figure 74. Resistance characteristics for fly ash and Dacron felt, inlet conc. 12 grains/ft.^{3}, filtration velocity 8.5 ft./min.

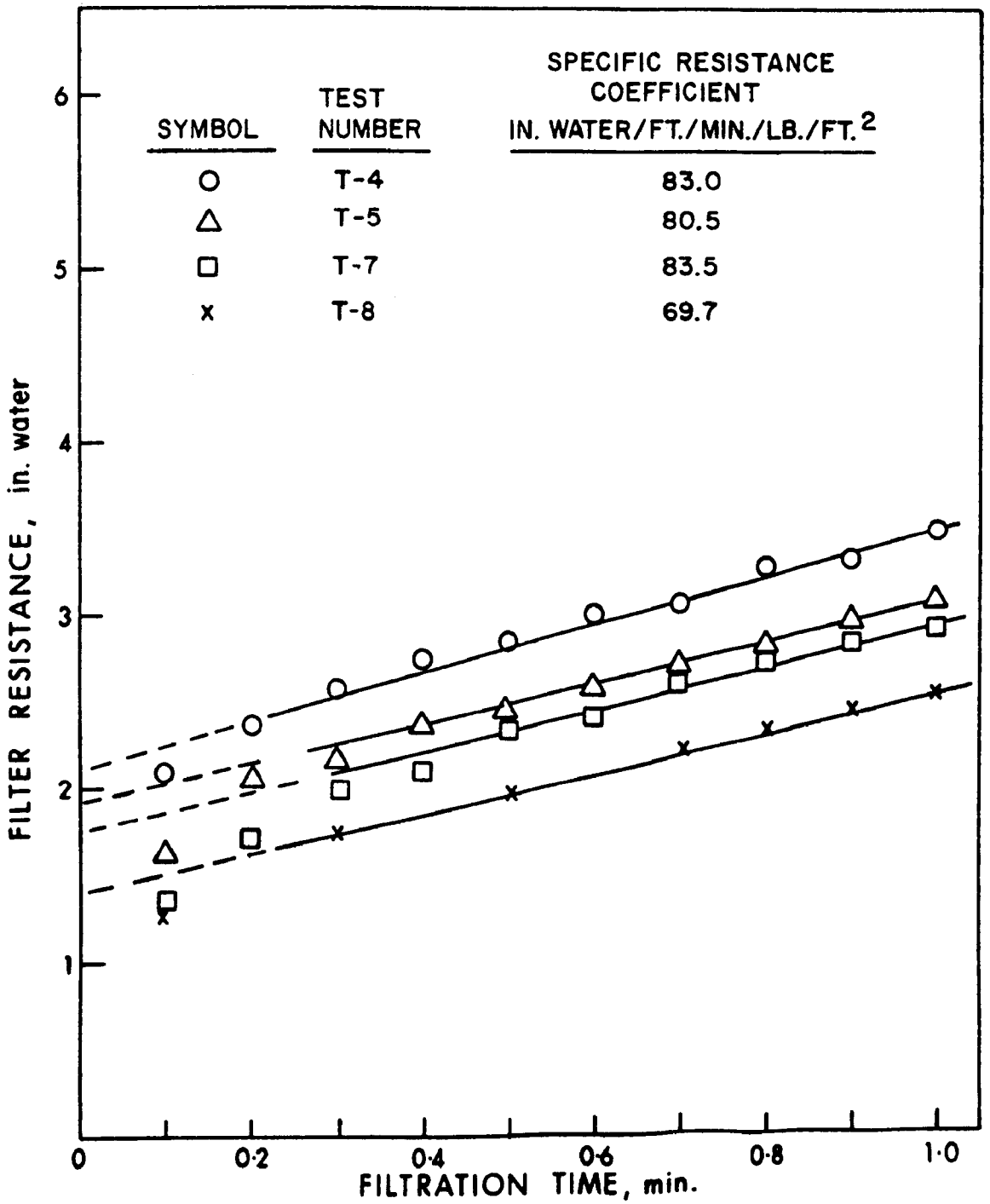

Figure 75. Resistance characteristics for talc and Dacron felt, inlet conc. 1.53 grains/ft.^{3}, filtration velocity 8.5 fpm

8 times lower. It is believed that because of the lower bulk density for talc the pore filling phase of the dust collection process is completed more rapidly. Under the latter circumstances, subsequent dust deposition is mainly superficial, which leads to an approximately linear relation between resistance rise and subsequent dust deposition.
In the following chapter, those operating factors that were expected to influence filter resistance are examined.

Compressed Air Pressure - Figure 76 indicates average filtration resistance for several measurements performed with a fly ash/Dacron system as a function of reservoir pressure. Operating filter resistance is seen to be roughly inversely proportional to reservoir pressure. In view of the limited amount of experimental data available, several variations in operating and/or cleaning parameters have been grouped for each reservoir pressure level for purposes of data smoothing. A comparison of direct and damped pulse measurements indicates an average resistance lowering of about 1-inch water when direct pulses are used. The corresponding impact on effluent concentration was much greater; i.e., a five fold increase in effluent concentration when using direct pulses according to Figure 55.

Pulse Interval - Selected data shown in Figure 77 indicate that extending the interval between pulses causes an essentially linear increase in average filter resistance. A few trials were performed in which the pulse intervals were reduced to very brief periods, ~ 0.06 to 0.1 minute. Operating resistances appeared to be higher during these tests than those for the 0.5 minute pulse intervals given in Figure 75. Presently, it is believed that some undefined instrument error led to these results. From a practical viewpoint, the reduction of pulse intervals to less than 0.5 minute for any one bag, would lead to prohibitive compressed air requirements, increased effluent concentrations as shown in Figures 58 and 59, and certainly increased air handling costs if in fact, the filter resistance actually increases for the very brief, ~ 0.06 to 0.5 minute pulse intervals.

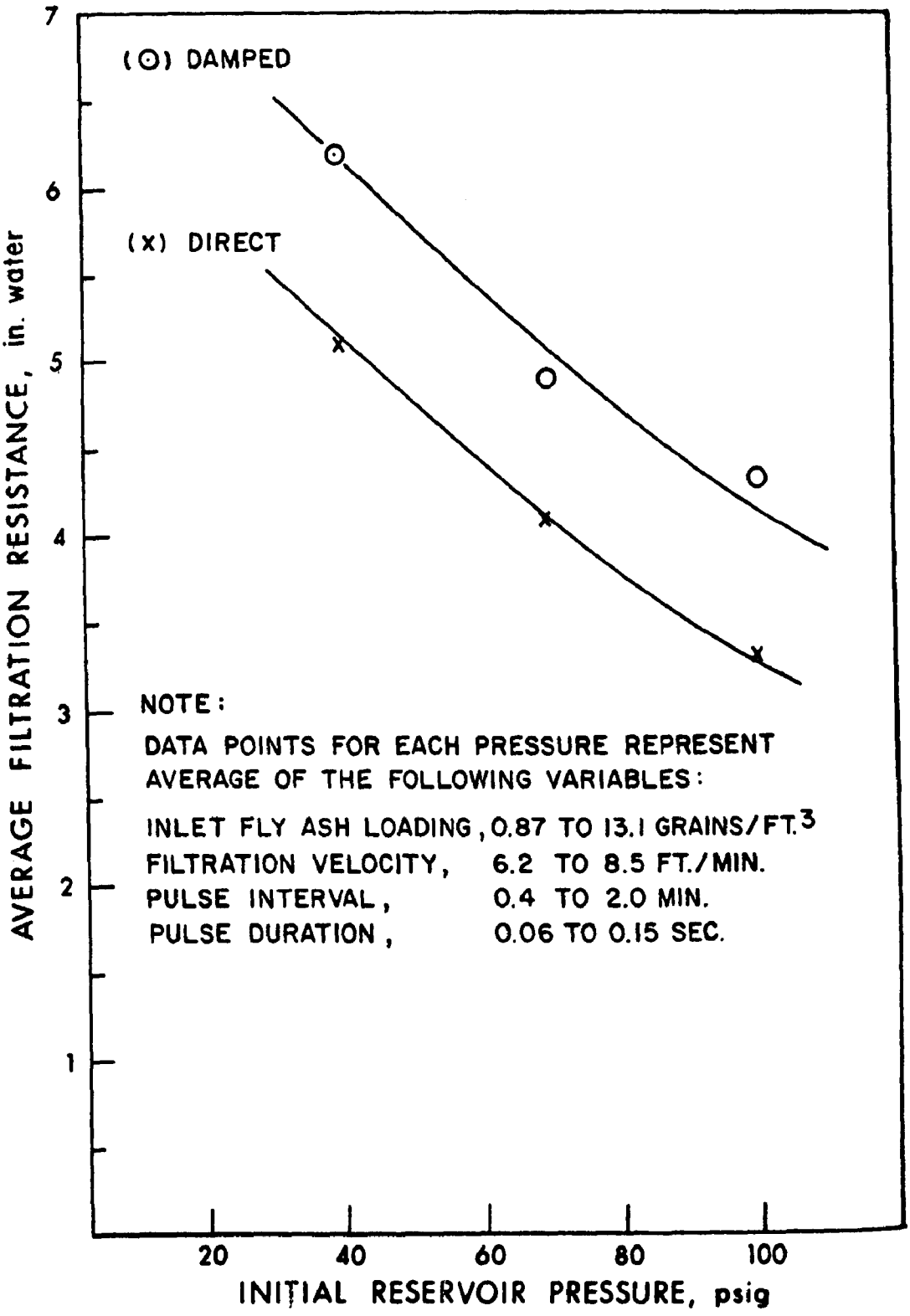

Figure 76. Average filter resistance versus reservoir pressure, direct and damped pulses, for fly ash filtration with Dacron felt

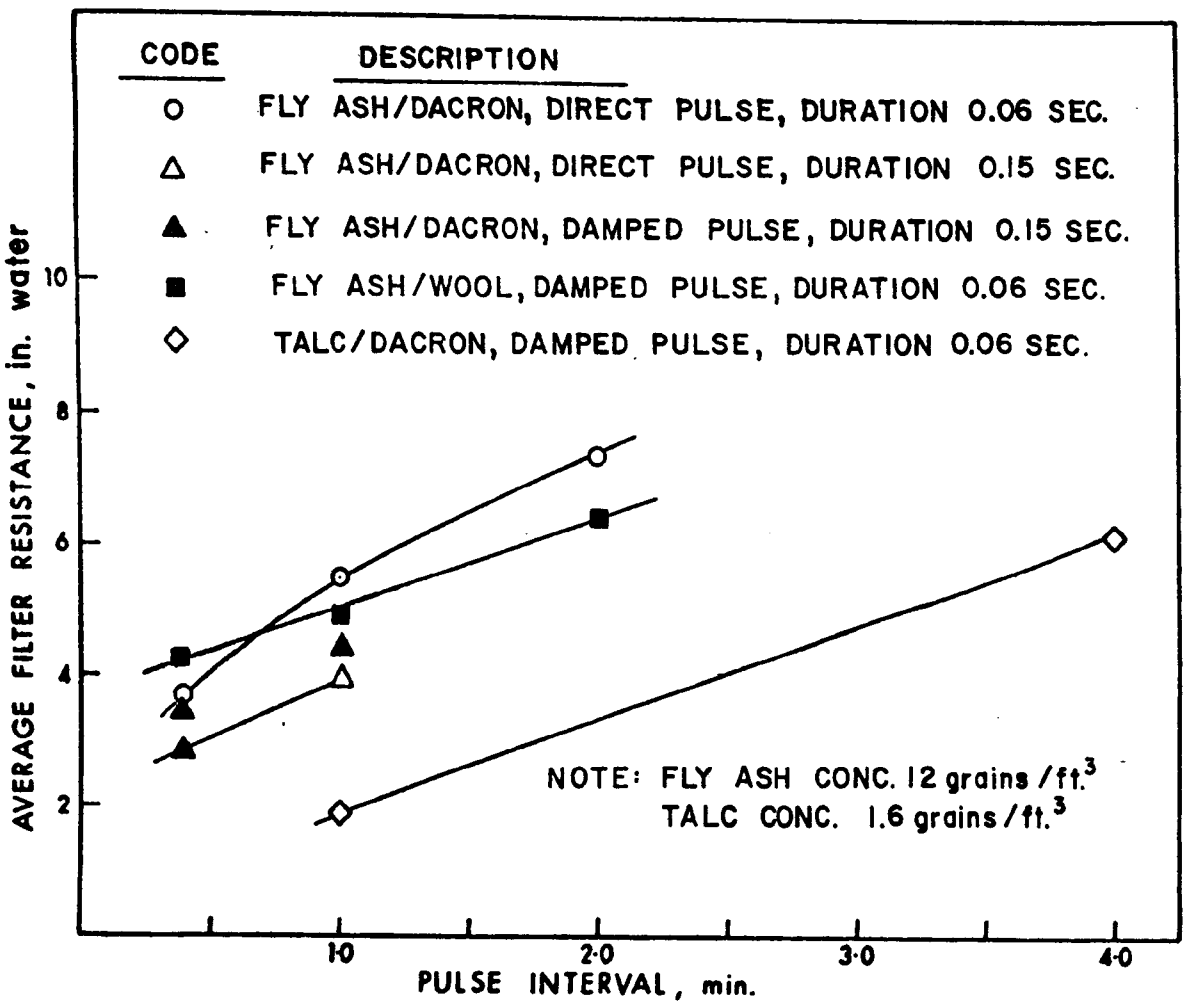

Figure 77. Effect of pulse interval on average filter resistance for 70 psig pulses

Pulse Duration - Although prior studies had indicated that pulse duration did not exert any strong effect on filter resistance,[3] it was believed that single bag tests might reveal some differences. However, according to data shown in Table 24 extended pulses have no significant effect on filter resistance, whereas they do lead to slightly higher particulate emissions. Only two tests in Table 24 suggest that there might be some advantage resistance-wise in extending the pulse duration. More tests will be required, however, to determine whether the resistance decreases are significant. From a practical viewpoint, it should be noted that the extended pulse duration represents a nearly threefold increase in compressed air demand. Additionally, prior measurements have also shown an adverse effect on emissions (> 60 percent increase in outlet concentration).

Felt Type - When wool felt was substituted for the Dacron media, the average operating resistance for fly ash was basically unchanged, Table 24. Since felts were similar in weight and permeability no large difference in filtration resistance was expected. In Figure 78 average resistance values for several fly ash/wool tests are shown for direct and damped pulses as a function of reservoir pressure. Inlet dust concentration, pulse interval and pulse duration were constant at 1.53 grains/ft.^{3}, 1 min., and 0.15 sec., respectively. There does not appear to be any significant difference in the resistance properties of wool and Dacron felts for damped pulse systems. Curves 2 and 4 represent the data for fly ash/Dacron systems given in Figure 76. The apparent difference indicated for direct pulses suggests a greater response to reservoir pressure for the fly ash/wool combination.

Dust Type - Although the reported resistance values for talc were lower during most tests than those observed for fly ash filtration it should be noted that the inlet loadings were also very much less, approximately 8 times. In order to place the resistance changes of fly ash and talc on a comparable basis they must be compared with the incremental dust deposit rates. This has been accomplished by calculating the specific

Table 24. EFFECT OF PULSE DURATION ON AVERAGE FILTER RESISTANCE FOR VARIOUS DUSTS AND FABRICS

Operating parameters	Average filter resistance, in. water					
	Direct pulses			Damped pulses		
	Pulse duration			Pulse duration		
	0.06 sec.	0.15 sec.	Ratio	0.06 sec.	0.15 sec.	Ratio
Wool felt, fly ash						
70 psig, pulse interval 1.0 min.	4.20	4.19	1.00	4.90	4.90	1.0
70 psig, pulse interval 1.0 min. reservoir and regulator interchanged	5.31	5.0	1.06	–	–	–
Dacron felt, fly ash						
70 psig, pulse interval 1.0 min.	5.5	4.3	1.28	4.9	4.9	1.0
Dacron felt, talc						
40 psig, pulse interval 1.0 min.	2.54	2.40	1.06	–	–	–
70 psig, pulse interval 4.0 min.	–	–	–	6.0	0.30 sec. / 4.7	1.28

Note: Inlet concentrations, fly ash 12 grains/ft.^{3}, talc 1.53 grains/ft.^{3}.

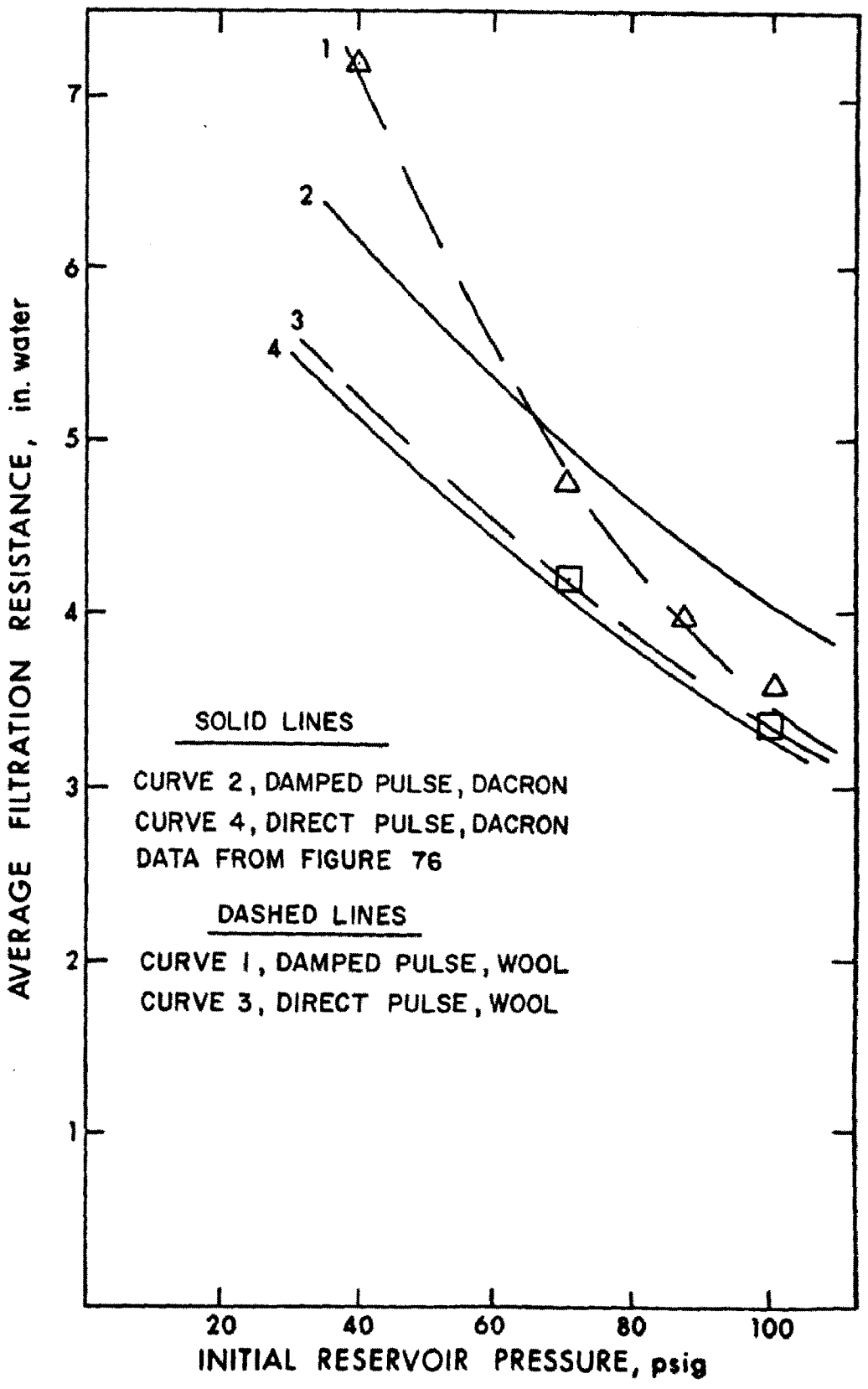

Figure 78. Comparative resistance properties of wool and Dacron fly ash filtration

resistance coefficients, K values, for the data presented in Figures 74 and 75. The average K values for fly ash actually were quite similar, ~ 13 to 16, to those found for fly ash filtration with woven cotton and Dacron fabrics in mechanical shaking systems. On the other hand, talc K values were generally about 2.5 times greater (80 versus 32) suggesting that the nature of the dust deposition must be different for the felt media. As stated previously, the increase in cloth loading over the first 0.4 minute of fly ash/felt filtration was the same as that for prior fly ash/cotton sateen at the end of 4 minutes. In both cases the slope of the resistance versus loading curves were linear beyond these points. However, the linear portions of the talc/Dacron felt curves appear to start at cloth loading levels greater than 10 times lower; i.e., < 4 grains/ft.^{2} rather than 40 grains/ft.^{2}. This behavior, which suggests that less talc dust penetrates the felt interstices, is confirmed by the lower residual dust holding for talc as compared to fly ash (330 versus 660 grains/ft.^{2}).

The fact that the K values are appreciably greater for talc is consistent with the effective size of the dusts as measured by cascade impactor; e.g., MMD = 8 μm for fly ash and 3.2 μm for talc. Since K values, in theory, are inversely related to the diameter squared for monodisperse particles, one should expect to find the K values for talc of the order of 6 times greater than those for fly ash.

Filtration Parameters - Although both decreased filtration velocity and inlet dust loading were shown to exert a significant effect on effluent concentration, Figure 55, their effects on average filtration resistance appear to be minimal, Table 25. This is somewhat surprising in that one might expect those filters with the lower dust holdings to show lower resistance.[6,8] Earlier tests by Dennis et al[3] indicated that average filter resistance rose approximately as the fourth root of the inlet concentration. The above measurements, however, were performed on a sequentially cleaned, 9 bag unit, such that considerable masking of any variable change should be expected. In the case of

Table 25. EFFECT OF INLET CONCENTRATION AND FILTRATION VELOCITY ON AVERAGE FILTER RESISTANCE FOR FLY ASH AND DACRON

Reservoir pressure	Average filter resistance, in. water			Adjusted[d] resistance
	Normal[a] filter cycle	Reduced[b] dust loading	Reduced[c] filtration velocity	
40	6.4 (281)[e]	6.5 (177)	4.7 (220)	6.5
70	5.3 (177)	5.0 (160)	4.4 (185)	6.1
100	4.9 (168)	3.01 (163)	3.8 (192)	5.2

[a] 12 grains/ft.^{3} inlet concentration. Cloth loading 51 grains/ft.^{2} at 0.5 min.

[b] 0.87 grains/ft.^{3} inlet concentration. Cloth loading 3.7 grains/ft.^{2} at 0.5 min.

[c] 9.9 grains/ft.^{3} inlet concentration. Cloth loading 30.5 grains/ft.^{2} at 0.5 min.

[d] Filter resistance adjusted to 8.5 ft./min.

[e] Number in parenthesis is residual dust loading in grams.

Note: All cleaning based on 1 minute pulse intervals, and 0.06 second pulses. Normal filtration velocity 8.5 ft./min. Reduced filtration velocity 6.2 ft./min.

reduced velocity, the observed resistances were significantly lower, but primarily because of the lowered filtration rate. Pro-rating these data to a velocity of 8.5 ft./min. actually indicated equal or slightly higher resistances despite the fact that the average filter weight gain was about 40 percent lower than for normal conditions. Because the inlet velocity was reduced, there is the possibility that a somewhat finer aerosol approached the filter due to increased hopper losses. Hence, some increases in filter resistance might be postulated.[9,10] It was also observed that the filter resistances recorded for the low loading tests rose almost immediately to the average (or 0.5 minute) value. Therefore, it appears reasonable to assume that system operation at reduced load levels may lead to more interstitial penetration of the dust. In

contrast, a high loading probably exerts a choking action that confines a larger fraction of the dust to the superficial region. The net result should be a higher operating filter resistance. Unfortunately, there are not sufficient data at this time to warrant any firm conclusions. The results are sufficiently interesting, however, to suggest strongly that further experiments be performed.

Design Modifications - The effect of equipment designs outlined in Table 23 upon particulate emissions has been discussed previously. In the following paragraphs, the modifications are treated in the same sequence starting first with those on the clean air side of the bag.

Pulse damping - clean air side - As pointed out previously, pulse damping produced on the average a 4- to 5-fold reduction in effluent concentration over the reservoir pressure range, 40 to 100 psig. If one equates reduced dust penetration with increased filter resistance, one should expect to see the higher resistance to air flow with damped pulse systems. This proved to be the case according to the data given in Figure 76, that shows an approximate 20 percent resistance rise when the damping approach is employed.

Despite the fact that test data are limited and subject to errors because of complex instrumentation problems, the pulse damping studies indicate that control of pulse form by mechanical or aerodynamic means is one avenue where power requirements might be optimized with respect to some pre-selected effluent standards.

Pulse generation - clean air side - By admitting the compressed air directly into the exit plenum chamber (1 $ft.^3$ volume) and removing the Venturi section from the exit end of the bag, the filter resistance was lowered by about 30 percent, Table 26. Although no significant increase in effluent concentration could be established, the compressed air requirement was increased by about 10 percent. In that the elimination

Table 26. FLY ASH EFFLUENTS FROM PULSED DACRON BAGS AS A FUNCTION OF PULSE FORM

Pulse type	Pulse interval (min.)	Pulse duration (sec.)	Average[a] outlet concentration (grains/ft.^{3} x 10^6)	Average filter resistance in. water
40/24[b] Plenum pulse, no nozzle. Vent opening 0.84 in.	0.1	0.1	1660	3.0
40/24[b] Large nozzle, I.D. = 0.622 in.	0.1	0.1	1840	4.6
40/24[b] Small nozzle I.D. = 0.364 in.	0.1	0.1	1000	6.2

[a]Particle concentrations estimated from B&L counter data.

[b]Reservoir pressure at beginning and end of pulse.

of Venturi elements and individual bag nozzles represents a simplification in collector design it appears important to explore further the possibilities of the plenum pulse approach.

Nozzle position - clean air side - Limited measurements, Table 23, Tests 62 and 63, indicated that elevating the 1/4-inch pulse jet nozzle permitted more effective bag cleaning, at least for those tests where the cleaning interval was extended to 2 minutes. Until the nozzle was raised 4 inches, the pulse failed to dislodge the dust from the upper section of the bag (6 to 10 in. from the top). In addition to decreasing the filtration resistance and permitting equilibrium operation, the effluent concentration increased as expected. These tests suggest that it is very important to determine at precisely what nozzle locations the best cleaning conditions can be obtained.

Baghouse volume - dirty air side - Eliminating about 57 percent of the housing volume on the dirty side of the bag (by closing a slide gate above the dust collection drum) resulted in a greater than 30 percent increase in operating resistance. The dirty side volume is apparently necessary to prevent excessive back-pressure on the dirty side of the bag during the pulse interval. Higher pressures on the dirty air side appear to attenuate the rate of reverse pressure rise. For example, the pressure rises for Tests 17 and 18, Table 23 were 1540-inch water/sec. and 1910-inch water/sec., respectively. Qualitatively, these values are in agreement with pressure rise/filter resistance relationships discussed later in this section. The same phenomenum is presumed to take place in a sequentially cleaned, multi-bag system, although the effect would be much less noticeable because of the far greater expansion volume.

Bag tension - dirty air side - An attempt was made to simulate what might be typical "uniformity of fit" conditions for the felt bags on the wire cage frame. Although the experimental data were confined to two measurements, the results appear to be in general agreement with what one would expect to find; i.e., the slack bag showing a lower average filter resistance, 4.6-inch water, compared to the tight bag, 5.2-inch water. The rational for the above is that a lowered resistance to motion in the slack bag should permit a greater acceleration rate. In turn, greater dust dislodgement and hence a lower residual filtration resistance should result.

Control of Operating Resistance

It has been shown that the average filter operating resistance depends on a variety of design and operating factors. In the following section, an attempt has been made to analyze several specific relationships; e.g., that between filter operating resistance and reservoir pressure, so

that the results of the test program may be extended beyond the boundaries of the limited dust/fabric combinations and operating parameters examined in the present study.

The following discussion relates the two components of average operating pressure, namely the residual and the transition pressures, each to their determining parameters. It is shown that residual pressure depends on the intensity of the cleaning pulse and on certain fabric and dust properties and that the transition pressure depends on the initial or just-cleaned state of the filter, on the K value of the dust, and on the amount of dust added between cleanings. With these simple relationships, the average operating pressure can easily be estimated.

Residual Resistance - As shown by Figure 74, the pressure differential immediately after cleaning changes so rapidly that it is difficult to measure accurately and, therefore, has little practical value. Most investigators prefer to use an "effective" residual pressure differential; i.e., the value obtained by extrapolating the linear portion of the p(t) curve back to time zero. This process was carried out for the pressure-time curves given in Figures 74 and 75. As stated previously, these curves achieved practical linearity after about 40 percent of the filter cycle had been completed. Pressure values from 0.1 to 0.3 minutes showed the characteristic rapid rise during the early phase of filtration. The average of 0.1 and 1 minute resistance values, however, was within a few percent of the 0.5 minute resistance. This indicated that except for highly unusual situations, the 0.5 minute "average" value was adequate for estimating power needs.

The filter pressure differential is due mainly to dust on or within the felt since the latter differential is about 25 times greater than that for a clean fabric at the same filter velocity. Residual pressure differential, therefore, must depend on the amount of dust on the filter after cleaning, and also on its distribution on and within the fabric structure. Several other factors, however, such as fabric properties,

dust properties, and system design characteristics must also be considered. An extensive discussion of filtration performance and its relationship to cloth-fabric structure has been presented recently by Draemel.[9]

In the following sections, experimental and theoretical approaches are discussed for estimating the amount of dust remaining on the fabric after cleaning.

Residual dust - Measurement of the dust remaining on the filter after cleaning were made by weighing the whole filter assembly (bag, cage, and Venturi). Because the dust weight represented only 5 to 10 percent of the assembly weight, accurate determinations of the dust weight could not be made. Consequently, caution should be exercized in applying the relationship between residual dust holding and residual resistance. On the basis of the data prescaled in Figure 71, it appeared that no valid distinctions could be made between the behavior of fly ash/Dacron, fly ash/wool, or talc/Dacron filter systems.

Talc filtration with Dacron felt gave results similar to those for fly ash, except that both resistance and dust holdings were about 1/3 lower. Although the relationship between residual dust weight and pressure is a fundamental one, it has no practical use because residual dust weight is not under the direct control of the filter operator. In order to characterize residual resistance, one must look beyond the residual dust weight to one or more characteristics of the cleaning process.

Pulse rise rate - It has already been shown that average operating resistance does not depend on the duration of the cleaning pulse, based on results obtained both in this study and in previous studies. Thus, the residual resistance fraction of the operating pressure is presumably independent of pulse duration. However, residual resistance does depend on pulse intensity, as will be demonstrated here and in the subsequent treatment of low pressure, reverse flow cleaning.

In the case of shaken bags, the amount of dust remaining on the bags after cleaning was found to correlate with the acceleration imparted to the fabric. This suggests that in pulse cleaning too, acceleration may determine the residual state of the filter. The maximum acceleration experienced by the bag can be estimated by Equation (3.2), whose development is given in Appendix L.

$$a_{max} = \frac{G}{\sqrt{\rho M}} \left(\frac{d(\Delta p)}{dt} \right)_{max} \qquad (3.2)$$

The terms G and M are the flexibility and stretch characteristics of the bag, respectively, and ρ is the gross mass per unit area of the filter (felt plus dust). The pressure expression is the rate at which the pulse differential pressure changes across the bag at the beginning of the cleaning pulse. One can infer from Equation (3.2) that the residual resistance of the filter depends on the rise rate of the pulse differential. The rise rate, when plotted against residual filter resistance, Figure 79, indicates that the residual filter resistance ΔP_{res} is described approximately by the following relation:

$$\Delta P_{res} = \frac{1.01 \times 10^4}{(d\ \Delta p/dt)} \qquad (3.3)$$

where both pressures are in inch water and time is in seconds. In its present form, Equation (3.3) applies only to the the specific dust/fabric combinations and operating parameters cited in Figure 79. The main value of this relationship lies in the fact that the rise rate of the pulse differential is determined by the bag dimensions and design of the pulse generating equipment, both controllable variables. By using conventional engineering calculations, one may predict the rise rate for a given system and, from equations similar to the above, estimate the residual operating filter resistance.

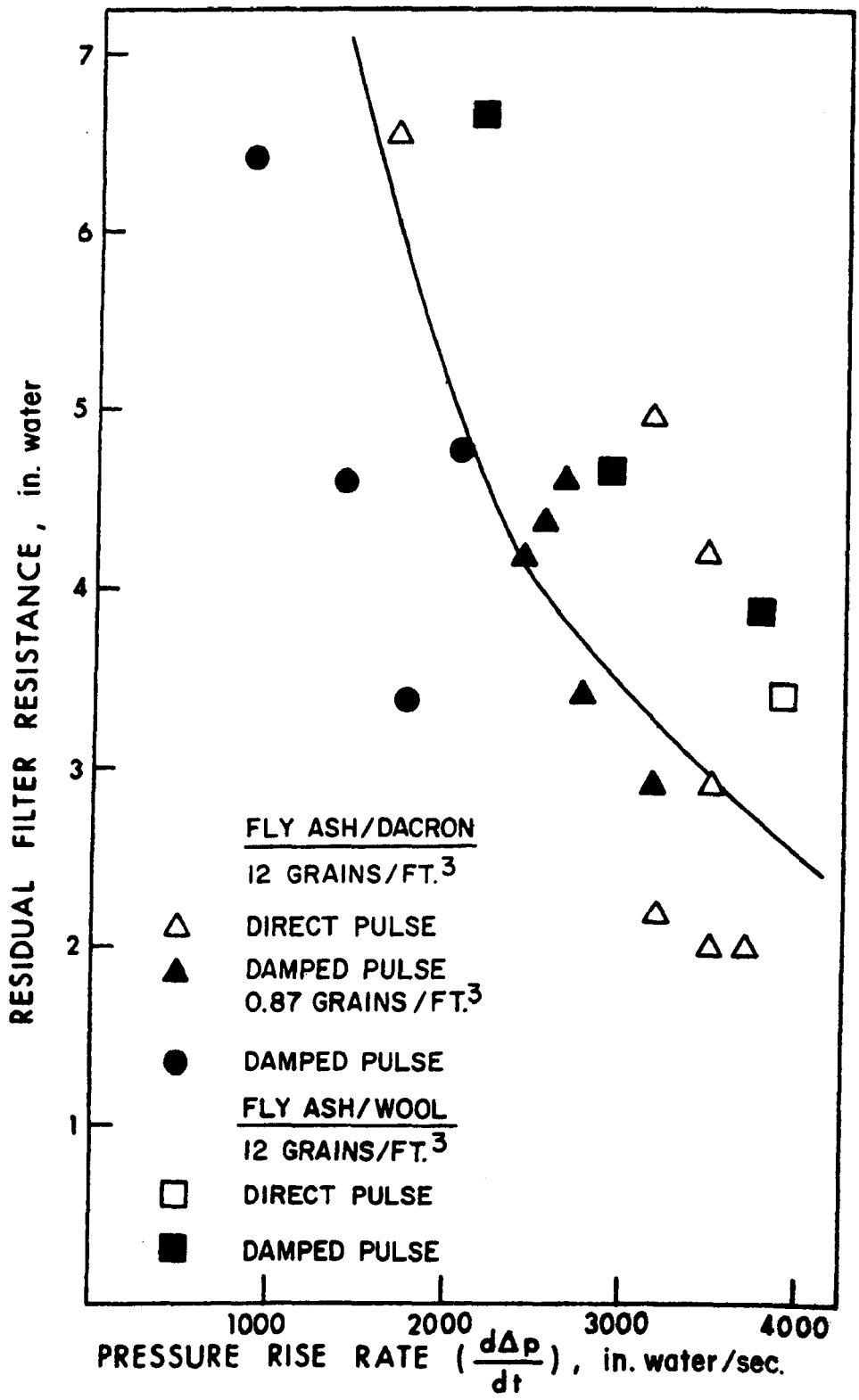

Figure 79. Relationship between rate of pressure rise and residual filtration resistance at 8.5 ft./min. filtration velocity

During fly ash tests, the rise rate ranged from 1500 to 3000-inch water/sec. for damped pulses and from 3000 to 4000-inch water/sec. for direct pulses. (Note that these values are a function of the design of the equipment and do not apply to longer bags nor to other pulse delivery configurations.)

If one refers to Figure 80, it can be seen that residual resistance is roughly inversely proportional to both pressure rise rate and reservoir pressure. This means that the pressure rise rate varies linearly with reservoir pressure for the systems studied, and, according to Equation 3.2, the maximum acceleration imparted to the bag varies linearly with reservoir pressure. Additionally, the residual filtration resistance is seen to vary inversely with bag acceleration for the pulse jet system. In contrast, the impact of acceleration on residual resistance in mechanical shaking systems appeared to be less, Figure 50 wherein residual resistance varied roughly as the inverse square root of the acceleration.

The data scatter in all these test results was greater than expected considering the care taken during the investigation to control all extraneous variables. One possible reason for the dispersion should be mentioned. If the flexibility of the felt, G, rises with improved cleaning, then the resulting greater fabric acceleration should further improve cleaning. Conversely, a heavier dust deposit would probably lower G, thus decreasing the acceleration and causing a still heavier deposit. In other words, the residual operating point may be unstable and dependent to some degree on the effect that dust within the filter matrix has on the filter properties.

Acceleration - In an effort to test the validity of Equation (3.2) that gives the acceleration of the fabric, several alternative measurement techniques were used (see APPARATUS, MATERIALS AND TECHNIQUES). The results in Table 27 suggest that a typical level of acceleration is about 250 g's, which is 25 to 50 times greater than that encountered in

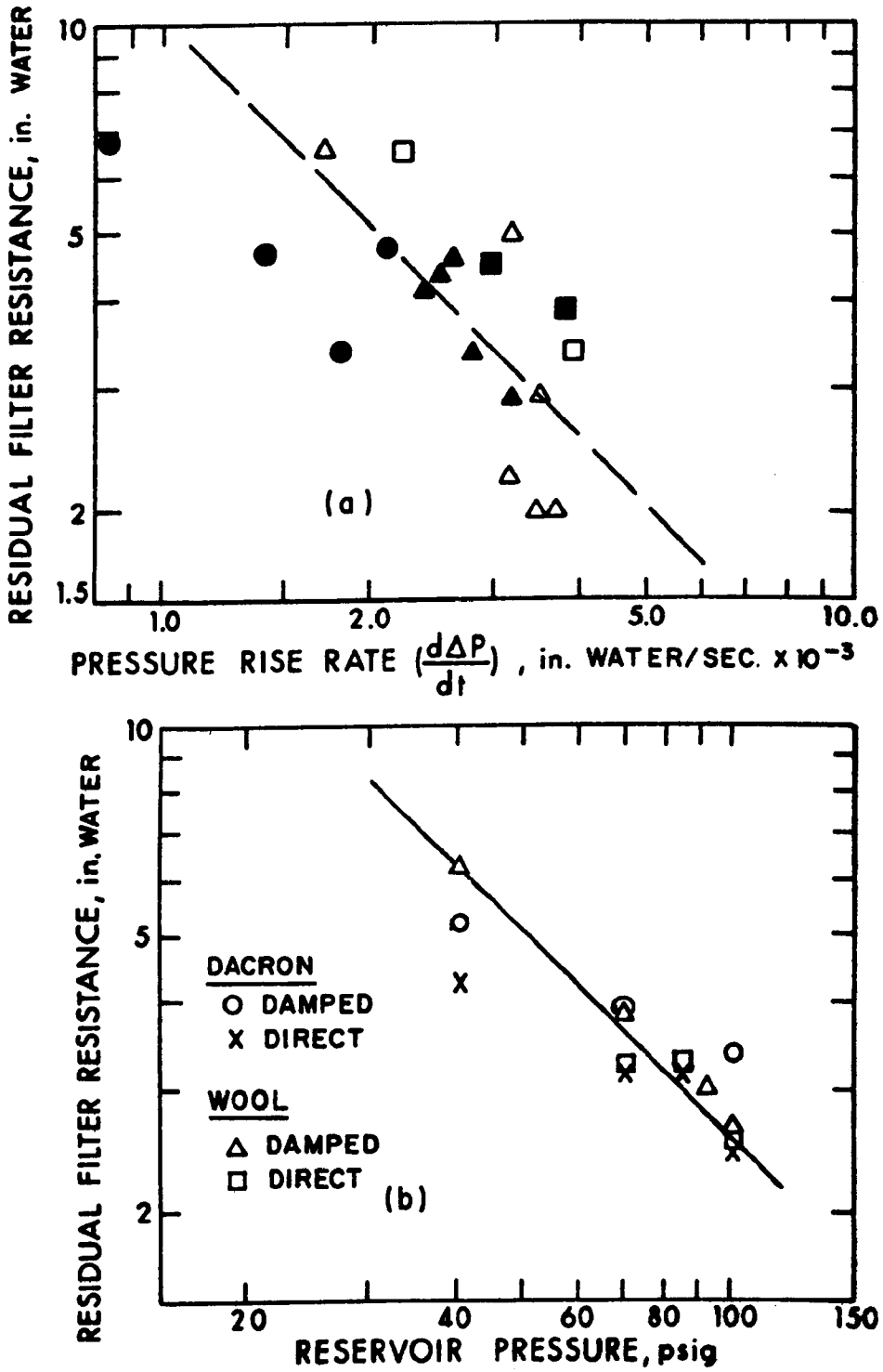

Figure 80. Residual filter resistance versus (a) pressure rise rate and (b) reservoir pressure (see Figures 76, 78 and 79, respectively)

Table 27. TYPICAL DESCRIPTORS OF PULSED BAG MOTION (DACRON FELT)

	Maximum displacement (inch)	Maximum velocity (ft./sec.)	Maximum acceleration g's
1. Static measurements			
Displacement versus pressure	0.26	--	--
2. High speed camera[a,b]			
Fabric	0.33	11.4	296
Dust	--	6.3	
3. Strain gauge[a]	0.24	6.55	272
4. Accelerometer[a]	--	--	225
5. Computations	0.26	4.35	252
Expansion modulus and pressure-time traces			
6. Dust trajectory	--	2.0	--

[a]Cleaning regime - 70 psi, 0.06 sec. pulse, 6 sec. intervals.
[b]Observed frequency - 133 cps.

shake cleaning. In the latter case, however, the bag was put through the acceleration process some 200 to 300 times. With repetitive shaking and particle loosening in conjunction with a statistical spread in particle adhesive and cohesive bonds, significant dust removal was accomplished despite the much lower acceleration. Substituting the characteristic parameters for Dacron and wool felts from Table 28 into Equation (3.2) in conjunction with the pressure rise term, $d\Delta p/dt$, calculated from oscilloscope pressure/time traces gave acceleration levels of 290 and 1870 "g's," respectively for Dacron and wool felts. The Dacron value checked reasonably well with the other measurements given in Table 27. There is some doubt as to the high acceleration level

estimated for wool because both resistance and dust penetration properties did not differ radically from those of the Dacron felt. Possible errors in the G or M parameter are suspected.

Table 28. PARAMETERS FOR USE IN EQUATION (3.2)

Fabric	G ft./(lb./ft.^{2})	ρ $\frac{\text{lb. sec.}^2}{\text{ft.}^3}$	M ft./(lb./ft.^{2})	$d\Delta p/df$ in.water/sec.	a_{max} g's
Dacron	0.00087	0.0070	0.000032	1000	290
Wool	0.0071	0.0070	0.000053	1000	1870

Pore size and dust removal - If one assumes a nominal bulk density of 2 gm/cc for the collected fly ash, an acceleration of 250 g's should be capable of dislodging an 8 μm thick planar deposit from the fabric surface. At the same acceleration level, a hemispherical deposit should be dislodgable from a hemispherical surface pore provided that the pore diameter is 48 μm or larger. In both cases, it is assumed that the adhesive strength is roughly 200 dynes/cm^2 as reported by previous investigators[8] and confirmed in the mechanical shaking tests discussed in Chapter II. Thus, it is expected that a large fraction of the dust removed during the pulse cleaning process should consist of agglomerates 50 μm in diameter or greater.

During a typical cycle of 1 minute at inlet concentrations of 12 grains/ft.^{3}, a dust layer with an average depth of 68 μm should be deposited. On the premise that surface pores smaller than 48 μm in diameter are permanently plugged, most dust probably deposits not uniformly but in select locations centered over previously cleaned locations. Therefore, in these regions, the deposit depth is probably nearer to 100 μm than the previously cited average value of 68 μm. Since, according to dust trajectory measurements most of the dislodged material fell within

the agglomerate size range of 100 to 120 μm average diameter, the concept of deposition cited above appears acceptable. It has also been indicated in earlier studies that pore diameters less than 10x greater than the characteristic particle diameter are readily bridged such that high collection efficiencies are attainable.[1,9,12] Thus with respect to nominal 5 μm MMD particles, it appears reasonable that most of the filtration should take place within those pore structures in excess of 50 μm diameter.

Microscopic examination of the filter in its residual state showed that much of the surface was still loaded with dust. Tunnel-like cavities of order 100 μm diameter were visible, however, from which dust had evidently been removed during the previous cleaning. It is probable that these cavities are responsible not only for most of the dust collection but also for most of the filter emission. Knowledge of the size distribution of all cavities above the theoretical pore size (an estimated 48 μm in this case) would permit computation of the residual pressure differential and improved estimates of dust penetration properties.

If a certain fraction of the fabric pores remain plugged for a specific filtration application, one can conclude that these areas are wasted. If it were possible to maintain a more uniform pore structure it would be possible to provide more active filtration channels for a selected gas handling capacity. Thus, although the superficial velocity would remain unchanged, the provision of more "active" pores will lead to a reduced interstitial velocity and a corresponding reduction in resistance. It is recognized, however, that the control of pore structure in fabric systems where the desired pore diameters, 50 to 100 μm, might not be much larger than nominal fiber sizes 20 to 30 μm, may be difficult.

Reverse drag cleaning - Another possible cause of dust removal, aside from acceleration, is the drag exerted on the dust deposit when the air

flows backwards through the fabric during the pulse. These drag stresses are indicated schematically in Figure 81. The dust deposit establishes a resistance to flow in proportion to the permeability of the deposit, the air velocity, and air viscosity. Integrating the deposit's resistance from the dirty side of the felt gives the approximate local stress in the dust deposit tending to detach it from the fiber matrix. This stress is offset throughout a good part of the felt layer by adhesive forces that depend on fiber, fabric and dust properties. When the removal stress exceeds the fiber holding strength, usually near the dirty filter surface, the dust will be removed.

In normal pulse cleaning, a reverse flow accompanies the mechanical (acceleration) stresses in every pulse. Thus, it is impossible to tell which mechanism is causing removal without highly sophisticated measurements. To isolate the separate effects of these mechanisms, two brief series of tests were made. In one series, the slackness of the bag was varied in order to change the acceleration of the fabric during the pulse without appreciably altering the pulse itself or the associated backflow. The cage diameter of the bag was reduced in one test, and in another a rod was wedged between the cage and the bag to tighten it. The results as shown below indicated that reducing the acceleration by constraining the bag and without changing the backflow did tend to raise the residual pressure differential, although not as much as anticipated. Unfortunately, the small differences and the limited data preclude drawing any firm conclusions.

Bag fit	Residual resistance in. water
Loose bag	3.53
Normal bag	3.70
Tight bag	3.78

Several tests discussed previously and presented in Table 23 and Figure 61 indicate that it is the intensity and not the length of

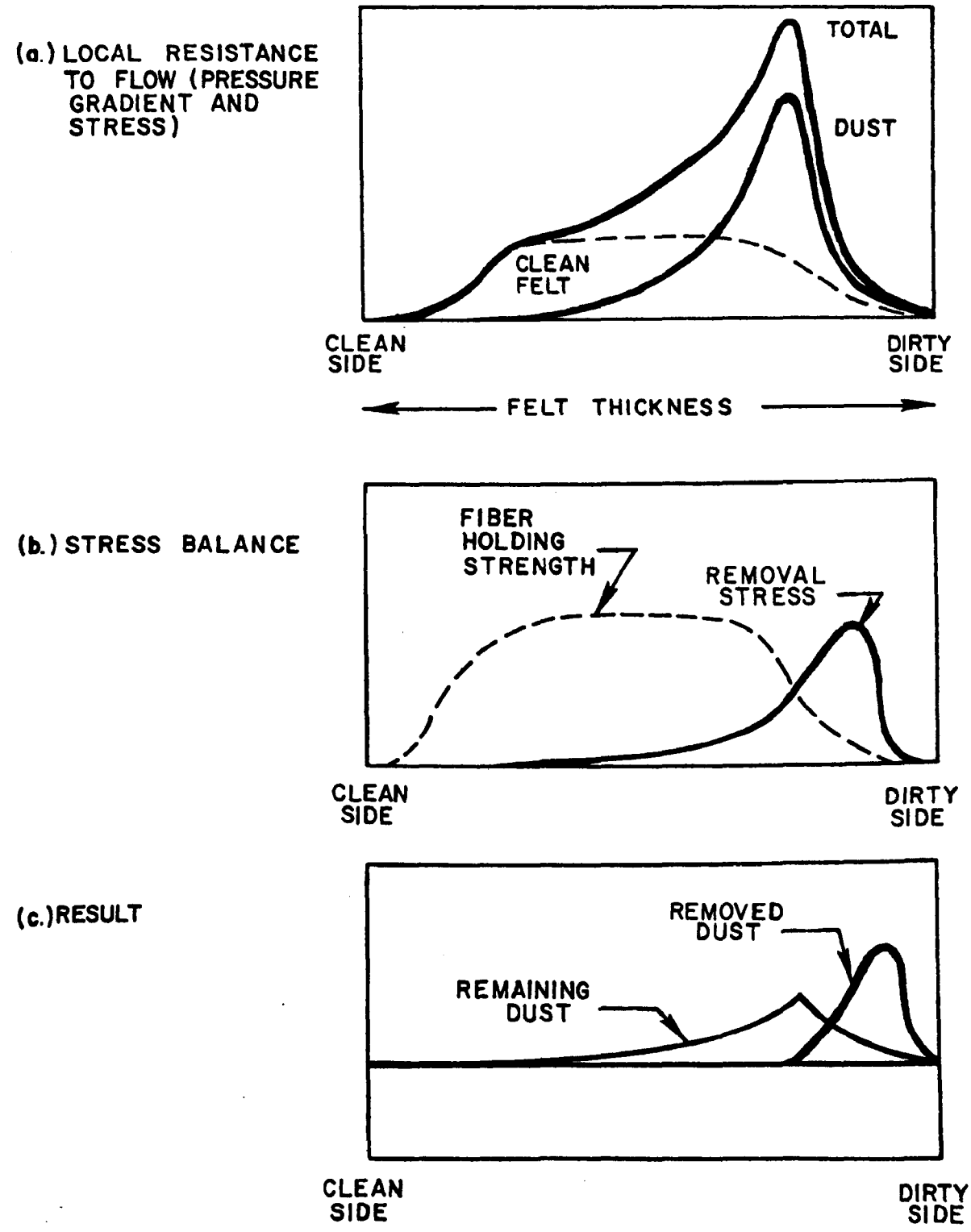

Figure 81. Postulated removal mechanism for reverse air drag through a loaded felt

the cleaning pulse that determines the amount of fabric cleaning. This conclusion is based on the fact that no resistance increase was observed when pulse durations were extended from 0.06 to 0.15 sec. and as much as 4 sec. in the case of talc, Table 23. The inspections of pressure/time traces describing the transient pressures over the duration of the pulse show that a pressure spike appears within the first 50 to 100 milliseconds followed by a rapid decay within the next 50 milliseconds to a nearly constant pressure differential across the bag for the remainder of the solenoid valve open time. The initial rapid decay in pressure is associated with the removal of the dust from the filter and the consequent decrease in filter resistance. The relative stability of the pressure differential during the remainder of the pulse interval suggests at best only minimal dust removal by the transient reverse flow phase when it is preceeded by a high energy pulse.

It is pointed out in Chapter IV, however, that introduction of a low pressure, reverse flow air at cloth velocities of the order of 40 to 60 ft./min. led to significant dust separation. The latter tests indicated, however, that the initial bowing or bonding of the bag by pressure differentials of the order of 15 inches was responsible for the dust dislodgement. This conclusion is based on the fact that dust removal determined over a threefold range of pressures were essentially the same. As stated previously it is believed that the primary role of the reverse flow air is to transport the dust dislodged by the pressure pulse away from the filter so that the larger agglomerates have an opportunity to fall towards the dust hopper.

Although fabric resistance to air flow does not appear to depend upon pulse duration, the particulate emissions show an apparent dependence; i.e., a 60 percent increase in effluent concentration when pulse duration was increased from 0.06 to 0.15 seconds. In the latter instance it appears that the extended pulse duration permits more time for settlement of the coarser particulate agglomerates. Accordingly, with

resumption of air flow a somewhat finer size spectrum with the potential for increased penetration appears at the dirty face of the filter.

Transport of agglomerates - The reverse flow of air through the filter may affect the trajectory and ultimate disposition of the agglomerates that are loosened from the filter by other means. The velocity and net displacement of the air reversing through the filter were estimated in various ways:

(a) Representative reverse pressure differentials of 15 inches water, and apparent residual filter resistances of 0.35 in.water/ft./min. indicate average reverse flow velocities of about 40 ft./min. Over a pulse duration of 0.06 seconds, this would produce a reverse displacement of air of less than half an inch through the filter. The true residual filter resistance may be much lower, however.

(b) Rough measurements of the reverse flow produced during the pulse showed that the aerosol was being forced backwards a typical distance of 2 feet in the ducting. Allowing for compression of the air inside the housing, this indicated a reverse displacement of air of about 1 inch through the filter during a typical pulse.

(c) Cinephotographic observations of the velocity of the dust cloud (Table 26) indicated particle velocities of about 380 ft./min. at the fabric surface.

From the above approaches, it appears that the air back flows through the filter a distance of the order of 1 inch during the pulse, with a maximum velocity of about 100 ft./min. With a single enclosed bag, as in the present test, the result is that the reverse air velocity in the vicinity of the bottom of the bag may increase to 1200 ft./min.

The possible consequences of this air movement are considered in Appendix K. Because the air movement reverses at the end of the pulse, assuming approximately the same flowlines as when it advances, the net

transport is essentially zero. However, the dust agglomerates may be projected across flowlines, resulting in an effective cleaning will occur under the following conditions.

- The flowlines are steep; i.e., nearly parallel to the bag. Use of baffles between bags that are not cleaned simultaneously and close bag packing should favor the above.
- The recovery of forward (normal) flow immediately following the pulse is gradual, resulting in a relatively long period in which the particles are airborne; e.g., damped pulses.
- The initial particle ejection velocity is high compared to the velocity of the air initially flowing backwards through the fabric.
- Short bags are used.
- Particles are dislodged from the fabric in the form of large, dense, agglomerates.

In Appendix K, a transport effectiveness parameter is developed based on the above concepts. This expression, presented below, is intended only for qualitative guidance until more definitive measurements on many dust/fabric combinations can be performed

$$\zeta = V_T \left[\frac{T_p}{L} + \frac{V_p T_p}{V_R L} + \frac{V_o}{dg} \left(\frac{V_T}{V_R} - 1 \right) \right] \tag{3.4}$$

where V_T = terminal falling velocity (Stokes velocity)

L = bag length

T_p = length of pulse (time)

V_o = initial particle ejection velocity

V_p = average pulse velocity

d = one-half the bag separation distance

g = gravity constant

V_R = average air velocity during resumption of flow

V_T = terminal (free-fall) velocity

The importance of having a large terminal velocity is evident. In the event that the V_T/V_R ratio is not very large, the pulse duration should be increased. This probably explains why extending pulse duration had little effect on fly ash filtration but was effective with talc; i.e., the talc agglomerates were lighter and fell more slowly such that settlement was enhanced by longer pulses.

Thetterminal falling velocity of agglomerated dust cannot always be given by simple Stokesian mechanics. If the agglomerates fall as a dense cloud rather than as isolated particles, the falling velocity may exceed the Stokesian velocity.[13] For example, dust loosened from the plates of an electrostatic precipitator often falls rapidly in the form of a single sheet of dust. Therefore, pulse cleaning a fabric in such a way as to remove the dust in a thin, dense layer should enhance dust transfer to the dust hopper.

In the following paragraphs, the controlling factors affecting residual filter resistance have been summarized.

- The residual filter resistance is determined by the amount of dust retained on the filter. Although a good quantitative correlation might be obtained, the difficulty in performing these measurements in any simple manner precludes practical use of this relationship.
- The residual pressure differential and the residual deposit weight are determined by the acceleration seen by the filter rather than by reverse (aerodynamic) drag.
- Filter acceleration is determined by the rise rate of the pressure pulse, and by flexibility, tension, and other properties of the fabric. Unfortunately, the amount of acceleration obtained may be unpredictable, depending on how the fabric properties change with the residual dust.

- Fabric acceleration levels are approximately 25 to 50 times those used in shake cleaning. In contrast to mechanical shaking, in which low, ~ 4 to 8 "g" acceleration levels are imparted to a filter some 200 times, only one high energy "shake" is given the bag cleaned by pulse jet air.
- Dust is removed as agglomerates having diameters of the order of 100 μm. Agglomerate size (and density) are important factors in determining how much of the dust falls to the hopper without being redeposited on the bag.
- In the absence of adequate falling velocity of the detached agglomerates, a longer pulse duration is necessary for effective cleaning. Other parameters; i.e., bag geometry, agglomerate ejection velocity, and filtering velocity are involved in this relationship.
- Pores in the surface of the felt with diameters less than approximately 48 μm appear to be permanently plugged for fly ash filtration. Because plugging reduces effective use of the fabric media with respect to filtration resistance, a better control of pore size is recommended.
- Most of the dust penetrating the filter escapes through the larger pores which are emptied and filled in almost every cycle of the filter.

Transition Pressure - Figure 70 shows that, beginning at a low residual pressure differential, the filter differential at first rapidly increases as the filter loads. At the end of the loading cycle, the differential has reached the terminal pressure. Evidently the terminal pressure depends on the residual level and on the amount and type of dust added during filtration.

It will be recalled from Chapter II that the rate of pressure differential increase given by

$$\frac{d\Delta p}{dt} = K C_i V^2 = KV \frac{dW}{dt} \qquad (3.5)$$

is a constant for a fixed specific filter resistance, K, a constant filtering velocity V and constant inlet concentration C_i. The main difference in pulse cleaning is that a constant rate of increase is not reached until about 40 percent of a 1-minute filtration cycle is completed (or about 20 percent of a 2-minute cycle). However, the resistance curves steadily approach linearity with less frequent cleaning such that they resemble those for mechanically shaken systems. Extrapolation of the linear portion of these curves to time zero permits estimation of the effective residual resistance.

The difference between the final and effective residual resistance values, which may be defined as the transitional pressure, is expressed by the following relation

$$\Delta P_{trans} = KVW = KC_iV^2t \qquad (3.6)$$

in which t is the filtration time. As pointed out previously, Equation (3.6) permitted convenient estimation of "K" values for the various dust/fabric combinations studied. Despite the deviations from linearity in resistance/time curves, use of the midpoint resistance value (that at 0.5 minutes for a 1-minute filtering cycle) actually provides a very good estimate of the average resistance with respect to determining fan power requirements. With few exceptions, selection of the midpoint pressure leads to a slightly conservative estimate of power requirements no more than 5 percent in excess of the time value.

Operating Resistance - The factors making up the filter operating resistance, the residual and transition pressures, respectively, have been discussed separately to permit a better understanding of the cleaning function and dust/fabric properties. From an operational viewpoint it is their summation, as depicted by a characteristic average value of the filtration cycle, that is essential to determining the contribution to total air handling costs chargeable to filter resistance. With respect to the dust and fabric combinations tested in this program,

average resistances were in the nominal 4 to 6 inch water range for pulse jet filtration at 8.5 ft./min. as compared to 1.5 to 4 inch water for mechanically shaken systems filtering at 3 ft./min. Based upon filter drag criterion, the average values of 0.6 and 0.9 inch water/ft./min., respectively, for pulse jet and mechanical shake systems indicate reduced air handling power for the former system.

Factors in the Selection of Optimum Operating Conditions

It has been stated previously in the analysis of mechanical shaking systems that, before any optimization of a filtration process can be undertaken, one must decide what constitutes an acceptable outlet concentration (or mass emission rate). Practically speaking, the target emission levels will ordinarily be dictated by Federal or State agencies and should include some built-in safety factor.

With respect to acceptable operating resistances, two basic constraints will probably apply. First, maximum resistance losses across the filter media should not exceed 10 inch water in any case. Secondly, unless special blowers of the turbo-compressor type are to be used for gas moving, the practical limit in operating static pressures will be in the range of 10 to 12 inch water. With some allowance made for resistance losses in hoods and ducting, it will probably be preferable to think in terms of 4 to 8 inch water for the typical filter resistance in a pulse jet system.

According to the results of this study, effluent concentrations vary approximately as the third power of the reservoir pressure, with all other filtration and cleaning parameters held constant. Conversely, the residual filter resistance varies inversely as the absolute reservoir pressure. When the pulse duration is increased, no observable reduction in filtration resistance is obtained. Therefore, except for the unusual case, it appears that it is advantageous to minimize pulse duration so as to minimize compressed air requirements.

On the other hand, if the pulse intervals are extended, for example, from 1 to 2 minutes, the average operating filter resistance is increased by the transitional resistance of the 1-minute pulse frequency system. Therefore, there appears to be an opportunity here to reduce the compressed air requirement by a factor of 2 while increasing air handling power needs by roughly 30 percent. If one is given an average allowable outlet concentration, reference to curves such as shown in Figure 62 indicate that low pressure direct or high pressure damped pulses will meet the effluent criterion. In almost every case, however, the added power requirement associated with the higher reservoir pressure used with a damped pulse will be much greater than any reduction attained in resistance to air flow.

It may be possible, however, to decrease the reservoir pressure with either direct or damped pulses so that the compressed air power is significantly reduced provided that the pressures are not less than 40 psig. To afford any advantage it is necessary that the increase in fan power due to higher filter resistance be more than offset by the decrease in compressed air demand. If the added filtration resistance does not tax the fan capacity, the above optimization path offers the added advantage of yielding lower effluent concentrations. Usually, the corresponding increase in fan power is less than that saved by reducing the compressed air volumes.

According to limited measurements, a 12 fold decrease in inlet loading had no effect on average filtration resistance suggesting that large variations in inlet dust loadings might be accommodated. In contrast to mechanically shaken systems, however, effluent concentrations correlate strongly with inlet concentrations. Thus, one must consider the fact that a large gain in dust handling capacity without significant cost penalties may be accompanied by higher effluent concentrations.

CONCLUSIONS TO PULSE JET CLEANING STUDIES

The conclusions that can be drawn from the pulse jet cleaning tests have been presented in essentially the same format as that used for the mechenical shaking studies. General conclusions are given first followed by more detailed conclusions on (1) particulate emission characteristics, (2) dust removal and filter resistance; and, (3) system design and operating factors. Insofar as possible, the behavior of experimental pulse jet systems has also been investigated with respect to system effectiveness in the collection of 1 μm particles or smaller. Consideration has also been directed to those factors affecting cost optimization for system operation once an emission criterion has been established.

General Conclusions

To avoid misinterpretation and unwarranted extrapolation of test results we present the following conclusions.

- Limits of data application - Unless clearly specified, test results should not be extrapolated beyond the bounds of the specific dust/fabric combinations studied and the actual filtration and cleaning parameters used. This caution is more important for the pulse jet studies than for the mechanical shaking studies because of the many probing tests performed in which the measuring techniques were deliberately of an approximate nature and where time did not always permit experiment replication.
- Need for further research - Aside from confirming the earlier observations that a dust/fabric interaction is often unique, it appears that the role of many variables identified and/or investigated that relate to collector geometry and cleaning system parameters require further study.
- Outlet versus inlet concentrations - It is necessary to make a very important distinction between the behavior of mechanically shaken and pulse jet cleaned fabrics. Whereas only minimal changes in effluent concentration and size properties are found in the former case for a huge range, 10^5, in inlet concentration, the emissions from pulse jet systems are strongly dependent upon the inlet concentration. Limited data suggest a linear relationship between effluent concentration and the nth

root of the inlet loading where n may vary from 0.5 to 1. Roughly speaking, this states that it is the collection efficiency and not the effluent concentration of pulse jet systems that is more apt to be nearly constant.

- Effluent particles from pulse jet systems contain many large particles such that there may not appear to be any significant size reduction during filtration even though the collection efficiencies are in the 99.9 to 99.99 percent range. The relative coarseness of effluent particles is attributed to the large fraction of agglomerates dislodged by the higher energy cleaning pulses. Upon resumption of filtration, re-entrained agglomerates from the fabric interstices as well as the transient penetration of those still in suspension on the dirty air side of the filter constitute a major part of the dust loading. It might be argued that the coarse nature of the pulse jet effluent may represent an advantage with respect to restricting its atmospheric transport.
- It is again emphasized that the concept of fractional particle size efficiency has no practical significance with respect to the pulse jet system. To begin with, the size and number concentrations change radically over a filtration cycle so that, at best, the only practical measurement is one depicting some long term average value. Secondly, the presence of agglomerates in the effluent (generated by the cleaning process) can lead to fictitious relationships between particle size and fabric collection efficiency.

Particulate Emissions

The conclusions presented in the following text describe the impact of system operating parameters, cleaning parameters and fabric type upon fly ash and talc dust emission.

- Fly ash and talc aerosols having roughly the same size properties can be filtered at efficiencies in the 99.9 to 99.99 percent range. Compared to the behavior of mechanically shaken cotton bags the average outlet concentrations were at least 2 to 3 orders of magnitude higher for pulse jet systems.
- The average outlet concentrations for the Dacron and wool felts, which were in the range of 0.001 to 0.0001 grains/ft.^{3} for both fly ash and talc, increased with increasing inlet dust loading as cited previously. Although the data were insufficient to establish a

precise quantitative relationship, the effluent loading appeared to depend on the inlet loading raised to some power between 0.5 and 1.0.

- The average outlet concentration showed a strong response, five fold decrease, to a 25 percent reduction in filtration velocity (8.5 to 6.2 ft./min.). Test data were too limited to justify any quantifying expression for the above results. It is believed, however, that the reduced reentrainment of agglomerates at the resumption of filtration may partially account for the lower loadings.
- The average outlet concentration varied directly with pulse intensity showing an approximate five-fold increase over the reservoir (pulse) pressure range of 40 to 100 psig.
- The average outlet concentration was affected by the waveform (pressure-time trace) as well as the intensity of the pressure pulse. By using a pulse damping technique in which the rate of pressure release from the bag was retarded, outlet concentrations were reduced approximately five-fold, irrespective of pressure intensity.
- The average outlet concentration was moderately dependent upon the duration of a pressure pulse increasing roughly as the square root of the pulse interval. One concludes that there is little merit to extending the pulse duration because of the adverse effects of increased particle discharge and increased compressed air usage. At the same time, no significant improvement in filter cleaning (and reduction in operating resistance) is attained.
- The average outlet concentration did not vary appreciably with the pulse frequency over the time intervals 0.4 to 4 min. These results indicate that the major dust emission occurs immediately following cessation of the pressure pulse.
- The apparent fractional particle size penetration appeared to be essentially independent of size for particles less than 5 μm in diameter for reservoir pressures up to 70 psig when direct pulses were used.
- The apparent fractional size efficiencies for particles 2 to 10 μm in diameter actually varied inversely with diameter with high energy, 100 psig pulses. This phenomenon was attributed to the large population of agglomerates dislodged from and penetrating the filter during the initial phase of filtration.
- The apparent fractional size efficiencies for damped pulse systems indicated the expected; i.e., a direct relationship between efficiency and particle diameter for the size range 1 to 10 μm. It is believed that the more gradual

bag deflation process reduces the "snap" or projection capacity of the bag when returned to service as well as eliminating the transient increased flow velocity. Both factors, the former by mechanical dislodgment and the latter by increased re-entraining power, favor increased emissions.

- Fractional particle size measurements for fly ash/wool systems under typical pulse cleaning conditions were essentially the same as those for the fly ash/Dacron combinations.
- No significant differences could be detected between the behavior of talc and fly ash with respect to fractional particle size measurements.
- Outlet particle concentrations (number basis) decreased rapidly during the filtration interval such that calculated mass concentrations varied by as much as 100 times. Although a similar pattern was established during mechanical shaking tests, the differences in the former case were often as much as 10^5 times. These results point out that the pulse jet filtration process has more deep bed collection characteristics compared to the "cake" type filtration found in many mechanical shaking systems.
- A relationships between effluent concentrations and average filter resistance was established. Similarly, the residual filter resistance was directly related, as expected, to the residual dust deposit.

Dust Removal and Filter Resistance

The following conclusions concern those measurements that relate to the key factors responsible for dust removal.

- The residual dust holding for a filter was inversely related to the intensity of the pressure pulse as determined by the reservoir pressure.
- The residual dust holding did not appear to vary significantly for direct and damped pulses and with the duration of the pulse.
- The residual dust holdings were approximately the same for the fly ash/Dacron and fly ash/wool systems. This was not surprising in that both felts had very similar properties and the collection efficiencies were about the same.
- The residual dust holdings for the talc/Dacron systems were about half those for the fly ash/Dacron (or wool) systems.

The difference is presently attributed to the much lower bulk densities observed for talc.

- The residual dust holding and residual resistance depend upon the acceleration imparted to the fabric. This suggests that the principal mechanism of dust removal is that of simple tensile forces exceeding those of adhesion and cohesion in essentially the same manner as predicted for mechanical shake cleaning.
- It is estimated that for many bags cleaned by pulse jet air the maximum fabric acceleration is directly proportional to the rate of rise of the pressure differential across the bag, ~1000 to 4000 in. water/sec.
- The residual resistance varies inversely with the rate of change of bag differential pressure and also with reservoir pressure. Thus, the rate of rise in bag pressure differential can be equated to reservoir pressure.
- Residual resistance values depend not only upon the rate of change in pressure differential across the filter but also upon the dust/fabric combination and the inlet loading to the filter. More tests are required to establish quantitative relationships that include the above factors.

The data presented in this report represent preliminary and, in many cases, exploratory measurements. Therefore, despite the many qualitative insights gained, we do not think the results should be extrapolated for design purposes unless the dust and fabric properties conform very closely to those tested in this study. On the other hand, the many relationships developed in this program, coupled with reliable field data from industrial sources, should provide useful guidelines for improvements in existing systems and for more extensive investigations of the variable influencing pulse jet system performance.

System Design and Operating Factors

The following conclusions relate to the probable impact of design and/or operating parameters.

- The location of a pulse jet nozzle may exert significant effects on system effluent and resistance properties by aiding or detracting from the uniformity of bag cleaning. Limited tests showed that secondary air flow induced by

the pulse jet should be entrained from the plenum region so that absolute pressure within the bag (clean air side) always exceeds that on the dirty side.

- Based upon observed effluent dust profiles, tests suggest that long filter bags may see inadequate cleaning in the lower region. The practical design limit should be established by controlled laboratory study because increased bag length can be advantageous from the perspective of equipment space requirements.
- Bag material should be flexible, light weight, and inelastic to obtain maximum acceleration. It should have sufficient weight (i.e., number of fibers per unit area) to present many targets for entering dust particles and the pore structure should be as uniform as possible.
- A large housing and hopper volume on the dirty side of the filter bag will minimize the pressure build-up in this region during the pulse, and thus enlarge the magnitude of the pulse differential. Likewise, any relief of the build-up pressure in this region during the pulse, including temporary stoppage of the incoming dirty air, will result in a larger pulse differential for the same compressed air energy expenditure. The larger pulse differential should be associated with a larger rise rate, and acceleration.
- The pulse delivered to the bag should begin as abruptly as possible with sufficient inflating flow to subject the entire bag length to a sudden pressure differential. It might be better if several concurrent pulses could be released at points long the bag, each with sufficient sharpness and volume to give the felt a maximum velocity per unit of pulse energy used.
- The back flow of air through the filter accompanying the pulse assists cleaning in several ways. It flushes agglomerates loosened by the acceleration from the pore structure. It can itself loosen agglomerates if the shock itself has been insufficient, although this appears to be a very inefficient use of compressed air. It also accelerates agglomerates that have already left the felt surface helping to convey them to the hopper.
- Pulse intensity should be as low as can be tolerated to save on compressed air (and reduce power needs) but sufficiently high to maintain an equilibrium cleaning process.
- Pulse duration should ordinarily be as short as possible. This will probably be limited by the care taken in designing the pulse generating and delivery system, particularly in the pressure release valving. In some operations, slightly longer pulses may be necessary to (1) inject sufficient air volume into the bag to enable the rise to develop

maximum acceleration along the entire bag; or, (2) to prevent redeposition and/or to promote transport of the agglomerates to the hopper.

- Optimum cleaning frequency is determined by the cost of fan power on one hand, and the cost of compressed air or the average emission requirement on the other hand.

REFERENCES

1. Billings, C. E. and J. E. Wilder. Handbook of Fabric Filter Technology. Volume 1: Fabric Filter Systems Study. GCA/Technology Division. Department A, Clearinghouse, U.S. Department of Commerce, Springfield, Va. 22151. Report Number GCA-TR-70-17-G, APTD-0690, Contract No. CPA-22-69-38, PB-200-648, December 1970.

2. Pulverizing Machinery Company, Summit, New Jersey. No Moving Parts Inside Hot Dust Collector. Chem. Eng., 64:188, August 1957.

3. Dennis, R. and L. Silverman. Fabric Filter Cleaning by Intermittent Reverse Air Pulse. ASHRAE J., 43:76, 1962.

4. Phillips, N. D. and R. J. Wright. A New Technique to Achieve Surface Renewal in Fabric Filtration. Presented at the 1969 Meeting, Air Pollution Control Association, Paper No. 69-201.

5. Berg, D. B. Dust Filter Reclaims 10,000 Pounds Per Hour of Hot Asphalt Plan Aggregate. Chemical Processing, 77, April 1968.

6. Spaite, P. and G. Walsh. Effect of Fabric Structure on Filter Performance. AIHA J., 24:357, July 1963.

7. Borgwardt, R. and J. Durham. Factors Affecting the Performance of Fabric Filters. 60th Annual Meeting AIHE, Paper No. 296, November 1967.

8. Herrick, R. A. Theory and Application of Filter Drag to Baghouse Evaluation. Air Engineering, 18, May 1968.

9. Draemal, D. Relationship Between Fabric Structure and Filtration Performance in Dust Filtration. Control Systems Laboratory, U.S. Environmental Protection Agency, Research Triangle Park, North Carolina, Report No. EPA-R2-73-288, July 1973.

10. Stephan, D., G. Walsh and R. Herrick. Concepts in Fabric Air Filtration, AIHA J., 21:1, 1960.

11. Williams, C. E., T. Hatch and L. Greenburg. Determination of Cloth Area for Industrial Air Filters. Heat Pipe and Air Cond., 12:259, 1940.

12. Winchester, S. C. and J. C. Whitwell. Multivariable Studies of Nonwoven Fabrics. J. Eng. for Ind., 89:1, 1967.

13. Fuchs, N. A. The Mechanics of Aerosols. The MacMillian Company, New York (1964).

CHAPTER IV

REVERSE FLOW STUDIES

OBJECTIVES AND APPROACHES

Based upon data provided in the Handbook of Fabric Filter Technology,[1] it is estimated that about 57 percent of existing commercial collector models are cleaned either by mechanical shaking (35 percent) or high pressure pulse jet air (22 percent). Another important approach, reverse flow cleaning, is used in about 25 percent of existing collector types based upon the statistics cited previously.[1] The latter category does not include those units cleaned by high pressure pulse jet air, as discussed in Chapter III, and those cleaned by continuous application of a high velocity air jet (traveling blow ring).

Data for low pressure-reverse air flow cleaning systems are quite limited with respect to their dust removal capabilities. In many cases, it appears that the reverse air flow functions mainly as an adjunct to the primary cleaning process; e.g., mechanical shaking as described previously or bag collapse as applied to highly tensioned, heavily laden glass bags. It should also be noted that as pressure levels increase and the rates of pressure and flow change become more rapid, it becomes progressively harder to differentiate between reverse flow and pulse jet cleaning processes.

Because the reverse flow concept is used in some 25 percent of available commercial equipment, and also because some operating features of reverse flow systems appear similar to those of the high pressure pulse

jet units, several exploratory measurements were performed in this area. In contrast to the more detailed studies of the better defined shaking and pulse jet cleaning systems, most of the experiments described in this section were simplified. The principal test objectives were as follows:

- Identify key variables that influence collection efficiency and operating resistance and postulate their relationships at least on a qualitative basis.
- Determine the apparent practical boundary conditions for the variables determining system performance.
- Develop a framework for the more effective evaluation and utilization of the reverse flow concept.

BACKGROUND

Postulated Cleaning Actions

Despite the different techniques used to create the dust separating forces for mechanically shaken and pulse jet systems, the data presented in Chapters II and III, respectively, suggest that tensile forces generated by rapid acceleration of the dust/fabric layer constitute the primary cleaning mechanism. When tensile forces exceed the adhesive and/or cohesive forces, dust is detached mostly in the form of large agglomerates at those locations where the binding forces are weakest or the acceleration forces the greatest. Visual observations indicate that the separation frequently occurs at the interface between the dust particles and the main fiber-structure.

The data presented in Chapter III indicated that a reverse air flow following pulse application serves to flush out loosened particles from fabric interstices. More important, however, is the transient arresting of system flow so that dislodged agglomerates can settle towards the collecting hopper. Based upon gravimetric measurements and filter resistance characteristics, there is little evidence to suggest any

significant removal of dust particles by aerodynamic action alone. The above findings are in agreement with those of Larson[2] who states that air velocities of the order of 200 ft./min. are required to remove a single 20 μm particle from a fiber and Zimon[3] who indicates that air velocities sweeping over a layer of dust (tangentially) must be in the 400 ft./min. range before any appreciable dust removal is attained. The latter observation explains why the reverse jet (traveling blow ring) system with constant slot velocities of 4000 to 6000 ft./min. constitutes an effective fabric cleaning method for felted media.

Since significant dust removal is attained in some reverse flow systems one must conclude that separating forces other than aerodynamic drag are involved. According to the drag approach, the separating force for a single particle produced by viscous drag should be essentially the same at any point within the filter if one assumes a constant interstitial velocity. At the same time, however, the pressure gradient produced by the reverse flow causes the filter to compress. Therefore, the normal adhesive forces between adjacent particles are actually increased as one moves radially from the dirty to the clean air side of the filter. The net effect is that any dust dislodgement is more likely to follow a simple spallation process with the adhesive bond failure occuring close to the dirty face of the filter. It should be noted that the above process is the opposite of that for cleaning by shaking or high energy pulse in which the dust/fabric experiences tension rather than compression when it is decelerated. From the practical viewpoint, reverse flow alone does not appear conducive to high dust removal unless air velocities are much higher than those used in typical reverse flow systems.

It should be noted, however, that a high reverse pressure gradient across the filter may also increase the lateral or hoop tension in the dust/fabric system so that many of the adhesive and cohesive bonds are disturbed. Given this situation, aerodynamic drag could be expected to flush out more loosened particles. Another adjunct to dust separation

is the flexure produced in the fabric when the flow is reversed. In many systems, sufficient bending or warping of the fabric surface occurs to cause a significant spallation at the dust/fabric interface. The effect is most pronounced for woven fabrics in which a larger fraction of the dust can appear as a superficial layer.

Basic Design Concepts

A comprehensive review of reverse flow cleaning processes has been presented by Billings and Wilder.[1] In contrast to cleaning methods discussed previously, it is more difficult to characterize rigorously many of the reverse flow cleaning systems. Generally, the reverse flow is produced by a gradual venting of low pressure air from a secondary fan rather than a compressed air source. Thus, there is usually no rapid rise in pressure, ~ 2000 in. water/sec., such as seen with a high pressure pulse jet system.

If the dust releases readily from the fabric, a reversal of flow in itself may suffice for adequate cleaning. In many cases, however, the reverse flow is used in combination with shaking, pulsing or bag collapse to facilitate dust removal. Because of its structural depth, and hence greater dust retentivity, a felted fabric is not usually cleaned by reverse flow.

When reverse flow is used as the sole method of cleaning, bag attrition is low provided that proper support structures are used to prevent excessive bag flexure. It is emphasized, however, that the rate of flexure is probably the controlling factor with respect to fabric (or fiber) failures. Thus, a gradual inflation or deflation process is unlikely to cause any serious fabric damage. Increased bag tension and reduced reverse flow rates also minimize the degree of flexure as well as preventing a complete flattening of the bag. Under the latter circumstances, there is no opportunity for loosened dust to fall to the hopper

nor is there a pathway for the reverse flow air. The insertion of restraining rings or a supporting cage eliminates complete bag collapse but introduces a potential problem of fabric chafing. Sewing the rings to the bag minimizes the chafing or attrition problem.

APPARATUS, MATERIALS AND TECHNIQUES

Experimentation with reverse flow cleaning was carried out with the shaking bag and pulse jet systems described in Chapters II and III after modifying the above units as shown schematically in Figures 82 and 83.

Modified Mechanical Shaking System

Figure 82 shows the arrangement by which a reverse air flow was produced with the mechanically shaken equipment. Since dusty air was delivered to the filter bag under positive pressure, flow reversal was accomplished by exhausting air from the dirty air side of the filter. As stated earlier in Chapter II, positive pressure operation facilitated the installation and use of special testing instrumentation.

During these experiments, Valve A was closed when the main fan was stopped. Concurrently, Valve B was opened and the reverse flow exhauster operated when the shaking cycle was in progress. In most cases, the Valve B solenoid drive was connected to the electrical circuit for automatic regulation of the shaking cycle.

Tests were performed with and without the installation of a flexible coil spring, diameter ~3 in., inside the bag to prevent its complete collapse when the flow was reversed. The static pressures cited during the actual reverse flow periods, which were measured by conventional manometers (liquid), reflect the negative pressure within the hopper (or dirty air chamber).

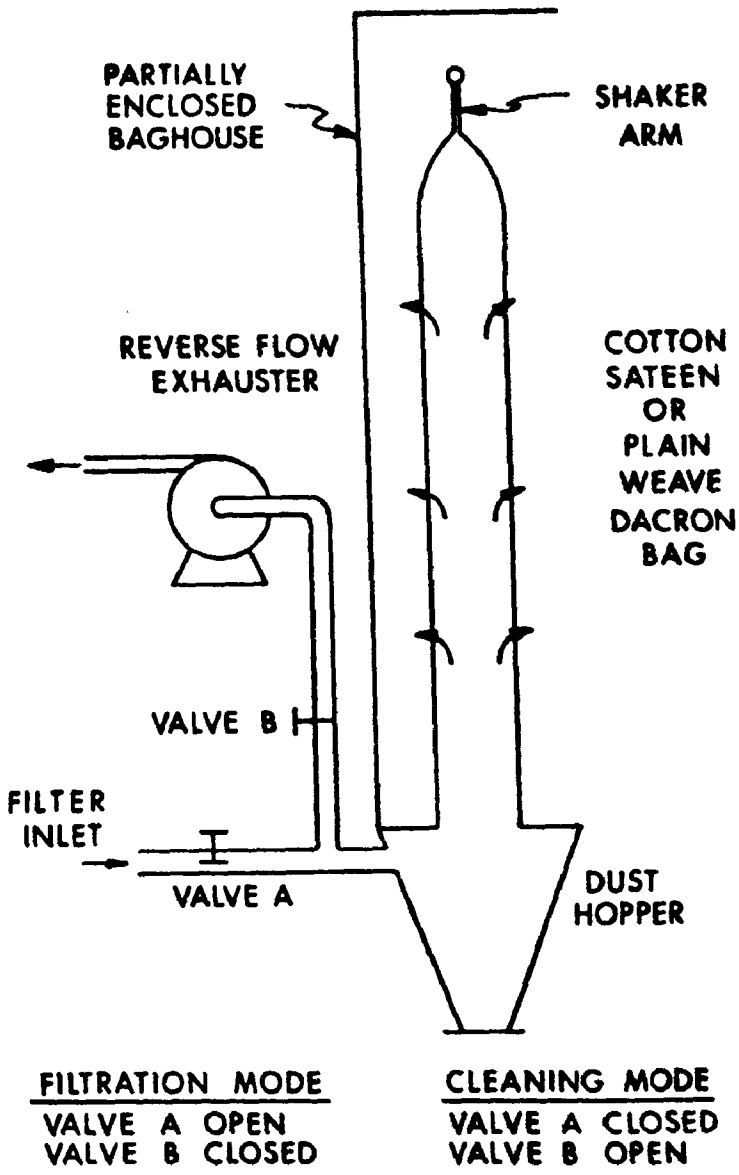

Figure 82. Schematic of mechanical shaking system as modified for reverse flow cleaning

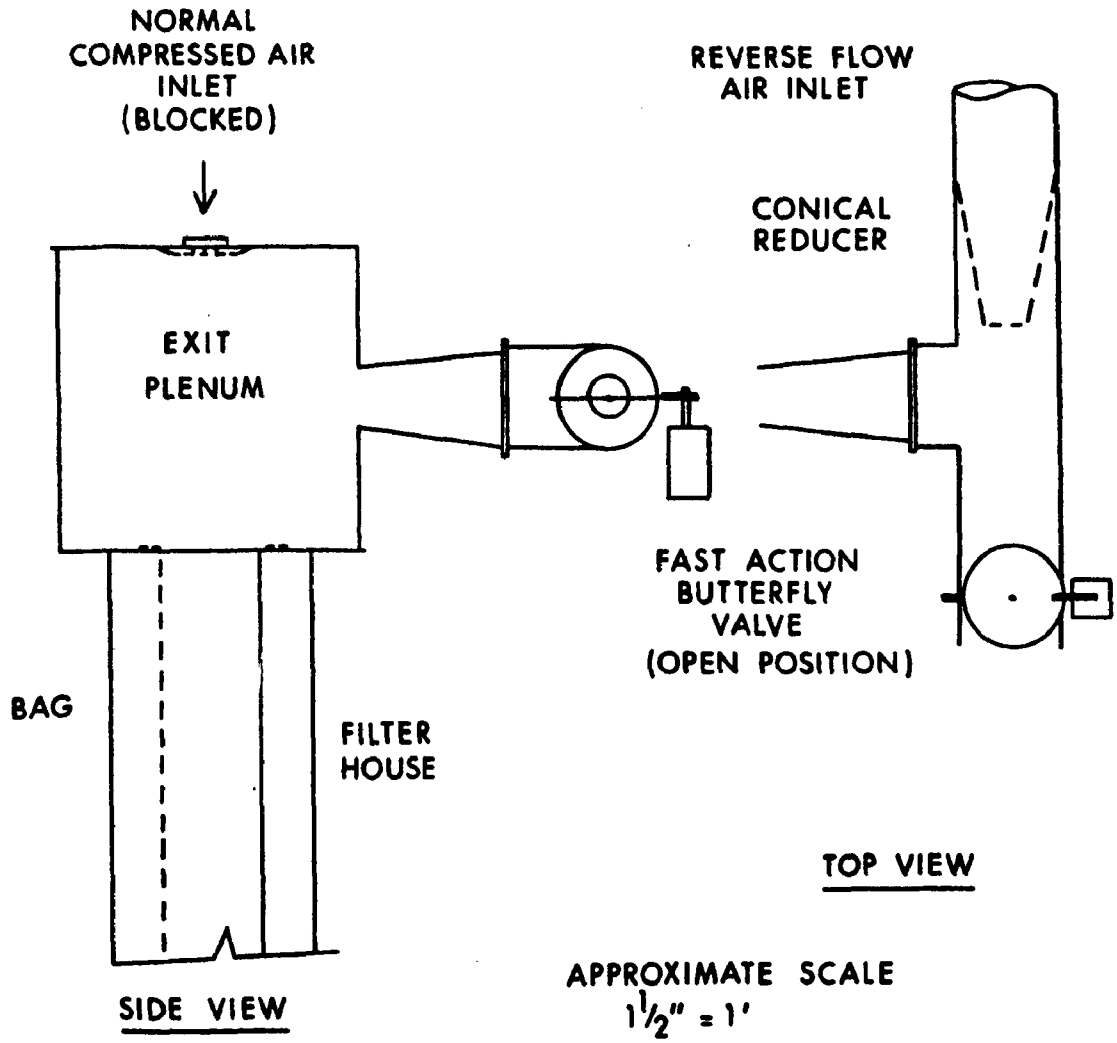

Figure 83. Schematic view, pulse jet assembly with low pressure reverse air and high pressure nozzle removed. No bag Venturi.

Modified Pulse Jet System

The evaluation of the effect of reverse flow cleaning for the wool and Dacron felts normally cleaned by pulsing was conducted using the basic equipment described in Chapter III. The system was modified as shown in Figure 83 by the addition of the same 600 ft.^{3}/min. blower used with the shaken bag unit. The ducting was arranged with the fan reversed to introduce a flow of air into the outlet plenum above the bag whenever a fast-acting damper closed. The damper was connected with the pulse solenoid, with a controlled time lag between them when desired. Alternatively the damper was used alone instead of the pulse solenoid, and controlled by the regular pulse timing system.

Because a commercial damper with sufficient size and response time could not be located, one was constructed on the butterfly valve principle. The shaft was turned by a powerful solenoid acting against a return spring. The rate of opening of the damper was regulated by attaching weights to the shaft, enabling a study of the effect of the rate of change of reverse flow.

When the damper closed, the primary system flow was temporarily blocked and, with sufficient pressure from the cleaning fan, the flow was reversed through the filter. Although the schematic arrangement of Figure 83 shows the pulse jet compressed air source as blocked off, several measurements were also made where the high pressure pulse was admitted directly to the plenum (plenum pulse as described in Chapter III) or by the conventional 1/4-inch nozzle with the Venturi element located in the bag exit.

The magnitude of the reverse pressure or reverse flow used during cleaning was regulated by damper control of the reverse flow fan. In most cases, the reverse flow fan was allowed to run continuously during operation, to minimize start-up delays. The fact that considerable power was wasted by this technique was immaterial from the experimental viewpoint.

Commercial equipment designed on these principles would, of course, utilize the reverse flow fan more efficiently because several compartments would be operated in parallel.

Test Fabrics

The filter fabrics used in this phase of the study included the woven and felted fabrics described in Chapter II, Tables 2, 3 and 17 and Chapter III, Table 19. The woven bags, well-used unnapped cotton sateen and plain weave Dacron, are normally cleaned by shaking. The term "well-used" refers to those bags that had been given about 2×10^7 individual shakes as part of their accelerated life testing. The wool and Dacron felt bags studied are normally cleaned by reverse pulse. The felted media were included, however, even though rarely used for reverse flow cleaning, to provide some data that is currently lacking in the filtration literature.

Measurements and Instrumentation

No new control and measurement techniques or concepts were introduced during the reverse flow tests. Primary system air flows and the recording of filter resistance as well as the timing of cleaning and filtering cycles were carried out with the same apparatus described in Chapters II and III. The initiation and regulation of the reverse flow processes were accomplished by making parallel or delayed time connections to the basic control circuits. Transient pressure differentials across the bag during the reverse flow intervals were again detected by paired Pitran transistors (see Chapter III) and displayed on an oscilloscope screen. This approach was particularly valuable for defining the pressure wave form and the rate of pressure rise for high and low pressure pulses.

Most dust concentration estimates for the effluent gas stream were performed with the RDM monitor discussed previously. Less emphasis was

placed on effluent characteristics during the reverse flow tests because the primary objective was to determine whether successful, steady state operation could be attained prior to any further evaluations.

Test Dusts

Fly ash (5 micrometer MMD), Table 4, was used exclusively as the test dust in this series of experiments. It was chosen because of the extensive amount of work done with fly ash in other phases of the program, because of its moderately good release properties and because reverse flow cleaning has also been used for industrial filtration of fly ash from oil and coal combustion sources.

RESULTS

Low Pressure, Reverse Flow with Mechanical Shaking

The use of reverse flow air in conjunction with the mechanically shaken apparatus shown in Figure 82 represents an augmentation approach in which the reverse air function is: (a) to flush out interstitially loosened dust; and (b) to hasten the removal of the finer aerosol fraction from the dirty air side of the bag.

Aside from the reverse flow modification, the basic filtration parameters for fly ash with unnapped cotton sateen and plain weave Dacron bags were essentially the same as described in Chapter II; i.e., 3 ft./min. filtration velocity and an inlet loading of 3.5 grains/ft.^{3} The shaking conditions were those indicated in Chapter II as a standard cleaning cycle; i.e., 8 cps, 1 in. amplitude and 360 shakes. The filtration period was approximately 20 minutes, as compared to the 30-minute period used previously.

Although the reverse flow fan had the capacity to exhaust air at 600 ft.^{3}/min., it was ordinarily throttled so that the typical range of

reverse flows was 20 to 220 ft.^{3}/min. Unless otherwise specified, the reverse flow fan and the shaker motor were operated simultaneously. Less than 5 seconds were required for the reverse flow fan to reach full speed.

According to the data summarized in Table 29, Tests 1 and 6, the base line (mechanical shaking only) tests were reasonable replications of prior measurements discussed in Chapter II. The resistance/time data shown in Figures 84 and 85 indicate that the base K values for fly ash/cotton and fly ash/Dacron, respectively, are 15 and 12 in. water/ft./min./lb./ft.^{2} The first reverse flow augmentation experiments in this series were conducted with bags that were not supported on the inner side. This led to varying degrees of collapse depending upon the vacuum (or differential pressure) across the bags during the reverse flow interval.

In the absence of internal support, increased reverse flow made it progressively more difficult to dislodge the dust and condition the filtering surface by the reverse flow. The result was that the K values also increased gradually, Table 29, Tests 1 to 3 and 6 to 8, and a similar increase in the amount of dust retained by the filters was also observed.

Upon the installation of an internal supporting structure (highly flexible helical coil) some reduction in filtration resistance was obtained as shown by Test 4. One is forced to conclude, however, that supplementing mechanical shaking with a low level reverse flow (plus support structure) afforded no advantage. Limited tests with reverse flow only and including an internal support showed much higher operating resistance and greater K values.

Although the weighings were considered to be rough, it was noted that the amount of dust dislodged (~ 200 grams) during Tests 1, 2 and 3, as shown in Table 29, was about equal to that deposited during the filtration cycle, one criterion for true steady state operation.

Table 29. FLY ASH FILTRATION WITH MECHANICAL SHAKING AND/OR LOW PRESSURE REVERSE FLOW CLEANING

Test number	Test conditions[a]	Filter resistance in. water			Reverse flow		Dust parameters		Effluent concentration gr./ft.^{3} x 10^3
		Initial	Effective residual (estimated value)	Terminal	Applied vacuum in. water	Estimated velocity ft./min.	Weight dislodged grams	Residual weight grams	
	Unnapped cotton sateen								
1	Shake only[b]	1.5	2.0	3.4	-	-	198	372	
2	Shake plus reverse flow	1.6	2.1	3.8	0.7-0.6	1.2	212	520	Estimated from Table 13
3	Shake plus reverse flow	1.4	2.1	4.0	2.2-1.8	4.3	203	535	
4	Shake plus reverse flow with support	1.4	2.0	3.4	1.0	2.1	-	-	2 x 10^{-2}
5	Reverse flow only with support[c]	1.3	2.5	6.2	5.2	12.0	-	290	
	Plain weave Dacron								
6	Shake only	0.2	1.0	2.1	-	-	208	414	6.6
7	Shake plus reverse flow	0.2	0.9	2.0	0.5-0.25	5.6	225	386	11.4
8[d]	Reverse flow only	-	-	6.7	4.5-4.3	-	50	1520	-
9[e]	Reverse flow only with support	3.1	3.5	7.0	0.75	0.7	80	1490	14.0
10	Reverse flow only with support	1.0	1.4	4.5	5.4	16.2	-	720	-

[a] 10 ft. x 6 in. diameter bags. Loaded to equilibrium at 3.5 grains/ft.^{3}, 3 ft./min. filter velocity.

[b] Shaking, 8 cps, 1 in. amplitude, 360 shakes.

[c] Reverse flow period, 45 seconds.

[d] No equilibrium attained.

[e] Near equilibrium.

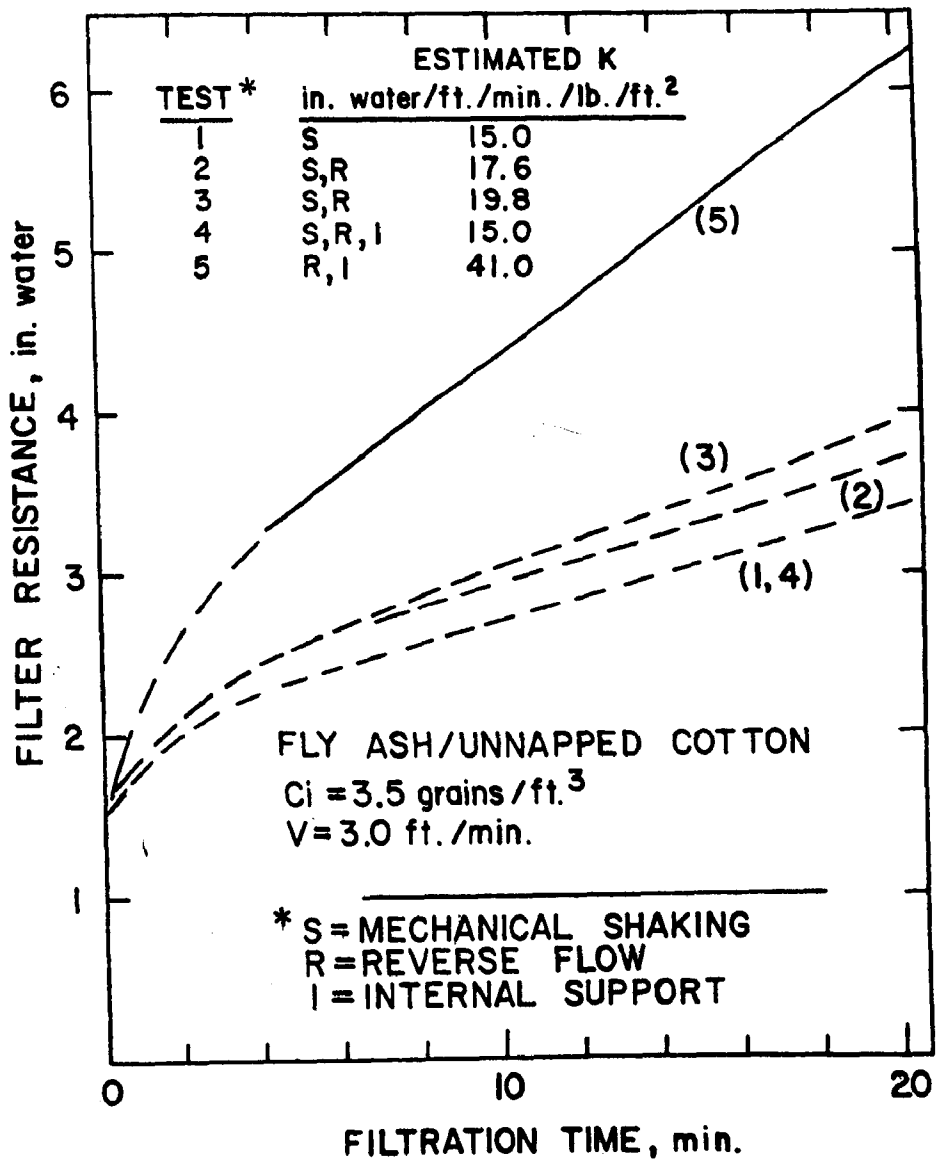

Figure 84. Resistance characteristics for fly ash/unnapped cotton filtration with mechanical shaking and/or reverse flow (shaking cycle, 8 cps, 1 in. amplitude, 360 shakes)

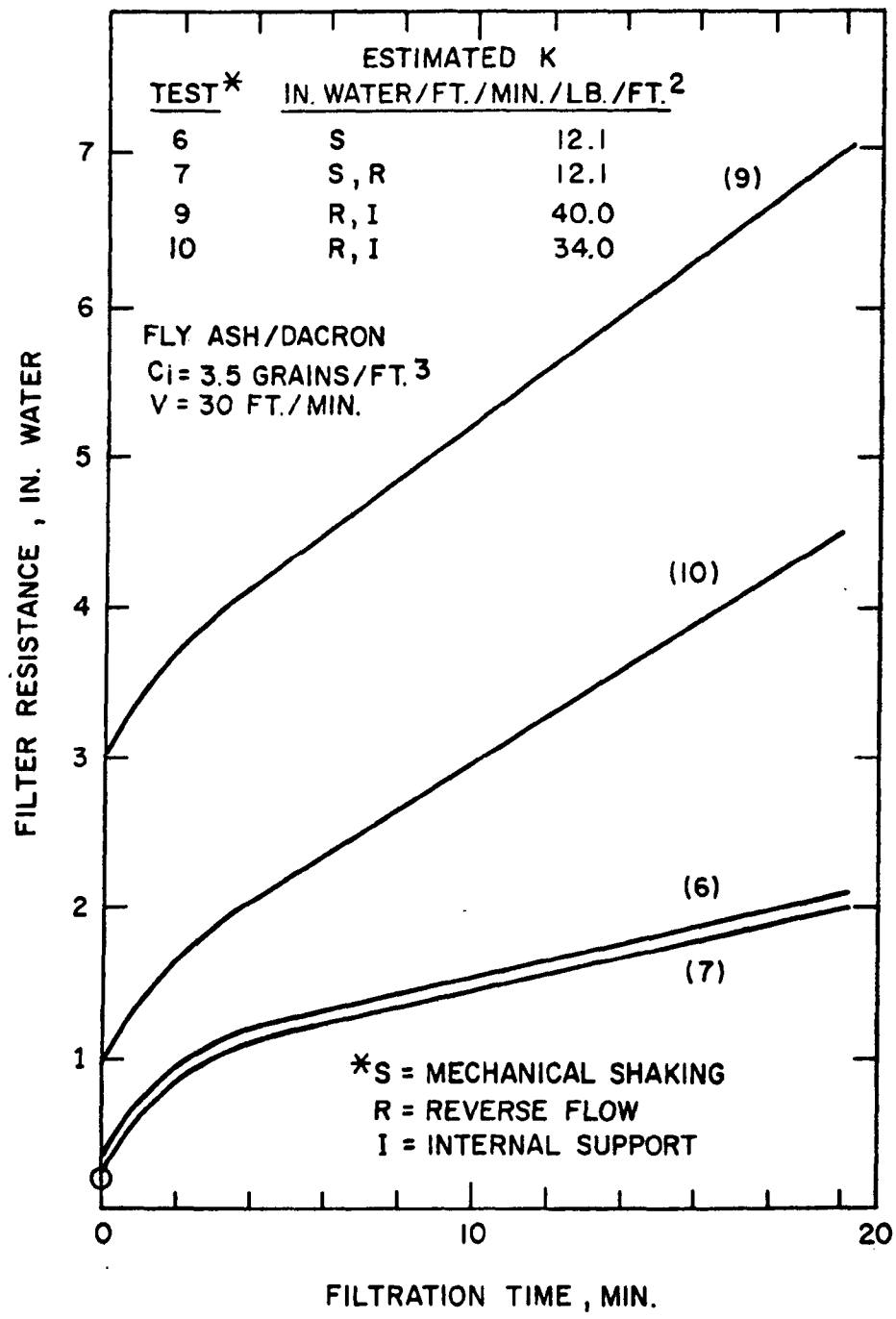

Figure 85. Resistance characteristics for fly ash/Dacron (plain weave) filtration with mechanical shaking and/or reverse flow. Shaking cycle, 8 cps, 1 in. amplitude, 360 shakes.

The fact that the K values increased, Figure 84, suggested that the collapse of the bag led to a nonuniform cleaning process. The latter effect, which was reported in this study (Chapter II), was also observed by Walsh and Spaite[4] in their mechanical cleaning tests when insufficient shakes, <150, were used. Although the residual resistance levels indicate good cleaning, the subsequent pressure rise shows a decreased holding capacity (or larger K value). Despite the fact that the tests reported in Table 29 show no benefits for reverse flow augmentation, it is emphasized that in other applications reverse flow has been used effectively. The present tests point out that once vigorous mechanical shaking has taken place there is little to be gained by the secondary treatment. In many operational systems, however, the compartment isolation valves may not completely stop filtration flow. Thus, during shaking there is a tendency not only for dust redeposition such as encountered with pulse jet cleaning but also for dust transport to the clean air side of the system. A gentle reverse flow in the latter case should prevent this dust penetration.

When the dust deposit is mainly superficial and the bag tension is high enough to minimize the collapse and internal blockage problems, the reverse flow approach has merit in low velocity filtration applications. In the present test series, it was not clearly defined what role the flexing of the fabric exerted relative to the dust removal by flexing. Some exploratory measurements are described in the next section that shed some light on the amount of dust removed by aerodynamic action.

Low Pressure, Reverse Flow With Pulse Jet Equipment

Ordinarily, felt bags and similar filter media are not used in simple reverse flow processes because of reportedly poor cleaning, usually attributed to complex dust/felt interactions. It was believed, however, that with the experimental equipment on hand it would be advantageous to carry out more detailed investigations of reverse flow processes to further the understanding of the physical mechanisms involved. Several

combinations of high and low level reverse flow pulses were investigated to establish possible relationships between shock and aerodynamic effects.

In a series of tests where reverse flow alone was used, the following factors were investigated with respect to filter cleanability.

- Slow inflation rate
- Rate of pressure rise (bag differential)
- Frequency of cleaning
- Flow duration

Separate test sequences were performed in which reverse pulse and reverse flow cleaning were combined.

Slow Inflation Rate, Reverse Flow Only - The exploratory tests summarized in Table 30 were designed to examine the effects of reverse flow velocity on dust removal from another perspective. As well as could be determined by the combination of reverse flow and mechanical shaking, Table 29, the aerodynamic removal of collected dust was probably of minor importance.

Several degrees of reverse pressuring of the clean air side of the bag were investigated with the pulse jet system. The test procedure was to load a Dacron or wool bag with fly ash under the routine filtering conditions used in many tests; i.e., inlet loading 11.6 grains/ft.^{3}, filter velocity 8.5 ft./min. and a 1-minute filtering interval. At the end of the filtering period, the main air flow was shut off completely. Reverse air was then admitted to the exit plenum chamber by the gradual opening of a valve installed in the compressed air delivery system such that the average rate of pressure increase on the clean air side of the bag was about 0.6 in./sec. The estimated acceleration in reverse flow velocity was 0.014 ft./sec.^{2} Once the indicated pressure levels were attained, Column 2, Table 30, the flow was held constant for 2 seconds and then gradually reduced to zero.

Table 30. DUST REMOVAL VERSUS REVERSE FLOW VELOCITY, VOLUME, PRESSURE AND DURATION. FLY ASH AND WOOL AND DACRON BAGS

Test[a] number	Reverse pressure differential in. water	Net dust removed grams	Reverse air[b]		Estimated cleaning time sec.
			Estimated maximum velocity ft./min.	Estimated total volume $ft.^3$	
11 W	3	4.1	4.3	0.50	12
12 W	4	4.6	5.7	0.83	15
13 W	6	4.5	8.5	1.70	22
14 W	8	5.4	11.4	2.90	29
15 W	3	4.5	5.6	0.80	28
16 W	4	5.4	5.7	0.83	15
17 W	6	6.3	8.5	1.70	22
18 W	7	2.3	9.9	2.3	25
22 D	5	9.9	7.1	1.23	19
23 D	10	10.4	14.2	4.36	35
24 D	14.6	8.4	20.7	9.08	51
19 W[c]	7	1.5	9.9	2.3	25
20 W[c]	7	0.7	9.9	2.3	25
21 W[c]	7	0.3	9.9	2.3	25

[a] W = wool; D = Dacron.

[b] Rate of change in cloth velocity during valve opening and closing, 0.014 $ft./sec.^2$.

[c] Three successive cleanings without reloading.

Note: Dust load applied at 11.6 $gr./ft.^3$ and 8.5 ft./min., filter cleaned first by reverse flow as indicated. Following measurements, filter cleaned by pulse jet, 70 psig damped, 0.06 sec. duration and 1 min. frequency, cycle then repeated.

Approximate values for maximum reverse cloth velocities and total reverse air volumes were based upon the terminal resistance value for the loaded filter, ~ 6 in. water. The above estimating process was used because only a small fraction, ~20 percent, of the 31 grams of dust added to the filter during the loading period was removed during each test. Thus, no large increase in overall permeability was expected. Additionally, the velocity estimates were also conservative.

It appears very clear from Table 30 that regardless of the pressure differential, the amount of reverse flow, and the flow velocity as determined by the pressure, the dust loss is very small and for all practical purposes a constant quantity. The only common factor that appears to afford a reasonable explanation for the constant removal is that the fabric surface was flexed once (dilate and contract) during each test. At the indicated range of pressures, the curvature assumed by the bag was probably the same and the change rate of curvature was dictated by a uniform expansion rate in each test. Thus, the adhesive and cohesive forces were diminished by the extent of the flexure so that even a minimal air motion sufficed to detach those particles not separated by gravity fall.

It had been observed that closing down the main fan in routine mechanical shaking tests, Chapter II, resulted in a 5 to 10 gram loss of dust as the woven cotton or Dacron bags collapsed. This loss was inconsequential relative to the ~300 grams dislodged during the shaking process, about 2.5 percent. The approximate time interval for the bag relaxation was 5 to 10 seconds such that the rate of flex corresponded to that of the tests summarized in Table 30.

The tests discussed in this section confirm the fact that even a very gentle bending of a fabric is sufficient to dislodge dust surface layers. Note that the rate of pressure increase for the Table 30 measurements, ~ 0.6 in./sec., was very small compared to that usually found for conventional pulse jet systems, ~2000 in./sec. They also appear to bear

out prior theories on adhesion[2,3] that indicate that air velocities must be in the 200 to 400 ft./min. range before aerodynamic forces become significant.

Pressure Rise Rate, Reverse Flow Only - The shape of the pressure pulse delivered to an equilibrated Dacron felt bag was varied by attaching weights to the damper used to divert the flow from the positive side of the high volume blower to the inner or clean side of the filter unit, Figure 83. This, in effect, retarded the opening and closing of the damper and reduced the rate of pressure change at both ends of the cleaning cycle. The wave forms of the pressure pulses across the bag are shown in the oscilloscope traces of Figure 86.

Each test shown in Table 31 was conducted at typical pulse jet filtration conditions; i.e., an inlet fly ash concentration of 11.6 grains/ft.^{3}, a filtration velocity of 8.5 ft./min. and a 0.5 minute cleaning frequency. As far as the general effect was concerned, the pressure changes produced in the filter system by the opening of the damper from the high volume blower were very similar to those resulting from pulse jet action. The major difference was that the rate of rise of differential pressure, $d\Delta p/dt$ at its maximum value of 750 in./sec. was 3 to 4 times less than that produced by a compressed air source. The actual maximum pressure differentials at steady state were roughly the same as those found for pulse jet systems, Chapter III.

Key test parameters for the measurements shown graphically in Figure 86 are given in Table 31. As expected, an inverse relationship between rate of pressure rise and average filter resistance was indicated. Similarly, a direct relation between average effluent concentration and

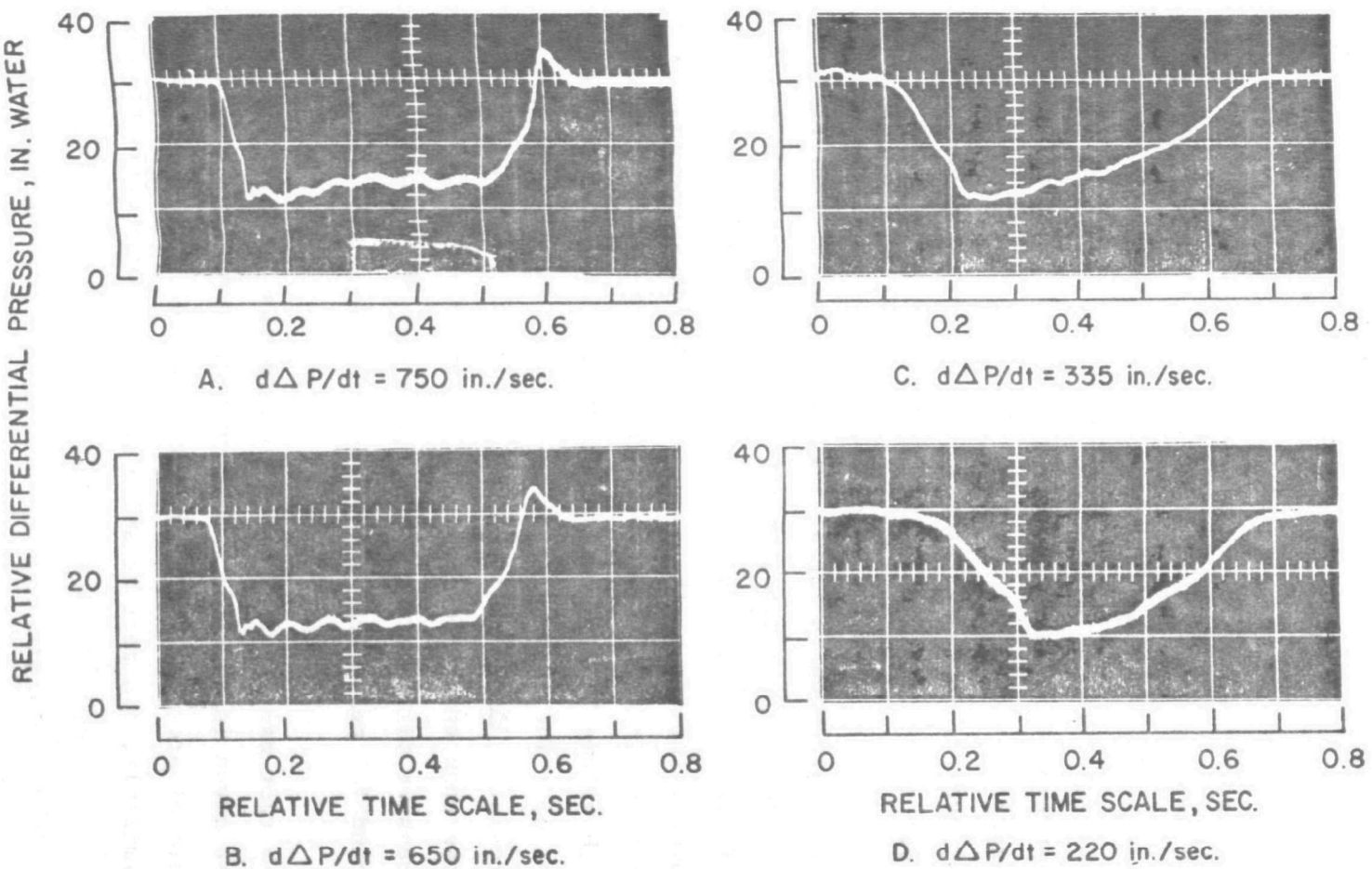

Figure 86. Controlled variations in rate of differential pressure change across felt bags (see Table 31)

Table 31. EFFECT OF VARYING RATE OF PRESSURE CHANGE ON FILTER RESISTANCE AND EFFLUENT CONCENTRATION. FLY ASH/DACRON SYSTEM, 11.6 GRAINS/FT.^{3} INLET LOADING, 0.5 MINUTE CLEANING INTERVALS.

Test number	Pressure change in./sec.		Bag resistance in. water			Effluent[a] concentrations gr/ft.^{3} x 10^3	Average reverse pressure in. water	Residual dust deposit grams	Air volume[b] per 0.2 sec. pulse ft.^{3}
	Rise	Fall	Residual	Average	Terminal				
25	750	520	7.5	7.8	8.1	0.85	17.0	145	0.30
26	650	545	7.4	7.6	7.8	0.35	18.0	213	0.32
27	335	140	9.5	10.6	11.6	0.17	14.0	263	0.20
28	220	140	10.1	10.9	11.6	0.04	20.0	268	0.16

[a] RDM measurement.

[b] Based on cloth velocity of 8.5 ft./min. at indicated residual resistance, cloth area of 4.7 ft.^{2} and persistence of maximum reverse pressure for 0.2 sec.

rate of pressure rise was consistent with the greater dust concentration expected for the lower resistant and more porous filter structure. The residual dust holding for the filter was also lowest when the pressure rise rate was the greatest.

Although the cleaning has been described as reverse flow because a low pressure fan was used in the above tests, the actual results were essentially the same as would have been obtained by the restricted venting of a compressed air source (slow acting solenoid valve). Despite the generally higher operating resistance, Test 25, Table 31, suggests that steady state operation can also be maintained with the lower energy pulses produced by the reverse flow system.

Discounting for the moment the size of the blower (up to 600 $ft.^3/min.$ capacity) used to provide the reverse flow by the mechanisms shown in Figure 83, the actual volumes used per 0.2 sec. pulse were in the 0.25 to 0.33 $ft.^3$ range STP. This is in the same range as the air volumes delivered by the pulse jet system at 70 to 100 psig for typical pulse durations, Figure 87. If one considers only the cost associated with the reverse air volume passing through the filter the relative power costs greatly favor the lower pressure fan by a factor of 50 to 100. Practically speaking, however, the low pressure system (up to 20 in. water) must be kept in operation to provide a fairly rapid reversal of air. Hence, the overall system must be designed as a multi-compartmented unit, order of 10 or more, so that by fast acting dampers, a single fan can service several compartments. The principle conclusion to be drawn from the tests summarized in Table 31 is that there appear to be alternative means to clean felted media that should be thoroughly investigated.

Frequency of Cleaning, Reverse Flow Only - Limited tests with the reverse flow system, Table 32, indicated that extending the filtration time to 1 minute between cleanings led to undesirably high operating resistances, ~ 11 in. water. Conversely, decreasing the cleaning

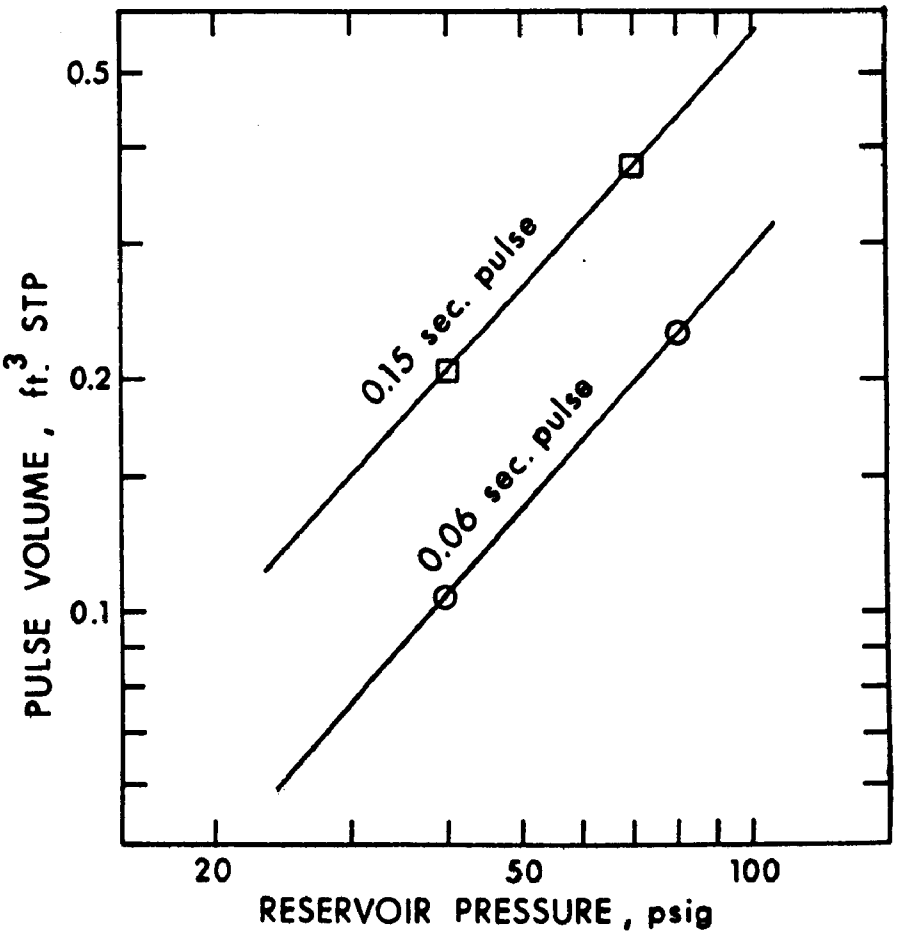

Figure 87. Air volume ejected per pulse with commercial 1/4-in. nozzle and solenoid valve assembly

Table 32. EFFECT OF CLEANING FREQUENCY ON FILTER RESISTANCE AND EFFLUENT CONCENTRATION WITH REVERSE FLOW CLEANING. FLY ASH/DACRON FELT AT 11.6 GRAINS/FT.^{3} AND 8.5 FT./MIN. VELOCITY.

Test number	Cleaning frequency min.	Bag resistance in. water			Effluent concentration gr./ft.^{3} x 10^3	Average reverse pressure in. water	Pressure rise rate in./sec.
		Residual	Average	Terminal			
29	0.25	7.8	7.9	8.00	0.35	15	615
25	0.5	7.5	7.8	8.1	0.85	17	750
30	1.0	9.5	10.8	12.0	0.61	17	900

interval to 0.25 min. did not show any improvement in resistance characteristics relative to a 0.5 min. cleaning frequency. A direct correlation between rate of pressure rise and the amount of dust deposited upon the filter between cleaning cycles was indicated. Tests reported in Chapter III showed large differences in the rate of pressure rise for a 10 to 12 fold range in inlet dust concentration.

Reverse Flow Duration - Reverse Flow Only - The effect of reverse flow duration was studied using reverse pulse equipment modified by the addition of the high volume blower. As in previous tests, the blower was operated continuously and the flow diverted by the damper into the Dacron filter bag during the cleaning cycle.

In the present test series, the filter was cleaned every 0.5 minute for time intervals ranging from 0.025 to 2 seconds as shown in Table 33. According to the pressure/time traces for these tests given in Figure 88, the wave forms for the 0.2 and 2 second pulse period. similar. Filter resistance characteristics also were similar but the effluent concentration was much greater for the 2 second pulse period. It is not believed that so large an increase is typical for the extended pulse. Based upon prior tests with conventional (compressed air) pulse jet systems, Chapter III, effluent concentrations appeared to increase

Table 33. EFFECT OF LOW PRESSURE PULSE DURATION ON FILTER RESISTANCE AND EFFLUENT CONCENTRATION. FLY ASH/DACRON SYSTEM.

Test number	Reverse flow[a] duration secs.	Bag resistance in. water			Effluent[b] concentration gr/ft.^{3} x 10^3	Reverse pressure in. water	
		Residual	Average	Terminal		Maximum	Average
31	2.0	8.4	9.4	10.1	4.4	20	16
32	0.2	8.8	9.0	9.7	0.61	20	16
33	0.05	9.3	9.9	10.6	0.57	19	12
34[c]	0.025	12.6	14.5	16.5	--	17	9

[a]Cleaning frequency, 0.5 min.

[b]Inlet concentration, 11.6 grains/ft.^{3}, filter velocity 8.5 ft./min.

[c]Air flow unsteady, fan capacity exceeded.

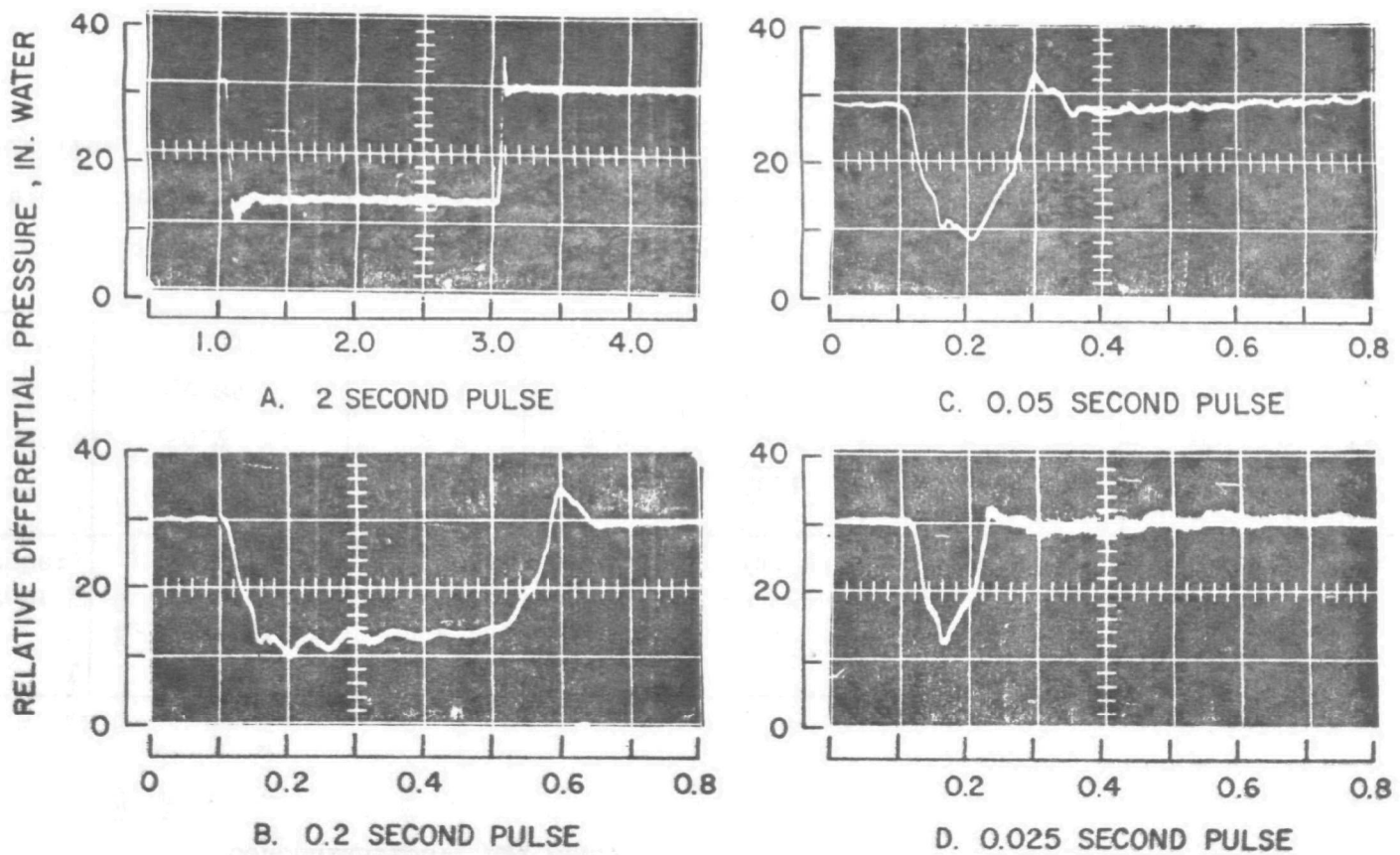

Figure 88. Characteristic pressure/time traces for variations in reverse pulse duration (see Table 33)

as the square root of the pulse duration. Hence, with respect to the 2 second pulse in Table 33, an emission of 2×10^{-3} grain/ft.^{3} might be nearer to the correct level. A small increase in filter resistance was noted for a 0.05 sec. pulse but the data are too limited to warrant any conclusions even though the pressure differential attained might suggest less effective cleaning. There does appear to be a lower limit for pulse duration, ~ 0.025 sec., at which dust removal falls off rapidly according to the high filter resistance observed. Although the rate of differential pressure rise was about the same, 700 in./sec., the maximum and average pressures displayed for the 0.025 sec. pulse were much lower. This test shows that not only the rate of pressure rise but the maximum value reached is also important in effective cleaning. The critical factor is that the impulse applied to the fabric must persist long enough for the fabric to experience full flexure. Continuation of pulses beyond this point appears to lead to higher effluent loadings and greatly increased reverse air demands.

Reverse Flow With Reverse Pulse Cleaning

A special sequence of tests was performed in which various combinations of reverse pulse and reverse flow cleaning, differing with respect to time phasing, were evaluated, Table 34. The basic test apparatus was that shown in Figure 83 except that the conventional 1/4 in. jet nozzle and Venturi section were re-installed in the system. Filtration was performed with a Dacron felt and an inlet concentration of 11.6 grains/ft.^{3} at 8.5 ft./min. filtration velocity.

The characteristic wave forms for the bag pressure differentials noted for these tests are given in Figure 89. Figures 89a and 89b, respectively, show the individual patterns for pulse jet and reverse flow alone, while Figure 89c indicates the effect of superposition of both cleaning processes. It should be noted that the combined pressure gradients are approximately equal to those of the pulse jet alone and not the algebraic sum of that produced by the high and low energy pulses.

Table 34. EFFECT OF PULSE JET AND/OR REVERSE FLOW CLEANING ON FILTER RESISTANCE AND EFFLUENT CONCENTRATIONS WITH A FLY ASH/DACRON FELT SYSTEM

Test number	Pulse jet parameters[a]			Reverse flow[b] parameters		Maximum[c] differential pressure in. water		Bag resistance[d] in. water			Effluent[e] concentration gr./ft.^{3} x 10^3
	Pressure, psig	Frequency, min.$^{-1}$	Duration, sec.	Duration, sec.	Phasing, sec.	Combined	Reverse flow only	Residual	Average	Terminal	
35	60	1	0.06	No reverse flow		19	-	2.7	4.3	5.9	2.0
36		No pulse		0.2	-	-	13	5.7	6.8	8.0	0.35
37	60	1	0.07	0.2	0.09	23	11	3.3	5.4	6.5	0.48
38	60	1	0.07	0.2	0.022	22	11	3.5	5.7	6.9	2.5
39	60	1	0.07	0.5	0.01	22	11	3.6	5.4	7.2	2.9
40	60	1	0.07	0.5	-0.05	20	10	3.8	5.3	6.8	2.7
41	60	1	0.07	0.5	-0.05	22	10	3.7	5.3	6.9	-
42	60	1	0.07	0.5	0.03	23	11	3.5	4.8	6.1	3.4
43	60	1	0.07	0.5	0.05	23	11	3.6	5.0	6.4	1.5
44	60	1	0.07	No reverse flow		22	-	3.9	5.1	6.3	-

[a] Direct pulses

[b] Minus sign means jet pulse initiated first.

[c] Average rate of pressure rise, 2300 in./sec. for pulse jet and 760 in./sec. for reverse flow.

[d] Based on inlet loading of 11.6 gr/ft.^{3} and filtration velocity of 8.5 ft./min.

[e] RDM measurement.

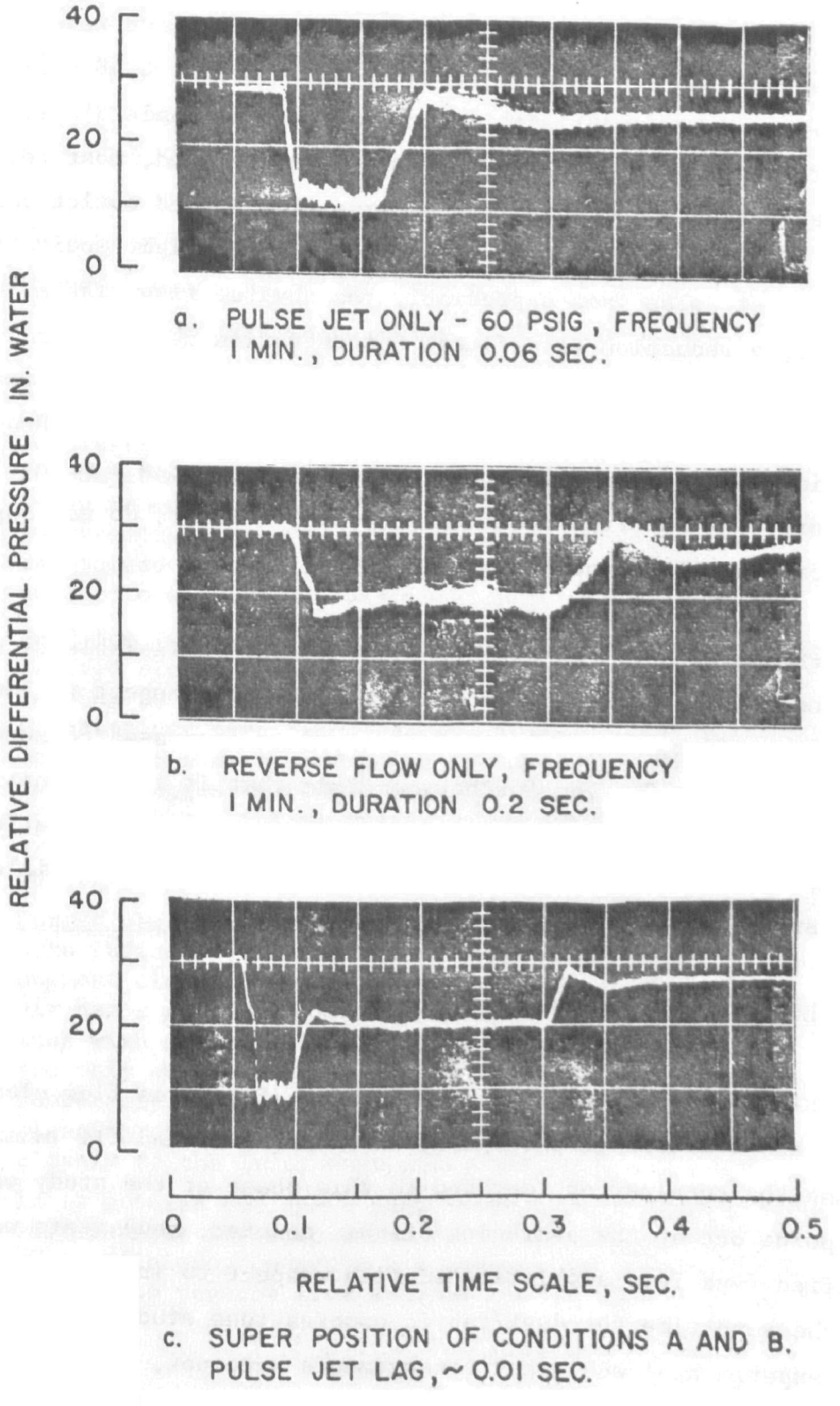

Figure 89. Differential pressures across Dacron felt bag for indicated cleaning conditions. Fly ash at 11.6 grains/ft.^{3}, 8.5 ft./min. inlet velocity.

Only one test was performed in this series in which reverse flow only was used. The indicated effluent concentration, 0.48×10^{-3} grains/ft.^{3} was in good agreement with values reported in Table 31, Tests 25 and 26, and Table 33, Tests 32 and 33. On the other hand, most tests in which pulse jetting accompanied the reverse flow showed outlet concentrations 5 to 10 times higher. There appears to be a slight indication that if the jet pulse lags appreciably the reverse flow, Table 34 Tests 37 and 43, a reduction in effluent concentration is obtained. It may be that prior removal of dust by the preceding reverse flow reduced the removal of interstitial deposits by the reverse pulse. Hence, the resulting dust/fabric collection surface constitutes a more efficient collector. The observed resistance values, however, do not appear to support the above theory.

For the most part, the test results summarized in Table 34 show that sequential pulsing affords no advantages with respect to lowered resistance or reduced emission but does lead to increased consumption of cleaning air. One can further conclude that it is the initial mechanical impulse given the fabric (and its resulting acceleration) that is responsible for dust removal. The role of aerodynamic dislodgement appears as a very minor factor.

CONCLUSIONS TO REVERSE FLOW CLEANING STUDIES

The studies performed under the heading of reverse flow cleaning differ from those discussed previously in Chapters II and III primarily because the total effort devoted to this phase of the study was limited. As point out at the beginning of this chapter, many tests were simplified (and less sophisticated with respect to instrumental techniques). At the same time the dust/fabric combinations studied were limited and the experimental equipment arrangements were not, in most cases, typical of commercial installations. Because of the constraints cited above, relatively few firm conclusions can be drawn and those that are

presented reflect probable relationships among key variables, rather than any specific operating guidelines.

General Conclusions

The conclusions set forth below are intended to place the results in proper perspective, to highlight the major experiments, and to suggest basic guidelines for further research.

- Limits of data application - Test results should not be extrapolated beyond those for the specific dust/fabric combinations studied. As a further constraint because the experimental apparatus was not necessarily modelled after commercial installations, no data scaling should be attempted. Although dimensional similarity was maintained in some cases, the tests were too few in number to warrant any statistical analysis.
- Need for further research - The tests performed in the limited study described here indicate that the factors leading to the successful application of reverse flow cleaning are even less understood than those for mechanical shaking and pulse jet systems. The results suggest strongly that the unique features of dust/fabric interactions, which prevent ready extrapolation to other dust/fabric systems, are equally important in reverse flow systems.
- Outlet versus inlet concentrations - Limited test data indicate that the use of reverse air flow to augment cleaning by mechanical shaking or pulse jet air has a negligible impact on base system performance. Thus with mechanically shaken systems, the effluents are only weakly dependent upon inlet dust loadings. Conversely, augmentation of conventional pulse jet cleaning processes, produces emissions that relate closely to the inlet dust concentrations.
- It is pointed out again that those factors necessitating very careful interpretation of any fractional particle size efficiency concepts are equally important with respect to reverse flow systems.

Augmentation of Mechanical Shaking by Reverse Flow

The use of reverse flow air alone or in combination with the mechanical shaking of woven fabric bags forms the basis for the following conclusions:

- No benefits were noted, resistance- or efficiency-wise, by reverse flow during the shaking interval even when an interior support was used to prevent a complete bag collapse. This appraisal may not apply to the use of reverse air in the field where failure of isolation valves to close completely can be compensated for by a separate source of reverse air. If one does not use a separate fan to provide a reverse flow (or at least a zero flow condition) some of the fine dust loosened during the shaking process may redeposit and the foward flow will also transport loosened particles more readily to the clean air side of the filter system.
- Not only were resistance and efficiency characteristics unchanged but as near as could be determined no dust removal was accomplished by aerodynamic action alone.
- The dust removal observed during tests with only reverse flow, with both sateen weave cotton and Dacron bags, was attributed to bag flexure alone. Despite the observed dust removal, the overall performance of the cleaned filters was highly unsatisfactory with a fly ash aerosol.
- The main role played by the reverse air appears to be that of preventing mechanical projection of dust into the clean air side of the system. Because the gas flow is stopped to the compartment undergoing cleaning for periods of about 1 minute before and after shaking, settlement alone enables most of the suspended dust to reach the collection hopper.
- Any attempt to use reverse flow air with shaking bag systems will be unsuccessful unless bag collapse can be prevented by means of internal support structures or high bag tensioning. It does not appear practical to use highly tensioned bags with shaking because other tests (Chapter II), have shown an adverse effect on emissions. One can also speculate that greater damage to fabric structure is also likely. Although the use of internal supports such as rings can prevent collapse, bag wear may result. More importantly, the

nature of the motion imparted to the bag by a shaker arm and the resulting cleaning action might be drastically altered.

Felt Bags Cleaned by Reverse Flow

The tests described in this section, despite their arbitrary classification as reverse flow cleaning experiments, do not depict the operation of standard commercial equipment. Although a conventional blower (thin scroll centrifugal with a static pressure capacity up to 30 in. water) was the reverse air source, its delivery characteristics were not radically different from those of a compressed air jet. Thus, some of the tests performed with the modified pulse jet apparatus more properly describe the influence of wave form on transient bag differential pressures.

- Dust Removal by Aerodynamic Drag - A controlled series of tests in which fabric acceleration was reduced by roughly 1000 times the level produced by high pressure jet pulse, indicated that reverse air velocities and air volumes ranging from 4.3 to 11.4 ft./min. and 0.5 to 2.9 $ft.^3$, respectively, had no effect on the amount of dust dislodged from the filter. The nearly constant removal of a few grams of dust was attributed solely to the flexing (slow dilation and slow contraction) produced by each air admission.
- Waveform and Dust Removal - The results of several tests in which the rate of rise of differential pressure across the bag was varied indicated that the primary dust removal was due to the acceleration imparted to the bag. The actual waveforms were nearly identical to those produced by high pressure jet pulses except for a less rapid rise in pressure (and hence lower fabric acceleration as described in Chapter III).
- Reverse Flow Duration - Except for those cases where the reverse flow was restricted to intervals less than 0.05 sec., increased pulse duration exerted no effect on average operating resistance. The only critical factor for a given rate of pressure rise is that the valve open time be sufficient for the full pressure differential to develop and the fabric to experience its maximum deflection.

- Sequential Pulsing - A series of tests in which low energy pulses produced by reverse flow were augmented by high energy compressed air pulses indicated that the filter performance with respect to resistance and efficiency was controlled mainly by the high energy pulse. At this time, there appears to be no particular advantage to using this technique which, for the most part, only increases the demand for cleaning air.

REFERENCES

1. Billings, C.E. and J.E. Wilder. Handbook of Fabric Filter Technology. Volume 1: Fabric Filter Systems Study. GCA/Technology Division. Department A, Clearinghouse, U.S. Department of Commerce, Springfield, Va. 22151. Report Number GCA-TR-70-17-G, APTD-0690, Contract No. CPA-22-69-38, PB-200-648, December 1970.
2. Larson, R.I. The Adhesion and Removal of Particles Attached to Air Filter Surface.AIHA Journal 19, 265 (1958).
3. Zimon, A.D. Adhesion of Dust and Powder. Page 112, Plenum Press, New York (1969).
4. Walsh, G.W. and P.W. Spaite. An Analysis of Mechanical Shaking in Air Filtration. Journal of the Air Pollution Control Association. 12, 57 (1962).

CHAPTER V

CONCLUSIONS AND RECOMMENDATIONS

The results of a detailed study of fabric filter cleaning processes used for industrial gas filtration are presented in this report. The information deriving from this program is intended to improve the performance and to further the application of fabric filters for control of particulate emissions. Although many factors are involved in assessing system behavior, the maximizing of gas handling capacity, collection efficiency, and service life of filter fabrics and other system components and the minimizing of power requirements related to gas handling and filter cleaning operations are considered to be key areas for performance improvements.

The conclusions and recommendations appearing in the following paragraphs are based mainly on the findings of the present study. The results of related studies by GCA/Technology Division or other groups, however, have also been used to support and/or clarify the experimental results provided in this report.

The conclusions presented in this chapter apply both to fabric filter systems as a class, irrespective of the method of cleaning, and to the comparative performance of devices that are cleaned by different dust removal methods. It is again emphasized that the major work in this study was with mechanically shaken and pulse jet cleaned fabrics. Generally, the experiments were designed to describe the behavior of existing gas cleaning systems and to develop operating parameters or at least

guidelines to improve their performance. The limited tests performed with various approaches to low pressure, reverse-flow cleaning were essentially exploratory. Therefore, the test results should not be extrapolated directly to real field situations.

All tests were carried out at typical ambient conditions which, in this study, were an air temperature of 70 $\pm$ 2°F and a relative humidity of 40 to 50 percent. It was assumed, therefore, that any observed differences in collector performance were not attributable to temperature or humidity changes. It should be noted that large changes in either variable can affect fabric filter performance significantly.

The terms "equivalent" and steady-state operation have been used in this report to describe any series of replicate tests in which no perceivable changes in system performance were observed over short term periods (days). Under these conditions, several parameters could be investigated, since, for all practical purposes, the effective residual and terminal drags remained constant for any set of fixed operating conditions. Over the long term, however; e.g., weeks to months, a gradual rise in fabric resistance properties may result from dust accumulating within the fabric pores.

CONCLUSIONS

Limits of Data Application

- Unless indicated to the contrary, the reader should assume that descriptive and operating parameters cited for a specific dust and fabric combination apply solely to that specified dust/fabric combination.

Outlet Versus Inlet Concentrations

- There is no simple relationship between typical outlet and inlet concentrations for fabric filters.

The average mass emission and its related particle size properties for a mechanically shaken filter when operating in a fixed mode with a specific dust/fabric combination is nearly independent of the concentration and size properties of the inlet dust.

- On the other hand, mass emissions from felted fabric filters cleaned by high pressure, reverse air pulse show a positive dependency on the inlet dust concentration.

Fractional Particle Size Efficiencies

- The concept of using fractional particle size efficiencies to predict filter performance based upon a knowledge of inlet dust properties can rarely be applied to a fabric filter system.
- In the case of mechanically shaken filters, the "apparent" measured efficiencies will depend upon the filter inlet loading and the instantaneous or average values of the effluent.
- Conversely, the "apparent efficiencies" for pulse jet systems may be independent of particle size due to the release of many agglomerated particles during the cleaning process.

Filter Effluent Concentrations

- Filter effluent concentrations for the same inlet dust may range from 10^{-7} to 10^{-3} grains/ft.^{3} for mechanical shaking systems with woven fabrics and from 10^{-3} to 10^{-2} grains/ft.^{3} for pulse jet systems using felted fabrics.
- The lower effluent concentrations found with shaken filter bags is due mainly to the much greater superficial dust deposit that results primarily from extended filtering periods (approximately 20 minutes) compared to approximately 1 minute intervals for felts cleaned by pulse jet air. At the same time, the somewhat larger pores and greater depth of the felts may require a longer period to fill the interstitial structure.

- The time required to fill the filter pore structure depends upon the dust deposition rate, the bulk density assumed by the interstitial dust deposits and the pore dimensions of the filter media compared to those of the dust.

Filter Cleaning Action

- Dust removal by both mechanical shaking and by high pressure air impulse is mainly the resulting interaction of tensile forces produced by acceleration of the dust-laden fabric and the characteristic dust adhesive and cohesive forces.
- The cleaning attained by mechanical systems, when defined in terms of residual resistance and dust holding capacity, can be related to the maximum acceleration seen by the shaker arm, the latter determined solely by its amplitude and frequency provided that the number of individual shakes is sufficient (200).
- By decreasing shaking amplitude and increasing shaking frequency a moderate reduction in effluent loadings (factor of 2) may be obtained while maintaining constant the acceleration level (and also the resistance and capacity properties).
- The cleaning (dust removal) afforded by pulse jet systems is best defined in terms of the residual and average filter resistance for a fixed cleaning cycle.
- The amount of dust removed during pulse jet cleaning depends upon the initial felt holding; inlet dust concentration; the magnitude, rate of rise and duration of the reverse air pressure; and the frequency of pulsing.
- The modulation of the pressure pulse waveform affords one means of controlling effluent concentrations.
- Aerodynamic forces play a very minor role in actual dust removal for pulse jet filter systems and also for mechanically shaken systems in which low velocity, low pressure reverse air flow is used as an adjunct to cleaning. The main role played by low velocity (100 ft./min.) reverse air is to flush out dust particles already loosened by high energy impulse. In the case of typical reverse jet systems extended pulse (reverse flow) periods usually had an adverse effect on effluent concentrations.

Energy Requirements and System Capabilities

- Requirements for mechanical shaking operations represent but a small fraction, 10 percent at the greatest, of the overall system power needs. For comparable gas handling capacity and filter resistance, typical power needs for high pressure pulse jet cleaning are roughly equivalent to those for gas handling.
- Pulse jet systems permit filter operation at high air-to-cloth ratios (three to five times higher than those for mechanically shaken systems) provide nearly constant ventilation rates at dust sources, adapt more readily to high loadings with respect to minimizing average filter resistance, and require smaller physical plants because of their higher air-to-cloth ratios.

RECOMMENDATIONS

Equipment Application and Operating Parameters for Mechanically Shaken Filters

- Fabric filter systems cleaned by mechanical shaking should be used whenever the particulate to be controlled is highly toxic. Sateen weave cotton fabrics or their equivalents in synthetic or mineral media in terms of fiber diameter, staple, weave and cloth weight will provide the best performance.
- Based upon laboratory pilot tests, a mechanical shaking frequency of 8 cps and a shaking amplitude not greater than 1-inch are recommended. Field observations have indicated, however, that some field filter installations may not have the structural rigidity to be shaken at this energy level.
- To provide improved dust removal and increased holding capacity with many existing filter systems (some of which operate at low amplitude and frequency; e.g., 0.25 in. and 4 cps), fabric acceleration should be increased by increasing the shaking frequency instead of the shaking amplitude to avoid resonance problems with the baghouse structure. As a fringe benefit, shaking at reduced amplitude also reduces particulate emissions.
- Filter bags should be tensioned so that the tensile force exerted at the top is roughly 0.5 lb. in excess of the combined weight of the bag with its residual dust.

- Approximately 200 individual shakes should be given a bag during a cleaning cycle to achieve the optimum dust removal for a fixed combination of bag shaking frequency and amplitude.
- The off-line period for the shaking of a single bag or filter compartment should represent only about 10 to 15 percent of the time allocated for filtration; e.g., 4 minutes versus 30 minutes.
- Any field measurements to define the average size properties and the average mass concentration of a filter effluent must include every phase of the cleaning and filtration cycles.
- No final design criteria should be submitted for a filter system until all possible interactions of the dust of interest and the selected fabric are known.
- The use of low velocity, reverse flow air as an adjunct to mechanical shaking is not ordinarily recommended except where the use of compartment isolation dampers fails to stop all air flow through the filter in the direction of normal filtration flow.

Equipment Applications and Operating Parameters for Pulse Jet Filter Systems

- Pulse jet systems should not be selected when it appears possible that mass emission rates for highly toxic materials may be exceeded.
- Pulse jet systems are recommended for application where process control or source ventilation needs require very constant air or gas flow rates assuming that emissions criteria are satisfied.
- Pulse jet systems are recommended for those applications in which inlet dust loadings are either variable and/or particularly high, approximately 15 to 20 grains/ft.^{3} assuming that emissions criteria are satisfied.
- Pulse jet systems must be operated with fast-acting valves so that a rapid change in differential pressure is obtained across the filter during the transient pulse, approximately 2000 to 4000 in. water/sec. The above levels are obtained routinely with commercial apparatus in which a 1/4-inch nozzle is located above each bag, the compressed air pressure is 70 to 100 psig and the valve opening time is of the order of 0.01 to 0.02 seconds.

- Approximately 200 individual shakes should be given a bag during a cleaning cycle to achieve the optimum dust removal for a fixed combination of bag shaking frequency and amplitude.
- The off-line period for the shaking of a single bag or filter compartment should represent only about 10 to 15 percent of the time allocated for filtration; e.g., 4 minutes versus 30 minutes.
- Any field measurements to define the average size properties and the average mass concentration of a filter effluent must include every phase of the cleaning and filtration cycles.
- No final design criteria should be submitted for a filter system until all possible interactions of the dust of interest and the selected fabric are known.
- The use of low velocity, reverse flow air as an adjunct to mechanical shaking is not ordinarily recommended except where the use of compartment isolation dampers fails to stop all air flow through the filter in the direction of normal filtration flow.

Equipment Applications and Operating Parameters for Pulse Jet Filter Systems

- Pulse jet systems should not be selected when it appears possible that mass emission rates for highly toxic materials may be exceeded.
- Pulse jet systems are recommended for application where process control or source ventilation needs require very constant air or gas flow rates assuming that emissions criteria are satisfied.
- Pulse jet systems are recommended for those applications in which inlet dust loadings are either variable and/or particularly high, approximately 15 to 20 grains/ft.^{3} assuming that emissions criteria are satisfied.
- Pulse jet systems must be operated with fast-acting valves so that a rapid change in differential pressure is obtained across the filter during the transient pulse, approximately 2000 to 4000 in. water/sec. The above levels are obtained routinely with commercial apparatus in which a 1/4-inch nozzle is located above each bag, the compressed air pressure is 70 to 100 psig and the valve opening time is of the order of 0.01 to 0.02 seconds.

- The compressed air jets must be located far enough above the bag exit (which may or may not contain a Venturi section) so that supplemental entrained air is extracted from the exit plenum and not from the dirty air side of the bag.
- In most cases, the duration of the pressure pulse should be only long enough to persist through the complete reverse inflation of the bag, roughly 0.05 second. With few exceptions it is not recommended that the cleaning pulse be longer as it only increases the compressed air demand and sometimes the exit dust concentration.
- It is suggested that the use of an auxiliary damping reservoir or a mechanical, electrical, or pneumatic regulation of the jet nozzle valves be used to reduce the particulate emissions. Laboratory measurements indicated that the damped pulses and the associated gradual venting of air from the bag at the end of the pulse resulted in a fivefold reduction in emissions and about a 20 percent rise in average filter resistance.
- A recommended alternative to the pulse damping procedure for reducing emissions is to reduce the cleaning pressure. In many cases, the lowering of compressed air requirements more than compensates for the increased resistance (and air moving) power requirement.

Research and Instrumentation Needs

- It is recommended that operating data be obtained through pilot plant testing and/or actual field measurements to determine representative "K" values for several commonly encountered dust/fabric combinations. This effort should also include an updating of related field and laboratory experience from as many sources as possible.
- It is recommended that fundamental studies be performed to determine what key particle and fiber parameters taken singly or in combination determine: (1) the K-value for a given dust/fabric combination and (2) the characteristic effective residual resistance for the above dust/fabric combination in conjunction with a specified fabric cleaning technique.

- It is recommended that mechanical shaking systems using using a spring loaded hanger arm (typical of many commercial bag suspension systems) be compared to systems with rigid shaker arms such as used in this study. The purpose of these tests is to determine whether the basic acceleration and dust removal relationships developed for systems with rigid arms apply to the spring loaded supports.

- It is recommended that other mechanical means of transmitting cleaning energy to the fabric be examined. Although simple mechanical shaking works, examination of many bags after shake cleaning showed surprisingly large amounts of dust adhering to the fabric as distinct patches. Since the latter material could often be removed by a very light flick of the finger, it appears that energy transmission by shaking is not sufficiently uniform nor as efficient as it might be.

- It is recommended that a simple method be developed to determine whether proper tension levels are maintained in mechanically shaken bags. Newly installed bags undergo rapid stretching such that frequent readjustment is necessary during the shake down and early service periods. Failure to re-tension will lead to excessive slackness causing bag plugging and physical damage.

- Controlled laboratory pilot testing (and field testing where practical) should be carried out with high temperatures and humid atmospheres to provide design parameters for difficult field applications.

- Rigorous tests should be performed, initially on a bench scale and later on a pilot scale, to determine how the following factors control or may be utilized to improve the filterability of various dusts: electrostatic charge, its presence or absence on particles and/or fibers; particle size distribution with shape factor constant; humidity control; particle size versus fabric pore size; surface deposition versus interstitial deposition; and the use of conditioning methods such as induced agglomeration.

- It is recommended that detailed tests be performed to determine the effects of variations in inlet concentration and filtration velocity on the performance of pulse jet cleaning systems.

- Further pilot testing should be performed to determine whether use of a simple plenum pulse system that eliminates individual valving for each bag offers advantages

over the pulse-per-bag approach investigated in detail in the present study.

- Definitive tests should be performed to determine what maximum bag length can be cleaned effectively by pulse jet systems.

APPENDIX A

AUTOMATIC FLOW CONTROL SYSTEM

To enable extended operation of the mechanical shaking equipment without close attention yet with precisely repeated timing of the cycles, an automatic control system was developed. This system uses a rotary cam-type timer to control the following operations:

1. Primary fan ON
2. Aerosolizing compressed air ON
3. Dust feeder ON
4. (Dust is collected for a prescribed time)
5 Dust feeder OFF
6. Aerosolizing compressed air OFF
7. Fan OFF
8. (Shaker Motor ON for prescribed time)
9. (Dust is permitted to settle for a prescribed time)
10. Cycle repeats.

The intervals between steps and the length of the overall cycle are adjustable to represent any standard shaking cycle. The system includes manual override switches for operation of the fan, dust feeder, compressed air, and shaker motor in any sequence or combination.

For cases where extended recycling is necessary, making unmanned operation desirable, certain fail-safe provisions are included in the system. These are designed to prevent damage to the equipment in case of malfunction. They are also intended to prevent data loss due to upsetting the status of the fabric and dust deposit, which may represent several

hours of previous operation. These criteria for unmanned operation include the following:

1. The main fan, dust feeder, and compressor supply to the air ejector cannot operate during the cleaning cycle, and vice versa.

2. Reduction of reservoir pressure within the compressed air tank below some preset level due to compressor failure; e.g., 90 psi will shut down the entire system.

3. If the flow adjustment damper can no longer control the flow rate either at the full-open or full-close position, the entire system is shut down. Failure to operate within the working range of the control valve indicates either a plugged bag (faulty cleaning) or a rapid decrease in bag resistance (excessive dislodgement of dust or holes in fabric).

4. Excessively high or low inlet dust concentrations to the collector as monitored by automatic light attenuation measurement will direct a system shut down.

5. Manual override at any time.

The system with fail-safe provisions is shown schematically in Figure A-1.

The system is designed to operate under a preset time cycle, recording continuously the pressure differential across the bag. Alternatively, with minor modifications, the system could be made to operate on reaching a preset upper pressure limit, with a varying time cycle. For flow control, a Bailey Meter Co. pneumatic system is used. This system senses the flow past a Stairmand disc in the 2-inch duct, amplifies the signal, and supplies 3 to 25 psig air to a diaphragm control valve in the 4-inch duct. The system also records primary flow and bag differential pressure on a 2-pen circular 24-hour recorder. Because the Bailey system is of standard industrial quality, it furnished only marginal control. The control system was calibrated by pitot static tube traverses believed to have been accurate to within 2 percent. The control provided by the system was steady from second to second. Over a typical

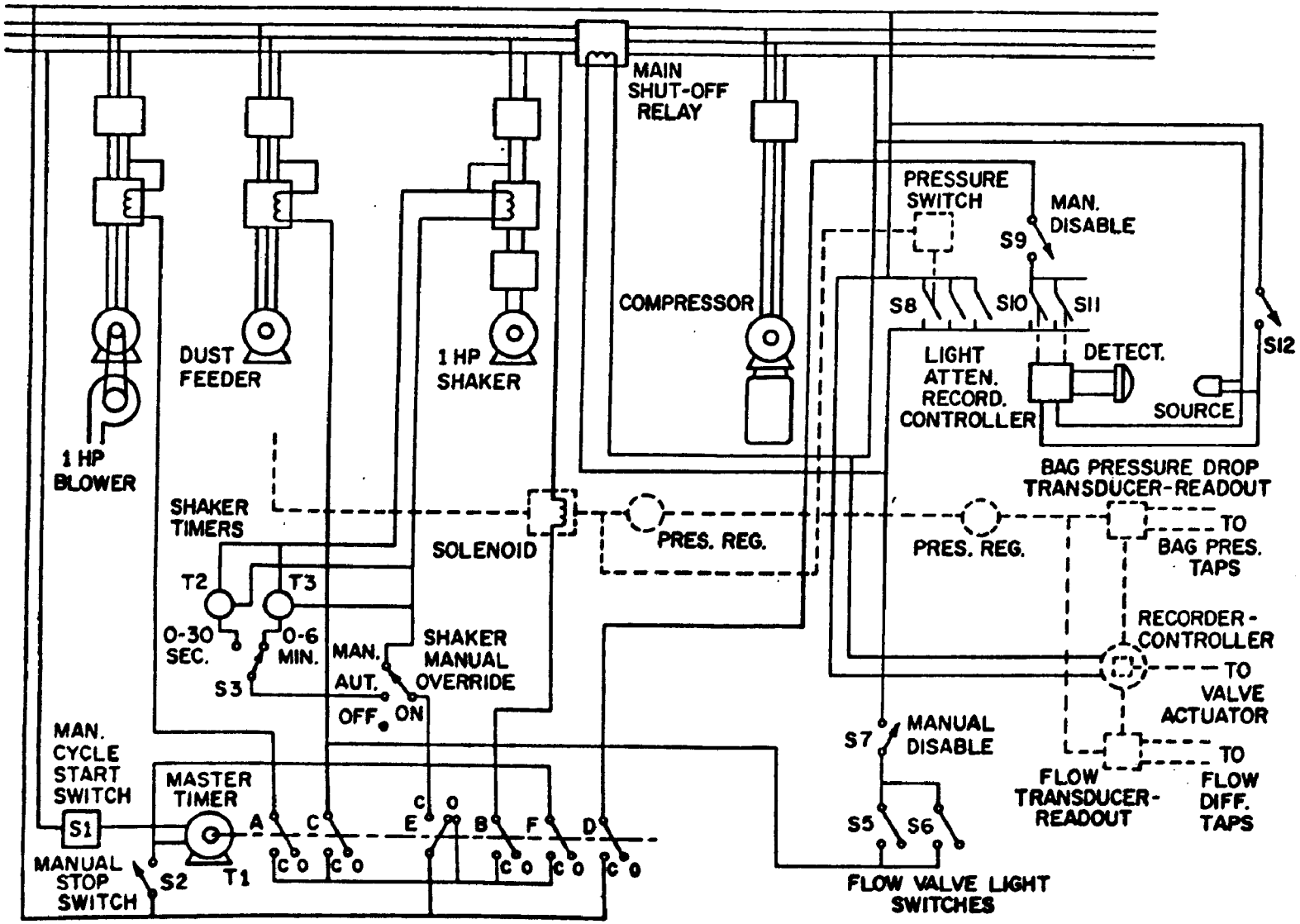

Figure A-1. Automatic flow control system

filtration cycle, during which the pressure differential across the filter increased by a few inches of water, the controlled flow decreased by a few percent due to an inability of the control system to hold exactly to the set point. This decrease in flow was usually negligible except when the pressure differential reached the neighborhood of 8 inches of water, at which point the flow began to drop rapidly. To compensate for this in the few experiments involving such high pressures, the recorded pressure differentials were adjusted to the preset flow conditions.

A further limitation of the flow control system was that a brief period of about 5 seconds was required for the flow to stabilize, following start-up or a sudden change of pressure differential as in pulse cleaning. This was associated with a tendency of the control system to hunt and overshoot the set point. To minimize any possible effects on the dust deposit of such an overshoot in pressure or flow, a damping resistance was used in the pressure line to the automatic control valve. This diminished the overshoot to, at most, a few percent at the expense of a slightly longer period required for stabilization. The stabilization period was only a problem when attempting to obtain true residual pressure differentials, especially in the case of pulse cleaning with its short intervals between pulses. The recorded residual pressure differentials were adjusted to reflect any abnormal flow at the moment of record.

In general, the control accuracy and precision provided by the Bailey system was adequate for this study. However, the system required so much extra attention and data correction that an improved better system is recommended.

Stable operation of the fabric filter system relies on a steady delivery of aerosol. A simple light scattering device was constructed (based on conventional stack instrumentation) in which a simple photocell detector and light source were mounted on opposite sides of the 2-inch diameter

inlet duct. A battery and Rustrak^{R} recorder produced a strip chart record of the photocell signal which was inversely proportional to the optical opacity of the aerosol stream. The record provided an excellent check of aerosol concentration stability, although no attempt was made to make the instrument quantitative. The photodetector and light source were not precisely flush with the walls of the duct and perhaps as a result, tended at first to become blinded by deep dust deposits. To minimize this, apertures approximately flush with the walls were placed in front of both detector and source. Air was blown slowly through both apertures into the duct at a velocity sufficient to prevent dust migration into the optical path.

APPENDIX B

FORCE AND VELOCITY MEASURING INSTRUMENTATION

FORCE AND PRESSURE MEASUREMENTS

A commercial load cell (Dynisco FTI-10) was used to measure top tension and bag weight in shaker tests and to measure bag weight in pulse tests. The mountings for the cell sketched and discussed in the text are shown here in more detail. The main difficulty with the early mounting in Figure B-1 was that the motion required to cock and partially jam the slide assembly was of the same magnitude as the motion produced during load cell compression, less than 0.001-inch. This made the cell unreliable for other than static vertical measurements.

The subsequent mounting in Figure B-2 was very nearly frictionless and thus responded at any angle or rate of shaking almost instantly. The difficulty with this second mounting was mainly that the left and right ends of the bag hanger (see side view) had different mechanical advantages to the load cell. Thus any swaying of the bag left and right, or any left and right motion at the lower end of the bag, appeared in the signal as tension changes. Nevertheless, the second mounting was preferred over the first for most measurements. By doubling the second design into a Watts linkage, it should be possible to produce a frictionless mounting with perfectly vertical motion. Refinements of the load cell mounting may yield diminishing returns however, because of the unpredictable mechanical properties of the bags. Because of these bag properties, the load cell systems were calibrated <u>in situ</u> with a bag of known weight suspended from the cell and with the bag "shaken

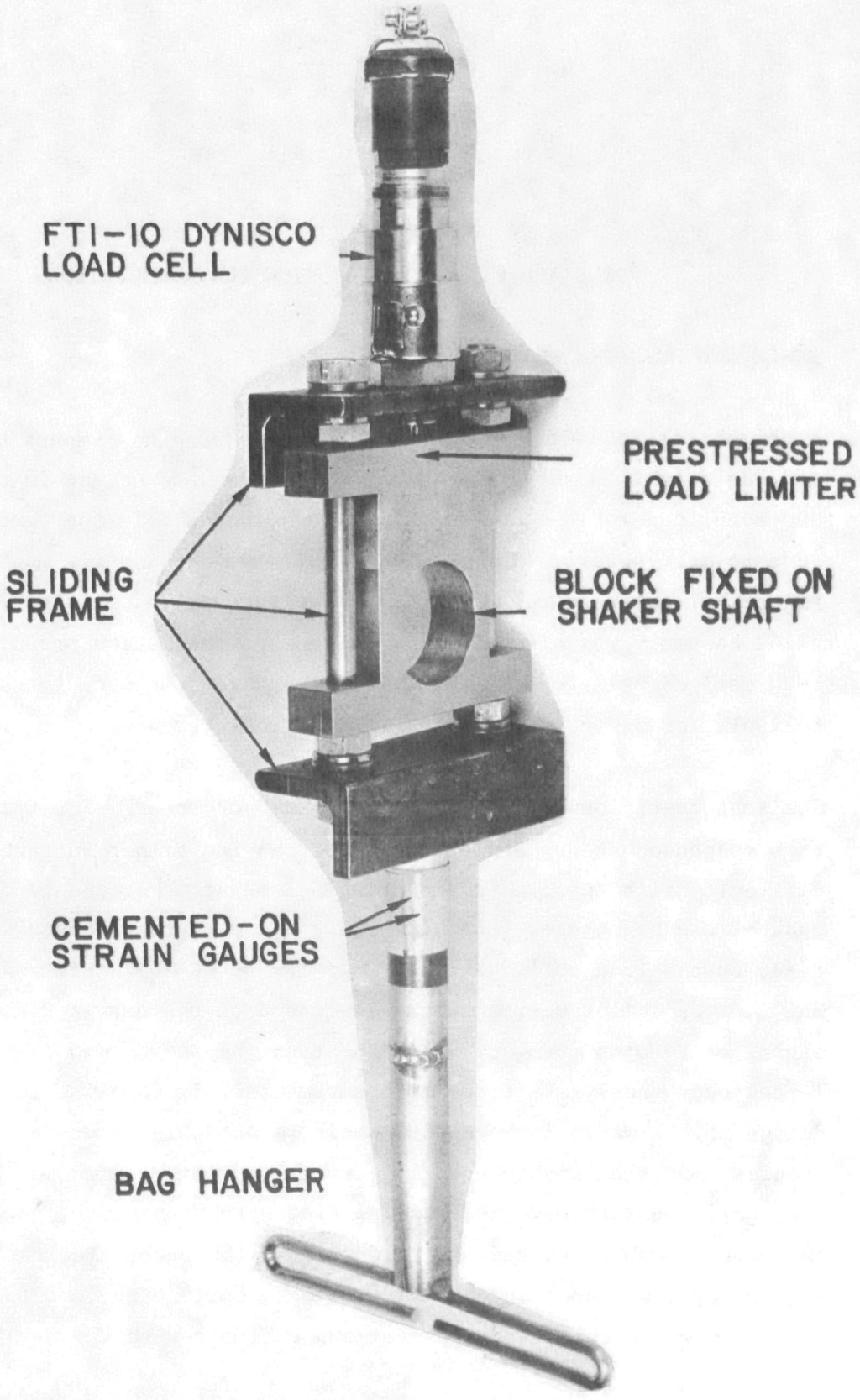

Figure B-1. Load cell mounting for shaken bags. Model 1

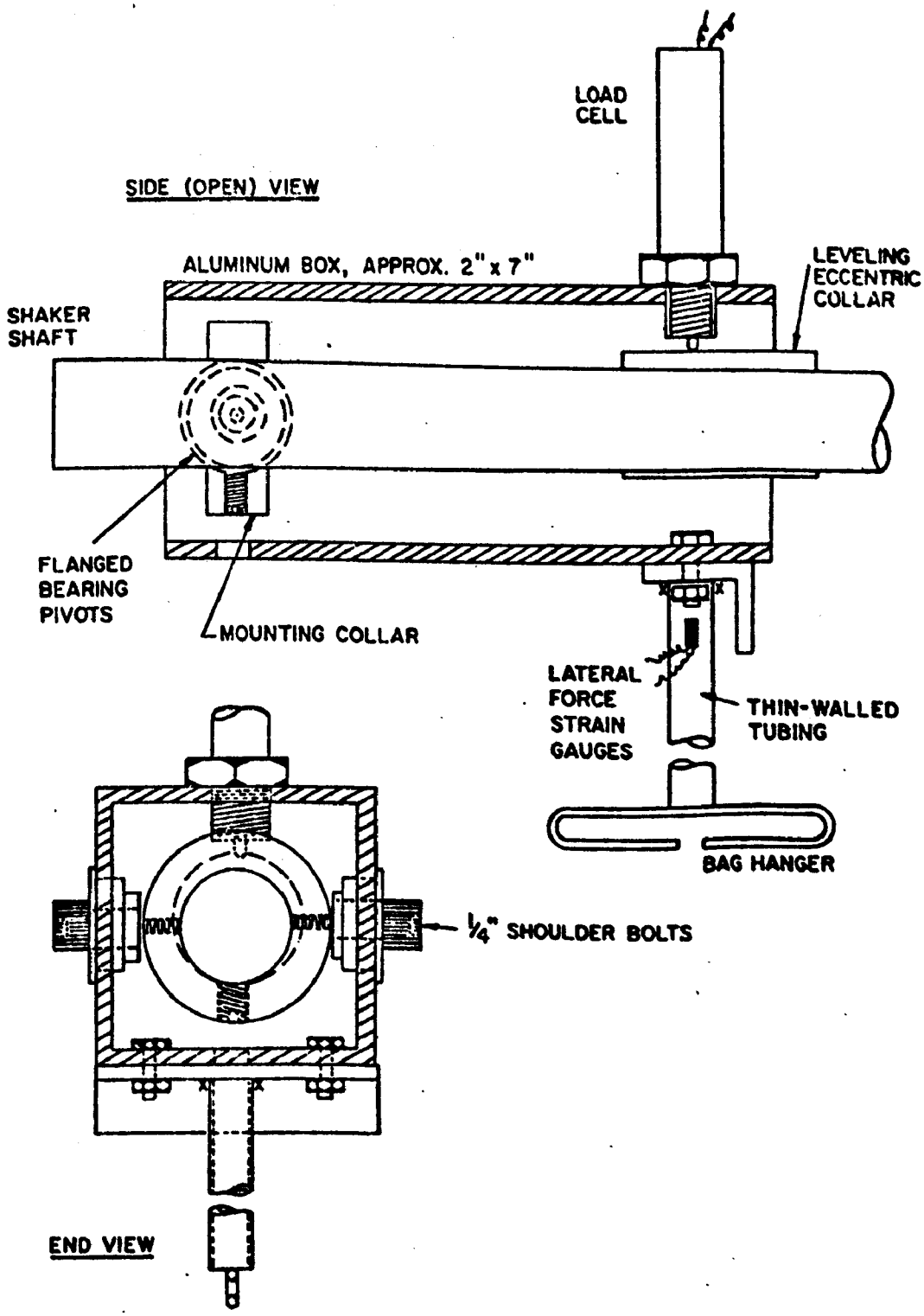

Figure B-2. Revised design for load cell mounting for shaken bags

in" to a steady configuration. Weights were then attached to the bottom of the bag for calibration.

The same load cell was used in the pulse cleaning studies to weigh the bag, dust, and mounting cage assembly as shown in Figure B-3. By releasing clamps sealing the upper end of the bag and cage assembly to the bottom of the upper plenum, the entire assembly was free to move upward. The external load cell mounting handle raised the load cell into contact with the bottom of the bag and slight additional lifting placed the entire weight on the load cell. The top of the bag assembly was restrained from tipping sideways by light, frictionless wire yokes (not shown). About the only difficulty with this arrangement was that other instrumentation attached to the bag and cage (pressure transducer, accelerometer, ...) required wires that affected the weighings. With accurate tares and care in aligning the wires, however, fairly reliable weights were obtained. They were checked from time to time by removing the entire assembly through the top of the upper plenum and weighing it on laboratory scales.

In all cases, the strain gauge bridge inside the load cell required the circuit shown in Figure B-4, a simple standard circuit with voltmeter readout. Oscilloscope readout was also obtained for studying instantaneous forces during the shaking cycle. In the latter case the voltmeter had to be disconnected from the circuit to eliminate a conflicting signal from the meter's armature assembly. The power supply voltage and circuit were adjusted to give exactly 1 voltmeter division per pound of force for convenience in data reduction. The calibration remained drift-free and constant through the entire program. The load cell-to-readout precision was about 0.01 pound. The force-to-load cell precision was not always this fine due to the mounting difficulties noted above, up to 0.1 pound.

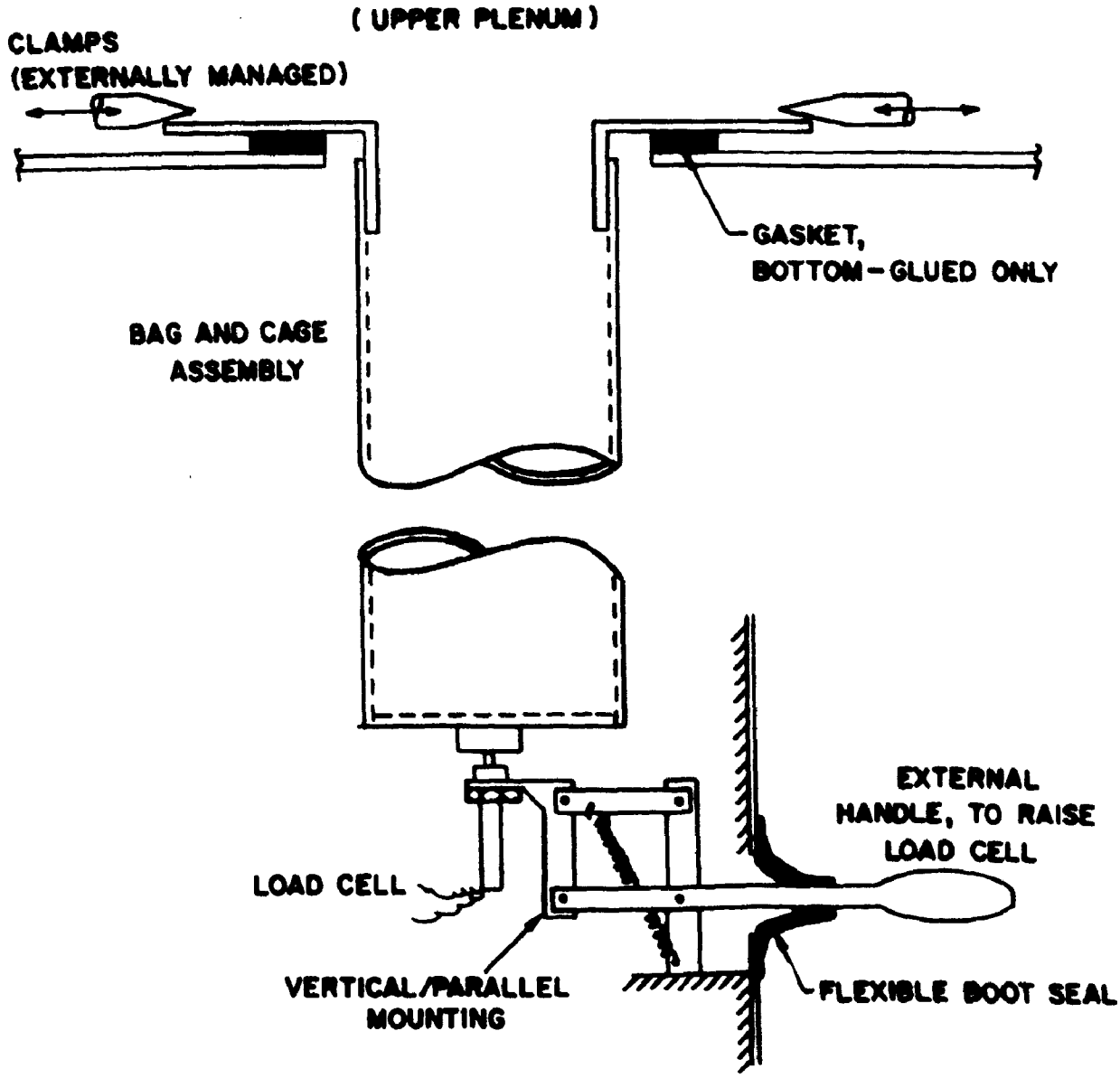

Figure B-3. Load cell mounting for weighing the pulsed bag assembly

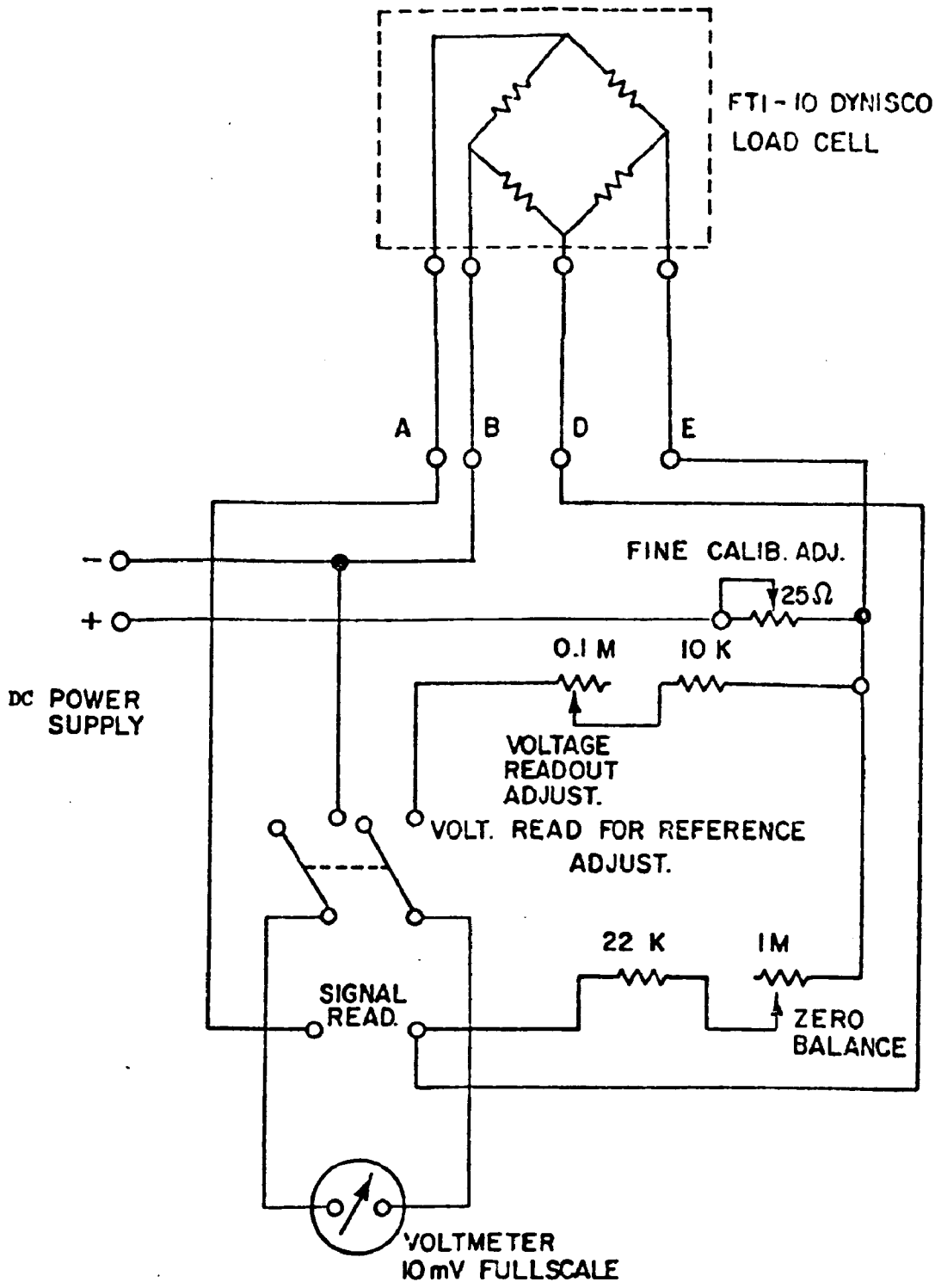

Figure B-4. Circuit diagram, signal output from load cell

As noted in the figures, strain gauges were cemented on the sides of the thin-wall tube that formed the bag hanger arm. Two of these strain gauges,

BLH SR-4 Epoxy Backed	BLH Electronics, Inc.
Type FAE - 18 12S6	Baldwin Lima Hamilton Corp.
Resistance: 120 ohms	Waltham, Mass. 02154
Gauge Factor: 2.04	617-894-6700
Dimensions: Overall: 3/8" x 9/16"	
Active: 1/16" x 3/16"	

were attached with Eastman 910 cement on opposite sides of the tube near the point of maximum bending moment. Thus as the tube bent slightly, one gauge compressed and the other stretched. The gauges were made part of an "opposed" bridge circuit, so that bending the tube resulted in a doubled effect. On the other hand, tension applied to the tube produced the same stretching in both gauges, and so the effects cancelled. Thus the circuit was sensitive to bending and insensitive to tension. Because the signal was small, it was amplified before transmission to the calibrating circuit similar to that in Figure B-4. The signal was read on an oscilloscope. Calibration was accomplished by turning the bag hanger arm to the horizontal and hanging known weights from it. The factor of order 30 mV/lb was drift-free through all experiments.

Thermal effects in the amplifier produced a wandering zero point, but since the average lateral force during shaking is zero, this was not a particular problem. Somewhat better shielding was required for this system than for the load cell system. With a sufficiently thin-walled hanger arm, the amplifier might become unnecessary.

If the two strain gauges were connected differently to the detection bridge the system would be sensitive to tension and insensitive to bending, taking the place of the load cell. Thus, using a switching arrangement, both lateral force and tension could be obtained with the same simple system, at least in principle.

VELOCITY MEASUREMENT

For precise analysis of the relationship between the position of the shaker arm at a given instant and the lateral and tension forces at the top of the bag, an electrical signal related to the arm position was needed. The first approach, that of using a photoelectric detector to describe arm motion, did not give an adequate time response. Attaching the rotor of a resistance potentiometer to the shaker shaft did not produce a reliable signal. Finally, a magnet was attached to the end of the shaker shaft, and a small stationary coil was positioned close to the magnet. The coil produced a clean, symmetric signal proportional to velocity from which the position of the arm was deduced to be 90 degrees out of phase with the velocity signal. This signal directly entered an oscilloscope on which the lateral and tension forces were being analyzed. Both Lisajou displays (one variable plotted against another) and time-based displays were studied.

APPENDIX C

PHOTOELECTRIC DETECTION OF SHAKEN BAG MOTION

This approach to monitoring the instantaneous position of the bag during shaking applies to a single point on the bag. The detector may be moved to other points, or several such systems may be used simultaneously. The system is very inexpensive and accurate and can be easily calibrated.

The system uses a rapidly responding photoconductor:

Clairex Photoconductor

Type 5H cadmium sulphide
Rise time at 23 foot candles: 0.004 sec.
Decay time at 23 foot candles: 0.0017 sec.
Approx. resistance at 23 foot candles: 3,000 ohms
Light Sensitivity: Approx. 1 percent per 1 percent
Dimensions: Approx. 0.5 in. dia. x 0.2 in.

Clairex Corp.
1239 Broadway
N.Y. N.Y. 10001
212-684-5512

As sketched in Figure C-1 the photocell senses the filament of the light source not obstructed by the bag. Motion of the bag normal to the line of sight is detected immediately by the cell, allowing for the time response limitations indicated above. The simple circuit shown requires only standard laboratory equipment. Calibration is accomplished by displacing the bag a known amount and observing the signal deflection on the oscilloscope. A moderately low level of room lighting, minimal shielding, and a sufficiently large battery for light source stability will ensure a fairly clean, steady signal. Elementary design will produce an essentially linear response. The signal may be recorded on an appropriate strip recorder for later analysis.

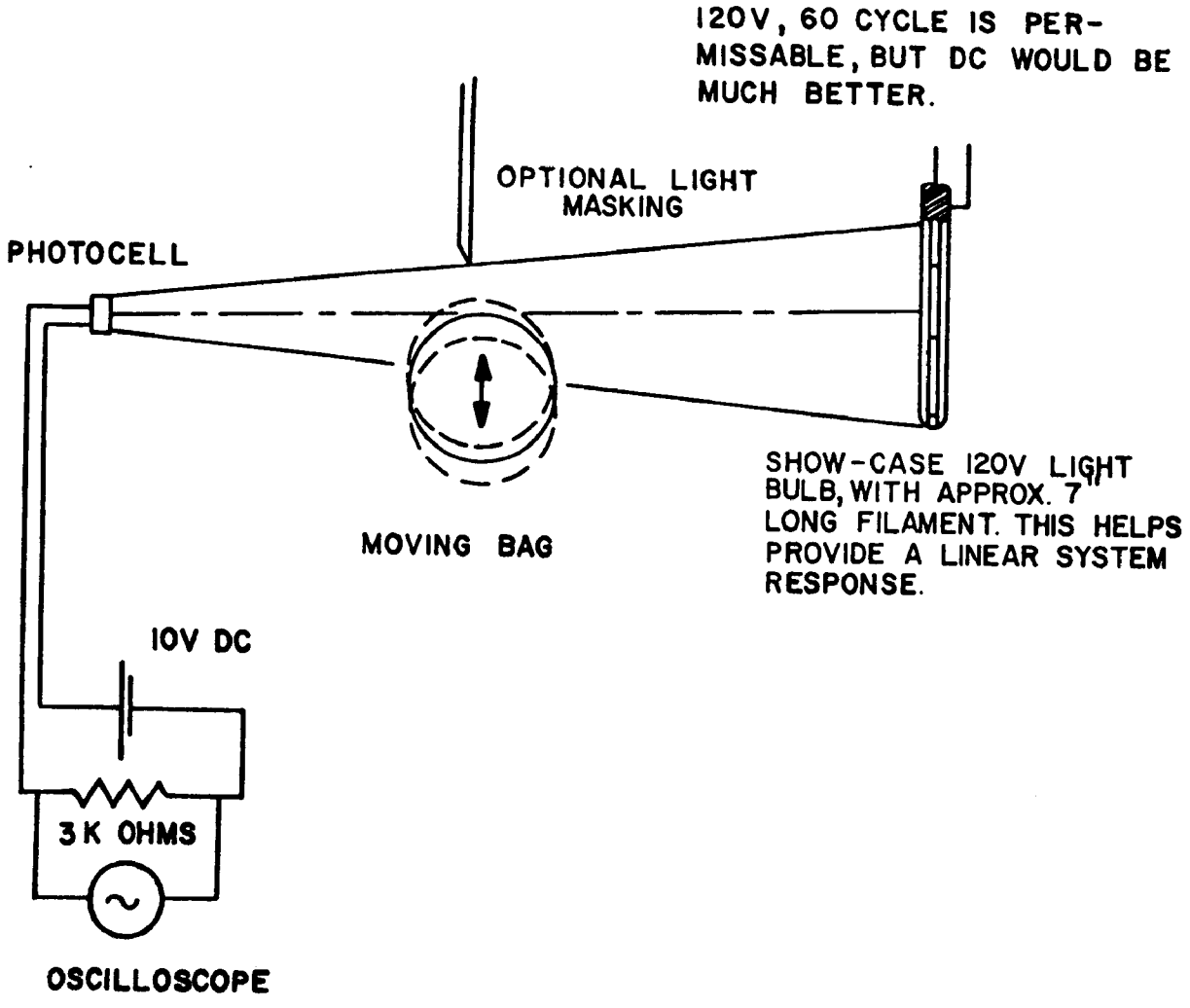

Figure C-1. Description of bag motion by interception of light beam

APPENDIX D

THEORETICAL AVERAGE WAVE VELOCITY

In a hanging bag with constant mass per unit length (ρ) and total length (L) the tension in the bag is given by

$$T_x = T_T - \rho_g (L - x)$$

where at the bottom of the bag x is zero and $T_{x=o}$ is whatever tension is applied at the bottom. Since the velocity of the wave at x is $\sqrt{T_x/\rho}$ the time required for the wave to travel down the bag is

$$t_L = \int_o^{t_L} dt = \int_L^o -\frac{dx}{V_x} = \int_L^o \frac{-dx}{\left(\frac{T_T - \rho g (L - x)}{\rho}\right)^{1/2}}$$

$$= \frac{2}{g\sqrt{\rho}} \left(\sqrt{T_T} - \sqrt{T_T - \rho g L} \right) \qquad \text{(D-1)}$$

where W is the total weight of the bag, ρgL. The effective overall average velocity is therefore:

$$\bar{V} = \frac{L}{t_L} = \sqrt{gL} \left[\frac{1}{2\sqrt{\frac{T_T}{W}} - 2\sqrt{\frac{T_T}{W}} - 1} \right] \qquad \text{(D-2)}$$

This compares with the wave velocity in a string under uniform tension:

$$V = \sqrt{gL} \cdot \sqrt{T/W} \qquad \text{(D-3)}$$

If the bag were assumed to have an average velocity based simply on the average tension, $(T_T - W/2)$, the velocity would then be:

$$\bar{V} = \sqrt{gL} \cdot \sqrt{\frac{T}{W} - \frac{1}{2}} \qquad \text{(D-4)}$$

The above assumption introduces an error in the exact expression, Equation (D-2), depending upon the dimensionless ratio (T_T/W):

T_T/W	$\bar{V}_{D-2}/\sqrt{gL}$	$\bar{V}_{D-4}/\sqrt{gL}$	% Error $= 100\left(\frac{\bar{V}_{D-3} - \bar{V}_{D-2}}{\bar{V}_{D-2}}\right)$
1.0	0.500	0.707	41.4%
1.1	0.683	0.775	13.5
1.2	0.772	0.836	8.3
1.5	0.968	1.00	3.1
2	1.21	1.22	0.8
3	1.57	1.58	0.6
5	2.11	2.11	~0

Since the tension at the top of the bag cannot be less than the hanging weight of the bag, the simpler expression Equation (D-4) results in a 41 percent maximum error in computing average velocities. As the bag is tightened at the bottom which increases the ratio of top tension to bag weight, the error diminishes rapidly. Thus the simpler expression may be adequate except when working with slack and near-slack bags.

The same comment applies in computing resonant frequencies, which depend on the effective overall average wave velocity:

$$f_N = \frac{N}{2\ t_L} = \frac{N\bar{V}}{2L} \qquad \text{(D-5)}$$

where f_N is the Nth resonant frequency of the bag.

Equation (D-5) was tested against a variety of shaken bags, observing the first few resonant frequencies on each bag and the associated tension.

The theoretical resonant frequencies were computed from Equation (D-5). In many cases, the computed f_N were about 1 cps lower than the observed f_N. This was attributed to the tacit and incorrect assumption that the bag behaved as an ideal string. Actually, since the bag has appreciable thickness while shaking, it also possesses stiffness. Hence, its wave velocity must exceed that for a simple string.* Determining the stiffness of a bag while shaking is extremely difficult because the cross section is neither circular nor flat, but somewhat oblate (Figure IV-4). Rather than compute the exact wave velocity, therefore, an empirical correction term was subtracted from the bag's length. This is to say, the bag behaves as if it were slightly shorter because of the higher wave speed. Equation (D-5) then becomes

$$f_N = \frac{N}{2L\left(1 - \frac{2D}{L}\right)} \sqrt{\frac{T_m}{\rho}} \qquad \text{(D-6)}$$

where $T_m = T_T - W/2$, and where the D/L ratio of the bag takes into account the bag's stiffness to a first approximation. The equation indicates that the stubbier the bag, the higher the resonant frequency.

The observed resonant frequencies were plotted against those computed by this method in Figure IV-5. The good agreement furnished a firm support to the theories of resonant frequency as applied to shaking bags.

*The wave velocity of a string with tension but no stiffness depends on the tension. The wave velocity of an elastic beam with no tension but with stiffness; i.e., with elastic modulus and bending moment, has a characteristic wave velocity that depends on the stiffness. A member with both tension and stiffness has a higher wave velocity due to the superposition of the separate effects.

APPENDIX E

BAG STRETCH AND TENSION DURING SHAKING

The problem is to determine the bag strain resulting from the added bag length when shaken according to the general wave form $y = Y\sin(2\pi x/\lambda)$.

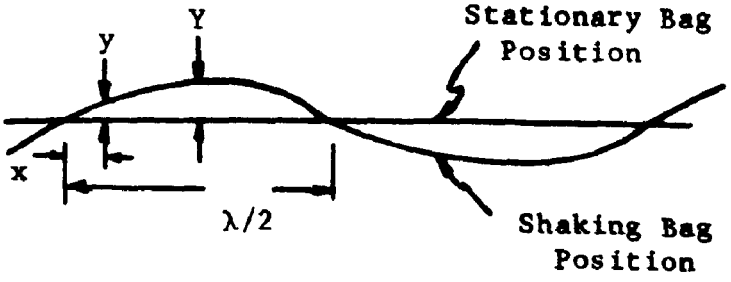

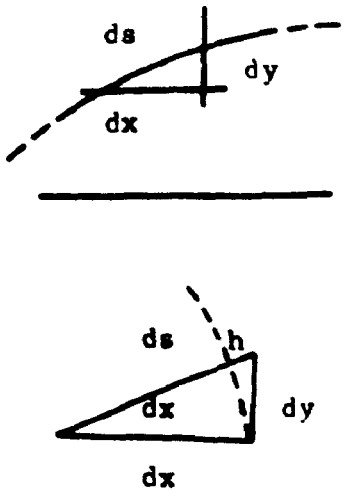

In the figure above,

$$dx^2 + dy^2 = (dx + h)^2 \ .$$

When reduced,

$$h = dy^2/2dx \ , \qquad \text{(E-1)}$$

provided that $h \ll 2\ dx$.

Since the stretched length $ds = dx + h$, the increase of the original length dx is h and the average strain along this increment of the bag is $h/dx = dy^2/2dx^2$. From the wave equation,

$$\frac{dy}{dx} = \frac{2\pi Y}{\lambda}\cos\left(\frac{2\pi x}{\lambda}\right) \qquad \text{(E-2)}$$

The average strain along the bag length $\lambda/2$ can be found by integration:

$$\bar{\varepsilon} = \frac{1}{\lambda/2} \int_{x=0}^{x=\lambda/2} \frac{1}{2}\left[\frac{2\pi Y}{\lambda} \cos\left(\frac{2\pi x}{\lambda}\right)\right]^2 dx \qquad \text{(E-3)}$$

$$= \left(\frac{\pi Y}{\lambda}\right)^2$$

That is, at the instant that the amplitude of the bag is Y, the average strain along the bag depends simply on Y and on the wavelength. This assumes that the bag has an integral number of wave nodes; otherwise, a more complicated dependency would apply.

The strain may vary with time. In a simple string oscillating with a standing wave

$$y = (Y \sin wt)\ (\sin 2\pi x/\lambda)$$

the average value of $(\pi Y/\lambda)^2$ can be shown to be one-half the maximum, so that the time-averaged value of the strain average along the string is

$$\frac{1}{2}\left(\frac{\pi Y}{\lambda}\right)^2$$

The motion in a shaken bag, however, is predominantly a downward traveling wave with the standing wave pattern less pronounced. In a traveling wave, the bag is under practically the same net elongation at all times. This is an over-simplification since the bag length is finite, and Y and/or the wave shape will be different at the ends of the bag. However, to a first approximation,

$$\bar{\varepsilon} = \left(\frac{\pi Y}{\lambda}\right)^2$$

describes the strain in a shaking bag averaged both timewise and along the bag. The strain is also defined by the simple relationship

$$\bar{\varepsilon} = T_d/ML$$

where T_d is the tension difference attributed to elongation, M the bag modulus and L the bag length.

Standing wave patterns and the process of reflection at the ends of the bag may be expected to cause variations in this average tension. Local tension variations will rapidly be distributed along the bag, however, because longitudinal waves travel much faster than lateral waves. The longitudinal wave velocity is $\sqrt{ML/(\rho)}$, which for a typical bag is approximately 750 ft/sec. This is $\sqrt{ML/T}$, or about 25 times faster than the lateral wave velocity. Thus, any local modification of tension distributes itself so rapidly along the bag, that the bag is virtually under uniform dynamic tension from end to end. The weight component of the tension of course still varies from end to end.

APPENDIX F

DAMPING AND AVERAGE BAG AMPLITUDE THEORY

The wave applied to the top of the bag diminishes as it travels down the bag, such that the maximum displacement seen by successive points down the bag may be given by $A\ e^{-\beta x}$. A is the wave's initial amplitude at $x = 0$ and β is a damping constant that depends on the rapidity with which the wave energy is dissipated. If β is large, the wave may, practically speaking, never reach the bottom of the bag, whereas for intermediate to low damping constants, the remaining amplitude at the bottom of the bag will be $A\ e^{-\beta L}$.

Since the dynamic shaking tension depends on the square of the bag amplitude, it is preferable to determine the average value of the amplitude squared, rather than the average value of the amplitude:

$$Y_1^2 = \frac{1}{L} \int_0^L \left(Ae^{-\beta x}\right)^2 dx = A^2 \left(\frac{1 - e^{-2\beta L}}{2\beta L}\right) \qquad \text{(F-1)}$$

Assuming that the wave reflected from the bottom of the bag has the initial amplitude $Ae^{-\beta L}$; i.e., there is no energy loss during reflection, then by a similar process of integration it can be shown that the average value of the amplitude squared for the reflected wave alone is

$$Y_2^2 = A^2\ e^{-2\beta L} \left(\frac{1 - e^{-2\beta L}}{2\beta L}\right) \qquad \text{(F-2)}$$

It is assumed here that the waves travel with the same extant mechanics, and do so independently of one another. By similar assumptions the Y^2's of the tertiary and any subsequent waves can be computed.

Let it now be assumed that the maximum amplitude seen by a given point on the bag is the sum of all such successive Y's, that is, sooner or later the waves will all combine constructively, resulting in a temporarily large bag displacement at that point.

$$Y^2 = A^2\left(\frac{1 - e^{-2\beta L}}{2\beta L}\right)\left(1 + e^{-2\beta L} + e^{-4\beta L} + \ldots\right)$$

$$= \frac{A^2}{2\beta L} \ldots \qquad \text{(F-3)}$$

The same conclusion could be reached directly from Equation (F-1) under the assumption that there is considerable damping, such that $e^{-2\beta L} \ll 1$, so that the first reflected wave is negligible.

From the definition of the shaking attenuation parameter called α,

$$\alpha \equiv \frac{Y}{A} = \frac{1}{2\beta L} \qquad \text{(F-4)}$$

For example, an average amplitude attenuation of 0.80 for a 10 foot bag corresponds to a damping constant β of 0.078 per foot. That is, the bag motion is expected to diminish at this rate in moving down the bag.

APPENDIX G

ENVELOPE PHOTOGRAPHS OF BAG MOTION

In this appendix, a series of photographs taken during a study of bag tension versus frequency have been hand-copied with scale adjustments to facilitate distance measurements. The maximum horizontal (envelope) excursions from the rest or non-shaking condition have been plotted for several locations over the length of the bag. The identifying photograph numbers refer to the frequency locations listed on the curve shown in Figure G-1. Examination of these photos, Figure G-2, shows that the lateral excursions are maximized and the model locations clearly delineated at the resonance points.

The above measurements were made with a used, unnapped cotton sateen bag, 10 ft. long and 6 in. in diameter. The shaking amplitude was 1 in. and the total weight of the bag and residual dust was 1.3 lbs.

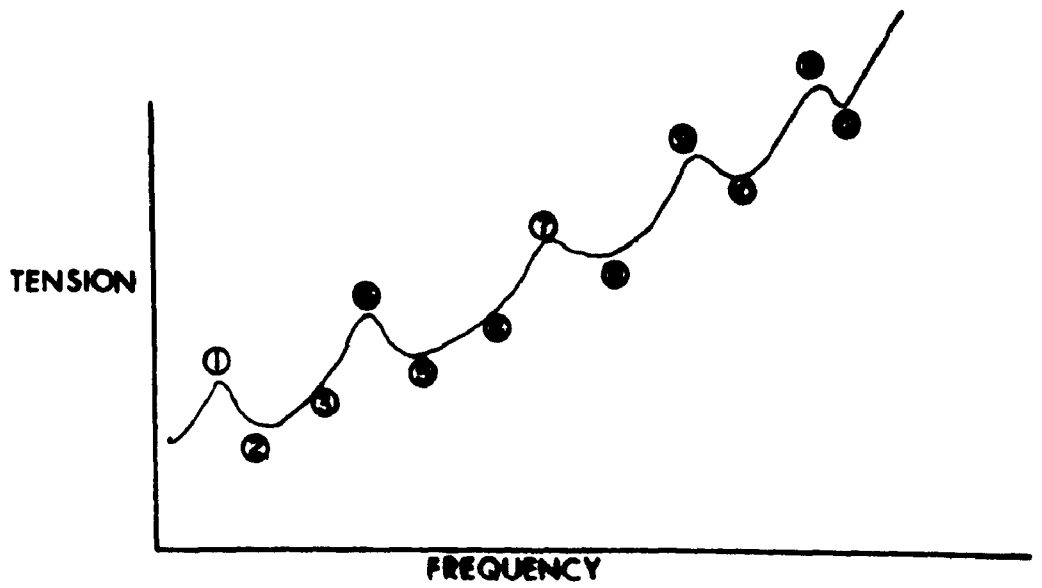

Figure G-1. Position of photographs relative to resonant frequencies

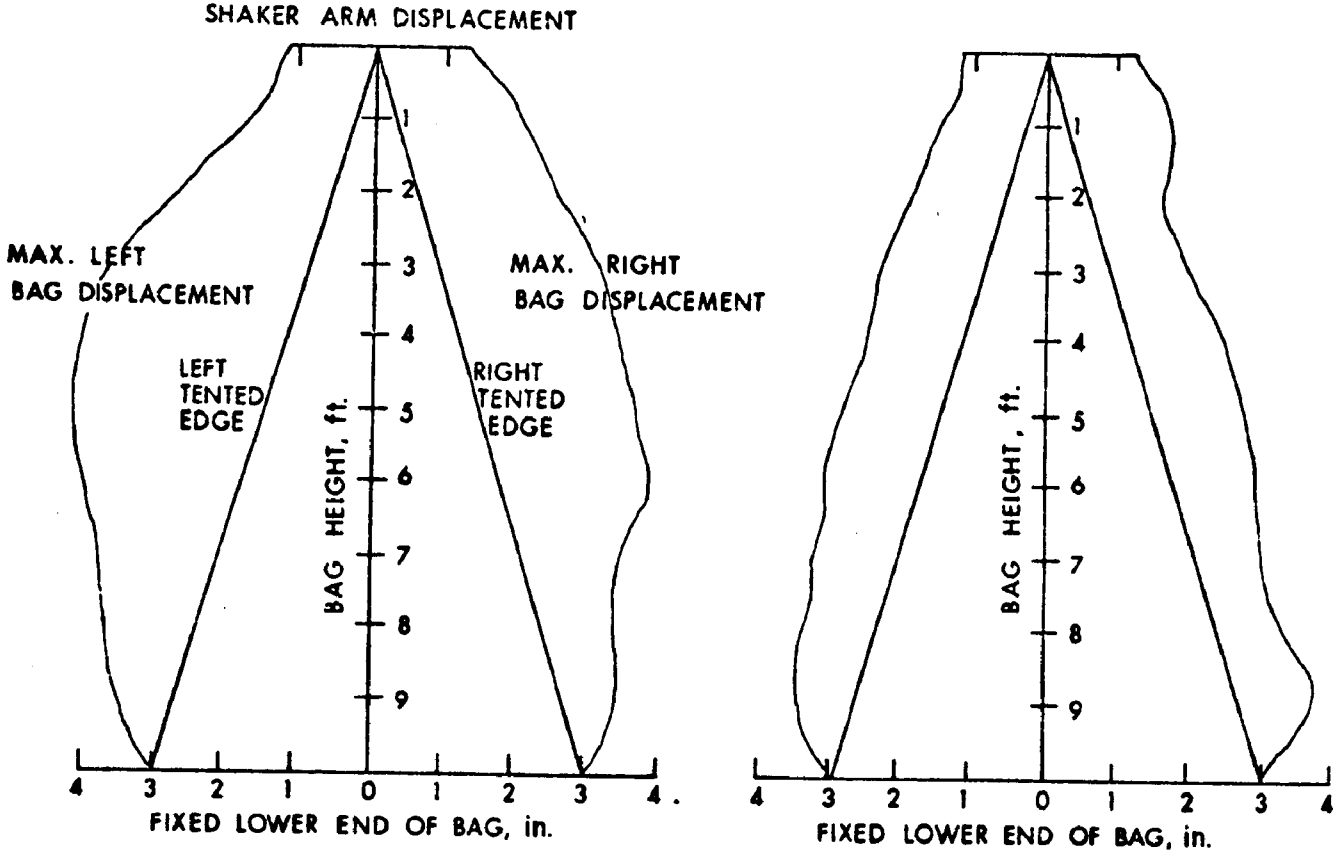

Photo no. 1: at first resonance; f = 1.8 cps; initial tension: 2.22 lbs, (arm ave.); shaking tension: 3.90 lbs, time ave. (max: 5.28; min: 2.52 lbs.)

Photo no. 2: f = 2.2 cps (anti-resonance); initial tension: 2.22 lbs.; shaking tension: 2.86 lbs. ave. (max: 3.50; min: 2.22 lbs.)

Figure G-2. Bag displacement versus shaking frequency

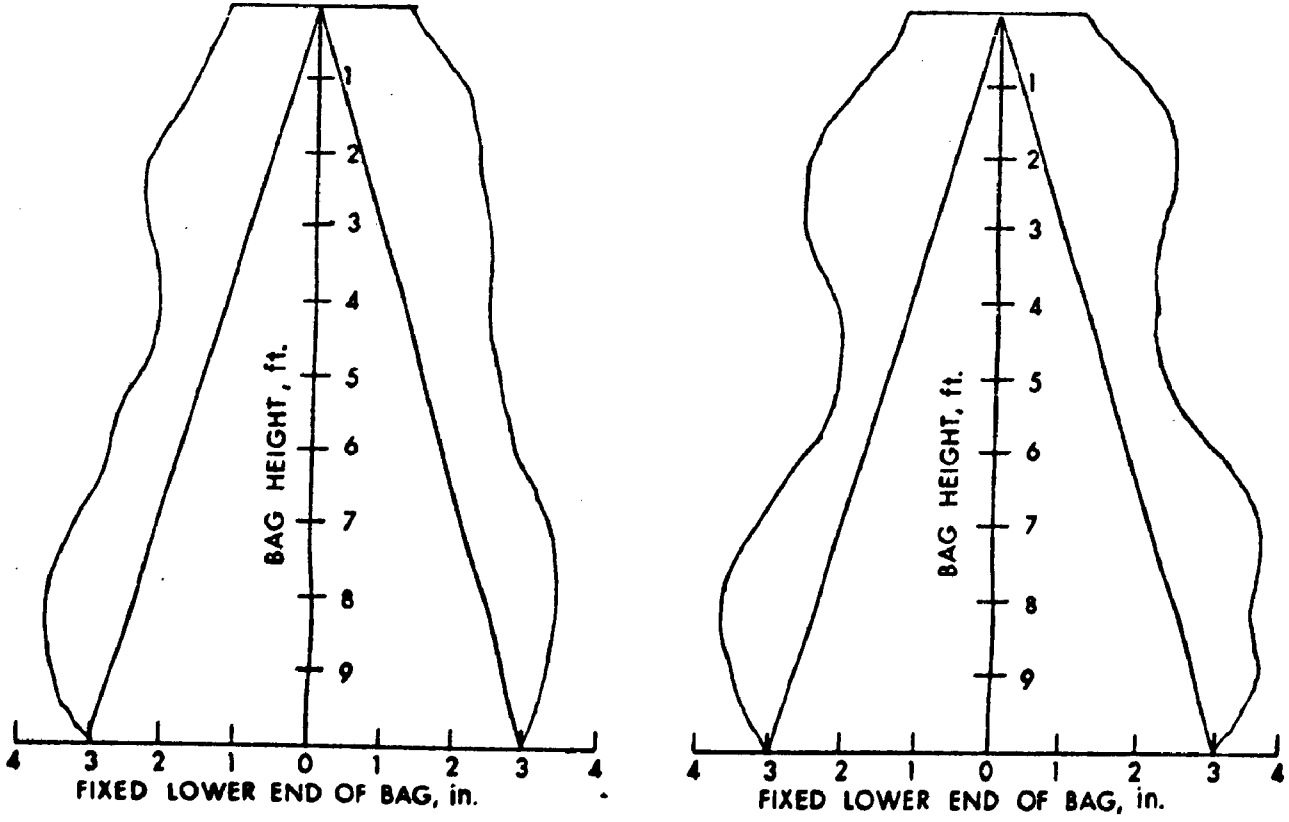

Photo no. 3: f = 3.3 cps (mid resonance); initial tension: 2.20 lbs.; shaking tension: 4.05 lbs. (max: 4.37; min: 3.73 lbs.)

Photo no. 4: f = 3.95 cps (second resonance); initial tension: 2.20 lbs.; shaking tension: 4.94 lbs. (max: 5.82; min: 4.06 lbs.)

Figure G-2 (continued). Bag displacement versus shaking frequency

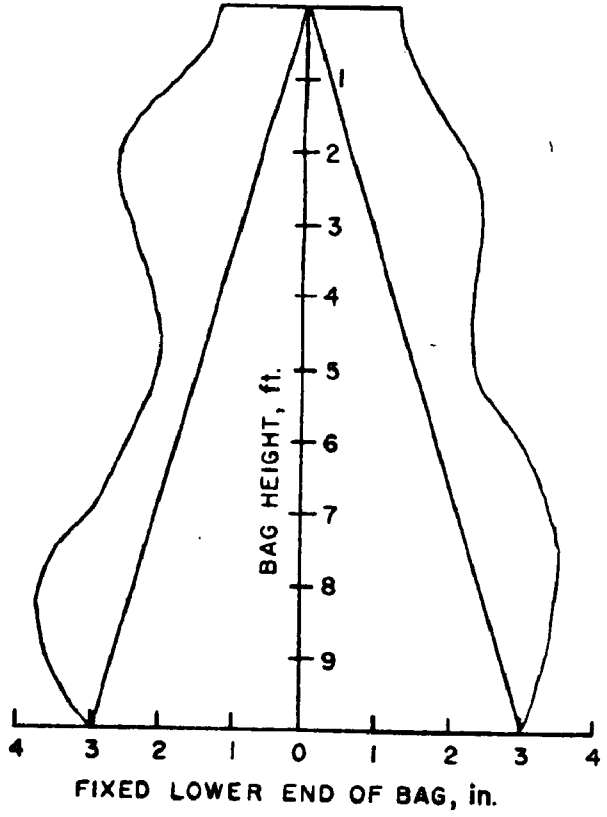

Photo no. 5: f = 4.1 cps (anti-resonance); initial tension: 2.15 lbs.; shaking tension: 4.13 lbs.; (max: 4.46; min: 3.80 lbs.)

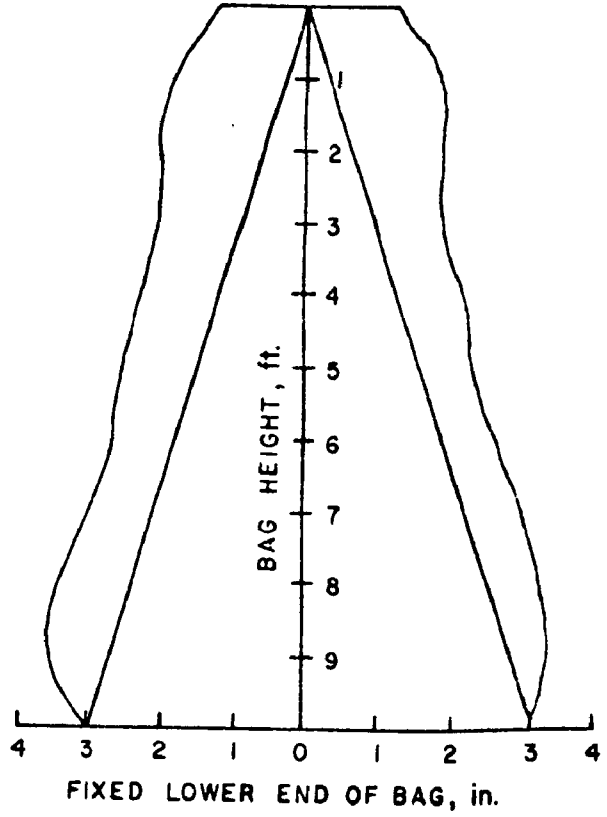

Photo no. 6: f = 5.4 cps (mid resonance); initial tension: 2.15 lbs.; shaking tension: 4.85 lbs.; (max: 5.41; min: 4.29 lbs.)

Figure G-2 (continued). Bag displacement versus shaking frequency

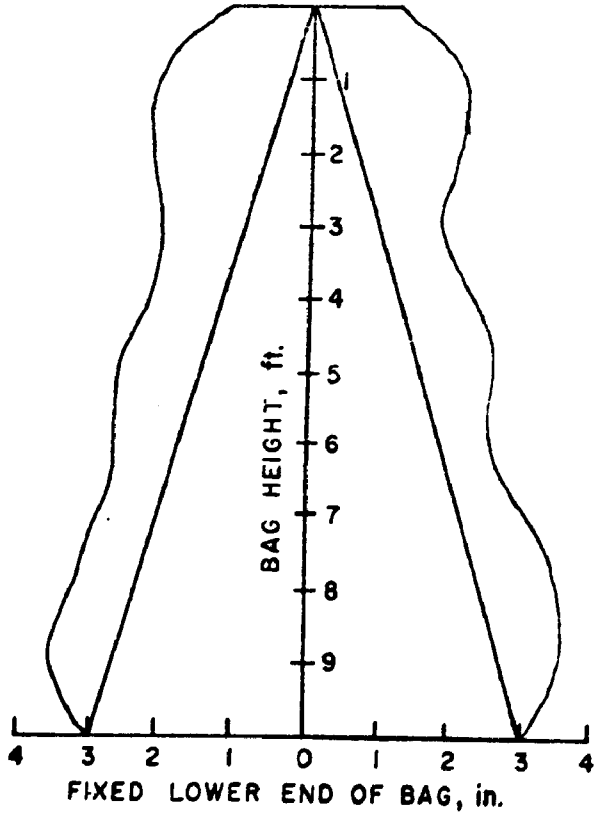

Photo no. 7: f = 5.95 cps (third resonance); initial tension: 2.10 lbs.; shaking tension: 5.42 lbs.; (max: 5.82; min: 5.02 lbs.)

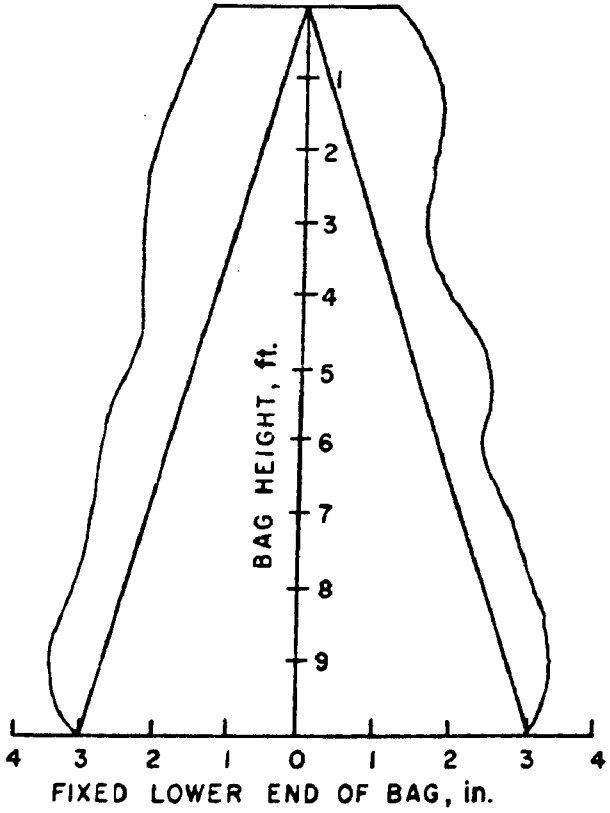

Photo no. 8: f = 6.4 cps (anti-resonance); initial tension: 2.10 lbs.; shaking tension: 5.26 lbs. (max: 5.42; min: 5.10 lbs.)

Figure G-2 (continued). Bag displacement versus shaking frequency

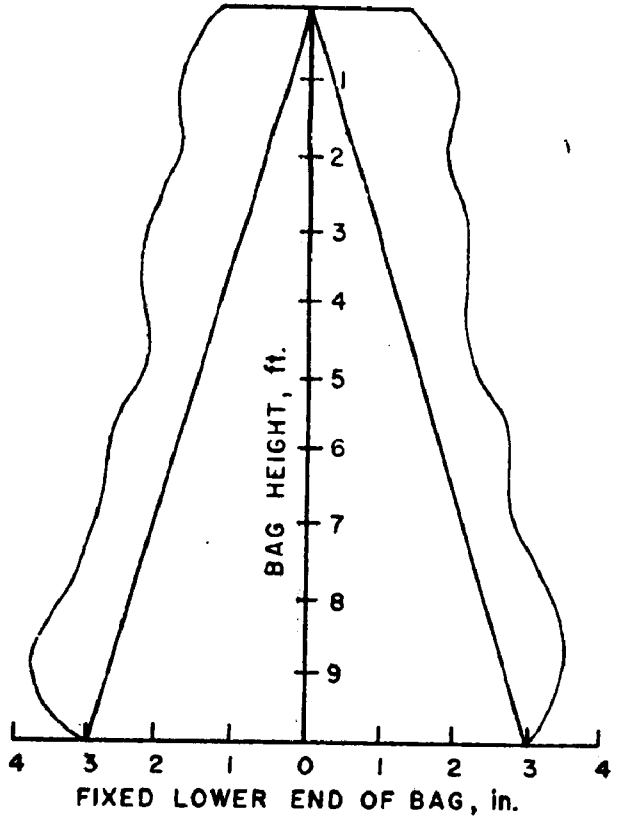

Photo no. 9: f = 8.6 cps (fourth resonance); initial tension: 2.10 lbs.; shaking tension: 6.70 lbs.; (max: 6.86; min: 6.54 lbs.)

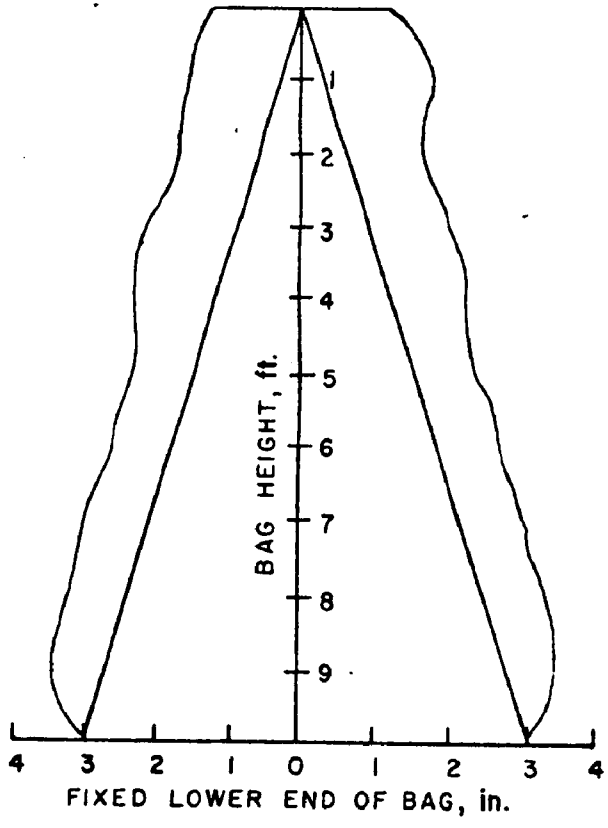

Photo no. 10: f = 8.9 cps (anti-resonance); initial tension: 2.10 lbs.; shaking tension: 6.06 lbs.; (max: 6.22; min: 5.90 lbs.)

Figure G-2 (continued). Bag displacement versus shaking frequency

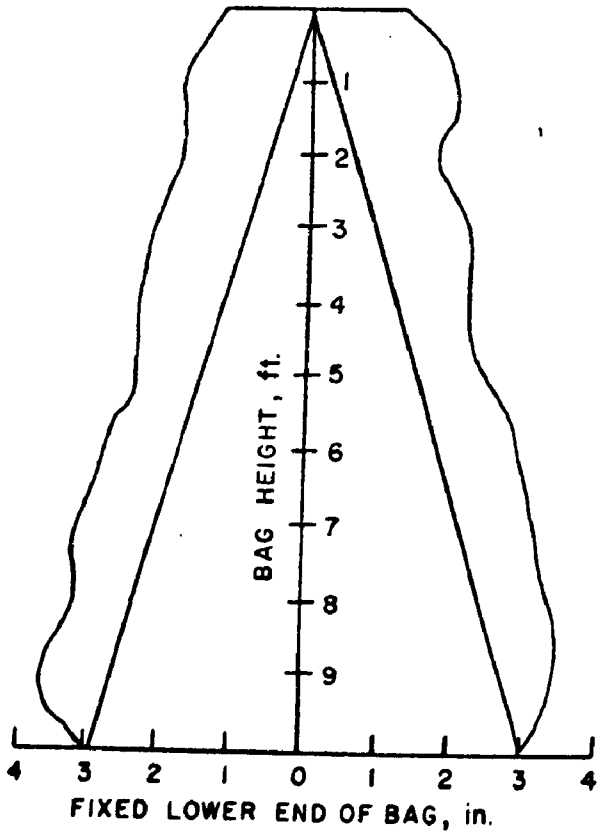

Photo no. 11: f = 11.0 cps (fifth resonance); initial tension: 2.10 lbs.; shaking tension: 7.80 lbs.; (max: 7.95; min: 7.65 lbs.)

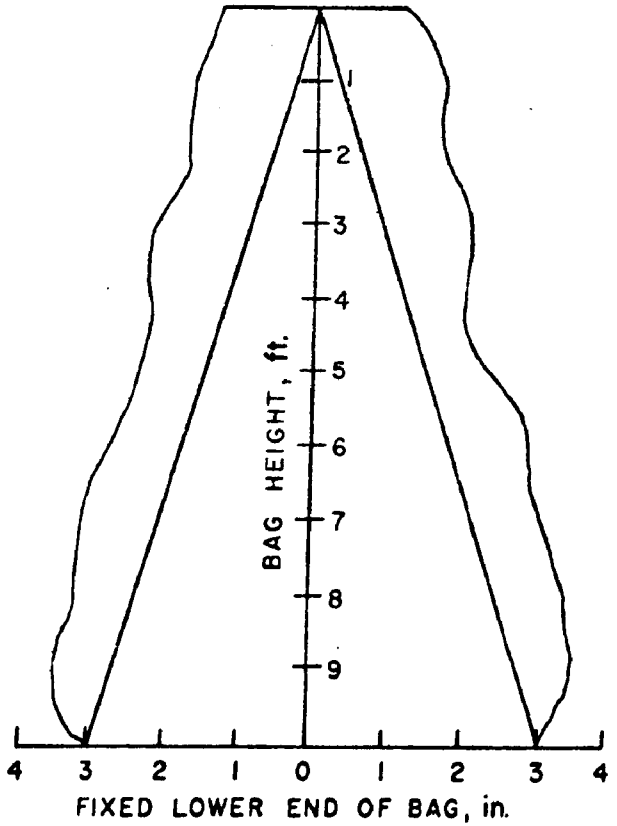

Photo no. 12: f = 11.4 cps (anti-resonance); initial tension: 2.10 lbs.; shaking tension: 6.86 lbs.; (max: 7.02; min: 6.70 lbs.)

Figure G-2 (continued). Bag displacement versus shaking frequency

APPENDIX H

DATA SHEETS FOR MECHANICAL SHAKING STUDIES

Because of the large number of original data and/or work sheets generated during this study, we have included in this section only the summary tables for test measurements in the following categories:

- Dynamic Tension Tests
- Dust Removal Tests
- Effluent Size Properties

Copies of the original data are on file in the Control Systems Laboratory of the Environmental Protection Agency.

DYNAMIC SHAKING TESTS

During dynamic tension measurements the bags were not ordinarily loaded with dust, except for some residual dust holding in certain instances. Although their weight did not change during these tests, they usually underwent some stretching.

Total tension at the top of the bag is tabulated against the shaking frequency. This is the time-averaged tension about which larger and smaller tensions occur during one complete shake. Usually the first two entries are:

Initial tension:	defined as the zero cps tension at the top of the bag when it is vertical;
0 ± 1 in.:	defined as the zero cps tension at the top of the bag when it is displaced left or right of vertical to the full amplitude being used in that series.

The last entry in each series is sometimes a "zero check," which is merely a re-measurement of the initial tension (vertical) after the series is completed. An apparent decrease in initial tension indicates bag stretching during the series.

Side force is also tabulated for some tests. This is the peak lateral force at the top of the bag directed perpendicularly to the shaker arm; i.e., the force causing the bag top to assume a sidewise motion. During one complete passage of the shaker arm, this side force is directed alternately to the right and to the left such that the average value is zero. A listing of these data sheets appears in Table H-1.

Dust Removal Tests

The following tabulations of original data describe the loading of a filter bag and the subsequent dust removal process under specified cleaning conditions. The data outlined below are included in the data sheets summarized in Table H-2. Figure H-1 represents a typical data sheet.

Loading Data:

Bag type, size, and general condition

Inlet dust loading and air flow to the bag, plus relative humidity.

Tension at the top of the bag, with vertical shaker arm, without inflation; "taut" = with the bottom of the bag clamped; "loose" = with the bottom unclamped; i.e., nominally the weight of the free bag (pounds).

Time, pressure differential across the bag, and total tension at the top of the bag due to this inflating pressure in addition to the previous "taut" value.

Cleaning Data:

Amplitude (one-half the full shaker arm stroke) and average frequency of the shaker arm;

Shaking Data: Cumulative seconds of shaking in several intervals; average shaking frequency observed in each interval; cumulative number of shaker cycles.

Table H-1. SUMMARY LISTING OF DATA SHEETS FOR TENSION/SHAKING FREQUENCY STUDIES

Test number	Shaking amplitude(s) (in.)	Bag parameters				
		Fabric	Dimension	Used or clean	Weight (lbs.)	Number
D 1	1	Unnapped cotton	10 ft x 6 in	Clean	1.11	4
D 2	1	Unnapped cotton	10 ft x 6 in	Used	1.33	4
D 3	1	Unnapped cotton	10 ft x 6 in	Used	1.33	4
D 4	1	Dacron 5 oz/yd^2	10 ft x 6 in	Clean	0.56	1913
D 5	1	Dacron 5 oz/yd^2	10 ft x 6 in	Clean	0.56	1914
D 6	1	Dacron 5 oz/yd^2	10 ft x 6 in	Clean	0.56	1916
D 7	1	Dacron plain weave	10 ft x 6 in	Clean	1.11	1915
D 8	1	Unnapped cotton	10 ft x 6 in	Used	1.33	-
D 9	1, 0.5	Unnapped cotton	10 ft x 6 in	Used	1.33	-
D 10	2	Unnapped cotton	10 ft x 6 in	Used	1.33	-
D 11	1, 0.5, 0.25	Unnapped cotton	5 ft x 6 in	Clean	0.6	-
D 12	1	Unnapped cotton	5 ft x 6 in	Clean	0.6	-
D 13	1, 0.25	Unnapped cotton	10 ft x 4 in	Clean	0.77	-
D 14	1	Unnapped cotton	10 ft x 6 in	Used	1.4	3
D 15	1	Dacron 5 oz/yd^2	10 ft x 6 in	Clean	0.56	-
D 16	1	Dacron plain weave	10 ft x 6 in	Used	1.33	36
D 17	1	Unnapped cotton	10 ft x 6 in	Clean	1.11	5

Table H-1 (continued). SUMMARY LISTING OF DATA SHEETS FOR TENSION/SHAKING FREQUENCY STUDIES

Test number	Shaking amplitude(s) (in.)	Bag parameters				
		Fabric	Dimension	Used or clean	Weight (lbs.)	Number
D 18	1	Unnapped cotton	10 ft x 6 in	Clean	1.11	a
D 19	1	Unnapped cotton	10 ft x 6 in	Clean	1.11	5
D 20	1	Unnapped cotton	10 ft x 6 in	Used	1.4	4

[a]Circular cap installed at top of bag.

TEST S1

Date: 4 May 71

DUST REMOVAL TEST

Test No. 2

LOADING DATA:	Bag No. 4	Bag type: 10'x6" cotton, Well Used	
Inlet conc.: 5 gr/ft^3	CFM: 43.8	% RH	
Initial Tension:[a]	Taut: 3.10	Loose: 1.90	Retaut:

Time (min)	Δ p (in.)	Filtering Tension
0	1.15	8.05
1.0	1.35	8.00
3.5	1.54	2.95
9.5	2.10	8.05
17.5	2.67	8.45
30	3.45	8.70

Notes:

CLEANING DATA: Amplitude: ± 1 inches Frequency: ~ 9 cps

Cum. seconds shaken	cps (increm't ave.)	Cum. no. shakes	Shake tension range[a]	Dust off (grams)	Cum. dust off	Cum. % dust off	Result, Δ p (in.)	Resulting tension[a]				Total dust wt.
								Taut	Loose	Net	Retaut	
0		0		0	0	0	3.45	3.35	2.70	0.65		706
5	9.-	45	7.5	128	128	18.1		3.18	2.46	0.72		
10	9.0	90	8.0	125	253	35.8		2.73	2.14	0.59		
15	9.0	135	-	36	289	41.0		2.89	2.06	0.83		
25	9.0	224	8.2	10	299	42.3		2.50	1.98	0.52		
45	8.9	402	8.13	12	311	44.0	1.25	2.48	1.93	0.55		414

Note: Weight loss based on free hanging bag weights = 2.70 - 1.93 = 0.77 lbs. or 350 grams.

SUPERCLEANING:

20	11.5	230	8.9-9.1				1.13	2.89	1.90	0.99		

[a]Tension in pounds at top of bag.

Figure H-1. Sample data sheet for dust removal tests

Table H-2. SUMMARY LISTING OF DATA SHEETS FOR TYPICAL FILTRATION AND MECHANICAL SHAKING TESTS

Test number	Shaking parameters		Tension lbs.		Filter[a] capacity grains/ft.^{2}	Operating parameters
	Amplitude frequency					
	in.	cps	Shaking	Static		
S1	1	9.0	7.9	3.1	326	Tests S1 through S37 Unnapped sateen weave cotton, equilibrated, Bag no. 4 Fly ash aerosol.
S2	1	7.0	7.1	2.9	246	
S3	1	10.0	8.3	2.5	414	
S4	1	6.2	6.8	2.2	264	
S5	1	8.1	7.4	2.7	312	
S6	1	7.2	6.8	2.2	289	
S7	1	7.8	7.1	1.9	314	
S8	1	7.5	9.5	6.1	289	
S9	1	7.7	7.5	2.1	304	
S10	0.75	7.7	6.0	2.9	202	
S11	1.15	8.0	8.1	2.5	350	
S12	0.50	7.9	4.5	2.0	31	
S13	1	7.5	7.2	2.1	310	
S14	1.50	7.8	11.9	2.6	336	
S15	1	5.9	6.4	2.5	179	
S16	1.50	6.0	8.4	2.0	300	
S17	2	5.7	14.3	1.9	348	
S18	1	4.7	5.1	2.0	61	
S19	1.5	4.5	10.4	2.0	233	
S20	2	4.1	9.4	1.6	197	
S21	0.50	10.9	3.9	1.6	83	
S22	0.75	10.7	5.4	1.6	255	
S33	1	7.8	7.8	2.9	372	
S34	1.50	8.0	13.0	2.8	315	
S35	1	8.0	8.8	3.1	315	
S36	1	7.8	6.0	1.4	197	
S37	1	9.1	6.0	3	241	
S38	1	8.0	6.3	2.1	153	Tests S38 through S49 as above but with bag dimensions of 10 ft. x 4 in.
S39	1	8.0	6.5	2.2	135	
S40	1	7.8	6.0	2.2	191	
S41	1	3.9	6.3	2.3	46	
S42	2	3.8	8.6	2.6	71	
S43	1.5	11.3	4.5	2.4	44	
S44[c]	1	7.9	4.9	2.4	248	
S45	1	7.8	4.9	2.3	213	
S46[d]	1	7.7	6.0	2.1	80	15 min.
S47[d]	1	7.7	6.3	2.4	385	60 min.
S48[d]	1	7.6	4.8	1.7	49	7.5 min.
S49[d]	1	7.9	5.7	2.1	470	60 min.

Table H-2 (Continued). SUMMARY LISTING OF DATA SHEETS FOR TYPICAL FILTRATION AND MECHANICAL SHAKING TESTS

Test number	Shaking parameters		Tension lbs.		Filter[a] capacity grains/ft.^{2}	Operating parameters
	Amplitude frequency					
	in.	cps	Shaking	Static		
						Tests S50, S51 plain weave Dacron, Bag 35
S50	1	8	5.0	2.7	291	New equilibrated
S51	1	8	5.3	2.7	267	After 2 x 10^7 shakes
						Tests S52, S53 crow foot Dacron bag 72
S52	1	8	4.0	2.3	300	New equilibrated
S53	1	8	>10.0	2.3	287	After 2 x 10^7 shakes
						Tests S54, S55 napped cotton bag 69
S54	1	8	8.4	2.5	309	New equilibrated
S55	1	8	>10	2.6	327	After 2 x 10^7 shakes
						Tests S56 through S59 unnapped cotton 2 x 10^7 shakes
S56	1	8	8.1	3.1	357	Bag 8
S57	1	8	8.6	3.8	357	Bag 8
S58	1	8	7.0	2.4	308	Bag 10
S59	1	8	7.7	3.1	323	Bag 10

Table H-2 (Continued). SUMMARY LISTING OF DATA SHEETS FOR TYPICAL FILTRATION AND MECHANICAL SHAKING TESTS

Test number	Shaking parameters		Tension lbs.		Filter[a] capacity grains/ft.^{2}	Operating parameters
	Amplitude in.	frequency cps	Shaking	Static		
						Talc aerosol 4 grains/ft.^{3}
S60	1	8	5.6	2.1	156	Unnapped cotton
S61[e]	1	8	4.9	2.2	313	Unnapped cotton
S63[f]	1	8	-	2.2	195	Unnapped cotton
S64	1	8	6.1	1.7	160	Napped cotton
S65	1	8	4.2	1.3	158	Plain Dacron
						Silica aerosol ~ 1.5 grains/ft.^{3}
S67	1	8	4.0	-	-	No equilibration, no useful data

[a]Filter capacity x 0.0021 = lbs. dust dislodged by cleaning action. Fly ash deposition rate per 30 min. cycle at 3.5 grains/ft.^{3} = 316 grains/ft.^{2} for 10 ft. x 6 in. bag.
Talc deposition rate per 20 min. cycle at 4.0 grains/ft.^{3} = 240 grains/ft.^{2}.

[b]Filtration velocity 3.0 ft./min. unless otherwise specified.
Bag dimensions 10 ft. x 6 in. unless otherwise specified.

[c]Filtration velocity 5 ft./min.

[d]Variable filtration time (and cloth loadings).

[e]Inlet concentration = 5.2 grains.ft.^{3}.

[f]Inlet concentration = 3.2 grains.ft.^{3}.

	Tension at the top of the bag during shaking averaged over complete shaker cycles, usually with tension variation from start to finish of the interval (pounds).
Dust Data:	Grams of dust removed in each interval; cumulative grams of dust removed in all intervals. Cumulative dust removed, expressed as a percent of the total dust initially on the bag including both the previous residual and the loaded dust. (Total given in last column.)
Pressure Drop:	The differential pressure across the bag, obtained by operating the fan at the same air flow used in loading the bag.
Resulting Tension:	Measured at the top of the bag with vertical shaker arm and without inflation; "taut" and "loose" the same definitions as during loading; "net" = the difference; i.e., the load applied at the bottom of the bag; "re-taut" = the tension obtained when the bottom was once again clamped (pounds).

Supercleaning Data:

The same as the above, during and resulting from a more intense cleaning, after the above test, in preparation for the next loading and cleaning test.

Effluent Size Properties

During a filtration period, the B&L light scattering particle counter was used to count the number of particles penetrating the bag. Data for a typical test is plotted on Figure H-2. For brief time intervals during the filter cycle (0.07 to 0.1 minute) all particles greater than a pre-set size were counted. For example, 1 minute after filtration began, during an interval of 0.07 minute, 110 particles larger than 0.5 micrometers were counted by the instrument, using an instrument sampling rate of 170 cc/min. This is equivalent to a concentration of

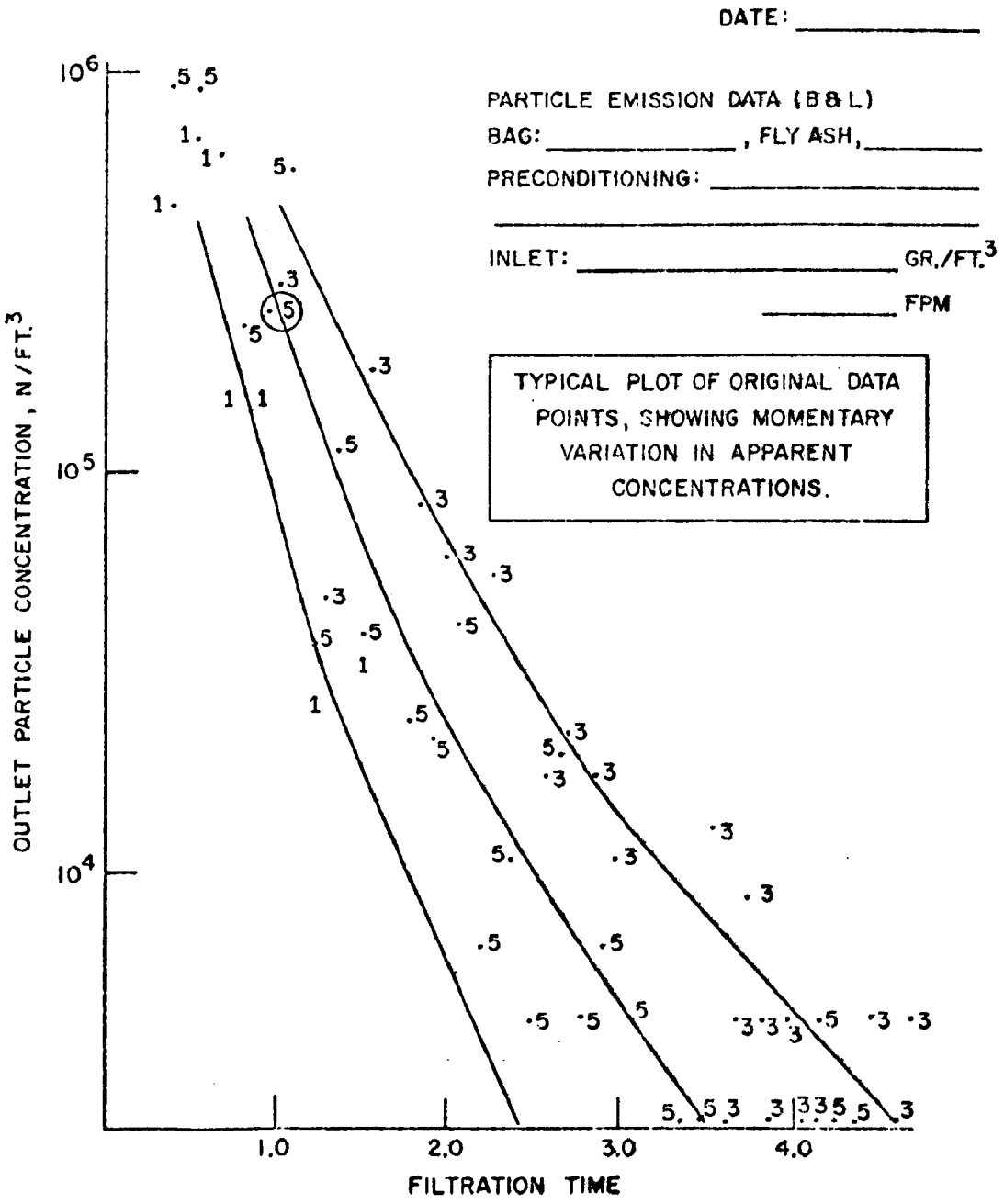

Figure H-2. Typical effluent concentrations versus particle size category and filtration time

2.62×10^5 particles per ft.^{3} for particles larger than 0.5 micrometers. These data are the coordinates for the encircled data point, 1.0 minute and 2.62×10^5 particles/ft.^{3}, shown on Figure H-2.

Similar measurements were continued over the filtration period, or as long as particles continued to be emitted. As may be seen from the resulting plot, the indicated concentrations vary by a factor of 2 to 3 from moment to moment due partially to experimental errors and probably partially to actual transient variations in concentration. Curves of best fit have been estimated visually to determine the average instantaneous size distribution of particles being emitted. The curves are not usually drawn above about 5×10^5 particles/ft.^{3} due to a limitation in counting ability of the instrument at high concentrations.

The curves of best fit were used to estimate mass concentrations emitted as a function of time as reported in the text of the report.

Three groups of data curves are depicted:

- Amplitude-frequency tests, with unnapped cotton sateen and fly ash
- Life tests, using six fabrics and fly ash
- Talc tests, using three fabrics

A listing of several curves similar to those of Figure H-2, along with descriptive operating parameters, is given in Table H-3.

Table H-3. SUMMARY LISTING OF DATA SHEETS FOR EFFLUENT SIZE AND CONCENTRATION PROPERTIES FOR VARIOUS DUSTS AND FABRICS

Test number	Bag number	Fabric	Dust	Shaking cycle		Bag life
				Freq. cps	Amplitude inches	Cumulative number of shakes
A1	-	Unnapped cotton	Atmos.	7.15	1.0	
A3	-	Unnapped cotton	Fly ash	7.15	1.0	
A3	-	Unnapped cotton	Fly ash	7.8	1.0	
A4	-	Unnapped cotton	Fly ash	7.8	1.0	
A5	-	Unnapped cotton	Atmos.	7.5	2.0	
A6	-	Unnapped cotton	Fly ash	7.5	2.0	Tests A1 through A10 $< 10^4$ shakes
A7	-	Unnapped cotton	Atmos.	4.3	1.0	
A8	-	Unnapped cotton	Fly ash	4.3	1.0	
A9	-	Unnapped cotton	Atmos.	11.3	1.0	
A10	-	Unnapped cotton	Fly ash	11.3	1.0	
B1	8	Unnapped cotton	Fly ash	8.0	1.0	5.8×10^6
B2	10	Unnapped cotton	Fly ash	8.0	1.0	5.8×10^6
B3	8	Unnapped cotton	Fly ash	8.0	1.0	10.4×10^6
B4	10	Unnapped cotton	Fly ash	8.0	1.0	10.4×10^6
B5	8	Unnapped cotton	Fly ash	8.0	1.0	16.0×10^6
B6	10	Unnapped cotton	Fly ash	8.0	1.0	16.0×10^6

Table H-3 (Continued). SUMMARY LISTING OF DATA SHEETS FOR EFFLUENT SIZE AND CONCENTRATION PROPERTIES FOR VARIOUS DUSTS AND FABRICS

Test number	Bag number	Fabric	Dust	Shaking cycle		Bag life
				Freq. cps	Amplitude inches	Cumulative number of shakes
B7	8	Unnapped cotton	Fly ash	8.0	1.0	20×10^6
B8	10	Unnapped cotton	Fly ash	8.0	1.0	20×10^6
B9	-	Napped cotton	Fly ash	8.0	1.0	$< 10^4$
B10	-	Plain Dacron	Fly ash	8.0	1.0	$< 10^4$
B11	-	Crow foot Dacron	Fly ash	8.0	1.0	$< 10^4$
B12	-	Napped cotton	Fly ash	8.0	1.0	20×10^6
B13	-	Plain Dacron	Fly ash	8.0	1.0	20×10^6
B14	-	Crow foot Dacron	Fly ash	8.0	1.0	20×10^6
C-1	-	Unnapped cotton	Talc	8.0	1.0	$< 10^4$
C-2	-	Napped cotton	Talc	8.0	1.0	$< 10^4$
C-3	-	Plain Dacron	Talc	8.0	1.0	$< 10^4$

APPENDIX I

THEORY FOR LATERAL FORCES IN SHAKING

The top of the suspended bag is assumed to have an instantaneous force diagram during shaking such as that sketched below:

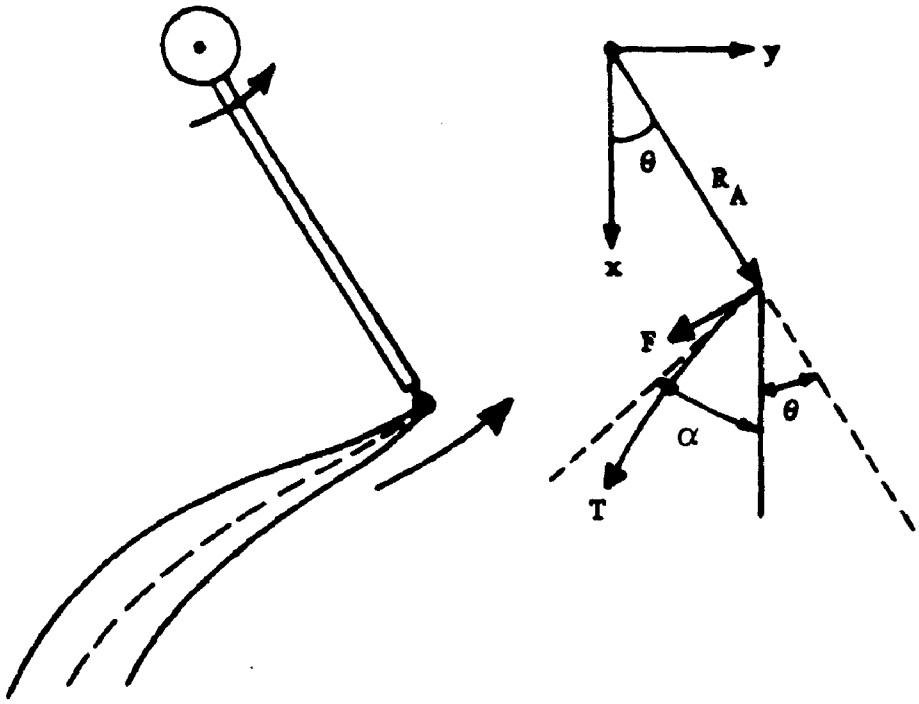

where F = the force at right angles to the shaker arm;

T = the tension in the bag;

θ = the angle of the shaker arm to the vertical;

α = the angle of the bag, and also of force T to the vertical.

Thus

$$F = T\sin(\alpha + \theta) \tag{I-1}$$

The angle θ is controlled by the shaking mechanism:

$$\theta = \sin^{-1}\left[\frac{A}{R_A}\sin wt\right] \tag{I-2}$$

where A is the maximum displacement of the arm and $w = 2\pi f$, the shaker frequency.

It is assumed that the pattern near the top of the bag is mainly that of the downward wave, $y = A\sin(wt + \beta - kx)$, where β allows for the fact that the bag is usually being pulled at an angle when the arm is vertical, and $k = 2\pi/\lambda$. Then since

$$\tan\alpha = \frac{dy}{dx} \text{ at } x = 0,$$

$$\alpha = \tan^{-1}\left[kA\cos(wt + \beta)\right] \tag{I-3}$$

Equations (I-2) and (I-3) permit an evaluation of the lateral force F from Equation (I-1). Equation (I-1) can be simplified under additional assumptions:

- that in typical shaking $\theta = \frac{A}{R_A}\sin wt$, since A/R_A is small, usually ~ 0.17 in the present equipment;
- that $\alpha = kA\cos(wt + \beta)$, since kA is small, usually 0.2 or less in the present study.

Hence,

$$F/T \approx \sin\left(\frac{A}{R_A}\sin wt + kA\cos(wt+\beta)\right) \tag{I-4}$$

Introducing another angle $\gamma = \tan kR_A$, for convenience, Equation (I-4) can be rewritten:

$$\frac{F}{T} = \sin\left(\frac{A}{R_A}\sqrt{1+(kR_A)^2}\sin(wt+\beta+\gamma)\right) \tag{I-5}$$

which shows that the instantaneous force ratio is periodic, with amplitude equal to $\sin\frac{A}{R_A}\sqrt{1+(kR_A)^2}$ and frequency w.

Further, since $(kR_A)^2 \ll 1$ in most cases, and since $\sin(\frac{A}{R_A}) \approx \frac{A}{R_A}$ in most cases,

$$\frac{F}{T} \approx \frac{A}{R_A}\sin(wt+\beta+\gamma) \tag{I-6}$$

For estimating the bag power consumption, the peak value of F is needed. It depends on the variation of T with time. T is approximately equal to T' (the average tension indicated by the load cell) because the angles α and θ are small. Oscilloscope observations indicate that

$$T \approx T' + \frac{MA^2}{4R_A}\sin(2wt+\delta) \tag{I-7}$$

where δ is another phase angle. Thus from the largest possible value of T and the largest possible value of F/T, the largest possible value of F is finally computed to be

$$\frac{F_{max}}{T'} = \left[1 + \left(\frac{MA^2}{4RT_a}\right)\right]\left(\frac{A}{R_A}\right) \qquad \text{(I-8)}$$

For example, if the shaking tension average is 5 lbs., A and R_A are 1 inch and 6 inches, respectively, and M is 16.5 lbs./in., F_{max} is computed to be 0.95 lbs. If the shaking amplitude is increased to 2 inches, F_{max} is estimated to become 2.6 lbs., and at 3 inches (many of the assumptions are weak), 5.6 lbs. The power consumption is expected to increase in the same proportions.

The following table lists the maximum lateral forces and average shaking tensions observed for a variety of bags, amplitudes, and frequencies. Comparison of their ratio with that predicted by Equation (I-8) indicates that the actual ratios are of the same magnitude as predicted, but about 50 percent higher. This suggests that the empirical formula be used to estimate F:

$$F_{max} \quad 1.5\ T_m \left(\frac{A}{R_A}\right)\left(1 + \frac{MA^2}{4\ R_A T_m}\right) \qquad \text{(I-9)}$$

Table I-1. COMPARISON OF MEASURED AND PREDICTED LATERAL FORCES

Bag type	f (cps)	A (in.)	T_{AVG} (lbs.)	F_{MAX} (lbs.)	F/T	F/T, Eq. (I-8)	F/T, Eq. (I-9)
5 oz. Dacron	4.9	1	5.10	1.11	0.22	0.27	0.40
	8.3	1	9.42	5.04	0.54	0.22	0.33
10 oz. plain Dacron	6.8	1	4.30	1.25	0.29	0.19	0.28
Unnap. cotton, 10' x 6", new	5.2	1	4.14	1.16	0.28	0.19	0.29
	6.5	1	4.77	1.38	0.29	0.19	0.29
	8.6	1	5.65	1.54	0.27	0.19	0.28
	10.0	1	7.97	2.23	0.28	0.18	0.27
	3.0	1/2	2.62	0.32	0.12	0.09	0.13
	8.9	1/2	6.21	0.74	0.12	0.09	0.13
	3.5	2	7.33	6.22	0.85	0.46	0.69
	7.0	2	9.72	3.71	0.38	0.43	0.74
	10.1	2	9.90	6.61	0.67	0.43	0.64
Same, 5' x 6"	8.0	1/4	1.58	0.21	0.13	0.04	0.07
	7.8	1/2	2.62	0.48	0.18	0.09	0.14
	8.0	1	3.42	1.58	0.46	0.23	0.35
Same, 10' x 4"	8.1	1/4	2.22	0.19	0.09	0.04	0.06
	8.1	1	3.82	0.69	0.18	0.18	0.28

APPENDIX J

SYSTEM PRESSURE DIFFERENTIAL VERSUS SINGLE ELEMENT PRESSURE DIFFERENTIAL

The problem of determining the overall pressure differential flow characteristics for a multicompartment baghouse has challenged investigators for some time. Even though the terminal resistance of each compartment (determined by the length of filtration period used) and the residual drag of each compartment (a function of cleaning) are completely under the operator's control, the sequential cleaning of several compartments means that the resistance of each compartment is different. Consequently, the filter velocity is at all times different in each compartment. Although the pressure differential across every compartment is essentially the same because they are connected in parallel, this pressure differential fluctuates between cleanings and is as hard to predict as filter velocity.

Typical variations in filtering velocity, pressure differential, and drag (or resistance) for a multicompartment baghouse are sketched in Figure J-1. Since the term T refers to the total time for N compartments to be cleaned, T/N indicates the time interval between the cleaning of any two compartments. It is customary to assume on the basis of experimental evidence, that the relationship of drag to dust deposited is linear. This is acceptable for low air/cloth ratios for which cake filtration is typical. For deep-surface fabrics or high air/cloth ratios in which cake type filtration may not be well established before cleaning, the assumption may not be acceptable. It is also customary to assume that the inlet dust concentration and the specific resistance coefficient of the dust are constant at all times and at all locations in the baghouse.

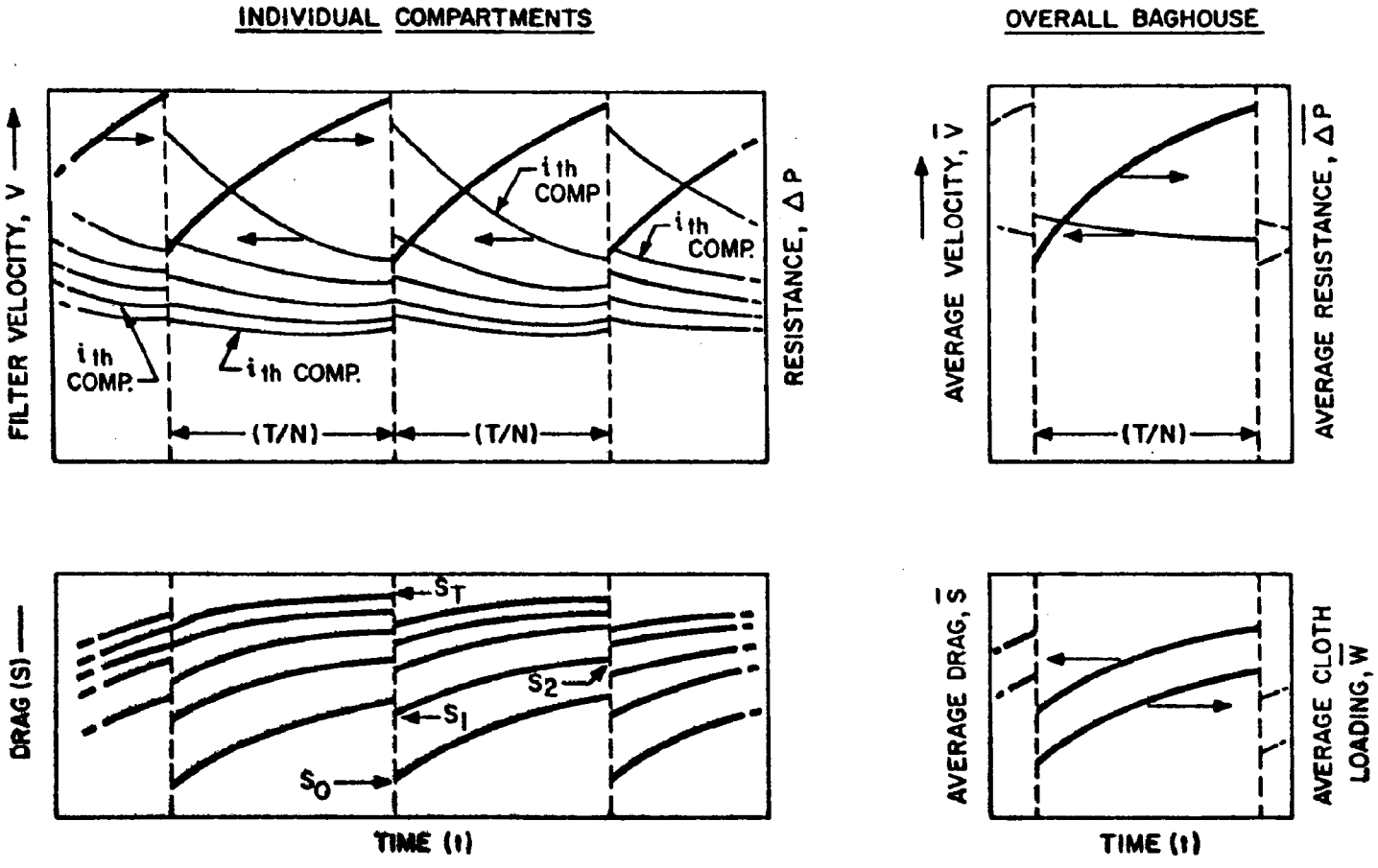

Figure J-1. Operating variables in a multicompartment baghouse. (Five compartments, negligible time for cleaning is assumed.)

In one of the first attempts at predicting the overall air flow resistance characteristics of a multicompartment baghouse, Robinson, Harrington, and Spaite* showed how the overall characteristics could be computed via a rather detailed process. Later Solbach+ developed an analytical process that was simplified by the use of nomograms. For the special case of a baghouse operating with constant pressure differential and varying flow, he showed that the filtration velocity in a single compartment was given as a function of time by

$$V = \left[\frac{2\,K\,C_i\,t}{\Delta p} + \frac{1}{\Delta p^2}\left(\frac{\Delta p}{V}\right)_o^2\right]^{1/2} \qquad \text{(J-1)}$$

where K = specific resistance coefficient of the dust

C_i = inlet dust loading

t = filtration time following cleaning

Δp = pressure differential (constant)

$(\Delta p/V)_o$ = drag of the filter at time zero. This is the effective residual drag. The author assumed that drag increases linearly with amount of dust deposited, as is customary

Solbach then showed that the filter velocity averaged for the entire baghouse over a full operating cycle of duration t' was given by

$$\bar{V} = \frac{\Delta p}{K\,C_i\,t'}\left\{\left[\frac{2\,K\,C_i\,t'}{\Delta p} + \frac{1}{\Delta p^2}\left(\frac{\Delta p}{V}\right)_o^2\right]^{1/2} - \left[\frac{1}{\Delta p^2}\left(\frac{\Delta p}{V}\right)_o^2\right]^{1/2}\right\} \qquad \text{(J-2)}$$

He might have simplified this relationship considerably since Δp was already assumed to be constant. By equating S_e to $(\Delta p/V)_o$ and rearranging terms,

*Robinson, J.W., R.E. Harrington, and P.W. Spaite. A New Method of Analysis of Multicompartmented Fabric Filtration. Taft Engineering Center, U.S. Public Health Service, Cincinnati, Ohio, paper for presentation at A.I.Ch.E. 58th Annual Meeting, Dallas, Texas, Feb. 1966.

+Solback, W., Derivation of a Computational Method for Multichamber Cloth Filters on the Basis of Experimental Results, Staub (English Trans.) 29 (1) 28, January 1969.

$$\left[\frac{K\ C_i\ T}{\Delta p}\ \bar{V} + \frac{S_e}{\Delta p}\right]^2 = \frac{2\ K\ C_i\ t'\ \Delta p}{\Delta p^2} + \frac{S_e^2}{\Delta p^2}$$

$$K\ C_i\ t'\ \bar{V}^2 + 2\ S_e\ \bar{V} = 2\ \Delta p$$

$$\frac{\Delta p}{\bar{V}} = S_e + \frac{KW_T}{2} \qquad \text{(J-3)}$$

where W_T is the weight of dust deposited over period t'. This equation states that a parameter rather similar to the average drag, $\overline{(\Delta p/V)}$, is equal to the residual drag plus half the drag increase from residual to terminal conditions. That is, baghouse drag is approximately linear with respect to dust input, just as for a single compartment.

The following independent analysis results in somewhat similar conclusions without the assumption that the pressure differential across the baghouse is constant. At any instant of time, the pressure differential is equal to the instantaneous product of drag filter velocity, both selected for any portion of the baghouse filter area:

$$\Delta p = S\ V \qquad \text{(J-4)}$$

Under the above assumption of linearity, drag is described only at conditions of loading by:

$$S = S_e + KW$$

$$\frac{dS}{dt} = K\frac{dW}{dt} = K\ C_i\ V \quad (K,\ C_i = \text{constants}) \qquad \text{(J-5)}$$

Using the above expression, the instantaneous pressure differential becomes

$$\Delta p = \frac{S}{K\,C_i}\frac{dS}{dt} = \left(\frac{S_e + KW}{C_i}\right)\left(\frac{dW}{dt}\right) \qquad \text{(J-6)}$$

It is implied, therefore, that the instantaneous pressure differential across any filter having a linear S/W characteristic is a simple function of S or of W. Since Δp is the same everywhere, the instantaneous drag times the rate of increase of drag is the same over every square inch of fabric operating in a baghouse, regardless of Δp, V, K, or C_i.

The average pressure differential over a time period t_1 to t_2 is:

$$\overline{\Delta p} \equiv \frac{1}{t_2 - t_1}\int_{t_1}^{t_2} \Delta p\, dt = \frac{1}{t_2 - t_1}\int_{S_1}^{S_2} \frac{S\, dS}{K\, C_i} = \frac{S_2^{\,2} - S_1^{\,2}}{2\,K\,C_i\,(t_2 - t_1)} \qquad \text{(J-7)}$$

In a baghouse with N identical compartments operating over a total cycle of T minutes, one compartment is cleaned every T/N minutes. It is convenient to average the pressure over this period because a complete cycle is depicted. The resulting average pressure is

$$\overline{\Delta p} = \frac{N\,\Delta S^2}{2\,K\,C_i\,T} \qquad \text{(J-8)}$$

which is the long-term average for the baghouse as well as that for any individual compartment.

Equation (J-2) says that over the time interval T/N, the quantity S^2 must be the same for every compartment. The only assumptions are that K and C_i be constant, that the S/W relationship be linear for each compartment, the operation be periodic, and the offline time be negligible during cleaning.

Equations (J-7) and (J-8) also apply to all locations in a single compartment, or all stations along a single bag. Since every point in the baghouse has the same average pressure differential, over any

time interval t_1 to t_2, every point in the baghouse undergoes the same increase with respect to the square of the drag. In this case, the resulting distribution of S^2 is not predictable, because of varying cleaning effectiveness along the bags.

In other words, over time interval T/N between cleanings, the various compartments undergo the following changes:

		Net Change of S^2		Resulting S
1st:	S_e to S_1	$S_1^2-S_e^2$	$= \Delta S^2$	$S_1 = (S_e + DS^2)^{1/2}$
2nd:	S_1 to S_2	$S_2^2-S_1^2$	$= \Delta S^2$	$S_2 = (S_e + 2\ DS^2)^{1/2}$
3rd:	S_2 to S_3	$S_3^2-S_2^2$	$= \Delta S^2$	$S_3 = (S_e + 3\ DS^2)^{1/2}$
...	...	...	...	...
Nth	S_{N-1} to S_T	$S_T^2-S_{N-1}^2$	$= \Delta S^2$	$S_T = (S_e + NDS^2)^{1/2}$
	Total	$S_T^2-S_e^2$	$= N\ \Delta S^2$	

This approach shows that Equation (J-8) might also be expressed as

$$\overline{\Delta p} = \frac{S_T^2-S_e^2}{2\ K\ C_i\ T} \qquad \text{(J-9)}$$

It signifies that the long-term average baghouse or compartment differential pressure depends simply on the residual and terminal drags between which each compartment is, in sequence, operating. Since these are up to the baghouse operator, depending on how he chooses to operate the cleaning mechanisms, this equation in effect determines what the time-averaged baghouse pressure drop will be.

Equation (J-9) can be simplified in the following manner:

$$\overline{\Delta p} = \left(\frac{S_T + S_e}{2}\right)\left(\frac{S_T-S_e}{K\ C_i\ T}\right) = \left(\frac{S_T + S_e}{2}\right)\left(\frac{KW_T}{K\ C_i\ T}\right) \qquad \text{(J-10)}$$

Since $W_T = C_i \int_0^T V\, dt = C_i \bar{V} T$,

$$\frac{\overline{\Delta p}}{\bar{V}} = \frac{S_T + S_e}{2} = S_e + \frac{KW_T}{2} \qquad \text{(J-11)}$$

This equation, which may be compared with Solbach's Equation, (J-3), cited previously, indicates that a slightly different parameter than his, but one still similar to the average drag, is still determined simply by the residual drag plus one-half the residual-to-terminal drag increase. In the present case, however, the equation applies to any baghouse, with no assumption of constant operating pressure.

If the plant situation requires filtering at a constant flow rate, typical of many industrial processes, then the left side of Equation (J-11) is equal to $\overline{(\Delta p/V)}$, which defines the average baghouse drag. The equation then says that under constant flow, the average baghouse drag is exactly half way between the residual and terminal drags between which each compartment is being operated.

Since each compartment acts as a resistance which is linear with respect to dust deposit, and since the baghouse is a passive assemblage of these resistances, it is perhaps to be expected that the resistance of the overall baghouse will also be linear with respect to deposit. Any passive system composed of linear elements has an overall linear characteristic. This overall linearity is indicated by Equation (J-11)

CONCLUSIONS

1. In each of three situations,
   - Constant pressure operation (Equation (J-3))
   - Varying pressure and varying flow operation (Equation (J-11))
   - Constant flow operation (Equation (J-11) using $\overline{(\Delta p/V)}$,

the long-term average resistance of the baghouse is described by the same simple expression with respect to dust filtered. It is therefore probable that every baghouse having linear S/W compartments, operating smoothly and periodically, has the same linear characteristic.

2. Over any given time interval, the increase of S^2 of every portion of the fabric is the same.

3. This in turn predicts that S^2 will vary in uniform steps from compartment to compartment at all times, since all compartments are cleaned periodically to the same residual level.

4. At any instant, the product of S and dS/dt is the same for every location in the baghouse.

5. By his control of the cleaning process, the baghouse operator determines the average operating pressure, via Equation (J-9).

6. The average operating pressure determines the average air/cloth ratio, via Equation (J-11).

Mathematical Model of a Five-Compartment Baghouse

To test the above predictions, a five-compartment baghouse was modeled by digital computation to predict the pressure and flow relationships for the overall baghouse as well as for the separate compartments. The following parameters were selected and held constant:

Number of compartments: 5
Inlet grain loading: 2.32 gr/ft.^{3} (exactly 1/3000 lb./ft.^{3})
Dust resistance coefficient: 10 in. H_2O/lb./ft.^{2}-ft./min.
Load cycle: 100 minutes overall, or 20 minutes between cleanings
Average air/cloth ratio: 3 ft./min.
Just-cleaned compartment drag: 1.0 in./ft./min.

Results

1. With constant inlet flow, making computations at 1-minute intervals, and cleaning one compartment every 20 minutes until the overall baghouse displayed a steady pressure cycle (equilibrated):

	Overall baghouse			Compartment being cleaned		
	Δp	V	S	Δp	V	S
Before cleaning:	4.800	3	1.600	4.800	2.41	1.992
Just cleaned:	4.162	3	1.387	4.162	4.16	1.000
Time average:	4.484	3	1.495	4.484	~3	1.495

2. Next, instead of holding flow constant, a fan curve was used to allow the flow to decrease into the baghouse as the pressure differential increased. The inlet flow-pressure characteristic was linearized using the points:

Δp	V
3.556	3.556
5.173	2.586

This fan "curve" supplies flow at about 3 ft./min. when the pressure differential is about 4.48 in.; i.e., the intention was to keep the average flow the same as above.

	Overall baghouse			Compartment being cleaned		
	Δp	V	S	Δp	V	S
Before cleaning:	4.645	2.883	1.606	4.645	2.32	1.992
Just cleaned:	4.308	3.106	1.388	4.308	4.308	1.000
Time average:	4.484	~3	1.495	4.484	~3	1.495

Thus, within a small margin of error, the average pressure differential does not depend on the slope of a linear fan curve, as long as the average operating point is the same. The pressure excursions are smaller when the flow is allowed to adjust to the pressure. Conversely,

the flow excursions are greater into the overall baghouse and also through each bag.

Incidentally, the drags of each of the five compartments were the same with both fixed and variable flows:

	C 1	C 2	C 3	C 4	C 5	
Before cleaning:	1.253	1.473	1.664	1.836	1.99193	
After cleaning:	1.253	1.473	1.664	1.836	1.000	
After 20 min.:	1.473	1.664	1.836	1.992	1.253	, etc.

Note that ΔS^2 = 0.565 = constant, as predicted

3. Next, instead of holding the increment of computation at 1.0 minute, both 0.5- and 5.0-minute increments were tried:

No. of calculations per 100-minute cycle	Overall time-average drag and Δp			
50	Δp:	4.47670	S:	1.49223
100		4.48383		1.49461
500		4.48950		1.49650

It appears that with more computation steps, the average drag approaches the theoretical value 1.50000, which is half way between the initial and terminal drags for any compartment.

Perhaps the biggest practical limitation to the above is the tacit assumption that during cleaning of one compartment, the other compartments undergo no filtration. Otherwise, the equations would be more complicated and the results less clear. For equipment which is cleaned quickly in comparison with the interval between cleanings, and which does not utilize appreciable reverse flow volume to assist the cleaning, the indicated approaches are applicable without modification.

APPENDIX K

DUST TRANSPORT DURING PULSE CLEANING

In pulse cleaning, as in any filter cleaning operation, collected particles must not only be dislodged from the filter medium, but they must be removed from the air flow system so that redeposition on the fabric is minimized. The time allowed for settling is small in the case of pulse cleaning, and the transport of particles by the pulse and airstream during pulsing and the subsequent resumption of filtration may have considerable impact upon the effectiveness of particle removal.

In this analysis, the three transport processes associated with pulse cleaning, particle ejection, air flow transport, and settling, are sketched as vectors in Figure K-1. It is assumed that the three processes are additive to a first approximation. The slanting lines to the right of the filter bag indicate the flow lines taken by the reversal air, first as the air leaves the bag and blows back toward the hopper, and then as the same air returns to the bag and is refiltered. The average angle of these lines depends on the length of the bag and the proximity of the bag either to a solid wall, to a vertical stagnation line between two bags being pulsed simultaneously, or to a bag that is still filtering.

Particles of all sizes are probably ejected from the bag horizontally because the fabric motion is horizontal, and also because the air passes through the bag essentially horizontally since the vertical air pressure gradients inside and outside the bag are small. It is hypothesized that the particles leave the fabric with a velocity greater than that

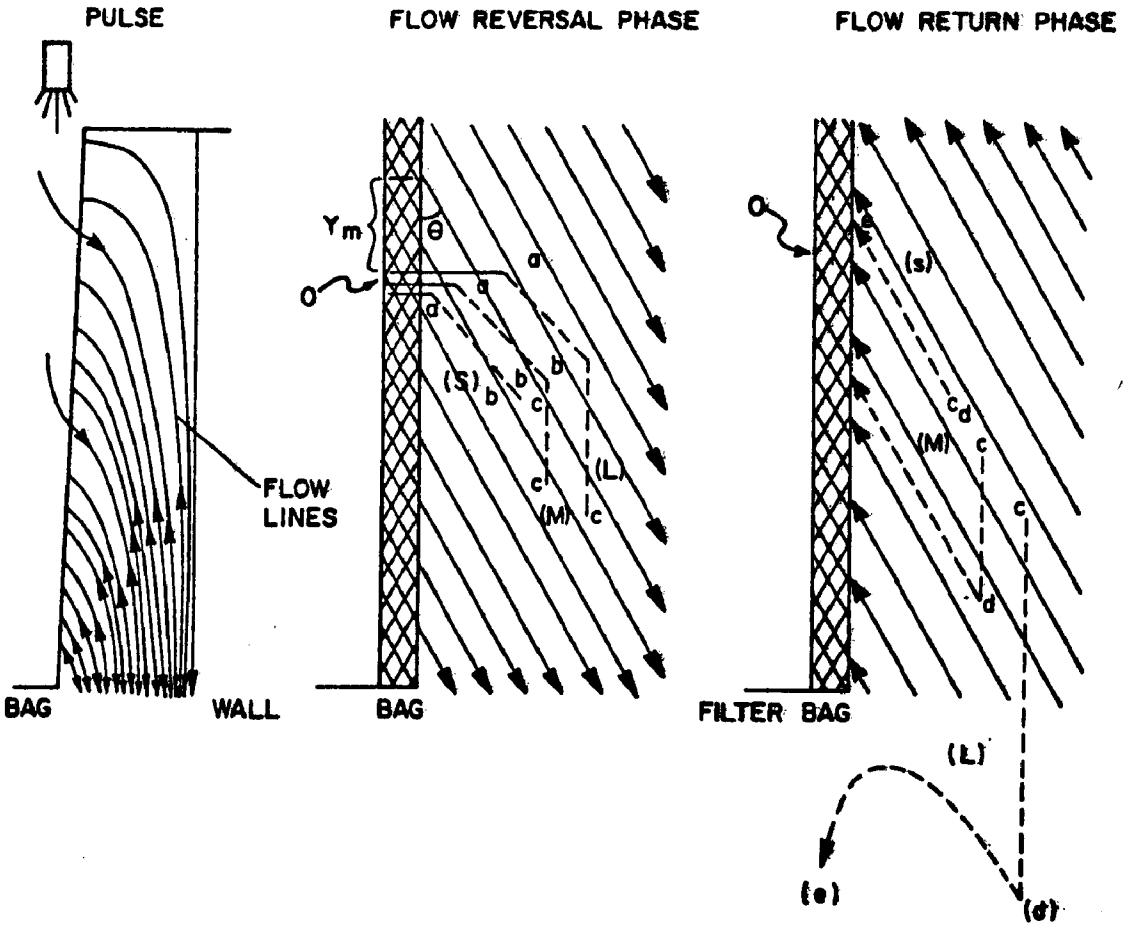

Figure K-1. Transport effects on particle disposition; s: small particles, M: medium particles, L: large pargicles. Path o-a: initial momentum due to pulse; path a-b: air transport during the reversed flow; path b-c: gravity settling during flow return; path d-e: air transport during flow return; point e: final deposition point; path o-e: net change of position on filter bag.

of the accompanying air. With an initial horizontal momentum rapidly reduced by air viscosity, the particles travel a "stopping distance" to point (a) in Figure K-1, the distance depending on the particle inertia. During this same time and until the flow reverses, all particles are transported in effect along the air flow lines through the distance vectors (a-b). This is the distance that the air moves backwards from the instant the particles are removed. Again during the same time period, the particles settle due to gravity a distance vector (b-c). This is determined approximately by the settling velocities in Figure K-2.* Thus under the concurrent action for momentum, aerodynamic transport, and settling, the particles reach points (c) by the time the air stops moving backwards.

Shortly thereafter, the flow reverses and follows approximately the same flow lines back to the filter. This time, the net result is the sum of two distance vectors. Until the particles reach the filter they continue to settle. Because the larger particles have farther to travel back to the filter, point (c) is farther from the filter for the larger particles. They settle even farther (c-d) than during the flow reversal phase. The transport distances (d-e) are also longer for the larger particles. In fact, many of them will have reached a point (d) so low in the system that they miss the filter bag, and continue to fall into the hopper. On the other hand, the smaller particles are seen to be slightly lifted up the bag by the cleaning process. This may partially account for the occasional observation of a very heavy accumulation of dust near the top of the filter bag.

The foregoing discussion is based on potential laminar flow. Actually, the flow is to some extent turbulent, and many secondary air currents

*There are additional inertial considerations associated with sudden changes of the direction of the air, but because the air reverses itself, these tend to cancel.

may be present. Although Figure K-1 indicates the average disposition of particles, turbulence will cause considerable mixing in the flow region. Some small particles will be carried even higher on the bag than indicated in Figure K-1.

Reexamination of the five distance vectors in Figure K-1 shows that as long as the air returns via the same flow lines, the settling process depends only on the free-fall terminal velocity of the particles, V_T and on the time available for fall. This time from the instant the particles leave the felt surface until they return is approximately equal to the duration of the pulse, T_p, plus the time required, T_R, to return to the filter surface. The initial momentum of the particles increases the distance the particle must travel to return to the fabric surface. The initial momentum also has an adverse effect, Y_m, on the net vertical distance, because it drives the particles over to flow lines which terminate at a higher location on the fabric. Consequently, the net vertical distance traveled is

$$y = V_T (T_p + T_R) - Y_m \qquad \text{(K-1)}$$

The pulse duration, T_p, is determined by the design and operating characteristics of the equipment. The time, T_R, is given by $T_p \frac{V_p}{V_R}$, where V_R is the average return air velocity, and V_p is the average pulse velocity, plus the time, T_m, gained by virtue of the momentum of the ejected particle. T_m is given by $Y_m/\bar{V}$, where $\bar{V}$ is the vertical component of the return air velocity. To a first approximation $\bar{V}$ and V_R may be equated to each other and the normal upward velocity in the dust collector; i.e., the filtering flow divided by the cross-sectional area carrying dirty air. The adverse effect of the momentum of the particle, Y_m, is given by m cot θ where m is the length of the path (o-a) in Figure K-1, and θ is the angle made by the flow lines with the vertical. Length, m, the stopping distance of the particle having initial outward velocity, Vo, is given by

$$m = \frac{V_o \rho D^2}{18} = \frac{V_o V_T}{g} \qquad \text{(K-2)}$$

using the approximation for V_F given in Figure K-2. With these substitutions, Equation (K-1) becomes

$$y = V_F \left[\left(T_P + \frac{V_p T_p}{V_R} + \frac{V_o \cot \theta}{g} \left(\frac{V_T}{V_R} - 1 \right) \right) \right] \qquad \text{(K-3)}$$

The equation indicates an advantage in having steep flowlines in the dust collector, such as might be obtained by using baffles between bags not cleaned simultaneously. An advantage in having a slow recovery of flow immediately following the pulse is also indicated; i.e., low V_R. If the dislodged particles are small (low V_T/V_R ratio), then a long pulse time may be advantageous. Conversely, agglomerates with a sufficiently high falling velocity should reach the hopper regardless of the pulse time, as expected. The hypothesized high initial dislodgement velocity is advantageous in minimizing redeposition of dust on the fabric.

As an example, consider agglomerates having diameters of 10, 30, 100, and 300 microns, with the same specific density of 1.0. The fall velocities are respectively, 0.011, 0.09, 0.82 and 3.3 ft./sec. Given the same ejection velocities of 2 ft./sec. by a pulse 0.06 seconds in duration in a system with an average upward flow velocity of 0.5 ft./sec. and $\theta = 1/12$ (e.g., 4 ft. bags surrounded by an average 4 in. clearance), the estimated shifts of particles along the bag during a single pulse are

10 : y = 0.011 (0.06 + 0.24 + (0.67) (0.022-1)) = 0.0039 feet upwards
30 : y = 0.09 (0.06 + 0.24 + (0.67) (0.18-1)) = 0.023 feet upwards
100 : y = 0.82 (0.06 + 0.24 + (0.67) (1.64-1)) = 0.60 feet downwards
300 : y = 3.3 (0.06 + 0.24 + (0.67) (6.6-1)) = 15.5 feet (i.e., 100%)

The theory thus predicts an intermediate agglomerate size which is lifted, or at least apt to settle less than either smaller or larger particles.

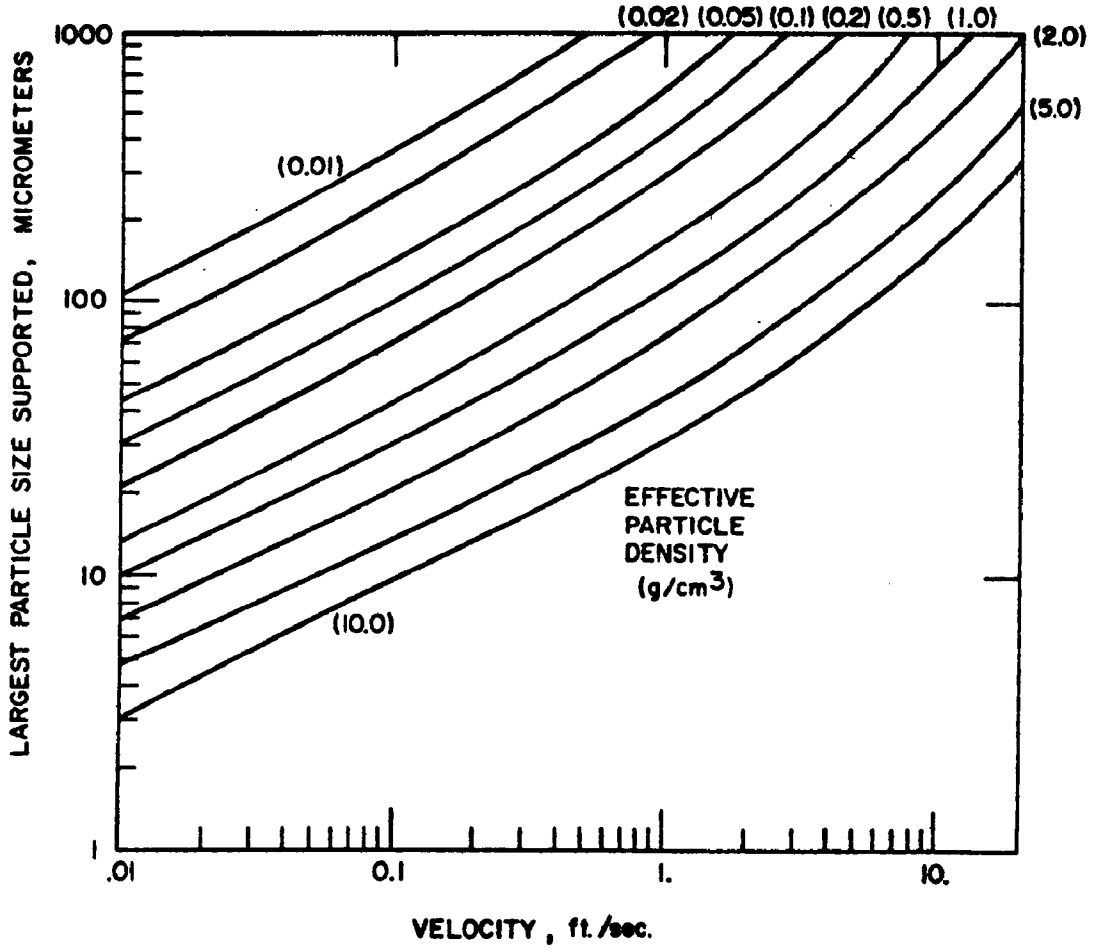

Figure K-2. Particle (or agglomerate) sizes which are supported by upward air flow. (Spherical particles; equivalent to terminal settling velocities and sizes.)

Also, agglomerates must be larger than 100 microns before the transport process is very effective.

An effectiveness ratio may be defined as y/L where L is the length of the bag. Since (cot θ) is approximately given by L/d where d is the average distance between the bag and the flow stagnation wall, the Equation can be rewritten:

$$\zeta = \frac{y}{L} = V_T \left(\frac{T_p}{L} + \frac{T_p}{L} \frac{V_p}{V_R} + \frac{V_o}{dg} \left(\frac{V_T}{V_R} - 1 \right) \right) \qquad \text{(K-4)}$$

Short bags, or bags packed close together, would apparently be cleaned more effectively than longer or more separated bags. Bags packed close together must be cleaned simultaneously, however.

Particles falling in clusters or clouds may fall faster than when falling individually, depending on the cloud density. The possible effects of this phenomena on the operation of pulse cleaned equipment have not been investigated.

APPENDIX L

FABRIC ACCELERATION IN PULSE CLEANING

In this appendix, estimates are made of the maximum acceleration seen by the filter bag during the cleaning pulse. The derivation is based on the mechanical properties of the bag and the pulse pressure differential.

In this study, dust was collected on the outside of the bag, with the bag supported by a cage composed of ten longitudinal rods 1.25 in. apart. During filtering, the bag draped inward between the rods under an inward pressure. The slackness of the bag, its stiffness, and the inward pressure determined the amount of drape; i.e., the distance the fabric was moved radially inward. This was of the order of 0.3 inches from the fully outward position. In both the inward and the outward positions, the bag was a geometric cylinder; i.e., it had negligible curvature in the longitudinal direction.

When the pressure reversed at the beginning of the pulse, the bag moved from its initial draped configuration outward until taut, where in stopping it experienced a sharp deceleration. This was larger than any other deceleration or acceleration seen at any other time during the cleaning pulse. To a first approximation, the magnitude of the deceleration depended on the velocity of outward movement and on the inelasticity of the fabric that stopped its motion. This will be clarified in the following paragraphs.

MECHANICAL PROPERTIES OF THE BAG

One major characteristic of the bag is the static position that it assumes as a function of pressure differential across the fabric. This geometry was measured using an auxiliary fan and Variac with the results shown in Figure L-1. Beginning at zero pressure differential it takes very little pressure to move the bag either inward or outward to the extent of the slackness. The pressure only has to overcome the frictional stiffness of the filter. However, after the slackness is removed, the inelasticity of the fabric takes over from the stiffness, and the displacement is greatly retarded. In changing from an increasing to a decreasing pressure differential, hysteresis is evident, due to friction internal to the fabric and dust matrix. However, because the cleaning process mainly involves a one-way movement (inflation), only the lower curve for each bag is relevant.

The inflation curves of Figure L-1 are to a first approximation characterized by a steep slope near zero differential pressure, and a nearly flat slope at fully inflated pressure. These slopes, which are termed G, the flexibility, and M, the elasticity of the bags, respectively, are delineated in the following sketch.

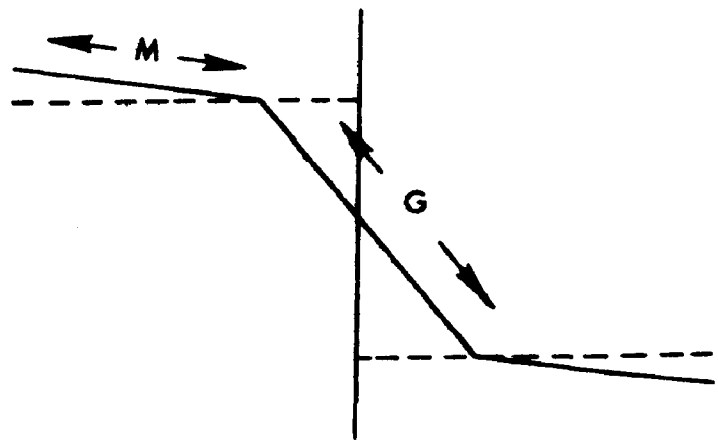

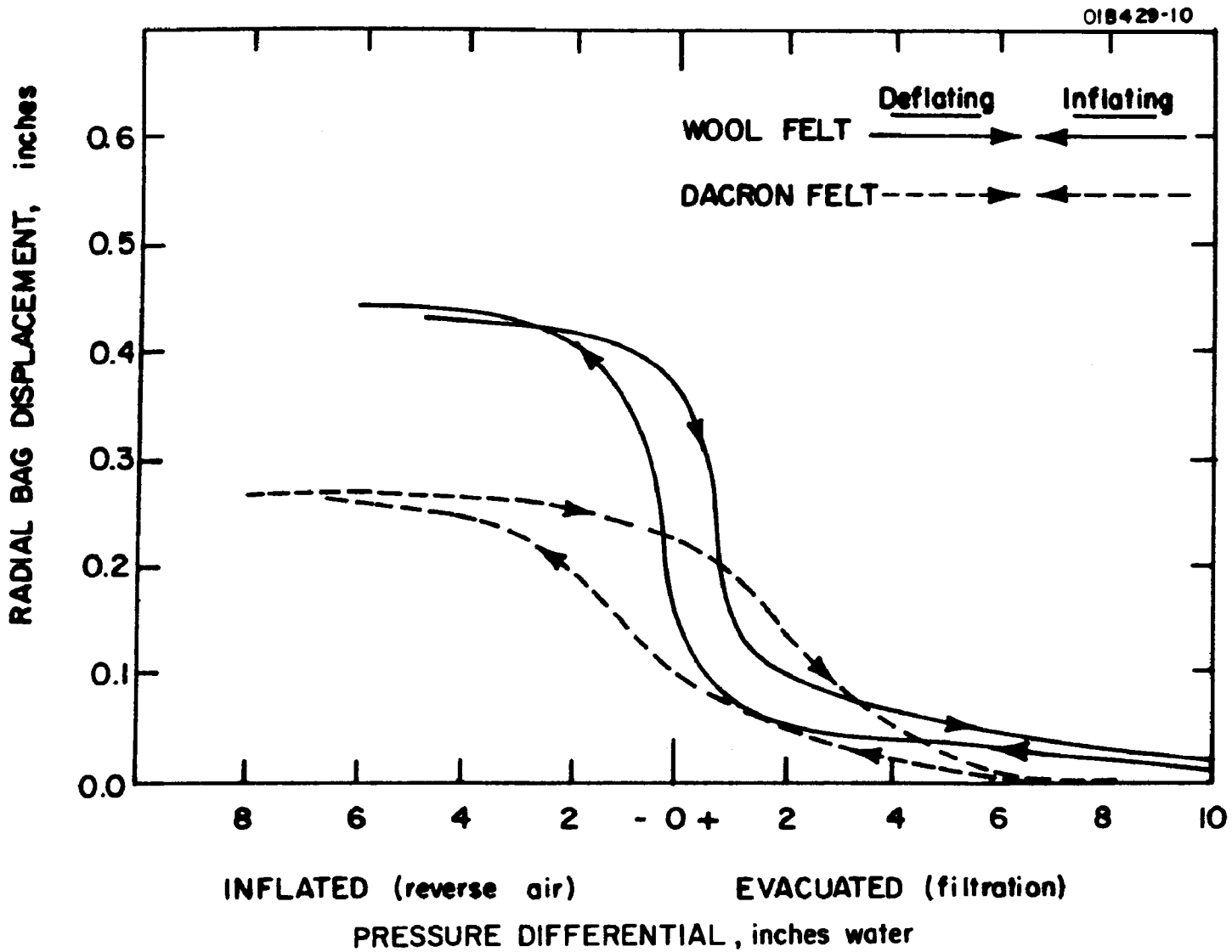

Figure L-1. Static displacement of fabric surface at constant differential pressure, used bags

	Flexibility, G		Elasticity, M	
	in/in. H_2O	ft./(lb./ft.^{2})	in/in. H_2O	ft./(lb./ft.^{2})
Wool bag with dust	0.44	0.0071	0.0033	0.000053
Dacron bag with dust	0.054	0.00087	0.0020	0.000032

The woolen felt with its residual dust is seen to be much more flexible and slightly more stretchable than the Dacron felt plus dust.

Dynamics of Bag Motion

In moving radially approximately 0.3 inches and draping between rods 1.25 inches apart, the motion of the bag is essentially one-dimensional. The equation of motion is:

$$\rho \frac{d^2r}{dt^2} + \sigma_r = \Delta p(t) \qquad \text{(L-1)}$$

The first term is the mass per unit area times the radial acceleration of the fabric. The second term is the force per unit fabric area which is resisting motion at an instantaneous bag displacement, r. σ_r has the units of pressure and is assumed to be given by Figure L-1 at an identical fabric displacement. The third term is the instantaneous pressure differential across the fabric.

Point-by-point solution of this equation was obtained, using a typical pulse and the Dacron inflation curve from Figure L-1. It was found that the felt began to move outward with a peak acceleration of 22 g's, reached a maximum velocity of 4.6 feet/second and then stopped with a maximum deceleration of 266 g's 0.01 seconds after the pulse began. The felt then continued to expand slowly and oscillated slightly in the inflated position with negligibly small oscillation amplitude and

accelerations. This computed motion was in good general agreement with the motions detected by laboratory means.

The point-by-point solution method was laborious and not at all suited to field application. Therefore, a simplified method of estimating the peak deceleration of the fabric was developed.

Estimating Fabric Deceleration

The fabric can be viewed as a mass traveling radially outward until it is stopped by a spring. The stopping deceleration depends on the maximum velocity acquired in the outward travel. There are several ways of estimating the maximum velocity, depending on the time taken for the fabric to reach maximum velocity compared with the pulse rise time. Most of the fabric's velocity is acquired during the flip-flop, or steep portion of the curve describable by:

$$\rho \frac{d^2 r}{dt^2} + \frac{r}{G} = \Delta p(t) \qquad \text{(L-2)}$$

This has a characteristic oscillation period $2\pi\sqrt{G\rho}$ seconds, which means that full velocity is characteristically developed from a dead start in about $1.6\sqrt{G\rho}$ seconds. If this characteristic time is shorter than or similar to the time required for the pulse to attain maximum pressure differential, the fabric is either fairly light or flexible and tends to move with the pulse. If the characteristic time is much longer than the pulse rise time, the fabric acts sluggish and cleaning may be poor until the pulse is lengthened.

STIFF, LIGHT FABRICS

The filter bags tested in this study appeared to be of the type, such that during the outward travel the position of the fabric was mainly

dependent on the stiffness of the fabric rather than on its mass. That is, the second term of the dynamics equation was much larger than the first term. Using the linearized equation (L-2) above, the maximum fabric velocity will be:

$$V_{max} = \frac{dr}{dt} = G \frac{d\sigma}{dt} = G \frac{d\Delta p}{dt} \qquad \text{(L-3)}$$

For example, a linear pulse with a rise rate of 1000 in. H_2O/sec. acting on the Dacron bag described above, would produce a maximum fabric velocity of about 54 in./sec.

At this peak velocity, the bag will move its full 0.3 inches in roughly 0.011 seconds. Since the pulse travels the full length of the bag in about 0.004 seconds (4 feet, at sonic velocity) the entire length of the bag must inflate almost simultaneously. Much stiffer bags will inflate as a cylinder, with no difference from top to bottom. Bags having a faster inflation velocity (minimal stiffness) will inflate in ripple fashion, with the ripple traveling from top to bottom at approximately sonic velocity.

Because the Dacron bag is estimated to develop a velocity of 54 in./sec. after about 0.0055 seconds, the associated acceleration is of the order of 82.0 ft./sec.^{2} (2.6 g's). Because the weight per unit area was 0.225 lb./ft.^{2} for this bag, the first term in the equation of dynamics is only about 1 in. H_2O compared with values of the second term of several in. H_2O. This justifies the earlier statement that the Dacron bag behaved like a stiff, light fabric.

Flexible, Heavy Fabrics

The inflating motion of flexible, heavy fabrics is resisted by the inertia of the fabric rather than the stiffness. The second term in the equation

of dynamics is negligible compared with the first term during development of the maximum outward velocity. Consequently,

$$V_{max} = \frac{1}{\rho} \int_0^T \Delta p(t)\, dt$$

$$= \frac{1}{\rho}\left(\Delta p_o T - \alpha \frac{T^2}{2}\right), \text{ for } \Delta p = \Delta p_o - \alpha t \qquad \text{(L-4)}$$

describes the velocity obtained by the fabric under a linear pulse after T seconds. T is limited either by the length of the pulse or by the fabric reaching the limit of its slackness, whichever happens first.

Moderately Stiff, Moderately Heavy Fabrics

In case neither the first nor the second term of the dynamics equation is negligible compared to the other one, both must be included in the solution. The most reliable solution is the numerical one already mentioned, in which point-by-point values of acceleration, velocity, and displacement are computed. A simpler approximation is the piece-wise linear method, in which the three straight parts of the characteristic curve are represented by analytic functions.

For the special case in which the characteristic time of the fabric motion is similar to the pulse rise time, the fabric may be expected to travel about one half its full displacement in the characteristic time, giving a rough estimate of the maximum velocity attained of

$$V_{max} = \frac{s}{3.2\sqrt{G\rho}} \qquad \text{(L-5)}$$

where s is the distance of travel, approximately 0.3 inches in this case.

With an estimate of the maximum outward velocity attained by the fabric during the beginning of the pulse, it is possible to estimate the deceleration of the fabric as it stops in the fully outward position. The fabric stops when its kinetic energy is fully converted to elastic energy:

$$1/2\ \rho V^2_{max} = 1/2\ M\ \sigma^2_{max} \qquad \text{(L-6)}$$

where simplifying assumptions of linear elastic stretching and negligible frictional energy loss have been made. From the above,

$$a_{max} = \frac{\sigma_{max}}{\rho} = \frac{V_{max}}{\sqrt{\rho M}} \qquad \text{(L-7)}$$

For the case of stiff, light fabrics, this equation becomes

$$a_{max} = \frac{G}{\sqrt{\rho M}} \cdot \frac{d\Delta p}{dt}\ , \qquad \text{(L-8)}$$

For example, $G = 0.00087$ ft./(lb./ft.^{2})

$M = 0.000032$ ft./(lb./ft.^{2})

$\rho = 0.0080$ lb. sec.^{2}/ft.^{3} (area mass density)

$\frac{d\Delta p}{dt} = \alpha = 1000$ in. H_2O/sec. $= 5200$ lb./ft.^{2}-sec.

$a_{max} = 8920$ ft./sec.$^2 = 279$ g's.

in good agreement with laboratory values.

Velocity of Removed Agglomerates

It is of interest to know as much as possible about the velocity of the material that is ejected from the fabric, since the velocity determines in part the disposition of the material; i.e., to the hopper or back onto

the fabric. In simple harmonic motion, the maximum acceleration occurs at the end of the stroke, when the velocity is zero. Differentiation of equation (L-1) and setting the acceleration term equal to zero, results in:

$$\frac{d\Delta p}{dt} - \frac{d\sigma_r}{dt} = \rho \frac{d^3 r}{dt^3} = 0$$

$$\frac{d\Delta p}{dt} = \left(\frac{d\sigma_r}{dr}\right)\left(\frac{dr}{dt}\right) = \left(\frac{1}{M}\right)\left(V\right) \qquad \text{(L-9)}$$

In other words, the deceleration is maximum when $V = M\, d\Delta p/dt$, approximately. Using the numerical example above, at the instant that the deceleration is 279 g's, the velocity is estimated to be 0.167 ft./sec. or 10 ft./min. The maximum velocity when the acceleration was zero or at least too small to remove much dust was 4.5 ft./sec. Thus, all the dust is estimated to leave the fabric at velocities between 4.5 and 0.167 ft./sec. depending on the levels of acceleration necessary to cause separation. These ejection velocities are referenced to the collector cage, not to the bag which is moving at similar but decelerating velocities.

In addition to these ejection velocities, reverse air is moving through the filter at approximately 0.5 ft./sec. Thus Stokes drag will tend to change the ejection velocities ultimately to 0.5 ft./sec.

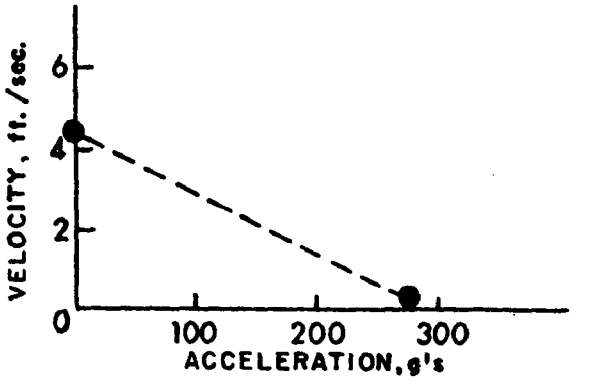

APPENDIX M

SUPPLEMENTARY DATA ON PRECISION OF MEASUREMENT TECHNIQUES

ANDERSEN "OUTSTACK" IMPACTOR

The Andersen impactor design for sampling ambient atmospheres (Particle Fractionating Sampler) was used for assessing inlet and outlet dust concentrations during filtration studies. Small duct diameters as well as the need to collect as much dust as possible precluded use of the "in-stack" model. Current use of the "outstack" device on another test program provides some useful statistics on the reliability of this device. Figure M-1 indicates that the results of parallel sampling of a resuspended foundry dust (MMD ~ 1 μm) by filters and impactors were in fair agreement.

Deviations from the regression line are attributed to errors introduced by sample transfer from probes, weighing errors, and fluctuations in sampling flow. Practically speaking, these results probably typify the expected field performance for these units.

Two sets of impactor stages, consisting of Petri dishes lubricated with a petroleum jelly and weighing about 20 to 21 grams were allowed to stand in a dessicator for 3 days between successive weighings. No special precautions other than routine care were exercised in the weighings. The reported weight differences shown in Table L-1 are based upon the original sample weights.

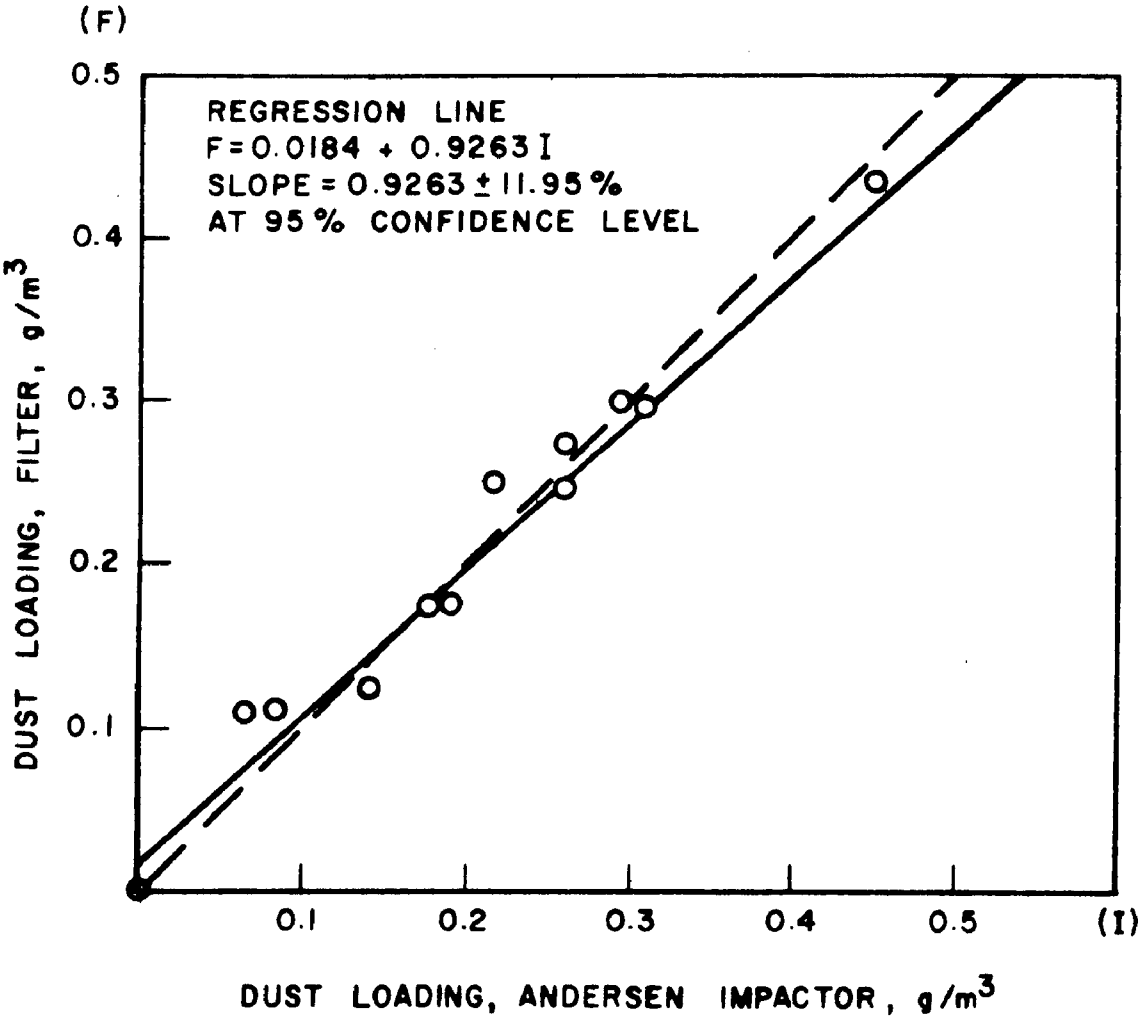

Figure M-1. Comparative mass loading measurements with all-glass filters and Andersen impactor (foundry dust, MMD = ~ 1 μm)

Table M-1. WEIGHT LOSSES FOR LOADED LUBRICATED, PETRI DISH IMPACTOR STAGES AFTER REPEATED WEIGHINGS

Weight loss milligrams		
Stage	Set 1	Set 2
1	0.3	0.1
2	0.1	0.2
3	0.2	0.2
4	0.0	0.3
5	0.1	0.2
6	0.3	0.5

Since the estimated standard deviation for the above 12 measurements was 0.13 mg. stage weights should probably be within $\pm$ 0.26 mg. of the true weight at least 95 percent of the time.

TECHNICAL REPORT DATA *(Please read Instructions on the reverse before completing)*		
1. REPORT NO. EPA-650/2-75-009	2.	3. RECIPIENT'S ACCESSION NO.
4. TITLE AND SUBTITLE Fabric Filter Cleaning Studies		5. REPORT DATE January 1975 6. PERFORMING ORGANIZATION CODE
7. AUTHOR(S) Richard Dennis and John Wilder		8. PERFORMING ORGANIZATION REPORT NO. GCA-TR-74-6-G
9. PERFORMING ORGANIZATION NAME AND ADDRESS GCA Technology Division Burlington Road Bedford, MA 01730		10. PROGRAM ELEMENT NO. 1AB012; ROAP 21ADJ-049 11. CONTRACT/GRANT NO. 68-02-0268
12. SPONSORING AGENCY NAME AND ADDRESS EPA, Office of Research and Development NERC-RTP, Control Systems Laboratory Research Triangle Park, NC 27711		13. TYPE OF REPORT AND PERIOD COVERED Final 14. SPONSORING AGENCY CODE
15. SUPPLEMENTARY NOTES		

16. ABSTRACT The report gives results of a detailed study of fabric filter cleaning mechanisms. A highly instrumented, pilot plant system was built to operate as a single- or multiple-bag unit for the investigation of cleaning by mechanical shaking, pulse jet air, and reverse flow air. Four woven bag types (cotton and Dacron) and two felt bag types (wool and Dacron) were evaluated with resuspended fly ash and talc dusts. Analysis of cleaning by both mechanical shaking and pulse jet air indicated that the tensile forces generated by bag acceleration were the main cause of dust removal; aerodynamic re-entrainment played only a minor role. Residual fabric drag, fabric holding capacity, and dust penetration characteristics were predictable, based on such cleaning parameters as shaking frequency, amplitude, pulse jet pressure, and rate of pressure rise. Based on inlet concentration of 3-10 gr/cu ft, effluent concentration for mechanically shaken, woven fabrics ranged from 10 to the minus 7th power to 0.001 gr/cu ft, in contrast to 0.001-0.01 gr/cu ft for felted media cleaned by pulse jet air. Effluent concentrations for both systems decreased significantly as filtration progressed. Caution should be exercised before extrapolating test results to dust/fabric combinations other than those investigated, until more data is available.

17. KEY WORDS AND DOCUMENT ANALYSIS			
a. DESCRIPTORS		b. IDENTIFIERS/OPEN ENDED TERMS	c. COSATI Field/Group
Air Pollution	Wool	Air Pollution Control	13B
Air Filters	Woven Fabrics	Stationary Sources	13K
Cleaning	Felts	Fabric Filters	13H
Dust	Fly Ash	Mechanical Shaking	11G, 21B
Cotton Fabrics	Talc	Pulse Jet Air	11E, 08G
Polyester Fibers	Kinetics	Reverse Flow Air	20K

18. DISTRIBUTION STATEMENT	19. SECURITY CLASS *(This Report)*	21. NO. OF PAGES
Unlimited	Unclassified	438
	20. SECURITY CLASS *(This page)* Unclassified	22. PRICE

EPA Form 2220-1 (9-73)